

ACTA PHYSIOLOGICA SCANDINAVICA
Supplement 442

THE RENIN ANGIOTENSIN
SYSTEM AND KIDNEY FUNCTION
A REVIEW OF
CONTRIBUTIONS TO A NEW THEORY

BY
PAUL P LEYSSAC

COPENHAGEN
1976

ACTA PHYSIOLOGICA SCANDINAVICA
Supplement 442

*The University Institute for Experimental Medicine
Copenhagen, Denmark.*

THE RENIN ANGIOTENSIN
SYSTEM AND KIDNEY FUNCTION
A REVIEW OF
CONTRIBUTIONS TO A NEW THEORY

BY
PAUL P LEYSSAC

COPENHAGEN
1976

Table of Content

Introduction	5
The two alternative model	7
a) the classical theory	7
b) the alternative hypothesis	9
c) working hypothesis	11
Evidence obtained with the occlusion time technique	13
The problem of proximal lumen diameter variations	17
Inter-tubular hydrostatic pressure variations	20
The effective filtration pressure	21
Physiological factor adjustment of proximal reabsorption rate and plasma flow dependence of GFR	24
The effect of anhydrites on the functional status of the kidney	28
Effect of angiotensin on osmotic transport and epithelial transport	31
The intraluminal effect of endogenous angiotensin	33
Tubuloglomerular feedback	35
Summary and concluding remarks	37

Table of Content

Introduction	5
The two alternative model	7
a) the classical theory	7
b) the alternative hypothesis	9
c) working hypothesis	11
Evidence obtained with the occlusion time technique	13
The problem of proximal luminal diameter variations	17
Inter tubular hydrostatic pressure variations	20
The effective filtration pressure	21
Physiological factor adjustment of proximal reabsorption rate and plasma flow dependence of GFR	24
The effects of anesthetic on the functional states of the kidney	28
Effect of angiotensin on isosmotic trans epithelial transport	31
The role of renal effects of endogenous angiotensin	33
Tubulo-glomerular feedback	35
Summary and concluding remarks	37

Introduction

Over the last decade considerable effort has been directed towards clarifying the local physiological role of the renin-angiotensin system for the intrarenal regulation of kidney function, in particular for the regulation of salt and water excretion, glomerular filtration rate (GFR) and renal blood flow (RBF).

The question concerning the contribution of the renin system to the regulation of the functions is necessarily related intimately with the phenomenon itself of so-called glomerulo-tubular balance, i.e. the fact that GFR is closely interrelated with the absolute rate of overall absorption of salt and water over a fairly wide range of variations both under physiological and experimental physiological conditions. Since the proximal absorption amounts to 70-75% of the total tubular absorption of salt and water (and of GFR) and repeatedly has been shown to vary in parallel with GFR under the conditions (e.g. Ley 1961; Schnemann et al 1963; Rodin et al 1969; Leitch et al 1968; Dirks et al 1965) the focus of research in this context has been directed to the mechanism of coupling between the rate of proximal reabsorption and filtration. Thus the fundamental question is how the proximal absorptive capacity is regulated and adjusted to the filtration process and vice versa.

Two views have been advocated. The first is the theory proposed by Rowe (1951) and accepted by most investigators, that the rate of proximal absorption is automatically adjusted by changes in the filtered load; several mechanisms for which a response have been proposed. The other concept is that of the Copenhagen point of view, the underlying hypothesis is that the proximal absorptive capacity is primarily independent of the load per

Introduction

Over the last decade considerable effort has been directed toward clarifying the local physiological role of the endocrine system in the intrarenal regulation of kidney function in particular for the regulation of salt and water excretion, glomerular filtration rate (GFR) and renal blood flow (RBF).

One question concerning the contribution of the renin-angiotensin system to the regulation of these functions is necessarily related intimately with the phenomenon often referred to as "glomerulo-tubular balance", namely the fact that GFR is closely parallel with the absolute rate of overall absorption of salt and water over a fairly wide range of variation both under physiological and several pathological conditions. Since the proximal tubule absorption accounts for 70-75% of the total tubular reabsorption of salt and water (and of GFR) and reportedly has been shown to vary parallel with GFR under these conditions (e.g. Ley, 1963; Schoermermann et al., 1968; Rodicio et al., 1969; Laine et al., 1968; Dix et al., 1963) the focus of most interest in this context has been directed to the mechanism of coupling between the rate of proximal reabsorption and filtration. Thus the fundamental question is how the proximal absorptive capacity is regulated and adjusted to the filtration pressure and vice versa.

Two alternative concepts have been advocated. The classical theory is credited by some (Smith (1951)) and accepted by most investigators in the field of proximal absorption: (i) automatic adjustment by changes in filtered loads; several mechanisms for such automatic responses have been proposed. The other concept is based on the Copenhagen point of view to the effect that the proximal absorptive capacity is physiologically independent of the filtered

significant change in GFR are secondary to hormonally mediated alterations in tubular reabsorption - predominantly in proximal tubular reabsorption (for comprehensive review of the evidence leading to this hypothesis the reader is referred to Loysac 1966)

The vast and expanding literature relating to these problems and the methodology utilized for their elucidation has been critically reviewed by several investigators (e.g. Mollin & Burg 1971; Wright and Giebisch 1972; Gottschalk and Leib 1973; Easley and Schrier 1973; Wardene 1973; Gutter and Boylan 1973; Leib 1975). However, the results of these surveys are rife with the implication of considerable uncertainty and divergence between concepts favoured by the various authors; controversy maintained partly in part due to the differences in personal valuations of the possible influence of errors and artifact and hence of the significance of the individual but mutually conflicting results. Many of the artifacts have now been recognized and some of them not until recently motivated re-evaluation of the overall problem.

In addition, one of the basic hydrodynamic characteristics of the nephron, namely the relatively high flow resistance offered by tubular segments distal to the proximal tubule has largely been neglected in considerations on the dynamics of glomerular filtration. In my opinion, this neglect has contributed to much unnecessary misunderstanding and continued disagreement.

Equally important is the distinction between the various concepts of a so-called central report on the local interrenal actions of dogenous and exogenous angiotensin which contribute to the motivation for re-evaluation of the problem obtained in the many attempts to clarify the complex of problems outlined above.

The purpose of the present paper is not to give a comprehensive review of literature pertaining to publication available on this subject but to refer to the above-mentioned views in particular to the relevant chapters in Handbook of Physiology (Section 8, 1973 on Renal Physiology) and to the recent review on renal mechanisms by Davison & Fries (1976). For the sake of clarity and comprehension I have preferred to limit mainly those contributions which I consider to be the most significant contribution on the way towards generally acceptable dogmatically on this theory.

by mean of the taps denoted by (A) and (E) representing the resistance of the afferent and efferent arterioles respectively. A long side-pipe representing the tubule is connected with the main pipe. A filter is inserted in the connecting link. The pressure inside the main-pipe at the level of the filter is the ultrafiltration pressure (P_{UF}) may be varied by change in the distance (A) and (E) i.e. by contraction and dilatation of the arterioles. P_{UF} is defined as $(P_{cap} - COP)$; P_{cap} is the hydrostatic pressure in the glomerular capillaries and COP is the colloid osmotic pressure.

The filter represents a certain resistance represented by the tap (G). The given value of this resistance gives a given pressure drop across the filter. The magnitude of which is a function of the resistance (G). This pressure drop equal to the filtration pressure minus the hydrostatic pressure at the proximal section of the side-pipe ($P_{UF} - P_{prox}$) determines the GFR and is referred to as the effective filtration pressure (EFFP).

The side-pipe (tubule) consists of two sections: proximal and a distal section separated by a tap (H) representing the resistance of the loop of Henle. A set of adjustable pipes connected to each section of the long side-pipe representing tubule reabsorption proximally (R_{prox}) and distally (R_{dist}) respectively.

It is self-evident that the proximal lumen hydrostatic pressure is maintained constant if a primary change in tubular reabsorption in GFR automatically cause parallel increase in proximal reabsorption, i.e. such that the tap (R_{prox}) remove equally much more fluid from this segment as is added by the change in filtration rate. This constancy of proximal intratubular pressure implies that basal tubular reabsorption is a fundamental assumption and implication.

The other fundamental assumption is that the glomerular reabsorption is the effective filtration pressure is relatively high; i.e. the order of 10-40 mm Hg (cf Pitts 1963; McKim and Gilmo 1973). This would imply that the very modest change in proximal intratubular pressure, which might occur due to hypothetical primary change in proximal reabsorptive capacity would significantly influence the magnitude of the effective filtration pressure (GFR). Such primary change in tubular reabsorption if it occurs at all then could only be responsible for changing the pressure drop (EFFP) of few per cent. The effective filtration would most likely be determined

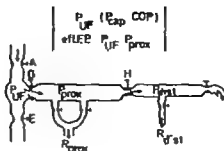
ined by the magnitude of and change in the ultrafiltration pressure (P_{UF}) is by glomerular vascular factors.

It is assumed that the automatic (physiologically determined) parallel adjustment of the proximal reabsorptive capacity and hormonal regulation of fluid reabsorption rate by this segment would of course appear accordingly according to this theory.

It is believed that the mechanism responsible for the assumed automatic adjustment of the rate of proximal reabsorption was the repletion by active sodium transport at maximum capacity of a limiting concentration difference across the proximal epithelium (Weinman, Anslow and Smith 1948; Smith 1951). Thereby any increase in the delivery of fluid into the tubule by filtration would not abolish the concentration difference so that the absolute filtration would tend to increase as pari passu with the filtration rate and vice versa when the GFR was reduced. However, it is important to note that though first suggested by the classical study of Maikler, Mott, Oliver and McDowell (1941), it has been beyond any doubt that such a limiting concentration difference cannot obtain in this tubular segment of the nephron under normal conditions (Lassiter, Gottschalk and Mylle 1961; Windhage and Liebowitz 1961; Ullrich et al. 1963). Furthermore, the theory was seriously questioned by results obtained in dilution studies (Bojarski 1954). Supported by results obtained by Selkurt's studies on perfused kidneys (Selkurt, Hall and Spencer 1949; Selkurt 1951), Bojarski interpreted his data as evidence that indirectly suggests that the rate of reabsorption does not depend linearly upon the load on the unit, but is delayed of about 10-15 minutes before any change in the rate of absorption and glomerular filtration (and RBF) could be detected.

The limiting hypothesis

On increasing the load of the concentrated solution, the rate of filtration and consequently of the reabsorption in the proximal part of the tubule does not change very rapidly as a function of the filtered load of fluid. The rate of reabsorption of concentration of the proximal tubular fluid is independent of the load on the tubule. The rate of reabsorption of fluid is independent of the load on the tubule. The rate of reabsorption of fluid is independent of the load on the tubule.



Alternative

Reabs.prox (load-independent)
(Im)

OFR L(reabs)

LP_{prox} variable
($\neq P_{UF}$)

2 eUEP low
(30-45 mmHg)

3 Reabs.prox hormonal
regul.

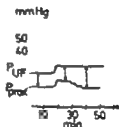


Fig. 2

The 1 ma we hypothesize the low gth of the curve shows
two of 1 p sec curve A adds small incre i the fi
on pr ur (P_p) ac separated i i lly by qual w
se prox mal lch 1 pre ur (P_{pro}) The d sac b two
he we pre ur level i the effective filt ion pre
if r p ree i uncharged i it lly Af 10 min P_{prox}
pre down q due in reased ab rption whil P_{UF} i
re said i d Th secondary charge i P_{prox} i the cause
f t delayd re se if r p e f rate plan ion ee

The logic of this conclusion is very simple. Let us consider by
way of example a 5% increase in the filtration pressure (P_{UF}).
This change will tend to increase the rate of filtration. However,
if initially the proximal reabsorption does not change
automatically in response to the change in P_{UF} , in other words if
no reabsorption is moved from this segment by the tap (R_{prox})
(cf. Fig. 2); secondly, if the tap (H) at the end of this
segment is also closed because of the large resistance to flow
in the loop of reabsorption and the resistance, it follows that the
proximal reabsorption will increase directly in parallel
with the filtration pressure. Hence filtration will be filtered that
the required to the stable reabsorption and to in

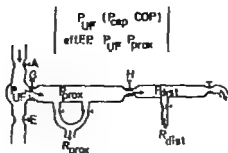
in the pressure that this high level. The effective filtration pressure will not change to any measurable degree not initially at least. Not until the proximal reabsorptive capacity has increased and more fluid is removed from this tubular segment will the luminal pressure fall down again. In this case it is the change in the rate of reabsorption which determines the change in the pressure drop across the glomerular membrane is in the effective filtration pressure (GFR).

It is evident that this concept are three fundamental features: 1) firstly the proximal intratubular pressure is not constant but variable; varying primarily in parallel with the filtration pressure (P_{UF}). 2) Secondly the modest change in proximal luminal pressure which can be caused by alterations in the rate of absorption must be sufficiently large to account for the relatively large range of variation in GFR which actually can be observed. Thus this alternative to the classical theory implies a prerequisite that the effective filtration pressure must be considerably lower than previously believed - i.e. about the same value as the proximal luminal pressure (about 10-15 mm Hg or less). 3) Thirdly it is known that the rates of reabsorption and filtration actually do change in parallel within 10-15 minutes in response to induced changes in P_{UF} . Also RBF changes roughly in parallel with GFR under the conditions. Consequently some factor(s) such as this secondary and delayed change in reabsorptive capacity must exist.

The unique structure of the nephron with its ascending limb of Henle making close contact with both the afferent and efferent arterioles of the affiliated glomerulus (Paasrup 1965; Sauer 1970) is worthy of attention. This feature which is a characteristic of all nephrons throughout the mammalian kingdom suggests the existence of feedback loops; and the region of this tubuloglomerular contact obviously is a key-point for the recognition of any concomitant adjustment of the proximal reabsorptive capacity and filtration pressure. At this very region is the juxtaglomerular apparatus (JGA) the primary site of synthesis and release of

A working hypothesis

It is the first hypothesis is alternative to the classical theory of renal regulation. The validity of working hypothesis 1 which has been suggested is systematically evaluated (Lays et al 1966). The essence of this hypothesis is with following (cf fig 3):



Alternative

Reabs.prox. load-independent
(T_m)

GFR ↓ (reabs.)

P_{prox} variable
($\neq P_{UF}$)

2. effLEP low
(30-35 mmHg)

3. Reabs.prox. hormonal
regul.

mmHg

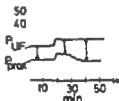


Fig. 2

The alternative hypothesis. The lower left (the figure shows) is the initial pre-renal curve. A sudden small increase in the filtration pressure (P_{UF}) accompanied initially by an equal increase in proximal tubular pressure (P_{prox}). The difference between the two pressures is the effective filtration pressure (P_{eff}) remains unchanged initially. At 10 minutes P_{prox} goes down as does the rate of reabsorption while P_{UF} is maintained. The secondary change in P_{prox} is the cause of the delayed response of P_{eff} . For further explanation see the text.

The logic of this conclusion is very simple. Let us consider by way of example a sudden increase in the filtration pressure (P_{UF}). This change will tend to increase the rate of filtration. However, if first of all the rate of proximal reabsorption does not change automatically in response to the change in P_{UF} , in other words if no more fluid is moved from this segment by the time P_{prox} (cf. Fig. 2); and secondly if the time (H) at the end of this segment is increased by the time P_{prox} is increased, then it follows that the proximal tubular pressure will increase closely in parallel with the filtration pressure. No more fluid will be filtered than that required to maintain the tubular pressure and to maintain

real the assurance that this higher level. The effective filtration pressure will not change to any measurable degree. Initially, at least, not until the proximal reabsorptive capacity has increased and no fluid is removed from this tubular segment will the luminal pressure fall down again. In this case it is the change in the rate of reabsorption which determines the change in the pressure drop across the glomerular membrane in the effective filtration pressure (GFR).

It is evident that implied in this concept are three fundamental features: 1) firstly the proximal intratubular pressure is not constant but variable; varying primarily in parallel with the filtration pressure (P_{UF}). 2) Secondly the modest change in proximal luminal pressure which can be used by iterations in the rate of absorption must be sufficiently large to account for the relatively large changes of variation in GFR which actually can be observed. Thirdly, it is intuitive that the classical theory implies as a prerequisite that the effective filtration pressure must be considerably lower than previously believed. About the same value as the proximal luminal pressure (about 10-15 mm Hg in the rat) or lower. 3) Thirdly it is known that the rate of reabsorption and filtration actually do change in parallel within 10-15 minutes in response to induced changes in P_{UF} . Also RBF change roughly in parallel with GFR under these conditions. Consequently one factor in using this theory and delayed change in reabsorptive capacity must be taken into account.

The unique structure of the nephron with its ascending limb extending making close contact with both the afferent and efferent arterioles of its affiliated glomerulus (Furup 1965; Sjöberg 1970) is worthy of attention. This feature which is characteristic of all nephrons throughout the mammalian kingdom suggests the existence of feedback loops and the glomerular tubulovascular contact obviously is a prerequisite for the recognition of any ion concentration of the proximal absorptive capacity in variable filtration pressure. At this region is the juxtaglomerular apparatus (JGA) the primary site for further end and related.

Working hypothesis

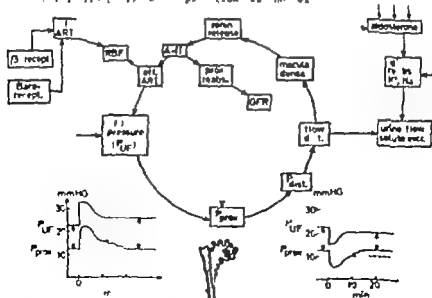
I wish to put forward an alternative theory for the regulation of the glomerular filtration rate which is based on the following principles (Layman 1966). The essence of this hypothesis is as follows (Fig. 1).

Renal rate as is upset & under conditions in which the filtration pressure tends to decline (of also recent view by Davis and Freeman 1976) A drop in P_{UP} is immediately accompanied by an equally large drop in the proximal intratubular pressure (P_{pro}); consequently, the rate of delivery of tubular fluid into the distal tubule decreases and the distal intraluminal pressure goes down. As a result, urine flow decreases.

The reduced delivery of fluid from the ascending limb of the 1 stimulates natriuresis, which is a feedback response possibly with macula densa & angiotensin II subsequently formed. Angiotensin II might have two effects: 1) Firstly the well known vasoconstrictory effect. If this were an effect predominantly on the post-glomerular vessels, a likely possibility since the efferent vessel would be the first smooth muscle containing its role met by the endogenous angiotensin II liberating it. A really - the post-glomerular vascular resistance would increase thereby counteracting the primary drop in P_{UP} . The proximal intratubular pressure would therefore increase somewhat but not necessarily completely back to the original value. In addition the efferent vessel constriction modified by angiotensin II would contribute to the reduction in renal blood flow (RBF).

Fig. 1

The way in which the body responds to a fall in renal blood flow



2) Secondly a hypothetical inhibitory effect of angiotensin on the proximal reabsorptive capacity could be postulated. Inhibition of proximal reabsorption itself would further lower the proximal luminal pressure which then would return right back to the control level. It is apparent that this latter part of the interstitial pressure increase is the major determinant of the resulting reduction in the effective filtration pressure and hence in GFR. Furthermore in this fashion the two angiotensin effects would influence the distal tubular pressure in the same direction and assist each other in maintaining the stability of the pressure.

As a result of such feedback mechanism MBF, proximal reabsorption itself and GFR would vary in parallel as observed; and proximal intratubular pressure and thereby the delivery of fluid to the distal tubular segment would be maintained in stable state. According to this working hypothesis complete correspondence and agreement with the classical theory is reached in the majority of tests. Even load-dependency of proximal reabsorptive capacity is an essential characteristic in both concepts being a direct and automatic dependency according to the one but being an indirect dependency according to the other concept. Thus the present working hypothesis may be considered a unifying hypothesis. Only the mechanisms by which change in the system is accomplished differently from the classical theory; there is fundamental difference in the sequence of events.

In the following sections the following concepts of the new working hypothesis versus the classical theory are reviewed. The heart of the problem was to obtain direct evidence establishing whether the absolute rate of proximal reabsorption is automatically a direct function of the filtered load, or whether it is primarily independent of GFR. The central question was whether or not angiotensin II may inhibit the proximal reabsorptive capacity and add an extra effect on the flow.

Evidence obtained with the use of iron-59 as a tracer

A relatively simple, unique and able to give some of the unique results provided with the introduction of the use of iron-59 as a tracer in the study of proximal reabsorption. The results of the study (Lay, 1963) will be discussed in the following section. The results observed with the use of iron-59 as a tracer are completely different from the results obtained with the use of inulin. As the results of the study are presented in the following table.

filtration process stops instantaneously whilst the proximal reabsorption continues until the lumen is re-occluded and totally occluded. The time interval from arterial clamping until the proximal lumen has disappeared is recorded and denoted by the occlusion time (OT). The time of occlusion was proved to collapse time in order to distinguish the gradual luminal occlusion due to reabsorption from the sudden collapse of the proximal lumen resulting from applying too much suction to an inverted collecting micropipette.

If reabsorptive capacity is constant during the luminal occlusion then

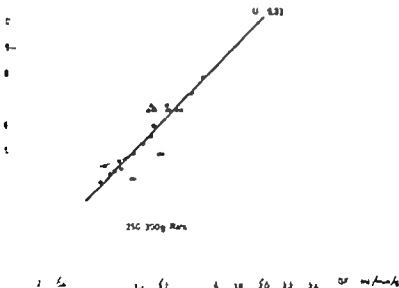
$$C = \frac{U}{OT}$$

in which C represents the proximal reabsorptive capacity and the luminal radius r . For any given luminal diameter the OT will be proportional to the length of the reabsorptive unit. Conversely the more the tubule is distended the longer the OT for any given value of C . Thus knowing the luminal radius the absolute rate of proximal reabsorption can be calculated from the measured OT.

Fig. 1

Proximal reabsorptive capacity C is proportional to the
OT is the occlusion time
is hydroponic (Ley et al.)

$$U = \frac{100}{OT} \text{ (mm}^2\text{) (sec}^{-1}\text{)}$$



Result equal to those given in fig 4 obtained within the range of spontaneous variations in insulin clearance from 0.7 to 2.0 ml min⁻¹ per g of kidney weight (k w) in rats demonstrated that the reciprocal of the GFR varied linearly and in direct proportion to the GFR measured just before the sort was suddenly lapsed (Leyssac 1963). In addition it was documented that under the conditions the proximal lumen radius was on an average 13.14 μ m in section of quickly frozen non-diuretic rat kidneys independent of the insulin clearance rate above 0.7 ml min⁻¹ g k w⁻¹. These results demonstrated the phoromoc of glomerulo-tubular balance. But the crux and significance of this experiment was that the identical values of absolute proximal reabsorption rates were found when calculated both from the insulin clearance and the proximal fractional reabsorption, the latter known from free flow micropuncture data and from the measured lumen radius and the GFR. This line agreement seemed to justify the conclusion that proximal tubular reabsorption continues throughout the occlusion time as an unchanged rate even though the filtration rate drops to a critical and direct piece of evidence indicating that the fractional reabsorption does not change automatically in response to a variation in GFR had the apparently been obtained.

Further it has been documented that proximal occlusion time can be quantitatively related to the other parameters dependent on proximal tubular reabsorption, that is measured in free flow such as transit time (t_{tr}) of the front of bolus of filtered diamine green and proximal fractional reabsorption (and hence the tubular fluid plasma inulin concentration $(T/P)_{T_1}$). The unique relationship between GFR, occlusion time (TT) and TT_{TR}/P_{TR} has also been derived (Björk and Leyssac 1963):

$$\frac{TT}{GFR} = \ln\left(\frac{P}{P_{TR}}\right)$$

which is correct on the condition that the retrograde flow of fluid from the peritubular capillary space into the proximal tubule during the proximal occlusion phenomenon is quantitatively greater between all occluded and directly measured inulin clearance (Cl_{TR}). TT/P is a constant, TT corrected GFR and lumen radius has been found over the range of spontaneous variation (Björk and Leyssac 1963). It is noted that an equally low quantitative relationship between the occlusion time obtained by the inverse of the rate of inulin clearance and the difference of the logarithm of the plasma and tubular inulin concentration ($\ln(P/P_{TR})$) is found. The relationship between the occlusion time and the occlusion

filtration process top in the transiently whilst the proximal reabsorption continues until the lumina is emptied and totally occluded. The time interval from aortic clamping until the proximal lumina have disappeared is recorded and denoted by the occlusion time (OT). The true occlusion time was preferred to collapse time in order to distinguish the gradual luminal occlusion due to reabsorption from the immediate collapse of the proximal lumen resulting from applying too much suction to the inserted occluding micropipette.

If absorptive capacity is constant during the luminal occlusion then

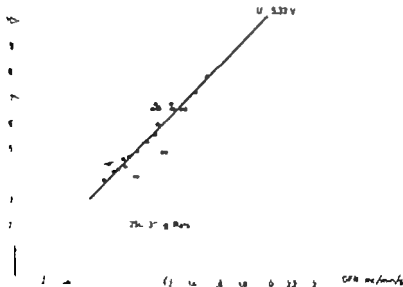
$$C = \frac{r}{OT}$$

in which C represents the proximal reabsorptive capacity and the luminal radius. For any given luminal radius the OT will be more rapid the larger the absorptive rate. Conversely the more the tubule is distended the longer the OT for a given value of C. Thus knowing the luminal radius the absolute rate of proximal reabsorption can be calculated from the measured OT.

Fig. 4

Relationship between the rate of proximal reabsorption and the occlusion time (OT) for a given luminal radius. The rate of reabsorption is expressed in $\mu\text{mol}/\text{cm}^2/\text{min}$ and the OT in seconds.

$U = \frac{r}{OT} \times 60$ (sec)

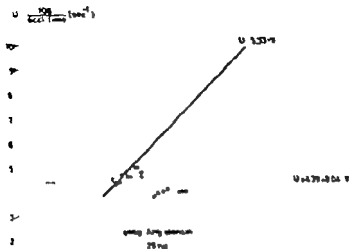


For its eqn 1 to those given in fig 4 obtained with the angle of spontaneous filtration inulin clearance from 0.7 to 2.0 ml min⁻¹ per g of kidney weight (k w) in rats. It was demonstrated that the reciprocal of the OT varied linearly and in direct proportion to the GFR measured just before the aorta was suddenly clamped (Layssac 1963). In addition it was documented that under the condition the proximal luminal radii were on an average 13-14 μ m. In section of quick frozen non-diuretic rat kidneys independent of the inulin clearance it also above 0.7 ml min⁻¹ g k w⁻¹. These results demonstrated the phenomenon of glomerulo-tubular balance. But the crux and significance of this experiment was that identical values of absolute proximal absorption were found when calculated both from the inulin clearance and the proximal fractional reabsorption the latter known from free flow micropuncture data and from the measured luminal radii and the OT. This close agreement seemed to justify the conclusion that proximal tubular reabsorption continues throughout the occlusion time at unchanged rate, though the filtration rate drops to zero. A further direct piece of evidence indicating that the rate of absorption does not change tonically in response to the occlusion is GFR had then apparently been obtained.

Further it has been documented that proximal occlusion time can be quantitatively related to the other parameters dependent on proximal tubular absorption, that is measured in free flow such as transit time (if the dye front of bolus of filtered substance) and proximal fractional absorption (and hence the tubular fluid to plasma ratio $(T/P)_{T_0}$). The unique relationship between OT and its time (TT) and TT_{IN}/T_{IN} has also been derived (Boje and Leys 1969):

$$\frac{TT}{OT} = 1 + \left(\frac{T/P}{F} \right)_{T_0}$$

With proper occlusion of the renal artery (12%) retrograde flow of fluid from the peritubular space of the proximal tubule during the proximal occlusion phenomenon has been quantitatively demonstrated between calculated and directly measured values of $(T/P)_{T_0}$ and $(C/P)_{T_0}$. If P is a constant TT correct OT and luminal radius has been found over the time angle of spontaneous occlusion (Boje and Leys 1969). It is thus equally quantitative relationship between the rate of occlusion and by the inverse of OT and OT and OT condition (see the 1 and 2 in cell 1 in the expansion table 1). The following table will show that OT method has been obtained and it can be used



6.3 6.4 6.5 6.6 6.7 6.8 6.9 6.10 6.11 6.12 6.13 6.14 6.15 6.16 6.17 6.18 6.19 6.20 6.21 6.22 6.23 6.24 6.25 6.26 6.27 6.28 6.29 6.30 6.31 6.32 6.33 6.34 6.35 6.36 6.37 6.38 6.39 6.40 6.41 6.42 6.43 6.44 6.45 6.46 6.47 6.48 6.49 6.50 6.51 6.52 6.53 6.54 6.55 6.56 6.57 6.58 6.59 6.60 6.61 6.62 6.63 6.64 6.65 6.66 6.67 6.68 6.69 6.70 6.71 6.72 6.73 6.74 6.75 6.76 6.77 6.78 6.79 6.80 6.81 6.82 6.83 6.84 6.85 6.86 6.87 6.88 6.89 6.90 6.91 6.92 6.93 6.94 6.95 6.96 6.97 6.98 6.99 7.00 7.01 7.02 7.03 7.04 7.05 7.06 7.07 7.08 7.09 7.10 7.11 7.12 7.13 7.14 7.15 7.16 7.17 7.18 7.19 7.20 7.21 7.22 7.23 7.24 7.25 7.26 7.27 7.28 7.29 7.30 7.31 7.32 7.33 7.34 7.35 7.36 7.37 7.38 7.39 7.40 7.41 7.42 7.43 7.44 7.45 7.46 7.47 7.48 7.49 7.50 7.51 7.52 7.53 7.54 7.55 7.56 7.57 7.58 7.59 7.60 7.61 7.62 7.63 7.64 7.65 7.66 7.67 7.68 7.69 7.70 7.71 7.72 7.73 7.74 7.75 7.76 7.77 7.78 7.79 7.80 7.81 7.82 7.83 7.84 7.85 7.86 7.87 7.88 7.89 7.90 7.91 7.92 7.93 7.94 7.95 7.96 7.97 7.98 7.99 8.00 8.01 8.02 8.03 8.04 8.05 8.06 8.07 8.08 8.09 8.10 8.11 8.12 8.13 8.14 8.15 8.16 8.17 8.18 8.19 8.20 8.21 8.22 8.23 8.24 8.25 8.26 8.27 8.28 8.29 8.30 8.31 8.32 8.33 8.34 8.35 8.36 8.37 8.38 8.39 8.40 8.41 8.42 8.43 8.44 8.45 8.46 8.47 8.48 8.49 8.50 8.51 8.52 8.53 8.54 8.55 8.56 8.57 8.58 8.59 8.60 8.61 8.62 8.63 8.64 8.65 8.66 8.67 8.68 8.69 8.70 8.71 8.72 8.73 8.74 8.75 8.76 8.77 8.78 8.79 8.80 8.81 8.82 8.83 8.84 8.85 8.86 8.87 8.88 8.89 8.90 8.91 8.92 8.93 8.94 8.95 8.96 8.97 8.98 8.99 9.00 9.01 9.02 9.03 9.04 9.05 9.06 9.07 9.08 9.09 9.10 9.11 9.12 9.13 9.14 9.15 9.16 9.17 9.18 9.19 9.20 9.21 9.22 9.23 9.24 9.25 9.26 9.27 9.28 9.29 9.30 9.31 9.32 9.33 9.34 9.35 9.36 9.37 9.38 9.39 9.40 9.41 9.42 9.43 9.44 9.45 9.46 9.47 9.48 9.49 9.50 9.51 9.52 9.53 9.54 9.55 9.56 9.57 9.58 9.59 9.60 9.61 9.62 9.63 9.64 9.65 9.66 9.67 9.68 9.69 9.70 9.71 9.72 9.73 9.74 9.75 9.76 9.77 9.78 9.79 9.80 9.81 9.82 9.83 9.84 9.85 9.86 9.87 9.88 9.89 9.90 9.91 9.92 9.93 9.94 9.95 9.96 9.97 9.98 9.99 10.00 10.01 10.02 10.03 10.04 10.05 10.06 10.07 10.08 10.09 10.10 10.11 10.12 10.13 10.14 10.15 10.16 10.17 10.18 10.19 10.20 10.21 10.22 10.23 10.24 10.25 10.26 10.27 10.28 10.29 10.30 10.31 10.32 10.33 10.34 10.35 10.36 10.37 10.38 10.39 10.40 10.41 10.42 10.43 10.44 10.45 10.46 10.47 10.48 10.49 10.50 10.51 10.52 10.53 10.54 10.55 10.56 10.57 10.58 10.59 10.60 10.61 10.62 10.63 10.64 10.65 10.66 10.67 10.68 10.69 10.70 10.71 10.72 10.73 10.74 10.75 10.76 10.77 10.78 10.79 10.80 10.81 10.82 10.83 10.84 10.85 10.86 10.87 10.88 10.89 10.90 10.91 10.92 10.93 10.94 10.95 10.96 10.97 10.98 10.99 11.00 11.01 11.02 11.03 11.04 11.05 11.06 11.07 11.08 11.09 11.10 11.11 11.12 11.13 11.14 11.15 11.16 11.17 11.18 11.19 11.20 11.21 11.22 11.23 11.24 11.25 11.26 11.27 11.28 11.29 11.30 11.31 11.32 11.33 11.34 11.35 11.36 11.37 11.38 11.39 11.40 11.41 11.42 11.43 11.44 11.45 11.46 11.47 11.48 11.49 11.50 11.51 11.52 11.53 11.54 11.55 11.56 11.57 11.58 11.59 11.60 11.61 11.62 11.63 11.64 11.65 11.66 11.67 11.68 11.69 11.70 11.71 11.72 11.73 11.74 11.75 11.76 11.77 11.78 11.79 11.80 11.81 11.82 11.83 11.84 11.85 11.86 11.87 11.88 11.89 11.90 11.91 11.92 11.93 11.94 11.95 11.96 11.97 11.98 11.99 12.00 12.01 12.02 12.03 12.04 12.05 12.06 12.07 12.08 12.09 12.10 12.11 12.12 12.13 12.14 12.15 12.16 12.17 12.18 12.19 12.20 12.21 12.22 12.23 12.24 12.25 12.26 12.27 12.28 12.29 12.30 12.31 12.32 12.33 12.34 12.35 12.36 12.37 12.38 12.39 12.40 12.41 12.42 12.43 12.44 12.45 12.46 12.47 12.48 12.49 12.50 12.51 12.52 12.53 12.54 12.55 12.56 12.57 12.58 12.59 12.60 12.61 12.62 12.63 12.64 12.65 12.66 12.67 12.68 12.69 12.70 12.71 12.72 12.73 12.74 12.75 12.76 12.77 12.78 12.79 12.80 12.81 12.82 12.83 12.84 12.85 12.86 12.87 12.88 12.89 12.90 12.91 12.92 12.93 12.94 12.95 12.96 12.97 12.98 12.99 13.00 13.01 13.02 13.03 13.04 13.05 13.06 13.07 13.08 13.09 13.10 13.11 13.12 13.13 13.14 13.15 13.16 13.17 13.18 13.19 13.20 13.21 13.22 13.23 13.24 13.25 13.26 13.27 13.28 13.29 13.30 13.31 13.32 13.33 13.34 13.35 13.36 13.37 13.38 13.39 13.40 13.41 13.42 13.43 13.44 13.45 13.46 13.47 13.48 13.49 13.50 13.51 13.5

Fig. 2

Reciprocal of ft is 1/1000 of angle is 1/11 diff
 measure of small vs 1/1000 measure angle of 1/11
 measure of immediately before the advent of ion of mg 1 The
 ray ion line 0 33 4 1 th out line can rol
 not a ve angle 1 (Ray ad 1965)

developed by Gottschalk and Lassit (1973) that the OT method was applied correctly in a simple and accurate measurement providing quantitatively correct data on absolute rate of proximal absorption seems justified.

It follows that the percent that proximal suboptive rats are
primary risers and percent of the GFR per unit must be equally
constant.

This is the methodology it was shown that oxygenation
 is increased in the early part of the ureter and blood
 flow is controlled in the same manner as in the other
 organs. It is immediately (1-3) after the passage of
 the blood through the kidney. The results (given in fig 5) were
 interpreted as indicating that the oxygenation of the
 blood is a very important factor in any high level down to
 the lowest level of the cord within the ureter.
 The results of the study (Ley 1964 1965) It should be
 noted that the inhibitory tubular effect of oxygenation
 could be a result of the high point of the ureter or of
 the low level of the cord (cf. Ley 1965). The inhibitory

effect of angiotensin was dose-dependent while equipressor dose of noradrenaline had no immediate effect on the OT (Leyssac 1963)

The problem of proximal luminal diameter variations provoked apparently in part at least by the evidence obtained with the OT technique several groups of investigators engaged themselves in obtaining the result with more sophisticated micropuncture methodology. The inability of the earlier report to reproduce the Copenhagen results created some confusion and great difficulties in explaining the discrepancies. Almost all other groups consistently found that the proximal luminal radius varied linearly with the rates of filtration such that the luminal volume per unit of tubular length () is related in direct proportion to GFR. In addition results obtained with the split-oil drop method introduced by Geck (1963) showed that the reabsorptive half time ($t_{1/2}$) was constant and independent of filtrations in varying renal pressure and GFR (Gertz et al 1963). According to Geck:

$$\frac{0.693}{t_{1/2}} = -\frac{C}{C_r}$$

in which C represents the proximal reabsorptive capacity. Based on these findings Geck proposed that C was usually related to the luminal volume per unit of length () such that any increase in tubular dilatation resulting from increases in GFR automatically will induce parallel change in the rate of absorption. This hypothesis was widely accepted by most investigators in the field; however, it was considered firmly established by supporting evidence from the split-oil drop and anit time experiments (Rector et al 1966; Brunne et al 1966; Rector et al 1967; Schnemann et al 1968). Apparently the earlier report (Leyssac 1963) that equally large variations in proximal reabsorption could be observed without any variation in the luminal diameter was disregarded even though it would present strong arguments against the concept that there is change physiologically in proximal reabsorption in response to changes in filtration. The question was then further investigated and improved techniques and blind experiments (Blumhert Gottschalk and Leyssac 1968) in vivo micropuncture have made of fecal collection of kidney dialysate collection possible and have demonstrated that the rate of reabsorption is ready to change from passive to active in the case of the renal tubule. This is confirmed by the origin of the

variation = change in proximal tubular diameter could be detected over the range of spontaneous variations; at lower values of GFR the radius actually tended to increase. Not until later was it generally recognized that the results obtained from split-oil drop experiments were due to artifacts (cf. recent review of the method by Orloff and Burg, 1971, and by Gottschalk and Leibertz, 1973) which can readily be explained (cf. Ley and Bojse, 1966).

Seriously challenging the occlusion time method Kahl et al (1967) in their labor theory reported that the course of reduction in proximal tubular radius during the occlusion phenomenon measured by photomicrographs taken at intervals was a linear function of time. Even though the intercept of the adi (plotted on the ordinate) could be obtained only during the first 6 seconds the slope of the linearly increasing adi as a function of time was sufficient to calculate the initial rate of absorption and the decline in radius. Extrapolation of the linear starting from a radius (r_0) of about 10 μ m intercepted the abscissa at a point equal to the measured OT. If reabsorption rate had remained constant during the minimal occlusion curved line should be obtained. Therefore the authors were interpreted as evidence that the rate of reabsorption continuously and constantly decrease rapidly with the decrease in diameter caused by GGT. However the problem involved in measuring the proximal luminal diameter by photomicrographs had not been considered. Measurements of the proximal diameter normally did not include the refractional correction present in photomicrographs at the margin of the tubular lumen giving a radius of about 10 μ m also found by others (Bain et al 1968). The problem solved in getting the rate by taking photographs made of a Plexiglas tube with unpolarized light surface ultraviolet light and exposed with ultraviolet light thus imitating the condition which enables us to obtain or obtain a photographed in vivo (Bain and Loefer 1969). The photomicrographs disclosed that the refractive index of the polarizing microscope which gives photomicrographs of Bain and his associates were used to indicate the refractive index proportional to the refractive index found in agreement with the linear relationship of quick frozen kidney (Layman 1969) and with the refractive index calculated by Pugh et al (1967). Thus the adi at time zero (r_0) of 10 μ m will be corrected the correct value is 10 μ m which corrected curve

and the initial slope of the line an extrapolation intercepts the abscissa at 19-20 sec. Beyond the measured OT of 13-14 sec. However, calculated curve describing constant rate of absorption given by the initial slope and starting from radius of 14 μ m intercept the abscissa at value of 13-14 sec equal to the measured OT. Thus in allity the data reported by Wahl and his colleagues were compatible with Gert hypothesis while as they lend strong support to the occlusion time method and the present working hypothesis.

Also checking the interpretation of the results obtained from occlusion time experiments to verdat obtained in proximal tubule microperfusion experiments by Wiederholt and his associates (1967). The results suggested that while the luminal diameter increased with perfusion rate going from 10 to 24 nano-l per min reabsorption rate increased proportionally since the collected perfate/infused fluid ratio remained unchanged. A loss only 1 of this data disclosed however that likely artifact could explain their results (if discussion by Bojlen and Layman 1969); and later studies by Morgan and Berline (1969) using the same methodology were unable to confirm the result of Wiederholt et al. The rate of proximal reabsorption remained unaffected by large changes in the luminal perfusion rate. As pointed out by O'Leary and Burg (1971) the method of microperfusion is of limited value excluding the influence of the glomerulus itself on net reabsorption. The result obtained by Morgan and Berline therefore add additional evidence indicating that the proximal absorptive capacity is independent of tubular load presented to the luminal side. It is thus Steven (1974a) lived to the same conclusion from results obtained by the method of constant flow section during collection of proximal tubule fluid from the distal microtubule of single nephron filtration rate (GFR). A 30% reduction in proximal luminal pressure generated SNGFR by 50% and $\text{ml}^{-1} \text{g} \text{Kw}^{-1}$ while $\text{TF} \cdot \text{P} \cdot \text{I} \cdot \text{L} \cdot \text{I}$ decreased by 0.5 (from 2.44 to 1.94). The absolute rate of proximal absorption remained unchanged.

Finally, the present work was designed by Gert et al. to perhaps to do it to the validity of the occlusion time method and the question whether or not change in GFR lowly occurs is addressed by proportionally changing in proximal luminal radius. The line graph of anit time (TT) vs. $\text{P} \cdot \text{I} \cdot \text{L} \cdot \text{I}$ could only remain constant if GFR varied proportionately. Gert concluded that the TT would be constant

variation of change in proximal tubular diameter could be detected over the range of spontaneous variations; at lower values of GFR the radius actually tended to increase. Not until late was it generally recognized that the results obtained from split-oil drop experiments were due to artifacts (for critical reviews of the method by Orloff and Burg 1971 and by Gottschalk and Lassiter 1973) which can readily be explained (of Laysac and Bojesen 1966).

Seriously challenging the occlusion time method Wahl et al (1967) in Thurnau laboratory reported that the course of reduction in proximal tubular radius during the occlusion phenomenon measured in photomicrographs taken at 1 sec interval was linear function of time. Even though exact measurements of the radius (plotted on the ordinate) could be obtained only during the first 6 sec the slope of the line relating radius to time was sufficiently exact for the calculation of the initial rate of reabsorption and of the decline in radius. Extrapolation of the lines starting from radius (r_0) of about 10 μ m intercepted the abscissa at a point equal to the mean r_0 . If absorption rate had remained constant during the luminal occlusion curved line should be obtained. Therefore these data were interpreted as evidence that the rate of reabsorption continuously and automatically decreases pari passu with the decrease in radius as suggested by Gertx. However the problems involved in measuring the proximal luminal radius in photomicrographs had not been considered. Measurements of the proximal radius generally did not include the refractile line (or) present in photographs of the outer margin of the tubular lumen giving radius of about 10 μ m as also found by others (Baines et al 1969). The problem was lived in a great part at least by studying photographs made of a Plexiglas tube with unpolished luminal surface submerged into water and exposed with incident light thus imitating the conditions in which renal surface convolutions are photographed in vivo (Bojesen and Laysac 1969). The photograph disclosed that the refractile line is part of the lumen. When the original photographs of Baines and his colleagues were re-measured to include the refractile one proximal radius of 13-14 μ m was found in agreement with the earlier measurements obtained in sections of quick-frozen kidneys (Laysac 1963) and also with the electrical radius calculated by Reguel Pröbst and Wick (1967). Thus the radius at time zero (r_0) = 10 μ m given by Wahl et al is incorrect; rather the corrected radius should be close to 14 μ m. Using this corrected value

cant change in arteri l plasma oncotic pre ur (COP) g ve rise to a modest but significant immedi t proximal lumen l p ssu e l vation ave ging l l mm Hg which pe i ted throughout th in fusion (l ml) Thi pr ure incr ment w ascribed to the re lting change in plasma volume Infusion of an amount Π = lloid f ee solution (0 ml) whi h gave the same pl sma volume xpansion as timated from the change in hematocrit caused more mark d immedi t proximal lumen l p ssu e l decrease to an ave ge f J & mm Hg and a drop in plasma COP Th diff r ce i the arly int atubul p ssu e increas t 2.7 mm Hg lmo t exactly equal d the re ear d drop in COP of 3.6 mm Hg Sin the latt r change in COP qual the diff ence in filter tion pre ure caused by the dilution f plasma protein the Π ults we di ct evi dence indic ting that th proximal luminal hydrost tic p ur i initially clos ly in pa l l l with the filter tion pre ur (P_{ur}) in acco dance with the ltern tive wo king hypothe is In addition it w documented th Π the ly intr lumen l p chang were g dually compensat d f i an undel ting renne The Π ur w gui ted back to exactly the p e-infusion lve within 10-15 minut in close greement with Boj sen i terpretation of hi l a ance data (1954) and in acco dance with the data obt ined by Gottschalk and Myll (1954)

V ry ce tly Knox (1973) ported lt obtained in dog demon t ti g est lly the amp h nome on infusion f ac tyl choli i to th n l t ry acut ly ugment d RBF and markedly inc d th p oximal i t tubul p n Si gl neph on fil t tion te (RNGFR) and hence th ff ctive filt ation pr s remained unchanged whil ff re t rt i l oncoti Π re de ased ignifi tly

The eff ct ve filtration pr s

Π lous indi ct that f glomerul epill ry hydro t ti p and permeabil ty f on l ing dat arp Π lvely ewed by Re ki nd G lmo (1973) l pertinent fts the d velopne Π no d ct method fo statig the ope tive f pon tbi f glomerul lt falt tion These l tt method and the i obt ined by thei t l l tion have rece t ly le criti lly lewed by La lce (1975) The impo tance in n p sen on t f h f mation p ovided in the tudi m Π f ur ry t thi pol t i ho t p tendi g t add b i l l he p ent ion give My Las it l n l l d ccun g m ing de lce n l g y f d ct co di g f hyd out t p

ure in microvasculature in a mutant Wistar strain of rat (the Munich strain) with several glomeruli located just underneath the capsule Brenne Troy and De Gharthy (1971) first succeeded in measuring directly the glomerular capillary pressure (P_{cap}) in rats P_{cap} averaged 45 mm Hg in hydropenic control rats. This value has been confirmed repeatedly with similar methodology both by Brenne and his associates (Brenne et al 1972; Robertson et al 1972; Dean et al 1973b) and by Blantz and associates (Blantz et al 1972; Blantz 1974). Ultramicro-protein determinations on systemic arterial and afferent arteriolar plasma the latter collected from the efferent vessels yielded efferent () and afferent () arteriolar oncotic pressures of 20 mm Hg and 35 mm Hg respectively with a hydrostatic pressure in Bowman's capsule equal to about 10-12 mm Hg as usually recorded in early proximal convoluted tubule during \bar{P}_{eff} ultrafiltration. The effective filtration pressure is 13-15 mm Hg at the efferent end of the glomerular capillaries and 0 mm Hg or slightly negative at the afferent end; hence filtration equilibrium is achieved a short time before the end of the glomerular capillaries. Accordingly the mean effective filtration pressure is about 10 mm Hg. This value may be somewhat underestimated however. The problems of correct sampling of efferent arteriolar blood and the technical difficulties in the ultramicro-chemical protein measurement were emphasized by Laszlo. Further Allison Wilson and Gottschalk (1975) have shown that during a micropuncture experiment the systemic plasma protein concentration of rats gradually declining in their experiments from about 5.7 g/dl before surgery to about 4.6 g/dl within 150 minutes after surgery corresponding to a reduction in calculated oncotic pressure from 17.5 to 12.5 mm Hg. Unpublished observations in our laboratory have confirmed, in all subjects, a slight reduction in directly measured systemic oncotic pressure (COP) following surgery. Immediately following anaesthesia the values of 18-19 mm Hg were recorded while during the micropuncture experiments COP declined and averaged 17.2 ± 0.6 and 16.1 ± 0.3 mm Hg respectively in two series of experiments (Leyssac, Frederiksen and Skinnar 1975). If similar values apply to Brenne's estimate, questionable whether filtration equilibrium actually had been achieved in his experiments.

Using the method of stop-flow pressure measurement (SFP) indirect estimates of glomerular capillary pressure can be obtained since P_{ap} should equal SFP plus \bar{P}_{eff} . The validity of correct estimation of P_{cap} in this fashion depends on certain assumptions, as Laszlo

correctly appraised in particular on the assumption that the reduction in flow to the distal tubule by the oil blockade has no significant hemodynamic effects. In view of the evidence (ideally indicating a feedback mechanism in the macula) and the resulting low value of GFR from distal collections (with intact flow to the macula) the flow proximal to the collection in distal measurement of $P_{\text{C}}/P_{\text{A}}$ may be subject to an artifactual over-

estimate at least under certain conditions and should be evaluated with caution. Using this indirect approach Allison, Lippman and Gottschalk (1972) found a glomerular capillary pressure of 52 mm Hg calculated from a RPF of 37.5 ml Hg and a renal plasma COP of 14.7 mm Hg. Källskog and associates (1975) in Ulfendahl's laboratory reported similar RPF of 38 mm Hg in the rat. As using a plasma protein concentration of 6 g% equal to a COP of 20 mm Hg they calculated P_{C} to be 58 mm Hg. However a COP of 20 mm Hg is probably an overestimate; from more likely loss of 16 mm Hg applying to the condition prevailing during their procedure $P_{\text{C}}/P_{\text{A}}$ would be 54 mm Hg in accordance with Allison and her colleagues. Källskog et al. were also able to measure the glomerular capillary pressure directly in their Sp aqueous. Davley et al. The reported value of 62 mm Hg is markedly higher than those measured by B. Nene and others in Munich. Wistner's data but probably is higher than the indirect estimate of $P_{\text{C}}/P_{\text{A}}$ in their own rat Sp aqueous. Davley et al. suggesting that specific differences cannot explain the differences which probably remain an underestimated technical problem.

Even though explicit answers to the glomerular capillary hydrostatic pressure in non-diluted tubules have not been reached, it is evident the bulk of evidence definitely shows that it is much lower than previously assumed. A mean value of about 50 mm Hg would appear likely. Although the renal plasma oncotic pressure of about 16 mm Hg does not oppose the condition, it is so small values give a filtration fraction (FF) of 0.1 the effective oncotic pressure will be less than 27 mm Hg. The renal glomerular oncotic pressure will be 22-23 mm Hg. The proximal limit is probably less and these conditions are about 12 mm Hg but the pressure in the proximal convoluted tubule is slightly higher than the pressure in the proximal convoluted tubule of the rat kidney (Källskog et al. 1975). Loss of about 14 mm Hg may be ascribed to a glomerular filtration coefficient of 1.0 ml/min/g of 11 mm Hg. The pressure in the tubule is the usual loss of the pressure in the renal artery according to the data of the animal model.

range of variation corresponding to the spontaneous variations in GFR ($0.7 \pm 0.1 \text{ ml min}^{-1} \text{ g kw}^{-1}$ in hydroponic rat)

In conclusion it has been established that the effective filtration pressure is low in the order of 10-15 mm Hg demonstrating much lower flow resistance across the glomerular membrane than previously suspected. Thus a change in proximal luminal pressure of only 2 mm Hg could be used by a primary change in the reabsorptive capacity of otherwise all other factors being equal will result in a 15-20% change in the rate of filtration.

Physical factors adjustment of proximal reabsorptive rate and plasma flow dependence of GFR

Recognizing the failure in demonstrating an automatic and direct dependency of proximal reabsorptive capacity on the filtered load presented luminally and the successive rejections of the hypothesis firstly of gradient limitation secondly of luminal flow velocity and thirdly of tubular distension (Purkinje) most investigators in the field felt dissatisfied for reasons not directly apparent by the idea that physical factors including hydrostatic pressure (Kaley, Martino and Friedler 1966) and in particular the oncotic pressure (Levy and Windhager 1968; Windhager, Levy and Spitze 1969; Spitze and Windhager 1970) in the peritubular environment significantly control the rate of net proximal transfer of solutes and water. The concept as outlined by Windhager and adopted by Brannan and his group was that primary changes in GFR and thereby in the filtration fraction (FF) elevate the effective oncotic pressure; this change in Starling force across the peritubular capillary wall would facilitate the net uptake from the interstitial space and thereby somehow effect (increase) the net flux of fluid across the epithelium automatically. It was believed that glomerulo-tubular balance could be explained by such physical mechanisms. It is worth noting that most of the early evidence taken as support for this idea was obtained with the split-oil drop method (Levy and Windhager 1968; Windhager, Levy and Spitze 1969; Spitze and Windhager 1970); and as was also the case with the α -hypothesis while it was popular many investigators found and found supporting evidence in what would appear fortuitous co-variances and reproducible artifacts. However given the premise first that change in fluid delivery into the proximal tubule by filtration (or otherwise) does not influence the reabsorptive capacity; second that the flow resistance of the glomerular capillary membrane is much lower than has been inferred by the nephron segments distal to the

surrounding the proximal convolutions in steady state must be very small. Evidence obtained in vitro as well as in vivo suggests that the sensitivity of the proximal tubules to changes in oncotic pressure of the surrounding medium is rather modest. Elvatiq, the protein concentration, in the bath to twice normal in raised net water and sodium flux out of isolated micropipette segments of proximal convolutions by about one third in Isai and Kokko experiments (1972) while Gauthier et al. (1972) were unable to detect any effect on absorption rate by hyperoncotic bathing solutions. In both studies marked depression in net fluid transport rate was observed when normal serum in the bath was replaced by completely colloid free ultrafiltrate. A low sensitivity to increase in hydrostatic pressure was also noted. An inhibitory effect on net transport by colloid free peritubular media may not even be due to the reduction in GFR. H. Rate et al. (1973) reported that replacement of bath serum by ultrafiltrate of homologous serum prepared with membrane excluding solutes with molecular weights greater than 14,000, in contrast to ultrafiltrates prepared with membranes excluding solutes with molecular weights greater than 50,000, caused no depression of fluid absorption. The authors concluded that factors other than the oncotic pressure were responsible for observed changes in net fluid transport. Disregarding the mutually conflicting results obtained with the split-oil drop method, several more recent results obtained in vivo by peritubular microperfusion with colloid free perfusates have failed to demonstrate any significant effect on proximal absolute rate of reabsorption (e.g. Cong, Bartoli and Early, 1973; Solgrve and Schier, 1975; Steven, 1974b). In other studies, any consistent correlation between the rate of proximal reabsorption and the oncotic pressure and/or the filtration fraction could not be detected (e.g. Arrizurieta-Machnik et al., 1969; Leymar, Frederiksen and Skinner, 1975); and Blantz and Tucker (1975) were unable to find any correlation between the net interstitial pressure (P_{1-P_2}) and the passive driving force across the proximal tubular epithelium and measured absolute rates of proximal reabsorption in the steady state of hydropic and following volume expansion with plasma. Finally, changes in the oncotic pressure of the peritubular environment had any significant influence on net absorption. The rate of reabsorption should be progressively depressed during proximal tubular occlusion following interruption of the blood supply because of dilution by the reabsorbed fluid. The evidence of constant rate of reabsorption during the tubular occlusion and the quantitative agreement between reabsorption

rates measured under free-flow conditions and the calculated f on the OT provide strong argument against the physical factor hypothesis.

Currently considerable interest has been taken in the possibility of filtration equilibrium mainly because it is believed apparently necessary to explain the observation of parallel change in renal blood flow and GFR without change in the filtration fraction and thereby without change in effective renal plasma flow. Within the framework of the concept in which the peritubular "environment" controls the net interstitial fluid transport across the proximal tubule by hydrostatic and oncotic forces (Dean Robertson and Branner 1973), single nephron glomerular filtration rate (SNGFR) will vary in proportion to change in plasma flow rate when filtration pressure equilibrium occurs (Dean Robertson and Branner 1972). In accordance with experimental data (Daugherty et al. 1972), proximal tubule absorption rate should remain unaffected by plasma flow-dependent variation in SNGFR following glomerular expansion with plasma which would increase the effective and effective oncotic pressures unchanged. Apart from the question raised above (p. 19) concerning the validity of the occurrence of filtration equilibrium, previous equilibrium appears not to have been generally obtained. Thus Blant Rees and Seidman (1974) found filtration equilibrium in the dog with furosemide but not in another; neither Allison Wilton and Gottschalk (1974) nor Killip et al. (1973) found evidence of filtration equilibrium in the rat. In the dog, Dawley et al. (1974) found filtration equilibrium did not occur in the dog investigated by Knox (1975).

However, in view of the hydrodynamic resistance of the entire nephron, the idea that SNGFR can be directly plasma flow-dependent is equally logically inconsistent. The idea that a primary change in SNGFR can occur in the post-glomerular segment and thereby the proximal absorption rate is affected by filtration equilibrium may be reached before the effective flow of the glomerular capillaries and the effective oncotic pressure of the plasma flow, which move the point of equilibrium, are altered. If the effective renal plasma flow is altered, the effective oncotic pressure followed by an immediate and parallel increase in the proximal tubule flow rate, we have the dog's glomerular filtration rate will not be changed. In the single nephron rate, the effective renal plasma flow is altered, the effective oncotic pressure is altered, and the effective renal plasma flow is altered.

the filtration pressure can be directly plasma flow-dependent. The same criticism also applies to the various other models of glomerular ultrafiltration dynamics recently published (Gustave and Ströbak 1974; Hus Marsh and Kalaba 1975); though recognizing the brilliancy of the quantitative formulations of their value in determining filtration coefficients, relative resistance, and the influences of the various parameters on the filtration pressure, these models are of little value in predicting which factors actually are the main limiting determinants of the SNGFR in the intact nephron in vivo (or even in vitro). The model only describes the events under conditions of presumed constancy of the proximal intertubular pressure, thus disregarding the flow resistance of the various tubular segments. The likelihood of misleading the reader by omitting considerations of the determinant sequence of events would be less if authors of such models were more stringent in the use of the term SNGFR (or GFR). Rather they should use the term glomerular filtration pressure, unless it can be demonstrated on the accompanying changes occurring in the tubular pressure permitting valid quantitative evaluation of the actual changes in the effective filtration pressure and their time course.

The experimental finding by Daugherty et al. (1972) that SNGFR did in fact increase in proportion to plasma flow following plasma infusion without change in either the effective oncotic pressure or proximal absolute reabsorption rate may be explained by the conditions of their micropuncture experiment. A likely artifact is that the fluid for determination of SNGFR was collected in such a fashion that the proximal luminal pressure was maintained the same under the hydropneumatically controlled condition and following volume expansion. A more correct experiment would have been in the control period to collect the fluid under controlled luminal pressure equal to the free flow pressure; then to infuse the plasma and measure the rise in proximal luminal pressure resulting from the volume expansion and finally to re-collect fluid at this new intratubular pressure.

The effect of natriuretic hormones on the function of the kidney. Even though serious criticisms have failed to invalidate the OT-method so far, it remained a fact that other investigators (Horst et al. 1966; Lovitt, Sturpe and Ochwadt 1969) were unable to reproduce the inhibitory effect of angiotensin on proximal tubular function in vivo observed originally in OT-experiments. All that

of both anesthetic measured in plasma of anaesthetized rats (about 5×10^{-4} M) was almost 10 times higher concentrations of Amytal were required for comparable degree of inhibition. At concentration of 5×10^{-4} M Amytal had no effect on fluid absorption. Furthermore changes in fluid absorption due to the gall bladder induced by Amytal were reversible and accompanied by parallel change in oxygen consumption. In contrast, Ictin induced depression of net fluid transport was irreversible and not accompanied by any change in oxygen consumption. A different conclusion was reached by Devitt (1973) in Munich who were able to obtain adequate anaesthesia with administration of somewhat smaller dose of Inactin (10-15 mg per 100 g of body weight (b.w.) than that used by Elms (12-25 mg per 100 g b.w.). Devitt and his associates found no difference in GFR in proximal tubular reabsorption rates between rats anaesthetized with Inactin and Amytal; nor could they detect any relation between the proximal reabsorptive rate and the dose of Inactin. They concluded that anaesthetic doses of Inactin did not interfere with tubular function and that there was no difference between Amytal and Inactin in this aspect. However, plasma barbiturate concentration was not measured; larger plasma tarry dose of Amytal were given intravenously rather than intraperitoneally; and the use of animal studied by Devitt was small. Hence the data are not directly comparable with Elms (1973) as it. The problem was therefore re-investigated by Leyssac and his group excluding for the sake of comparison all rats which could not keep adequately with the total dose of Inactin of at most 15 mg/100 g b.w. (Leyssac, Frederiksen and Skinnar, 1975). In complete agreement with the data reported by Devitt et al. it was found that within this narrow range of Inactin dose (12.5-15.0 mg per 100 g b.w.) proximal fractional reabsorption was slightly but significantly higher than previously observed. Moreover, absolute rate of proximal absorption measured in Inactin anaesthetized rats were within the range of values obtained in the Amytal series; and the well established correlation between the rate of absorption and the dose of Inactin administered. However, comparison of the data obtained in the Inactin anaesthetized animal with those observed in Amytal anaesthetized showed significant differences. In the latter group the range of proximal reabsorption rate was nearly all less than in the lower half of the range of values measured in Amytal anaesthetized rats; and more important, a moderate increase in intravenous (equal to 1% of b.w.) failed to increase the proximal reabsorptive capacity in the Inactin group. In volume expansion with line

sed highly significant increase (on an average by 27%) in proximal tubular function (and GFR) in the group of animals anaesthetized with Avertin. Thus even low doses of Inactin appear to inhibit and limit the proximal reabsorptive capacity such that the response to physiological stimulus is abolished or at least blunted.

Another difference between Inactin and oxybarbiturate anaesthetics was reported by Steven (1974) in a micropuncture study. Under conditions of sodium pentobarbital anaesthesia a 3 mm Hg reduction in proximal intratubular pressure achieved by controlled suction caused significant increases in SNGFR where in Inactin anaesthetized rats a small reduction in luminal pressure was unable to augment the SNGFR because the lumen collapsed. The latter partially proximal to the collecting pipette. The observation indicates that the proximal tubule will be profoundly changed by Inactin being more collapsible compared to tubules under conditions of oxybarbiturate anaesthesia which would explain why observation of the proximal lumen radius with GFR has consistently been found over the entire range of filtration rate in tubules on Inactin anaesthetized rats. Finally it has most recently been shown that Inactin in contrast to oxybarbiturate impairs the autoregulation of RBF both in the rat and dog (Cong and Burk 1976). Thus the choice of the anaesthetic Inactin for studies on proximal tubule function and its regulation would appear to be most unfortunate in particular in studying an inhibitory effect of angiotensin (Rosenblatt 1966; Lovitz et al 1969) which has been detectable only at the highest spontaneous rates of proximal absorption obtained in Avertin anaesthetized rats.

The results of these studies which seem to solve long-lasting controversy emphasize that the effect of the anaesthetic itself should be taken into consideration when evaluating the literature and that we must recognize the effects of the anaesthetic route be matter of continuing concern as emphasized also by Laszlo (1975).

Effect of angiotensin on sodium transport with distal transport. There is increasing evidence that angiotensin II may influence tubular sodium transport of sodium and water in the distal tubule primarily by direct effect. Dahl and Mandarinos (1970) demonstrated a significant effect of angiotensin II (10^{-10} g/ml) on intracellular fluid volume of the y-intercepted preparations in vivo. It is tipped into the lumen of the tubule by previous neph-

rectomy and adrenalectomy angiotensin I has dose-dependent biphasic action on net fluid transport; low concentration (10^{-11} to 10^{-12} g ml $^{-1}$) stimulated whilst higher concentration (10^{-9} to 10^{-8} g ml $^{-1}$) depressed net fluid transport (Davies Munday and Parsons 1970). These latter observations were confirmed by Hornykch Mays and Millie (1973) who also showed that the biphasic response to angiotensin was dependent upon the previous nephrectomy-adrenalectomy. Angiotensin used an increase in sodium and water flux across mucosa from ascending colon of normal rat whereas it inhibited net fluxes across mucosa from descending colon at all dose levels (10^{-11} to 10^{-6} M). In later studies by Bolton and his associates (Bolton et al 1975) a biphasic effect of angiotensin on jejunal net fluid absorption in vivo was demonstrated in normal rat; again subpressor doses (0.59 nano-g kg $^{-1}$ min $^{-1}$) stimulated whilst high pressor doses (5.9 nano-g kg $^{-1}$ min $^{-1}$) inhibited absorption. Evidence that the stimulatory effect of angiotensin on colonic transport apparently depends on protein synthesis is the theoretical suggestion has been provided (Davies Munday and Parsons 1972) suggesting that the mechanism of this effect differs profoundly from the rapid inhibitory effect of angiotensin on proximal tubular function (Leyssac 1964). An inhibitory effect of angiotensin II on in vitro fluid absorption by gall bladders from normal rabbits was reported by Leyssac and his group (Leyssac et al 1974); the onset of this effect was rapid and the maximum effect was obtained within 30 minutes. Any stimulating effect of angiotensin could not be detected in this preparation. The effect of angiotensin on the gall bladder was due to inhibition of the active component of the transport process leaving the passive osmotic-to-mucosal flow of sodium and the potential difference unaffected. Osmotic resistance increased slightly (by 10%) in response to ion transport on isolated segments of proximal tubules in vitro Burg and Orloff (1968) were unable to detect any significant effect of angiotensin (2×10^{-6} M) on net fluid transport. However, net fluid transport rates were less in vitro than in vivo and the dose applied was extremely large either of which factors might have concealed potentially physiological effects.

More important in this context therefore was microperfusion study by Stuv (1974b) in which the inhibitory effect of angiotensin on proximal tubular reabsorption was reproduced in vivo in pentobarbitol anaesthetized rat. Lat proximal tubular fluid was collected from flow lumina prepared intrinsically from different tubular segments. Proximal tubular apical microperfusion

20 nano-1 min⁻¹ with angiotensin cont 1 ing solution (20 nano-g ml⁻¹) or with saline. Absolute fluid reabsorption rate was significantly depressed by 7.4 nano-1 ml⁻¹ g x w⁻¹ and tubular fluid/plasma inulin ratio significantly decreased by 0.79 during angiotensin perfusion. Peritubular microperfusion with saline had no effect on proximal reabsorption rate as compared to values obtained with out peritubular perfusion in the same kidney. The direct effect of angiotensin on isosmotic fluid transport by various epithelia in vitro and in vivo has been demonstrated; and its inhibitory effect on proximal tubular reabsorptive capacity has been directly verified utilizing different methodology than that used for its first demonstration. The inverse relationship between log plasma renin concentration and/or activity and the proximal rate of reabsorption found in Auyt 1 same relationship over the large range of absorption rate (and GFR) including the range occurring physiologically (Elmer et al 1973) well than induced by moderate saline loading (Layman et al 1973) is consistent with the hypothesis that the endogenous activity of angiotensin modulate proximal absorption rate under these conditions. Moreover such an inverse relationship is absent in rats anaesthetized with Inactin which was shown to inhibit and limit the proximal absorptive function.

The interrelationship of effect of endogenous angiotensin in II

Within the framework of the classical theory it might be conceivable that endogenous angiotensin could play a regulatory role of GFR and RBF by an action predominantly on the pre-glomerular arterioles. In accordance to this concept the rate of filtration is almost exclusively determined by the filtration pressure (Starling forces) glomerular dynamics. Thus, Thoreau advocates the view that the activity of the angiotensin system is regulated by feedback mechanisms in the macula densa which may then be stimulated by distal sodium concentration markedly sodium reabsorption at the distal renal tubule circuit (Thoreau 1972, Thurman and Mason 1973). Thus, glomerular pressure decreases tubular function (nephronally) and it is possible that the macula densa by increasing the distal NaCl-concentration and/or fluid flow it would stimulate the juxtaglomerular apparatus. It is local angiotensin formation on the afferent arteriole could be stimulated by decreasing GFR and tubular fluid delivery to the distal nephron segments. The distal tubule is therefore open to the effect of the tubular reabsorption by the distal tubule and conceivably

also by the early distal tubule directly load-dependent probably by gradient limitation (e.g. Anagnostopoulos Kinn y and Windhager 1971; Kunau Webb and Borman 1974). Thus any outflow in the delivery of fluid to the loop and the macula densa should stimulate the renin system. Contrary to this view is the well known fact that such an increase in loop and distal tubule fluid flow used e.g. by an acute intravenous saline load depresses renin release within few minutes (e.g. Leyaert 1975) while adding a reduction in filtration pressure and thereby in tubular pressure and flow to stimulates renin release immediately and continuously even in the isolated perfused kidney (e.g. Hofbauer et al 1974). After a period of reduced filtration pressure and ischemia, distal sodium concentration is increased indicating impaired function of the tubular epithelium as shown by Thurau et al (1967) in particular that of the diluting segment i.e. the ascending limb of Henle; most likely therefore the reabsorptive capacity of the macula densa cells should also be impaired under this condition which should depress renin release according to Thurau's concept; but it seems to stimulate the release according to measurement.

Apart from these apparent difficulties for accepting Thurau's view Gros and his associates have obtained indirect evidence of an effect of endogenous as well as exogenous angiotensin predominantly on the post glomerular circulation. Using an isolated perfused kidney preparation these investigators found marked increases in GFR and the filtration fraction following the addition of renin substrate to substrate-free perfusion medium (Krahn, Scharf and Gros 1970) or addition of angiotensin II to the medium (Krahn, Scharf and Gros 1971). Similar increases of GFR and FF were reported by Hulme and Bloor (1975) after infusion of the renin angiotensin I to the systemic circulation of rats where equipressor doses of no adrenaline or adrenaline had but little effect on the FF and GFR. More direct evidence of a post glomerular vascular action of endogenous angiotensin has recently been obtained by St van Peitubul micropuncture of angiotensin II containing perfusate ($20 \text{ nano-l min}^{-1}$) used dose-dependent increments in the luminal hydrostatic pressure of adjacent proximal convolutions ranging from 1 to 6 cm H_2O in pentobarbital anaesthetized rats (St van 1974b). Since the intratubular pressure closely reflects acute changes in the filtration pressure the measured pressure increase could be due either to pre-glomerular vasoconstriction or to post-glomerular

Schnemann, P. and Agerup 1973) or with diuretics known to interfere with loop and distal tubule electrolyte reabsorption (Wright and Schnemann 1974) suggesting that the feedback response depends upon the transepithelial transfer of electrolytes from the macula densa. Also it has been shown that albumin is an essential component of the perfusion fluid for the feedback response to occur (Burk et al 1974). The response appeared to be asymmetrical since changes in loop perfusion rate below the predetermined normal level had no detectable influence on the filtration pressure as estimated either from measurements of SNGFR collected at experimentally fixed intratubular pressure (Schnemann et al 1970; 1973); from measurements of proximal intratubular pressure change (Nierholm et al 1974); or from direct measurements of glomerular capillary hydrostatic pressure (Blant et al 1972). Further indirect evidence that the feedback response to increased fluid flow is to the distal tubule involve the renin-angiotensin system has been obtained. Dietary salt intake modified the sensitivity of the feedback mechanism; salt loading which reduces the renal renin content and release diminished the response (Dev Dresher and Schmermann 1974); blockers of the renin-angiotensin system (saralasin and converting enzyme inhibitor) also blunted the response reported by Schmermann (1975). Direct evidence indicating that the renin system is involved in the feedback mechanism has not been obtained.

The operation of such a feedback system under normal hydropenic conditions predicts that occlusion of the proximal convoluted tubule and thereby of fluid flow into the early distal tubule should lower the filtration pressure. Proximal occlusions of fluid free flow pressure for measurement of SNGFR should therefore give values of SNGFR higher than those obtained in the same kidney by occlusions of fluid from distal tubule. This prediction has been confirmed in several studies (e.g. Schmermann et al 1971; Davis, Schnemann and Harte 1972; Nwari et al 1974) while other investigators have been unable to detect such a difference in SNGFR dependent on the site of fluid collection (e.g. Morgan 1971; Bartoli and Earley 1973; Knox et al 1974). Taking into consideration the technical difficulties and likely artifacts inherent in micropuncture technique the influence on the feedback system of previous salt intake and of the physiological state of the animal during the experiment including anaesthesia and dose of anaesthetic is highly surprising the conflicting results have been reported. Collectively these studies do provide strong

and direct evidence indicating the existence of a feedback control mechanism which senses changes in a flow dependent signal (the level of the early distal tubule) and which in response adjusts the glomerular capillary hydrostatic pressure.

The question of how change in delivery of tubular fluid into the early distal tubule is sensed and converted to an effector response remain a matter of speculation.

Evidence has suggested firstly that trans-epithelial transport of electrolytes across the macula densa may be of great significance; secondly that the reabsorptive rate of this tubular segment is directly flow-dependent. Recently studies on cell release in vitro (Frederiksen, Luyssens and Skinner 1975; Kaubach, Luyssens and Skinner 1975) have indicated that the cells containing juxtaglomerular cells may respond to small osmotic challenges with passive changes in cell volume. Based on the hypothetical assumptions firstly that the tubule-glomerula feedback is mediated by the renin-angiotensin system; secondly that the passive cell volume-dependent renin release observed in vitro may be of physiological importance in regulation of basal cell volume; and thirdly that these findings suggest to the other unifying hypothesis according to this hypothesis — the macula densa is part of the juxtaglomerular cell (JG-cell) could function as a systemic barometer. While the same time cell volume-sensing coupling could include both the baroreceptor and chemoreceptor concepts of volume regulation (for review by Davi and Norman 1976) and accounts for feedback response. Thus the hypothesis predicts that an increase in flow would lead to an increase in reabsorption by the macula densa of flow. This would lead to a decrease in delivery of fluid to the tubule segment would increase the level of distal fluid osmolality. This hyperosmolarity in turn would cause cell shrinkage and thereby depress renin release.

Summary and concluding remarks (cf. figs 1, 2 and 3)

- 1) It has been established that proximal absorptive capacity is primarily a function of flow rate (the filtered load) of the tubule. It is well known that the rate of flow is provided by the glomerular pressure. This high pressure is maintained by the glomerular pressure.
- 2) It is well known that the pressure in the glomerular capillaries is primarily a function of the flow rate. The pressure in the glomerular capillaries is primarily a function of the flow rate.

tates It has been demonstrated that the proximal luminal pressure is a constant parameter

3) It has been shown indirectly as well as directly that the pressure drop across the glomerular membrane - the ultrafiltration - driving force - effective filtration pressure - is low in the order of 10-15 mm Hg or less. Hence small changes in proximal intratubular pressure with all the factors being equal will cause large changes in GFR.

4) A tubulo-glomerular feedback mechanism which responds to changes in distal fluid flow directly with changes in the filtration pressure has been demonstrated directly

5) It has been shown and interpreted with different direct techniques that angiotensin II has, presumably direct tubular action which inhibits the proximal reabsorptive capacity of isotonic fluid

6) Direct evidence has been provided indicating that the vascular effect of endogenous angiotensin is predominantly an effect on the afferent arteriole; and that the resistance of this arteriole is controlled in vivo by the local activity of angiotensin II. Thus the tubular effect of angiotensin acts in the same direction on the proximal intratubular pressure

It would seem, therefore, that the fundamental assumption of the present working hypothesis as well as its implications have been verified and established. Furthermore each link in the chain of events in the hypothesis has been confirmed by results obtained in several laboratories and by utilization of various techniques. On this background the term working hypothesis may now be dismissed in my opinion; rather it should be regarded as a new theory replacing the disproved and more or less local theory.

The new theory is in complete harmony both with the anatomical structure of the nephron and with the special localization of the reabsorption system. In addition it offers an explanation of the large development of the proximal tubular segment in mammalian homeotherms as mammals are with high blood pressure and a vascular system with arterioles which react to many stimuli unrelated to the salt and water balance. Their filtration pressure will be relatively unstable, varying over a range of several mm Hg. According to the theory the proximal tubular segment of the nephron and the reabsorption system functions in part to be set by means of feedback mechanism in a feedback system which can rapidly stabilize

th intratubular pressure in spite of variable propulsive pressure

In this fashion a stable delivery of tubular fluid both to the loop of Henle and to more distal tubular segments is insured; and it can be easily understood that large pressure changes can be compensated for with larger proximal absorptive capacity and variability of the effluent tubular resistance.

A stabilized fluid flow to the segment distal to the proximal tubule is a desirable necessity if the distal tubule is to be maintained partly because the optimal function of the concentrating mechanism in the loop of Henle depends upon the maintenance of tubular flow rates within relatively narrow ranges; and partly because the absorptive capacities of distal tubule and collecting duct by which the excretion of fluid is finally regulated is small and slowly adjustable (e.g. by mineralocorticoids).

Thus within the framework of this theory the renin system and the proximal tubule segments play a central role for the compensation of the maintenance of body salt and water balance and hence of renal blood pressure. But it should be strongly emphasized that quite evidently we do not know but a few of the probably many factors including internal factors which may possibly regulate its excretion; and the significance of other factors in part unknown perhaps which may influence and limit the proximal reabsorptive capacity under various conditions also remains undefined. But the basis for further progress in this field may be improved I hope. Obviously the new theory has a bearing also upon pathophysiology but hopefully it may influence future research on the pathogenesis of hypertension and disease of the renal filter in a positive direction.

Acknowledgement

The present work has been supported during the years 1961-1974 by grants from the Danish Medical Research Foundation, the Carlsberg Foundation, the Tuborg Foundation, the Danish Foundation of the Advancement of Medical Science, the Erik Iulius Foundation, the Novo Foundation, the American Export Association, Johnson and Hansen Weismann's Legacy, the P. A. Brandt's Legacy and Ebba Celinder's Legacy, of which the author expresses his gratitude.

- BOJKEW E The renal mechanism of dilation diuresis and salt excretion in dogs Acta Physiol Scand 1954 22 129-145
- BOJKEW and P P LEYSSAC Proximal tubul reabsorption in the kidney studied by the occlusion time and lissamine green renal time technique Acta Physiol. Scand 1969 76 213-235
- BOLTON J E A. MUNDAY R J PARSONS and D. YORK Effect of angiotensin II on fluid transport transmembrane potential difference and blood flow by the jejunum in vivo J. Physiol. (Lond) 1975 253 441-456
- BRUNNER M L. TROY T M. DAUGHARTY The dynamics of glomerular ultrafiltration in the rat J. Clin. Invest. 1971 50 1776-1780
- BRUNNER M. J L TROY T M DAUGHARTY R OCK and C R. FORBESON Dynamics of glomerular ultrafiltration: the effect of renal plasma flow dependence of GFR Amer. J. Physiol. 1972 223 1184-1190
- BRUNNER P P C RECTO and ELOIN Mechanism of glomerulotubular balance. I: Regulation of proximal tubular reabsorption by tubular volume as studied by stopped flow microperfusion J. Clin. Invest. 1966 45 603-611
- BUMS R and ORLOFF Control of fluid absorption in the renal proximal tubule J. Clin. Invest. 1968 47 2016-2024
- BURKE L. HAAR R. CLAP and ROBINSON Response of single nephron glomerular filtration rate to single nephron microperfusion Kidney Int. 197 6 23-241
- CHRISTENSEN P L. S. HANSEN and LEYSSAC The effects of Atrial and Aortic on osmotic and fluid transport in the rabbit gall-bladder in vitro Acta Physiol Scand 1973 87 55-64
- CONGER, D and BURKE Effect of anesthesia upon the autonomic regulation of renal hemodynamics in the rat and dog Amer. J. Physiol 1966 220 452-457
- CONGER, J D R. BARTOLI and EARLEY No effect of peritubular plasma protein on proximal tubular volume absorption during apical microperfusion 5th Ann. Meet. Am. Soc. Nephrol. Washington D C 1973 25 (Abstr.)
- DAUGHARTY M. UKE D. M. COLAS and D.M. BRUNNER, Comparative renal effect of ouabain and ouabain free volume expansion in the rat Amer. J. Physiol 1972 222 125-135
- DAVIS and FREEDMAN Mechanism of regulation of renal plasma flow Physiol. Rev. 1966 46 1-35

- ELMER M P C RSKILDSEN L-S KRISTENSEN and P H LEYERAC
A comparison of renal function in the anaesthetized with
Inactin and sodium Amytal Acta Physiol scand 1972 86
41-58
- ELMER, M L-S KRISTENSEN and P H LEYERAC Proximal luminal
diameters and cell volume in rats anaesthetized with In-
actin and Amytal Acta physiol. scand. 1973 88 226-233
- HAARUP P On the morphology of the juxtaglomerular apparatus
Acta anat. 1965 80 20-38
- FREDERIKSEN O H LEYERAC and S L SKINNER Sensitive
osmometer function of the juxtaglomerular cells in vitro
J. Physiol. (Lond) 1975 252 669-679
- GERKE H R Trans tubulär Natrium- und Wasserfluss und Perme-
abilität für Nichtelektrolyte im proximalen und distalen
Konvolutede Nierentubulus Arch ges Physiol
1963 276 336-356
- GERKE H and J W BOLTAN Juxtaglomerular-tubule balance
In Handbook of Physiology Section 8 Renal Physiology
Eds Oloff J R. Baltimore The Williams Wilkins
Co Baltimore 1973 Chapter 23 763-790
- GERKE H R J WANDERS G BRADY and H PAGEL On the
glomerular tubule balance in the rat kidney Pflügers
Arch ges Physiol 1969 285 360-372
- GOTTSCHEALK C W and W E LAMSTER Microperfusion methodology
In Handbook of Physiology Section 8 Renal Physiology
Ed Oloff J R. Baltimore The Williams Wilkins
Co Baltimore 1973 Chapter 6 139-144
- GOTTSCHEALK C W and M HYLLIE Microperfusion study of pres-
sures in proximal tubules and peritubular capillaries of
the rat kidney and their relation to arterial and renal
venous pressure Amer. J. Physiol. 1956 185 430-439
- GRANTHAM B GOALISIA and L-W MILLING Influence
of serum proteins on net fluid reabsorption of isolated
proximal tubules Kidney Int. 1972 2 64-73
- KROHL, H E FRÖMTER and T WICK Die elektrischen Wand-
widerstände des proximalen Konvolutede Nierentubulus
Pflügers Arch ges Physiol 1967 274 274-280
- KIERHOLZER K R MÖLLER-SOHN H-U GUTCHER M BOTS and
I LICHTENSTEIN Filtration in the glomeruli
regulated by flow through the loop of Henle Pflügers
Arch ges Physiol 1974 272 315-337
- ROSLAGER M SCHIEDRICH RACHENTHAL and M CROSS
Function of the renal angiotensin system in the isolated
perfused kidney Circ. Res. 1974 suppl 34 22
193-201

- LASSITER E The Kidney *Ann Rev Physiol* 1975 27, 371-393
- LASSITER W E C W GOTTSCHALK and M WYLIE Mi report re study f net transtubul movemen f wate and re in oedema i mammalian kidney *Amer Physiol* 1961 201 1139-1146
- LEVINE D I G LIEBER FISCHBACH and E THORAU Micro-puncture studies on the dog kidney II Reabsorptive characteristics f the proximal tubul during spontaneous and xpe isemal variation in GFR and during drug induced nat iore i *Physiol Rev* 1968 30 365-372
- LEVY J E and E E WINTERHAKE Peri tubula control f proximal tubular fluid reabsorption in the rat kidney *Amer. J. Physiol* 1948 21 943-954
- LEYSSAC P P Dependence of glomerular filtration rate on proximal tubule reabsorption f salt i *Acta Physiol Scand* 1963 28 238-243
- LEYSSAC P P The in vivo effect f angiotensin on the proximal tubular reabsorption f salt i rat kidney *Acta Physiol Scand* 1964 32 436-448
- LEYSSAC P P The in vivo effect f angiotensin and sodium saline on the proximal tubular reabsorption f salt i mammalian kidneys *Acta Physiol Scand* 1965 34 167-175
- LEYSSAC P P Regulation f proximal tubular reabsorption in the mammalian kidney *Acta Physiol Scand* 1966 70 suppl 291
- LEYSSAC P Renal salt and water movement i different states f an intact control system *Proc Roy Soc Med* 1969 62 1111-1116
- LEYSSAC P and E BJÖRSTEN Is dependence between glomerular filtration and tubular reabsorption i the process f proximal salt and water turnover *Proc 3rd Int Congr Nephrol* Washington 1966 1 110-120 (Karger Basel/New York 1967)
- LEYSSAC O FREDERIKSEN and S L SHAPIRO The effect on total renal and tubular function and plasma renin f moderate sodium chloride load on the rat *Am J Physiol* 1975 22 42-48
- LEYSSAC P P L S KRISTENSEN P CHRISTENSEN and E BJÖRSTEN The effect f angiotensin on isosmotic fluid absorption by the rabbit gall-bladder in vivo *Acta Physiol Scand* 1976 32 508-516
- LOWTTS M D R H STUMPF and B OCHSADT report re study f the action f angiotensin i on tubular osmotic

- SCHULMAN J J M DAVIS P MUNDERLICH D I LEVINE and M ROOSTER Technical problems in the micropuncture determination of nephron filtration rate and their functional implications Physiol Rev 51 Physiol 1971 322 307-320
- SCHULMAN J D I LEVINE and M ROOSTER A direct valuation of the Gert hypothesis on single proximal tubular flow: influence of the tubular volume on the renal determinant of the reabsorptive rate Physiol Rev 1969 302 149-165
- SCHULMAN J A G PERSSON and S ÅKERSTEDT Tubuloglomerular feedback: nonlinear relation between glomerular hydrostatic pressure and loop of Henle perfusion rate J. Clin. Invest. 1973 52 842-849
- SCHULMAN J M WALKER LIEBOWITZ and S FISCHER Balance between tubular flow rate and net fluid absorption in the proximal convolution of the kidney: I. Dependency of reabsorptive net fluid flux upon proximal tubular flow: a spontaneous variation of filtration at Physiol Rev 1968 304 90-103
- SCHULMAN J F S WRIGHT J M DAVIS V STACKELBERG and G GRILL Regulation of superficial nephron flow rate by tubulo-glomerular feedback Physiol Rev 1970 318 147-175
- SELKURT E Effect of pulse pressure and mean arterial pressure modification on renal hemodynamic and electrolyte and water excretion Circulation 1951 4 441-451
- SELKURT E E FRANK M HALL and M P SPENCER Influence of graded arterial pressure decrement on renal excretion of renin, p-aminopyridine and sodium Amer. J. Physiol. 1949 152 369-378
- SMITH E W The Kidney Oxford 1 Press New York 1951 pp 1049
- SPITZER A and E WINDHAGER Effect of peripheral vascular pressure change on proximal tubular fluid reabsorption Ann. N.Y. Acad. Sci. 1970 21 1188-1193
- STEIN E Influence of nephron GFR on proximal absorption of p-aminopyridine: an experimental study Kidney Int. 1974a 6 204-213
- STEIN E Effect of peripheral vascular pressure change on proximal nephron function Kidney Int. 1974b 6 73-80
- STEIN E Angiotensin II: tubular and renal regulatory pressure regulation in the rat Submitted to Publ. Physiol Rev 1976

- STEVEN K and B STIPPER Basal corporeal hydrodynamic
 Milt 1 compute imulation Physiol. Arch. exp. Physiol.
 1974 348 317 331
- THURAU K The juxtaglomerular apparatus its 1 in the
 form on f the 1 gls nephron unit In Modern Diabetic
Therapy 1 the Treatment of Cardiovascular and Renal
 Dis. at 1 t Congr Serl no 268 Excerpt Med
 Amsterdam 1972 84-92
- THURAU K and RASCHKE Renin-angiotensin loc 1 det
 Nizam f glomerul fil t on in Pathophysiol of
Hypertension In Congr Serl no 302 Excerpta Med
 Amsterdam 1973 33 37
- THURAU K J SCHREIBER M RAGEL N ROBERTS and M MARL,
 corpus on f ubular fil d the macula densa secret
 factor gult t th fur on f the jux glomerul
 ppe Exp. Phys. 196 suppl 17 20-21 7 88
- ULLICH K J SCHMIDT NIELSEN R ODELL G PERLING
 C M GOTTSCHALK M E LASSITER and M RYLL Microscop-
 re study of corpus on f proximal ad distal tubula
 fil d k dney Am. J. Physiol. 19 3 281 527 531
- MARL M G LIEBOW M FISCHBACK and J SCHREIBER Balance
 betwee ubular flow its and net fluid absorption in
 the proximal convolution f the k dney II Reab-
 sorptive cha ac co d eq con ion f the
 ex i rry Physiol. Arch. exp. Physiol. 1968 304
2 314
- ARL M ARLE M FISCHBACK and THURAU On the ppl
 on the cories on the we had for measurem ts f
 dia 1 net fil ac the pro nal corrol on f the t
 dney Physiol. Arch. exp. Physiol. 196 278 161 173
- MARLY A M B A DOTT OLIVER and MACDONELL To col
 1 st on and analysi f fil id f on single neph con f the
 nappia an k dney Am. J. Physiol. 1 61 214 340-3 5
- WILSON L ANELON J and M WHITE The
 re on f deo (autolyt Path. M. T. Acad. Med. 1948
21 8 06
- STEARNS M R BIRNBAUMER E WYCHACE and LEBACH
 reyo (as on way 1 id ab drpt on pr 1
 ab f k wry Am. J. Physiol. 1 1 211
0 618
- WIRCHACE and G FRISCH M reyo ur why f conal
 ut an f od on 1 de he Am. J.
Physiol. 1 2 81
- CE K LEWY and A T E Int or l
 ut 1 reab rpt on od an and
Am. J. 1 5

ACTA PHYSIOLOGICA SCANDINAVICA

SUPPLEMENTUM 443

**Muscle Strength,
Fibre Types and Enzyme Activities
in Man**

BY

ALF THORSTENSSON

STOCKHOLM 1976

ACTA PHYSIOLOGICA SCANDINAVICA
SUPPLEMENTUM 443

**From the Department of Physiology
Gymnastik och idrottshögskolan, Stockholm**

**Muscle Strength,
Fibre Types and Enzyme Activities
in Man**

**BY
ALF THORSTENSSON**

STOCKHOLM 1976

INTRODUCTION	7
METHODOLOGICAL ASPECTS	
Subjects	11
Statistics	11
Strength measurements	13
Strength training	16
Muscle sampling	16
Histochemical methods	17
Biochemical methods	18
Isozyme analysis	20
Single fibre analysis	21
RESULTS AND COMMENT	
Force velocity relationships in the knee extensor muscles	22
Force velocity relationships and muscle fibre composition	23
Fatigability and muscle fibre composition	26
Contractility enzymes and muscle fibre types	27
Isozymes of contractility enzymes and muscle fibre types	29
Effects of strength training	31
GENERAL DISCUSSION	33
SUMMARY	36
ACKNOWLEDGEMENT	37
REFERENCE	

INTRODUCTION

The present study is an attempt to relate the histochemical profiles and biochemical characteristics of human skeletal muscle to its mechanical properties

The speed of muscle shortening is known to be inversely related to the load against which it shortens. This basic finding in muscle mechanics was first made by Fenn and Marsh (1935) and formulated in mathematical terms by Hill (1938). This force velocity relationship applies to both smooth and striated muscle (for refs see Sonnenblick 1962) even human elbow flexors during voluntary co-contractions (Hill 1940 Wilkie 1950 Astruc et al 1965 Komi 1973). In these studies either resistance or velocity was kept constant. A new method has been designed based on Perrine's work (Perri 1968) in which different constant velocity levels are easily achieved. The force output of different muscle groups during maximal contractions can then be conveniently studied at different muscle shortening velocities.

More than a century ago Ranvier (1873) observed differences in the force velocity properties of rabbit skeletal muscles of differing gross morphology. Links between the contractile properties of a muscle and its metabolic and morphological characteristics in terms of the distribution of distinct muscle fibre types were firmly established subsequently (see Close 1972 and Burke et al 1973). Experiments initially involving histochemical analyses of whole muscles with fast or slow contraction times and later direct studies of single motor units led to the conclusion that motor units can be classified into two main types: fast twitch (FT) and slow twitch (ST) (otheromenclatures are also used; see Close 1972). The muscle fibres belonging to each type of motor unit have been shown to be homogeneous (Edström and Kugelberg 1968 Burke et al 1973) and can be conveniently identified by histochemical means (see Methodological Aspects). Maximal tetanic tension appears to be higher for FT motor units than for ST units even when the tension is related to the cross sectional area (see Burke and Teasdale 1973 Barry and Close 1971). Due to methodological difficulties this latter difference is also well established (cf Close 1972). The motor units display a high susceptibility to fatigue upon

repeated electrical stimulation than ST units (Edström and Kugelberg 1968 Burke et al 1973) However the fatigability within the FT motor unit pool varies and appears to be inversely related to the oxidative capacity of the fibres These differences led to a subdivision of FT fibres into two types one which is comparably resistant to fatigue and another which fatigues rapidly (Barnard et al 1971 Burke et al 1973) Both types possess a high glycolytic potential in contrast to ST fibres which have a low glycolytic and high oxidative capacity

For obvious reasons much less detailed information is available about motor units in human muscle than in animals However autopsy (e.g. Johnson et al 1973 Edgerton et al 1975) and biopsy (e.g. Engel 1962 Gollnick et al 1972) studies have shown that most human skeletal muscle consists of a mixture of muscle fibre types histochemically classifiable as ST (type I) or FT (type II) fibres Metabolic studies of human skeletal muscles using both mixed muscle homogenates and single muscle fibres have essentially confirmed the findings from animal muscles (e.g. Schmalbruch and Kamieniecki 1974 Essén et al 1975) One striking feature of human skeletal muscle is the inter individual variation in the proportion of FT and ST fibres within any given muscle Data on the contractile properties of human skeletal muscle are limited Two types of motor units were postulated on the basis of the twitch contraction times recorded for single motor units (Sica and McComas 1971); a slower contraction velocity has been reported for fibre bundles containing a high percentage muscle fibres rich in mitochondria (presumably ST) (Buchthal and Schmalbruch 1970)

Contractile activity in muscle is controlled by regulation of the Mg^{2+} stimulated ATPase (adenosine triphosphatase) of the actomyosin of the myofibrils (Parry 1974) The validity of Mg^{2+} activated actomyosin ATPase in this respect is supported by most in vitro studies (see Barany 1967) A high correlation exists between the speed of contraction and activity of Mg^{2+} activated ATPase in both myosin and actomyosin (Barany 1967 Barany and Close 1971) The activity of this enzyme may therefore be one of the controlling factors in contraction velocity At present it is not known whether or not this enzyme is related also to muscle tension e.g. by controlling the number of activated cross bridges

The fast ATP hydrolysis during vigorous muscle contractions calls for rapid resynthesis of ATP. This can be accomplished from local stores of creatine phosphate via the reaction catalyzed by creatine phosphokinase (CPK) (for refs see Karlsson 1971). A higher level of activity of this enzyme in FT muscle fibres than in ST fibres has been reported for rabbit and human skeletal muscle (see Pette and Bücher 1963, Sherwin et al. 1969). The myokinase (MK) reaction transforming 2 ADP to ATP and AMP can also provide this rapid ATP replenishment (Cain and Davies 1962). However, the link between the activity of this enzyme and muscle contraction has been less firmly established (Hoda 1973). The characteristics of the MK reaction are likely to be of relevance in the regulation of the rate of glycolysis since the ATP:ADP:AMP ratio is known to regulate the activity of the key enzymes glycogen phosphorylase and phosphofructokinase (see Atkinson 1968).

More detailed information about the action of an enzyme can be obtained if a analysis of isozyme distribution is combined with determinations of total enzyme activity. Isozymes of several enzymes including CPK and MK have been demonstrated in human muscle tissue (for refs see Watts 1973, Hoda 1973 and Markert 1975). These multiple varieties of an enzyme catalyzing the same reaction are thought to enable the cell to cope with various metabolic conditions. These conditions may occur at different sites within the same cell or in different cells, e.g. FT and ST muscle fibres. A good example of this has recently been demonstrated for lactate dehydrogenase in human skeletal muscle (Ljüdin 1976). Muscle fibre specificity of CPK isozyme distribution has been indicated for the skeletal muscle (Sherwin et al. 1967). MK has not been studied in this respect.

The possibility of differential expression of FT and ST muscle fibres by myoelectric elements such as training is currently the subject of investigation. The physiological relationships such as cross innervation and innervation density of myoelectric elements lead to changes in contractile properties of fast and slow muscles and concomitant alterations in metabolism (see Close 1971, Lowy et al. 1974). However, the physiological significance of yet one more factor affecting the isozyme pattern of myoelectric ATP re-forming the basis for the classical

fication of FT and ST muscle fibres (for refs see Burke and Edgerton 1975) There is much evidence in support of the view that the distribution of the two main fibre types is largely governed by genetic factors (cf Komi et al 1978) The predominance of one fibre type in a given category of athletes e.g. ST fibres in endurance athletes (Gallnick et al 1972) would then be the consequence of selection However long term effects for systematic training can not be ruled out completely at this stage

The metabolic properties of a muscle can be altered by physical training Endurance training has been shown to cause substantial increases in the oxidative potential of both animal and human skeletal muscle (for refs see Holloszy 1973 Saltin 1978) These oxidative changes appear to be confined mostly to the ST fibre type and a selective hypertrophy of this fibre type has been observed with endurance training (Gollnick et al 1973) Evidence for an increase in the oxidative capacity of FT fibres has also been noted (e.g. Bernard 1970) Changes in the isozyme pattern of lactate dehydrogenase after endurance training have been found for both fibre types (Sjödén et al 1978) No information is available on corresponding muscular adaptations in response to strength training

The main object of the present series of experiments was to investigate the relationship in human skeletal muscle between contractile properties such as force, velocity and fatigability on the one hand and the quality of the muscle in terms of its distribution of FT and ST muscle fibres and the related activities and isozyme patterns of Mg^{2+} stimulated ATPase, CPK and MK on the other hand plus the adaptation of these muscle properties to strength training

METHODOLOGICAL ASPECTS

Subjects

Subjects in studies I and III VI were recruited among healthy habitually active men mostly students of physical education. In one study (III) Swedish elite athletes in various sport events participated along with a group of sedentary subjects with no experience of systematic physical training. In all cases the subjects agreed to participate after being informed about all aspects of the experiments. Most of the subjects were between 20 and 30 years of age (total range 17-39 Table I). Although muscular strength is known to vary with age, the age variation in the present material was so small that it was considered to be of no significance to the results. Some anthropometrical data for the groups of subjects examined are presented in Table I. Muscle strength was mainly measured as torque (see below) which is theoretically proportional to L^3 (L = linear dimension). To circumvent the influence of body dimensions on the strength measurements the muscle strength was expressed per kg of body weight (also proportional to L^3) or in relative terms as a percentage of maximal isometric strength (for reference age and dimension: see Astrand and Rodahl 1970).

Statistics

Conventional statistical methods were employed to calculate standard deviations (σ), standard error of the means (SE) and linear correlation coefficients (r). Determination of linear regression was performed using the method of least squares. Intraindividual differences and differences between mean values were tested for significance using dependent and independent Student's t tests respectively. The level of significance is denoted with p values. The method for a defined as the Bonferroni significance level calculated from the Bonferroni ratio according to the following formula:

$$\sqrt{n} \alpha / (1 - \alpha)$$

where n is the difference between the two groups and α is the nominal level of significance.

In the text the method error will be expressed as coefficient of variance (C V) i.e. $SD/x \times 100$ where x the mean

Table I: Characteristics of subject groups in studies I III and VI Mean values and ranges are given

Study	n	Age yrs	Height cm	Weight kg	Category
I	25	24	178	70.9	habitually active men
		17-37	165-191	51.7-95.0	
II	9	24	187	77.8	jumpers and sprinters
		19-34	181-194	73-86.0	
	6	21	178	68.4	downhill skiers
		19-25	174-181	67.0-75.0	
	7	27	178	64.5	competition walkers
		17-36	175-187	61.0-67.0	
	7	25	181	68.5	orienteers (cross country runners)
		22-29	174-185	63.5-74.5	
	10	26	184	75.1	sedentary men
		22-29	170-190	61.1-95.0	
III	10	30	180	69.5	habitually active men
		25-39	165-185	62.5-77.0	
VI	14	24	179	74.2	habitually active men
		19-31	168-186	59.6-88.3	

Strength measurements (I-III)

Maximal muscle strength in the left knee extensor muscles was recorded as torque output during maximal voluntary knee extensions with constant angular velocity. The subject was sitting in an experimental chair and the lower leg moved the lever arm of the isokinetic dynamometer (Cybex II Lumex Inc. New York). The pivot point of the lever arm was aligned with the knee joint. The angular velocity was controlled at the pre-set level by an internal resistance which accommodates to the muscular force applied [see Parrine 1965, Haislop and Parrine 1967, Thistle et al. 1967]. The experimental setup is illustrated in Fig. 1 and the different components are described. The range of motion encompassed knee angles from 90 to 0 degrees¹⁾. Isometric strength was measured at selected knee angles whereas concentric strength was recorded over the whole range of motion. Angular velocities could be selected between 0 and 180 degrees/s²⁾. Two attempts were allowed at each knee angle and velocity and the highest values were noted.

A representative recording of torque output³⁾ during a maximal isokinetic contraction is shown in Fig. 2. Peak torque is identified and will be the principle measurement used for comparative analyses of muscle strength. One advantage of assessing muscle strength by means of torque output in addition to its functional connection is the independence of the location on the body segment at which moment is recorded. The length of the lever arm was therefore kept constant in the present series of experiments. However, the location of the knee joint could not be accounted for. Nor were individual differences in this or other anatomical parameters such as leg length of the participant considered.

Finally, the validity of the isokinetic dynamometer has been established to be high (Moffrid et al. 1963). Torque values dis-

¹⁾ The angular velocity was preset at 30 degrees (0.5 π radians) per second fully extended to the knee joint.

²⁾ The angular velocity was preset at 180 degrees/s (100 degrees/s).

³⁾ The torque values were recorded in kgm.



Fig re 1 The experimental setup for the gth measurement
A adjust bl h i ith upper t f houlders hip nd l g;
B i h i ti dy anomet (Cyb II) with ve t ea ka H
leve re C p d l t H H f oplifi ra E UV-
record r (H eywell 201)

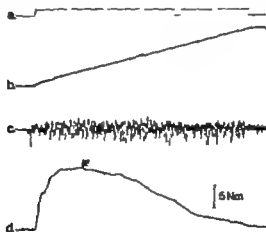


Fig re 2 Repres t t ve re rdig of ne inal i l ti on
tr tion t t ng l vel ty f 50 degre /
eve t g t vary 15th d gre f mot b pot t met
re rd g f ng l l ity EPG signal re rd from th
cont t g astua l t l i d t r q re rdig d tes p k
t r q

played a linear increase in response to increasing weights attached to the lever arm for calibration. The test-retest reliability coefficient for repeated applications of various loads was $r = 0.995$ ($n = 70$). Maffroid et al. also reported high values for the constant velocity ($r = 0.985$, $n = 34$) which was confirmed in the present study for the greater part of the range of motion. At onset of motion there is an unavoidable time lag before the preset constant velocity is reached. This time lag (0.05 s) was large at the high test velocity (180 degrees/s).

The reliability of subject ability to produce maximal torque at each velocity and knee angle was investigated in 3 different situations: a) in consecutive attempts; b) in randomized effort interrupted by contraction at other velocities; c) as in b) but on two separate days. These investigations produced the following over-all coefficients of variation (C.V.) for the whole torque curve: i.e. from 7 knee angles in the arc of motion and at 8 different velocities: 8.4% (a, $n = 8$), 8.5% (b, $n = 9$), and 13.7% (c, $n = 8$) respectively. The C.V. for peak torque produced according to a) ranged from 3.2 to 4% in a total of 38 subjects. These results were complemented by a study of 25 habitually active healthy men (aged 17-27 yrs) who completed the test programme according to c). The C.V. for peak torque (the highest values recorded on two separate days) in this group ranged from 4.1 to 5.5% and for subsequent peak loads the same conclusion (2.1 to 4.7%). No systematic differences between the two testing sessions were observed irrespective of the programme (a, b or c) which were found.

The influence of fatigue caused by the testing procedure was checked by repeating the initial test protocol after the completion of the entire programme. 10 subjects. No systematic difference was found between these determinations. The effect of fatigue is considered negligible with the present test battery in line with up to 22 maximal contractions at various speeds interrupted by rest intervals of 30-45 s.

Muscular fatigue was assessed in a preliminary experiment with repeated maximal contractions performed on the isokinetic dynamometer. Angular velocity was set at 180 degrees/s. The subjects were instructed to perform repeated contractions with maximal effort and to resume the starting position passively between each contraction. Every contraction lasted 0.5 s and the passive phase approximately 0.7 s. In an average of about 50 contractions was performed per min.

All subjects were tested on two separate days one day performing 50 and the other 100 knee extensions. The averaged peak torque for the 48 50th contraction in percent of the corresponding value for the initial 3 contractions was taken as the fatigue index. The C V for this measure was calculated at $\pm 2\%$ ($n = 10$).

The maximal knee extension velocity was estimated from the time interval between microswitches at 7° and 15° knee angle during knee extension against no external load. The best of 5 attempts was used. Day to day variation for this measurement amounted to $\pm 5\%$ (C V).

Strength training (VI)

The training programme consisted of exercises used by athletes to achieve optimal improvements in maximal strength. The programme included mainly maximal or close to maximal exercises (3 sets of 6 repetitions) for the leg extensor muscles carried out in the form of squats with knee bands and extensions with weights on the shoulders. The load was progressively increased over a training period lasting 8 weeks (3 sessions of about 1 h per week). The programme also included various jumping regimens e.g. vertical jumps. The effects of this programme was tested by a variety of performance tests comprised one repetition maximum in squats, vertical jump, standing broad jump and determination of maximal isometric force during two leg extension (Karlsson and Öllander 1972). The isokinetic device was not used in this study.

Muscle sampling (I-VI)

Skeletal muscle samples were obtained from resting vastus lateralis muscle using the needle biopsy technique as described by Bergström (1962). The vastus lateralis was chosen because it is a major contributor to the force generated during knee extension (cf Fig. 2) and is also located at a site convenient for muscle biopsy sampling. The other muscles engaged in the generation of measured total knee extensor strength were not biopsied. In one of the studies (IV) surgical biopsies were obtained from human papillary and soleus muscles for comparison of isozyme patterns (see below).

Histochemical methods [I VI VI]

Muscle specimens for muscle fibre typing and area determination were trimmed of fat and connective tissue mounted in histoclad and frozen in isopentane cooled with liquid nitrogen. When not analyzed immediately samples were stored in a freezer at -80°C . Cross sections $5\text{ }\mu\text{m}$ thick were cut in a cryostat and applied onto microscopic cover glass slips subsequently incubated in specific staining solutions.

The myofibrillar ATPase method (Padykula and Herman 1955) as modified by Guth and Samaha (1969) was used for muscle fibre classification. The reactions were carried out at pH 9.4 following alkaline preincubation (pH 10.3). Using this procedure two distinct fibre types can be distinguished one staining dark and the other with a light staining intensity. In the present study these two main fibre types are referred to as fast twitch (FT) and slow twitch (ST) muscle fibre types respectively (cf Gollnick et al 1972). The number of fibres of each type was counted from photomicrographs of the stained cross sections and the relative distribution of FT and ST fibres was determined. A sample was discarded whenever the number of fibres failed to exceed 200. Determinations of the percent of FT fibres in duplicate biopsies from the same muscle yielded a C.V. of 10% (n = 10). The biopsies were obtained at a depth of 3.4 cm into the muscle belly. This standardization of sampling depth was not especially important since the distribution of FT and ST fibres appears homogeneous throughout the depth of the muscle (Edgerton et al 1975).

Fibre areas were determined from serial cross sections of each biopsy stained for NADH diaphorase (Novikoff et al 1961). This histochemical procedure was used to avoid fibre shrinkage due to dehydration. 10 fibres of each type (identified with the ATPase staining) were selected from an area of the photomicrograph where the cross section appeared perpendicular to the fibre orientation. Planimetry was used to calculate the mean FT and ST areas in study I and VI (cf Gollnick et al 1972). In study II a simpler method was used in which the prints of the fibres were cut out, pooled together and weighed. By weighing of photopaper with known areas an averaged area could be calculated for each fibre type. Close agreement was found between the two methods and the methodological error was calculated at 4% (C.V.).

Fibre area determinations on biopsies obtained from the same muscle on two different occasions revealed a C V of 15.1% for the absolute areas of FT and ST fibres respectively. When the FT/ST area ratio was considered the corresponding figure was 9%. The great variation in absolute values might have been due to a difference in degree of contraction caused by the sampling procedure. The FT/ST area ratio was concluded to be a more reliable measure of muscle fibre area relationships. This quotient is also included along with the relative number of fibres in the computation of relative muscle fibre area (Gollnick et al 1972).

Biochemical methods (IV-VI)

Muscle specimens for enzyme activity analyses were trimmed quickly, froze in liquid nitrogen and stored in a freezer at -80°C . On the day of analysis the muscle samples were weighed in a cryostat (Karlsson 1971) and homogenized by sonication in 0 M KCl. The homogenate was further diluted in buffer before 20 μl aliquots were added to 1 ml of test medium.

The enzyme activity determinations were performed with fluorometric techniques using a Farrand ratio fluorometer-2 (Farrand Optical Co. New York). The reactions catalyzed by the enzymes under investigation were coupled to NAD/NADP linked reactions and the changes in NADH or NADPH were monitored according to principles outlined by Lowry (Lowry and Passonneau 1972). The initial rate of these changes was taken as the measure of enzyme activity. The measurements were made under V_{max} conditions i.e. with an excess of substrate(s). By running standard curves with known amounts of fluorescence the experimental readings could be quantified. The three major enzymes investigated in the present study were Mg^{2+} stimulated ATPase (E.C. 3.6.1.4), creatine phosphokinase (CPK, E.C. 2.7.3.2) and myokinase (MK, E.C. 2.7.4.3). These three enzymes will henceforth be referred to as contractility enzymes. The composition of the test media and the methodological errors estimated from duplicate determinations made using the same homogenate are listed in Table II.

Table II Summary of the reagents used for enzyme activity determinations

3)

Reagent

Enzyme

Mg²⁺ stimulated ATPase

8 %

0.05 M Tris (pH 8.1) 0.2 mM ATP 0.5 mM
 p-enol pyruvate 0.015 mM NaOH 0.02 % BSA
 50 mM KCl 3 mM MgCl₂
 auxiliary enzymes HLDH (0.54 U/ml) pyruvate
 kinase (0.20 U/ml)

Myokinase

4 %

0.1 M Tris (pH 8.0) 0.2 mM ADP 2.8 mM
 glucose 0.1 mM NADP 0.02 % BSA 5 mM MgCl₂
 1.0 mM glutathione
 auxiliary enzymes hexokinase (0.70 U/ml)
 glucose 6-phosphate dehydrogenase (0.14 U/ml)

1) Creatine phosphokinase

4 %

0.1 M tri-ethanolamine buffer (pH 7.0) 35 mM
 creatine phosphate 1.0 mM ADP 20 mM glucose
 0.8 mM NADP 10 mM AMP 10 mM Mg acetate
 9.0 mM glutathione
 auxiliary enzymes hexokinase (≈ 1.2 U/ml)
 glucose 6-phosphate dehydrogenase (≈ 1.2 U/ml)

1) Adapted from Lowry Biochemicals were obtained from Sigma Chem Co St Louis USA and enzymes from
 Boehringer Mannheim GmbH W Germany except for HLDH that came from Worthington
 Biochem Corp NJ USA

2) CPK activated MONOTEST (cat No 15873) Boehringer Mannheim GmbH W Germany Before use the reagent
 was diluted 1:10 in 0.1 M Tris buffer (pH 7.5)

3) Coefficient of variation calculated from duplicate determinations on the same muscle homogenate

RESULTS AND COMMENTS

Force-velocity relationships in the knee extensor muscles (I II III)

The isokinetic muscle strength measurements made possible a comparison of maximal muscle force output both with respect to the position in the arc of motion and to different velocities of movement.

With few exceptions individual peak torque values occurred at knee angles between 50 and 70 degrees (cf Fig 2). This knee angle tended to be smaller with increasing angular velocity due at least in part to the design of the apparatus (see Methodological aspects). The position for peak torque output was in close agreement with values previously reported for knee extension (Williams and Stutman 1959, Maffroid et al 1969) and reflects optimal relationships between muscle length and leverage at the knee joint.

At each of the selected knee angles the torque produced was higher for isometric than for dynamic contractions. With increasing angular velocities the torque produced decreased. This was true throughout the range of motion although less pronounced at the small knee angles.

For comparative analyses the peak torque values at each velocity were selected resulting in torque velocity curves with the general shape of those in Fig 3. The peak isometric torque output ranged from 5.4-6 Nm/kg bw in a material comprising 5 physical education students. The group mean of 3.45 Nm/kg bw was somewhat higher ($p < .05$) than the value obtained for an age matched group of sedentary men (mean 3.1 Nm/kg bw, $n = 10$). Among the elite athletes the total range in peak isometric torque amounted to

7.5-10 Nm/kg bw. The values obtained by downhill skiers and sprinters/jumpers (3.9 and 3.8 Nm/kg bw) were significantly ($p < .05$) higher than the averages of 3.1 achieved by the orienteers (cross country runners). Competition walkers did not differ significantly from any of the other categories with respect to peak isometric torque (mean 3.4 Nm/kg bw). The present values are in accordance with values of about 3.0 Nm/kg bw reported for college men by Williams and Stutman (1959).

At the highest motion velocity studied i.e. 180 degrees/s the peak torque output ranged from 1.13 to 3.20 Nm/kg bw (n = 74). The mean value obtained in the group of sprinters and jumpers (2.73 Nm/kg bw) was significantly ($p < 0.01$) higher than in any other group of subjects whereas the mean values for endurance athletes and physical education students did not differ significantly from the 1.9 Nm/kg bw value for sedentary men.

An average of about 55% of the maximal isometric torque remained at 180 degrees/s. Consequently the highest angular velocity offered by the apparatus was far from the maximal motion velocity which is defined as the maximal speed that can be achieved with 0 load (see Hill 1938). The estimated maximal knee extension velocity ranged 600-825 degrees/s (n = 16). Thus the highest applied isokinetic velocity corresponded to less than 30% of maximal motion velocity (Fig. 3). Extrapolation of the torque velocity curve to the approximated maximal velocity values resulted in curves (Fig. 3) similar to those previously reported by e.g. Wilkie (1950) and Asmus et al. (1985).

Force-velocity relationships and muscle fibre composition (I, II, III)

As indicated by the large ranges in the torque produced at the different velocities there were inter-individual differences in torque-velocity curves. The values shown in Fig. 3 suggest that muscle fibre composition might be a factor determining the individual shape of the torque-velocity curve. Although the groups of subjects investigated were small, the figure illustrates some of the worthy tendencies. Thus at 0 velocity i.e. isometric contraction no difference could be obtained between individuals with high and low percentages of FT fibres. This lack of correlation between fibre composition and maximal voluntary isometric strength also persisted if the total number of subjects as well as when two leg isometric strength was considered (VI). This finding indicates that both FT and ST motor units are involved in isometric force development as suggested by e.g. Gydikov and Kjaerov (1973) and/or that the isometric force produced is equal for both fibre types (cf. Close 1972). Thus the quantity of muscle (in terms of mass) and not the quality of muscle in terms of muscle fibre related properties could be decisive to maximal shortlasting isometric strength performance (cf. Ikai and Fukunaga 1986).

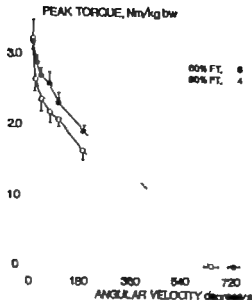


Figure 3 Peak torque values expressed as percentage of body weight versus angular velocity in degrees per second for subjects differing in fibre composition. The torque-velocity curves were plotted at the approximate 1/3 of maximal velocity for the ten subjects.

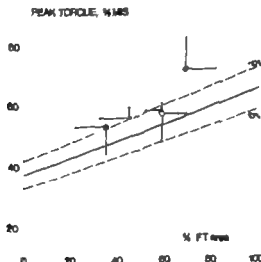


Figure 4 Peak torque expressed as percentage of maximal isometric strength versus the relative area of fast twitch fibre. The regression lines ($r = 0.29$, 38 , 0.46 , $p < 0.05$) were drawn from individual values of 2 habitually trained male (avg 32.6% FT are) and 8 plotted at the tempo of 1.5 included in the competition with 1.5 (4.7) down all kilg (1.8) and 1.5 and jump (1.8) and 1.5 and 1.5 group of detraining (1.8).

Considering the other extreme point of the concentric force velocity curve i.e. maximal velocity a difference due to muscle fibre composition was indicated (Fig 3). Higher velocities were attained by individuals with a high percentage of FT fibres. The correlation found between the percent of FT and maximal velocity was subsequently supported in a similar analysis using the isopot equipment (Selapöt Saloom AB Mölndal Sweden) (unpubl results from this department). These results are in accordance with findings in animals (see Burke and Edgerton 1975) and earlier indirect evidence from human skeletal muscle (Buchthal and Schmalbruch 1970).

The curves in Fig 3 also point to a difference in peak torque output during dynamic contractions depending on muscle fibre composition. However this difference was less consistent. Peak torque output could only be related to fibre composition at the highest velocity applied (180 degrees/s). Thus in a fairly homogenous material comprising 10 habitually active subjects a positive correlation ($r = 0.73$ $p < 0.05$) was demonstrated between peak torque at 180 degrees/s and the percent of FT fibres (Fig 5). Tendencies towards similar relationships were also present in the more heterogeneous groups participating in studies I and II.

However when peak torque output at the highest velocity was expressed in relation to the maximal isometric strength (MIJ) of each subject a significant positive correlation was obtained between this value and the proportion of FT muscle fibres (Fig 4). This relationship was also supported by the experiments on the different groups of athletes (Fig 4). Although the linear correlation coefficients were relatively low the aggregate results underline the importance of a high proportion of FT muscle fibres to force output at fast motion speed. Thus the high relative area of FT fibres in the elite athlete of sprinting and jumping would be advantageous for their specific performance with respect to force output.

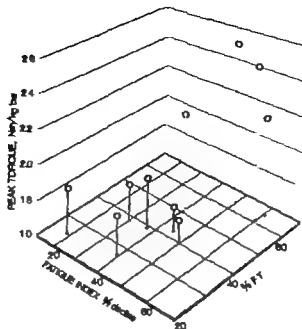


Figure 5 Three dimensional diagram showing the relationships between the percentage of fast twitch fibres (% FT) the percentage of peak torque for 50 up to 100 maximal tetanic tension at 150 degree / (fast twitch fibres) and peak torque in Nm/kg of body weight (Nm/kg bw) produced in the gluteal muscle at 150 degree / for 10 habitually active men

fatigability and muscle fibre composition (III)

Animal experiments have shown that repetitive stimulation of muscles containing mainly FT fibres causes a rapid decline in force produced. In the ST counterparts on the other hand tension output is maintained over long periods of time. This has been shown to apply to both single twitches and brief tetani (for refs see Burke 1973).

From the above it seems reasonable to assume that FT motor units are responsible for the major part of muscle force production during fast voluntary maximal contractions. Repetitions of this kind of contraction could consequently provide some indication as to the interrelationship between fatigability and muscle fibre types in human skeletal muscle.

Thus experiments were performed on 10 habitually active men. Their peak torque values displayed a gradual decline from about the 5th to the 45th contraction; values thereafter then reached a fairly stable plateau even up to 100 contractions. However the magnitude of the decrease in peak torque varied between individuals. The decline after 50 repetitions called the fatigue index demonstrated a positive correlation ($r = 0.86$ $p < 0.01$) with the percentage of FT fibres (Fig. 5). Thus a high proportion of FT fibres in the muscle appears to limit the ability to maintain maximal force at a high speed of motion. This could be a factor to consider when evaluating the range in fibre compositions found among the elite athletes in sprinting and jumping events (II).

Contractility enzymes and muscle fibre types (V-VI)

Our approach in the study of the contractile mechanisms in human muscle was to examine the Mg^{2+} stimulated ATPase activity of the muscle. A correlation between high activity for Mg^{2+} stimulated ATPase and a high percentage of FT fibres in the investigated muscle biopsy homogenates of 14 subjects was not found until after a 8 week period of strength training. The explanation for this finding is not known at present. In experiments on pooled single muscle fibres a higher activity of Mg^{2+} stimulated ATPase was found in FT fibres (Fig. 6). The FT/ST ratio was approximately 3:1. In

human skeletal muscle there is a higher activity for actomyosin ATPase in FT fibres (e.g. Bernard et al. 1971, Guth and Semah 1989) and a similar relationship exists in human skeletal muscle for the ATPase activity of purified myosin (Taylor et al. 1974).

The activities of CPK and MK were determined to assess the capacity of the muscle to replenish ATP rapidly. No correlation was found between CPK activity and fibre composition in mixed muscle homogenates. This was in conformity with previous findings for human skeletal muscle (Gollnick et al. 1974) but contrasted with the reports of Sherwin et al. (1987 and 1988) on guinea pig and human skeletal muscle indicating a significantly higher CPK activity in FT than in ST muscles. Reproducing the CPK activity determinations in pools of FT and ST muscle fibres disclosed a 30%

greater activity in FT fibres a difference which could escape detection in the analysis of muscle homogenates with only a rather limited range of muscle fibre compositions

On the other hand a muscle fibre dependency could be observed for MK activity both by examination of mixed muscle homogenates and pooled single muscle fibres showing higher values in FT muscle fibres. This finding has subsequently been confirmed by results on biopsies obtained using a larger number of subjects (Thorstensson to be published)

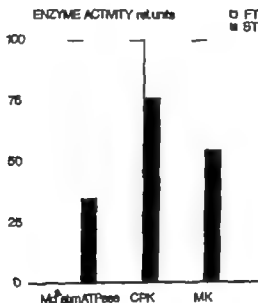


Figure 6 Enzyme activities of Mg²⁺ stimulated ATP phosphorylation (CPK) and myokinase (MK) in pooled single FT and ST muscle fibres dissected out from freeze dried biopsy material. The activity of each enzyme in FT fibres as a percentage of the total 100.

Iszymes of contractility enzymes and muscle fibre types (IV V)

The classification of human skeletal muscle fibres as FT or ST is based upon differences in pH lability between different forms of myofibrillar ATPase. Several investigators have attributed these differences to the occurrence of two different isozymes of the myofibrillar ATPase (of e.g. Trayer and Perry 1965, Sreter et al 1965, Lowey and Risby 1971). However the techniques of protein separation used in the present study did not permit the conclusive demonstration of this difference in myofibrillar ATPase isozymes in human muscle fibre types.

Two bands could be demonstrated that possessed CPK activity after isoelectric focusing of crude muscle homogenates: the pI values averaged 7.2 and 6.9 respectively. Comparison of isozyme staining density disclosed no difference in isozyme pattern between muscle samples from heart, soleus or vastus lateralis muscle. The most alkaline band always predominated, constituting about 70% of total stain density. Also when a ministration of vastus lateralis biopsy specimens of different fibre compositions was performed no indications of a fibre specificity in CPK isozyme pattern were present. These observations were confirmed by similar experiments on pooled single FT and ST muscle fibres. The results were consistent with the finding of two CPK isozymes tentatively identified as the MM and MB forms in human heart and skeletal muscle (Dawson and Fife 1967, Somer and Konttinen 1972). However other authors (e.g. Roberts et al 1974) have reported the existence of only one CPK isozyme form (the MM form) in human skeletal muscle. Methodological differences might account for these discrepancies. The muscle fibre specificity in CPK isozyme pattern found for rabbit skeletal muscle (Sherwin et al 1987) was not confirmed by the present results from human muscle.

In the case of MK two isozyme bands could be demonstrated after isoelectric focusing. Both were in the alkaline region of the gel: pI values averaged 9.6 (MK 1) and 8.9 (MK 2) respectively. MK 1 was the predominant isozyme irrespective of the source of muscle samples. The relative portion of MK 2 varied however and

attained higher values in the vastus lateralis than in soleus and heart muscle. These findings are in close agreement with those obtained by Russell et al (1974) for human tissues using similar techniques. They even suggested a heart and a skeletal muscle specific MK isozyme. When the relative proportion of MK 2 in vastus lateralis muscle samples was related to the actual variation in muscle fibre composition a positive correlation was observed with respect to the percentage of FT fibres (Fig. 7). The indicated fibre specificity in MK isozyme pattern was substantiated in experiments on pooled single FT and ST muscle fibres (Fig. 7). The isozyme MK 2 made up 27% of total stain density in the FT fibres and 13% in the ST fibres respectively.

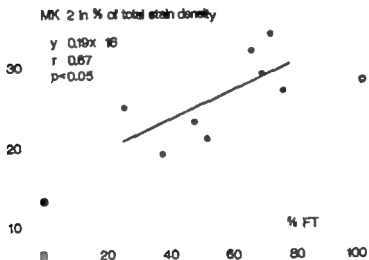


Figure 7 The total density of myokines 2 (MK 2) relative to total stain density vs the percentage of FT fibres in 13 individual biopsies including the 1 total of pooled single FT (●) and ST (●) muscle fibres determined from freeze sectioned biopsies.

Effects of strength training (II - VI)

The 8 week period of systematic progressive strength training caused significant ($p < 0.01$) improvements in isometric and dynamic strength. The relative increases in the various performance tests ranged from 13 - 67%.

The percentage distribution of FT and ST muscle fibres was not altered by 8 weeks of strength training. This is in accordance with other training studies on animals (for refs see Edgerton 1976) and human beings (Gollnick et al 1973 see also Prince et al 1976). The results support the view that fibre distribution based on myofibrillar ATPase is governed by largely genetic factors (Komi et al 1976).

However, the relative volume of fibre types in a muscle can still be altered by a change in the FT/ST area ratios. This ratio was increased by strength training (Fig. 8) indicating specific hypertrophy of FT fibres due to the training stimuli. Similar results were obtained after an attempt with strength training of primates (Edgerton 1976). Thus, the high FT/ST area ratios found in sprinters and jumpers (Fig. 8) may be the result of a lengthy period of strength training. Similar results were obtained in weight lifters (Edström and Ekblom 1972, Prince et al 1976).

The effect of strength training on the activity of the selected enzymes was insignificant except in the case of MK for which a small increase was observed. In a later study involving the same type of strength training, no significant changes in the activities of any of the co-traility enzymes were obtained (Thorstensson et al 1976). However, the observed V_{max} of the enzymes does not exclude the possibility of changes in the kinetic properties or isozyme patterns. Studies are now in progress to evaluate this possibility. The exact nature of the strength training programme also appears to influence the effect on the enzyme activities. This was indicated by the increased activity observed for CPK and MK after a strength training programme carried out as a sprint training (Thorstensson et al 1975). It is likely that higher demands are placed on rapid ATP synthesis under conditions in which fast maximal contractions are repeated 5-6 times with brief rest intervals as in sprint training.

attained higher values in the vastus lateralis than in soleus and heart muscle. These findings are in close agreement with those obtained by Russell et al (1974) for human tissues using similar techniques. They even suggested a heart and a skeletal muscle specific MK isozyme. When the relative proportion of MK 2 in vastus lateralis muscle samples was related to the actual variation in muscle fibre composition a positive correlation was observed with respect to the percentage of FT fibres (Fig 7). The indicated fibre specificity in MK isozyme pattern was substantiated in experiments on pooled single FT and ST muscle fibres (Fig 7). The isozyme MK 2 made up 27% of total stain density in the FT fibres and 13% in the ST fibres respectively.

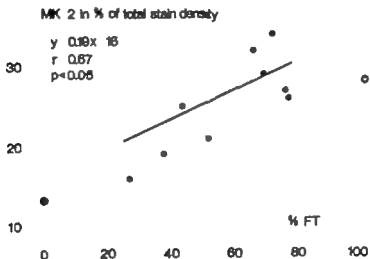


Figure 7 The relationship of myokinase (MK 2) relative to total stain density vs the percentage of FT fibres in individual biopsies. Pooled material from single FT (○) and ST (●) muscle fibres did not differ from the biopsies.

GENERAL DISCUSSION

The present study has shown that force output and fatigue in voluntary contractions can be correlated to the proportion of FT muscle fibres on the one hand and that differences exist between FT and ST muscle fibres with respect to contractility enzymes and their isozymes on the other hand.

The fact that high proportion of FT fibres is essential to a high force output during fast muscle contractions may be due to several different circumstances. The most likely cause is the short contraction time of FT fibres which is related to higher intrinsic speed of shortening as well as a higher rate of rise in tension in a tetanus (Close 1984). A higher rate of tension development should yield higher force output at the optimal angle in the arc of motion in the present experiment. Furthermore a higher intrinsic speed of shortening in FT fibres should if the shape of the force velocity curves are roughly similar lead to a divergence of the curves for FT and ST fibres and higher force output for FT fibres at high contraction velocities even if there is a difference in maximal isometric force between fibre types (cf Fig 3).

It is conceivable that the rate of hydrolysis of ATP at the cross bridge between actin and myosin in the muscle is one of the main factors controlling the speed of shortening and thus even the tension produced at high contraction velocities. This ATP hydrolysis is brought about by the enzymatic activity of myosin. The higher sensitivity of this enzyme found in FT fibres would therefore provide a basis for the differences obtained in contractile properties. Our increased knowledge about the morphology and biochemistry of muscle excitation-contraction coupling is difficult to incorporate into our models of control such as the release and uptake of transmitter at the neuromuscular junction as well as of the relationships between the sarcoplasmic reticulum and the contractile apparatus. Differences between FT and ST motor units in this respect have already been demonstrated (for ref. see Berk & Edgert 1975).

The potential of a faster hydrolysis of ATP in FT muscle fibres was matched by higher activity for the enzymes CPK and MK both serving to catalyze reactions providing rapid resynthesis of ATP. The fact that both these pathways are open has been demonstrated during single contractions of frog muscle (Cain and Davies 1962). The extent to which they are decisive to the speed and force of contraction is unknown at present. The presence of isozymes of both CPK and MK in the human muscle cell is interesting in this context. Thus the MM form of CPK has been shown to bind specifically to the M band of the contractile apparatus (Turner et al 1973). Similar relationships for the MK isozymes have not been investigated although the last traces of MK have been very difficult to remove in preparations of myosin (Node 1973).

The differences in MK activity between fibre types is also likely to be of significance in the regulation of the overall metabolism of the two kinds of muscle cells. The ratio between the adenylate nucleotides involved in the MK reaction regulates the activity of several key enzymes in the energy yielding processes (cf Atkinson 1988). The effects of AMP on the glycolytic regulatory enzyme phosphofructokinase has been emphasized in this respect (Newsholme 1971). The higher activity of MK in human FT muscle fibres also coincides with a higher anaerobic capacity of this fibre type (e.g. Essén et al 1975, Sjödin 1976). Extended studies of the kinetics and localization of MK and its isozymes are required in order to clarify their role in connection with muscle contraction.

The anaerobic metabolic profile of FT muscle fibres may explain for the greater fatigability of this fibre type. Repeated activation of FT motor units are likely to create local conditions in the FT muscle fibres such as a decrease in pH or available substrates detrimental to continued usage. Differences in oxidative potential within the FT motor unit pool might affect the resistance to fatigue. This appears to be the case in animal muscle in which two FT motor unit types can be identified. The one with a high oxidative capacity is comparatively resistant to fatigue whereas the other displays a low oxidative potential and is easily fatigued (see Burke and Edgerton 1975). The extent to which subgroups of human FT muscle fibres characterized by histochemical means

(cf Brooks and Keifer 1970 Edgerton et al 1975 Essén et al 1975) are affecting the susceptibility to fatigue and other contractile properties is at present unclear. The possibility of a difference in fatigueability confined to other parts of the neuromuscular system such as the properties of the axons or the neuromuscular junction cannot be excluded completely (see Burke 1973). Support for the latter possibility has been presented by Stephens and Taylor (1972). They concluded that neuromuscular junction fatigue was most important during the initial phase (about 1 min) of maintained maximal contractions whereas the fatigue confined to the contractile elements increased with longer contraction times.

The metabolic, morphological and contractile properties of motor units appear to be intimately related with the pattern of motor unit recruitment during different movements. It is generally accepted that motor units under most conditions are activated according to size i.e. small motoneurons prior to large ones. This size principle was first postulated by Henneman et al (1965) and corroborated and has since been supported in studies on various animals including man (e.g. Milner-Brown et al 1973). These investigations were performed mainly using isometric contractions with relatively low tensions or dynamic contractions with a slow increase in tension at a constant rate. However, an increasing amount of evidence demonstrates that the order of motor unit recruitment is not a strictly fixed (see review by Burke and Edgerton 1975). The central nervous system appears to be able to adjust the sequence of motor unit recruitment to selectively involve large units (presumably FT) when very forceful and/or rapid movements are required (cf Grimby and Hoyer 1968 Wasmuth and Engel 1972). The fast maximal isometric contractions used in the present study appear to be good examples of such movements. Furthermore, if it is accepted that the greatest hypertrophy occurs in muscle fibres with the greatest at rest fibre size, then the present results comprising an inverse FT/ST area ratio with strength training as well as a high FT/ST area ratio value in athletes in explosive events would lend support to the view that relative involvement of different motor unit types can be changed during movement training for both great force and speed.

SUMMARY

Force velocity relationships were identified by studying isokinetic contractions of the knee extensor muscles of healthy male individuals of varying proficiency and varying degrees of strength training

No correlation was found between force output and muscle fibre composition except at the highest angular velocity applied. A positive correlation between peak force and the percentage of fast twitch muscle fibres was noted at this velocity

The susceptibility to fatigue during repeated fast maximal voluntary contractions was shown to be related to muscle fibre composition; high fatigability coincided with a high percentage of fast twitch fibres

Examination of elite athletes in explosive strength events disclosed a wide variation in the percent of fast twitch fibres but a significantly higher fast to slow twitch fibre area ratio than in sedentary subjects and endurance athletes

The fast to slow twitch fibre area ratio increased after a period of systematic strength training indicating a specific effect for the heavy training loads on the fast twitch muscle fibres. However the training effect on selected enzyme activities was slight irrespective of any large gains in strength performance

Alysis of mixed muscle homogenates indicated higher activity for Mg^{2+} stimulated ATPase and myokinase in fast than in slow twitch muscle fibres. This indicated fibre specificity was confirmed for both enzymes in alysis of pooled single freeze dried muscle fibres

The distribution of isozymes of myokinase separated by isoelectric focusing was shown to be related to fibre type distribution in muscle homogenates. Similar results were obtained when applying this procedure to pooled single freeze dried muscle fibres. A corresponding fibre dependency could not be found for the distribution of isozymes of creatine phosphokinase

ACKNOWLEDGEMENTS

I wish to express my gratitude to

Professor Per-Olof Astrand Head of the Department of Physiology Gymnastik och idrotts högskolan Stockholm for working facilities and generous support;

Professor Erik Hohwö Christensen former Head of the Department for originally introducing me to the field of work physiology and for most valuable advice;

Associate Professor Jan Karlsson who initiated the present investigation for stimulating guidance and never failing enthusiasm;

Associate Professor Sten Grillner for constructive criticism in the preparation of the manuscript;

My colleagues for rewarding collaboration and stimulating discussions;

Mr Kersti Elvi Mrs Inger Hallbäck and Mrs Berit Sjöberg for skillful technical assistance;

Mr Harry Höglin and Mr Eddy Karlsson for invaluable help in keeping the instrument functioning;

Mrs Marie-Louise Ekstrand for doing all the typing;

All the subjects who volunteered for the different studies;

The tireless staff of the Department of Physiology GIH whose tireless efforts and enthusiasm made the working environment pleasant and stimulating.

The investigations were supported by grants from the Swedish Medical Research Council and the Research Council of the Swedish Sports Federation.

SUMMARY

Force velocity relationships were identified by studying isokinetic contractions of the knee extensor muscles of healthy male individuals of varying proficiency and varying degrees of strength training

No correlation was found between force output and muscle fibre composition except at the highest angular velocity applied. A positive correlation between peak force and the percentage of fast twitch muscle fibres was noted at this velocity.

The susceptibility to fatigue during repeated fast maximal voluntary contractions was shown to be related to muscle fibre composition; high fatigueability coincided with a high percentage of fast twitch fibres.

Examination of elite athletes in explosive strength events disclosed a wide variation in the percent of fast twitch fibres but a significantly higher fast to slow twitch fibre area ratio than in sedentary subjects and endurance athletes.

The fast to slow twitch fibre area ratio increased after a period of systematic strength training indicating a specific effect for the heavy training loads on the fast twitch muscle fibres.

Over the training effect on selected enzyme activities was slight irrespective of any large gains in strength performance.

✓ Analysis of mixed muscle homogenates indicated higher activity for Mg^{2+} stimulated ATPase and myokinase in fast than in slow twitch muscle fibres. This indicated fibre specificity was confirmed for both enzymes in analysis of pooled single freeze dried muscle fibres.

The distribution of isozymes of myokinase separated by isoelectric focusing was shown to be related to fibre type distribution in muscle homogenates. Similar results were obtained when applying this procedure to pooled single freeze dried muscle fibres. A corresponding fibre dependency could not be found for the distribution of isozymes of creatine phosphokinase.

- BURKE R E and V R EDGERTON Motor unit properties and selective involvement in movement In *Exercise and Sport Sciences Reviews* Acad Press New York 1975 Vol 3 pp 31 81
- BURKE R E and P TSAIRIS Anatomy and innervation ratios in motor units of cat gastrocnemius *J Physiol (Lond)* 1973 234 749 765
- BURKE R E D N LEVINE P TSAIRIS and F E ZAJAC III Physiological types and histochemical profiles in motor units of cat gastrocnemius *J Physiol (Lond)* 1973 234 723 748
- CAIN D F and M E DAVIES Breakdown of adenosine triphosphate during a single contraction of working muscle *Biochem Biophys Res Commun* 1982 8 381 386
- CLOSE R Dynamic properties of fast and slow skeletal muscles of the rat during development *J Physiol (Lond)* 1984 173 74 95
- CLOSE R I Dynamic properties of mammalian skeletal muscles *Physiol Rev* 1972 52 129 196
- DAWSON D M and I H FINE Creatine kinase in human tissue *Arch Neurol* 1987 16 175 180
- EDGERTON V R Neuromuscular adaptation to power and endurance work *Can J Appl Sport Sciences* 1976 1 48 56
- EDGERTON V R J L SMITH and D R SIMPSON Muscle fibre type populations of human leg muscles *Histochem J* 1976 7 259 288
- EDSTRÖM L and B EKBLOM Differences in sizes of red and white muscle fibres in vastus latialis of musculus quadriceps femoris of normal individuals and athletes Relation to physical performance *Scand J clin Lab Invest* 1972 30 175 181
- EDSTRÖM L and E KUGELBERG Histochemical composition distribution of fibres and fatigueability of single motor units *J Neurol Neurosurg Psychiat* 1968 31 424 433

- ENGEL W K The essentiality of histo and cytochemical studies of skeletal muscle in the investigation of neuromuscular disease Neurology (Minneapolis) 1962 12 778 784
- ESSEN B E JANSSEN J HENRIKSSON A W TAYLOR and B SALTIN Metabolic characteristics of fibre types in human skeletal muscle Acta physiol scand 1975 85 153 165
- FENN W M and B S MARSH Muscular force at different speeds of shortening J Physiol (Lond) 1935 85 277 287
- GOLLNICK P D R B ARMSTRONG C W SAUBERT IV ■ PIEHL and B SALTIN Enzyme activity and fibre composition in skeletal muscle of untrained and trained men J appl Physiol 1972 33 312 319
- GOLLNICK P D R B ARMSTRONG ■ SALTIN C W SAUBERT IV W L SEMBROWICH and R E SHEPHERD Effect of training on enzyme activity and fiber composition of human skeletal muscle J appl Physiol 1973 34 107 111
- GOLLNICK P D B SJÖDIN J KARLSSON E JANSSEN and B SALTIN Human soleus muscle: a comparison of fiber composition and enzyme activities with other leg muscles Pflügers Arch 1974 348 247 257
- JIMBY L and J HANNERZ Recruitment order of motor units of voluntary contraction changes induced by proprioceptive afferent activity J Neurol Neurosurg Psychiat 1968 31 565 73
- GUTH L and F J SAMAHA Qualitative differences between actomyosin ATPase of slow and fast mammalian muscle Eptl Neurol 1969 25 138 152
- GYDIKOV A ■ and D KOSAROV Some features of different motor units in human biceps brachii Pflügers Arch 1974 347 75 88
- HENNEMAN E G SOMJEN and D O CARPENTER Functional significance of cell size in spinal motoneurons J Neurophysiol 1965 28 580 580

HILL A V The heat of shortening and the dynamic constants of muscle Proc Roy Soc ■ (Lond) 1938 126 138 185

HILL A V The dynamic constants of human muscle Proc Roy Soc ■ (Lond) 1940 128 263 274

HISLOP H J and J J PERRINE The isokinetic concept of exercise Physical Therapy 1967 47 114 117

HOLLOSZY J D Biochemical adaptations to exercise Aerobic metabolism In Exercise and Sport Sciences Reviews (ed J H Wilmore) Acad Press New York 1973 Vol 1 pp 48 71

IKAI ■ and T FUKUNAGA Calculation of muscle strength per unit cross sectional area of human muscle by means of ultrasonic measurement Int J angew Physiol einschli Arbeitsphysiol 1968 28 28 32

JOHNSON ■ A J POLGAR D WEIGHTMAN and ■ APPLETON Data on the distribution of fibre types in thirty six human muscles An autopsy study J neurol Sci 1973 18 111 129

KARLSSON J Lactat and phosphagen concentrations in working muscle of man Acta physiol scand 1971 Suppl 358

KARLSSON J and ■ OLLANDER Muscle metabolites with exhaustive static exercise of different duration Acta physiol scand 1972 86 308 314

KOMI P V Measurement of the force velocity relationship in human muscle under concentric and eccentric contractions In Medicine and Sport Vol 8 Biomechanics III 1973 pp 224 229

KOMI P V J T VIITASALO ■ HANU A THORSTENSSON and J KARLSSON Physiological and structural performance capacity effect of heredity I Int Ser Biomech Vol 1A Biomechanics V A Univ Park Press Baltimore 1976 pp 116 123

- LEWIS D M C J C KEAN and J D McGARRICK Dynamic properties of slow and fast muscle and their trophic regulation Ann N Y Acad Sci 1974 228 105 120
- LOWEY S and D RISBY Light chains from fast and slow muscle myosins Nature 1971 234 81 85
- LOWRY O H and J V PASSONNEAU A flexible system of enzymatic analysis Academic Press New York 1972
- LOWRY O H N J ROSEBROUGH A L FARR and R J RANDALL Protein measurement with the folin phenol reagent J Biol Chem 1951 193 265 275
- MARKERT C L (ed) Isozymes I Molecular structure Acad Press New York 1975
- MILNER BROWN H S R B STEIN and B YEMM The orderly recruitment of human motor units during voluntary isometric contractions J Physiol (Lond) 1973 230 359 370
- MOFFROID M R WHIPPLE J HOFKOSH E LOWMAN and H THISTLE A study of isokinetic exercise Physical Therapy 1969 49 735 746
- LWSHOLME E A The regulation of phosphofructokinase in muscle Cardiology 1971 6 22 34
- NODA L Adenylate kinase In The Enzymes (ed P D Boyer) 3rd ed Academic Press New York 1973 Vol XIII pp 278 305
- NOVIKOFF A B W Y SHIN and J DRUCKER Mitochondrial localization of oxidative enzymes Staining results with two tetrazolium salts J Biophys Biochem Cytol 1961 9 47 61
- PADYKULA H A and E HERMAN The specificity of the histochemical method for adenosine triphosphatase J Histochem Cytochem 1955 3 170 195

- PERRINE J J Isokinetic exercise and the mechanical energy potentials of muscle J Health Phys Educ Res 1968 4 40 44
- PERRY S V Calcium ions and the function of the contractile properties of muscle Biochem Soc Symp 1974 39 115 132
- PETTE D and T BUCHER Proportionskonstante Gruppen in Beziehung zur Differenzierung der Enzymaktivitätsmuster von Skelett Muskeln des Kaninchens Z physiol Chem 1983 331 180 195
- PRINCE F P R S HIKIDA and F C HAGERMAN Human muscle fibre types in power lifters distance runners and untrained subjects Pflügers Arch Eur J Physiol 1978 383 19 26
- RADOLA B J Isoelectric focusing in layers of granulated gels I Thin layer isoelectric focusing of proteins Biochim Biophys Acta 1973 295 412 428
- RANVIER L Propriétés et structures différentes des muscles rouge et des muscles blanc chez les lapins et chez les roies Compt Rend 1873 77 1030 1043
- RIGHETTI P and J W DRYSDALE Isoelectric focusing in gels J Chromatography 1974 88 271 321
- ROBERTS R P D HENRY B A G J WITTEVEEN and B E SOBEL Quantification of serum creatine phosphokinase isoenzyme activity Am J Cardiology 1974 33 650 654
- RUSSELL Jr P J J M HORENSTEIN L GOINS D JONES and M LAYER Adenylate kinase in human tissue Organ specificity of adenylate kinase isoenzymes J Biol Chem 1974 249 1874 1879
- LTIN M K NAZAR O I COSTILL M STEIN E JANS ON B ESSEN and P D COLLNICK The effect of the training response peripheral and central adaptation to legged exercise Acta physiol scand 1976 98 88 305

ACTA PHYSIOLOGICA SCANDINAVICA
Supplementum 444

SODIUM AND ANGIOTENSIN II
IN THE CENTRAL CONTROL OF FLUID BALANCE
A study in conscious goats

BY
LEA ERIKSSON

HELSINKI 1976

ISBN 951-99092-3-8

Helsingin yliopiston monistuspalvelu, offset 1976

This thesis is based on the following publications:

- I Andersson B L Eriksson O Fernander C -G Kolmodin and R Oltner Centrally mediated effects of sodium and angiotensin II on arterial blood pressure and fluid balance Acta physiol scand 1972 85 398-407
- II Eriksson L Effect of lowered CSF sodium concentration on the central control of fluid balance Acta physiol scand 1974 91 61-68
- III Eriksson L Negligible role of CSF cations other than Na^+ in the central regulation of ADH release Acta physiol scand 1976 97 398-400
- IV Eriksson L and P Fyhrquist Plasma renin activity following central infusion of angiotensin II and altered CSF sodium concentration in the conscious goat Acta physiol scand 1976 98 209-216
- V Eriksson L and P Fyhrquist A comparison between the central effects of angiotensin II and its fragments des_1 -angiotensin II and des_{1-2} -angiotensin II Acta physiol scand 1976 96 134-136

These articles will be referred to by their Roman numerals

Abbreviations used

ADH = antidiuretic hormone	ECF = extracellular fluid
CH_2O = renal free water clearance	ICV = intracerebroventricular
CNS = central nervous system	PRA = plasma renin activity
CSF = cerebrospinal fluid	SFO = subfornical organ

CONTENTS

INTRODUCTION	5
THE PURPOSE OF THE STUDY	7
METHODS	8
RESULTS AND COMMENTS	10
1 Centrally mediated effects of angiotensin II and sodium on fluid balance and blood pressure	10
2 Effects of lowered CSF Na^+ concentration on the central control of fluid balance	13
3 Effect on PRA of ICV infusions of angiotensin II and altered CSF Na^+ concentration	16
4 A comparison between the centrally mediated effects of angiotensin II and its fragments des_1 -angiotensin II and des_{1-2} -angiotensin II	18
GENERAL DISCUSSION	20
Osmoreceptors versus sodium sensitive receptors	21
The entry of angiotensin into the brain and the angiotensin sensitive areas	22
Cerebral receptors controlling renal Na^+ excretion	25
SUMMARY AND CONCLUSIONS	28
ACKNOWLEDGEMENTS	29
REFERENCES	30

INTRODUCTION

Verney's classical experiments (1947) in unanesthetized dogs form the basis for the theory of an osmometric regulation of the antidiuretic hormone (ADH) release. He found that infusions of hypertonic solutions of sodium salts or sucrose into the carotid artery caused antidiuresis in hydrated dogs whereas hypertonic urea was ineffective. Verney postulated that there are osmoreceptors in the brain, probably in the anterior hypothalamus, which regulate the release of ADH (Verney 1947, Jewell and Verney 1957). He inferred that the adequate stimulus for the osmoreceptors is not a rise in blood tonicity as such but rather changes in the composition of the extracellular fluid (ECF) which, by dehydration, reduce the volume of the receptors. This would explain why an elevation of ECF osmolality induced by a highly diffusible substance like urea did not stimulate the ADH release. ADH release and drinking serve a common purpose, i.e. they maintain the water balance. When Andersson (1953) found that injections of small amounts of hypertonic NaCl solution into the antero-medial hypothalamus elicited drinking in the goat, he postulated that cerebral osmoreceptors also participate in the regulation of water intake.

The possible influence of brain barrier systems was not taken into consideration in these original investigations. Later studies in the conscious goat suggest that changes in cerebrospinal fluid (CSF) sodium concentration are much more effective in influencing the central control of fluid balance than are changes in CSF osmolality. Therefore, a possible alternative to osmoreceptors in Verney's sense would be sodium sensitive receptors near the third cerebral ventricle (cf. Andersson 1971). Here, the concept of specific cerebral sodium sensitivity will be discussed in relation to the results of the present experimental studies.

The physiological importance of the renin-angiotensin system had originally been related only to the peripheral effects of angiotensin II (vasoconstriction, stimulation of aldosterone secretion). However, in 1961 Rickertson and Buckley demonstrated that angiotensin II can produce a centrally mediated rise in

blood pressure Previous to this Linazasoro and co-workers (1954) had observed that injections of kidney extracts elicit drinking in rats The association between the renin-angiotensin system and the thirst mechanism has been further studied by Fitzsimons and co-workers (cf Fitzsimons 1972) The effects of systemically administered angiotensin II and hypertonic NaCl solution are additive in the rat (Fitzsimons and Simons 1969) The dipsogenic effect of angiotensin is centrally mediated Administration of intravenously inactive amounts of this peptide into the anterior hypothalamus in rats (Epstein Fitzsimons and Simons 1969) or into the third ventricle in goats (Andersson and Westbye 1970) elicits drinking Furthermore angiotensin II stimulates the release of ADH from the neurohypophysis (Severs et al 1970 Bonjour and Malvin 1970) Even this effect is due to an action of the octapeptide at the hypothalamic level of the brain (Andersson and Westbye 1970)

Studies on the centrally mediated effects of angiotensin have given interesting results in recent years (for review see Severs and Daniels-Severs 1973) Particularly the discovery of an intrinsic renin-angiotensin system in the brain (Ganten et al 1971 Fischer-Perraro et al 1971) supports the contention that angiotensin II may be physiologically important within the central nervous system (CNS)

Electrical stimulation of different brain loci and intracerebroventricular (ICV) perfusion with low $[Na^+]$ CSF in turn have furnished evidence that the CNS participates in the control of renin release from the kidney (for review see Davis and Freeman 1976) Davis and Freeman (1976) divide the mechanisms controlling renin release into following groups: the intrarenal receptors the sympathetic nerves and humoral agents Humoral regulators include sodium and potassium ions angiotensin II and ADH Angiotensin and ADH inhibit the secretion of renin probably by a direct action on the juxtaglomerular cells (see Davis and Freeman 1976) In addition to this short-loop negative feedback angiotensin II has been postulated to suppress the renal renin release by raising the blood pressure in part via central nervous action (Oparil and Haber 1974)

THE PURPOSE OF THE STUDY

The principal aims of the experimental work in this thesis were to study in conscious goats:

- the role of CSF sodium concentration in the control of fluid balance (papers II III and IV)
- the influence of ICV infusions of angiotensin II and of its fragments des_1 -angiotensin II and des_{1-2} -angiotensin II on fluid balance (papers I IV and V)
- the importance of CSF sodium concentration for centrally mediated responses to angiotensin II (paper I)

blood pressure Previous to this Linasasoro and co-workers (1954) had observed that injections of kidney extracts elicit drinking in rats The association between the renin-angiotensin system and the thirst mechanism has been further studied by Fitzsimons and co-workers (cf Fitzsimons 1972) The effects of systemically administered angiotensin II and hypertonic NaCl solution are additive in the rat (Fitzsimons and Simons 1969) The dipsogenic effect of angiotensin is centrally mediated Administration of intravenously inactive amounts of this peptide into the anterior hypothalamus in rats (Epstein Fitzsimons and Simons 1969) or into the third ventricle in goats (Anderson and Westbye 1970) elicits drinking Furthermore angiotensin II stimulates the release of ADH from the neurohypophysis (Seyers et al 1970 Bonjour and Malvin 1970) Even this effect is due to an action of the octapeptide at the hypothalamic level of the brain (Anderson and Westbye 1970)

Studies on the centrally mediated effects of angiotensin have given interesting results in recent years (for review see Seyers and Daniels-Seyers 1973) Particularly the discovery of an intrinsic renin-angiotensin system in the brain (Ganten et al 1971 Fischer-Ferraro et al 1971) supports the contention that angiotensin II may be physiologically important within the central nervous system (CNS)

Electrical stimulation of different brain loci and intra cerebroventricular (ICV) perfusion with low $[Na^+]$ CSF in turn have furnished evidence that the CNS participates in the control of renin release from the kidney (for review see Davis and Freeman 1976) Davis and Freeman (1976) divide the mechanisms controlling renin release into following groups: the intrarenal receptors the sympathetic nerves and humoral agents Humoral regulators include sodium and potassium ions angiotensin II and ADH Angiotensin and ADH inhibit the secretion of renin probably by a direct action on the juxtaglomerular cells (see Davis and Freeman 1976) In addition to this short loop negative feedback angiotensin II has been postulated to suppress the renal renin release by raising the blood pressure in part via central nervous action (Opairil and Haber 1974)

pressure transducer. The mean and systolic/diastolic blood pressure and the heart rate were recorded on an ink-writing polygraph. Entry of blood into the catheter and blood clotting during testing was prevented by infusing isotonic NaCl solution slowly (0.1 ml/min) into the catheter system.

Radioimmunoassay of PRA and plasma angiotensin II concentration
Blood samples were taken via a Braunule cannula from the jugular vein into prechilled centrifuge tubes with 0.3 M EDTA solution as an anticoagulant. Immediately cooled and centrifuged at $+4^{\circ}\text{C}$. The plasma was stored at -20°C until radioimmunoassayed.

Radioimmunoassay of PRA (Fyhrquist et al. 1976) was modified for the assay of goat PRA. The optimal pH for angiotensin II generation in goat plasma was found to be 6.2. Therefore samples were incubated at pH 6.2 in the presence of OH-quinoline 3.5 mM and $\text{Na}_2\text{-EDTA}$ 15 mM. There was no change of pH during the 2 hour incubation at $+37^{\circ}\text{C}$.

Radioimmunoassay of plasma angiotensin II concentration was made according to Fyhrquist et al. (1972).

Special reagents

The angiotensin analogues used were:

- angiotensin II (val^5 -angiotensin II-asp- γ -amide Hypertensin^R Ciba)
- angiotensin III (des_1 - ileu^5 -angiotensin II Schwarz-Mann)
- $\text{des}_{1,2}$ - ileu^5 -angiotensin II (Schwarz-Mann)

T

RESULTS AND COMMENTS

I Centrally mediated effects of angiotensin II and sodium on fluid balance and blood pressure (paper I)

When angiotensin II (0.8 or $0.4 \text{ ng kg}^{-1} \text{ min}^{-1}$) was infused in hypertonic NaCl (0.25 or 0.33 M) solution into the third cerebral ventricle of hydrated goats for one hour conspicuous dipsogenic antidiuretic hypertensive and natriuretic responses were obtained. If the CSF $[\text{Na}^+]$ was simultaneously lowered by infusing angiotensin dissolved in isotonic d-glucose the effects of the octapeptide were markedly reduced. Angiotensin in 0.14 M NaCl solution or merely the hypertonic NaCl gave moderate responses. In the following sections the different effects of the infusions are considered separately.

Water intake

In order to avoid over-hydration hydrated goats were not allowed to drink more than 500 ml . During the combined infusion of angiotensin and hypertonic NaCl all goats drank the total amount of water available. The latency time for drinking was short and thirst outlasted the infusion period by up to 30 min . Infusion of angiotensin in 0.14 M NaCl or of hypertonic NaCl alone induced drinking in most cases but the latency time was longer and drinking stopped within 10 min after the infusion. None of the goats drank during the infusion of angiotensin in isotonic glucose but some goats sipped water after termination of the infusion. In non-hydrated goats it is not necessary to withhold water. In such animals simultaneous infusion of angiotensin and hypertonic NaCl results in a marked potentiation of the dipsogenic effect (Andersson and Westbye 1970). Andersson and co-workers (Andersson, Leksell and Rundgren 1975) have recently shown that such potentiation also may be obtained when the infusion of angiotensin and hypertonic NaCl are not concurrent. Angiotensin dissolved in 0.3 M glucose failed to elicit drinking but it markedly accentuated the dipsogenic and antidiuretic effects of the subsequent infusion of hypertonic NaCl. This delayed effect of angiotensin would suggest the possibility that angiotensin remains at periventricular receptor sites and continues to interact with Na^+ thereby eliciting thirst and ADH release for about

half an hour. Another possibility is that a sustained angiotensin-induced receptor activation is implicated. In the rat injections of angiotensin II dissolved in solutions with various

ionic composition directly into the septal and preoptic areas of the brain have given partially divergent responses (Svensson, Sharpe and Griffin 1973). Hypertonic NaCl mixed with threshold doses of angiotensin was found to potentiate drinking. On the other hand, there was no decrease in the dipsogenic effect when angiotensin was injected in Na^+ -free solution.

In hypertonic KCl was infused with angiotensin a marked reduction of water intake was seen.

Inhibition of water diuresis

A strong and long lasting antidiuretic effect was obtained by the infusion of angiotensin II in hypertonic NaCl. The antidiuresis seen in response to the infusion of angiotensin in 0.14

NaCl was of shorter duration. No antidiuretic response or only a weak one was observed during the ICV infusion of angiotensin in isotonic glucose. However, a distinct post-infusion inhibition of the water diuresis was seen after the infusion.

A delayed response may indicate that the receptors activated by angiotensin remain in the activated state which is unmasked when glucose no longer reduces the CSF $[\text{Na}^+]$.

Evidence that the inhibition of the water diuresis elicited by these stimuli is actually due to release of ADH was first obtained indirectly. It was shown that the ICV infusion of hypertonic NaCl (Andersson, Dalsman and Olsson 1969) and angiotensin II (paper I) no longer caused an antidiuresis when the hypothalamo-neurohypophyseal connections were interrupted by radiofrequency lesions in the median eminence. Recently Lishajko and Andersson (1975) have bioassayed the ADH in urine following the infusion of angiotensin II and hypertonic NaCl into the ventricular system of the hydrated goat. Plasma samples obtained during infusions in the later studies (papers IV and V) were analyzed for ADH with a sensitive direct radioimmunoassay method (Fyhrquist, Eriksson and Wallenius 1976). Plasma ADH concentrations rapidly rose during infusions of angiotensin II and hypertonic NaCl.

Olsson and Kolmodin (1974) have further studied the angiotensin- Na^+ synergism by giving these stimuli via different

routes. Infusions of angiotensin II into the lateral cerebral ventricle in amounts which had negligible antidiuretic and no diuretic activity on their own potentiated the antidiuretic and diuretic effect of simultaneous intracarotid infusions of hypertonic NaCl in hydrated goats.

Hypertensive and natriuretic effects

During the ICV infusion of angiotensin II in hypertonic NaCl the blood pressure began to rise within 5 min reaching its maximum increment (25-45 mmHg) within 20 min and remained elevated 50 to 90 min after cessation of the infusion. Also with angiotensin in 0.14 M NaCl the rise of blood pressure was rapid (maximum increment 15-35 mmHg) but the pressure started to decline with the smaller doses before the infusion was completed. The blood pressure rose slowly during the infusion of hypertonic NaCl alone reaching the highest increment (15-30 mmHg) at the end of the infusion period. Infusion of angiotensin in isotonic glucose had no noticeable effect on the blood pressure. These experiments strongly suggest that an angiotensin- Na^+ sensitive receptor system may contribute to the central regulation of the arterial blood pressure.

Bergmann et al (1971) have postulated that Na^+ may form a complex with angiotensin and thus a biologically more active molecule. This could explain the Na^+ -angiotensin synergism observed in the goat. To reexamine this possibility angiotensin II was pre-incubated in saline before it was infused with glucose (paper I). The effect was not enhanced. Furthermore the intravenous injection of angiotensin II in glucose caused the same rise in carotid blood pressure as when it was injected in isotonic NaCl.

Although great variations were seen between animals the magnitude and the duration of the natriuretic response to the different infusions were generally correlated to the rise in blood pressure. It has previously been shown that the natriuresis induced by hypertonic NaCl applied into CSF is accompanied by an increase in the glomerular filtration rate (Andersson Dallman and Olsson 1969). The correlation between the hypertensive and natriuretic effect in the present study also indicates that changes in renal hemodynamics may have contributed to the natriuretic response.

In the present study it was found that the local Na^+ concentration determines the degree to which angiotensin II applied in the third ventricle affects the fluid balance and elevates the blood pressure. It is therefore suggested that angiotensin II may act via a Na^+ -sensitive receptor system near the third ventricle. Angiotensin II may either make the receptors more sensitive to the environmental Na^+ concentration or facilitate the entry of Na^+ to the receptor sites.

Recordings of action potentials in different brain loci have shown that angiotensin II has a direct effect on many central neurons (Nicoll and Barker 1971, Wayner, Ono and Molley 1973 and Felix and Akert 1974). Furthermore, Wayner et al (1973) have found that some of the Na^+ -sensitive neurons which all were sensitive to angiotensin II displayed a pronounced potentiation of discharge frequencies when both stimuli were applied simultaneously. They suggest that angiotensin facilitates membrane Na^+ permeability. Angiotensin II is known to affect toad bladder sodium flux (McAfee and Locke 1967) and intestinal electrolyte transport (e.g. Davies, Munday and Parsons 1970). The study of Gubash et al (1972) gives good evidence that angiotensin stimulates Na^+ transport in the tissues where it is acting. They found that angiotensin II increases microsomal $(\text{Na}^+ - \text{K}^+) - \text{ATPase}$ activity in the hypothalamus, the mucosa of colon and the adrenal cortex.

2 Effects of lowered CSF Na^+ concentration on the central control of fluid balance (papers II and III)

Water diuresis

The concentration of CSF $[\text{Na}^+]$ was artificially lowered by infusing isotonic or hypertonic non-electrolyte solutions into the cerebral ventricular system of goats in normal water balance. Either the third ventricle was infused for 40 min at 10 or 20 $\mu\text{l}/\text{min}$ or the lateral ventricle was infused for one hour at 20 $\mu\text{l}/\text{min}$. All isotonic non-electrolyte solutions caused water diuresis and so did hypertonic (0.45 or 0.6 M) solutions of carbohydrates. Hence the increase in renal free water clearance ($\text{C}_{\text{H}_2\text{O}}$) was not caused by reduced osmolality of CSF.

more likely by dilution of the CSF $[Na^+]$. These infusions obviously inhibit the release of ADH normally occurring in the non-hydrated animal. In the first place there was no increase in renal osmotic clearance. Secondly intravenous injection of 5 mU of ADH interrupted this water diuresis.

The infusions of non-electrolyte solutions into the ventricular system also reduced the relative concentrations of other ions in the CSF to the same degree as the Na^+ concentration. Therefore it could be argued that the diuretic effect of these infusions may have been due to a reduced concentration of some ion or solute other than Na^+ . Control infusions however and previous studies in the same species seem to rule out this possibility. Infusions of isotonic saline alone or saccharides in isotonic saline which maintain the CSF $[Na^+]$ but reduce the concentrations of other ions did not produce water diuresis. However after the combined infusions some increase in C_{H_2O} was often seen. Osmotically these hypertonic solutions may have drawn water into the CSF thereby reducing the Na^+ concentration and making a postinfusion reduction of the ADH release apparent. On the basis of earlier studies in the goat (Andersson et al 1967) it is unlikely that reduced CSF Cl^- concentration was of crucial importance.

In order to reduce the CSF $[Na^+]$ without reducing the normal concentration of other cations isotonic saccharides with K^+ (3 mmol/l), Ca^{2+} (1.3 mmol/l) and Mg^{2+} (1 mmol/l) were infused into the ventricular system (paper III). These infusions caused water diuresis on most occasions. However when the cations were infused together with d-glucose the renal C_{H_2O} sometimes failed to turn positive. It was found that glucose with Ca^{2+} and Mg^{2+} consistently induced water diuresis while glucose with K^+ did not always do so. This latter result with K^+ and glucose does not disprove the crucial role of Na^+ . It is possible that glucose with K^+ in some way activated the Na^+ transport in periventricular tissues and choroid plexuses. Brändstedt (1970) has studied the transport of various sugars from CSF. He found a carrier-mediated transport of glucose which seems to be connected with the active transport of Na^+ and K^+ . The net fluxes of Na^+ and K^+ showed that if one molecule of K^+ passes from the perfusate into surrounding tissues 3-10 molecules of Na^+ would

pass in the opposite direction. Recent studies in goats have given additional information concerning the periventricular sodium receptors (Olsson 1976; Leksell, Lishajko and Rundgren 1976). ICV infusions of isotonic NaCl dissolved in heavy water (D_2O) elicit in spite of initially sufficient CSF $[Na^+]$ a pronounced water diuresis in the non-hydrated goat (Leksell et al 1976). Deuterated water is an inhibitor of (Na^+-K^+) -ATPase (Ahmed and Foster 1974). It appears possible that ICV infusions of deuterated water inhibit the release of ADH by affecting the Na^+ transporting enzyme system and so reducing the Na^+ sensitivity of the periventricular receptors. Substances which stimulate this enzyme system could thus increase the Na^+ sensitivity. This may be the situation with glucose together with K^+ .

In most of the studies reported perfusion of the cerebral ventricular system with artificial CSF low in Na^+ has a diuretic effect. In chloralose-anesthetized dogs a brisk water diuresis ensues (Lousen and Lacroix 1961). In conscious sheep urine flow rate shows a tendency to increase sometimes markedly (Mouw et al 1974). On the other hand pentobarbital-anesthetized dogs have a high initial plasma ADH concentration which does not show any consistent change during low $[Na^+]$ CSF perfusion (Mouw and Vander 1971). It is known that several anesthetics increase the secretion of the ADH (cf Walker 1957).

Renal Na^+ excretion

Artificial lowering of CSF $[Na^+]$ exerts varying effects on the renal electrolyte excretion. In pentobarbital-anesthetized dogs (Mouw and Vander 1970) and in conscious sheep (Mouw et al 1974) urine Na^+ excretion decreased during ventricular perfusion with low $[Na^+]$ CSF. However when a water diuresis developed as in the present study in chloralose-anesthetized dogs (Lousen and Lacroix 1961) and occasionally in the sheep (Mouw et al 1974) there was no consistent antinatriuresis. This dissimilarity of responses raises the question of a possible interrelationship between the renal sodium and the renal water excretion. In order to keep urine flow stable while lowering the CSF $[Na^+]$ isotonic fructose was also infused into the CSF in hydrated goats (paper IV). Na^+ excretion did not decrease. Thus an increase in urine flow could not explain the lack of antinatriuretic response to the ICV fructose infusion in non-hydrated goats. On the other

hand there was some decrease in the renal K^+ excretion

3 Effect on PRA of ICV infusions of angiotensin II and altered CSF Na^+ concentration (paper IV)

Angiotensin II

Infusion of angiotensin II dissolved in 0.15 M NaCl in doses from 0.5 to 1 μ g into the lateral cerebral ventricle caused a marked decrease of PRA. The direct inhibitory effect of angiotensin on the renal renin release (cf Davis and Freeman 1976) was excluded in these experiments since the plasma angiotensin II concentration did not rise after the infusions. However the infusions also raised arterial blood pressure (25-30 mmHg) released ADR and increased renal Na^+ excretion. Any one of these effects may have influenced renin release.

Centrally applied angiotensin II is thought to increase the sympathetic outflow (cf Severs and Daniels-Severs 1973). In view of this Vollmer et al. (1974) have suggested that an angiotensin II-induced increase in adrenergic outflow may stimulate the renal renin production. On the other hand Oparil and Haber (1974) have assumed that the centrally mediated pressor effect of angiotensin may be of considerable importance in the negative feedback of angiotensin on renin release. The present study indicates that angiotensin II applied into the CSF suppresses PRA but does not unmask the underlying mechanism.

Hypertonic NaCl

Like the infusions of angiotensin II infusion of 0.5 M NaCl solution at a rate of 20 μ l/min for 30 min caused a definite reduction of PRA. As expected from earlier studies in this species (Andersson et al. 1967) these infusions also caused antidiuresis, natriuresis and some drinking. Blood pressure response was variable. In some experiments ($n = 2$) there was no appreciable change in blood pressure whereas in other recordings ($n = 2$) blood pressure rose slowly and reached the highest increment (10-15 mmHg) at the end of the infusion. At that time PRA was already suppressed. Because of the rather long half-life of renin in circulating blood (10-20 min) it seems unlikely that the rise

in blood pressure could be of importance to the PRA suppression in these experiments. On the other hand the infusion of 0.3 M NaCl caused a large rapid increase in plasma ADH concentration (Fyhrquist, Eriksson and Wallenius 1976). ADH is known to inhibit renin release from the kidney (see Davis and Freeman 1976). It therefore appears probable that the increasing of CSF $[Na^+]$ suppressed PRA by stimulating ADH release.

In conscious rats Morris, Campbell and Pattinger (1976) have recently reported results similar to our data. Injection of hypertonic (2 M) NaCl into the third ventricle of the rat caused a decrease in serum renin activity, a rise in blood pressure and natriuresis. In contrast, high $[Na^+]$ CSF perfusion of the ventricular system in Na^+ -depleted conscious sheep influenced neither blood pressure nor plasma renin concentration (Abraham et al 1976). The varying Na^+ balance may readily explain the apparently diverging results. The hyperactive state of the renin-angiotensin system following Na^+ -depletion in the sheep may not be suitable for the demonstration of renin suppression with hypertonic NaCl applied into the cerebral ventricle. Hyponatremia and hypovolemia may be too effective peripheral stimuli for renin release to be suppressed by a rise in CSF $[Na^+]$.

Lowered CSF Na^+ concentration

Lowering of CSF $[Na^+]$ by infusing isotonic fructose into the lateral cerebral ventricle at a rate of 20 μ l/min during one hour elevated PRA. The result agrees with the studies of low $[Na^+]$ CSF perfusion in pentobarbital-anesthetized dogs (Mouw and Vander 1970) and in conscious sheep (Mouw et al 1974). In the non-hydrated goats the infusion of fructose induced water diuresis without any consistent change in renal Na^+ excretion in agreement with earlier studies (paper II). In the hydrated goats the urine flow rate was stable but yet there was no obvious reduction of renal Na^+ excretion following the infusion of fructose. However, both in hydrated and non-hydrated goats renal K^+ excretion decreased somewhat.

Infusion of isotonic NaCl into the lateral ventricle during one hour caused some increase in PRA. This result cannot be explained at present. It should be stressed however that the

rise in PRA after the infusion of saline was small (35 %) compared with that following the infusion of fructose (155 % in hydrated and 125 % in non-hydrated goats)

The efferent pathway by which the lowered CSF $[Na^+]$ influences the juxtaglomerular apparatus remains unclear. The blood pressure was stable during the infusion (paper II). Thus the renal baroreceptor mechanism would appear not to be responsible for the change in PRA. The decrease in plasma ADH could allow for a rise in PRA. However in hydrated goats too PRA rose in spite of initially suppressed ADH. Furthermore in pentobarbital-anesthetized dogs Mouw and Vander (1971) found an increase in PRA even though the plasma ADH was high and did not show any consistent changes. In our study there were no changes in renal Na^+ excretion which would explain the stimulation of renin release. The role of decreasing renal K^+ excretion due to infusion remains to be settled. Mouw and Vander (1971) showed that the renal nerves are not necessary for the antinatriuretic effect of low $[Na^+]$ CSF perfusion. On the other hand their study did not exclude the renal nerves as one possible pathway to the juxtaglomerular cells during lowering of CSF $[Na^+]$. In anesthetized cats Schad and Saller (1975) reported that high $[Na^+]$ CSF perfusion of the ventricular system produced an increase in renal sympathetic activity whereas a low $[Na^+]$ perfusion decreased it. It would appear necessary to evaluate whether CSF $[Na^+]$ can have an effect on the juxtaglomerular cells via the renal nerves.

4 A comparison between the centrally mediated effects of angiotensin II and its fragments des_1 -angiotensin II and des_1-2 -angiotensin II (paper V)

As expected from previous studies in the hydrated goat (paper I) infusion of angiotensin II in 0.15 M NaCl into the lateral ventricle at a rate of 50 ng/min during 30 min caused drinking, antidiuresis and natriuresis. In contrast infusion of des_1 -angiotensin II (angiotensin III) at an equimolar concentration did not induce any drinking or antidiuresis and had no obvious influence on renal Na^+ excretion. When a more concentrated angiotensin III solution was infused at a rate of 0.35 µg/min

during 5 min three out of six animals drank water. There was some inhibition of water diuresis after every infusion and CH_2O became negative in 5 out of 8 experiments. These responses as well as the rise in blood pressure were definitely smaller than those following infusion of angiotensin II of half the molar strength. Infusion of des_{1-2} -angiotensin II the hexapeptide had no effect on water balance.

Fitzsimons (1971) studied the dipsogenic action of various angiotensin analogues. He found that the des_1 -angiotensin II retains about 50 % of the dipsogenic activity of the octapeptide when infused into the angiotensin sensitive regions in the rat's diencephalon. In the present study des_1 -angiotensin II appeared dipsogenic although to a lesser degree. However the data cannot be readily compared. In the goat intraventricular infusion of $\text{des}_1\text{-ileu}^5$ -angiotensin II was used whereas Fitzsimons (1971) applied $\text{des}_1\text{-val}^5$ -angiotensin II directly into the brain tissue.

In the present study the same latency time was observed for the antidiuresis induced by angiotensin II and III. This was taken as indication that both polypeptides act on a common presumably membrane located receptor. Gagnon, Sirois and Park (1975) have studied in vitro the neurohypophyseal receptors for angiotensin II and suggested that cyclic AMP may be involved in the stimulation of ADH secretion from incubated rat neurohypophyses. They also found that a much longer incubation period was needed with des_1 -angiotensin II than with angiotensin II before ADH was released. They assumed that the altered binding affinity for the receptor may contribute to a delay in the action. Following longer incubation periods the heptapeptide was capable of producing neurohypophyseal effects comparable to those induced by angiotensin II. After intravenous injection of labelled angiotensin II high concentrations of radioactivity were found in the pituitary (Osborne et al. 1971, Johnson 1975). This may be one route of entry for the blood-borne angiotensin into the CNS particularly as a releaser of ADH. These studies raise the question of the possible existence of two kinds of angiotensin receptors affecting ADH release. There probably are receptors higher up in the hypothalamic neurohypophyseal system. In addition the neurohypophysis itself may contain receptors.

GENERAL DISCUSSION

Several reviews have recently been published concerning the central actions of angiotensin II (Severs and Daniels-Severs 1973) central control of fluid homeostasis (Andersson 1974) and control of drinking (Fitzsimons 1972 Peters Fitzsimons and Peters-Raefelt 1975) Therefore only aspects closely related to the present study will be discussed in this chapter

The current opinion is that the fluid balance is principally controlled by osmometric and volumetric mechanisms acting synergistically to maintain the composition and volume of the body fluids. There is much evidence that atrial and some other vascular receptors monitor the blood volume and exert a reflex inhibitory tone on the release of ADH (for review see Gauer Henry and Behn 1970 Goetz Bond and Bloxham 1975). The renal renin-angiotensin system forms an important humoral link in the volume regulation by its influence on aldosterone secretion but apparently also by its effect on central mechanisms involved in the control of fluid balance. Experiments in the goat indicate that these centrally mediated effects of angiotensin II are Na^+ dependant. Therefore it has been suggested that angiotensin II may act by sensitizing periventricular Na^+ receptors to existing CSF $[\text{Na}^+]$ (Andersson 1971). Angiotensin II appears to be dipsogenic in all species tested. However many consider that the doses of angiotensin which have been studied are unphysiologically high (e.g. Abraham et al 1975). Thus the question to what degree the renin-angiotensin of renal origin contributes to the volumetric control of thirst remains open.

Various species of animals have been used in the studies concerning the central control of fluid balance. This may have been a factor causing some of the divergencies in the results obtained. The goat like other ruminants has the voluminous forestomachs acting as a large reservoir for water and electrolytes. The dog in contrast is a monogastric carnivore which eats at long intervals. Furthermore the modulating effect of anaesthetics and surgical stress should be kept in mind.

Osmoreceptors versus sodium sensitive receptors

The main evidence for the osmoreceptor theory in the central control of water balance has been obtained by studying the effects of altered solute composition of the blood plasma (Verney 1947). Later studies have given additional support for this concept (see Blass 1973). In Verney's original investigations the blood-brain and the blood-CSF barriers have been disregarded. However, the responses to the administration of various hypertonic solutions into the central nervous system of the goat from either side of the blood-brain barrier seem to contradict the osmoreceptor theory. A rise in the carotid blood osmolality obtained by infusion of NaCl or fructose acts as a much more potent stimulus for ADH release and thirst than the equivalent rise elicited by infusions of urea, glycerol or glucose (Eriksson, Fernández and Olsson 1971, Olsson 1972) although a rather effective blood-brain barrier seems to exist for all of the latter substances (Crone 1965, Yudilevich and de Rose 1971). On the other hand, the infusion of hypertonic sucrose solution into the third cerebral ventricle elicits neither ADH release nor thirst, in contrast to corresponding infusion of hypertonic NaCl (Olsson 1969). These observations make the existence of osmoreceptors unlikely, at least inside the blood brain barrier. The other possibility, that cerebral osmoreceptors are outside the blood brain barrier, or in a region where the barrier is lacking, also appears unlikely. Slow infusions of iso- or hypertonic solutions of non-electrolytes into the lateral ventricle repress the dipsogenic, antidiuretic and natriuretic responses to intracarotid infusions of hypertonic NaCl (Olsson 1973). This would hardly be the case if the intracarotid infusion of hypertonic NaCl acted via receptors located outside the blood brain barrier.

A possible alternative to hypothalamic osmoreceptors may be a sodium sensitive receptor system in the close vicinity of the third cerebral ventricle (cf. Andersson 1971). The following results have been taken as evidence for this concept. Slow infusions of hypertonic NaCl solution into the third or lateral ventricle elicit drinking, antidiuresis and natriuresis in hydrated goats (cf. Andersson and Olsson 1973). However, no

drinking or antidiuretic responses are obtained by similar infusions of hypertonic sucrose (Olsson 1969). Rather the lowering of CSF $[Na^+]$ by infusing saccharide solutions caused a water diuresis in the non-hydrated goat (paper II). This also happened on most occasions when saccharides were infused together with K^+ , Ca^{2+} and Mg^{2+} (paper III) whereas during infusions of isotonic NaCl or saccharides in isotonic NaCl water diuresis did not develop (paper II). The results of combined intracarotid/intraventricular infusions also support the Na^+ -receptor hypothesis. Infusions of saccharides into the lateral ventricle suppressed the dipsogenic antidiuretic and natriuretic responses to intracarotid infusions of hypertonic NaCl. Corresponding infusions of 0.14 M NaCl or isotonic glucose in 0.14 M NaCl did not have this suppressive effect (Olsson 1973).

McKinley, Blaine and Denton (1974) reexamined the concept of brain osmoreceptors in thirst regulation in the conscious sheep by making injections into the third ventricle of hypertonic NaCl and saccharide solutions in artificial CSF. In an attempt to minimize apart from osmolality the alteration in CSF composition, hypertonic saccharide solutions in water did not elicit drinking, while hypertonic saccharides in artificial CSF, hypertonic NaCl in artificial CSF and hypertonic NaCl in water were dipsogenic. These results were taken as support for combined cerebral osmotic and sodium sensitivity. Thus the studies in the sheep lend support to the osmoreceptor theory but do not rule out specific sodium sensitivity, since hypertonic NaCl in artificial CSF caused much more drinking than hypertonic saccharides in artificial CSF.

The entry of angiotensin II into the brain and the angiotensin sensitive areas

It appears that in order to act centrally circulating angiotensin II must enter the brain. However, the blood-brain barrier effectively restrains angiotensin II (Volicer and Loew 1971, Osborne et al. 1971). The other possible routes are via the choroid plexuses into the CSF or an action in areas where the blood-brain barrier is lacking. There is no consensus of opinion as to whether angiotensin II penetrates the blood-CSF barrier.

Volicer and Loew (1971) studied the distribution of ^{14}C -angiotensin II in the brain of mice after systemic intravenous injection. The volume of distribution was larger than the plasma volume. Furthermore, autoradiographs showed radioactivity in choroid plexuses in the lateral and third ventricles and in the aqueduct but not in the fourth ventricle. The results were however criticized (Abraham 1974) because of the supra-physiological doses of angiotensin and the incubation method used. Using lower doses of tritiated angiotensin II of relatively high specific activity, Johnson (1975) studied in detail the distribution of intravenous angiotensin in rat brain. Radioactivity was high in the ventricular spaces, periventricular tissues, choroid plexuses, pituitary, pineal, subfornical organ (SFO) and area postrema. Abraham (1974) found the CSF of normal sheep to contain angiotensin II but the levels were not elevated above 5 ng/100 ml when the blood angiotensin II concentrations were raised up to 15-70 ng/100 ml by intravenous infusion. As a possible explanation, a rapid uptake of angiotensin II from the CSF in physiological situations was taken into consideration.

Among the areas where a blood-brain barrier is lacking, the area postrema, SFO and pituitary are of special interest. There is much evidence that blood borne angiotensin II stimulates central pressor activity in the area postrema, whereas the periaqueductal grey (subnucleus medialis) is the site where angiotensin applied into CSF raises blood pressure (for review see Severs and Daniels-Severs 1973).

Circulating angiotensin II may act directly on the neurohypophysis, since high radioactivity was observed in the pituitary after intravenous injection of labelled angiotensin II (Osborne et al. 1971, Johnson 1975). The finding of high renin (Kaulice et al. 1975) and angiotensin converting enzyme activity (Yang and Neff 1972) in the hypophysis points to the possibility that also local production of angiotensin II may play a role in the release of ADH. Cagnon et al. (1975) have studied the rat neurohypophysis in vitro and observed that angiotensin II stimulates ADH secretion, possibly via cyclic AMP.

The SFO has been claimed by Simpson and Routtenberg (1973) to be the most sensitive locus to angiotensin as a diuretic.

This periventricular organ is in close contact with both blood and CSF. Although there is much evidence supporting this concept the SFO apparently is not the only site where angiotensin elicits thirst. It is for instance possible to stimulate drinking in spite of massive damage of the SFO if the entry of angiotensin into the anterior part of third ventricle is guaranteed (Buggy et al 1975). During remapping of angiotensin sensitive brain loci Johnson and Epstein (1975) observed that angiotensin II induced thirst if cannula traversed the anterior cerebral ventricles thus allowing the injected material to enter the ventricular system. On the basis of this result and of autoradiographic findings (Johnson 1975) they maintain that angiotensin II may use the ventricular route to gain access to the sensitive periventricular sites.

It has to be emphasized that in the earlier experiments high doses of angiotensin II were used. However Epstein and Hsiao (1975) and Trippodo, McCaa and Guyton (1976) claimed on the basis of their recent studies that angiotensin II acts diplogenically also in physiological doses. In addition to the blood-borne angiotensin the existence of the intrinsic renin-angiotensin system in the brain (Ganten et al 1971, Fischer-Ferraro et al 1971) has focused interest on the possible physiological role of central effects of angiotensin. The hypothalamic region close to the third ventricle and the brain stem contain the highest level of angiotensin I and II (Fischer-Ferraro et al 1971). The centers which control fluid balance and blood pressure are located here. Different regimens of treating animals were found to change the renin activity and angiotensin I content of the brain. Systemic administration of aldosterone decreased cerebral renin activity (Ganten et al 1971). On the other hand, administration of hypertonic NaCl (Maulice et al 1975) or sar¹ileu⁸-angiotensin II, an angiotensin II antagonist (Sen, Ferrario and Bumpus 1974) increased this activity. Furthermore hypovolemia increased the concentration of angiotensin I in the brain stem whereas Na⁺-loading decreased it (Slaven 1975). Taken together these data would indicate that systemic changes in the electrolyte and fluid balance affect not only the renal but also the cerebral renin release.

Cerebral receptors controlling renal Na^+ excretion

Most studies concerning the central control of Na^+ homeostasis favor the view that a Na^+ -sensitive system in the brain operates in the regulation of the renal Na^+ output. Elevation of the Na^+ concentration in the CSF of the cerebral ventricular system has been found to increase renal Na^+ excretion in many species. Perfusion experiments with low $[\text{Na}^+]$ CSF indicate that reduced basal activity of these receptors may play a role in initiating Na^+ -sparing during salt depletion. The physiological basis for this concept lies in a study with Na^+ -depleted and normal sheep (Mouw et al 1974). Progressive Na^+ -depletion was associated with a significant reduction of CSF $[\text{Na}^+]$ and the Na^+ concentration in CSF and blood were closely related. In pentobarbital anesthetized dogs (Mouw and Vander 1970) and in conscious sheep (Mouw et al 1974) hypotonic low $[\text{Na}^+]$ perfusion of the cerebroventricular system caused antinatriuresis and a rise in plasma renin. In the present work in conscious goats CSF $[\text{Na}^+]$ was lowered by ICV infusions of isotonic fructose. The PRA rose in accordance with the previous studies but renal Na^+ excretion showed no consistent changes. Instead urine flow rate increased and water diuresis developed. Similar responses in urine excretion have been reported by Leusen and Lacroix (1961) in chloralose-anesthetized dog during low $[\text{Na}^+]$ perfusion of ventricular system. In some of their sheep Mouw et al (1974) also observed a marked increase in urine flow during low $[\text{Na}^+]$ perfusion and in these instances Na^+ excretion did not decrease. In some way the behavior of renal Na^+ excretion thus appears to depend on the degree of diuresis. One possibility is that the presence of ADH may be an important factor in renal Na^+ -sparing. In the present work renal K^+ excretion was found to decrease to some extent. This may reflect a diminished Na^+ load at the distal nephron.

Intracarotid infusions have also been used to study the postulated central Na^+ receptors. Such infusions of hypertonic NaCl solution always induce a more pronounced natriuresis than equivalent intravenous infusions. In the conscious goat intracarotid infusion (1.5 ml/min) of hypertonic (2 M) fructose had a negligible natriuretic effect when compared with hypertonic

(1 M) NaCl infused at a same speed (Olsson and Kolmodin 1974) Similarly in anesthetized cats (Thornborough Passo and Rothballer 1973) intracarotid infusion of hypertonic sucrose in normal saline and in anesthetized dogs (Zucker and Kaley 1976) infusion of hypertonic glucose failed to increase renal Na^+ excretion In conscious sheep on the other hand Blaine et al (1975) observed a definite natriuresis following intracarotid infusion (1.6 ml/min) of hypertonic sucrose or fructose (2 M) but the response to intravenous infusion was delayed and weak Hence the latter authors expressed the belief that osmoreceptors control the Na^+ excretion

The efferent pathway from the brain to the kidney mediating the effects on Na^+ excretion has not been ascertained There are several possible partly interrelated mechanisms These are

- (1) alterations in renal hemodynamics including vasomotor autoregulation
- (2) changes in renal nerve activity and
- (3) humoral factors such as aldosterone ADH and natriuretic factor

1 The natriuresis following elevated CSF $[\text{Na}^+]$ in the third ventricle is accompanied by a rise in the glomerular filtration rate (Andersson et al 1969 Zucker Levine and Kaley 1974) In the present study the infusion of hypertonic NaCl into the third ventricle caused a slowly developing rise in blood pressure concurrently with the natriuretic response (paper I) Similar results have been reported in anesthetized rats (Dorn et al 1969) cats (Chiu and Sawyer 1974) and dogs (Zucker et al 1974) The changes in renal hemodynamics may thus contribute to the increased Na^+ excretion (cf Guyton et al 1974) On the other hand the rise in blood pressure following intracarotid infusion of hypertonic NaCl is inconsistent and not well correlated to natriuresis (Blaine et al 1975 Thornborough et al 1973 Zucker and Kaley 1976) Furthermore during antinatriuresis following the lowering of CSF $[\text{Na}^+]$ there were no significant changes in blood pressure The redistribution of renal blood flow is another possible mechanism often discussed but not yet established

2 There is much evidence that the renal nerves may be involved in the tubular reabsorption of Na^+ (e.g. Slick et al 1975; for review see Gill 1969). However the evidence that the changes in Na^+ excretion following stimulation of brain Na^+ receptors are mediated via renal nerves is meager. By means of renal denervation McKinley, Blaine and Denton (1973) were able to inhibit the natriuresis following the injection of hypertonic NaCl into the third ventricle of conscious sheep. However in anesthetized cats (Chin and Sawyer 1974) and dogs (Zucker et al 1974) renal denervation did not prevent an increase in Na^+ excretion after infusion of hypertonic NaCl into the third ventricle. Furthermore the antinatriuresis during low $[\text{Na}^+]$ CSF perfusion was not abolished by renal denervation (Mouw and Vander 1971).

3 Although the plasma levels of aldosterone decrease during elevated CSF $[\text{Na}^+]$ (Abraham et al 1976) this apparently is not essential for natriuresis since natriuresis develops rapidly and aldosterone pretreatment does not inhibit the response (Andersson et al 1969). During low $[\text{Na}^+]$ CSF perfusion blood aldosterone concentration was unchanged (Mouw et al 1974). Thus aldosterone probably did not mediate the antinatriuretic response.

Stimuli which elicit natriuresis are known to release ADH. While high doses of ADH are natriuretic the importance of this hormone for Na^+ excretion has been much debated (e.g. Macfarlane et al 1967, Blaine et al 1973). The release of ADH however cannot alone explain the effect since experimental diabetes insipidus does not abolish the natriuretic response (Andersson et al 1969). Pretreatment with ADH like that with aldosterone could not inhibit the natriuretic effect following intracarotid infusion of hypertonic NaCl (Thornborough et al 1973, Zucker and Kaley 1976). Lowering of CSF $[\text{Na}^+]$ was in most cases found to decrease ADH release and this may have contributed to the antinatriuresis observed (Mouw et al 1974). However in anesthetized dogs antinatriuresis developed even though the plasma ADH concentration was high (Mouw and Vander 1971).

In spite of an intense search for a natriuretic factor conclusive proof of its existence is still lacking (Mashat 1974).

REFERENCES

- ABRAHAM E F The central nervous system and sodium and water homeostasis Thesis University of Melbourne 1974
- ABRAHAM S F R M BAKER E H BLAINE D A DENTON and M J MCKINLEY Water drinking induced in sheep by angiotensin - a physiological or pharmacological effect? J comp physiol Psychol 1975 88 503-518
- ABRAHAM S F J R BLAIR-WEST J P COGHILAN D A DENTON D R MOUW and B A SCOGGINS Aldosterone secretion during high sodium cerebrospinal fluid perfusion of the brain ventricles Acta endocr (Kbh) 1976 81 120-132
- AHMED K and D FOSTER Studies on the effects of $^2\text{H}_2\text{O}$ on $\text{Na}^+ \text{K}^+$ -ATPase Ann N Y Acad Sci 1974 242 280-292
- AKERLUND L -E I ANDERSSON and K OLSSON A cannula system for frequent infusions into the CSF of the cerebral ventricles of the goat Physiol Behav 1973 10 161-162
- ANDERSSON B The effect of injections of hypertonic NaCl-solutions into different parts of the hypothalamus of goats Acta physiol scand 1953 28 188-201
- ANDERSSON B Thirst - and brain control of water balance Amer Scientist 1971 59 408-415
- ANDERSSON B Central control of body fluid homeostasis Proc Aust Physiol Pharmacol Soc 1974 5 139-152
- ANDERSSON B M F DALLMAN and K OLSSON Evidence for a hypothalamic control of renal sodium excretion Acta physiol scand 1969 75 496-510
- ANDERSSON B L G LEKSELL and M RUNDGREN Duration of central action of angiotensin II estimated by its interaction with CSF Na^+ Acta physiol scand 1975 93 472-476
- ANDERSSON B and K OLSSON On central control of body fluid homeostasis Conditional Reflex 1973 8 147-159
- ANDERSSON B K OLSSON and R G WARNER Dissimilarities between the central control of thirst and the release of anti-diuretic hormone (ADH) Acta physiol scand 1967 71 57-64
- ANDERSSON B and B WESTBYE Synergistic action of sodium and angiotensin on brain mechanisms controlling fluid balance Life Sciences 1970 Part I 2 601-608

- BERGMANN J P OEHME J JELINEK and J H ~~CR~~ *Journal of*
of angiotensin and eledoisin activities by ~~and~~ *Life Sciences*
Life Sciences 1971 Part I 10 969-975
- BICKERTON R Y and J P BUCKLEY Evidence for a ~~mechanism~~
mechanism in angiotensin-induced hypertension *Exp Biol (NY)*
exp Biol (NY) 1961 106 834 836
- BLAINE E H D A DENTON M J MCKINLEY and S ~~central~~
central osmosensitive receptor for renal ~~excretion~~ *J Physiol (Lond)*
J Physiol (Lond) 1975 244 497 509
- BLASS E M Cellular-dehydration thirst: Physiological and behavioral correlates In *The neurobiology of thirst*
of thirst New findings and advances in ~~conduct~~ *Epstein H R Kissileff and E Stellar V H W*
Epstein H R Kissileff and E Stellar V H W
Washington D C 1973 pp 37-72
- BOLJOUR J P and R L MALVIN Stimulation of ~~the~~ *the*
the renin-angiotensin system *Amer J Physiol* 1971 155-1559
- BRONSTED M Z Transport of glucose sodium potassium between the cerebral ventricles and ~~tissues~~ *Acta physiol scand* 1970 73 2
- BUOGY J A E FISHER W E HOFFMAN A K JOEL ~~PHILLIPS~~
PHILLIPS Ventricular obstruction effect on ~~angiotensin~~ *1975 190 72 74*
1975 190 72 74
- CHIU P J S and W H SAWYER Third ventricular ~~hypertonic~~ *hypertonic*
hypertonic NaCl and natriure is in cat *Amer J Physiol* 1974 226 463 469
- CROWE C The permeability of brain capillaries to ~~electrolytes~~ *Acta physiol scand* 1965 64 407 417
- DAVIES N T K A MUNDAY and B J PARSONS The effect of angiotensin on rat intestinal fluid transfer *J Physiol (Lond)* 1974 248 39-46
- DAVIS J B and R H FREEMAN Mechanisms regulating ~~release~~ *Physiol Rev* 1976 56 1-56
- DORN J B N LEVINE G KALEY and A B ROTHBART ~~sis~~ *sis*
sis induced by injection of hypertonic saline ~~in~~ *cerebral ventricle of dogs Proc Soc exp Biol Med*
cerebral ventricle of dogs *Proc Soc exp Biol Med* 1969 131 240 242

REFERENCES

- ABRAHAM S F The central nervous system and sodium and water homeostasis Thesis University of Melbourne 1974
- ABRAHAM S F R M BAKER E H BLAINE D A DENTON and M J McKINLEY Water drinking induced in sheep by angiotensin - a physiological or pharmacological effect? J comp physiol Psychol 1975 88 503-518
- ABRAHAM S F J R BLAIR-WEST J P COGHLAN D A DENTON D R MOON and B A SCOGGINS Aldosterone secretion during high sodium cerebrospinal fluid perfusion of the brain ventricles Acta endocr (Kbh) 1976 81 120-132
- AHMED K and D FOSTER Studies on the effects of $^2\text{H}_2\text{O}$ on $\text{Na}^+ \text{K}^+$ -ATPase Ann N Y Acad Sci 1974 242 280-292
- AKERLUND E -E I ANDERSSON and K OLSSON A cannula system for frequent infusions into the CSF of the cerebral ventricles of the goat Physiol Behav 1973 10 161-162
- ANDERSSON B The effect of injections of hypertonic NaCl-solutions into different parts of the hypothalamus of goats Acta physiol scand 1953 28 188-201
- ANDERSSON B Thirst - and brain control of water balance Amer Scientist 1971 59 408-415
- ANDERSSON B Central control of body fluid homeostasis Proc Aust Physiol Pharmacol Soc 1974 5 139-152
- ANDERSSON B M P DALLMAN and K OLSSON Evidence for a hypothalamic control of renal sodium excretion Acta physiol scand 1969 73 496-510
- ANDERSSON B L G LEXSELL and M RUNDGREN Duration of central action of angiotensin II estimated by its interaction with CSF Na^+ Acta physiol scand 1975 93 472-476
- ANDERSSON B and K OLSSON On central control of body fluid homeostasis Conditional Reflex 1973 8 147-159
- ANDERSSON B K OLSSON and R G WARNER Dissimilarities between the central control of thirst and the release of anti-diuretic hormone (ADH) Acta physiol scand 1967 71 57-64
- ANDERSSON B and O WESTBYE Synergistic action of sodium and angiotensin on brain mechanisms controlling fluid balance Life Sciences 1970 Part I 9 601-608

- GANTEN D J L MINKICH F GRANGER K HAYDOK H M BRECHT
A BARBEAU R BROUCHER and J GENEST Angiotensin-forming
enzyme in brain tissue Science 1971 173 64-65
- GAUER O H J P HENRY and C BERN The regulation of extra-
cellular fluid volume Ann Rev Physiol 1970 32 547-595
- GILL J R Jr The role of the sympathetic nervous system in
the regulation of sodium excretion by the kidney In Frontiers in neuroendocrinology Eds W F Ganong and L Martini
Oxford University Press New York 1969 pp 289-305
- GOETS K L G C BOND and D D BLOKHAM Atrial receptors and
renal function Physiol Rev 1975 55 157-205
- GUTHAN Y Y SHAMIR D GLUSHEVITSKY and B BOCHMAN Angio-
tensin increases microsomal ($Na^+ - K^+$)-ATPase activity in
several tissues Biochim Biophys Acta 1972 273 401-405
- GUYTON A C T G COLEMAN A W COWLEY Jr R D MANNING Jr
R A NORMAN Jr and J D FERGUSON A systems analysis ap-
proach to understanding long range arterial blood pressure
control and hypertension Circulat Res 1974 35 159-176
- HAULICE I B D BRANISTEANU V ROSCA A STRATONE V BERSE-
LEU G BALAN and L IONESCU A renin-like activity in pineal
gland and hypophysis Endocrinology 1975 96 508-510
- JEWELL P A and E B VERHEY An experimental attempt to deter-
mine the site of the neurohypophysial osmoreceptors in the
dog Phil Trans roy Soc (Lond) B 1957 240 197-324
- JOHNSON A K The role of the cerebral ventricular system in
angiotensin-induced thirst In Control mechanisms of drinking
Eds G Peters J T Fitzsimons and L Peters Haefeli
Springer-Verlag Berlin 1975 pp 117-122
- JOHNSON A K and A M EPSTEIN The cerebral ventricles as the
avenue for the diuretic action of intracranial angiotensin
Brain Res 1975 86 399-418
- LEKSELL L G F LISHAJKO and M KUNDGREN Negative water
balance induced by intracerebroventricular infusion of
deuterium Acta physiol scand 1974 97 142-144
- LEUSEN I and E LACROIX Changes in osmolarity in the cere-
bral ventricles and diuresis Endocrinology 1961 58 719-721
- LIMASABORO J M C JIMENEZ DIAZ and H CASTRO MENDOZA The
kidney and thirst regulation Bull Inst Med Res Madrid
1954 7 53-61

- SLICK E L A J AQUILERA E J ZAMBRASKI G F DIBONA and
E J KALOYANIDES Renal neuroadrenergic transmission Amer
J Physiol 1975 229 60-65
- SWANSON L W L G SHARPE and D GRIFFIN Drinking to intracere-
bral angiotensin II and carbachol: dose-response relationships
and ionic involvement Physiol Behav 1973 10 595-600
- THORNBOROUGH J R S S PASSO and A B ROTHBALLER Receptors
in cerebral circulation affecting sodium excretion in the
cat Amer J Physiol 1973 225 138-141
- TRIPPODO N C R E McCAA and A C GUYTON Effect of prolonged
angiotensin II infusion on thirst Amer J Physiol 1976
230 1063-1066
- VERNEY E B The antidiuretic hormone and the factors which de-
termine its release Proc roy Soc B 1947 135 25-106
- VOLICER L and C G LOEW Penetration of angiotensin II into
the brain Neuropharmacol 1971 10 631-636
- VOLLMER R J P BUCKLEY T A SOLOMON and H S JANDHYALA
Central hypertensive actions of angiotensin Acta physiol
latinoam 1974 24 582-586
- WALKER J M Release of vasopressin and oxytocin in response
to drugs In The Neurohypophysis Ed H Heller Butter-
worths London 1957 pp 221-229
- WAYNER M J T ONO and D HOLLEY Effects of angiotensin II on
central neurons Pharmacol Biochem Behav 1973 1 679-691
- YANG H -Y T and N B NEFF Distribution and properties of an-
giotensin converting enzyme of rat brain J Neurochem
1972 19 2443-2450
- YUDILEVICH D L and N de ROSE Blood-brain transfer of glucose
and other molecules measured by rapid indicator dilution
Amer J Physiol 1971 220 841-846
- ZUCKER I H and G KALEY Natriuresis induced by intracarotid
infusion of hypertonic NaCl Amer J Physiol 1976 230
427-433
- ZUCKER I H M LEVINE and G KALEY Third ventricular injec-
tion of hypertonic NaCl: effect of renal denervation on
natriuresis Amer J Physiol 1974 227 35-41

ISBN 951-95092-3-0

Helsingin yliopiston monistuspainos, offset 1976

ACTA PHYSIOLOGICA SCANDINAVICA
Supplement 421

APPARENT REGIONAL TENSION OF
ACETYLCHOLINE IN VISCERAL MUSCLES

METHODOLOGICAL AND FUNCTIONAL ASPECTS

BY
AGNETA NORDBERG

ISSN 0302 2994

Printed in Sweden 1977

TEXTgruppen i Uppsala AB

The present survey is based on the following papers, which will be referred to by their Roman numerals.

- I. Nordberg, A. and A. Sundwall, Effect of pentobarbital on endogenous acetylcholine and biotransformation of radioactive choline in different brain regions. In: *Cholinergic Mechanisms*. Ed. P G Waser Raven Press, New York. 1975 229-239
- II. Nordberg, A. and A. Sundwall, Effect of oxotremorine on endogenous acetylcholine and on uptake and biotransformation of radioactive choline in discrete regions of mouse brain *in vivo* *Biochem. Pharmacol.* 1976. 25 135-140.
- III Nordberg, A. and A. Sundwall, Biosynthesis of acetylcholine in different brain regions *in vivo* following alternative methods of sacrifice by microwave irradiation. *Acta physiol. scand.* 1976. 98. 307-317
- IV Nordberg, A. and A. Sundwall, Effect of sodium pentobarbital on the apparent turnover of acetylcholine in different brain regions. *Acta physiol. scand.* 1977 99 336-344
- V Nordberg, A., Effect of oxotremorine and sodium pentobarbitone on the pharmacokinetics of intravenous tracer doses of radioactive choline. *J Pharm. Pharmacol.* 1977 29 96-98.
- VI Nordberg, A. and G. Wahlström, Effect of long-term forced oral barbital administration on endogenous acetylcholine in different rat brain regions. *Eur J Pharmacol.* 1977 (accepted for publication).
- VII. Nordberg, A., Effect of oxotremorine on the apparent regional turnover of acetylcholine in mouse brain. In manuscript.

Contents

1	Introduction	7
2	Microwave irradiation as a rapid method of enzyme inactivation and sacrifice of small rodents	9
2.1	Some basic facts	9
2.1.1	Generation of microwaves	9
2.1.2	Waveguide	10
2.1.3	Applicator	10
2.2	Heating by microwaves	10
2.3	Sacrifice of small rodents by microwave irradiation	11
2.4	Brain temperatures following microwave irradiation	13
2.5	Enzyme inactivation following microwave irradiation	14
3	Steady state levels of acetylcholine in brain tissue	16
4	Steady state levels of choline in brain tissue	26
5	Apparent rate of turnover of acetylcholine in brain regions	28
5.1	Definitions	28
5.2	Previous results	28
5.3	Biotransformation of radioactive choline in brain regions	28
5.4	Differences in the <i>post mortem</i> stability of endogenous and radioactive acetylcholine	32
5.5	Rate of turnover of acetylcholine in brain tissue determined by different methods of calculation	34
6	Effect of pentobarbital and oxotremorine on the apparent turnover of acetylcholine in different brain regions	39
7	General summary	43
8	Acknowledgements	45
9	References	46

The term turnover is defined as the renewal of a substance at steady state (Zilversmit *et al.* 1943).

Measurements of the turnover of a neurotransmitter such as acetylcholine (ACh) in brain regions will give more information about functional relationships than will be obtained by measuring static levels. A change in the release, for example, may leave the steady state unaltered but affect the rate of biosynthesis. Turnover changes in different brain regions may be masked in whole brain studies.

To measure the ACh turnover choline (Ch) may be given intravenously and the time course of the specific radioactivities (SA) of the precursor (Ch) and product (ACh) followed in the brain. Labelled choline (Schubert *et al.* 1969 Jenden 1973, Saelens *et al.* 1974) or phosphorylcholine (PhCh) (Cheney *et al.* 1975b) has been given to mice and rats either by intravenous (i.v.) pulse injection (Schubert *et al.* 1969 Hanbrich *et al.* 1975) or intravenous infusion (Saelens *et al.* 1973b Racagni *et al.* 1974).

This method necessitates the assumption that the brain handles the Ch in a way which may be described in terms of an open single compartment model, that there is instant mixing of the labelled and unlabelled compounds and that steady state conditions prevail (Zilversmit 1960).

The turnover values obtained will necessarily be rather approximate. The most obvious limitation is our lack of knowledge about the compartmentation of Ch and the size of the Ch pool available for ACh synthesis (Sparf 1973 Jenden 1976).

In order to avoid this uncertainty Domino and Wilson (1972) measured the ACh turnover from the rate of depletion of the ACh after intracerebroventricular administration of hemicholinium (HC 3), a quaternary drug which inhibits ACh synthesis by blocking Ch transport. Richter and Crossland (1949) measured the initial rate of restitution of the ACh after depletion by electroshock. However in these cases steady state conditions were not obtained.

Both the ACh and Ch levels in brain are extremely labile (for review see MacIntosh and Collier 1976). This is a serious obstacle and a limiting factor for work on brain regions. During recent years great progress has been made in the development of methods of getting rapid inactivation of brain enzymes without preventing accurate dissection. When the present study was initiated in 1971 Stavinocha and co-workers (1970) had recently introduced microwave irradiation as a rapid method of enzyme inactivation and sacrifice of small rodents, a method which allowed accurate dissection of the brain.

The aims of the present investigation were-

1. to evaluate the importance of the time of enzyme inactivation for ACh and Ch values in brain tissue-
2. to study the precursor-product relationship of Ch and ACh in different brain regions

by following the time courses of the specific radioactivities of Ch and ACh after an intravenous tracer dose of Ch

- 3 to apply the data to different models of turnover calculation
- 4 to study the functional role of ACh in different brain regions by measuring the effect of barbiturates and oxotremorine on the apparent regional ACh turnover

2. Microwave Irradiation as a Rapid Method of Enzyme Inactivation and Sacrifice of Small Rodents

2.1 Some basic facts

For detailed information about microwave physics, see Püschner (1966), Thomas (1972), Copson (1962) and Okress (1968).

Microwaves are electromagnetic waves with a wavelength varying between 0.001 and 1 m. The most commonly used wavelengths have dimensions of 0.328 and 0.122 m (915 and 2450 MHz).

Non-metallic materials can be heated by microwave irradiation, since the energy-rich electromagnetic waves can pass into materials and convert their energy into heat. For microwave heating a system consisting of at least three components is necessary 1) a generator of microwave energy 2) a waveguide and 3) an applicator

2.1.1 Generation of microwaves

For the generation of microwaves with an effect of less than 10 kW a magnetron is used. This consists of a vacuum diode with a cathode in the centre surrounded by a cylindrical anode containing several resonant cavities (Fig. 1). The cathode consists of a material which emits electrons at increased temperature. The emitted electrons are affected by the force from both a magnetic field (parallel to the cathode) and an electric field (applied voltage between anode and cathode). The electrons are only attracted to the parts of the anode which are positively charged by the electromagnetic oscillation. Subsequently in the interaction space between cathode and anode the emitted electrons travel in spiral paths to form the spokes of a wheel which rotate. In the resonance cavities high frequency oscillation microwaves are excited by the passing spokes of electrons. The generated microwaves can then be transmitted from one of these resonance cavities to the waveguide.

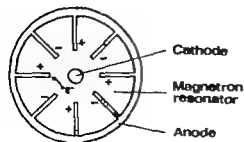


Fig. 1 Magnetron, a diagrammatic drawing.

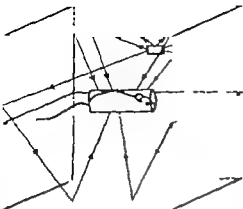


Fig. 2a. Applicator for whole body irradiation of mice. The electromagnetic waves are reflected by the walls of the exposure chamber (oven) to penetrate into the mouse body

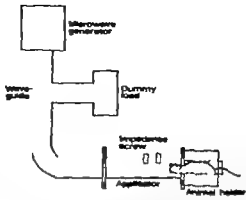


Fig. 2b. Diagrammatic drawing of the microwave system Metaboheat 4104. The mouse's head is placed in the applicator and exposed to microwaves.

2.1.2 Waveguide

The waveguide can be a rectangular metal channel, with the same dimension as the wavelength of the microwaves and constitutes the transmission line for propagation of the microwaves from the generator to the applicator

2.1.3 Applicator = exposure chamber (Figs. 2a 2b).

2.2 Heating by microwaves

A dielectric material with polar properties may be regarded as an electric dipole with a positive and a negative charge (q) separated by a distance l (Fig. 3). If an electric field is applied, the dipole will be oriented in the direction of the field and a dipole moment will be induced ($q \times l$). A change in the direction of the electric field will alter the orientation of the dipoles. If the electric field alternates with a high frequency the dipoles will also oscillate very rapidly and by friction will convert oscillation energy into heat. The dipoles respond with a short delay to the change in the electric field and during this relaxation time the dielectric loss occurs. There are also free charged particles which are able to produce heat by friction. The heat produced per volume can be described by the following equation, where the first term represents the dielectric heat and the second the joule heat.

$$p = \frac{E^2}{2} \pi f \epsilon \epsilon_0 \tan \delta + E^2 \sigma \quad (1)$$

dielectric heat + joule heat

- | | |
|------------------------------------|---------------------------------------|
| p = power | ϵ_0 = permittivity of vacuum |
| E = electric field | $\tan \delta$ = loss factor |
| f = frequency | σ = conductivity |
| ϵ = relative permittivity | |

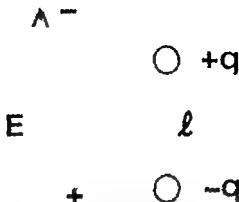


Fig. 3. Orientation of a dipole in an electric field (E). The positive and negative charges of the dipole (q) are separated by a distance l.

The ϵ value is a characteristic of the material and is determined by the force and number of dipoles per volume. Permanent dipoles, e.g. water are independent of an electric field. The value for the loss factor ($\tan \delta$) is determined by the friction of the dipoles.

By the conventional heating methods the surface of the material first becomes heated, and the deeper parts are then heated by means of conduction and convection. With microwave irradiation, electromagnetic energy passes into the material more rapidly and more uniformly than the passage of heat by conduction and convection. However the amount of microwave energy delivered decreases during penetration. From the following equation the depth at which the developed heat has decreased to 14% can be calculated.

$$\frac{c}{\pi f \sqrt{\epsilon} \tan \delta} = \text{depth of penetration} \quad (2)$$

c = velocity of light

f = frequency

ϵ = relative permittivity

$\tan \delta$ = loss factor

It is seen that the depth of penetration is inversely related to the frequency. The dielectric data change with frequency, temperature, and salt concentration. The depth of penetration into water at 2450 MHz is about 11 mm and in a solution of 0.1 M NaCl about 9 mm.

2.3 Sacrifice of small rodents by microwave irradiation

In study III a Husqvarna 241® oven with an effect of 1.3 kW and a frequency of 2450 MHz was used for sacrificing mice weighing about 20 g, by whole body exposure. The mouse was held in a plastic holder and placed in the middle of the oven as shown in Fig. 2a. The waves are reflected by the walls and thus penetrate from many directions. A mode stirrer "stirs" the waves and distributes them more uniformly. A simplified illustration of the process is given in Fig. 2a. A correlation was found between the duration of exposure and the brain temperature.

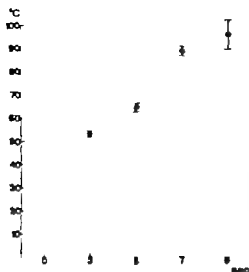


Fig. 4 Mice were sacrificed by whole body microwave irradiation (1.3 kW) for 3, 5, 7 or 9 s or by dislocation of the spine. The brain temperature was measured within 11 s. Each point represents the mean of 3-5 experiments. Vertical bars indicate S.E.

completion of the exposure (Fig. 4). The mice are dead after 3 s of exposure (brain temperature 53°C), while denaturation of proteins is found after 7 s of exposure (brain temperature 89°C). The body weight is crucial. The energy required to heat a mouse weighing 20 g from 38°C to 89°C within 7 s can be calculated from the following equation (Lin *et al* 1973)

$$W = \frac{\Delta T}{t} \frac{4186}{c} \rho \quad (3)$$

ΔT = change in temperature (°C)

W = absorbed power density (mW g⁻¹)

c = specific heat (J g⁻¹ °C⁻¹)

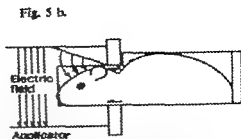
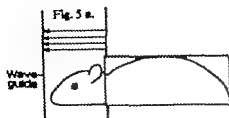
ρ = density (g cm⁻³)

t = time of exposure (s)

With $c = 0.83$ J g⁻¹ °C and $\rho = 0.96$ g cm⁻³ as given by Lin *et al* (1973) (using a phantom modelling material for brain tissue) it is found that 0.5 kW is required (38% of the 1.3 kW generated by the magnetron).

To be able to increase the brain temperature even more rapidly Stavinocha *et al* (1973) modified a conventional microwave oven and placed the animal so that the head lay in the centre of the waveguide and the microwaves were admitted on the top of the head (Fig. 5a). Essentially the same arrangement has since been used by Guidotti *et al* (1974), Heubrich and Wang (1976) and Schmidt (1976).

A microwave system (Mctabostat 4104² Gerling Moore, California, USA maximal power 5 kW 2450 MHz) specially built for sacrificing small rodents was used in studies III IV and VII (Figs. 2b, 3b). The animal holder consists of a small tube to hold the head and a larger one for the rest of the body. Only the small tube with the head can be inserted into the applicator (Fig. 5b). Owing to the design of the applicator the brain will be exposed preferentially to the microwaves. Microwaves that are not absorbed by the head



are reflected to a dummy load (containing water) in order to prevent damage to the magnetron by returning microwaves. To ensure that maximal power will be absorbed by the head, the impedance match between the power source and the head must be optimized. This adjustment (tuning) can be performed by exposing an animal to low-efficiency microwaves (10 mW) and adjusting the impedance screws on the applicator until a minimum of power is reflected toward the power source.

According to equation 3, the depth of penetration ($f=2450$ MHz) into the head will be about 1 cm.

As described in paper III, a brain temperature of $85-90^{\circ}\text{C}$ is obtained in the frontal cortex 10 s after termination of a 0.25 s exposure of 5 kW. A comparable brain temperature was obtained in the rat by Butcher *et al.* (1976) with the same type of instrument after 17 s of exposure. Theoretically (eq. 3), 17 kW is required to increase the temperature of the head of a mouse (2.5 g) by about 50°C in 0.25 s.

A somewhat different type of high power microwave instrument has recently been constructed by Stavinoha and co-workers (Modak *et al.* 1976). By exposure of the head of a mouse for 0.30 s a brain temperature of 90°C is obtained. With their instrument the microwaves are admitted on the top of the head. The instrument allows an individual adjustment of the impedance match for each mouse (Stavinoha 1976).

2.4 Brain temperatures following microwave irradiation

The relation between exposure time and brain temperature is shown in Fig. 4 and in paper III. It was not possible to measure the temperature at a shorter interval than 10 s after completion of the irradiation, as the animal had to be taken out of the animal holder, the vault of the skull removed and a thermistor probe inserted into the brain tissue to measure the temperature. The choice of probe is important. Probes with a large diameter tend to give lower temperature readings than those with a smaller diameter. A probe with a diameter of 0.5 mm was used. In study III a brain temperature of $85-90^{\circ}\text{C}$ was recorded in mice 10–11 s after completion of both whole body irradiation for 7 s (1.3 kW) and irradiation of the head for 0.25 s (5 kW). The temperature then decreased by about 5°C per 15 s during the interval 10 to 45 s after irradiation. It may therefore be assumed that the brain temperature might have been somewhat higher immediately after completion of irradiation. There was no difference in the time course of the brain temperature between the two methods of microwave exposure (paper III).

With the aim of discovering possible temperature gradients due to uneven heating of

the brain, the time course of the temperature was followed in different brain regions (paper III). The temperature was measured at four well-defined points at three different depths at intervals of 15 to 60 s after termination of exposure. Readings from different points at the same depth tended to show the same temperature. However readings from the superficial structures (depth 1 mm) were lower (about 10 per cent) than those from deeper structures (depth 1.5 mm, 2.5 mm). There are two possible explanations. Central parts, such as the striatum, may be more efficiently heated than outer parts, such as the cortex and medulla oblongata. This could happen after irradiation of the head with the microwaves "focused" on the head. However these lower outer temperatures were found after both types of exposure (paper III, Nordberg 1976, unpublished observations). The second explanation therefore seems more plausible, namely that the superficial parts cool more rapidly. However this is to some extent speculative, as temperature gradients may have occurred before the first time point of measurement. These possible gradients might have been levelled out by conduction of heat during the initial 10–15 s.

In studies III, IV and VII the brain temperature was measured routinely in all animals at a well-defined site. Only brain tissues with a temperature of 85–90°C were included in further analyses (about 2/3 of the irradiated animals).

2.5 Enzyme inactivation following microwave irradiation

Most enzymes are thermolabile and irreversibly inactivated at high temperatures. Studies have shown that acetylcholinesterase (AChE) is completely inactivated at 70°C (Silver 1974) and incubation of brain homogenates at 90°C for some seconds inactivates both AChE and choline acetyltransferase (CAT) (Stavinoha *et al.* 1973). Following microwave irradiation of the mouse or rat, almost complete inactivation of brain CAT and AChE has been noted when the brain temperature has increased to 70–90°C (Schmidt *et al.* 1972, Stavinoha *et al.* 1973, Butcher *et al.* 1976, Schmidt 1976 paper III).

It is a disadvantage that the enzyme activities cannot be measured at the very instant of completion of microwave irradiation. In study III the enzyme activities were measured 1–2 min after termination of irradiation. With use of the low power instrument (paper III) it cannot be excluded that the enzymes might be active during a part of the 7 s exposure time. The enzyme activities might even be accelerated during some part of the temperature increase. This is very difficult to measure. In addition it is possible that the enzymes may be more stable *in vivo* than can be observed in studies *in vitro* (for CAT see Prempeh *et al.* 1972). From this point of view it would seem advantageous to shorten the irradiation time from 7 s to 0.25 s.

The influence of the time of enzyme inactivation on values of ACh and Ch in brain tissue was investigated in study III by using three methods of sacrifice, viz. *dislocation of the spine* (7 min before inactivation of enzymes in trichloroacetic acid (TCA)), *whole body microwave irradiation for 7 s* (1.3 kW brain temperatures 85–90°C 11 s after completion of irradiation), and *irradiation of the head for 0.25 s* (5 kW; 85–90°C 10 s

after completion of irradiation). Although it is not known whether the time of enzyme inactivation is absolutely identical with the duration of microwave irradiation, the three inactivation times will be referred to in the following as 7 min, 7 s and 0.25 s.

3. Steady State Levels of Acetylcholine in Brain Tissue

Decapitation with rapid dissection, and freezing in liquid nitrogen (N_2), have until recently been the methods of sacrifice for measurement of the steady state concentrations of ACh in the brains of small rodents. From the time of decapitation until the brain tissue is homogenized and extracted in an acid medium, the enzymes acetylcholinesterase (AChE) and choline acetyltransferase (CAT) are active and may cause changes in the ACh level *post mortem*. The time that elapses before the enzymes are inactivated is therefore probably critical. The time taken for decapitation, dissection and homogenization of whole mouse or rat brain cannot be reduced to less than 30–60 s. The interval before enzyme inactivation can be shortened somewhat by freezing. The brain is frozen *in situ* by dropping the whole animal into liquid nitrogen (-196°C), or the animal is decapitated and the head frozen. The time required for freezing depends on the size. The superficial parts of the brain are cooled more rapidly than the deeper parts. Takahashi and Aprison (1964) immersed rats weighing about 200 g into liquid nitrogen and found that the temperature of the cerebral cortex had dropped to 0°C after 24–40 s, while in the thalamus the corresponding time was 68–83 s. On submersion of the head and thorax a temperature of 0°C was reached in the thalamus after only 31 s (Stavinoha *et al.* 1967). Mice are cooled more rapidly and the cerebral cortex, thalamus, and pons medulla reach a temperature of 0°C after 2–4 s, 6–13 s and 13–24 s, respectively (Ferrendelli *et al.* 1972).

Recently brain blowing has been developed (Veech and Hawkins 1974). By an air blast (1–1.5 atm. pressure), the brain tissue between the olfactory bulbs and the superior colliculi is removed and frozen in liquid nitrogen. The whole procedure takes less than 1 s.

To be able to dissect the brain into different regions, Takahashi and Aprison (1964) introduced the near freezing technique. By dipping the rat into liquid nitrogen for only 10 s, the brain is cooled to almost 0°C without being frozen.

Table I summarizes data from the literature on ACh in whole brain following four different methods of sacrifice, namely decapitation, freezing, near freezing, and brain blowing. It is seen that values ranging from 7 to 31 nmol g⁻¹ brain tissue have been reported and results obtained by different research groups have varied even when the same method of sacrifice has apparently been used. However different extraction media have been used and this is another parameter which might influence ACh values. Toru and Aprison (1966) found higher values in rat brain tissue extracted with formic acid-acetone (31.2 nmol g⁻¹) than when acid-ethanol (21.6 nmol g⁻¹) or trichloroacetic acid (15.1 nmol g⁻¹) was used. Domino *et al.* (1976) reported higher values with acetonitrile (25.8 nmol g⁻¹) than with acid-ethanol (18.7 nmol g⁻¹).

The method of assay is a third parameter which may affect ACh values. Until ten

years ago, ACh was mainly assayed by biological methods, using such tissues as guinea-pig ileum, the dorsal muscle of the leech and the frog rectus abdominis muscle, for example. Several chemical, gas chromatographic, and radioenzymatic methods have recently been developed. The different assay methods available are listed in Table II, together with the sensitivity limit for each method. As seen in Table I, Stavinocha and Ryan (1965) and Domino *et al.* (1976), when using the same extraction media, obtained higher ACh values in rat brain by gas chromatography (21.0 nmol g^{-1} 18.7 nmol g^{-1}) than by use of guinea-pig ileum (14.6 nmol g^{-1}) and frog rectus abdominis muscle (9.5 nmol g^{-1}).

Differences in species, strain, age and the time of day of sacrifice are further parameters that may influence the ACh values (Sackens *et al.* 1973a, Hann *et al.* 1970, Saito *et al.* 1975). Hann *et al.* (1970) reported a higher ACh content in rat whole brain during the light period of the day (39.6 nmol g^{-1} 2 h of light) than during the dark period (20.5 nmol g^{-1} 6 h of darkness). This diurnal variation was only observed in decapitated rats and not in rats frozen in liquid nitrogen.

For measuring the ACh content in discrete brain regions both decapitation and near freezing have been used. Decapitation followed by dissection of the brain into regions increases the time interval before enzyme inactivation by minutes. More rapid inactivation should be obtained by the near freezing method (Aprison and Takahashi 1964). Table III summarizes some data on ACh in different brain regions obtained by these two methods of sacrifice. No clear difference between the methods is seen and the values vary considerably even with the same method. In the striatum, for example, ACh contents from 23 nmol g^{-1} (rat) to 40 nmol g^{-1} (mouse) have been obtained.

Thus several factors may influence the measured ACh values, and none of them can be disregarded as unimportant (Tables I–III). To improve one of these parameters, the time of enzyme inactivation, the use of the microwave technique as a rapid method of sacrifice has increased progressively during recent years (Stavinocha *et al.* 1970, 1973 1974 Schmidt *et al.* 1972, Sethy *et al.* 1973 Butcher and Butcher 1974 1976, Grudotti *et al.* 1974 Longoni *et al.* 1974 Haubrich *et al.* 1975 Freeman *et al.* 1975 Racagni *et al.* 1974 Nordberg and Sandwall 1975 Atweh and Kuhar 1976 Modak *et al.* 1976, Sethy 1976, Speth *et al.* 1976, Zeila *et al.* 1976, Cohen and Wurtman 1976, Karlén *et al.* 1976, papers III, IV VII).

Table IV presents a summary of published values for ACh in whole brain following alternative methods of microwave irradiation. Values for mouse and rat brain vary from 18–29 and 20–25 nmol g^{-1} respectively. The values obtained by microwave irradiation are usually somewhat higher than those obtained after decapitation.

There appears to be no clear cut relationship between presumed inactivation time and ACh content in whole brain. The values reported by Stavinocha *et al.* (1973) and Modak *et al.* (1976) are almost identical (25.5 nmol g^{-1} and 24.2 nmol g^{-1}) (mouse) despite the differences in power source and exposure time (1.2 kW for 6 s and 6 kW for 0.30 s).

Stavinocha *et al.* (1973) found an approximately 80 per cent higher content of ACh (25.4 nmol g^{-1}) in rats following head irradiation (1.2 kW) for 6 s than following decapitation ($13.18 \text{ nmol g}^{-1}$). Freeman *et al.* (1975) noted a 20 per cent higher ACh

TABLE I. Endogenous ACh in whole body - comparison of published values (nmol g⁻¹)

Method of sacrifice	Species	Extraction media	Assay method	Content of ACh	Reference
Decapitation	Rat	Acid leech Ringer phosphate veronal	Leech muscle	19.0 ± 2.8 (S.D.)	Elkott and Henderson 1951
	Mouse	Potassium acid	Radioenzymatic	16.1 ± 1.1 (S.E.)	Frerguson and Sackem 1969
	Rat		Gas chromatography	28.9 ± 2.95 (S.D.)	Hagan et al. 1970
	Rat			20.2 ± 2.9 (S.E.)	Sethy et al. 1973
	Mouse		Mass fragmentography	16.1 ± 0.3 (S.E.)	Karlén et al. 1975
	Rat		Fluorometric	11.5 ± 2.4 (S.D.)	Browning 1972
	Rat	Acid-ethanol	Bleedway Heart of class	15.2 ± 1.88 ^a (S.D.)	Takahashi and Aperia 1964
	Rat		Guinea pig liver	14.6 ± 0.6 (S.D.)	Starvinola and Ryan 1965
	Rat		Gas chromatography	21.0 ± 0.5 (S.D.)	Starvinola and Ryan 1965
	Rat			18.7 ± 0.4 (S.L.)	Donaleo et al. 1976
	Rat		Frog rectus abdominis	9.5 ± 0.5 (S.E.)	Donaleo et al. 1976
	Mouse	Total acid-acetone	Radioenzymatic	9.0 ± 0.8 (S.E.)	Sackem et al. 1970
	Rat	Trichloroacetic acid	Gas chromatography	13.7 ± 1.70 (S.D.)	Starvinola et al. 1973
	Mouse		Leech muscle	14.4 ± 0.57 (S.E.)	Nordberg and Sandwall 1975 (Paper 1)
	Rat	Boiling acid Ringer + urichloroacetic acid	Frog rectus abdominis	15.7 ± 0.9 ^b (S.D.)	Garnica and Pepes 1962
	Rat	Acetonitrile	Galera pig liver	24.8	Szilagyi et al. 1972
	Rat		Gas chromatography	26.4	Szilagyi et al. 1972
	Rat			25.8 ± 0.4 (S.E.)	Donaleo et al. 1976
	Rat	Buffered saline	Frog rectus abdominis	6.7 ± 0.7 (S.D.)	Richter and Crowland 1949
Freezing	Rat		Leech muscle	8.5 ± 1.5 (S.D.)	Richter and Crowland 1949

	Rat	Acid malino-oxalate	Frog rectus abdominals	17.1 ± 1.9	(S.D.)	Crowland et al. 1955
	Rat	Exhausted saline		15.0 ± 1.6	(S.D.)	Takizuki et al. 1961
	Rat	Trichloroacetic acid		7.0 ± 1.9	(S.D.)	Richter and Crowland 1949
	Rat		Cat blood plasma	10.9 ± 2.4	(S.D.)	Richter and Crowland 1949
	Mouse		Leach ascites	17.4 ± 1.0	(S.E.)	Lundholm and Speer 1975
	Rat	Acid-ethanol	Gulben p/g flexus	15.1 ± 0.6	(S.D.)	Tors and Aprison 1966
	Rat		Heart of clam	18.7 ± 1.25 ^d	(S.D.)	Takizuki and Aprison 1964
	Rat		Frog rectus abdominals	15.8 ± 0.3	(S.E.)	Domino et al. 1976
	Rat	Formic acid-acetone	Gulben p/g flexus	21.6 ± 1.1 ^d	(S.D.)	Tors and Aprison 1966
	Rat			31.2 ± 1.5 ^d	(S.D.)	Tors and Aprison 1966
	Rat	Perchloric acid	Radioenzymatic	26.5 ± 2.2	(S.E.)	Aprison et al. 1974
	Rat		Gas chromatography	15.8 ± 0.77	(S.E.)	Hazin et al. 1970
	Rat	Acid-ethanol	Heart of clam	18.7 ± 1.58 ^d	(S.D.)	Takizuki and Aprison 1964
	Rat	Formic acid-acetone	Radio-enzymatic	25.7 ± 0.9	(S.E.)	Aprison et al. 1974
	Rat			24.2 ± 1.1	(S.E.)	Sarlsen et al. 1973a
	Mouse			14.5 ± 1.0	(S.E.)	Sarlsen et al. 1973a
	Rat	Acetonitrile + trichloroacetic acid	Gas chromatography	19.5 ± 1.2 ^c	(S.D.)	Vocch and Hawkins 1974
	Rat	Perchloric acid a/l. formic acid-acetone		12 ± 1.8 ^d	(S.E.)	Goldetti et al. 1974
Nose freezing						
Brain blowing						

^d Excluding carboxyls, methyl oblongita, procs

^b Excluding carboxyls

^c Brain tissue between the olfactory bulbs and the superior colliculi

TABLE II *Methods for ACh assay*

	Sensitivity pmol	Reference
Frog rectus abdominis	200 - 1000	Marchbank 1975
"	25	Whittaker 1963
Leech muscle	5	Whittaker 1963
Guinea pig serum	10	Whittaker 1963
Cat blood pressure	5 - 10	Whittaker 1963
Venous heart	0.5	Whittaker 1963
Radioenzymatic	<100	Hamberich and Reid 1974
"	2	Goldberg and McCann 1974
"	20	Aprison et al. 1974
"	10	Sackens et al. 1973a
Gas chromatography demethylation	50	Jenden and Hanin 1974
Gas chromatography pyrolysis	14 - 138	Green and Schlegel 1974
Gas chromatography ion pair extraction, demethylation	1000	Karlén et al. 1974
Mass fragmentography ion pair extraction, demethylation	5	Karlén et al. 1974
Polarographic	100	Maslove 1974
Fluorometric	500	Speeg 1974
	100	Browning 1972

content (22.4 nmol g^{-1}) after head irradiation (5 kW) for 1.2 s than after decapitation (18.6 nmol g^{-1}). However following whole body irradiation of rats for 40 s Sethy *et al.* (1973) found no significant change in the ACh content (22.2 nmol g^{-1}) as compared with rats killed by decapitation (20.2 nmol g^{-1}).

ACh levels in mouse *brain regions* were measured with variations in the time of enzyme inactivation (7 min, 7 s and 0.25 s; paper III). A markedly higher value was obtained with an interval of 0.25 s than with a 7 s interval (Table V). All variables, except the method of sacrifice, were kept constant. Following whole body irradiation (7 s, 1.3 kW) a significant increase in ACh was obtained only in the cortex (+ 39%). After the more efficient irradiation (0.25 s), the increase in cortex was markedly higher (+ 83%) and, moreover significantly higher values were obtained in the striatum (+ 103%), medulla oblongata (+ 47%), and midbrain (+ 39%) in comparison with decapitated animals. A markedly higher ACh content has also been found by Weintraub *et al.* (1976) in the striatum and cortex following head irradiation of rats (6 s, 1.2 kW) in comparison with decapitation. In the other brain regions, however lower ACh values were obtained in irradiated rats (Weintraub *et al.* 1976).

Table VI summarizes values for ACh in brain regions obtained by various research groups using different types of microwave equipment and different procedures.

TABLE III. Steady state concentrations of endogenous ACh in different brain regions - comparison of published values (nmol g⁻¹)

Endogenous ACh nmol g ⁻¹	Takahashi and Ageton 1964	Campbell and Jeandem 1970	Selby <i>et al.</i> 1973	Neuberg and Burchwell 1975 (Paper I)	Cosato <i>et al.</i> 1976
Method of sacrifice and analysis	New freezing- blotting heart of chas- vans mar- saria	Decapitation, postmorte - 5% C ₁₀ gas chromato- graphy	Decapitation, postmorte - 5% C ₁₀ gas chromato- graphy	Dissection of the spine, blotting beach article	Decapitation + near freezing rad locomotion sawing
Brain region	Rat M ⁻ ± S.D.	Rat M ⁻ ± S.E.	Rat M ⁻ ± S.E.	Mouse M ⁻ ± S.E.	Rat M ⁻ ± S.E.
Cerebellum	2.3 ± 0.74	4.1 ± 0.5	4.7 ± 0.5	4.3 ± 0.30	3.7 ± 0.5
Brain stem		Mitochondria-post- medulla			
Olfactory bulb (oblongata)	12.3 ± 2.39	22.6 ± 2.6	20.0 ± 0.8	21.6 ± 0.65	Diencephalon 24.0 ± 0.4
Midbrain	Diencephalon 22.3 ± 1.84	Thalamus 31.7 ± 2.0	27.7 ± 1.3	20.7 ± 1.47	Metencephalon 19.2 ± 1.0
Hypothalamus	Metencephalon 14.7 ± 2.68	20.5 ± 1.3	34.0 ± 3.8	-	28.8 ± 0.7
Striatum	37.3 ± 2.69	23.2 ± 3.8	37.0 ± 3.1	40.1 ± 1.71	18.4 ± 0.7
Hippocampus	-	-	20.4 ± 2.0	17.0 ± 0.90	13.9 ± 0.7
Cortex	-	13.5 ± 1.6	9.8 ± 1.2	13.3 ± 0.95	

TABLE II *Methods for ACh assay*

	Sensitivity pmol	Reference
Frog rectus abdominis	200 - 1000	Marchbank 1975
"	25	Whittaker 1963
Leech muscle	5	Whittaker 1963
Guinea pig ileum	10	Whittaker 1963
Cat blood pressure	5 - 10	Whittaker 1963
Venous heart	0.5	Whittaker 1963
Radioenzymatic	<100	Haubrich and Reid 1974
	2	Goldberg and McCann 1974
	20	Aprison et al. 1974
	10	Sachdev et al. 1973a
Gas chromatography demethylation	50	Jenden and Hanin 1974
Gas chromatography pyrolysis	14 - 138	Green and Szilagyi 1974
Gas chromatography ion pair extraction, demethylation	1000	Karlén et al. 1974
Mass fragmentography ion pair extraction, demethylation	5	Karlén et al. 1974
Polarographic	100	Matlova 1974
Fluorometric	500	Speeg 1974
	100	Browning 1972

content (22.4 nmol g⁻¹) after head irradiation (5 kW) for 1.2 s than after decapitation (18.6 nmol g⁻¹). However following whole body irradiation of rats for 40 s Sethy *et al.* (1973) found no significant change in the ACh content (22.2 nmol g⁻¹) as compared with rats killed by decapitation (20.2 nmol g⁻¹).

ACh levels in mouse *brain regions* were measured with variations in the time of enzyme inactivation (7 min, 7 s and 0.25 s paper III). A markedly higher value was obtained with an interval of 0.25 s than with a 7 s interval (Table V). All variables, except the method of sacrifice, were kept constant. Following whole body irradiation (7 s, 1.3 kW) a significant increase in ACh was obtained only in the cortex (+ 39%). After the more efficient irradiation (0.25 s), the increase in cortex was markedly higher (+ 83%) and, moreover significantly higher values were obtained in the striatum (+ 103%), medulla oblongata (+ 47%), and midbrain (+ 39%) in comparison with decapitated animals. A markedly higher ACh content has also been found by Weintraub *et al.* (1976) in the striatum and cortex following head irradiation of rats (6 s, 1.2 kW) in comparison with decapitation. In the other brain regions, however lower ACh values were obtained in irradiated rats (Weintraub *et al.* 1976).

Table VI summarizes values for ACh in brain regions obtained by various research groups using different types of microwave equipment and different procedures.

TABLE III. Steady state concentrations of endogenous ACh in different brain regions — comparison of published values (nmol g^{-1})

Endogenous ACh nmol g^{-1}	Takahashi and Aprison 1964	Campbell and Jennison 1970	Batley <i>et al.</i> 1973	Nordberg and Sundvall 1975 (Paper I)	Corrado <i>et al.</i> 1976
Method of synthesis and analysis	New freezing bloomy heart of clean, young mice	Decapitation, perfuse -5°C , gas chromatog- raphy	Decapitation, perfuse -5°C , gas chromatog- raphy	Dislocation of the spine, bloomy fresh muscle	Decapitation + new freezing and biochemical study
Brain region	Rat $M\bar{V} \pm S.D.$ 2.3 ± 0.74	Rat $M\bar{V} \pm S.E.$ 4.1 ± 0.5	Rat $M\bar{V} \pm S.E.$ 4.7 ± 0.5	Mouse: $M\bar{V} \pm S.E.$ 4.3 ± 0.30	Rat $M\bar{V} \pm S.E.$ 3.7 ± 0.5
Cerebellum		Midbrain-pont- medulla			
Brain stem (Medulla oblongata)	12.3 ± 2.39	22.6 ± 2.6	20.0 ± 0.8	21.6 ± 0.65	
Midbrain	Diencephalon 22.3 ± 1.84	Thalamus 21.7 ± 2.0	27.7 ± 1.3	20.7 ± 1.47	Diencephalon 24.0 ± 0.4
Hypothalamus	Mesencephalon 16.7 ± 2.68	20.5 ± 1.3	34.0 ± 3.8	—	Mesencephalon 19.2 ± 1.0
Striatum	37.5 ± 2.69	23.2 ± 3.8	37.0 ± 3.1	40.1 ± 1.71	28.8 ± 0.7
Hippocampus	—	—	20.4 ± 2.0	17.0 ± 0.90	18.4 ± 0.7
Cortex	—	13.5 ± 1.6	9.8 ± 1.2	13.3 ± 0.95	13.9 ± 0.7

TABLE IV: Steady state concentrations of endogenous ACh in whole brain following sacrifice by microwave irradiation - comparison of published values ($\mu\text{mol g}^{-1}$)

Microwave irradiation	Extraction media	Assay method	Acetylcholine ($\mu\text{mol g}^{-1}$) $M \pm S.E.$	Reference
Whole body irradiation				
Rat (242 g); 1.25 k W; 20 \pm 8.5 $^{\circ}\text{C}$ (15-20 s after completion of irradiation)	acetonitrile + TCA	gas chromatography	19.91 ± 0.91	Schmidt et al. 1972
Head irradiation				
Rat (225-275 g); 40 g; 1.2 k W	perchloric acid	gas chromatography	22.2 ± 3.2	Sethy et al. 1973
Rat (100-200 g); 1.2 k W; 6 \pm 9.2 $^{\circ}\text{C}$	acetonitrile + TCA	gas chromatography	25.4 ± 1.49 (S.D.)	Starinova et al. 1973
Mouse (18-22 g); 1.2 k W; 3 \pm 8.5 $^{\circ}\text{C}$	acetonitrile + TCA	gas chromatography	25.5 ± 2.63 (S.D.)	Starinova et al. 1973
Rat (200-280 g); 5 k W; 1.2 g	formic acid-acetone	gas chromatography/ mass spectrometry	22.4 ± 1.4	Freeman et al. 1975
Mouse (20-25 g); 1.3 k W; 3-3.6 g	formic acid-acetone	radioenzymatic	29 ± 3	Hasbrieh and Wang 1976
Mouse (20-25 g); 2.0 k W; 1.4 g	perchloric acid	gas chromatography	18 ± 0.56	Trebacchi et al. 1975
Mouse (19-26 g); 2.5 k W; 0.62 g	perchloric acid	mass fragmentography	26.1 ± 4.1 (S.D.)	Karika et al. 1976
Mouse (20-30 g); 6 k W; 0.300 \pm 90 $^{\circ}\text{C}$	formic acid-acetone	pyrolysis-gas chromatography	24.2 ± 1.8 (S.D.)	Modak et al. 1976

TABLE V: Endogenous ACh and Ch (nmol g⁻¹) in different mouse brain regions following 3 months of microflora.

	Acetylcholine		Choline	
	Dyslocation of the axons		Microwave irradiation	
		Whole body 7 g	Head 0.25 g	Whole body 7 g
Cerebellum	3.7 ± 0.38 (11)	4.6 ± 0.97 (3)	5.2 ± 1.05 (4)	39.0 ± 4.49 (6)
Medulla oblongata	19.8 ± 1.07 (12)	20.8 ± 3.01 (3)	29.1 ± 1.10 (4)***	44.0 ± 7.24 (5)
Midbrain	21.1 ± 1.24 (14)	23.2 ± 1.47 (5)	29.4 ± 1.65 (4)***	39.3 ± 4.76 (7)
Pons	37.1 ± 2.06 (14)	40.4 ± 3.73 (5) ^a	73.3 ± 1.84 (3)***	48.8 ± 6.50 (6)
Hypothalamus	15.8 ± 0.83 (14)	17.1 ± 1.77 (5)	20.8 ± 2.25 (4)	43.8 ± 5.37 (6)
Cortex	13.2 ± 0.74 (12)	18.4 ± 1.55 (5)***	24.2 ± 1.52 (4)***	30.4 ± 2.80 (6)

MF ± S.E. (n) number of experiments. * p<0.05 ** p<0.01, *** p<0.001

^a In an additional sample 70.3 nmol g⁻¹

^b In an additional sample 48.7 nmol g⁻¹

TABLE VI. *Steady state concentrations of endogenous ACh in different brain regions following*

Endogenous acetylcholine nmol g ⁻¹	Schmidt et al., 1972	Nordberg and Sundwall 1976 (Paper III)	Stravinska et al., 1973 1974
Method of microwave irradiation, tissue extrac- tion and analysis	WHOLE BODY	IRRADIATION	HEAD
	Rat (115 g) 1.25 kW 15 s, 96° (15–20 s after completion of irradiation)	Mouse (18–22 g); 1.3 kW 7 s; 88– 89° C (11 s after completion of irradiation)	Rat (200–250 g); 1.2 kW 6 s; 92° C;
	acetonitrile + TCA gas chromatography	TCA leech muscle	formic acid- acetone pyrolysis-gas chromatography
Brain region	M \bar{x} ± S.E.	M \bar{x} ± S.E.	M \bar{x} ± S.D.
Cerebellum	6.55 ± 0.93	4.6 ± 0.97	7.2 ± 2.0
Brain stem (Medulla oblongata)	27.37 ± 1.22	20.8 ± 3.01	30.9 ± 4.7
Midbrain	30.69 ± 1.22	23.2 ± 1.47	—
Hypothalamus	34.12 ± 1.67	—	—
Striatum	46.96 ± 2.22	40.4 ± 3.73	55.4 ± 4.7
Hippocampus	24.24 ± 0.51	17.1 ± 1.77	25.8 ± 2.7
Cortex	18.95 ± 0.46	18.4 ± 1.55	21.1 ± 3.0

Although the values for the striatum vary between 40 and 88 nmol g⁻¹ it is worthy of note that values from 77 to 88 nmol g⁻¹ have been obtained with the presumably more efficient equipment (5 to 6 kW).

sacrifices by microwave irradiation — comparison of published values ($\mu\text{mol g}^{-1}$)

Modak et al., 1976	Schmidt, 1976	Zafra et al., 1976	Butcher et al., 1976	Nordberg and Sandwall, 1977 (Paper IV)
-----------------------	---------------	-----------------------	-------------------------	---

IRRADIATION

Mouse (20–30 g); 6 kW 0.300 s; 90°C;	Rat (150–200 g); 1.25 kW 2.5 s; 95°C;	Rat (100–120 g); 2.0 kW 2 s;	Rat (230–250 g); 5 kW 1.7 s; 87°C;	Mouse (20–24 g), 5 kW 0.25 s; 85°C; (10 s after completion of irradiation)
formic acid-acetone pyrolysis-gas chromatography	toluene-ether pyrolysis-gas chromatography	perchloric acid gas chromatography	formic acid-acetone, gas-chromatography/mass spectrometry	TCA leech muscle
$\text{M}\bar{\text{v}} \pm \text{S.D.}$	$\text{M}\bar{\text{v}} \pm \text{S.E.}$	$\text{M}\bar{\text{v}} \pm \text{S.E.}$	$\text{M}\bar{\text{v}} \pm \text{S.E.}$	$\text{M} \pm \text{S.E.}$
16.6 \pm 2.4	6.8 \pm 0.2	—	6.3 \pm 0.6	5.2 \pm 1.05
44.1 \pm 1.9	31.9 \pm 1.2	34 \pm 2.0	31.9 \pm 0.9 (including milkbinder)	29.1 \pm 1.10
33.8 \pm 2.2	35.3 \pm 2.0	—	—	29.0 \pm 1.80
—	32.3 \pm 1.3	—	31.3 \pm 1.0	—
81.0 \pm 1.9	64.4 \pm 2.1	31 \pm 1.9	88.3 \pm 4.0	76.8 \pm 1.78
31.0 \pm 1.9	29.0 \pm 0.6	25 \pm 1.6	28.4 \pm 0.9	21.2 \pm 2.32
25.7 \pm 3.4	27.6 \pm 1.3	16 \pm 1.2	21.8 \pm 1.0	24.8 \pm 1.44

4. Steady State Levels of Choline in Brain Tissue

The values reported for free Ch in brain vary considerably. Sparf (1973) summarizes the data for free Ch published up to 1973. Values ranging from 600 nmol g⁻¹ (Smith and Saelens 1967) to 21.5 nmol g⁻¹ (Eade *et al.* 1973) are given. It has been suggested that the rapid *post mortem* increase in free Ch (Schuberth *et al.* 1970a) is caused by a breakdown of glycerylphosphorylcholine and/or phosphatidylcholine (Dross and Kewitz 1972, Dross 1975) or to interruption of the venous drainage (Kewitz *et al.* 1973). The lowest values, 21.5–35.0 nmol g⁻¹ (Eade *et al.* 1973) and 39.3 nmol g⁻¹ (Ewetz *et al.* 1970), were obtained after sacrifice by total freezing and are in fairly good agreement with the value obtained by extrapolation of the *post mortem* increase in Ch (27.5 nmol g⁻¹ Dross and Kewitz 1972) and the *in vivo* concentration of Ch calculated by Hanin and Schuberth (30–40 nmol g⁻¹) from data on dilution of the brain Ch pool by deuterium-labelled Ch (d-Ch).

Near freezing tends to give higher Ch values (64.0 nmol g⁻¹ Aprison *et al.* 1974). Following microwave irradiation of the head values of 26.3 nmol g⁻¹ (Stavitskha and Weintraub 1974) and 24.2 nmol g⁻¹ (Freeman *et al.* 1975) for the rat and 28 nmol g⁻¹ (Hanbrich and Wang 1976), 33 nmol g⁻¹ (Trabucchi *et al.* 1975), 32.4 nmol g⁻¹ (Nordberg 1975 unpublished observation) and 49.1 nmol g⁻¹ (Karlén *et al.* 1976) for the mouse have been obtained.

Data for Ch in different brain regions following microwave irradiation are given in Table VII. Values between 14 and 45 nmol g⁻¹ have been reported. There is no consistent difference between brain regions. The Ch contents of the striatum given in Table VII are much lower than those obtained after decapitation and freezing (152.5 nmol g⁻¹ Butcher *et al.* 1976, 127 nmol g⁻¹ Sethy *et al.* 1973, 96.1 nmol g⁻¹ Ladinsky *et al.* 1976). In study III no marked difference in the Ch contents of different brain regions was found when the time of microwave exposure was reduced from 7 s to 0.25 s.

TABLE VII. Steady state concentrations of endogenous ^{22}Na in different brain regions following sacrifice by irradiation of the head - comparison of published values (nmol g^{-1})

Microvire irradiation	Sizemba et al., 1973 1974 Rat: 1.2 kW- 6 $\leq 92^\circ\text{C}$ $\text{M} \pm \text{S.D.}$	Schmidt, 1976 Rat: 1.25 kW- 2.5 $\leq 95^\circ\text{C}$ $\text{M} \pm \text{S.E.}$	Bulcher et al., 1976 Rat: 5 kW- 1.7 $\leq 87^\circ\text{C}$ $\text{M} \pm \text{S.E.}$	Zaia et al., 1976 Rat: 2.0 kW- 2 \leq $\text{M} \pm \text{S.E.}$	Norberg and Sandwell 1976b (Paper IV) Monkey: 5 kW 0.25 $\leq 85^\circ\text{C}$ $\text{M} \pm \text{S.E.}$
Brain regions					
Cerebellum	17.6 \pm 4.2	30.0 \pm 1.8	17.1 \pm 2.7	-	32.8 \pm 4.63
Brain stem (Medulla oblongata)	34.7 \pm 5.8	29.3 \pm 1.8	14.3 \pm 0.4 (excluding subdura)	36 \pm 4.4	43.8 \pm 4.30
Midbrain	-	28.1 \pm 1.6	-	-	33.8 \pm 3.56
Hypothalamus	-	28.2 \pm 2.1	26.9 \pm 0.4	-	-
Striatum	43.0 \pm 1.7	32.0 \pm 1.5	24.9 \pm 1.7	39 \pm 3.4	38.2 \pm 3.11
Hippocampus	36.0 \pm 9.7	24.0 \pm 1.4	26.3 \pm 1.5	45 \pm 5.5	28.2 \pm 3.18
Cortex	22.1 \pm 1.8	28.4 \pm 2.5	17.6 \pm 2.6	26 \pm 3.5	33.8 \pm 3.34

4. Steady State Levels of Choline in Brain Tissue

The values reported for free Ch in brain vary considerably. Sparf (1973) summarizes the data for free Ch published up to 1973. Values ranging from 600 nmol·g⁻¹ (Smith and Sæviens 1967) to 21.5 nmol·g⁻¹ (Eade *et al.* 1973) are given. It has been suggested that the rapid *post mortem* increase in free Ch (Schuberth *et al.* 1970a) is caused by a breakdown of glycerylphosphorylcholine and/or phosphatidylcholine (Dross and Kewitz 1972, Dross 1975) or to interruption of the venous drainage (Kewitz *et al.* 1973). The lowest values, 21.5–35.0 nmol·g⁻¹ (Eade *et al.* 1973) and 39.3 nmol·g⁻¹ (Ewetz *et al.* 1970), were obtained after sacrifice by total freezing and are in fairly good agreement with the value obtained by extrapolation of the *post mortem* increase in Ch (27.5 nmol·g⁻¹ Dross and Kewitz 1972) and the *in vivo* concentration of Ch calculated by Hann and Schuberth (30–40 nmol·g⁻¹) from data on dilution of the brain Ch pool by deuterium-labelled Ch (d-Ch).

Near freezing tends to give higher Ch values (64.0 nmol·g⁻¹ Aprison *et al.* 1974). Following microwave irradiation of the head values of 26.3 nmol·g⁻¹ (Stavimoha and Weintraub 1974) and 24.2 nmol·g⁻¹ (Freeman *et al.* 1975) for the rat and 28 nmol·g⁻¹ (Haubrich and Wang 1976), 33 nmol·g⁻¹ (Trabucchi *et al.* 1975), 32.4 nmol·g⁻¹ (Nordberg 1975 unpublished observation) and 49.1 nmol·g⁻¹ (Karlén *et al.* 1976) for the mouse have been obtained.

Data for Ch in different brain regions following microwave irradiation are given in Table VII. Values between 14 and 45 nmol·g⁻¹ have been reported. There is no consistent difference between brain regions. The Ch contents of the striatum given in Table VII are much lower than those obtained after decapitation and freezing (152.5 nmol·g⁻¹ Butcher *et al.* 1976, 127 nmol·g⁻¹ Sethy *et al.* 1973, 96.1 nmol·g⁻¹ Ladinsky *et al.* 1976). In study III no marked difference in the Ch contents of different brain regions was found when the time of microwave exposure was reduced from 7 s to 0.25 s.

TABLE VIII. Turnover rate $\int ACh$ (nmol g^{-1} min $^{-1}$) in whole brain determined by tracer techniques - comparison of published values

Turnover rate nmol g^{-1} min $^{-1}$	Species	Labelled precursor	Method of sacrifice	Reference
5	Mouse	Intravenous pulse injection of 25 μ mol kg^{-1} H-Ch	Decapitation	Schmobarth et al. 1970b
10				
20	Mouse	Intravenous pulse injection of 25 μ mol kg^{-1} H-Ch	Liq. N ₂	Sparf 1973
6.5	Mouse	Intravenous pulse injection of 35 μ mol kg^{-1} C-Ch	Liq. N ₂ 3.5 s	Saunders et al. 1974
14.8				
5	Mouse	Intravenous pulse injection of 20 μ mol kg^{-1} d ₄ -Ch	Decapitation + liq. N ₂	Jendren 1973 Jendren 1974 Jendren et al. 1974
7.5				
14; 7.9				
6	Mouse	Intravenous pulse injection of 5 μ mol kg^{-1} C-PtCh	Microwave irradiation of the head 1.4 s (2 kW)	Trabuacchi et al. 1975

5 Apparent Rate of Turnover of Acetylcholine in Brain Regions

5.1 Definitions

Turnover The renewal of a substance in a tissue at steady state.

Turnover rate The quantity of a substance in a tissue that is renewed per unit of time.

Turnover time The time taken for a whole pool of a substance present in a tissue to be renewed.

The principles for the use of radioactive precursors for measurements of turnover as formulated by Zilverman (1960) require the assumption of a system with the following properties

- it behaves like an open single compartment
- radioactive and endogenous substances are handled in the same way by the system
- no distinction is made by the system between old and newly synthesized substances
- existence of steady state conditions (the rate of synthesis of the substance equals the rate of disappearance).

5.2 Previous results

A summary of published values for turnover of ACh in whole brain or brain regions obtained by the use of tracer techniques is given in Tables VIII and IX. Values obtained by other means are summarized in Table X. With the tracer techniques the turnover rate in whole brain has varied between 1 and 20 nmol g⁻¹ min⁻¹ (Table VIII). Although different precursors, modes of sacrifice and methods of turnover calculations have been used, each research group has obtained at least one turnover value within the range of 5 to 8 nmol g⁻¹ min⁻¹. The value (38 nmol g⁻¹ min⁻¹) calculated by Richter and Crossland from the initial rate of resynthesis of ACh after partial depletion of ACh in the brain by electroshock is much higher than all other values given for the whole brain (Tables VIII, X). But it is rather close to the maximal capacity of CAT in 1 g brain tissue to synthesize ACh *in vitro* (60 nmol g⁻¹ Schrier and Shuster 1967). For different brain regions (Tables IX, X) turnover rates of between 1 and 55 nmol g⁻¹ min⁻¹ have been reported. The turnover rate seems to be highest in the striatum (6–55 nmol g⁻¹ min⁻¹), although the values differ between research groups (Table IX, X). It is, however, worth noting that the apparent turnover values obtained in paper study IV (Table IX, this survey) by a tracer technique and the values calculated by Stavinocha *et al.* (1976) (Table X) when the accumulation rate of ACh in different brain regions is measured after i.v. injection of dichlorvos (15 mg kg⁻¹) in rats are quite identical.

5.3 Biotransformation of radioactive choline in brain regions

Not only the steady state concentrations of ACh and Ch but also the kinetics of tracer doses of ³H Ch might be dependent on the time of enzyme inactivation. A comparison

TABLE VII. Turnover rate of ACh (nmol g⁻¹ min⁻¹) in whole brain determined by tracer techniques - comparison of published values

Turnover rate nmol g ⁻¹ min ⁻¹	Species	Labelled precursor	Method of sacrifice	Reference
5	Mouse	Intravenous pulse injection of 25 μ mol kg ⁻¹ H-Ch	Decapitation	Schubert et al. 1970b
10				
20	Mouse	Intravenous pulse injection of 25 μ mol kg ⁻¹ H-Ch	Liq N ₂	Spurr 1973
6.5				
16.8	Mouse	Intravenous pulse injection of 35 μ mol kg ⁻¹ C-Ch	Liq N ₂ 3.5 s	Sehrens et al. 1974
5				
7.5	Mouse	Intravenous pulse injection of 20 μ mol kg ⁻¹ d ₄ -Ch	Decapitation + liq N ₂	Jendren 1973 Jendren 1974 Jendren et al. 1974
1.4				
7.9				
6	Mouse	Intravenous pulse injection of 5.1 μ mol kg ⁻¹ C- ¹⁴ Ch	Microwave irradiation of the head 1.4 s (2 kW)	Tsiboev et al. 1975

TABLE IX. Turnover rate of ACh (nmol g⁻¹ min⁻¹) in different brain regions obtained by tracer techniques - comparison of published values

Brain region	Cerebellum	Brain stem	Midbrain	Striatum	Hippocampus	Cortex
Reference						
Labelled precursor						
Method of sacrifice						
Series <i>et al.</i> 1972b	-	5.0	8.4	-	-	20.9
1. infusion 0.016 μ mol kg ⁻¹ min ⁻¹ [11-C]ACh, i.v., decapitation						
Series <i>et al.</i> 1974	1.34	3.63	6.25	-	-	6.64
1. infusion 3.5 μ mol kg ⁻¹ [14-C]ACh, resuscitate N ₂ 3.5						
Ravenhill <i>et al.</i> 1974	-	1.5	-	21.7	-	3.3
1. infusion 0.63 μ mol kg ⁻¹ min ⁻¹ [3-C]ACh, 2-8 min, i.v., head irradiation, 2 s (2 kW)						
Cheney <i>et al.</i> 1975a	-	-	-	5.1	-	1.4
1.7 infusion 0.63 μ mol kg ⁻¹ min ⁻¹ [3-C]ACh, 6 min, i.v., head irradiation, 3 (2.5 kW)						
Zade <i>et al.</i> 1976	-	4.2	-	12.7	8.8	3.2
1.7 infusion 2.5 μ mol kg ⁻¹ min ⁻¹ [3-C]ACh, 6 min, i.v., head irradiation, 2 s (2 kW)						
Woodberg and Sundin 1977 (Paper IV)	(2)	10	11	55	21	27
1. infusion 0.75 μ mol kg ⁻¹ [11-C]ACh, mouse, head irradiation, 0.25 s (5 kW)						
Frederick <i>et al.</i> 1975		-	-	18	-	5
1. infusion 0.3 μ mol kg ⁻¹ [11-C]ACh, rat, head irradiation, 4.5 (1.3 kW)						

TABLE X. Turnover rate of ACh (nmol g⁻¹ min⁻¹) in brain tissue determined by non-tracer techniques - comparison of published values

Turnover rate nmol g ⁻¹ min ⁻¹	Brain tissue	Species	Method	Reference
3.8	Whole brain	Rat	Calculation of the initial rate of ACh re-synthesis after partial depletion of the ACh content in brain following electroshock	Richter and Cronlund 1949
1.2	Whole brain	Rat	Calculation of the rate of induced ACh depletion after an intraventricular dose of hemicholinium (20 µg)	Domboi and Wilson 1972
0.15	Cerebral cortex	Cat	Calculation of the rate of ACh release from the cortex when the synthesis of releasable ACh was blocked by topically applied hemicholinium (1 µg ml ⁻¹)	Szabo et al. 1970
49.5 27 18.5 14.8 7.7 7.2	Striatum Hippocampus Cerebral cortex Medulla-pons Midbrain Thalamus	Rat	Calculation of the <i>in vivo</i> acetylcholinesterase rates of ACh following treatment with diisopropyl (15 mg kg ⁻¹ i.v.)	Starisobya et al. 1976

tional properties and/or different access to AChE (Fig. 7). When animals are killed by decapitation the ACh released in the synaptic cleft at the moment of sacrifice will be rapidly destroyed by AChE in the cleft. Rapid inactivation of AChE and/or rapid tissue fixation might prevent the enzymatic hydrolysis of released ACh. Several studies indicate that newly synthesized ACh might be released preferentially (for review see MacIntosh and Collier 1976). This might explain the higher content of ^3H ACh after 7 s of microwave irradiation (preservation of a pool of ACh with high specific radioactivity pool b_2 , Fig. 7b). The higher steady state concentration of total ACh found after 0.25 s of microwave irradiation might represent an intraneuronal pool of ACh (very low specific radioactivity pool b_1 , Fig. 7a) that is destroyed by AChE unless the time of enzyme inactivation is extremely short, 0.25 s.

There is a corresponding decrease in ^3H -Ch content with increased content of ^3H ACh, but it is difficult to understand why there is no clear decrease in endogenous Ch with increased concentration of ACh.

A higher steady state concentration of ACh in rat brain was obtained by Hanin *et al.* (1970) during the light period of the day than during the dark period. Is this diurnal variation in ACh due to a change in the stable pool a or the labile pool b_1 of ACh (Fig. 7a)? The higher ACh values were found only in rats sacrificed by decapitation and not following freezing in liquid nitrogen (Hanin *et al.* 1970).

Endogenous ACh in the hippocampus was also found by Atweh and Kuhar (1976) to be more labile to destruction than ^3H ACh. Their data are, however, different from the results of the present study (paper III), since they found no change in the ratio ^3H ACh/ ^3H -Ch in rats sacrificed by microwave irradiation of the head for 3 s (1.3 kW) in comparison with decapitation. But they obtained a higher steady state concentration of ACh after microwave irradiation (28 nmol g $^{-1}$) than after decapitation (22 nmol g $^{-1}$).

5.5 Rate of turnover of acetylcholine in brain tissue determined by different methods of calculation

When the specific radioactivities (SA) of a precursor and a product are plotted at different time points after intravenous administration of the precursor the time courses of the SA of the precursor and product intersect at the maximum of the product SA. According to Zilversmit (1960) this is an important criterion (but not the only one) that must be fulfilled for establishment of such a relationship. The absence of this criterion is taken as a sign of non-existence of such a relationship.

Curves indicating a precursor-product relationship between Ch and ACh have been presented for whole brain by Dross and Kewitz (1972), Sparf (1973), Jenden *et al.* (1974) and Karlén *et al.* (1975) following sacrifice by decapitation and freezing in liquid nitrogen and by Cheney *et al.* (1975b) following microwave irradiation (2.5 kW 1 s).

Plots of the SA of Ch and ACh versus time in different brain regions with the two times of enzyme inactivation 7 s and 0.25 s are shown in Fig. 8a-b. Only at the shorter inactivation time is a precursor-product relationship indicated (papers III and IV). However in the cerebellum no relationship was found. The assumption of instant

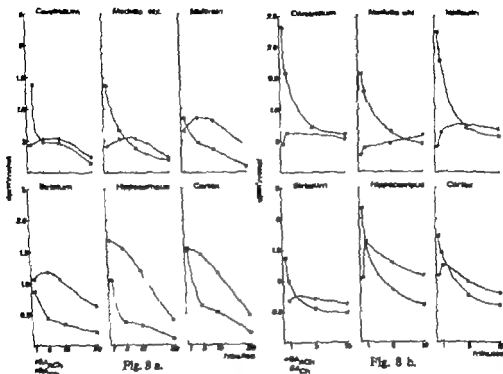


Fig. 8. The specific radioactivities of ACh and Ch are expressed as ^3H -ACh and ^3H -Ch in per cent of the total radioactivity (^3H to ^3H) per nmol endogenous ACh and Ch, respectively.

TABLE XI. Turnover rate of ACh ($\text{nmol g}^{-1} \text{ min}^{-1}$) in the striatum, hippocampus and cortex calculated by five different methods from the same experimental data obtained at different time intervals after the injection of ^3H -Ch.

For a description of the different methods, see text (section 5.3).

Turnover rate of ACh ($\text{nmol g}^{-1} \text{ min}^{-1}$)			
Striatum	Hippocampus	Cortex	Calculation method
51	60	14	I
23	9	17	b
41	43	17	II
51	5	6	III
13	5	17	a
59	7	104	III
		14	II
55	21	27	IV
37		—	V

mixing of unlabelled and labelled Ch and subsequently a true precursor-product relationship may however be questioned, since endogenous ACh and ^3H -ACh show different post mortem stabilities (3.5.3). All the same, it would be of interest to calculate an

labelled Ch can be calculated from the slope of the line obtained when plotting $d(\text{labelled ACh})/dt$ against $SA_{\text{Ch}} - SA_{\text{ACh}}$ for each time point (method III, Table XI). For whole brain Jenden *et al* (1974) found that two lines with different slopes could be drawn corresponding to 1.4 and 7.9 nmol g⁻¹ min⁻¹ (Table VIII). They concluded that these slopes represented different pools of ACh in the brain.

In the present study data from the drawn SA curves (Fig. 8b) at 0.25 min intervals ranging from 0.5 to 2.75 min were plotted (Fig. 10). In the striatum a line with a slope of 59 nmol g⁻¹ min⁻¹ was obtained (Fig. 10). In the hippocampus a linear relationship between the points was found only at the time interval 1.25–2.5 min (7 nmol g⁻¹ min⁻¹). In the cortex two lines with different slopes were obtained (10.4–14 nmol g⁻¹ min⁻¹) (line a 0.5–1.25 min line b 1.25–2.5 min).

Schuberth *et al* (1969) found that the time course of the ratio ³H ACh/³H-Ch increased fairly linearly up to 1 min after an intravenous pulse injection of ³H-Ch. This was also the case in the brain regions studied (paper IV). Assuming that the Ch pool is known, a rough estimate of the turnover can be made (method IV Table XI).

Instead of assuming that the total free Ch pool is used for ACh synthesis, Saelens *et al* (1974) calculated the size of the specific Ch pool from the peak value of the ratio ³H ACh/³H-Ch and the endogenous content of ACh. By using this theoretical Ch pool value they estimated the turnover according to Schuberth *et al* (1969). As shown in Table XI in this presentation, this method (V) could only be used for the striatum (37 nmol g⁻¹ min⁻¹), since no peak value in the ratio ³H-ACh/³H-Ch could be found up to 10 min after ³H-Ch injection in the hippocampus and cortex (paper IV).

As seen in Table XI higher turnover values are obtained when calculations are made at time points before the SA_{ACh} has reached its maximum. This is clearly seen for the hippocampus. However since the SA curves were drawn by hand, they must be approximative (experimental data at 0.5 1.5 10 min after ³H Ch injection).

The values calculated in the present study by the finite difference method (method II, Table XI) are somewhat higher especially in the cortex, than those obtained by Racagni *et al* (1974) (Table IX) with the same method of calculation.

6. Effect of Sodium Pentobarbital and Oxotremorine on the Apparent Turnover of Acetylcholine in Different Brain Regions

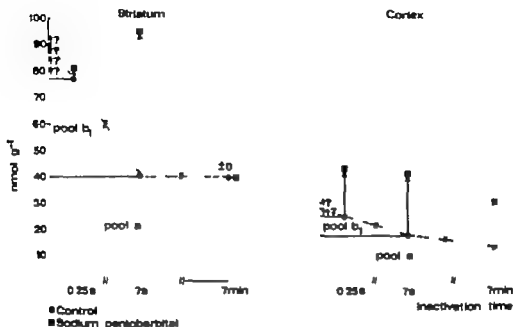
Barbiturate anesthesia increases the steady state concentration of ACh in whole brain in experimental animals (Tobias *et al.* 1946, Richter and Crossland 1949 Elliott *et al.* 1950, Glarman and Pepen 1962, paper I, Modak *et al.* 1976). It also decreases both the ACh release from the cortex (Mitchell 1966) and the apparent rate of turnover of ACh in whole brain (Schubert *et al.* 1969 Trabucchi *et al.* 1975). The ACh concentration increases in a dose-related manner with a threshold dose of 30 mg/kg for sodium pentobarbital given intraperitoneally (I.p.) (paper I). The maximal increase in ACh occurs about 15 min after injection of the barbiturate (Modak *et al.* 1976). The ACh content is normal within 7 min after reappearance of the righting reflex (paper I).

In the present studies endogenous ACh was not affected to the same extent in all brain regions. Sodium pentobarbital (60 mg/kg¹ I.p.) significantly increased the ACh content only in the midbrain, hippocampus and cerebral cortex (papers I and IV). Similar results were obtained after sacrifice by dislocation of the spine as after microwave irradiation of the head (0.25 s) (papers I and IV). However when the intermediate enzyme inactivation time (7 s) was used, a significant increase in ACh was also observed in the medulla oblongata and striatum (Nordberg and Sundwall 1975 unpublished data). In pentobarbital treated animals the ACh content was essentially the same following both types of microwave irradiation, but the values for the two groups of controls differ (data for the striatum and cortex are given in Fig. 11). Trabucchi *et al.* (1975) found that sodium pentobarbital increased the endogenous ACh in the striatum from 54 to 89 nmol/g¹ in rats subjected to head irradiation for 2 s (2.5 kW). The results are fairly similar to those obtained after whole body irradiation for 7 s. However Modak *et al.* (1976) found also in mice treated with sodium pentobarbital and sacrificed by microwave irradiation for 0.30 s (6 kW), a significant increase of ACh from 81 to 117 nmol/g¹ in the striatum. The findings in the present studies—different control values but similar ACh values after pentobarbital treatment following both types of microwave irradiation—might indicate that pentobarbital stabilizes a very labile pool of ACh (Fig. 11). The increased ACh content in the striatum of pentobarbital treated mice following sacrifice by microwave irradiation for 0.30 s (6 kW) (Modak *et al.* 1976) is different from the finding of the present author (at inactivation time 0.25 s) and is difficult to explain.

Sodium pentobarbital decreased the apparent rate of turnover of ACh (paper IV) selectively in the hippocampus and cortex, but had no effect on the turnover in the striatum (Table XII). A similar relative effect on the turnover in the cortex and striatum was reported by Trabucchi *et al.* (1975), though their absolute values were lower.

Recent studies indicate that the high affinity uptake of Ch by the cholinergic nerve terminal might be the rate-limiting and regulatory step in the synthesis of ACh (Haga,

Fig. 11 EFFECT OF SODIUM PENTOBARBITAL ON ACh AT DIFFERENT TIMES OF ENZYME INACTIVATION



and Noda 1973 Barker and Mittag 1975 Mulder *et al* 1974 Simon *et al* 1976). The latter authors found that sodium pentobarbital anesthesia significantly decreased the sodium-dependent uptake of ³H-Ch in synaptosomes from cortex and hippocampus, while the uptake in striatal synaptosomes was unchanged.

The data available thus indicate that sodium pentobarbital has a selective effect on the hippocampus and cortex. A decreased release of ACh into the synaptic cleft might decrease the high affinity uptake of Ch by the neuron and reduce the synthesis of ACh. The increased steady state concentration of ACh indicates a latency between these processes.

On long-term administration of a non anesthetic dose of barbital to rats in the drinking fluid (250 mg kg⁻¹ day⁻¹) for 30 weeks no effect was seen on the brain steady state concentration of ACh when the barbital was administered up to the time of decapitation (paper VI). When the drug was withheld for 3 days a significant decrease in ACh was found only in the striatum. On the 12th day of such an abstinence a decrease in ACh was found both in the striatum and brain stem + cerebellum. No effect was found in the cortex + hippocampus in either of the two time points of the abstinence. The findings are in contrast to the effect of a single anesthetic dose of sodium pentobarbital.

Like pentobarbital, the muscarinic agonist *oxotremorine* increases the steady state concentration of ACh in the brain (Holmstedt *et al* 1963 Cox and Potkonjak 1969 Sethy *et al* 1973) and decreases the apparent turnover of ACh (Schubert *et al* 1969

TABLE XII Effect of sodium pentobarbital (60 mg kg⁻¹ l.p.) and oxotremorine (1 mg kg⁻¹ l.p.) on the apparent rate of turnover (nmol g⁻¹ min⁻¹) of ACh in different mouse brain regions

Brain region	Control	Sodium pentobarbital	Oxotremorine
Cerebellum	(2)	(2)	—
Medulla oblongata	10	7	—
Midbrain	11	9	5
Striatum	55	59	44
Hippocampus	21	6	7
Cortex	27	10	8

Trabucchi *et al.* 1975). In contrast to pentobarbital it also increases the steady state concentration of endogenous Ch in the brain (Schubert *et al.* 1969 Ladinsky *et al.* 1974 Trabucchi *et al.* 1975). Szerb and Somogyi (1973) found that oxotremorine *in vitro* decreased the release of ACh from the cerebral cortex.

Oxotremorine selectively increases the endogenous ACh concentration in the cortex, hippocampus and striatum while no effect is found in the midbrain, medulla oblongata and cerebellum (Campbell and Jenden 1970, Choi *et al.* 1973 papers II, VII). In the striatum, however its effect on ACh is less pronounced in animals sacrificed by microwave irradiation than in decapitated animals (Cheney *et al.* 1976, Karlén *et al.* 1976, papers II, VII).

The effect of oxotremorine on the biosynthesis of ³H ACh in the striatum was also found to differ following the two methods of sacrifice (papers II, VII Karlén *et al.* 1976). Following dislocation of the spine the biosynthesis of ³H ACh was increased and the effect could not be counteracted by pretreatment with atropine (paper II). Following microwave irradiation the biosynthesis was decreased and the effect was counteracted by pretreatment with atropine (paper VII). Oxotremorine decreased the ³H ACh biosynthesis in the other brain regions following both methods of sacrifice, and the effect was prevented by pretreatment with atropine (papers II, VII).

A possible reason for these different effects on both ³H ACh and endogenous ACh in the striatum is that oxotremorine might have a stabilizing effect on the labile ACh pool(s) which is/are destroyed by AChE in untreated animals unless the enzyme is not instantly inactivated by microwave irradiation.

Increased values of endogenous Ch have been obtained in mouse brain regions following oxotremorine treatment (Karlén *et al.* 1976, paper VII). As discussed in paper VII this might be due to a combined central and peripheral effect (hemodynamic effect, see below). A solely peripheral effect is less likely due to the finding of Lundgren *et al.* (1976) that pretreatment with methylatropine prevented the increase of Ch in plasma but not in brain.

In study VII oxotremorine decreased the apparent rate of turnover of ACh in the cortex, hippocampus, midbrain and striatum (the only brain regions studied in this respect) (Table XII). This is in agreement with the decreased ACh turnover in the lower brain stem, diencephalon, striatum and cortex found by Choi *et al.* (1973) following decapitation and in the striatum observed by Karlén *et al.* (1976) following microwave irradiation.

Simon *et al* (1976) reported a decreased *in vitro* uptake of ^3H -Ch in synaptosomes from hippocampus of oxotremorine treated rats. Preliminary observations by the present author indicate that the uptake is also decreased in the cortex and striatum (Nordberg 1977 unpublished observations). The effect of oxotremorine thus seems to be different from the effect of pentobarbital, where no effect was found on the ^3H -Ch uptake in striatal synaptosomes. A stimulating effect of oxotremorine on the ACh receptors might lead to a diminished release of ACh into the synaptic cleft, a reduced neuronal high affinity uptake of Ch and a reduced synthesis of ACh in the neuron.

The possibility may not be overlooked that drug treatment might influence the kinetics of the injected radioactive Ch. After treatment with sodium pentobarbital (60 mg kg⁻¹), the initial brain uptake of intravenously administered ^3H Ch and the brain concentration of unmetabolized ^3H -Ch were lower (by 20–40%) than in the controls (paper V). A correspondingly (40%) lower concentration of unmetabolized ^3H -Ch was also found in the plasma of pentobarbital treated animals (paper V). These findings indicate that sodium pentobarbital might, by hemodynamic effects, influence the kinetics of a tracer dose of ^3H -Ch.

Oxotremorine (1 mg kg⁻¹), on the other hand, increased the plasma concentration of ^3H -Ch (by 70%) as well as the initial brain uptake of ^3H -Ch (by 50%) and the brain concentration of unmetabolized ^3H -Ch (by 80%) (papers II–V). Karlén *et al* (1971) found a higher content of oxotremorine in the plasma and brain of rats treated with oxotremorine alone than in those treated with methylatropine and oxotremorine combined, and concluded that oxotremorine might decrease its volume of distribution. Higher plasma values of intravenously injected radioactive dextran (^3H -dextran) were also found in oxotremorine treated mice (paper II). It therefore seems plausible that the effect of oxotremorine on the brain ^3H -Ch content may be explained by hemodynamic changes. Higher steady state concentrations of Ch have also been found in the plasma and brain in rats treated with oxotremorine (Karlén *et al* 1976 Schuberth *et al* 1969 Ladinsky *et al* 1974). The increase in the brain content of endogenous Ch caused by oxotremorine might partly be due to peripheral (hemodynamic) effects (Lundgren *et al* 1976, paper VII).

When the apparent turnover of ACh was calculated in studies IV and VII no compensation was made for extracerebral radioactivity in the blood remaining in the brain tissue (Aquilonius and Eckernäs 1976). Thus, the hemodynamic effects of pentobarbital and oxotremorine might alter the calculated turnover values of ACh. In study II ^3H -dextran was given intravenously and from the data obtained, the volume of the blood remaining in the cortex is calculated to be 20 $\mu\text{l g}^{-1}$. Taking into account the content of unconverted ^3H -Ch in remaining blood of the brain, the turnover in the cortex is calculated to be 35 nmol g⁻¹ in control animals and 11 nmol g⁻¹ in oxotremorine treated animals. The turnover values are thus a little higher than those obtained without compensation for extracerebral ^3H -Ch (76 nmol g⁻¹ and 8 nmol g⁻¹ respectively paper VII). However a 70% decrease in the rate of turnover of ACh is found to follow oxotremorine treatment with both methods of calculation.

The importance of the time of enzyme inactivation for the steady state concentrations of ACh and Ch, and the biotransformation of a tracer dose of ^3H -Ch have been systematically investigated in six well-defined parts of the mouse brain. To get a shorter time of enzyme inactivation than with conventional killing two methods of microwave exposure were used. Whole body irradiation for 7 s (1.3 kW) or head irradiation for 0.25 s (5 kW) increased the brain temperature to 85–90°C. The time courses of the temperature after completion of irradiation were similar.

A markedly higher content of ^3H ACh was preserved, especially in the striatum, when the time of enzyme inactivation was reduced from 7 min (decapitation) to 7 s. A comparable increase in the steady state concentration of ACh was obtained on reducing the time of inactivation further to 0.25 s. The findings indicate the existence of several pools of ACh in the brain.

- a. A fairly stable pool which is not changed during the time interval of some seconds to some minutes after sacrifice.
- b₁ A very labile pool which is destroyed by AChE unless the time of enzyme inactivation is extremely short. This pool constitutes about half the total ACh content in the striatum.
- b₂ A pool of newly synthesized (^3H ACh) which is more stable than pool b₁. This pool is also easily demonstrated in the striatum.

Although these studies indicate that ACh in a brain region is not homogeneous, plots of the specific radioactivities (SA) of ACh and Ch at different time points after injection of ^3H -Ch indicated a precursor-product relationship in all brain regions (except in the cerebellum) at the shorter time of enzyme inactivation (0.25 s).

The data obtained were applied to different models of turnover calculations. The calculated turnover rate values must be considered rather approximate (apparent) owing to our lack of knowledge of the size of the Ch pool available for ACh synthesis. Higher values were found when the calculations were made at time points before SA_{ACh} had reached its maximum. The turnover values differed between the brain regions and the highest rate of apparent turnover was found in the striatum (55 nmol g⁻¹ min⁻¹). In the cortex and hippocampus this value was approximately half and in the midbrain and medulla oblongata approximately a fifth.

Sodium pentobarbital and oxotremorine increased the steady state concentrations of ACh selectively in the brain. A marked increase in ACh was found in the cortex and hippocampus after treatment with both drugs. Oxotremorine also increased the content of ACh in the striatum. A plot of the SA of ACh and Ch indicated a precursor-product relationship in the brain regions also for drug treated animals. This motivated a calculation of an apparent turnover rate of ACh. Sodium pentobarbital decreased markedly

apparent rate of turnover of ACh only in the cortex and hippocampus. The effect of oxotremorine was less selective and a decreased rate of turnover was obtained in all four brain regions studied in this respect.

Pentobarbital and oxotremorine treatment appeared to have a stabilizing effect on the labile ACh pools (b_1 and b_2).

In rats treated with barbital for 30 weeks and the barbital was withheld for 3 days a decrease in the steady state concentration of endogenous ACh was obtained specifically in the striatum while no change was found in the cortex + hippocampus.

8. Acknowledgements

This study was performed at the Department of Pharmacology Faculty of Pharmacy University of Uppsala.

I wish to express my sincere thanks to

Professor Anders Sundwall, my teacher for his excellent guidance, generous support and inspiring enthusiasm

Professor Göran Wahlström for highly stimulating collaboration

Mrs Birgitta Öhman Mrs Ingrid Blomquist, Mr Ulf Ullström and Miss Maria Astin for skilful technical assistance and for their interest in this research

Mrs Karin Anter and Mrs Ellen Erbes for excellent assistance in the preparation of manuscripts

Mr Karl-Erik See-Knudsen for generous advice concerning theoretical and practical problems with the microwave technique

Mrs Mand Marsden for correcting the English Mr Manne Fredriksson for the photographic work

Numerous other friends for help and stimulating discussions.

The financial support of the Swedish Medical Research Council (project No. 2879), the Swedish Tobacco Company The Swedish Academy of Pharmaceutical Sciences, the C.D Carlsson Foundation, the L.F Foundation for Pharmaceutical Research and the Swedish Association for Medical Research is gratefully acknowledged.

References

- Aprison, M.H., P.A. Shea and J.A. Richter. Methodology for a radioenzymatic assay of acetylcholine and choline — from the living animal to the measurement in extracts of CNS tissue. In: *Choline and acetylcholine: handbook of chemical assay methods*. Ed. I. Hanin. Raven Press, New York, 1974. 63–80.
- Aquilone, S.M. and S.-Å. Eckermls. Cortical and striatal *in vivo* uptake and metabolism of plasma choline in the rat: effects of haloperidol and apomorphine. *Acta Pharmacol. et Toxicol.* 1976. **39** 129–140.
- Atweh, S.P. and M.J. Kuhar. Effects of anesthetics and septal lesions and stimulation on ³H acetylcholine formation in rat hippocampus. *Eur. J. Pharmacol.* 1976. **37** 311–319.
- Barker, L.A. and T.W. Mering. Comparative studies of substrates and inhibitors of choline transport and choline acetyltransferase. *J. Pharmacol. Exp. Ther.* 1975. **192** 86–94.
- Browning, E.T. Fluorimetric oxoyase assay for choline and acetylcholine. *Anal. Biochem.* 1972. **46** 624–638.
- Butcher, S.H. and L.L. Butcher. Acetylcholine and choline levels in the rat corpus striatum after microwave irradiation. *Proc. West. Pharmacol. Soc.* 1974. **17** 37–39.
- Butcher, L.L. and S.H. Butcher. Brain temperature and oxoyase histochemistry after high intensity microwave irradiation. *Life Sci.* 1976. **19** 1079–1088.
- Butcher, S.H., L.L. Butcher, M.S. Hanna and D.J. Jenden. Fast fixation of brain *in situ* by high intensity microwave irradiation: application to neurochemical studies. *J. Microwave Power* 1976. **11** 61–65.
- Campbell, L.B. and D.J. Jenden. Gas chromatographic evaluation of the influence of osotremorine upon the regional distribution of acetylcholine in rat brain. *J. Neurochem.* 1970. **17** 1697–1699.
- Cheney, D.L., E. Costa, I. Hanin, G. Racagni and M. Trabucchi. Acetylcholine turnover rate in brain of mice and rats: Effects of various dose regimens of morphine. In: *Cholinergic Mechanisms*. Ed. P.G. Waser. Raven Press, New York, 1975a. 217–228.
- Cheney, D.L., E. Costa, I. Hanin, M. Trabucchi and C.T. Wang. Application of principles of steady-state kinetics: the *in vivo* estimation of acetylcholine turnover rate in mouse brain. *J. Pharmacol. Exp. Ther.* 1975b. **192** 288–296.
- Cheney, D.L., G. Racagni, G. Zella and E. Costa. Differences in the action of various drugs on striatal acetylcholine and choline content in rats killed by decapitation or microwave radiation. *J. Pharm. Pharmacol.* 1976. **28** 75–77.
- Choi, R.L., M. Roch and D.J. Jenden. A regional study of acetylcholine turnover in rat brain and the effect of osotremorine. *Proc. West. Pharmacol. Soc.* 1973. **16** 188–190.
- Cohen, E.L. and R.J. Wurtman. Brain acetylcholine: control by dietary choline. *Science* 1976. **191** 561–562.
- Crescino, S., S. Buschi and H. Ladinsky. Effect of carbamazepine on cholinergic parameters in rat brain areas. *Neuropharmacology* 1976. **15** 653–657.
- Copson, D.A.. Microwave heating — in freeze-drying, electronic ovens and other applications. *The Art Publishing Company* Westport, Conn. 1962.
- Cox, B. and D. Potkinjak. The relationship between tremor and change in brain acetylcholine concentration produced by injection of tremorine or osotremorine in the rat. *Br. J. Pharmacol.* 1969. **33** 295–303.
- Crosland, J. H.M. Pappas and K.A. Elliott. Acetylcholine content of frozen brain. *Amer. J. Physiol.* 1955. **183** 27–31.
- Domino, E.F., M.R. Vaslo and A.E. Whalen. Mixed depressant and stimulant actions of morphine and their relationship to brain acetylcholine. *Life Sci.* 1976. **18** 361–376.

- Domino, E.F. and A.B. Wilson, Psychotropic drug influences on brain acetylcholine utilization. *Psychopharmacologia* (Bari). 1972. 25 291-298.
- Dross, K., Effects of α -isopropylthiochosphatate on the metabolism of choline and phosphatidylcholine in rat brain. *J Neurochem.* 1975. 24 701-706.
- Dross, K. and H. Kewitz, Concentration and origin of choline in rat brain. *Nordens Schmelzberg & Arch. Pharmacol.* 1972. 274 91-106.
- Eade, L. C. Webb and S.P. Mann, Free choline levels in the rat brain. *J Neurochem.* 1973. 20 1499-1502.
- Ellott, K.A.C. and N. Henderson, Factors affecting acetylcholine found in excised rat brain. *Amer J Physiol.* 1951. 165 365-374.
- Ellott, K.A.C., R.L. Swank and N. Henderson, Effects of anesthetics and convulsants on acetylcholine content of brain. *Amer J Physiol.* 1950. 162. 469-474.
- Ewetz, L., B. Sparf and B. Sörbo, Enzymatic determination of choline in brain with choline phosphokinase and 32 P-labelled ATP Symposium on *In vitro* Procedures with Radiolabels in Medicine in Vienna 1969. Ed. International Atomic Energy Agency 1970. *SM 124/59* 175-183.
- Feigenson, M.E. and J.K. Seelens, An enzyme assay for acetylcholine. *Biochem. Pharmacol.* 1969. 18. 1479-1486.
- Ferrandelli, J.A., M.H. Gray W.G. Seidwick and M.M. Cheng, Quick freezing of the murine CNS: comparison of regional cooling rates and metabolite levels when using liquid nitrogen or freon-12. *J Neurochem.* 1972. 19 979-987.
- Fremont, J.J., R.L. Choi and D.J. Jenden, The effect of hexicholinium on behavior and on brain acetylcholine and choline in the rat. *Psychopharmacology Communications.* 1975. 1 15-27.
- Gierman, N.J. and G. Pepes, Drug-induced changes in brain acetylcholine. *Br. J Pharmacol.* 1962. 19 226-234.
- Goldberg, A.M. and R.E. McCann, An enzymatic method for the determination of picomole amounts of choline and acetylcholine. In: *Choline and acetylcholine: handbook of chemical assay methods*. Ed. I. Hanin. Raven Press. New York. 1974. 47-61.
- Orren, J.P. and F.A. Szilagyi, Measurement of acetylcholine by pyrolysis gas chromatography. In: *Choline and acetylcholine: handbook of chemical assay methods*. Ed. I. Hanin. Raven Press. New York. 1974. 151-162.
- Goldotti, A., D.J. Cleary M. Trabacchi, M. Dottochi and C. Wang, Focused microwave radiation technique to minimize post mortem changes of cyclic nucleotides, dopamine and choline and to preserve brain morphology. *Neuropharmacology* 1974. 13 1115-1122.
- Haga, T. and H. Noda, Choline uptake systems of rat brain synaptosomes. *Biochimica et Biophysica Acta.* 1973. 291 564-573.
- Hanin, I., R. Massarelli and E. Costa, Environmental and technical preconditions influencing choline and acetylcholine concentrations in rat brain. In: *Drugs and cholinergic mechanisms in the CNS*. Eds: E. Hellstrom and A. Winter. Föreläsningssamlingar. Almqvist & Wiksell. Stockholm. 1970. 33-54.
- Hanin, I. and J. Schubert, Labelling of acetylcholine in the brain of mice fed on a diet containing deuterium labelled choline: studies utilizing gas chromatography-mass spectrometry. *J Neurochem.* 1974. 23 819-824.
- Hanin, D.R. and W.D. Reid, Use of choline kinase in the radioisotopic estimation of brain choline and acetylcholine. In: *Choline and acetylcholine: handbook of chemical assay methods*. Ed. I. Hanin. Raven Press. New York. 1974. 33-45.
- Hanin, D.R. and P.F.L. Wang, Inhibition of acetylcholine synthesis by juglone and 4-(1-naphthylvinyl)pyridine. *Biochem. Pharmacol.* 1976. 25. 669-672.
- Hanin, D.R., P.F.L. Wang, R.L. Herman and D.E. Clody, Acetylcholine synthesis in rat brain: dissimilar effects of clozapine and chlorpromazine. *Life Sci.* 1975. 17 739-743.
- Holmstedt, B., G. Lundgren and A. Sundwall, Tremorine and atropine effects on brain acetylcholine. *Life Sci.* 1963. 10 731-736.
- Jenden, D.J. The use of gas chromatography-mass spectrometry to measure tissue levels of acetylcholine. In: *Advances in Biochemical Psychopharmacology* 7 Eds: E. Costa and B. Hol. Raven Press. New York. 1973. 69-81.

- Jenden, D.J. Effects of chlorpromazine on acetylcholine turnover *in vivo*. In *The Phenothiazines and Structurally Related Drugs*. Eds. S. Forrest, C.J. Carr, E. Usdin. Raven Press, New York, 1974. 769-777.
- Jenden, D.J. Approaches to the study of acetylcholine turnover in brain. *Proc. First Pharmacol. Soc. 1976* 19 1-7.
- Jenden, D.J., L. Choi, R.W. Silverman, J.A. Strihorn, M. Roch and R.A. Booth, Acetylcholine turnover estimation in brain by gas chromatography/mass spectrometry. *Life Sci.* 1974, 14 55-63.
- Jenden, D.J. and I. Hanin, Gas chromatographic microestimation of choline and acetylcholine after N-demethylation by sodium benzenesulfonate. In *Choline and acetylcholine: handbook of chemical assay methods*. Ed. I. Hanin. Raven Press, New York, 1974. 135-150.
- Karlén, B., G. Lundgren, B. Lundholm, I. Nordgren and B. Holmstedt, Acetylcholine turnover in mouse brain *in vivo* studied with a mass fragmentographic technique. In *Cholinergic Mechanisms*. Ed. P.G. Waser. Raven Press, New York, 1975. 99-105.
- Karlén, B., G. Lundgren, I. Lundin and B. Holmstedt, Effects of oustermorine on synthesis of acetylcholine in striatum and whole brain of mice killed by various techniques. *Life Sci.* 1976. (Submitted for publication.)
- Karlén, B., G. Lundgren, I. Nordgren and B. Holmstedt, Ion-pair extraction and gas phase analysis of acetylcholine and choline. In: *Choline and acetylcholine: handbook of chemical assay methods*. Ed. I. Hanin. Raven Press, New York, 1974. 163-179.
- Karlén, B., L. Triskman and F. Sjöqvist, Decreased distribution of oustermorine to brain after pharmacological blockade of its peripheral acetylcholine-like effects. *J. Pharm. Pharmacol.* 1971. 23. 758-764.
- Kewitz, H., K. Dross and O. Piehl, Choline and its metabolic successors in brain. In *Central Nervous System - Studies on Metabolic Regulation and Function*. Eds. E. Gemazzani and H. Herken. Springer Verlag, Berlin, 1973. 21-32.
- Ladinsky, H., S. Consolo, S. Bianchi and A. Jori, Increase in striatal acetylcholine by picrotoxin in the rat: evidence for a gabergic-dopaminergic-cholinergic link. *Brain Res.* 1976. 108. 351-361.
- Ladinsky, H., S. Consolo and G. Peri, Effect of oustermorine and physostigmine on choline levels in mouse whole brain, spleen and cerebellum. *Biochem. Pharmacol.* 1974. 23 1187-1193.
- Lo, J.C., A.W. Gray and G.H. Kraft, Microwave selective brain heating. *J. Microwave Power* 1973. 8 275-286.
- Longoni, R., A. Miles and G. Pepen, Drug effect on acetylcholine level in discrete brain regions of rats killed by microwave irradiation. *Brit. J. Pharmacol.* 1974. 52 429P (abstract).
- Lundgren, G., B. Karlén and B. Holmstedt, Acetylcholine and choline in mouse brain. Influence of peripherally acting cholinergic drugs. *Biochem. Pharmacol.* 1976. (Submitted for publication).
- Machtsos, F.C. and B. Collier, Neurochemistry of cholinergic terminals. In: *Neuromolecular Junction. Handbook of Experimental Pharmacology* New Series. 42. Ed. E. Zaima. Springer Verlag, Berlin and New York, 1976. 99-228.
- Marchbanks, R.M., Biochemistry of cholinergic neurons. In *Handbook of physiology*, vol. 1, Eds. L. Iversen, S.D. Iversen and S.H. Snyder. Plenum Press, New York and London, 1975. 247-326.
- Maslouva, A.F., Quantitative determination of acetylcholine in biological tissues by the method of polarographic analysis utilizing a rotating platinum electrode. In *Choline and acetylcholine: handbook of chemical assay methods*. Ed. I. Hanin. Raven Press, New York, 1974. 215-230.
- MacNeil, J.F. Acetylcholine release from the brain. In: *Mechanisms of release of biological amides. Proceedings of an International Hemon-Gren Center Symposium, Stockholm 1965*. Hemon-Gren Center International Symposium series vol. 5. Eds. U.S. Eider, S. Rosen and B. Uvåks. Pergamon Press, London and New York, 1966.
- Modak, A.T., S.T. Wentracht, T.H. McCoy and W.B. Stanisha, Use of 300 mWc microwave irradiation for enzyme inactivation: a study of effects of sodium pentobarbital on acetylcholine concentration in mouse brain regions. *J. Pharmacol. Exp. Ther.* 1976. 197 245-252.
- Molander, A.H., H.I. Yamamura, M.J. Kuhar and S.H. Snyder, Release of acetylcholine from hippocampal

- altes by potassium depolarization dependence on high affinity choline uptake. *Brain Res.* 1974. 70. 372-376.
- Neff, N.H. P.F. Spano, A. Groppetti, C.T. Wang and E. Costa, A simple procedure for calculating the synthesis rate of norepinephrine, dopamine and serotonin in rat brain. *J. Pharmacol. Exp. Ther.* 1971. 176. 701-710.
- Nordberg, A. and A. Sundwall, Endogenous acetylcholine and biotransformation of labelled choline in brain regions *in vivo* following sacrifice by microwave irradiation. Sixth International Congress of Pharmacology Helsinki. 1975. 502 (abstract).
- Oliver, E.C. (Ed.), *Microwave power engineering vol. 2* Academic Press, London and New York. 1968.
- Prentiss, A.B.A., A.K. Prince and E.O.J. Hyde, The reaction of acetylcoenzyme A with choline acetyltransferase. *Biochem. J.* 1972. 129. 991-994.
- Pischner, H., Heating with microwaves - fundamental components and circuit techniques. Philips technical Library The Netherlands. 1966.
- Racagni, G., D.L. Cheney, M. Tribucchi, C. Wang and E. Costa, Measurement of acetylcholine turnover rate in discrete areas of rat brain. *Life Sci.* 1974. 15. 1961-1975.
- Richter, D. and J. Crossland, Variation in acetylcholine content of the brain with physiological state. *Amer. J. Physiol.* 1949. 159. 247-255.
- Selms, J.K., M.P. Allen and J.P. Sluka, Determination of acetylcholine and choline by an enzymatic assay. *Arch. Int. Pharmacodyn.* 1970. 186. 279-286.
- Selms, J.K., J.P. Sluka, M.P. Allen and C.A. Conroy, Measurement of choline (Ch), acetylcholine (ACh), and their metabolites by combined enzymatic and radioisotopic techniques. In: *Methods of Neurochemistry*. 4. Ed. R. Fried. Marcel Dekker New York. 1973a. 69-95.
- Selms, J.K., J.P. Sluka, M.P. Allen and C.A. Conroy, Some of the dynamics of choline and acetylcholine metabolism in rat brain. *Arch. Int. Pharmacodyn.* 1973b. 203. 305-312.
- Selms, J.K., J.P. Sluka, J. Schuman and M.P. Allen, Studies with agents which influence acetylcholine metabolism in mouse brain. *Arch. Int. Pharmacodyn.* 1974. 209. 250-258.
- Seki, Y., I. Yamashita, K. Yamazaki, F. Okada, R. Setani and T. Fujieda, Circadian fluctuation of brain acetylcholine in rats. *Life Sci.* 1975. 16. 281-288.
- Schmidt, D.E., Regional levels of choline and acetylcholine in rat brain following head focused microwave modifier effect of (+) amphetamine and (-) pargoline. *Neuropharmacology* 1976. 15. 71-84.
- Schmidt, D.E., R.C. Speth, F. Welch and M.J. Schmidt, The use of microwave radiation in the determination of acetylcholine in the rat brain. *Brain Res.* 1972. 38. 377-389.
- Schrier, B.K. and L. Shester, A simplified radiochemical assay for choline acetyltransferase. *J. Neurochem.* 1967. 14. 977-985.
- Schoberth, J., B. Spier and A. Sundwall, A technique for the study of acetylcholine turnover in mouse brain *in vivo*. *J. Neurochem.* 1969. 16. 695-700.
- Schoberth, J., B. Spier and A. Sundwall, Determinations of choline. In: *Drugs and cholinergic mechanisms in the CNS*. Eds. E. Heffernan and A. Wiener. Föreläsningssamling, Almqvist & Wiksell, Stockholm. 1970a. 15-25.
- Schoberth, J., B. Spier and A. Sundwall, On the turnover of acetylcholine in nerve endings of mouse brain *in vivo*. *J. Neurochem.* 1970b. 17. 461-468.
- Sethy V.H., Effects of chronic treatment with neuroleptics on striatal acetylcholine concentration. *J. Neurochem.* 1976. 27. 325-326.
- Sethy V.H., R.H. Roth, M.J. Kohar and M.H. van Woert, Choline and acetylcholine: regional distribution and effect of degeneration of cholinergic nerve terminals in the rat hippocampus. *Neuropharmacology* 1973. 12. 819-823.
- Sethy V.H. and M.H. van Woert, Antimuscarinic drugs - effect on brain acetylcholine and tremors in rats. *Biochem. Pharmacol.* 1973. 22. 2685-2691.
- Silver, A., The biology of cholinesterase. In: *Frontiers of biology* 36 Eds. A. Newberger and E.L. Tatum. North-Holland Publishing Company London and New York. 1974.

- Simon, J.R., S. Atweh and M.J. Kuhar. Sodium dependent high affinity choline uptake: a regulatory step in the synthesis of acetylcholine. *J Neurochem* 1976, 26 909-972.
- Smith, J.C. and J.H. Sackles. Determination of tissue choline with choline acetyltransferase. *Fed. Proc* 1967 26, 296 (abstract).
- Sparf, B. On the turnover of acetylcholine in the brain - an experimental study using intravenously injected radioactive choline. *Acta physiol. scand.* 1973, suppl. 397 7-47
- Sparf, B. and B. Ljungholm. The effect of atropine on the turnover of acetylcholine in the mouse brain. *Eur J Pharmacol.* 1975 32 287-292.
- Speng, K.V. A sensitive and specific fluorometric method for the determination of acetylcholine. In *Choline and acetylcholine - handbook of chemical assay methods*. Ed: I. Hamn. Raven Press, New York, 1974. 129-133
- Speth, R.C., D.E. Schmidt, B.V. Rama Sastry and D.M. Burbaum. *In vivo* and *in vitro* effects of bromoacetylcholine on rat brain acetylcholine levels and choline acetyltransferase activity. *Neuropharmacology* 1976, 15 287-290.
- Starinoha, W.B. Personal communication to A. Sved all. 1976.
- Starinoha, W.B., B.R. Endecott and L.C. Ryan. Freezing techniques to prepare brain tissue for analysis of acetylcholine. *Pharmacologist*. 1967 9 252 (abstract).
- Starinoha, W.B., A.T. Modak and S.T. Westraub. Rate of accumulation of acetylcholine in discrete regions of the rat brain after dichlorvos treatment. *J Neurochem.* 1976, 27 1375-1378.
- Starinoha, W.B. B. Pepelko and P.W. Smith. Microwave radiation to inactivate cholinesterase in the rat brain prior to analysis for acetylcholine. *Pharmacologist* 1970, 12 257 (abstract).
- Starinoha, W.B. and L.C. Ryan. Estimation of the acetylcholine content of rat brain by gas chromatography. *J Pharmacol. Exp. Ther* 1965 150, 231-233
- Starinoha, W.B. and S.T. Westraub. Choline content of rat brain. *Science* 1974 183 964-965
- Starinoha, W.B., S.T. Westraub and A.T. Modak. The use of microwave heating to inactivate cholinesterase in the rat brain prior to analysis for acetylcholine. *J Neurochem* 1973, 20, 361-371
- Starinoha, W.B., S.T. Westraub and A.T. Modak. Regional concentrations of choline and acetylcholine in the rat brain. *J Neurochem.* 1974 23 885-886.
- Szerb, J.C., H. Malik and E.Q. Hunter. Relationship between acetylcholine content and release in the rat's cerebral cortex. *Can. J Physiol Pharmacol.* 1970, 48 780-790
- Szerb, J.C. and G.T. Somogyi. Depression of acetylcholine release from cerebral cortical slices by cholinesterase inhibition and by isoproterenol. *Nature New Biology* 1973 241 121-122.
- Szidgyi, P.J.A., J.P. Green, O.M. Brown and S. Margols. The measurement of nanogram amounts of acetylcholine in tissues by pyrolysis gas chromatography. *J Neurochem.* 1972, 19 2555-2566.
- Takahashi, R. and M.H. Aprison. Acetylcholine content of discrete areas of the brain obtained by a pear freezing method. *J Neurochem* 1964 11 887-898.
- Takahashi, R., T. Nasa, T. Tanaka and T. Kariya. Relationship of ammonia and acetylcholine levels to brain excitability. *J Neurochem.* 1961 7 103-112.
- Thomas, H.E. Handbook of microwave techniques and equipment. Prentice Hall Inc. Englewood Cliffs, NJ 1972.
- Tobias, J.M., M.A. Lipton and A.A. Lepoint. Effect of anesthetics and convulsants on brain acetylcholine content. *Proc Soc exp. Biol (N.Y)* 1946 67 31-34
- Torn, H. and M.H. Aprison. Brain acetylcholine studies: a new extraction procedure. *J Neurochem.* 1966, 13 1533-1544
- Trabacchi, M. H. L. Cheney, I. Hamn and E. Costa. Application of principles of steady state kinetics to the estimation of brain acetylcholine turnover rate. Effects of isoproterenol and physostigmine. *J Pharmacol. Exp. Ther* 1975 194 57-64
- Verch, R.L. and R.A. H. Sims. Brain Blowing: A technique for *in vivo* study of brain metabolism. In *Research Methods in Neurochemistry* 2 Ed. N. Mark and R. Rodnight. Plenum Press, New York, 1974 171-18..
- Westraub, S.T. A.T. Modak and W.B. Starinoha. Acetylcholine post mortem increase in rat brain regions. *Brain Res* 1976 103 179-183

- Watteler, V.P. Identification of acetylcholine and related esters of biological origin. In: *Handbuch der Experimentellen Pharmacologie Ergänzungswork* VI Ed. G.B. Koelle Springer Verlag Berlin, 1963, 1-39.
- Zahn, G., D.L. Cheney and E. Costa. Regional changes in the rate of turnover of acetylcholine in rat brain following diazepam or meprobamate. *Kenneth Schrammberg's Arch. Pharmacol.* 1976, 94: 251-254.
- Zierman, D.B., The design and analysis of isotope experiments. *Amer. J. Med.* 1960, 29: 81-84.
- Zierman, D.B., C. Eisenman and M.C. Fahlner. On the calculation of "turnover time" and "turnover rate" from experiments involving the use of labeling agents. *J. Gen. Physiol.* 1943, 26: 325-331.

OBSERVATIONS ON THE MORPHOLOGY
AT THE TRANSITION BETWEEN THE PERIPHERAL
AND THE CENTRAL NERVOUS SYSTEM IN THE CAT

T Carlstedt

I. A preparative procedure useful for electron microscopy of the
lumbosacral dorsal rootlets.

C. H. Berthold and T. Carlstedt

II. General organization of the transitional region in S₁ dorsal
rootlets.

C. H. Berthold and T. Carlstedt

III. Myelinated fibres in S₁ dorsal rootlets.

T. Carlstedt

IV. Unmyelinated fibres in S₁ dorsal rootlets.

C. H. Berthold and T. Carlstedt

V. A light microscopical and histochemical study of S₁ dorsal
rootlets in developing kittens.

MATERIALS METHODS AND EVALUATION NORMS

Twenty-three adult cats (see Fig. 1) were anesthetized intraperitoneally with pentobarbital, 40 mg/kg BW and artificially ventilated with 100% oxygen. The lower spinal cord and its roots were fixed by vascular perfusion through the thoracic aorta, using a controlled intermittent pressure which varied from 0 up to 70-100 mm Hg (see Berthold, 1968 a). After a laminectomy the lower lumbar and the first sacral cord segments together with their dorsal roots were removed. Each root was carefully separated with the aid of watchmaker's forceps along the cleavage planes offered by the rootlets. After trimming with a razor blade the specimens consisted of the proximal one third of the rootlet and its attachment to the spinal cord with a small piece of the surrounding white matter.

In the case of immersion fixation (see Fig. 1) the specimens were removed from the animal after a laminectomy carefully placed on strips of filter paper and then immediately put in the various ice-cold fixatives (see below). The tonicity of all solutions were tested on a Knauer osmometer.

For light-microscopic survey pictures, specimens obtained after the perfusion fixation were frozen, longitudinally sectioned into 15-20 μ m thick slices in a cryostat at -30°C and stained in alkaline toluidine blue (1% toluidine blue in a 1% solution of NaHCO₃, pH 8) heated on the glass slide.

Preparative experiments

1. *The original preparative method (cf. Berthold, 1968 a, 3 cat. see Fig. 1):* The perfusate consisted of 5% glutaraldehyde in a 300 mOsm phosphate buffer pH 7.2-7.4 prepared according to Millonig (1.8 g NaH₂PO₄ · H₂O 23.25 g Na₂HPO₄ · H₂O and 5 g NaCl dissolved in 1000 ml of distilled water see Karlsson and Schultz, 1965) containing 2.7% Dextran T70 (Pharmacia, Uppsala, Sweden) (cf. Berthold 1968 a, Bohman and Magnusson 1970). After a postfixation at 4°C for 4 hours in a solution of the same composition as the perfusate the roots were rinsed overnight at 4°C in a 300 mOsm Millonig buffer osmoticated for 4 hours at 4°C in 2% OsO₄ 300 mOsm Millonig buffer and then again rinsed for 0.5 hours at 4°C in a 300 mOsm Millonig buffer. The specimens were dehydrated at room temperature (cf. Sternberg and Napolitano, 1971) in 50 70 80 90 and 95% acetone water mixtures (one hour in each concentration) and in absolute acetone (two hours) and were embedded in Vestopal W (Ryter and Kellenberger 1968). Filtration was performed in 25, 50 and 75% Vestopal acetone mixtures for 3-4 hours in each step and in 100% Vestopal overnight at room temperature. Polymerization took place first at 4°C for 24 hours and then at 60°C for 48 hours. Each of the various steps in the preparative procedure given above was submitted in consecutive order to a set of tests. A schedule of the various experiments is given in Fig. 1.

2. *Immersion fixation (3 cats see Fig. 1 and Table I):* 5% glutaraldehyde was used. The fixative vehicle consisted of the Millonig buffer (100-300 mOsm) with the addition of sucrose (0-500 mOsm) or NaCl (0-500 mOsm).

3. *Perfusion fixation (8 cats see Fig. 1 and Table II):* The perfusates tested consisted of 5% glutaraldehyde in a 300 mOsm Millonig buffer containing 7% dextran. Sucrose (0-250 mOsm) and/or NaCl (0-300 mOsm) were added in different concentrations.

4. *Rinsing and osmication (4 cats see Fig. 1 and Table III):* Specimens obtained after perfusion fixation in 5% glutaraldehyde in a 300 mOsm Millonig buffer containing 2.7% dextran and 200 mOsm sucrose were rinsed in 300 mOsm Millonig buffer and osmicated in 2% OsO₄ dissolved in 300 mOsm Millonig buffer. Sucrose (0-400 mOsm) was added in different concentrations to the rinsing solution used after glutaraldehyde fixation and to the osmium solution.

5. *Dehydration (6 cats see Fig. 1 and Table IV):* Specimens perfused fixed as described under (1), rinsed in 200 mOsm Millonig buffer with the addition of 200 mOsm sucrose and osmicated in 2% OsO₄ in 300 mOsm Millonig buffer were dehydrated in acetone. The dehydration procedure was varied with respect to dehydration time number of dehydration steps and the concentration of acetone in the different steps. In one case the specimens were dehydrated continuously from 0 to absolute acetone for eight hours.

6. *Embedding* (3 cats see Fig. 1): Specimens processed as described in section 5 and submitted to a stepwise and prolonged dehydration (N in Table V) were embedded in Vestopal W or Araldite (Glavert *et al.*, 1966) or Epon (Luft, 1961) or Spurr (Spurr 1969). Specimens intended for embedding in Araldite or Epon were dehydrated in ethanol either in a prolonged and stepwise way (N in Table V) or with only few steps (*cf.* Luft, 1961) and after dehydration soaked for 0.5 hours in propyleneoxide. Infiltration in the different resins took place in 25, 50 and 75% solutions for 3-4 hours and in 100% resin overnight at room temperature. Polymerization of Araldite, Epon and Spurr was performed for 3 days and at 60°C.

7. *Additional experiments* (4 cats): These experiments were all minor modifications of the final procedure given in Table I.

(a) Digitonin (Sigma, USA) was added to a concentration of 0.5% to the glutaraldehyde-fixative solution, and the subsequent rinsing solution (*cf.* Napolitano and Scallen, 1969).

(b) The perfusate contained 4% glutaraldehyde and 1% formaldehyde instead of 5% glutaraldehyde as fixative agent. The postfixative solution was of the same composition as the perfusate.

(c) Ethanol was used instead of acetone as a dehydration agent (Vestopal embedding). The specimens were then rinsed in styrene and infiltrated in a 1:1 styrene-Vestopal mixture under a moderate vacuum according to Kurtz (1961).

(d) The water-miscible embedding medium Raform I (resorcinol formaldehyde resin) (Robertson and Parsons, 1970; Hildebrand, 1974) and glycol methacrylate (Rosenberg *et al.*, 1960; Ledoc and Bernhard, 1967) were used instead of dehydration in acetone and embedding in Vestopal. Before embedding the specimens were cut into 0.1 mm-thick transverse slices on a Smith-Farquhar TC-2 tissue sectioner (Borvall, USA). The slices intended for embedding in Raform I were stained *en bloc* in a solution of 1% uranyl acetate in 300 mM Veronal-acetate buffer for 1 hour (for details see Hildebrand, 1974).

The length of six roots were measured in between each step of the preparative sequence of the usual methods (see Fig. 1) using a preparatory microscope with fixed scale. This was done in order to determine the degree of shrinkage.

Preparative steps performed after polymerization

These steps remained unchanged throughout the investigation. The specimen blocks were trimmed to a pyramid using a high-speed dental burr and razor blades and sectioned on a LKB 4800 Ultratome. Semithin sections (0.5 μ m thick) were placed on glass slides and stained with alkaline toluidine blue. The sections were examined and photographed in a Leitz photomicroscope (Ortholux).

Ultrathin sections (the interference colour of which varied from gray to white-yellow corresponding to a thickness of approximately 500-1000 Å *cf.* Peuchey 1968) — were placed on one-hole copper grids (Veeco, Germany) coated with a carbon-stabilized formvar film. After

double staining with uranyl acetate (Brody 1969) and lead citrate (Reynolds, 1963) the sections were examined in Philips EM 300 electron microscope operated at 80 kV and equipped with a 30 μ m objective aperture.

Evaluation norms

The current criteria for an acceptable ultrastructural preservation of a tissue in general (see *inter alia* Palade, 1963; Maunsbach, 1966 a, b; Sjostrand, 1967; Millonig and Marinuzzi, 1968) and of nervous tissue in particular (among others see Webster and Spiro, 1960; Elfvig, 1961; Williams and Landon, 1963; Landon and Williams, 1963; Webster and Collins, 1964; Karlsson and Schultz, 1968; Johnston and Roots 1967; Berthold, 1968 a, b; Hildebrand, 1971; Schultz and Karlsson, 1972; Karlsson *et al.*, 1975; Kallmo, 1976) were adopted. Thus the tissue of the transitional region should appear free from empty torn spaces, myelin sheath splitting defects in cellmembranes and disarranged cytoplasmic constituents if its preservation was to be considered as useful.

Brief comments on the methods

Glutaraldehyde was used in view of its well documented superiority as an ultrastructural fixative in general (Sabatini *et al.*, 1963; Maunsbach, 1966a, Millonig and Marinuzzi 1968; Hopwood, 1969, 1972) and in particular with regard to nervous tissue (Karlsson and Schultz, 1965; Berthold 1968a; Conradi, 1969; Hildebrand, 1971). The concentration of the glutaraldehyde was kept at 5% in all but one experiment (7b) in order to avoid a poor tissue penetration when using a too low concentration (Hopwood, 1969) and a hypertonic effect of too high a concentration (cf. Berthold, 1968a; Hildebrand, 1971). Likewise because of already demonstrated advantageous preparative effects, the phosphate buffer containing 0.5% NaCl (Millonig 1961; Maunsbach, 1966; Millonig and Marinuzzi 1968) and 2.7% low molecular dextran (Berthold, 1968a, Bohman and Maunsbach, 1970) as well as the method of administering the fixative by vascular perfusion (Palay *et al.*, 1962; Maunsbach, 1968a) were without further testing adopted from the so-called 'original preparative method' (Berthold, 1968a). Immersion fixation was used when studying the effects of different vehicular toxicities.

The results of the experiments were evaluated for each set of tests by examining two or more specimens from each cat. The modification within a test group that rendered the least artifactual appearance was classified as the 'relatively best' method and was selected for further experiments now in combination with various modifications of the consecutive step in the preparative sequence. In this way a final series of modified preparative steps was obtained, which when taken together constituted what was referred to as the 'useful methods' (see Fig. 1).

RESULTS

General description of the transitional region

A cross section through the transitional region reveals two concentric compartments separated at the PNS-CNS borderline, an outer PNS compartment and an inner CNS compartment (Figs. 2, 3, 4). The CNS compartment discloses an 'inner core zone' showing the arrangements of a central fibre tract and an outer covering 'mantle zone' consisting of astrocytes and nerve fibres (Figs. 3, 4). The transition of a myelinated nerve fibre from the peripheral to the central nervous type (Figs. 5 and 6) occurs in the mantle zone at a node of Ranvier the borderline node (for a full description and definition of terms see Berthold and Carlstedt, 1977).

Preparative experiments

Original preparative method (Exp. 1 Figs. 1, 4, 5). As shown in Figs. 4 and 5 the appearance of the PNS compartment of the transitional region corresponded to that of a successfully performed preparation.

In the CNS compartment and particularly in the mantle zone the appearance of the tissue was far from satisfactory. The myelin sheaths of the large and medium sized fibres (4-5 μ m in diameter) and of most small fibres revealed splitting, which was most severe close to the borderline nodes (i.e. at the termination of the central internode). Moreover there occurred comparatively large empty spaces both outside and inside the myelin sheaths (Fig. 4). Empty spaces and disarranged astrocytes were also noted at the borderline nodes of Ranvier. The node gaps appeared as if they had been torn open and they contained randomly arranged Schwann cell and glial processes (Fig. 5).

Modifications of the original steps in the preparatory procedure (Exp. 2, 3, 4, 5, 6). The progression of this step-by-step development is given in Fig. 1. The preservation quality of the PNS-compartment was in all experiments superior to that of the CNS-compartment. The artifacts noted in the different experiments (2-6) all belonged to the same general pattern of disarrangement as disclosed by the TR after treatment according to the 'original preparative method' and represented exaggerations or mitigations of this very pattern.

Immersion fixation (Figs. 6-14, Table 1) in a normotonic or slightly hypertonic Millonig buffer (Figs. 8, 10, 11, 13) gave the relatively best results of experiment group 2. Immersion fixation as such seemed to exaggerate the disarrangements (compare Figs. 6 and 8 with Figs. 4 and 5). Treatment with equimolar 5% glutaraldehyde solutions containing either NaCl or sucrose gave distinctly different preservation patterns when the tonicities of the added substances exceeded 300 mOsm (compare Figs. 12 and 14).

The next two sets of experiments: perfusion fixation (exp. 3; Table II, Figs. 15-18) and rinsing and osmication (exp. 4; Table III, Figs. 19-20) showed that the addition of 200 mOsm sucrose to the perfusate and to the rinsing solution gave the relatively best results respectively. An addition of more than 200 mOsm sucrose to the rinsing solution gave rise to a serious and generalized splitting of all central myelin sheaths (Fig. 19).

The testing of different modes of dehydration (Table IV, Figs. 21-26) showed that a procedure that started in 10% acetone and progressed in 10%-steps for 1-hour intervals to 100% acetone rendered the relatively best preservation. As compared to Vestopal W (Fig. 25) no improvements were obtained by embedding in Epon, in Araldite (Fig. 27), or in Spurr (Fig. 28). The latter two media gave rise to a considerable disarrangement of the CNS-compartment.

To sum up, a degree of preservation classified as useful was obtained by vascular perfusion with 5% glutaraldehyde in 300 mOsm Millonig buffer with the addition of 200 mOsm sucrose and 2.7% low molecular dextran, postfixation in the same medium for 4 hours; a rinse overnight in 300 mOsm Millonig buffer with the addition of 200 mOsm sucrose; osmication in 2% OsO_4 in 300 mOsm Millonig buffer; a slow and extensive stepwise dehydration in acetone and embedding in Vestopal W. In specimens treated according to this procedure, the myelinated nerve fibres of the core zone appeared almost free of both myelin splitting and tissue defects in the adjoining glia. Small discrete and solitary myelin fissures and splittings were present in the mantle zone and large myelin sheaths appeared somewhat wavy or serrated (Figs. 3, 26). Borderline nodes were closely surrounded by astrocytic elements, contained Schwann and glial processes and only a few small torn, empty-looking defects were noted. Small fibres constantly revealed a better preservation than did larger ones.

The longitudinal shrinkage of the specimens was about 10% (Table V).

Additional experiments (exp. 7): In this set of experiments the useful method was submitted to minor modifications.

The addition of digitonin (7a) to the fixative and rinsing solutions (Fig. 29) gave well preserved myelin sheaths but introduced serious disarrangements of glial, Schwann cell and axon membranes. Neither the use of a formaldehyde-glutaraldehyde fixative (7b; Fig. 30) nor dehydration in ethanol prior to Vestopal embedding (7c; Fig. 31) improved the preservation. Embeddings in water-soluble media (7d) were likewise without success. GMA (Fig. 32) provoked severe myelin splitting and glial shrinkage. Reform I (Fig. 33) gave a very weak positive contrast after staining *en bloc* in uranyl acetate. A negative contrast pattern appeared after section staining with lead. Here myelin sheaths were easily identified as light rings on a black background (Fig. 33). Glial cells, Schwann cell and axons, however, all required high magnification in order to be visualized. Myelin sheath splitting was minute. The sections showed a strong tendency to disintegrate when exposed to the electron beam.

DISCUSSION

The present study has shown that certain modifications of the original preparative methods did improve the ultrastructural appearance of the transitional region — notorious for the difficulties involved in its preservation (cf. Foncin, 1961; Maxwell, 1967; Maxwell *et al.* 1969; Ross and Burkel, 1971; Steer 1971). Considerable improvements were noted with regard to the following very troublesome artifacts, which all seemed to be aggravated as fibre size increased: loss of paranodal CNS-myelin sheath compactness; high occurrence of CNS-myelin sheath fissures; large empty spaces outside and inside CNS-myelin sheaths; empty spaces between glial processes and torn and disrupted nodes of Ranvier. Nevertheless, minor defects presumably induced by myelin lipid extraction and the high osmotic pressure of the useful method (see below) still remained. These artifacts appeared in the form of tiny spaces outside central nervous myelin sheaths, as also did small fissures in the terminal (close to node) segments of the largest myelin sheaths and a more or less corrugated appearance of CNS-myelin sheaths. These aberrations being more pronounced in larger fibres and particularly in the mantle zone were less pronounced in the core zone and were quite rare in the PNS compartment.

A comparison between the performance of the individual steps of the original preparative methods and that of the useful one shows that the improvements of the preservation is connected with the following steps: (a) the addition of 200 mOsm sucrose to the fixative; (b) the addition of 200 mOsm sucrose to the rinsing solution after glutaraldehyde fixation; and (c) the use of a prolonged and extensive stepwise dehydration. The present study also added much support to the view that vascular perfusion fixation is superior to immersion fixation (cf. Figs. 5 and 6).

It is well known that the tonicity of a fixation solution is highly significant as regards the tissue preservation obtained (Palade 1952; Robertson 1964; Holt and Hicks 1961; Elfvin 1962; Karlsson and Schultz, 1963; Maunsbach, 1966b; Millonig and Marinuzzi, 1968; Berthold 1968a, Hildebrand, 1971). With regard to myelinated nerve fibres the use of isotonic or slightly hypertonic vehicles has proved to give the best results (Webster and Collins 1964; Schultz and Karlsson, 1963; Berthold 1968a, Hildebrand, 1971). Usually NaCl and/or sucrose are used to regulate the osmotic pressure (Holt and Hicks 1961; Maunsbach, 1966b; Brunk and Eriksson, 1972).

The total osmotic pressure of the fixative employed in the useful method is theoretically close to 1000 mOsm. In terms of effective osmotic pressure — some 60–100% of the theoretical tonicity of the fixing agent, here containing 5% glutaraldehyde — is considered to be osmotically ineffective (cf. Schultz and Karlsson, 1963; Maunsbach, 1966b; Bone and Denton, 1971; Brunk and Eriksson, 1972; Penttilä *et al.* 1974) — this should correspond to 500–700 mOsm, i.e. a pressure about twice that of serum. The observation that such a comparatively high total tonicity renders a useful preservation of the CNS compartment of the transitional region is nevertheless in full agreement with the data of Hildebrand (1971) on feline spinal cord white matter. Thus Hildebrand added 150–200 mOsm NaCl or 200 mOsm sucrose to the 300 mOsm Millonig buffer. In the present study however sucrose was found to be superior to NaCl as osmotically active agent. The choice of the former substance was made because although quite comparable to NaCl with regard to the better preservation of the core zone it consistently gave a somewhat better preservation of the mantle zone characterized by fewer myelin fissures, fewer glial defects and less torn node gaps (Figs. 15 and 18).

The rationale behind the differentiated influence of equiosmolar additions of sucrose and NaCl to 5% glutaraldehyde in a standard vehicle as shown in Figs. 12 and 14 is obscure. In this context there are however some sparse data of interest which have mostly been derived from fixation model systems such as pure protein solutions, tissue cultured cells and sea urchin eggs (see Millonig and Marinuzzi,

1968, Penttilä *et al.* 1974). Unfortunately all these are far from possessing the complexity displayed by the highly intricate system of densely packed and interwoven high-lipid low water (myelin) and high-water low-lipid (cytoplasm and endoneurial space) elements that constitute the transitional region.

In the first place NaCl dissociates into charged particles and sucrose does not. The great significance of the ionic strength with regard to the stability of the myelin sheath has been demonstrated by Robertson (1964), who showed that the severe myelin sheath splitting evoked by osmotic shock in distilled water could not be reversed by pure osmotic forces (sucrose) but responded promptly to a change in ionic strength (see also Worthington and Blaurock 1969). Since the 300 mOsm Millionig buffer contains some 100 mOsm NaCl and the advantageous effects of sucrose addition were noted at a tonicity of 100-200 mOsm, the possibility exists that an osmolarity ratio of 0.5-1 between NaCl and sucrose is optimal with regard to myelin sheath stability during fixation of the mantle zone. Moreover as shown by Millionig and Marinuzzi (1968) NaCl and sucrose are strikingly different in their capacity to catalyse the fixation reactions as estimated from swelling times. The former substance was by far the more active one. The membrane protective action of sucrose is well known and is in fact exploited in most EM histochemical procedures (cf. Brunk and Eriksson, 1973).

From the observation of a low content of vessels in the transitional region (Berthold and Carlstedt, 1977) it might be expected that the rapid penetrating abilities of formaldehyde would be advantageous when using a formaldehyde-glutaraldehyde mixture as fixative (cf. Karnowsky 1965). However no improvement in preservation of the tissue was noted with this modification (Fig. 30). This might be due to the fact that formaldehyde, although it rapidly penetrates a tissue, is a slow-acting fixative the effects of which are reversible (Millonig and Marinuzzi, 1968; Hopwood, 1977).

The dehydration step means substitution of an anhydrous organic solvent for water as well as a considerable extraction of lipids such as cholesterol, cholesterol esters triglycerides and free fatty acids (Adams and Bayliss, 1968). During dehydration the interlamellar distance of myelin decreases by about 30% (from 180 Å to 120 Å) and about 40-50% (from 160 Å to 110-80 Å) in the PNS and the CNS respectively (Fineman 1953, 1960 a,b; Fernandez-Moran and Fineman, 1967; Moretz *et al.*, 1969 a,b; Hildebrand and Müller 1974). Thus the whole myelin sheath shrinks some 30-50% in the radial direction but as found here (Table V) only about 10% in the longitudinal direction. This is a situation where mechanical stresses and shearing forces are apt to develop at those sites where the ordered high-lipid low water compartment of compact myelin is interfered by the low-lipid high-water compartments of cytoplasm and extracellular space, i.e. at the interfaces between a sheath and its surroundings. The incisures of Schmidt-Lanterman and the nodes of Ranvier are particularly noteworthy here, since at these sites tiny compartments of cytoplasm are more or less secluded in the compact myelin.

The use of a slow and stepwise dehydration that started at 10% acetone and included passage through several concentration steps below 50% proved to be the modification of the originally used preparative procedure that yielded the comparatively greatest improvement. Conceivably a slow progression from low to high concentrations would induce less drastic fluid fluxes and less stress in the tissue than would a procedure starting at 50% acetone.

Accounting for the facts that lipid loss and radial myelin sheath shrinkage are more or less restricted to the highest acetone concentrations (Mählentaler 1958; Sternung and Napolitano 1971) and that these higher concentrations were used both in the original preparatives and in the useful method, it seems probable that the lower acetone concentrations of the adopted dehydration schedule might actually have increased the stability of in particular the myelin sheaths.

This recalls the earlier use of acetone as a primary fixing agent in light microscopy (Pearse, 1961) as well as in the leather tanning industry in that case in combination

with aldehydes (Gustavsson 1956). Although the effects of dehydrating agents as a rule are treated in terms of mere water substitution their possible role as post fixatives has been discussed by among others, Johnston and Roots (1967) and Schultz and Karlsson (1972). In line with those workers and taking into account the present results, it seems reasonable to ascribe some sort of myelin sheath post fixation property to the acetone as used here.

Embedding in water miscible media like glycol methacrylate and recorcinol formaldehyde whereby dehydration is avoided, were not successful. Neither were there noted any further improvements by the addition of digitonin — a cholesterol-protective agent (Napolitano and Scallen 1969; Sterzing and Napolitano 1971) — to the fixative nor through the use of ethanol as a dehydrating agent, a procedure claimed to diminish lipid extraction (Sterzing and Napolitano 1971) or through the embedding of specimens that had been acetone dehydrated to 90-95%. In full agreement with Condie *et al.*, (1961) Vestopal W appeared to be a highly reliable nerve fibre embedding medium.

The best preservation was always noted in the PNS-compartment where the myelinated fibres constituted individual units distributed in a large more or less empty-looking endoneural space. A less satisfactory preservation was obtained in the core zone of the CNS-compartment where the fibres are densely packed, often with thin rim-like demarcations of glial cytoplasm between them. The least satisfactory results were constantly found in the mantle zone where the paranodal segments of the central fibres are found surrounded by comparatively large areas of astrocytic cytoplasm.

Two facts emerge when one looks for the rationale behind the differences noted in the preservation of the PNS and CNS compartments. (a) the CNS-compartment lacks blood vessels (see Berthold and Carlstedt, 1977); (b) there are differences in the chemical composition of PNS and CNS myelin (Evans and Finean, 1965; Wolfgram and Kotori, 1968 a,b). The ultrastructural preservation of a vulnerable tissue compartment that lacks blood supply undoubtedly offers great problems and it might be asked whether vascular perfusion really is at all meaningful for the fixation of the transitional region. However the comparatively high occurrence of blood vessels in the PNS compartment and their distribution along the PNS-CNS borderline (Berthold and Carlstedt, 1977) speak in favour of a fixation administered via the vascular route. This is supported by the successful use of perfusion and the complete failure to obtain acceptable preservation by immersion fixation in the present work.

PNS and CNS myelin are known to differ with regard to both proteins and lipids. (Finean 1960 a; Hildebrand and Müller 1974). X-ray diffraction analysis has shown that the interlamellar myelin sheath period of unfixed and of fixed, dehydrated and embedded PNS and CNS specimens is 180 Å and 120 Å and 160 Å and 80-110 Å respectively (Evans and Finean, 1974; Wolfgram and Kontori, 1968 a,b). In the case of a myelin sheath of 130 lamellae (fiber size 15-20 µm) this differentiated shrinkage on the two sides of the borderline node implies that the radial shrinkage on the CNS side is about 1.6 times that on the PNS side. This gives in absolute figures a fibre shrinkage of more than 2 µm in the CNS as compared with 1.2 µm in the PNS. Consequently the CNS fibres should be more exposed than the PNS fibres to mechanical stress and shearing forces during preparation.

While it seems possible to argue that the general differences in PNS-fibre ultrastructural preservation as compared with that of CNS-fibres are likely to be due to differences in the chemical composition of the myelin this explanation is hard to adopt with regard to the differences noted between the mantle- and the core-zones. These two regions are occupied by the same internodes and there are no data available that support the idea that the fundamental myelin sheath composition varies along one and the same internode. On the other hand, the CNS paranodal region (cf Hildebrand, 1971) might well in analogy with PNS paranodes, be a particularly vulnerable fibre region. However since distortion of CNS-paranodes, as seen in feline spinal cord white matter (Hildebrand, 1971) can be considerably

reduced by the use of a fixative solution that has been made by the addition of either 100-200 mM NaCl or sucrose and that addition of fixative had little effect as regarded the CNS borderline paranodes — sucrose being more effective agent — other factors seem to influence the preservation of myelin. One such additional factor could be the position of the paranode at the interface between two tissue compartments with different shrinkage properties.

Why then does not the PNS borderline paranode become distorted like the to the borderline as the CNS paranode. This brings up the question of the arrangement of the nerve fibres in the PNS compartments and the myelinated neighbour fibres by the endoneurial space; a connective tissue containing some bundles of collagen fibres a few fibroblasts and a structureless ground substance. In the mantle zone the myelinated fibres is completely occupied by a mosaic of myelin processes. Hence, there is a superficial resemblance between the myelinated environment. In the PNS, however each tube appears to be able to change shape within rather wide limits without seriously distorting the structureless extracellular space of the endoneurial compartment prevents the tracing of such changes in the electron microscope. On the other hand, the intervening space is in principle exposed to osmotic influence. It is further supplied by all families as well as by a number of specific structural proteins. Concerning shrinkage in the mantle zone should then give rise to the formation of torn components and splitting.

To sum up, it can be suggested that the difficulties met with in the transitional region for electron microscopy should be due to factors; a difference in the chemical properties of CNS and PNS which give rise to a sharp shrinkage gradient in the PNS-CNS borderline of the mantle zone. The formation of torn empty-looking myelin and splitting were to a considerable extent prevented by the use of a hypertonic postfixation rinse and careful dehydration.

ACKNOWLEDGEMENTS

This investigation was supported by grants from Karolinska Institute and from The Swedish Medical Research Council (projects on the myelin sheath). I am indebted to Doctor Claes-Henric Barthold for discussions and to Dr. Bengtström, Mrs Eva Björkner and Mrs Anna-Edna Höfner for technical assistance.

oly-
tion

(± 1)

Table I

Experiment II Immersion fixation in 5% glutaraldehyde dissolved in a phosphate buffer containing different tonicities of sucrose and NaCl. The quality of the preservation is rated in terms of relatively bests (+) and not usefuls () (MHI = Millonig buffer)

Type and tonicity of osmotically active addition Tonicity of buffer	SUCROSE mOsm						NaCl mOsm					
	0	100	200	300	400	500	0	100	200	300	400	500
100 mOsm MHI	-	-	-	-	-	-	-	-	-	-	-	-
300 mOsm MHI	+	+	+	-	-	-	+	+	+	-	-	-
500 mOsm MHI	-	-	-	-	-	-	-	-	-	-	-	-

Table II

Experiment III Perfusion fixation in 5% glutaraldehyde dissolved in 300 mOsm phosphate buffer containing different tonicities of both sucrose and NaCl. The quality of the preservation is rated in terms of relatively bests (+) and not usefuls ()

Tonicity of sucrose (mOsm)	Tonicity of added NaCl (mOsm)				
	0	100	150	200	300
0					
150	+	-	-		-
200	+		-	-	
250	-				

Table III

Experiment IV Rinsing and osmification. The quality of the preservation as seen after treatment with the different solutions is rated in terms of relatively bests (+) and not usefuls ()

	Addition of sucrose (mOsm)				
Rinse	0	200	200	400	400
Osmification	0	0	200	0	400
Rating	-	+	+	-	-

Table IV

Experiment V Dehydration. The quality of the preservation as seen after using different acetone concentrations and dehydration times is rated in terms of relatively best (+) and not useful (-)

Acetone %											Specimen	Rating
10	20	30	40	50	60	70	80	90	95	100		
										120	A	-
								30	0	0	B	-
								60	0	120	C	-
						60	60	60	0	120	D	-
					10	10	10	10	0	30	E	-
					30	30	30	30	0	0	F	-
					30	30	30	30	30	0	G	-
					180	180	180	180	0	720	H	-
				15	0	15	15	15	0	15	I	-
				60	0	60	60	60	60	120	J	-
				30	0	30	30	30	30	120	K	-
		5	0	5	5	5	5	5	5	5	L	-
5	5	5	5	5	5	5	5	5	5	5	M	-
60	60	60	60	60	60	60	60	60	60	120	N	+
480 (continuous)											O	-

Table V

Mean values and (SD) of the length (mm) of the proximal parts of six S₁ dorsal roots from three cats as found during treatment according to the useful methods

Rinse		Acetone %			After polymerization
70	80	90	95	100	
15 (± 0)	14,3 ($\pm 0,2$)	14,2 ($\pm 0,1$)	14,0 ($\pm 0,1$)	13,9 ($\pm 0,1$)	13,9 ($\pm 0,1$)

REFERENCES

- Adams, C.W. and Bayliss O.B. (1968) Histochemistry of myelin. VI Solvent action of acetone on brain and other lipid-rich tissues. *The Journal of Histochemistry and Cytochemistry* 16, 116-8.
- Berthold, C. H. (1968a) A study on the fixation of large mature feline myelinated ventral lumbar spinal root fibres. *Acta Societatis Medicorum Upsaliensis* 73, Suppl. 9, 1-36.
- Berthold, C.-H. (1968b) Ultrastructure of the node-paranode region of mature feline ventral lumbar spinal-root fibres. *Acta Societatis Medicorum Upsaliensis* 73, Suppl. 9 37-70.
- Berthold, C.-H. and Carlstedt, T. (1977) Observations on the morphology at the transition between the peripheral and the central nervous system in the cat. II. General organization of the transitional region in S₁ dorsal rootlets. *Acta Physiologica Scandinavica* Suppl. 446, 23-42.
- Bohman, S.-O. and Maunsbach, A.B. (1970) Effects on tissue fine structure of variations in colloid osmotic pressure of glutaraldehyde fixatives. *Journal of Ultrastructure Research* 30 196-208.
- Bons, Q. and Denton, E.J. (1971) The osmotic effects of electron microscope fixatives. *The Journal of Cell Biology* 49 571-81.
- Bons, Q. and Ryan, K.P. (1972) Osmolarity of osmium tetroxide and glutaraldehyde fixatives. *Histochemical Journal* 4 331-47.
- Brody, L. (1969) The keratinization of epidermal cells of normal guinea pig skin as revealed by electron microscopy. *Journal of Ultrastructure Research* 2, 452-511.
- Brunk, U.T. and Ericsson, J.L.E. (1972) The demonstration of acid phosphatase in *in vitro* cultured tissue cell. Studies on the significance of fixation toxicity and permeability. *Histochemical Journal* 4 349-63.
- Condie, R.M., Howell, A.E. and Good, R.A. (1961) Studies on the problem of preservation of myelin sheath ultrastructure: Evaluation of fixation, dehydration, and embedding techniques. *The Journal of Biophysical and Biochemical Cytology* 9, 429-43.
- Conrad, S. (1969) Observations on the ultrastructure of the axon hillock and initial axon segment of lumbo-sacral motoneurons in the cat. *Acta Physiologica Scandinavica* Suppl. 332, 65-84.
- Elfvén, L.-G. (1961) Electron microscopic investigation of the plasma membrane and myelin sheath of autonomic nerve fibres in the cat. *Journal of Ultrastructure Research* 5, 388-407.
- Elfvén, L.-G. (1962) Electronmicroscopic studies on the effect of anisotonic solutions on the structure of unmyelinated splenic nerve fibres of the cat. *Journal of Ultrastructure Research* 7 1-38.
- Evans N. and Finean, J.B. (1965) The lipid composition of myelin from brain and peripheral nerve. *Journal of Neurochemistry* 12, 729-34.
- Fernandez-Moran, H. and Finean, J.B. (1967) Electron microscope and low angle X-ray diffraction studies of the nerve myelin sheath. *The Journal of Biophysical and Biochemical Cytology* 3, 725-48.
- Finean, J.B. (1965) Further observations on the structure of myelin. *Experimental Cell Research* 5 202-15.
- Finean, J.B. (1966a) Electron microscope and X-ray diffraction studies of the effects of dehydration on the structure of nerve myelin. I. Peripheral nerve. *The Journal of Biophysical and Biochemical Cytology* 8, 13-30.
- Finean, J.B. (1966b) Electron microscope and X-ray diffraction studies on the effects of dehydration on the structure of nerve myelin. II. Optic nerve. *The Journal of Biophysical and Biochemical Cytology* 8, 31-7.
- Foncin, J.-F. (1961) Structure fine de la zone de passage radiculomedullaire. *Revue Neurologique* 105 509-13.
- Glauret, A.M., Rogers, G.E. and Glauret, R.H. (1956) A new embedding medium for electron microscopy. *Nature* 178, 803.
- Gustavsson, K.H. (1956) *The Chemistry of Tanning Processes*. Academic Press, New York.
- Hildebrand, C. (1971) Ultrastructural and light microscopic studies of the nodal region in large myelinated fibres of the adult feline spinal cord white matter. *Acta Physiologica Scandinavica* Suppl. 364 43-84.
- Hildebrand, C. (1974) Embedding of myelinated nerve tissue in water soluble resorcinol-formaldehyde resins for light and electron microscopy. *Stain Technology* 49 281-86.
- Hildebrand, C. and Müller, H. (1974) Low-angle X-ray diffraction studies on the period of central myelin sheaths during preparation for electron microscopy. A comparison between different anatomical areas. *Neurobiology* 4 71-81.

- Holt, S. I. and Hicks, R.M. (1961) Studies on formalin fixation for electron microscopy and cytochemical staining purposes. *The Journal of Biophysical and Biochemical Cytology* 11, 31-45.
- Hopwood, D. (1968) Fixatives and fixation: a review. *Histochemical Journal* 1, 323-60.
- Hopwood, D. (1972) Theoretical and practical aspects of glutaraldehyde fixation. *Histochemical Journal* 4, 287-303.
- Holles, E. (1905) Beiträge zur Kenntnis der sensiblen Wurzeln der Medulla Oblongata beim Menschen. Arbeiten aus dem Neurologischen Institute an der Wiener Universität 13, 593-98.
- Johnston, P.V. and Root, B.J. (1967) Fixation of the central nervous system by perfusion with aldehydes and its effect on the extracellular space as seen by electron microscopy. *The Journal of Cell Science* 2, 377-86.
- Karlsson, U. and Schultz, R.L. (1965) Fixation of the central nervous system for electron microscopy by aldehyde perfusion. I. Preservation with aldehyde perfusates versus direct perfusion with osmium tetroxide with special reference to membranes and the extracellular space. *Journal of Ultrastructure Research* 12, 160-86.
- Karlsson, U., Schultz, R.L. and Hooker, W.M. (1975) Cation-dependent structures associated with membranes in the rat central nervous system. *Journal of Neurocytology* 4, 637-42.
- Katino, H. (1976) The role of the blood brain barrier in perfusion fixation of the brain for electron microscopy. *Histochemical Journal* 8, 1-12.
- Karnovsky, M.J. (1965) A formaldehyde-glutaraldehyde fixative of high osmolality for use in electron microscopy. *The Journal of Cell Biology* 27, 137A.
- Kurtz, B.M. (1961) A new method for embedding tissues in Vestopal W. *Journal of Ultrastructure Research* 5, 468-9.
- Landon, D.N. and Williams, P.L. (1963) Ultrastructure of the node of Ranvier. *Nature* 199, 676-7.
- Leduc, E., and Bernhard, W. (1967) Recent modifications of the glycol methacrylate embedding procedure. *Journal of Ultrastructure Research* 19, 196-9.
- Left, L.H. (1961) Improvements in epoxy resin embedding methods. *The Journal of Biophysical and Biochemical Cytology* 9, 409-14.
- Marrasbach, A.B. (1965a) The influence of different fixatives and fixation methods on the ultrastructure of rat proximal tubule cells. I. Comparison of different perfusion fixation methods and 1 glutaraldehyde, formaldehyde and osmium tetroxide fixatives. *Journal of Ultrastructure Research* 15, 242-69.
- Marrasbach, A.B. (1965b) The influence of different fixatives and fixation methods on the ultrastructure of rat kidney proximal tubule cells. II. Effects of varying osmolality ionic strength, buffer system and fixative concentration of glutaraldehyde solutions. *Journal of Ultrastructure Research* 15, 283-309.
- Maxwell, D.S. (1967) Fine structure of the normal trigeminal ganglion in the cat and monkey. *Journal of Neurosurgery* 28, 126-31.
- Maxwell, D.S., Kruger, L. and Pineda, A. (1968) The trigeminal nerve root with special reference to the central-peripheral transition zone. An electron microscopic study in the Macaque. *The Anatomical Record* 164, 113-26.
- Millonig, G. and Marinuzzi, V. (1965) Fixation and embedding in electron-microscopy. In *Advances in Optical and Electron Microscopy* (edited by Barer, R. and Conley, V.E.) 2, pp. 261-341. London, New York: Academic Press.
- Morita, R.C., Akers, C.K. and Parsons, D.F. (1969a) Use of small angle X-ray diffraction to investigate disordering of membranes during preparation for electron microscopy. I. Osmium tetroxide and potassium permanganate. *Biochimica et Biophysica Acta* 193, 1-11.
- Morita, R.C., Akers, C.K. and Parsons, D.F. (1969b) Use of small angle X-ray diffraction to investigate disordering of membranes during preparation for electron microscopy. II. Aldehydes. *Biochimica et Biophysica Acta* 193, 12-21.
- Mühlenthaler, K. (1967) Die Dehydratisierung. In *Vierter Internationaler Kongress für Elektronenmikroskopie* (edited by Bergemann, W., Möllenstedt, G., Niehrs, H., Peters, D., Rucke, E. and Wolpers, C.) 2, pp. 32-37. Berlin, Göttingen, Heidelberg: Springer Verlag.
- Napolitano, L.M. and Scallen, T.J. (1968) Observations on the fine structure of peripheral nerve myelin. *The Anatomical Record* 163, 1-6.
- Palade, G.E. (1953) A study of fixation for electron microscopy. *Journal of Experimental Medicine* 96, 285-307.
- Palay, S.L., McCee-Russell, S.M., Gordon, S. and Grillo, M.A. (1963) Fixation of neural tissues for electron microscopy by perfusion with solutions of osmium tetroxide. *The Journal of Cell Biology* 13, 386-8.

- Penchev I.D. (1958) Thin sections: I. A study of section thickness and physical distortion produced during microtomy. *The Journal of Biophysical and Biochemical Cytology* 4, 233-42.
- Pearse A.G.E. (1961) The chemistry of fixation. In *Histochemistry Theoretical and Applied* (edited by Pearse A.G.E.) 2, pp. 53-74. London: J. and A. Churchill Ltd.
- Penttilä, A., Kallimo H. and Trump, B.F. (1974) Influence of glutaraldehyde and/or osmium tetroxide on cell volume, ion content, mechanical stability and membrane permeability of Ehrlich ascites tumor cells. *The Journal of Cell Biology* 23, 197-214.
- Reynolds, E. (1963) The use of lead citrate at high pH as an electron-opaque stain in electron microscopy. *The Journal of Cell Biology* 17, 209-13.
- Robertson, J.D. (1964) Unit membranes: A review with recent new studies of experimental alterations and a new subunit structure in synaptic membranes. In *Cellular Membranes in Development* (edited by Locke M.) pp. 1-81. New York and London: Academic Press.
- Robertson, J.-G. and Parsons D.F. (1970) Myelin structure and retention of cholesterol in frog sciatic nerve embedded in a resorcinol-formaldehyde resin. *Biochimica et Biophysica Acta* 219, 379-87.
- Rosenberg M., Bartl, P. and Lesko, J. (1960) Water-soluble methacrylate as an embedding medium for the preparation of ultrathin sections. *Journal of Ultrastructure Research* 4, 298-303.
- Ross M.D. and Barkel, W. (1971) Electronmicroscopic observation of the nucleus, glial dome and meninges of the rat acoustic nerve. *American Journal of Anatomy* 130, 73-91.
- Ryter A. and Kellenberger E. (1958) L'inclusion au polyester pour l'ultramicrotomie. *Journal of Ultrastructure Research* 2, 200-14.
- Sabatini, D.D., Benach A. and Barnett, R.J. (1967) Cytochemistry and electron microscopy. The preservation of cellular ultrastructure and enzymatic activity by aldehyde fixation. *The Journal of Cell Biology* 17, 19-88.
- Schultz, R.L. and Karlsson, U. (1963) Fixation of the central nervous system for electron microscopy by aldehyde perfusion. II. Effect of osmolarity, pH of perfusate and fixative concentration. *Journal of Ultrastructure Research* 12, 187-206.
- Schultz, R.L. and Karlsson, U. (1972) Brain extracellular space and membrane morphology variation with preparative procedures. *Journal of Cell Science* 10, 181-95.
- Sjöstrand P.S. (1967) The structural patterns observed after fixation and the preserved structure in the living cell. In *Electron Microscopy of Cells and Tissues* (edited by Sjöstrand, P.) 1, pp. 393-412. New York, London: Academic Press.
- Spurr A.R. (1969) A low-viscosity epoxy resin embedding medium for electron microscopy. *Journal of Ultrastructure Research* 26, 31-43.
- Stear J.M. (1971) Some observations on the fine structure of rat dorsal spinal nerve roots. *Journal of Anatomy* 109, 457-63.
- Sternng, P.R. and Napolitano L.M. (1971) Tissue cholesterol preservation. Factors associated with retention of cholesterol in rat sciatic nerve fixed for electron microscopy. *The Anatomical Record* 173, 485-92.
- Webster H. de F. and Collins, G.H. (1964) Comparison of osmium tetroxide and glutaraldehyde perfusion fixation for the electron microscopic study of the normal rat peripheral nervous system. *Journal of Neuropathology and Experimental Neurology* 23, 169-88.
- Webster H. de F. and Spiro D. (1960) Phase and electronmicroscopic studies of experimental demyelination I. Variations in myelin sheath contour in normal guinea pig sciatic nerve. *Journal of Neuropathology and Experimentl Neurology* 19, 4-89.
- Williams, P.L. and Landon, D.N. (1963) Paranodal apparatus of peripheral myelinated nerve fibres of mammals. *Nature* 196, 870-3.
- Wolfgarm, F. and Kotoni, K. (1966a) The composition of the myelin proteins of the central nervous system. *Journal of Neurochemistry* 15, 1281-90.
- Wolfgarm, F. and Kotoni, K. (1966b) The composition of the myelin proteins of the peripheral nervous system. *Journal of Neurochemistry* 15, 1291-5.
- Worthington, C.H. and Blaurock, A.E. (1968) A low angle X-ray diffraction study of the swelling behavior of peripheral myelin. *Biochimica et Biophysica Acta* 173, 427-435.

LEGENDS TO FIGURES

A	astrocyte
BN	borderline node of Ranvier
C	central nervous fibre
CNS	central nervous system
CZ	core zone
EM	electron micrograph
Exp.	experiment
Glut.	glutaraldehyde
Im.	immersion fixation
LM	light micrograph
MIL	phosphate buffer (Millonig)
MZ	mantle zone
P	peripheral nervous fibre
Perf.	perfusion fixation
PNS	peripheral nervous system
SC	spinal cord
Sol.	solution
Sucr.	sucrose
U	unmyelinated axon
V	blood vessel
VC	vehicular composition

Fig. 1 A digest of material, methods and results.

The following pictures show the transitional regions of feline lumbosacral dorsal spinal rootlets. The fixation agent is 5% glut. unless stated otherwise.

Fig. 2 LM. Toluidine blue stained longitudinal cryostat section of material fixed only with glutaraldehyde. The CNS tissue appears light and protrudes like a cone into the darker stained PNS tissue. The dorsal root-spinal cord junction is in the upper right corner of the picture. The hatched line indicates the level corresponding to the cross section of Fig. 3 (x130).

Fig. 3 EM. Cross section. Useful methods. The CNS compartment occupies the centre of the micrograph. It is characterized by CNS closely spaced nerve fibres forming the core zone (CZ), and peripheral mantle zone (MZ) where there is comparatively large amount of glia cytoplasm. The surrounding PNS compartment is characterized by its more contrast-rich myelin sheaths and more loosely arranged nerve fibres. Blood vessels (V) are restricted to the PNS compartment (x750).

Fig. 4 EM. Cross section. Perfusion fixation according to the original preparative methods. The PNS compartment is seen on the right, the core zone in the middle of the picture. Myelinated fibres in the PNS compartment show minor fissures, while myelin sheath splitting, axonal retractions (x) and glial defects (*) are common in both the mantle and core zones of the CNS compartment (x1900).

Fig. 5 EM. Perfusion fixation according to the original preparative methods. Longitudinal section through a large myelinated fibre. Borderline node of Ranvier (BN) in the centre of the picture. The CNS part of the fibre is on the left. The PNS part of the fibre appears well preserved except for a minor empty space in the terminal cuff of the myelin sheath (arrow). The CNS part of the fibre shows multiple myelin fissures. There are large empty-looking spaces (x) outside the nodal region (x4200).

Fig. 6 EM. Immersion fixation in the same medium as in Fig. 4. Longitudinal section through large myelinated fibre. The CNS compartment is on the left. The PNS part of the fibre shows splitting in the myelin sheath at inclusions of Schmidt-Lanterman and close to the node (arrows), as well as axonal retractions from the inner contour of the myelin sheath (x). The CNS part of the fibre shows extensive myelin sheath splitting and shrinkage defects between the axon and the myelin sheath (*) and empty spaces between the myelin sheath and the surrounding glia cytoplasm (*). Note the difference in preservation quality between the CNS and PNS components (x1700).

The following pictures (Figs 7-33) are all electronmicrographs of cross sections demonstrating the preservation of the transitional region as obtained in some of the preparatory experiments. For details compare with the digest in Fig. 1. The PNS compartment is in the lower part of the pictures (1100).

Fig 7 Exp. 2. Immersion fixation. VC: 100 MILL, 0 sucrose 0 NaCl The ultrastructure of the CNS compartment is ruined. CNS myelinated fibres are almost completely destroyed and appear like whorls of myelin lamellae surrounding shrunken axons (arrows). The glial components appear swollen and vacuolated and show disrupted membranes. Note the comparatively good preservation of the PNS fibres (P).

Fig 8 Exp. 2. Immersion fixation. VC: 300 MILL, 0 sucrose 0 NaCl CNS fibres show myelin sheath splitting. The surrounding glial cytoplasm reveals some empty spaces. The degree of preservation was classified as being among the relatively best ones.

Fig 9 Exp. 2. Immersion fixation. VC: 500 MILL, 0 sucrose 0 NaCl Myelin sheaths are compact but show deformed contours. Several axons are seriously shrunken (x). Torn empty spaces (*) are prevalent outside the CNS fibres.

Fig. 10 Exp. 2. Immersion fixation. VC: 300 MILL, 100 sucrose 0 NaCl CNS myelin sheaths show minor fissures. Axonal retractions (x) from the inner contour of the myelin sheath are common. The preservation degree was classified as being among the relatively best.

Fig 11 Exp. 2. Immersion fixation. VC: 300 MILL, 200 sucrose 0 NaCl The CNS fibres show faint fissures in the myelin sheaths. Axonal retractions (x) are uncommon and the glia appears free of large empty spaces. The PNS fibres are well preserved. The preservation degree was classified as being among the relatively best.

Fig. 12 Exp. 2. Immersion fixation. VC: 300 MILL, 500 sucrose 0 NaCl The CNS fibres show large myelin fissures as well as general myelin sheaths splitting. The axons have shrunken to irregular star-shaped dark profiles. Glial cytoplasm has shrunk to a dark reticulum leaving large empty spaces in between the fibres. In contrast to this PNS myelin sheaths appear more or less intact, whereas the axons are seriously shrunken. Compare with Fig. 14.

Fig 13 Exp. 2. Immersion fixation. VC: 300 MILL, 0 sucrose 200 NaCl The CNS fibres show compact myelin sheaths. Axonal retractions (x) from the inner contour of the myelin sheath do occur. The PNS fibres appear well preserved. The preservation degree was classified as being among the relatively best.

Fig. 14 Exp. 2. Immersion fixation. VC: 300 MILL, 0 sucrose 500 NaCl The CNS fibres show compact myelin sheaths and axonal retractions are comparatively rare. The PNS fibres appear well preserved. Compare with Fig. 12.

Fig 15 Exp. 3. Perfusion fixation. VC: 300 MILL, 0 sucrose 150 NaCl The CNS fibres show large myelin fissures. Torn empty spaces are seen in the glia outside the myelin sheath (x). PNS myelinated fibres appear well preserved.

Fig 16 Exp. 3. Perfusion fixation VC: 300 MILL, 250 sucrose 0 NaCl In the CNS compartment there are many large myelin fissures. Torn empty spaces are rare in the glia. PNS myelinated fibres are well preserved.

Fig. 17 Exp. 3. Perfusion fixation. VC: 300 MILL, 200 sucrose 200 NaCl In the CNS compartment there is a generalized myelin sheath splitting. The axons have mostly retracted from the inside of the myelin sheaths (x) and the glia contains some large empty spaces (*). PNS myelinated fibres appear well preserved.

Fig 18 Exp. 3. Perfusion fixation VC: 300 MILL, 200 sucrose 0 NaCl In the core zone (CZ) the fibres appear with few and small fissures in the myelin sheaths and the glia appears more or less free of empty spaces. Glial defects (x) and myelin sheath splitting are seen in the mantle zone (MZ).

In the PNS compartment the fibres appear well preserved. The preservation degree was classified as being the relatively best one.

Fig 19 Exp. 4. Rinsing after glut. fixation. The rinsing solution was a 300 MILL buffer to which 400 sucrose had been added. CNS myelinated fibres show a pronounced and generalized myelin sheath splitting (cf. Figs. 12, 18 and 20). The PNS compartment appears well preserved.

Fig 20 Exp. 4. Rinsing after glut. fixation. The rinsing solution was a 300 MILL buffer to which 200 sucrose had been added. In both the core zone (CZ) and the mantle zone (MZ) the myelin sheaths show only small fissures. Empty spaces have to be searched for. PNS fibres are well preserved. The preservation degree was classified as being the relatively best one.

Fig. 21 Exp. 5. Dehydration. E in Table IV Short time in few acetone steps. In the CNS compartment most fibres show splitting in the myelin sheaths. Axonal retractions from the inner contour of the myelin sheath (x) as well as empty spaces outside the myelin sheath (*) are seen. The PNS compartment appears well preserved.

Fig. 22 Exp. 5. Dehydration. M in Table IV Short time in many acetone steps. CNS fibres show large multiple myelin fissures. The fibres in the PNS compartment are well preserved.

Fig. 23 Exp. 5. Dehydration. H in Table IV Long time in few acetone steps. In the CNS compartment splitting is seen in the myelin sheaths. The PNS compartment is well preserved.

Fig. 24 Exp. 5. Dehydration. O in Table IV Eight hours continuous dehydration. CNS fibres show large fissures. Axonal retractions from the inner contour of the myelin sheath (x) and defects in the surrounding glia cytoplasm (*) are prevalent. In the PNS compartment the fibres show fissures in some myelin sheaths.

Fig. 25 Exp. 5. Dehydration. P in Table IV Dehydration stopped in 90% acetone and embedding started here. In the CNS compartment the fibres appear collapsed with a thin dark condensed rim of cytoplasm surrounded by a well-preserved myelin sheath of low electron density. In the PNS compartment the fibres appear less collapsed. The myelin sheaths are well preserved and more electron-dense. The axoplasm is clear.

Fig. 26 Exp. 5. Dehydration. N in Table IV Long time in many acetone steps. The CNS compartment appears to be almost free of axonal retractions, of myelin sheath splitting and of tissue defects in the adjoining glia. The largest myelin sheaths, although quite compact, show a somewhat serrated outline. PNS fibres revealed occasional splittings at the incisures of Schmidt-Lanterman. The preservation degree was classified as being the relatively best one. This is also the procedure which finally was classified as the useful methods.

Fig. 27 Exp. 5. Embedding. Araldite. CNS fibres show axonal retractions (x) and generalized splitting in the myelin sheaths. Empty spaces are prevalent in the glia (*). PNS fibres are well preserved.

Fig. 28 Exp. 5. Embedding. Spurr. CNS myelin is of a comparatively low contrast. CNS myelin sheaths show generalized and severe splitting. PNS fibres are well preserved.

Fig. 29a Additional exp. Addition of 0.2% digitonin to the glut. post fixation and rinsing solutions in a preparative procedure otherwise analogous to that used in Fig. 26. The plasma membranes of the Schwann cell, axon and astrocyte (A) are disrupted and the cytoplasmic compartments contain vesicle-like entities (x) (x27100).

Fig. 29b Specimen treated according to the same preparative procedure as in Fig. 26 (x27100).

Fig. 30 Additional experiment. 1% formaldehyde and 4% glut. used as fixation agent. CNS axons have retracted from the inner contour of the myelin sheath (x). Myelin sheath splitting and glial defects (*) are prevalent. The PNS fibres appear less distorted (cf. Figs. 9 and 14).

Fig. 31 Additional experiment. Dehydration in ethanol. CNS fibres show a generalized and pronounced myelin sheath splitting. Axonal retractions (x) and glial defects (*) are prevalent. PNS fibres are well preserved.

Fig. 32 Additional experiment. Embedding in GMA. CNS fibres show extensive myelin sheath splitting. The glia is deformed and shrunken and contains large empty spaces (x). The PNS fibres are well preserved.

Fig. 33 Additional experiment. Embedding in resorcinol formaldehyd (Reform I) Stained en bloc in uranyl acetate and sectioned stained in lead citrate. The specimen revealed a negative contrast pattern with low-density myelin sheaths and high-contrast glia and axoplasm.

Figures at the end of this volume

Running title: EM preparation of the transitional region

Acta physiol. scand 1977 Suppl.448

From the Department of Anatomy Karolinska Institutet,
Stockholm Sweden

Observations on the Morphology at the Transition between the Peripheral and the Central Nervous System in the Cat. II

General organization of the transitional region in S₁ dorsal rootlets.

by

C. H. BERTHOLD and T. CARLSTEDT

ABSTRACT

C. H. BERTHOLD and T. CARLSTEDT *Observations on the morphology at the transition between the peripheral and the central nervous system in the cat. II. General organization of the transitional region in S₁ dorsal rootlets. Acta physiol. scand. 1977 Suppl. 448 23-42.*

The proximal segment of feline S₁ dorsal rootlets were investigated light and electronmicroscopically. A cone shaped protrusion of CNS tissue was found to extend distally into each rootlet for a distance of 100-1000 µm. That free segment of a rootlet which when cross sectioned revealed both CNS and PNS constituents was denoted the transitional region (TR). The TR was subdivided into an axial CNS compartment and a surrounding PNS compartment. The CNS compartment consisted of a core zone that showed the organization of CNS fiber tract, and of an outer astrocytic mantle zone which corresponded to the basement membrane that demarcated the endoneurial space from the glial space. The mantle zone constituted the PNS-CNS borderline. The mantle zone was rich in astrocytes and projected a large number of thin processes — the glial fringe — distally into the endoneurial space of the PNS compartment. There were large fenestration defects in the basement membrane that demarcated the endoneurial space from the glial space. The mantle zone contained many large myelinoid bodies and some encapsulated small dark unclassified cells. Similar cells, some covered by a basement membrane, were not found in the adjacent endoneurial space. The myelinated nerve fibres were equipped with a node of Ranvier at their borderline passage. During their course proximally in the TR the unmyelinated axons were redistributed from a random arrangement to a more or less segregated position superficially in the ventrolateral aspect of the rootlet. Crossing the borderline meant a considerable increase in the number of small myelinated nerve fibres on the CNS side and a corresponding decrease in the number of unmyelinated axons.

The occurrence of CNS tissue in the proximal parts of spinal roots and cranial nerves has been documented in a large number of lightmicroscopical investigations (see for instance Virchow 1858, Obersteiner and Redlich 1894, Hülse, 1906; Skinner 1931, Tarlov 1937 a, b). According to the reports on higher vertebrates and man the CNS tissue protrudes more peripherally in sensory than in motor nerves the eighth cranial nerve and the dorsal spinal root S₁ being equipped with particularly extensive CNS parts (Skinner 1931 Tarlov 1937 b). The contour of the PNS-CNS borderline is described as 'helmet like' (Tarlov 1937 b) or 'dome-shaped' (Skinner 1931), its convexity facing the PNS. The tissue zone forming the curved borderline has been reported to constitute a 'double lamina cribrosa' (Tarlov 1937 a), which outer part derives from the pia mater and covers an inner glial layer. Solitary 'islands' of glial tissue are reported to occur in the endoneurial space close to the PNS-CNS borderline. (Tarlov 1937 a, see also

General organization of the transitional region

Maxwell *et al.* 1969). The cell content of the transitional region is stated to be comparatively high (Tarlov 1937a) and oligodendrocytes have been suggested as the dominant glial element (Tarlov 1937a). The myelinated nerve fibres were found to be constricted as they pierced the *lamina cribrosa* and were claimed to lose their myelin for the first 10-50 μ m of their CNS part, this giving rise to the so-called *»Aufhellungszonen»* (Hülke, 1906). The first indication that the myelinated fibres were equipped with a node of Ranvier at their passage across the PNS-CNS borderline was given by Fricke (1961).

Electron-microscopic works on this region of the nervous system are for reasons which probably have to do with difficulties in obtaining good ultrastructural preservation quite sparse (Foncin 1961, Nataniel and Nataniel, 1963, Maxwell *et al.* 1969, Ross and Brökel, 1971, Steer 1971). In the first EM study on the transitional region Foncin (1961 — rat) demonstrated the PNS-CNS borderline nodes and clearly showed that the *»Aufhellungszonen»* was an artifact based on pronounced myelin sheath splitting on the CNS side (see also discussion in Carlstedt, 1977). More recent EM reports (Maxwell 1967, Maxwell *et al.*, 1969, monkey; Ross and Brökel, 1971-rat; Steer 1971-rat) have shown that the *pia mater* does not participate in the formation of the *lamina cribrosa*. Contrary to the light-microscopical opinions, oligodendrocytes were rarely observed, the dominating glial cell being the astrocyte which formed a feltwork of interwoven processes in the border layer corresponding to the external glial limiting membrane of the brain and the spinal cord.

It can be concluded that the ultrastructural organization of the very region where PNS tissue meets CNS tissue is far from fully explored and has not been investigated in the cat. This region holds points of great interest with regard both to neuroanatomy and to neuropathology and offers the unique opportunity to analysing one and the same axon as it appears in the peripheral as well as in the central nervous system. For an up to date review and discussion regarding the transitional region see Gamble (1978).

The organization of the transitional region seems furthermore to be of importance in *tabes dorsalis* (Obersteiner and Redlich, 1894) in primary myelin degeneration (Princeas *et al.* 1969) and in tumour development (Minckler 1972). A detailed knowledge of the ultrastructure of this region is a *sine qua non* when discussing and investigating the highly interesting issue of a possible immigration of Schwann cells into the CNS (see, for instance, Gilmore 1971, Ghatak *et al.* 1973, Hori 1973, Wood *et al.* 1975, Blakemore and Patterson 1975, Raine 1976).

The present work which makes use of a recently developed preparatory procedure (Carlstedt, 1977) deals with the general ultrastructural organization of the transitional region (TR) and investigates the distribution of cell units and nerve fibers in the TR.

MATERIAL AND METHODS

Eight adult cats were anaesthetized by intraperitoneal injection of pentobarbital 40 mg/kg BW and artificially ventilated with 100% oxygen. The lumbosacral spinal cord and its roots were fixed by vascular perfusion through the thoracic aorta with controlled intermittent pressure (Berthold, 1968). The fixative agent was 5% glutaraldehyde dissolved in a 300 mOsm Millonig buffer with the addition of 2.7% low-molecular Dextran and 200 mOsm sucrose. After laminectomy the specimens consisting of the first sacral spinal cord segment and its dorsal roots were removed.

Specimens intended for cryostat sectioning (2 cats) were, after a short rinse in 300 mM Osm Millonig buffer, frozen and longitudinal sections 15–20 μm thick were cut in a cryostat at -30°C . The sections were placed on glass slides and stained in alkaline toluidine blue (Carlstedt, 1977).

Specimens intended for Vestopal embedding (8 cats) were trimmed with a razor blade so the proximal part of each rootlet, about 15 mm, and its attachment to the spinal cord with a piece of the white matter were left for investigation. After a postfixation for 4 hours in an ice-cold solution of the same composition as used for the perfusion, the specimens were rinsed overnight, treated in a 2% OsO₄ phosphate buffer solution, dehydrated in a slow and stepwise way in acetone and finally embedded in Vestopal (for details see Carlstedt, 1977). The specimens were trimmed into masses 30 μm high using LKB 11800 Pyramitome and sectioned with a glass knife on a LKB 4800 Ultratome. The specimens were carefully orientated for cross-sectioning: the nerve fibres were cut perpendicularly to their longitudinal axis and then sectioned in the distal to proximal direction. Longitudinal sections parallel to the longitudinal axis of the nerve fibres were obtained by sectioning the rootlet in the dorso-ventral direction.

Sections for light microscopy (0.5 μm thick) were placed on glass slides and stained with alkaline toluidine blue and examined and photographed in a Leitz photomicroscope.

Besides several series of 25–100 consecutive ultra-thin cross and longitudinal sections, four long series of cross sections, comprising 10,000 (Rootlet 2, cat K1039) 6,000 (Rootlet 3, cat K1040) and 4,500 (Rootlet 1, cat K1038) sections respectively and four long series of longitudinal sections of 200–1000 consecutive sections each were cut. The section thickness was obtained from the ratio between mass height and the number of sections it yielded and was found to vary between 600 and 800 Å. The loss of sections was less than 1%.

The specimens used for the cross section series consisted each of rootlet comprising 100–400 myelinated fibres as determined before serial sectioning in the light microscope.

The sections were placed on one-hole copper grids coated with carbon-stabilized formvar film. After a double staining with uranyl acetate (Brody 1959) and lead citrate (Reynolds, 1963) the sections were examined in a Philips EM 300 electron microscope operated at 80 kV and equipped with a 30 μm objective aperture.

Definition of terms and quantitative estimations

The terms proximal and distal will be used with respect to the spinal root — spinal cord junction (Fig. 1).

Four main cross-sectional reference levels — A, B, C and D (see Fig. 1) — will be used with respect to position in the proximal part of the investigated rootlets. Their

A is that level where the rootlet meets the most caudal part of its corresponding spinal cord segment

B is level situated roughly halfway between A and C.

C is the level at which the glial fringe is situated and which separates the stereotype PNS part of a rootlet from its transitional region and

D is a level some 200–400 μm distally to level C i.e. situated well in the stereotype PNS part of the rootlet.

The additional level 0 is the level at which the tip of the CNS compartment is situated.

Each cross-sectional level — as it appeared in electronmicrographs at X 2000 magnification — was divided, with respect to its centre, into dorsal and a ventral part and each of these was divided in medial and lateral part. So each level was separated into four parts or quasi-quadrants (see Figs. 21a, 22a, 23a). In view of the unsymmetrical shape of the cross sections and the differences in shape between the various levels, true quadrants of comparable size could not be obtained. Hence, in order to make a comparison of the fibre distributions in different parts of a cross-sectional level and at different levels of the transitional region at all possible the area of each separate quasi-quadrant was estimated by planimetry and the relative occurrence of nerve fibres per unit area calculated (see legend to Fig. 24).

In order to evaluate the distribution of different fibre classes with respect to depth in the rootlet, each cross-section level was divided into four concentric areas: one central spot surrounded by three concentric zones of equal breadth and assimilated to the contour of rootlet (see Figs. 21f, 22f, 23f). For the same reason as given above, the areas spot and the surrounding zones were determined by planimetry

The nerve fibres were separated into myelinated and unmyelinated (C-) fibres. The former group was further separated into large ($>13\mu\text{m}$ thick), medium ($6-13\mu\text{m}$ thick) and small ($<6\mu\text{m}$ thick) fibres. The number and types of the fibres were determined on photocopies representing $20\mu\text{m}$ -intervals cross sections through the transitional region (see Figs. 21d, 22d, 23d). In addition to this the distribution of the fibres with respect to quasi-quadrants and concentric zones was estimated in the four main cross-section levels A-D (see Figs. 11, 23, e, f).

Schwann cells and fibroblasts were identified according to the criteria given by Thomas (1963). Glial cells were classified according to the principles of Magnaini and Walberg (1964) and Peters *et al.*, (1970). The number of the different cell types was estimated from the occurrence of cell nuclei at consecutive $20\mu\text{m}$ intervals along the transitional region, using photocopies of cross sections. The occurrence of astrocytes and oligodendrocytes was moreover checked every $2.5\mu\text{m}$ directly in the electron microscope. Hence it was possible to estimate the total number of these two cell types in the transitional region, as their cell nuclei are longer than $2.5\mu\text{m}$ (cf. Cammermeyer 1960).

RESULTS

General description of the transitional region and presentation of a terminology

The dorsal root S_1 ran more or less parallel with the spinal cord from its ganglion up to the lower level of the segment S_1 . At a distance of 5-10 mm from the spinal cord junction the root split into a fan of from five to ten differently sized rootlets which turned medially and lined up in the dorsolateral sulcus (Figs. 1-2). The angle between the length axis of the rootlets and the longitudinal axis of the spinal cord measured about 30° .

At a distance of 1-2 mm from the cord the larger rootlets split into 2-3 thinner fascicles, here denoted mini rootlets. These mini rootlets reunited again at the spinal cord junction (Fig. 3). Toluidine blue staining of frozen sections gave the peripheral myelin sheaths a dark blue colour that contrasted sharply against the pale blue staining of the central myelin (Fig. 3) (cf. Feigin and Cravioto 1961). This difference in the staining properties of the myelin greatly simplified the identification of the central nervous tissue, which extended for some 100-1000 μm from the spinal cord out into the rootlets (Fig. 3). In larger rootlets the CNS tissue showed a more rounded end than it did in thinner rootlets, forming a top angle of some 40° and some 20° respectively. The thinner the rootlets the shorter was the extension of CNS tissue.

The S_1 dorsal rootlets consisted of CNS tissue at the level of their spinal cord junction (see Fig. 1). In most cases the wedge shaped most proximal piece of a rootlet that connected it to the spinal cord (Fig. 1) did as well consist of PNS tissue. At a cross level about 100-1000 μm more distally (level C Fig. 1) the rootlet appeared completely free of CNS constituents. That segment of the free proximal end of a rootlet which contained both CNS and PNS constituents (i.e. the region found in between the reference levels A and C of Fig. 1) was referred to as the transitional region. TR (Figs. 4-5). According to this definition the connecting piece is outside the transitional region.

The transitional region (TR) consisted of two main parts: (1) A cone shaped CNS compartment which tapered to a tip (level 0 of Fig. 1) in the distal direction and which lacked an endoneural space. (2) A PNS compartment which covered and surrounded the CNS compartment. The PNS compartment contained an endoneural space and a fringe of glial processes which emanated from the CNS compartment, and tapered to a tip in the distal direction (reference level C of Fig. 1).

The interface between PNS compartments was denoted the PNS-CNS borderline. (Figs. 12, 13).

The CNS compartment of the TR disclosed two zones again concentrically arranged. (1) an inner core zone (Figs. 5-8) composed of closely packed central nerve fibres and a few scattered glial cells thus showing the arrangements of a central fibre tract and (2) an outer covering mantle zone 20-30 μm thick and built up of astrocytes and nerve fibres (Figs. 9-10). The astrocytes of the mantle zone gave off numerous fibriform cytoplasmic processes the glial fringe (Figs. 1-5) which ran distally in the endoneural space parallel to the nerve fibres of the PNS compartment.

The myelinated nerve fibres, adopted a more or less typical paranodal arrangement as they approached the CNS compartment. Just outside the mantle zone the peripheral myelin sheaths ceased and each fibre showed a node of Ranvier at the site where it crossed the PNS-CNS borderline: the borderline node of Ranvier (Figs. 5-8). The axons became again invested by myelin and penetrated the mantle zone in order to reach the central core and eventually the spinal cord. At the passage through the mantle zone the myelinated nerve fibres were loosely packed with comparatively numerous astrocytic perikarya situated in between them (Figs. 9-10).

Electronmicroscopic examination

PNS compartment

The PNS compartment was separated from the subarachnoid space by the root sheath. This, the outermost layer of the TR consisted of loosely arranged flattened cells and collagen fibres. No obvious demarcation was noted between the root sheath and the *pia mater* at the root-cord junction (Fig. 5). The endoneural space continued uninterrupted into the subpial space (cf. Haller *et al.*, 1972). The endoneural space of the PNS compartment was comparatively roomy and contained astrocytic processes, the glial fringe (Figs. 6-8, 7). The blood vessels of the endoneural space did not follow the course of the nerve fibres into the CNS compartment (see Table I). Instead the vessels deviated out from their submerged positions and joined vessels situated on the spinal cord surface at the attachments of the rootlets. The CNS compartment of the TR was always found completely free of vessels (Table I, Figs. 6-11).

The passage from the stereotype root region into the PNS compartment of the TR was signalled by the appearance of the cross-cut tip of the glial fringe (Fig. 7). The tip was formed by one single or just a few closely spaced cross-cut polygonal astrocytic processes which were demarcated from the endoneural space by a basement membrane. It was in all cases possible by making use of consecutive sections to ascertain that these seemingly isolated glial islands in fact originated from the mantle zone (see below).

More proximally in the TR the glial fringe occupied an increasingly large area of the cross section and its organization became more complex (Fig. 8). The number of astrocytic processes increased and the processes joined together forming fenestrated walls in the endoneural space. At a distance of 5-20 μm from the PNS-CNS borderline the glial walls united outside the fibres, separating them and enclosing them together with a minute concentric endoneural space in a tube- or holster-like fashion (Figs. 5-8, 9-10-12). In this way the paranodes of most myelinated fibres were found in a narrow endoneural *cul de sac* that extended up to the PNS-CNS borderline and which at its proximal blind end contained the borderline node of Ranvier (Fig. 5).

Extensive glial processes and comparatively deep endoneural *cul de sacs* characterized the glial fringe as far proximally as level II (Fig. 12). From this level onwards the length of the processes decreased and the endoneural *cul de sacs* became shallow measuring only a few μm in length. Hence proximally to level B, where the majority of the smaller fibres entered the CNS compartment, the CNS-PNS borderline was as a rule comparatively easy to observe (Fig. 13).

The astrocytic processes forming the glial fringe contained large bundles of glial fibrils, clusters of tubules, scattered glycogenlike particles, small mitochondria and numerous lysosomes, some of which had prismatic cristae (Fig. 16) (cf. Morales and Duncan 1971). In the case of one very thin rootlet analysed quantitatively (rootlet 1, Fig. 21b) four astrocytic perikarya were noted in the glial fringe. Otherwise the fringe was free of astrocytic perikarya.

The glial processes lay closely packed inside a basement membrane and were separated by a narrow empty-looking space 100-200 Å in width. Desmosomes and gap junctions (see Nabahima *et al.*, 1975) were common (Figs. 15-18). At some sites however there were larger spaces in a group of glial processes. Several such spaces contained longitudinally-orientated bundles of collagen fibres (Fig. 15). As found in series of consecutive sections the collagen bundles originated in the endoneural space and projected several µm into the glial space. At these sites the basement membrane that separated the endoneural space from the glial space was fenestrated, thus letting the collagen fibres through. Similar basement membrane defects but not associated with traversing collagen bundles, were rather common in the fringe close to the mantle zone (Fig. 18). Most collagen fibres measured 200-300 Å in diameter. At some sites and particularly in a zone adjacent to the CNS compartment the collagen fibres varied from 200-12000 Å diameter (Fig. 15).

The following familiar cell types were constantly noted as members of the PNS compartment: Schwann cells, fibroblasts and pericytes (Figs. 21a, 22a, 23a). To this was added the likewise constant occurrence of a cell type of unknown origin and of unknown classification. These unclassified cells were found in the glial fringe and superficially in the mantle zone (Fig. 19). They were dark, round, about 5 µm in size and contained a comparatively large, often deeply indented nucleus whose abundant chromatin was distributed in irregular clumps inside the nuclear membrane. The dark, finely granular cytoplasm formed a thin rim outside the nucleus. It contained few organelles and formed a few short processes. Several of these cells were equipped with a more or less intact basement membrane. In spite of careful serial section analysis it was not possible to demonstrate any contacts between unclassified cells and axons.

CNS compartment

Mantle zone. The mantle zone constituted the outer part of the CNS compartment (Fig. 5) and measured 20-30 µm in width. It contained the first CNS segments of passing nerve fibres, 95-100% of all astrocytic perikarya of the TR, a large number of myeloid bodies, a few cells of the unclassified type referred to above, and a dense outer feltwork of astrocytic processes which without clear delineation, projected distally into the endoneural space forming the glial fringe (Fig. 12). Desmosomes and gap junctions were prevalent.

At those rare sites where the plasma membrane of an astrocytic perikaryon directly faced the endoneural space (Fig. 13) it was covered by an incomplete basement membrane reflected on to it from penetrating nerve fibres and again lifted away by emerging fringe processes. Numerous electron-dense hemidesmosome-like specializations at the astrocytic plasma membrane were present subjacent to the basement membrane (for discussion regarding these entities see Bondareff and McLone, 1973).

The astrocytes were of the fibrillar type (Figs. 12, 13). Their perikarya measured 7-12 µm and contained a pale irregularly shaped nucleus, a well-developed Golgi complex, single strands of granular and smooth endoplasmatic reticulum, some small mitochondria (0.2 µm in size), fibrils, microtubules, electron-dense bodies 0.1 µm in size, of which some elongated ones revealed an interior of longitudinally orientated lamellae and numerous gliosomes 1-10 µm in size (cf. Mugnaini and Walberg 1964; Peters *et al.*, 1970) (Figs. 12, 13, 16, 17).

There were many myelinoid bodies in the mantle zone (Fig. 14). These bodies were irregularly shaped, measured $2-10\ \mu\text{m}$ in size, and revealed a lamellated texture. Intact regions showed an interlamellar period of $100\ \text{\AA}$. Most bodies disclosed some intralamellar splitting and crescent-like empty defects at their outer aspects. Some bodies were compact. Others showed a clear centre. The bodies were surrounded by astrocytes.

Core zone. In the core zone, unmyelinated and myelinated fibres were densely packed with scanty of glial cytoplasm in between them (Figs. 5, 9-10, 11, 20). Adjacent myelin sheaths sometimes formed an intraperiod dense line along their contact lines. Most myelinated fibres were separated by thin flat astrocytic processes containing bundles of filaments and gliosomes. Oligodendrocytes of an ultrastructure fully in line with the current picture (see Magnaini and Walberg 1964, Peters *et al.*, 1970 and legend to Fig. 20) were the dominant cell type. Other cells classified as microglia were occasionally found in the proximal parts of the core zone (Figs. 21a-23a). A few fibrillar astrocytes were also noted in the region close to or proximally to level A (Figs. 21b-23b).

Quantitative analysis

One small rootlet (rootlet 1) and two medium sized rootlets (rootlets 2, 3) were investigated quantitatively with regard to the occurrence of different cell types at different TR levels and to the size, shape and extent of the various TR compartments, as well as to the distribution of unmyelinated and myelinated fibres at different TR levels (Figs. 21-24).

The distance between the reference levels A and C — i.e. the length of the transitional region — was $340-460$ and $260\ \mu\text{m}$ respectively (Figs. 21-22, 23). The free length of the glial fringe — i.e. the distance between level C and the tip of the CNS compartment — was $140-40$ and $20\ \mu\text{m}$ respectively (Figs. 21d-23d).

In all three rootlets there extended a thin lateral crescent-shaped compartment of PNS tissue proximally to level A. In rootlets 1 and 2 the PNS crescent extended proximally for about $40\ \mu\text{m}$. It amounted to less than 5% of the total cross section area at level A. More than 95% of the myelinated fibres and most of the unmyelinated fibres has crossed the PNS-CNS borderline distally to level A (Figs. 21d, 23d).

In rootlet 3 the PNS crescent extended proximally for $120\ \mu\text{m}$. At level A it made up about 20% of the cross sectional area and contained some 20% myelinated fibres and a large number of the unmyelinated axons (Fig. 23d).

Mantle area of the CNS compartment

The CNS compartments of rootlets 1 and 3 were cone-shaped (cf. Figs. 21d, 23d). The size of the mantle area of this cone can be obtained approximately by calculating the mantle area of the cone the height of which is the length of the CNS compartment and the basis radius is obtained from the length of the circumference of the CNS compartment in level A assuming a circular cross section area (Table II). By this method the top angles of the two CNS compartments were estimated to be about 20° and 40° . The CNS mantle area was approximately 2.2×10^4 and $7.7 \times 10^4\ \mu\text{m}^2$ in rootlet 1 and rootlet 3 respectively.

In rootlet 2, where the CNS compartment extended distally for $420\ \mu\text{m}$, the CNS cross section area at level A and at a level $180\ \mu\text{m}$ more distally were about the same. Hence as shown in Fig. 22d, the shape of this CNS compartment is roughly that of a proximal cylinder $180\ \mu\text{m}$ in length which tapers off distally into a cone, $240\ \mu\text{m}$ in length the top angle of which can be calculated at about 40° and the mantle area of which is about $7.7 \times 10^4\ \mu\text{m}^2$ the total CNS mantle area being $18 \times 10^4\ \mu\text{m}^2$ (Table II).

Cell population

The cell population of the transitional region was dominated by Schwann cells (Figs. 21 a, b c 23a, b c) Astrocytes were with very few exceptions present only in the mantle zone. The number of astrocytes was 27 103 and 85 in rootlet, 1 2 and 3 respectively. Oligodendrocytes were restricted to the core zone. The number of oligodendrocytes was 6, 48 and 25 in rootlet, 1 2 and 3 respectively. Microglia and pericytes were few: the former restricted to the CNS compartment and the latter to the PNS compartment. Unclassified cells lodged in the fringe and in the outer part of the mantle zone. They were found at all levels. The highest occurrence of unclassified cells in one cross section was noted distally in the TR of rootlet 2, where seven individuals were found outside a CNS compartment whose cross section measured $4000\mu\text{m}^2$ (Fig. 22a).

Nerve fibres

The rootlets contained 441 1300 and 1359 axons, of which 104 350 and 349 respectively were myelinated at the level C. Thus about 25% of all fibres were myelinated. Of these roughly half the number were small and half the number were medium sized. Fibres $13\mu\text{m}$ or more in diameter i.e. large fibres, were rare and amounted only to a few per cent (Table I).

The number of axons at level A equalled that of level D or C. However at level A the number of unmyelinated fibres showed a decrease of about 5% as compared to level C. The myelinated fibres on the other hand showed a corresponding increase. Figs. 21e, f 23e, f and Table I show that this increase concerned only the group of small myelinated fibres which increased by 13 (25%) 46 (27%) and 41 (24%) members in rootlets 1 2 and 3 respectively.

The countings of the nerve fibres at $20\mu\text{m}$ intervals along the transitional region showed that the larger fibres entered the CNS distally to the thinner ones (Figs. 21d-24d). For example in rootlet 2 30% of the medium-sized and 55% of the small myelinated fibres together with some 90% of the C-fibres remained in the PNS compartment at the level where all (100%) large myelinated fibres appeared on the CNS side of the borderline.

The occurrence at different TR levels of the four investigated fibre classes — large, medium and small myelinated fibres and unmyelinated fibres — with regard both to quadrants and concentric zones is given in Figs. 21e, f - 23e, f. The large myelinated fibres showed a slight preponderance in the dorsal part of the rootlets both at level D and level A. At the latter level the large fibres seemed to aggregate in the outer zones of the dorso-medial part of the rootlets. Medium-sized fibres were somewhat more frequent in the inner zones of the rootlets. Small myelinated fibres showed at level D an even distribution both with respect to quadrants and with respect to concentric zones. At level A small myelinated fibres seemed to have concentrated in the outer zones of the lateral and, particularly of the ventrolateral aspects of the rootlets.

The unmyelinated fibres disclosed at a distal reference level either as in rootlet 3, a more or less random distribution or as in rootlets 1 and 2, a moderate concentration in the lateral half of the cross section. During the passage in the proximal direction to level A there was observed a clear-cut redistribution of the C-fibres. These axons more or less completely deserted the inner zones of the rootlets and became concentrated in the outer zone with a clear preponderance for its ventrolateral compartment. This is illustrated in Fig. 24 which gives the relative C-fibre occurrences at different sites in proximal and distal levels as calculated per unit area ($1000\mu\text{m}^2$) (See legend to Fig. 24). In rootlet 1 for example, the relative occurrence of C-fibres in the ventrolateral part of the cross section is 157 189 148 and 120 as estimated for the central spot to the outermost concentric zone, of the level C respectively. At the level A of the same rootlet the corresponding values are 0 40 150 and 355 respectively. Thus the C-fibre occurrence appears to have decreased to zero in the central zone, decreased by 80% in the adjacent zone and increased about three times in the outer zone.

DISCUSSION

Terminology

The place in a spinal root or a cranial nerve where the CNS meets the PNS carries many names: the *Aufhellungszone* (Obersteiner and Redlich 1894); the transition zone (Tarlov 1937; Maxwell *et al.* 1969) the entrance zone of Obersteiner and Redlich (Boony 1967); the glioschwannian junction (Minckler 1979); and the glia-Schwann cell border (McFarland and Friede 1971). The present work uses with its own definitions the designation »transitional regions» thereby referring to that most proximal free part of a rootlet which in one and the same cross section contains both CNS and PNS tissue. This designation has been adopted for the following reasons. »Regions» was preferred to such terms as zone, junction and border because it was felt to be associated with a more extended and spacious structure than is indicated by the other terms. »Transitional» was considered to give greater emphasis to the conceptual importance of the structural changes that take place at the crossing than does, for instance, the word »entrance». The use of designations like »glioschwannian junctions» and »glia-Schwann cell borders» appeared to be rather awkward, partly because they refer to only one aspect of TR organization and partly because electron microscopy revealed a very complex glia-Schwann cell border, i.e. the glial fringe where glial processes to a depth of up to 200 μm interdigitated with the Schwann cells. Such terms as »*Aufhellungszone*» and »*lamina cribrosa*» must be considered meaningless and should be avoided. Both are based on preparation artifacts: the *Aufhellungszone* develops as a result of extensive paranodal CNS myelin sheath splitting and the *lamina cribrosa* is the effect of myelin splitting in combination with astrocytic shrinkage (see Carlstedt, 1977).

The concept »transitional regions» as here defined includes besides the PNS-CNS borderline a PNS and a CNS compartment. Both these compartments reveal unique morphological features. Thus the PNS compartment shows a high cell-body content, profound fibre redistributions and the glial fringe. The CNS compartment is devoid of blood vessels, and carries a mantle zone rich in astrocytes. Moreover crossing the PNS-CNS borderline apparently implies quantitative changes in the number of unmyelinated and myelinated nerve fibres.

Blood vessels

The blood vessels of the PNS compartment did not accompany the nerve fibres into the CNS compartment. Nor did this compartment receive vessels from the spinal cord. The PNS vessels deserted the rootlet at its proximal end and joined superficial spinal cord vessels. The reason why the PNS vessels did not enter the CNS compartment is obscure. The observation, however recalls that there are data which indicate that the permeability properties of PNS and CNS vessels are quite different. Thus it has been shown that protein tracers injected intravenously into cats pass easily from the circulation into dorsal root ganglia and spinal nerve roots (Olsson, 1971). In the central nervous system, on the other hand, such extravasation is prevented by the endothelium of the CNS blood vessels ((Reese and Karnovsky 1967; Brightman and Reese, 1969). The lack of blood vessels means that the CNS compartment metabolism has to rely on the diffusion of nutrients and waste products for a distance that may exceed 0.1 mm (cf. rootlet 2).

Unclassified cells and basement membrane

The glial fringe and adjacent parts of the mantle zone contained solitary specimens of a small uncharacteristic cell type which it was found impossible to classify according to current criteria. The observation that several of these cells were invested by a more or less intact basement membrane suggests an epithelial connection and indicates that they may represent some sort of aberrant Schwann cells (cf. Blakemore and Patterson, 1975). However their origin remains for the time being as obscure as their significance.

General organization of the transitional region

The basement membrane which demarcated the astrocytic processes of the glial fringe and the mantle zone form the endoneurial space carried large fenestrations. These were at sites several μm in size and formed openings through which endoneurial collagen penetrated into the outer layers of the mantle zone. The possible barrier function of the basement membrane at those sites where it constitutes the PNS-CNS interface has been discussed mainly in connection with the occurrence of Schwann cells in the central nervous system (see for instance Gilmore and Duncan, 1969; Blakemore 1975). Obviously the basement membranes of the astrocytes cannot be of any importance as regards diffusion of macromolecular substances. Apart from the fact that it has large fenestrations both ferritin and peroxidase have been found to pass the basement membrane of the external glial limiting membrane (Brightman 1963; Brightman and Reese, 1969). According to Blakemore (1976) the presence of a basement membrane at the PNS-CNS border should prevent migrating Schwann cells from entering the CNS. The present observations suggest that one prerequisite for Schwann cell migration into the CNS — the basement membrane defects — already exists in the apparently healthy cat. Whether the other ingredients — the Schwann cells that are free of axons — are also present in the healthy animal, perhaps in the form of unclassified cells remains to be shown.

Proximal extension of the PNS compartment

In a recent communication Raine (1976) has reported on the occurrence in the rabbit lumbosacral spinal cord of rare small islands of PNS tissue characterized by a roomy collagen-containing endoneurial space, a lack of fibroblasts and a nerve fiber population restricted to unmyelinated and very small ($1.2\ \mu\text{m}$) myelinated axons. These PNS areas were described as being situated in close proximity to the entry zones of a few dorsal spinal roots. Since serial section analysis was not applied it cannot be decided whether the PNS areas represented true enclosed islands or whether they in fact are but central extensions of the PNS compartment of the TR of adjacent rootlets. The similarity in general organization of the PNS areas as shown by Raine (1976) superficially in the spinal cord of the rabbit, and that presently noted proximally in the PNS compartment of the TR in feline S₁ dorsal rootlets, the extension of the latter compartment in a few cases further proximally into the lateral



The mantle zone

The crossing of the CNS demarcation line means penetration of the external glial limiting membrane. This membrane measures $10\text{--}30\ \mu\text{m}$ in thickness, consists of a complex feltwork of interwoven fibrillar astrocytes and in the cat contains roughly $0.5\text{--}1$ astrocytic perikaryon per $10\ \mu\text{m}^2$ of CNS surface area (Williams, 1975; Carlstedt unpublished observation). In the transitional region, the mantle zone is the counterpart to the external glial limiting membrane.

In the present work the size of the mantle-zone area was obtained approximately by calculating the mantle area of the simple geometric figure to which the shape and the size of the CNS compartment could be extrapolated. In rootlets 1 and 3 the configuration of the CNS compartment corresponded roughly to that of a cone whose mantle area was 2.2×10^4 and $7.7 \times 10^4\ \mu\text{m}^2$ respectively. In line with the astrocytic occurrence ($0.5\text{--}1/10^4\ \mu\text{m}^2$) elsewhere in the external glial limiting membrane, the mantle zone of the two rootlets should contain 2.2 and 7.7 perikarya respectively. Since part of the penetration area is occupied by nerve fibres, it is reasonable to expect still lower values. Actually the mantle zone of rootlet 1 contained 22 astrocytic perikarya and that of rootlet 3 contained 33, i.e. the rootlets contained 12 times and 7 times as many astrocytes as expected respectively. In the case of rootlet 2 the CNS compartment appeared like a proximal cylinder that was

transformed distally into a cone of the same shape and size as that of rootlet 3. The total mantle-zone area was estimated at $18.7 \times 10^4 \mu\text{m}^2$ which gives a maximum of 19 expected astrocytes. Examination of sections at consecutive $2.5 \mu\text{m}$ intervals showed that the true value was 85 astrocytes which is about 5 times the expected maximum value. The distribution of the astrocytes in rootlet 2 was, in contrast to rootlets 1 and 3, strikingly irregular 85 perikarya were present in the mantle of the conical part (length $240 \mu\text{m}$, mantle area $7.7 \times 10^4 \mu\text{m}^2$) and 11 in that of the cylindrical part (length $180 \mu\text{m}$, mantle area $11 \cdot 10^4 \mu\text{m}^2$). This gives for the conical part an observed value 11 times that expected and for the cylindrical part precisely the expected value of 1.

In all three rootlets, the conical part of the CNS compartment received 85% or more of the myelinated fibres. This is, for instance, illustrated by rootlet 2, where on the other hand only 5-10% of the unmyelinated fibres enter the conical region. Here the majority of the C-fibres penetrate the astrocyte-poor mantle zone of the cylindrical CNS compartment.

Against this background it can be concluded that the mantle zone contains far more astrocytes than expected. This seems in particular to be true of those parts of the CNS compartment which receive the majority of the myelinated fibres. Here the astrocytic occurrence was calculated to be about 10 times the maximal expected value. As indicated by the organisation of the cylindrical part of rootlet 2, neither a CNS protrusion as such nor the penetration of hundreds of C-fibres seemed to require an increased number of astrocytes. The high occurrence of mantle-zone astrocytes in the conical part of all three rootlets — there is on average one astrocyte to every 5 myelinated fibres — is difficult to explain. It should, however be pointed out that myelinated fibres here mean nodes of Ranvier and that the distal parts of the CNS compartment are equipped with an extensive glial fringe of unknown significance.

Distribution of nerve fibres

The large and the medium-sized myelinated dorsal root fibres are known to project mono- or disynaptically to the motoneurons and to join the lemniscus pathways. Some fibres penetrate into the head of the posterior horn of the spinal cord grey matter where they ramify. The small myelinated and the unmyelinated fibres terminate on cells of the extralemniscus pathways or project polysynaptically on motoneurons, particularly on flexor neurons (see Ramon y Cajal, 1909; Szentagothai, 1964; Wall, 1964; Ralston, 1965).

Unmyelinated axons and small myelinated fibres occupy according to Ranson (1913 1914 a, b) and Ranson and Billingsly (1916) a lateral position in the proximal part of feline lumbosacral dorsal roots. Earle (1962) reports that unmyelinated feline dorsal root fibres as they approach the zone of entrance into the spinal cords become separated to the periphery of the root. Wall (1962) on the other hand in a study of feline lumbar dorsal roots doubts that there is any specific localization at all of fibres at the root entrance zone, and Szentagothai (1964) working on the cat and the dog has claimed that the small fibres are grouped both on the lateral and median edges of the rootlets. Sindou *et al.*, (1974) recently noted that, in man, the small myelinated and the unmyelinated fibres were localized in the ventrolateral part of lumbosacral dorsal rootlets.

In the present work the nerve fibres were found to redistribute during their course along the TR with regard to both concentric zone and quadrant position. Since myelinated fibres entered the CNS compartment at more distal levels than did unmyelinated fibres and since the majority of the large and medium-sized myelinated fibres crossed the borderline distally with regard to the majority of small myelinated fibres these, and, in particular unmyelinated axons became aggregated in a thin layer just below the surface of the rootlets between levels B and A. A second shift in position concerned the quadrant distribution of the C-fibres. The calculated values for the relative C-fibre occurrence in the outer zone of the ventrolateral quasi-

quadrant at level A was in all cases more than 1.6 times that of the other quadrants ($\times 2.4$, 1.9 and 1.6 in rootlets 1, 2 and 3 respectively). A comparison between distal levels (D in rootlet 2 and 3, C in rootlet 1) and level A shows that the relative C-fibre occurrence in the outer zone of the ventrolateral quasi-quadrant increases some 2-4 times. On the other hand these calculations (see Fig. 24 and its legend) shows clearly that comparatively large numbers of C-fibres are present in the outer zones of the other quadrants as well.

Our conclusions disagree with Wall's (1962) opinion that there is no particular segregation of the nerve fibres in the proximal parts of feline spinal rootlets. Nor do the present data lend support to the idea (Sindou *et al.*, 1974) that partial and superficial rhizotomy along the ventral aspects of lumbosacral dorsal roots should be accepted as a neurosurgical procedure to alleviate regional pain. This is a question which cannot be evaluated until the small fibre distribution in human dorsal rootlets has been thoroughly documented by electron microscopy.

Fibre number on the two sides of the PNS-CNS borderline

Countings of the number of nerve fibres at the different levels showed that although the total number of fibres was roughly the same at all levels, the number of small myelinated fibres increased by 25% between levels B and A. The increase in myelinated fibres was accompanied by a similar decrease in the unmyelinated fibres. This suggests either that some PNS C-fibres acquire myelin presumably as they enter the CNS or that some C-fibres never enter the proximal level of the TR, whereas on the other hand some small myelinated fibres must have branched as they reached the proximal TR level. No straightforward explanation is available at the present time. This would require numerical analysis performed on sections separated by only a few μm and could not, as in the present case, be based on sections separated by up to a hundred or more μm .

ACKNOWLEDGEMENTS

This investigation was supported by grants from Karolinska Institutet (Reservationsanlaget) and from the Swedish Medical Research council (projects No. 12x 3157 and 03157). We are much indebted to Miss Maj Berghman, Mrs. Anita Bergström, Mrs. Eva Björkner and Mrs. Anna-Stina Holjer for excellent technical assistance.

Table I

Number of unmyelinated and myelinated fibres and the occurrence of blood vessels at four cross levels of the free proximal part of S₁ dorsal rootlets in three cats. (I = large, II = medium, III = small fibres)

Specimen	Level	Number of unmyelinated fibres	Number of myelinated fibres Total	I	II	III	Number of vessels
Rootlet 1	II	—	—	—	—	—	—
	C	337	104	3	50	51	1
	II	337	104	3	50	51	0
	A	324	117	3	50	64	0
Rootlet 2	II	950	350	10	174	166	8
	C	950	350	10	174	166	8
	B	950	350	10	174	166	4
	A	904	398	10	174	212	0
Rootlet 3	D	1010	349	9	171	169	7
	C	1010	349	9	171	169	7
	B	1010	349	9	171	169	7
	A	989	390	9	171	210	0

Table II

Estimations of length and mantle area of the CNS compartment and its content of astrocytes

Specimen	Length of CNS compartment (µm)	Appr. area of the mantle zone (µm ²)	Expected number of astrocytes in the mantle zone ³⁾	Estimated number of astrocytes in the mantle zone
Rootlet 1	200	22321	2,2	26
Rootlet 2	420	187205	19	95
		(77406 ¹⁾)	(7,7 ¹⁾)	(85 ¹⁾)
		(109800 ²⁾)	(11 ²⁾)	(11 ²⁾)
Rootlet 3	240	77405	7,7	53

1) Conical part

2) Cylindrical part

3) Based on estimations of feline external glial limiting membrane (0.9 astrocyte nuclei per 10⁴ µm²)

REFERENCES

- Berthold, C. H. (1968) A study on the fixation of large mature feline myelinated ventral lumbar spinal-root fibres. *Act. Societatis Medicorum Upsaliensis* 73, Suppl. 9 1-38.
- Blakemore W.F. (1975) Remyelination by Schwann cells of axons demyelinated by intraspinal injection of 6-aminocaproic acid in the rat. *Journal of Neurocytology* 4, 745-57.
- Blakemore, W.F. and Patterson, R.C. (1973) Observations on the interactions of Schwann cells and astrocytes following X-irradiation of neonatal rat spinal cord. *Journal of Neurocytology* 4 573-85.
- Bondareff W. and McLone D.G. (1973) The external glial limiting membrane in macaca: Ultrastructure of a laminated glioepithelium. *The American Journal of Anatomy* 136 277-96.
- Bossy J. (1967) Les gaines de myéline au niveau de la jonction des racines des nerfs spinaux et de la moelle épinière chez l'homme et le Chacal. *Archives d'Anatomie, d'Histologie et d'Embryologie normales et expérimentales* 40 72-81.
- Brightman M.W. (1965) The distribution within the brain of ferritin injected into cerebrospinal fluid compartments. II Parenchymal distribution. *The American Journal of Anatomy* 117 193-219.
- Brightman, M.W. and Reese T.S. (1969) Junctions between intimately apposed cell membranes in the vertebrate brain. *The Journal of Cell Biology* 40, 648-77.
- Brody I. (1959) The keratinization of epidermal cells of normal guinea pig skin as revealed by electron microscopy. *Journal of Ultrastructure Research* 2, 482-511.
- Cassemeyer J. (1960) Differences in shape and size of neuroglial nuclei in the spinal cord due to individual, regional and technical variations. *Acta Anatomica* 40, 149-77.
- Carleton, T. (1977) Observations on the morphology at the transition between the peripheral and the central nervous system in the cat. I A preparative procedure useful for electron microscopy of the lumbosacral dorsal rootlets. *Act. Physiologica Scandinavica*, Suppl. 448, 6-22.
- Earle, K.M. (1952) The tract of Lissauer and its possible relation to the pain pathway. *The Journal of Comparative Neurology* 96, 93-111.
- Feigin I. and Cravito H. (1961) A histochemical study of myelin. A difference in the solubility of the glycolipid components in the central and peripheral nervous system. *Journal of Neuropathology* 20 245-54.
- Foncin, J.F. (1961) Structure fine de la zone de passage radiculomédullaire. *Revue Neurologique* 105, 509-13.
- Frada, R.L. (1961) *A Histochemical Atlas of Tissue Oxidation in the Brain stem of the Cat*. Basel, New York: S. Karger.
- Gamble H.J. (1976) Spinal and cranial nerve roots. In *The Peripheral nerve* (edited by Landon, D.N.) pp. 330-354. London: Chapman and Hall.
- Ghatak, N.R., Hirano A., Doron, Y. and Zimmerman H.M. (1973) Remyelination in multiple sclerosis with peripheral type myelin. *Archives of Neurology* 29 252-7.
- Gilmore S.A. (1971) Autoradiographic studies of intramedullary Schwann cells in irradiated spinal cords of immature rats. *The Anatomical Record* 171 517-28.
- Gilmore S.A. and Duncan, D. (1968) On the presence of peripheral-like nervous and connective tissue within irradiated spinal cord. *The Anatomical Record* 160 675-90.
- Haller F.R., Haller A.C. and Low F.N. (1972) The fine structure of cellular layers and connective tissue space of spinal nerve root attachments in the rat. *The American Journal of Anatomy* 133, 109-24.
- Hori, A. (1973) Über intraspinal Schwannosen der Zona terminalis (Lissauer). *Acta Neuropathologica (Berl)* 24, 89-94.
- Hollen, E. (1906) Beiträge zur Kenntnis der sensiblen Wurzeln der Medulla oblongata beim Menschen. *Arbeiten aus dem Neurologischen Institut der Wiener Universität* 13, 392-98.
- Maxwell, D.S. (1967) Fine structure of the normal trigeminal ganglion in the cat and monkey. *Journal of Neurosurgery* 26 127-31.
- Maxwell, D.S., Kruger L. and Pineda, A. (1969) The trigeminal nerve root with special reference to the central-peripheral transition zone: An electron microscope study in the Macaque. *The Anatomical Record* 164, 113-20.

- McFarland, D.E. and Friede, R.L. (1971) Number of fibres per sheath cell and internodal length in cat cranial nerves. *The Journal of Anatomy* 109 169-78.
- Mincier, J. (1972) Communication disorders. In *Pathology of the Nervous System* (edited by Mincier J.) 3, pp 2881-83. New York: McGraw Hill Book Company.
- Morales, R. and Duncan, D. (1971) Prismatic and other unusual arrays of mitochondrial cristae in astrocytes of cats and hamsters. *The Anatomical Record* 171 545-57.
- Mugnaini, E. and Walberg F. (1964) III. Ultrastructure of neuroglia. *Ergebnisse der Anatomie und Entwicklungsgeschichte* 37 194-236.
- Nabeshima, S., Reese, T.S., Landis, D. and Brightman, M.V. (1975) Junctions in the meninges and marginal glia. *The Journal of Comparative Neurology* 184 127-70.
- Natanziel, E.J. and Natanziel, D.R. (1963). Electron microscopic observations on the dorsal root-spinal cord junction. *The Journal of Comparative Neurology* 184 127-70.
- Obersteiner H. and Redlich, E. (1894) Über Wesen und Pathogenese der tabischen Hinterstrangsdegeneration. *Arbeiten aus dem Neurologischen Institute and der Wiener Universität* 1-3, 158-72.
- Olsson, Y. (1971) Studies on vascular permeability in peripheral nerves. IV. Distribution of intra-axonally injected protein tracers in the peripheral nervous system of various species. *Acta Neuropathologica (Berl)* 17, 114-26.
- Peters, A., Palay L.S. and Webster H. de F. (1970) *The Fine Structure of the Nervous System, The Cells and Their Processes*. New York, Evanston and London: Harper and Row Publishers.
- Ploess J., Balne, C.S. and Wisniewski H. (1969) An ultrastructural study of experimental demyelination and remyelination III. Chronic experimental demyelination and remyelination III. Chronic experimental allergic encephalomyelitis in the central nervous system. *Laboratory Investigation* 21 472-83.
- Raine, C.S. (1976) On the occurrence of Schwann cells within the normal central nervous system. *Journal of Neurocytology* 5 571-80.
- Ralston, H.J. (1955) The organization of the substantia gelatinosa Rolandi in the cat hemibuccal spinal cord. *Zeitschrift für Zellforschung* 67 1-23.
- Ramon y Cajal, C. (1909) *Histologie du Système Nerveux* 1 986. Paris: Maloine.
- Ranson, S.W. (1913) The course within the spinal cord of the nonmedullated fibres of the dorsal roots: A study of Lissauer's tract in the cat. *The Journal of Comparative Neurology* 23, 259-81.
- Ranson, S.W. (1914a) The tract of Lissauer and the substantia gelatinosa Rolandi. *The American Journal of Anatomy* 18, 97-126.
- Ranson, S.W. (1914b) An experimental study of Lissauer's tract and the dorsal roots. *The Journal of Comparative Neurology* 24, 631-45.
- Ranson, S.W. and Billingsly P.R. (1916) The conduction of painful afferent impulses in the spinal nerves. *The American Journal of Physiology* 40, 571-84.
- Reese T.S. and Karnovsky M.J. (1967) Fine structural localization of a blood-brain barrier to exogenous peroxidase. *The Journal of Cell Biology* 34, 207-17.
- Reynolds, E. (1963) The use of lead citrate at high pH as an electron-opaque stain in electron microscopy. *The Journal of Cell Biology* 17 209-13.
- Ross, M.D. and Burkel, W. (1971) Electron microscopic observations of the nucleus, glial dome and meninges of the rat acoustic nerve. *The American Journal of Anatomy* 130 73-91.
- Sandou, M., Quocq, C. and Baleydiar C. (1974) Fiber organization at the posterior spinal cord-rootlet junction in man. *The Journal of Comparative Neurology* 163, 15-25.
- Skinner H.A. (1931) Some histological features of the cranial nerves. *Archives of Neurology and Psychiatry* 25, 356-72.
- Steer J.M. (1971) Some observations on the fine structure of rat dorsal spinal nerve roots. *The Journal of Anatomy* 109 467-85.
- Szentagothai, J. (1964) Neuronal and synaptic arrangement in the substantia gelatinosa Rolandi. *The Journal of Comparative Neurology* 122, 219-39.
- Tarlov I.M. (1937a) Structure of the nerve root. I. Nature of the junction between the central and the peripheral nervous system. *Archives of Neurology and Psychiatry* 37 555-63.
- Tarlov I.M. (1937b) Structure of the nerve root. II. Differentiation of sensory from motor roots. Observations on identification of function in roots of mixed cranial nerves. *Archives of Neurology and Psychiatry* 37 1338-55.
- Thomas, P.K. (1963) The connective tissue of peripheral nerve: an electron microscope study. *The Journal of Anatomy (Lond)* 97, 35-44.
- Wall, P.D. (1962) The origin of spinal cord slow potential. *The Journal of Physiology* 164, 505-29.

- Wall, P.D. (1961) Presynaptic control of impulses at the first central synapses in the cutaneous pathway. In *Progress in Brain Research 12. Physiology of Spinal Neurons* (edited by Eccles, J.C. and Schäffé J.P.) Amsterdam London New York: Elsevier Publishing Company.
- Williams, V. (1975) Intercellular relationships in the external glial limiting membrane of the neocortex of the cat and rat. *The American Journal of Anatomy* 144, 4, 1-32.
- Virchow, R. (1858) Rückenmark und Gehirn. In *Die Cellular Pathologie in ihrer Begründung auf Physiologische und Pathologische Gewebelehre* pp 238-251 Berlin, Hirschwald.
- Wood, W.C., Rothman, I.M. and Nussbaum, B.E. (1975) Intramedullary neurolemmas of the cervical spinal cord. *Journal of Neurosurgery* 42, 465-8.

Fig. 4a. LM. Vestopal embedded specimen. Toluidine blue stained cross section of the dorso-lateral part of the spinal cord and a number of adjoining S dorsal rootlets. Arrow indicates the dorsomedial sulcus. One rootlet joins the cord in the dorsolateral sulcus (single-bar arrow). The pale central areas of the two medial rootlets are not artifacts but an effect of the different staining properties of CNS and PNS myelin ($\times 110$).

Fig. 4b. Higher magnification of the rootlet as marked out by double-bar arrow in Fig. 4a. The rootlet contains a darker stained outer compartment of PNS tissue (P) and lighter stained inner compartment of CNS tissue (C) ($\times 110$).

Fig. 5. EM. Survey picture of a longitudinally sectioned TR of a thin S dorsal rootlet. The spinal cord is situated in the lower aspect of the picture and the stereotypic PNS part of the root in the upper aspect of the picture. The five reference levels A, B, C, D (see Fig. 1) are indicated to the right of the picture. The interface between the PNS and CNS compartments of the rootlet is formed by the mantle zone (MZ), which gives off the glial fringe (GF) in distal direction. The glial fringe occupies part of the endoneurial space of the PNS compartment. The CNS compartment consists of a core zone (CZ) with closely packed myelinated fibres. Borderline nodes (BN) and CNS borderline paranodes together with astrocytes (A) constitute the mantle zone (MZ) ($\times 1300$).

Figs. 6-11. This sequence of electron micrographs shows six different cross levels selected from a complete series of consecutive cross sections through the proximal free part of a S dorsal rootlet in specimen K 1040. The orientation of the rootlet is given by the reference directions M (medial), V (ventral), L (lateral), D (dorsal) in the compass card given in the upper right corner of each picture. The section number (section thickness 700 Å) is given in the lower left corner. Seven fibres have been marked out, fibre 2 is a large fibre ($> 13 \mu\text{m}$), fibres 3 and 5 are medium sized (6-13 μm) and fibres 1, 4, 6 and 7 are small myelinated fibres ($< 6 \mu\text{m}$) ($\times 1500$). Inset shows higher magnification ($\times 6800$) of fibre 1.

Fig. 6. Stereotypic PNS part of the rootlet as seen in a cross section 340 μm distally to the proximal upper limit of the TR. This position corresponds roughly to the reference level D as given in Figs. 1 and 5. There is no clear segregation of various myelinated fibre types. Most of the unmyelinated (U) fibres occur superficially in the rootlet. The rootlet contains 2 vessels (Ve).

Fig. 7. Distal part of the TR as seen in a cross section 280 μm distally to the proximal limit of the TR. This position corresponds roughly to the reference level C (as given in Figs. 1 and 5). The whole cross section is occupied by the PNS compartment. CNS tissue constituents — the tip of the glial fringe — appear like several astrocytic processes in the immediate vicinity of fibre 1 (see inset). Fibre 2 shows paranodal crenation (PN). All fibres are of PNS type.

Fig. 8. Distal part of the TR as seen in a cross section 240 μm distally to the proximal limit of the TR. This position corresponds roughly to the reference level O as given in Figs. 1 and 5. There are several deeply crenated PNS borderline paranodes (PN) in between the areas occupied by the glial fringe. The borderline node of fibre 2 is found close to the centre of the picture. This appeared to be the most distal of all borderline nodes in this rootlet. There is a myelinoid body (MB) localized in the astrocytic compartment to the right of the borderline node.

Fig. 9. Distal part of the TR as seen in a cross section 210 μm distally to the proximal limit of the TR. This position corresponds to level in between the reference levels O-B. The PNS compartment encloses the CNS compartment. Most large fibres are of CNS type and localized in the centre of the picture. The main part of the smaller fibres are in the outer zone of the rootlet and are of PNS type. Note the high occurrence of unmyelinated fibres (U) in the most superficial zone of the rootlet. Fibre 1 shows paranodal configuration (PN). The core zone (CZ) discloses closely packed CNS myelinated fibres. The mantle zone (MZ) contains borderline nodes (BN) and CNS borderline paranodal segments as well as astrocytes (A). The glial fringe is situated between the paranodal parts of PNS myelinated fibres. There are no vessels in the CNS compartment.

Fig. 10. The section level is 10 μm more proximal than in Fig. 9. Fibre 1 which already at reference level C was surrounded by astrocytic processes has here some 60 μm further proximally shifted to the CNS type.

Fig. 11. Proximal limit of the TR. The position of the section corresponds to the level A of Fig. 1. Arrows point at the two most proximally situated borderline nodes. The rootlet is free of vessels.

Fig. 12 Cross section through the mantle zone (MZ) in the lower part of the picture and adjacent parts of the PNS compartment. The position of the section is about 20 μm proximally to reference level O (Fig. 1). The PNS-CNS borderline is marked out by the dotted line. A large CNS myelinated fibre and astrocytic perikarya are seen in the mantle zone. The glial fringe (GF) is extensive. Its astrocytic processes forms more or less complete walls between the PNS myelinated axons. Fibres 1 and 2, both cut through their PNS borderline paranodes, are bordered by the glial fringe, each together with a rim of endoneurial space that contains collagen fibres (x4000).

Fig. 13 Cross section through the mantle zone (lower half of the picture), and adjacent parts of the PNS compartment. The position of the section is about 20 μm distally to the proximal limit of the TR. The dotted line suggest the course of the PNS-CNS borderline. Two PNS myelinated fibres and collagen (Co) containing endoneurial space are enclosed in the thin rim of loosely packed astrocytic processes which forms the glial fringe at this proximal level of the TR (x4700).

Fig. 14 EM. Mantle zone. Two myelinated bodies (MB) are situated close to the borderline segment of a myelinated fibre (x) (x13000).

Fig. 15 Cross cut bundles of endoneurial collagen fibres separated by thin astrocytic septa. The astrocytic plasma membranes lacks its usual basement membrane cover. Continuity between the clear space occupied by the collagen and the endoneurial space of more distal levels was ascertained by serial section analysis. The size of the individual collagen fibres varies between 200 and 1200 \AA . Arrows indicate desmosomes between the astrocytic processes (x22000).

Fig. 16 EM. Cross cut glial fringe. The picture shows two apposed astrocytic processes (Ap, Ap'). The cytoplasm of each process contains many fibrils scattered micro tubules and one gliosome supplied with prismatic cristae (x71000).

Fig. 17 EM. Mantle zone. Large gliosome (2 μm) containing a fine granular matrix (x21000).

Fig. 18a, b EM. Cross section through the glial fringe showing a large defect in the basement membrane (between arrows) outlining the astrocytic processes. The gap between the two pictures is about 5 μm . Gap junction at the arrow with bar in Fig. 18a (x44000).

Fig. 19 EM. Cross section through the glial fringe. Unclassified cell (UC) surrounded by basement membrane (arrows) (x17000).

Fig. 20 EM. Cross sectioned core zone. In this part of the TR the tissue show the appearance of CNS fibre tract with closely packed nerve fibres and intervening glial elements. An oligodendrocyte (O) classified according to its characteristic appearance (Magnaini and Walberg, 1964; Peters *et al.*, 1970): a rounded, clear outline, large amounts of free ribosomes, microtubuli, heterogeneous dense bodies and mitochondria but no gliosomes. The cell body contacts the myelin of two adjacent fibres (arrows) (x5000).

Figs. 21, 22, 23 Quantitative estimations of various parameters in the proximal part of S₁ dorsal rootlet from each of three cats (Rootlet 1 K1037, rootlet 2 K1039, rootlet 3 K1040).

a) Number of fibroblasts, microglia, Schwann cells, unclassified cells and pericytes as found in cross sections 20 μm apart.

b) Number of astrocytes as found in 20 μm long segments of the transitional region. The numbers in the boxes represent astrocytes found in the core zone. All other astrocytes were parts of the mantle zone.

c) Number of oligodendrocytes as found in 20 μm long segments of the transitional region.

d) Occurrence of central myelinated fibres in sections 20 μm apart. The picture also gives the total area of the rootlet (statched line) and the area of the CNS compartment as found at 20 μm intervals (cf. Fig. 1).

e) Distribution of large (I), medium (II) and small (III) myelinated and unmyelinated (C) fibres in the four quasi-quadrants (DM - dorsomedial, DL - dorsolateral, VM - ventromedial, VL - ventrolateral) of the reference levels A, B, C, D (see Fig. 1). The area of each quadrant is given in arbitrary units. The key value is found in the central part of the picture. Schematic drawings of the cross contour of the rootlet at the diverse reference levels and with the different quasi-quadrants are in the central part of the picture.

f) Distribution of fibres as found in three concentric zones and the central spot of the reference levels A, B, C, D (see Fig. 1). Same arbitrary area scale as in Fig. e. Note that each rootlet has its own area key value.

Fig. 4a L.M. Vestopal embedded specimen. Toluidine blue stained cross section of the dorso-lateral part of the spinal cord and a number of adjoining S₁ dorsal rootlets. Arrow indicates the dorso-medial sulcus. On rootlet joins the cord in the dorso-lateral sulcus (single-bar arrow). The pale central areas of the two medial rootlets are not artifacts but an effect of the different staining properties of CNS and PNS myelin (x110).

Fig. 4b Higher magnification of the rootlet as marked out by double-bar arrow in Fig. 4a. The rootlet contains a darker stained outer compartment of PNS tissue (P) and lighter stained inner compartment of CNS tissue (C) (x110).

Fig. 5 EM Survey picture of a longitudinally sectioned TR of a thin S₁ dorsal rootlet. The spinal cord is situated in the lower aspect of the picture and the stereotypic PNS part of the rootlet in the upper aspect of the picture. The five reference levels A, B, C, D, E (see Fig. 1) are indicated to the right of the picture. The interface between the PNS and CNS compartments of the rootlet is formed by the mantle zone (MZ), which gives off the glial fringe (GF) in distal direction. The glial fringe occupies part of the endoneurial space of the PNS compartment. The CNS compartment consists of a core zone (CZ) with closely packed myelinated fibres. Borderline nodes (BN) and CNS borderline paranodes together with astrocytes (A) constitute the mantle zone (MZ) (x1300).

Figs. 6-11 This sequence of electron micrographs shows six different cross levels selected from a complete series of consecutive cross sections through the proximal free part of a S₁ dorsal rootlet in specimen h 1040. The orientation of the rootlet is given by the reference directions M (medial), V (ventral), L (lateral), D (dorsal) in the compass card given in the upper right corner of each picture. The section number (section thickness 700 Å) is given in the lower left corner. Seven fibres have been marked out, fibre 2 is a large fibre (13 µm), fibres 3 and 5 are medium sized (8-13 µm) and fibres 1, 4, 6 and 7 are small myelinated fibres (6 µm) (x1500). Inset shows higher magnification (x8800) of fibre 1.

Fig. 6 Stereotypic PNS part of the rootlet as seen in a cross section 340 µm distally to the proximal upper limit of the TR. This position corresponds roughly to the reference level D as given in Figs. 1 and 5. There is no clear segregation of various myelinated fibre types. Most of the unmyelinated (U) fibres occur superficially in the rootlet. The rootlet contains 2 vessels (V).

Fig. 7 Distal part of the TR as seen in cross section 280 µm distally to the proximal limit of the TR. This position corresponds roughly to the reference level C (as given in Figs. 1 and 5). The whole cross section is occupied by the PNS compartment. CNS tissue constituents — the tip of the glial fringe — appear like several astrocytic processes in the immediate vicinity of fibre 1 (see inset). Fibre 2 shows paranodal crenation (PN). All fibres are of PNS type.

Fig. 8 Distal part of the TR as seen in cross section 240 µm distally to the proximal limit of the TR. This position corresponds roughly to the reference level B as given in Figs. 1 and 5. There are several deeply crenated PNS borderline paranodes (PN) between the areas occupied by the glial fringe. The borderline node of fibre 2 is found close to the centre of the picture. This appeared to be the most distal of all borderline nodes in this rootlet. There is a myelin body (MB) localized in the astrocytic compartment to the right of the borderline node.

Fig. 9 Distal part of the TR as seen in a cross section 210 µm distally to the proximal limit of the TR. This position corresponds to a level in between the reference levels B and C. The PNS compartment encloses the CNS compartment. Most large fibres are of CNS type and localized in the centre of the picture. The main part of the smaller fibres are in the outer zone of the rootlet and are of PNS type. Note the high occurrence of unmyelinated fibres (U) in the most superficial zone of the rootlet. Fibre 1 shows paranodal configuration (PN). The core zone (CZ) discloses closely packed CNS myelinated fibres. The mantle zone (MZ) contains borderline nodes (BN) and CNS borderline paranodal segments as well as astrocytes (A). The glial fringe is situated between the paranodal parts of PNS myelinated fibres. There are 2 vessels in the CNS compartment.

Fig. 10 The section level is 10 µm more proximal than in Fig. 9. Fibre 1 which already at reference level C was surrounded by astrocytic processes has here, some 60 µm further proximally shifted to the CNS type.

Fig. 11 Proximal limit of the TR. The position of the section corresponds to the level A of Fig. 1. Arrows point at the two most proximally situated borderline nodes. The rootlet is free of vessels.

Acta physiol. scand 1977 Suppl. 446

From the Department of Anatomy Karolinska Institutet,
Stockholm, Sweden

Observations on the Morphology at the Transition between the Peripheral and the Central Nervous System in the Cat.

III.

Myelinated fibres in S dorsal rootlets.

by

C H. BERTHOLD and T. CARLSTEDT

ABSTRACT

C H. BERTHOLD and T. CARLSTEDT *Observations on the morphology at the transition between the peripheral and the central nervous system in the cat. III. Myelinated fibres in S dorsal rootlets* Acta physiol. scand. 1977 Suppl. 446, 43-60.

Myelinated nerve fibres were analysed at their passage of the PNS-CNS borderline in the transitional region (TR) of the S₁ dorsal rootlets by means of light and electron microscopy. At the borderline, PNS internodal length was 30% shorter than noted further distally in the root. Analysis of variance based on the numerical estimation of various fibre parameters did not support the current idea that a myelinated nerve fibre decreases in diameter as it passes from the PNS into the CNS. There was a rough rectilinear correlation between axon size and number of myelin lamellae in small and medium sized fibres. In large fibres the number of myelin lamellae was highly variable and could not be predicted from axon size. The nodes of Ranvier found at the borderline showed an organization that could be described as compound node where the PNS-CNS demarcation line runs across the nodal axon segment in the midst of the node gap. Branching at the borderline nodes was a very rare phenomenon. The length of the nodal axon segment, the nodal axon membrane area and the amount of paranodal mitochondria were similar to earlier presented data of feline ventral root fibres. The hypothesis that the elements of the paranodal apparatus of PNS fibres compensate for the lack in the PNS of nodally connected astrocytes is presented and discussed. A small number of the fibres lacked a borderline node. In these cases the CNS myelin sheath projected uninterrupted for hundreds of μm into the PNS compartment where it was enclosed by a Schwann cell and PNS myelin. This rare arrangement was referred to as a transitional internode.

Somatic myelinated nerve fibres of the mammalian peripheral nervous system (PNS) either originate or terminate in the central nervous system (CNS). Hence, they all have to cross the PNS-CNS borderline. This passage implies profound rearrangements of the axonal surroundings. In the PNS one Schwann cell attends a restricted segment of one single axon and supplies the internodal ends with the components of the paranodal apparatus: mitochondria and node-gap microvilli (for references see Landon and Williams, 1963, Williams and Landon, 1963; Berthold, 1968b; Biechoff and Thomas, 1976; Landon and Hall 1976). In the CNS one oligodendrocyte gives rise to several internodal myelin sheath segments belonging to different axons. There are no paranodal accumulations of mitochondria, and node-gap microvilli are few and poorly developed (see review by Bunge, 1968; Hildebrand, 1971). Thus one of the most intriguing features of PNS-fibre organization — the paranodal apparatus — appears to be virtually absent in the CNS.

Myelinated fibres in the transitional region

Available data indicate that the transition from one nervous tissue compartment to the other as seen in a myelinated fibre takes place at a node of Ranvier — the borderline node — where an internode of PNS origin meets one of CNS origin (Foncin, 1961; Friede 1961; Maxwell *et al.*, 1969). Whether the borderline node consists of a typical PNS half and a typical CNS half or shows a preponderance of either pattern or whether it possesses certain unique features is unknown. In connection with the PNS to CNS transition of myelinated fibres the current literature supplies conflicting data as regards such functionally significant parameters as axon size, myelin sheath thickness and degree of fibre branching (Maxwell *et al.*, 1969; Ross and Burkel, 1971; Fraher 1976; see review by Gamble, 1976). In no case have comparisons been performed at CNS and PNS levels of the same axon. A direct serial section analysis of the myelinated fibres as they appear in the transitional region itself would then obviously provide straight forward information on many an obscure issue.

The present study deals in qualitative and quantitative terms with the myelinated nerve fibres of the dorsal root S₁ transitional region (TR) as observed light and electron-microscopically in the adult cat (see Berthold and Carlstedt, 1977). In short, the results — intended to serve as a standard for future work on the development of the TR — show that there is no difference in axon size on the two sides of the borderline node, that a recalculation of axon sizes and myelin sheath thickness to the native condition gives similar CNS and PNS values, that besides borderline nodes there are also transitional internodes and that the organization of the borderline node discloses unique features, some of which might be taken to support the idea that the paranodal apparatus might be the PNS counterpart of astrocytes related to the nodes of Ranvier in the CNS.

MATERIAL AND METHODS

Eight adult cats were anaesthetized intraperitoneally with pentobarbital, 40 mg/kg BW and artificially ventilated with 100% oxygen. The lower spinal cord was fixed by vascular perfusion of a solution containing 5% glutaraldehyde for 20 minutes. The specimens, consisting of the segment S₁ and its dorsal roots, were removed by a laminectomy which required 10-15 minutes of preparative work (see Carlstedt, 1977).

Teased specimens

Specimens of 4 cats were after perfusion fixation rinsed for a short time in the buffer and the roots were carefully teased under a dissecting microscope into individual fibres.

Estimation of internodal length Teased specimens were osmicated for 2 hours in 2% OsO₄ in 300 mM Millonig buffer and mounted in glycerine on glass slides. In order to avoid pressure on the specimens strips of adhesive tape 80 μ m thick were placed on the glass slides to support the cover glass. Internodal length and fibre diameter were determined in the proximally situated peripheral internodes and in internodes of the mid part of the root, using a scale in the eyepiece of a Leitz light microscope.

NADH₂-diaphorase activity Teased specimens were incubated at 37°C for 30 minutes in a medium containing NADH as a substrate and Nitro BT as reagent (Becker *et al.*, 1960; Berthold and Skogland, 1967). Specimens incubated in a medium without substrate served as controls. After incubation the specimens were briefly rinsed in the Veronal buffer, mounted in glycerine on glass slides and examined and photographed in a Leitz photomicroscope.

Vestopal embedded specimens

Specimens of 4 cats were processed according to a method described in detail elsewhere (see Carlstedt, 1977). The specimens were, after postfixation, osmication and Vestopal-embedding trimmed iteratively into 30 μ m high mesas using a LKB 11800 Pyramitome and then sectioned on LKB 4800 Ultratome. The specimens were carefully orientated for cross sectioning so that the nerve fibres were cut perpendicularly to their longitudinal axis and sectioned in the distal to proximal direction. Longitudinal sections parallel to the longitudinal axis of the nerve fibres were obtained by sectioning the rootlets in the dorsoventral direction.

Three series of consecutive ultra thin cross-sections (average thickness 700 Å) were cut comprising 10,000, 6000, 5,500 sections, respectively and four series of longitudinal sections of 200-1000 consecutive sections each. The average section thickness which was obtained from the ratio between mesa height and the number of sections, varied between 600-800 Å. The loss of sections was less than 1%. The sections were placed on one hole copper grids coated with a carbon-stabilized formvar film. After double staining with uranyl acetate (Brody, 1966) and lead citrate (Reynolds, 1963) the sections were examined in a Philips EM 300 electron microscope operated at 80 kV and equipped with a 30 μ m objective aperture.

Sections for light microscopy (0.5 μ m thick) were placed on glass slides and stained with alkaline toluidine blue, examined, and photographed in a Leitz photomicroscope.

Quantitative estimations

Each cross-section series was photographed at consecutive 10 μ m intervals and the myelinated fibres were identified and marked out by numbers on the photocopies. Proper identification was ascertained by the checking of intervening sections in the EM.

The myelinated fibres were classified as large, type I (D = 12 μ m), medium, type II (D = 13 μ m) and small, type III (D = 8 μ m) fibres. Since this classification corresponds to the three groups of afferent fibres as separated by Lloyd (1943) with regard to conduction velocity the proper classification of the present material can be performed first after the fiber size of the unprocessed fibres (D = native fibre size) has been calculated. This was done here by adding together the axon diameter (d), compensated for by a factor of shrinkage = 1.1 (see Berthold, 1968b, Carlstedt, 1977) and the double myelin sheath thickness as obtained from the number of myelin lamellae (n) times the original myelin period given as 180 Å (see Finean, 1960) and 160 Å (see Hildebrand and Møller 1974) in the PNS and CNS respectively. Thus DPNS = 1.1 dPNS + 2x180 nPNS, DCNS = 1.1 dCNS + 2x160 nCNS. The PNS and the CNS size of one and the same fibre were estimated 100 μ m distally and proximally to the PNS-CNS borderline respectively.

The axon size (σ) was determined both as the length of the axon circumference (σ_{circ}) measured with map distance reader and as the size of the axon cross-section area (σ_{area}) as estimated by planimetry. A third estimate of axon size, σ_{ratio} was obtained by the ratio of cross section area to length of circumference.

The number of myelin lamellae was estimated from the number of major dense lines in each sheath. The myelin period was measured as the mean distance between the midpoints of 10 successive major dense lines. The measurements were performed in regions of the myelin sheaths where the lamellar pattern was regular and distinct and where the course of the lamellae was parallel to the direction of sectioning. Sharply curved parts of the sheaths were excluded (cf. Gusterson, 1968).

The hypothesis that there is a difference in fibre size between the investigated PNS and CNS levels was tested by an analysis of variance. First, the difference in axon size was tested using each of the three estimates (σ_{circ} , σ_{area} and σ_{ratio}) separately. Then the native calculated D-values were tested once, using the σ -estimate which according to the analysis of variance showed the smallest CV value. Not surprisingly this turned out to be the ratio which has the higher information content. The analysis of variance was performed with the aid of computer (IBM 370/155) and a standard statistical programme.

The number of Schwann cell mitochondria was estimated by counting on photocopies of different paranodal and internodal levels (see Fig 6 and Table III). The number of mitochondria was then plotted to scale in a diagram with reference to the distance from the borderline node. Since the sum of the area between the plotted line and the base line expresses the amount of mitochondria given in arbitrary units, this latter parameter was estimated by planimetry. These estimations were performed on 27 fibres (3 fibres of each type animal).

The length of the nodal axon segment (nl) was measured as the length of the undercoated axon membrane as seen in series of longitudinal sections. The parameter is given as the mean value of six measurements performed on each side of the axon in three sections: one median section and two paramedian sections located symmetrically between the median section and the axon perimeter. In the same way the mean values of the length of the terminal PNS and CNS myelin sheath segments were also estimated. The nodal axon diameter (nd) was measured in the median section and corrected by the shrinkage factor of 1.1. Assuming that the nodal axon segment is a cylinder its membrane area (A) is very simple to calculate, viz. $A = \pi \cdot nd \cdot nl$. These estimations were performed in 18 fibres (2 fibres of each type in each of 3 animals).

RESULTS

Internodal length

The internodal length measured 200-1000 μm in PNS borderline internodes. Halfway between the spinal cord and the spinal ganglion the internodes measured 300-1600 μm . At both levels internodal length was linearly correlated to fibre size with a correlation coefficient of 0.95 (Fig. 1). In several cases it was noted that the internodal length along one and the same fibre increased gradually in the proximal to the distal direction as seen from the PNS-CNS borderline and for a distance corresponding to 3-4 internodes.

Distribution of NADH₂-diaphorase activity

The distribution of the enzyme activity in the PNS compartment of the TR corresponded, with the exception of the PNS borderline paranode, to that given elsewhere for feline dorsal root fibres (Berthold and Skoglund, 1967; Berthold, 1968a). PNS borderline internodes thus revealed the rather stereotype pattern of a enzyme activity concentrated at the Schwann cell perikaryon, extending proximally and distally like delicate longitudinal stripes that broadened paranodally and terminated, still arranged like stripes, close to the node (Fig. 7b). At PNS-borderline paranodes, however, the bluish-black stripes coalesced and lost their identity some 5-10 μm away from the node. This gave the picture (Fig. 7a) of paranodal bulbe that contained irregularly-shaped pools of enzyme activity that extended up to and sometimes covered the node gap.

Proximally to the borderline node the intensity of the staining was low and its distribution was uncharacteristic.

All controls were negative.

Fibre parameters on the two sides of the PNS-CNS borderline

Axon diameter. The analysis of variance (Table 1) showed a low significance ($p < 0.05$) with regard to a PNS-CNS difference in axon size as estimated from the \bar{x}_{circ} and the \bar{x}_{area} . In the case of the \bar{x}_{ratio} there was no difference between PNS and CNS size. A comparison between the three \bar{x} -variables using the coefficient of variation (CV, Table 1) showed that the \bar{x}_{ratio} had a smaller CV and hence was the test variable to be preferred to \bar{x}_{circ} and \bar{x}_{area} .

Myelin lamellae. In peripheral myelin sheaths the number of myelin lamellae varied between 20 and 130 (Fig. 4) and in the central myelin sheaths between 10 and 180 (Fig. 3). There was a more or less linear relationship between number of lamellae and axon size in small fibres where the number of lamellae varied between 20-100 in the PNS and between 10-90 in the CNS. Larger fibres contained a highly variable number of lamellae.

When comparing the number of lamellae in the peripheral and the central myelin sheath on the same axon (Fig 4) it was noticed that the smallest fibres (small group III fibres $4\text{ }\mu\text{m}$) had fewer lamellae in the CNS than in the PNS and that the situation was the reverse in medium and large fibres. The PNS myelin period (Table II) was $120\text{ }\text{\AA}$ (± 5) in all fibres alike. The CNS myelin period varied between 81 and $117\text{ }\text{\AA}$, being inversely related to fibre size (cf. Hildebrand, 1972).

Fiber size. Recalculation of myelin sheath thickness and of axon size to the native condition enabled the whole fibre size (D) to be estimated. Fig 5 shows that the PNS D-values of the smallest fibres ($4\text{ }\mu\text{m}$) are larger than the corresponding CNS D-values. Fibres more than $4\text{ }\mu\text{m}$ in size show a more or less contrary situation. As seen in Table II the mean values for the whole fibre population with regard to the PNS and CNS D-values indicated that the CNS part of a fibre might be somewhat thicker than its PNS part. This difference is also evident when using the analysis of variance (Table I).

The borderline segment

This part of a myelinated fibre found at the crossing of the PNS-CNS borderline consisted in the vast majority of fibres of a PNS (distal) borderline paranode, a CNS (proximal) borderline paranode and, an intervening borderline node of Ranvier. A few fibres lacked a borderline node in which cases an uninterrupted CNS myelin sheath crossed the borderline. This arrangement was referred to as a transitional internode.

PNS borderline paranodes In all but the smallest fibres ($4\text{ }\mu\text{m}$) the paranodes were characterized by a high content of Schwann cell mitochondria (Figs. 6, 8b, 12) and by longitudinal myelin sheath crests (Fig. 8a). The smallest fibres seemed to lack a paranodal Schwann cell mitochondrion accumulation (see below and Table III). The length of the paranodes varied from about $10\text{ }\mu\text{m}$ in small fibres to about $40\text{ }\mu\text{m}$ in large ones.

The paranodes together with a surrounding narrow *cul de sac* of the endoneural space, were as a rule isolated from neighbouring fibres inside a holster of closely-packed astrocytic processes (Figs. 8a, 10a) (cf. Bertold and Carlstedt, 1977). The processes were part of the glial fringe and derived from the astrocytic perikarya of the mantle zone. The borderline node was situated at the bottom (proximal end) of the endoneural *cul de sac*. The larger the fibre the longer (or deeper) was the holster its length varying from 20 down to only a few μm . The lumen of a holster adapted its shape to that of the enclosed paranode. The intervening endoneural gap measured about one μm in width (Figs. 8a, 10a). This arrangement restricted or eliminated the perinodal space, the latter being more or less replaced by the feltwork of astrocytic processes.

In contrast to ordinary PNS paranodes borderline paranodes showed myelin crests that disappeared several (5-10) μm from the node (Fig. 8b). Proximally to this level the cords of Schwann cell cytoplasm of more distal levels joined and often formed a more or less common cytoplasmic compartment very rich in mitochondria (Figs. 8b, 12). In several cases this compartment extended close to the node. At some nodes it covered part of the node gap (Fig. 12). In the latter cases Schwann cell microvilli projected from the mitochondrion-rich compartment straight into the node gap.

The highest numbers of paranodal Schwann cell mitochondria were noted in cross sections $3\text{--}7\text{ }\mu\text{m}$ from the node gap (Fig. 6). The countings were here about 300-200 and 30 mitochondria per cross section in average large, medium and small fibres respectively. The amount of paranodal mitochondria, as expressed in arbitrary units (Table III and Fig. 6) was in the same fibre types 100-200, 40-80 and 1-10 respectively. The smallest fibres showed no clear accumulation of paranodal mitochondria. In addition to mitochondria, the paranodal Schwann cell cytoplasm

contained electron-dense granules 200-300 Å in size (presumably glycogen), myelinoid bodies 2.5 µm in diameter and bodies 0.5-2 µm in diameter consisting of a homogeneous low-density material lacking a limiting membrane presumably lipid droplets (cf. Berthold, 1988b)

CNS paranodes. The contour of cross cut paranodal CNS myelin sheaths was rounded and lacked myelin crests (Fig. 8d). The paranodes pierced the mantle zone and were surrounded by astrocytic processes and astrocytic perikarya (Figs. 8, 9). Both the processes and the perikarya were rich in gliosomes. Myelinoid bodies up to 10 µm in size were common outside the CNS paranodes (Fig. 8d) (cf. Berthold and Carlsfeldt, 1977)

Borderline nodes The node-gap content was as a rule disarranged to some extent by tiny empty-looking torn spaces. The gaps contained in their distal part a corona of closely packed Schwann cell microvilli and in their proximal part some irregularly-shaped astrocytic extensions (Figs. 8c, 9 10a, b). The processes were surrounded by a finely granular node gap matrix substance. The two kinds of processes radiated towards the nodal axon plasma membrane, terminated 50-100 Å away from it and occupied each about half of its area (Table IV)

The axon diameter was reduced to less than half of its internodal size in those segments where the PNS-CNS-myelin sheaths terminated and in the intervening nodal segment. The cross-section contour was almost circular. The constricted axon segment contained tubules, filaments, scattered mitochondria and vesicles. The axon segment related to the PNS-myelin sheath termination, and adjacent parts of the nodal axon segment contained an accumulation of 200-300 Å-large electron dense granules (Fig. 9) (cf. Berthold, 1988b). The length of the nodal axon segment was about 1 µm in all fibres and its membrane area measured 11.20 7.9 and 2.5-5 µm² in large, medium and small fibres respectively (Table IV)

The borderline segment of the smallest (4 µm) fibres was of a similar general outline to that described above. The node gap appeared however more roomy and contained broad Schwann cell and astrocytic processes (Fig. 11). The peripheral paranode showed few and low myelin crests and the outer Schwann cell compartment contained comparatively few mitochondria (Table III, Fig. 6).

In two cases out of about 1000 investigated fibres axon bifurcation was noted at the borderline node (Fig. 13). Apart from the bifurcation the borderline segments of such fibres were morphologically similar to ordinary ones. The branches were thinner than the parent fibre.

Transitional internodes Each rootlet contained superficially in its PNS compartment one or two medium sized axons (i.e. less than 1% of the myelinated fibres) which for about 150-200 µm were equipped with both a central and a peripheral myelin sheath (Fig. 14a). The CNS-myelin sheath was telescoped inside the PNS-myelin sheath, both surrounding the axon.

Such aberrant fibres consisted of the following concentric layers as traced in the centripetal direction: basement membrane, outer cytoplasmic compartment of the Schwann cell, peripheral myelin sheath, inner Schwann cell compartment, astrocyte cytoplasm, central myelin sheath, a thin, presumably oligodendrocyte cytoplasmic layer and a central axon (Figs. 14a, b). The plasma membranes of the inner Schwann cell compartment and the astrocyte cytoplasm were separated by a space 200-300 Å wide. These two cytoplasmic compartments were missing at some sites and the central and peripheral myelin sheaths apposed each other forming a myelin-sheath intraperiod line at the zone of contact (Fig. 14c).

The peripheral myelin sheath terminated at the surface of the mantle zone. It formed cytoplasmic pockets which were attached to the underlying central myelin sheath (Fig. 14d). The Schwann cell contained in this position more mitochondria than were observed internodally and the proximal end of the outer Schwann cell

compartment formed a few short and broad processes. Fissures, both in the myelin sheaths and in the surrounding glia were common at the borderline passage of transitional internodes.

DISCUSSION

The problems of obtaining ultrastructurally well-preserved myelinated nerve fibres at their passage between the PNS and CNS compartments in feline S₁ dorsal rootlets are great and have been dealt with in a preceding communication (Carlstedt, 1977). Although that report showed that it was possible to improve the preservation of the myelin sheaths and the glia considerably none of the preparatory methods tested also gave a fully satisfactory preservation of the node-gap ultrastructure. Torn spaces and disarranged Schwann cell and glial processes were constantly noted at least at some sites in the gaps of large and medium-sized fibres. Hence, estimations of node-gap volume and the number and the area of the node gap processes cannot be performed. The preservation outside the node gaps may on the other hand, be regarded as satisfactory (cf Carlstedt, 1977) and the data obtained from measurements of such parameters as myelin-sheath period, axon size, length of nodal axon segment and so forth (see under Material and Methods) are considered reliable enough to be used below without further comment.

Axon size. Axon size (a) was estimated in three ways: a_{circ} , a_{area} and a_{ratio} as the length of the axon circumference, as the axon cross-section area and as the area to circumference ratio respectively. Using these three a -variables the hypotheses concerning a difference between a_{PNS} and a_{CNS} of the same axons was tested in an analysis of variance. Even if the cats are considered as fixed effects (Table I) there is very little support of a difference ($p = 0.05$) of a_{circ} and a_{area} and there is no significant difference when testing a_{ratio} . As shown by the coefficients of variation (Table I) a_{ratio} shows the smallest value and is the variable to be preferred of the three tested. Hence our data do not seem to support the idea (see Todorov 1937 Gamble, 1976) that passage into the CNS means a decreased axon size. Instead they indicate that axon size remains unchanged.

Myelin sheath and whole fibre diameter. The plotting of PNS-axon diameter (from a_{ratio}) against the number of surrounding myelin lamellae gave a more or less rectilinear relationship in axons 1-4 μm in size where the number of lamellae varied between 20-100. Rectilinearity was lost in the group of larger axons 4-12 μm in size where several fibres carried about the same number of about a hundred lamellae in spite of a threefold variation in axon diameter. A maximum number of 130 lamellae was noted outside two axons 10.6 and 12.6 μm thick. In the CNS a rough rectilinearity was present in axons up to 3 μm thick carrying 10-80 lamellae. CNS axons more than 4-5 μm thick were equipped with a highly variable number of lamellae, ranging between 100-160. A maximum of 170-180 lamellae was noted outside the largest axons (10-13 μm). Thus it appears as if a myelin sheath thickness of 100-200 lamellae would give sufficient insulation in both PNS and CNS axons which are 4-13 μm in diameter.

In a series of works on mouse and rat peripheral nerves using electron microscopy Friede and coworkers (1967 1968, 1972) found that axon size and number of myelin lamella are rectilinearly related throughout the fibre spectrum. Superficially this is in contrast to the situation in feline dorsal roots. However since in the mouse 100 lamellae is about the maximum number found outside the largest axons some 6-7 μm thick, there seems to be fairly good agreement between mouse fibres in general and small to medium-sized feline axons. The larger axons which in the cat carry highly variable number of lamellae and invalidate rectilinearity are simply not present in the mouse.

Fibres belonging to group I and II ($> 6 \mu\text{m}$) carried an average of 20-30 additional CNS lamellae. In small group III fibres ($< 4 \mu\text{m}$) transition into the CNS meant a loss of 10-15 lamellae corresponding roughly to 25% of the PNS number. The larger group III fibres (fibre size $4-6 \mu\text{m}$) did on average acquire some additional lamella in the CNS. Hence it appears as if axons more than $2 \mu\text{m}$ in size roughly increased their number of myelin lamellae by an average of 20-25% as they reached into the CNS. Whether the higher number of myelin lamella along the CNS part of an axon is significant in terms of impulse transmission remains to be shown. In fact, several fibres showed no CNS-PNS lamellar difference or even a negative one.

The common preparative procedure used in electron microscopy includes dehydration and plastic embedding, during which the interlamellar distance of myelin shrinks by about 40-50% (from 180 Å to 80 Å) and about 30% (from 180 Å to 120 Å) in the CNS and the PNS, respectively (Finean, 1960; Karlsson, 1966; Hildebrand and Möller 1974). So in the embedded condition there are in fact few fibres that reveal a CNS myelin layer that is thicker than the PNS one (cf. Table II). The difference between the CNS and the PNS in interlamellar distance of fresh myelin means that the CNS part of a fibre has to carry 13% additional lamellae if the CNS and PNS-myelin-sheath thicknesses are to be equal in the unfixed condition. In larger fibres where the preparative CNS myelin shrinkage is 50%, this means that a PNS-myelin sheath of 100 lamellae which when unfixed is of the same thickness as a 113-lamellar CNS sheath will after processing appear to be about 25% thicker. Thus the CNS myelin in question must, if it in the embedded condition is to be of a thickness equal to that of its PNS counterpart consist of 150 lamellae. It is then obvious that CNS and PNS myelin sheath thicknesses cannot be compared unless they are recalculated to the unfixed condition. Maxwell *et al.* (1969) who stated in general terms, that myelin sheath thickness decreases as the fibres enter the CNS based their conclusions on very small monkey fibres. As is also found in the cat (Fig. 4) very small fibres ($< 4 \mu\text{m}$) decreased in myelin sheath thickness as they reached into the CNS. Recalculated values for the whole fiber population indicated that CNS D-values may be somewhat larger than the corresponding PNS values in fibres larger than $4 \mu\text{m}$ (Fig. 5, Table II). Comparisons between dorsal root and spinal-cord calibre spectra (among others see Skoglund and Romero, 1965; Hildebrand and Skoglund, 1971a) show however that the group of large CNS fibres definitely are thinner than the PNS ones. Conduction velocity is also reported to slow down after passage into the CNS (Lloyd and McIntyre, 1950; Collins and Randt, 1961; Petit and Burgess, 1968; Brown, 1968). These differences between CNS and PNS fibres are currently explained by fibre branching at the CNS entrance. Yet since branching was an exceptional observation in feline dorsal root borderline nodes it must in the cat be a phenomenon of more centrally located nodes.

Internodal length. The rectilinear increase in internodal length with increasing fibre size is well known and is considered to be of the same magnitude in CNS and PNS fibres alike (Vizoso and Young 1948; Thomas and Young 1949; Ohlrich and McDonald, 1974). The internodes found in the PNS compartment of the transitional region i.e. the most proximally located PNS internode of a fibre, revealed a length 30% shorter than expected from fibre size and the situation noted more distally in the root (see Fig. 1). In most fibres the decrease in internodal length was not sudden but gradual, comprising the last 2-4 PNS internodes. Provided that other fibre factors remain equal, a gradually decreased internodal length should mean a gradually increased depolarizing nodal current and a comparatively most advantageous situation as regards the safety factor in that part of the fibre where the passage into the CNS takes place (Tasaki, 1953). This brings up the issue of the borderline node.

The borderline node As already pointed out in the introduction, there are striking differences between the structural organization of CNS and PNS node-paranode regions and it is questionable whether the term paranodal apparatus is at all relevant in the CNS. Two of the three most characteristic features of the paranodal apparatus are simply not found in the CNS and the third is only indicated. Thus paranodal myelin-sheath crenation and mitochondrion accumulation have proven to be exclusively a PNS specialization (cf. Berthold, 1968 b; Hildebrand, 1971). The node-gap corona of densely packed Schwann cell microvilli that interconnects the immediate vicinity of the nodal axon membrane with the mitochondrion pools is in the CNS replaced by a few rudimentary-looking astrocytic processes. Moreover the node gaps of the PNS are surrounded by a comparatively voluminous extracellular space: the endoneurial room. In the CNS the extracellular space is very much restricted and forms a labyrinthine system of extremely flat spaces (cf. Bunge, 1968). Features that, on the other hand appear to be common to both CNS and PNS nodes are a coated nodal-axon membrane which varies from $3\mu\text{m}$ to $25\mu\text{m}$ with increasing fibre size (cf. calculations by Berthold, 1968 b; Hildebrand, 1971) a node-gap substance that gives a positive reaction to tests on acid mucopoly-saccharides, and node-gap walls formed by myelin-sheath terminal cytoplasmic pockets (Elfvin, 1961; Berthold, 1968 b; Langley and Landon, 1969; Hildebrand, 1971; Hildebrand and Skoglund, 1971 b). Hence, since the principle of impulse conduction are considered to be the same in the CNS and PNS (Rasminsky and Sears, 1972) available data seem to imply that the elaborate paranodal apparatus should actually be insignificant in terms of impulse generation and propagation.

The present results indicate that the borderline node-paranode region in several respects resembles what might be called a PNS-CNS compound node. This is clearly demonstrated in series of sections where the separation line runs in the middle of a node gap which in its peripheral half lodges a microvilli corona that more distally is transformed into a mitochondrion-rich paranodal Schwann cell compartment and which in its central half reveals a few blunt astrocytic processes. The size and shape of the nodal axon resembled those of genuine PNS and CNS nodes.

In contrast to ordinary peripheral paranodes, those of the borderline segment were holstered and isolated from their neighbours by astrocytic processes: their myelin crests were less developed close to the node and paranodal accumulations of Schwann cell mitochondria extended very close to the node gaps, at some sites even covering parts of the gap (see Fig 12). Beside its relation to astrocytic perikarya (see below) the CNS-borderline paranode appeared similar to paranodes as seen elsewhere in white matter. Taking into account these differences as well as the short length of the adjoining PNS paranode, it can be concluded that the borderline node of Ranvier is a compound PNS-CNS node with some unique features.

Calculations of the amount of mitochondria in large (group I) borderline PNS-paranodes and of ordinary alpha-fibre paranodes of a corresponding size show roughly equal values (Berthold, 1968b). Comparisons with regard to group II and III fibres cannot be performed because of the absence of reference data. The variation with fibre size in the amount of mitochondria of the PNS borderline paranodes is in line with the previously made suggestion that A fibres constitute two main groups, one comprising small fibres with a poorly developed paranodal apparatus (here small — D $4\mu\text{m}$ — group III fibres) and the other the larger fibres with well developed apparatus where, for instance, the amount of mitochondria increases rapidly with fibre size (here group I and II fibres) (cf. Berthold, 1968b; Phillips *et al.*, 1972).

A comparatively high number of astrocytic perikarya occurred in close relation to the paranodes of the mantle zone. As pointed out in a previous communication on the transitional region (Berthold and Carlstedt, 1977), the mantle-zone corresponds to the external glial limiting membrane which is formed by a complex feltwork of astrocytes and it was calculated that the occurrence of

Table II

Myelinated fibre parameters as estimated the same cross-sectioned dorsal root fibres on the two sides of the borderline node.¹⁾

Axonal fibre type	Axon diameter calculated from circumference		Axon diameter calculated from area		No. of myelinated fibres		Myelin period		Calculated fixed myelin sheath thickness		Calculated active myelin sheath thickness		Calculated active total fibre diameter	
	Mean value μm PNS	Mean value μm CNS	Mean value μm PNS	Mean value μm CNS	Mean value (SD) PNS	Mean value (SD) CNS	Mean value (SD) PNS	Mean value (SD) CNS	Mean value (SD) PNS	Mean value (SD) CNS	Mean value (SD) PNS	Mean value (SD) CNS	Mean value, μm PNS	Mean value, μm CNS
I	12.73	12.44	11.66	11.43	10.74	10.52	123.30	83.6	1.43	1.77	2.08	2.25	19.99	18.80
K 1027	II	6.69	6.86	8.53	8.21	4.59	118.82	108.37	1.07	1.12	1.62	2.05	8.96	10.06
		3.19	2.94	2.42	2.20	1.84	170.22	111.44	0.49	0.32	0.74	0.54	3.48	3.17
		12.00	11.66	11.16	10.97	9.92	122.18	90.62	1.42	1.34	2.11	2.37	15.13	15.72
K 1039	II	7.36	7.67	8.40	8.91	8.22	123.69	91.98	1.26	1.23	1.84	2.18	9.43	10.95
		3.34	3.67	2.69	2.41	1.72	123.70	103.3	0.66	0.60	0.80	0.86	3.49	3.96
		12.36	11.78	10.47	10.17	8.86	116.10	90.8	1.33	1.10	2.08	1.93	13.95	13.96
K 1040	II	8.33	7.84	6.78	6.69	6.60	117.40	91.4	1.20	1.00	1.84	1.71	9.79	10.72
		2.36	2.07	1.79	1.64	1.27	116.7	101.4	0.40	0.26	0.69	0.40	2.96	2.34
		12.36	12.07	11.11	10.60	9.94	124.43	120.2	1.40	1.21	2.09	2.18	15.03	15.45
K 1038	II	7.53	7.28	6.26	6.31	6.33	121.07	116.86	1.17	1.11	1.77	1.97	9.38	10.28
		2.96	2.71	2.24	2.18	1.83	120.87	106.38	0.84	0.36	0.71	0.61	3.17	3.16
		12.36	12.07	11.11	10.60	9.94	124.43	120.2	1.40	1.21	2.09	2.18	15.03	15.45

¹⁾ The axon data from 80 myelinated fibres on the two sides of the borderline node will be supplied on request.

Table III

Numerical estimations of mitochondria in the PNS borderline paranodes

Animal	Fibre type	Amount of paranodal mitochondria in arbitrary units (see Fig. 6)	Highest number of mitochondria in the paranode	Distance from the borderline node of the highest number of mitochondria (μm)	Number of mitochondria 100 μm distal to the borderline node
K 1027	I	106	264	10	12
		153	347	4	12
		169	320	4	11
	II	44	168	4	6
		55	217	4	6
		49	182	4	4
	III	9	81	2	2
		3	17	4	4
		1	6	4	2
	I	100	264	4	8
		147	282	7	22
		77	227	4	14
K 1039	II	81	114	16	10
		47	146	4	8
		34	202	4	10
	III	2	60	4	4
		2	60	4	10
		1	4	4	2
	I	178	271	10	36
		130	220	6	14
		100	260	4	25
	II	81	155	10	34
		32	110	4	4
		68	214	7	10
K 1040	III	3	12	4	4
		1	39	4	4
		2	61	4	5

Table 1)

Myelinated fiber parameters as estimated: the same cross-sectioned dorsal root fibres on the two sides of the borderline node.¹⁾

Animal	Fibre type	Axon diameter calculated from circumference		Axon diameter calculated from area		Axon diameter calculated from circumference		No. of myelin lamellae		Myelin period		Calculated flat myelin sheath thickness		Calculated native myelin sheath thickness		Calculated native total fibre diameter	
		Mean value μm	PMS	Mean value μm	PMS	Mean value μm	PMS	Mean value (SD)	PMS	Mean value (SD) μm	PMS	Mean value (SD) μm	PMS	Mean value (SD) μm	PMS	Mean value μm	PMS
K 1027	I	12.75	12.44	11.08	11.43	10.74	10.82	105.80 (24.36)	140.80 (22.72)	123.20 (17.16)	53.6 (2.76)	1.43 (0.11)	1.77 (0.21)	2.08 (0.18)	2.26 (0.36)	15.08	16.00
	II	8.86	8.20	8.86	8.53	8.21	4.86	89.64 (8.18)	118.82 (40.86)	108.27 (32.66)	68.09 (2.66)	1.07 (0.13)	1.12 (0.17)	1.82 (0.17)	2.08 (0.32)	8.86	10.08
	III	3.18	2.94	2.42	2.20	1.94	1.80	41.22 (8.07)	32.11 (27.76)	120.52 (8.12)	111.44 (33.66)	0.49 (0.06)	0.32 (0.16)	0.74 (0.14)	0.54 (0.26)	3.48	3.17
K 1038	I	12.00	11.96	11.16	10.87	9.62	9.44	117.28 (8.31)	148.18 (18.08)	122.18 (6.87)	90.62 (4.12)	1.43 (0.12)	1.34 (0.18)	2.11 (0.18)	2.37 (0.31)	15.13	15.72
	II	7.26	7.87	6.40	6.81	8.22	8.27	102.33 (9.07)	134.33 (19.26)	123.86 (14.26)	81.78 (2.71)	1.26 (0.11)	1.23 (0.17)	1.84 (0.16)	2.18 (0.31)	9.43	10.06
	III	3.34	3.57	2.86	2.41	1.72	1.62	43.28 (11.34)	84.20 (26.63)	123.70 (1.77)	103.3 (6.34)	0.65 (0.37)	0.30 (0.28)	0.80 (0.18)	0.86 (0.42)	3.46	3.96
K 1040	I	12.26	11.78	10.47	10.17	8.68	8.81	116.10 (2.78)	120.60 (10.64)	118.1 (6.87)	90.6 (4.07)	1.33 (0.04)	1.10 (0.08)	2.08 (0.17)	1.93 (0.31)	13.96	13.96
	II	8.23	7.84	6.78	6.68	8.58	8.60	102.00 (7.68)	110.10 (17.26)	117.4 (8.18)	81.4 (2.34)	1.20 (0.13)	1.00 (0.14)	1.84 (0.14)	1.71 (0.28)	8.78	10.22
	III	2.38	2.07	1.73	1.64	1.27	1.21	32.7 (8.82)	24.4 (8.37)	118.7 (4.22)	101.4 (8.34)	0.40 (0.07)	0.26 (0.07)	0.86 (0.12)	0.40 (0.18)	2.56	2.34
K 1027	I	12.26	12.07	11.11	10.80	9.84	9.68	113.07 (26.20)	134.43 (21.24)	120.2 (13.1)	88.43 (4.42)	1.40 (0.11)	1.21 (0.18)	2.09 (0.13)	2.18 (0.34)	16.03	16.48
	II	7.83	7.28	6.36	6.21	8.33	8.40	97.97 (10.30)	121.07 (21.13)	118.98 (8.78)	90.42 (3.42)	1.17 (0.18)	1.11 (0.17)	1.77 (0.16)	1.97 (0.06)	8.36	10.28
	III	2.86	2.71	2.34	2.16	1.63	1.64	38.77 (9.78)	37.40 (23.47)	120.87 (4.86)	106.36 (7.42)	0.36 (1.1)	0.36 (0.26)	0.71 (0.18)	0.81 (0.38)	3.17	3.16

¹⁾ The crude data from 80 myelinated fibres on the two sides of the borderline node will be supplied on request.

REFERENCES

- Becker N.H. Goldflaber S., Shih, W. Y. and Novikoff, A.B. (1960) The localization of enzyme activities in the rat brain. *The Journal of Biophysical and Biochemical Cytology* 8, 649-653.
- Berthold, C.-H. (1968a) A study on the fixation of large mature feline myelinated ventral lumbar spinal-root fibres. *Acta Societatis Medicorum Upsalienis* 73, Suppl. 9 1-36.
- Berthold, C.-H. (1968b) Ultrastructure of the node-paranode region of mature feline ventral lumbar spinal-root fibres. *Acta Societatis Medicorum Upsalienis* 73, Suppl. 9 37-78.
- Berthold, C.-H. and Carlstedt, T. (1977) Observations on the morphology at the transition between the peripheral and the central nervous system in the cat. II. General organization of the transitional region. *Acta Physiologica Scandinavica*, suppl. 446, 23-42.
- Berthold, C. H. and Skoglund, S. (1967) Histochemical and ultrastructural demonstration of mitochondria in the paranodal region of developing feline spinal roots and nerves. *Acta Societatis Medicorum Upsalienis* 72, 37-70.
- Blahoff, A. and Thomas, P.K. (1975) Microscopic anatomy of myelinated nerve fibres. In *Peripheral Neuropathy* (edited by Dyck, P.J., Thomas, P.K. and Lambert, E.H.) pp. 104-130 Philadelphia, London, Toronto: W.B. Saunders.
- Blakemore, W.F. and Patterson, R.C. (1975) Observations on the interrelation of Schwann cells and astrocytes following x-irradiation of neonatal rat spinal cord. *Journal of Neurocytology* 4, 573-585.
- Brody L. (1959) The keratinization of epidermal cell of normal guinea pig skin as revealed by electron microscopy. *Journal of Ultrastructural Research* 2, 483-511.
- Brown, A.G. (1968) Cutaneous afferent fibre collaterals in the dorsal columns of the cat. *Experimental Brain Research* 5, 293-306.
- Bunge, R.P. (1968) Glial cells and the central myelin sheath. *Physiological Reviews* 48, 197-251.
- Carlstedt, T. (1977) Observations on the morphology at the transition between the peripheral and the central nervous system in the cat. I. A preparative procedure useful for electron microscopy of the lumbosacral dorsal rootlets. *Acta Physiologica Scandinavica*, Suppl. 446, 446, 5-22.
- Collins, W.F. and Randt, C.T. (1961) Fibre size and organization of afferent pathways. *Archives of Neurology* 5, 202-4.
- Elfvén L.-G. (1961) The ultrastructure of the nodes of Ranvier in cat sympathetic nerve fibres. *Journal of Ultrastructural Research* 5, 374-87.
- Fineman, J.B. (1960) Electron microscope and X-ray diffraction studies of the effects of dehydration on the structure of nerve myelin. I. Peripheral nerve. *The Journal of Biophysical and Biochemical Cytology* 8 13-30.
- Foncem, J.P. (1961) Structure fine de la zone de passage radicoclonodulaire. *Revue Neurologique* 106, 509-13.
- Fraser J.P. (1976) The growth and myelination of central and peripheral segments of ventral motorneuron axons. A quantitative ultrastructural study. *Brain Research* 106, 193-211.
- Friede, R.L. (1961) *A Histochemical Atlas of tissue Oxidation in the brainstem of the Cat*. Basel, New York: S. Karger.
- Friede, R.L. (1972) Control of myelin formation by axon calibre (with a model of the control mechanism) *The Journal of Comparative Neurology* 144, 233-62.
- Friede R.L. and Samorajski, T. (1967) Relation between the number of myelin lamellae and axon circumference in fibres of vagus and sciatic nerve on mice. *The Journal of Comparative Neurology* 130 223-32.
- Friede R.L. and Samorajski, T. (1968) Myelin formation in the sciatic nerve of rat. A quantitative electron microscopic, histochemical and radioautographic study. *The Journal of Neurophysiology and Experimental Neurology* 27 548-71.
- Gambel H.J. (1976) Spinal and cranial nerve roots. In *The Peripheral Nerve* (edited by London D.N.) pp. 330-54. London: Chapman and Hall.
- Hildebrand, C. (1971) Ultrastructural and light-microscopic studies of the nodal region in large myelinated fibres of adult feline spinal cord white matter. *Acta Physiologica Scandinavica* Suppl. 384 43-61.
- Hildebrand, C. (1972) Evidence for a correlation between myelin period and number of myelin lamellae. Fibres of the feline spinal cord white matter. *Journal of Neurocytology* 1 223-32.
- Hildebrand, C. and Müller H. (1974) Low-angle X-ray diffraction studies on the period of central myelin sheaths during preparation for electron microscopy. A comparison of different anatomical areas. *Neurobiology* 4, 71-81.

- Hildebrand, C. and Skoglund, S. (1971a) Calibre spectra of some fibre tracts in feline central nervous system during postnatal development. *Acta Physiologica Scandinavica* Suppl. 364, 5-43.
- Hildebrand, C. and Skoglund, S. (1971b) Histochemical studies of adult and developing feline spinal cord white matter. *Acta Physiologica Scandinavica* Suppl. 364, 145-73.
- Karlsson, U.L. (1966) Comparison of the myelin period of peripheral and central origin by electron microscopy. *Journal of Ultrastructure Research* 15, 451-68.
- Landon, D.N. and Williams, P.L. (1963) Ultrastructure of the node of Ranvier. *Nature* 199, 575-7.
- Landon, D.N. and Hall, S. (1976) The myelinated nerve fibre. In *The Peripheral Nerve* (edited by Landon, D.N.) pp. 1-105. London: Chapman and Hall.
- Langley O.K. and Landon, D.N. (1969) Copper binding at nodes of Ranvier: a new electron histochemical technique for the demonstration of polyanions. *The Journal of Histochemistry and Cytochemistry* 17, 68-9.
- Lloyd, D.P. (1943) Nerve patterns controlling transmission of ipsilateral hind limb reflexes in cat. *The Journal of Physiology* 6, 293-315.
- Lloyd, D.P. and McIntyre, A.K. (1950) Dorsal column conduction of group I muscle afferent impulses and their relay through Clarke column. *The Journal of Neurophysiology* 13, 39-54.
- Maxwell, D.S., Kruger, L. and Pineda, A. (1969) The trigeminal nerve root with special reference to the central-peripheral transition zone. An electron microscopic study in the Macaque. *The Anatomical Record* 184, 113-36.
- Ohlrich, G.D. and McDonald, W.J. (1974) Demyelination in the central nervous system of the cat studied by single fibre isolation. *Proceedings of the Australian Association of Neurologists* 11, 77-87.
- Petit, D. and Burgess, P.R. (1968) Dorsal column projection of receptors in cat hairy skin supplied by myelinated fibres. *The Journal of Neurophysiology* 31, 849-55.
- Phillips, D.D., Hulse, R.G., ElHach, J.P. and Shapiro, H. (1972) An electron microscopic study of central and peripheral nodes of Ranvier. *The Journal of Anatomy* 111, 229-38.
- Rasminsky, H. and Sears, R.A. (1972) Internodal conduction in undiseased demyelinated nerve fibres. *The Journal of Physiology* 227, 232-50.
- Reynolds, E. (1963) The use of lead citrate at high pH as an electron-opaque stain in electron microscopy. *The Journal of Cell Biology* 17, 209-13.
- Ross, M.D. and Burkel, W. (1971) Electronmicroscopic observation of the nucleus, glial dome, and meninges of the rat acoustic nerve. *The American Journal of Anatomy* 130, 73-91.
- Samorajski, T. and Friede, R.L. (1966) A quantitative electron microscopic study of myelination in the pyramidal tract of rat. *The Journal of Comparative Neurology* 134, 323-38.
- Skoglund, S. and Romero, D. (1965) Postnatal growth of spinal nerves and roots. A morphological study in the cat with physiological correlations. *Acta Physiologica Scandinavica* Suppl. 260, 1-50.
- Tarlov, I.M. (1937) Structure of the nerve root. I. Nature of the junction between the central and the peripheral nervous system. *Archives of Neurology and Psychiatry* 37, 558-83.
- Tasaki, I. (1953) *Nervous Transmission*. Springfield, Ill. Charles C. Thomas, Publisher.
- Thomas, P.K. and Young, J.Z. (1949) Internode lengths in nerves of fishes. *The Journal of Anatomy* 83, 336-60.
- Williams, P.L. and Landon, D.N. (1963) Paranodal apparatus of peripheral myelinated nerve fibres of mammals. *Nature* 198, 670-3.
- Vino, A.D. and Young, J.Z. (1948) Internodal length and fibre diameter in developing and regenerating nerves. *The Journal of Anatomy* 82, 110-34.

LEGENDS TO FIGURES

Abbreviations used in Figs. and legends

A	astrocyte
Ax	Axon
B	Basement membrane
BN	borderline node of Ranvier
C	central myelinated fibre
CM	CNS myelin
E	endoneurial space
EM	electron micrograph
G	glial fringe
LM	light micrograph
MB	myelinoid body
N	node of Ranvier
P	peripheral myelinated fibre
PM	PNS myelin
S	Schwann cell

Fig. 1 Internodal length and fiber diameter in the S₁ dorsal root of four different cats as measured in the most proximally situated peripheral internode (DRP) and in internodes situated half way between the pinal cord and the dorsal root ganglion (DRM). The regression line for DRP is, $y = 40.748x - 184.664$ and for DRM, $y = 83.697x - 354.007$.

Figs. 2, 3 Number of myelin lamellae plotted against axon diameter as calculated from the ratio between axon area and length of circumference on the PNS (Fig. 2) and CNS (Fig. 3) side of the transitional nodes in 90 fibres of three cats. The symbols refer to the different animals.

Fig. 4 Difference in number of myelin lamellae between the CNS and PNS parts of a fibre plotted against axon diameter (calculated from the ratio between axonal area and length of circumference). Same fiber population as Figs. 2 and 3.

Fig. 5 Calculated native CNS fibre diameter (D_{CNS}) plotted against calculated native PNS fibre diameter. The solid line indicates where $D_{CNS} = D_{PNS}$. Same fibre population as in Figs. 2 and 3.

Fig. 6 Occurrence of Schwann cell mitochondria within 100 μ m from the borderline node (NoR) in one group I fibre ($D = 16.7 \mu$ m), one group II fibre ($D = 9 \mu$ m) and two group III fibres ($D = 6 \mu$ m and 2.5μ m indicated by a single and a double hatch respectively). For comparison data of a large feline ventral root fibre (hatched line) was included (fibre No. 3 from Berthold, 1968b).

Fig. 7 a, b LM Tensid S₁ dorsal rootlet. Incubation for NADH-tetrazolium reductase activity. The pictures show the proximal (a) and the distal (b) ends of the PNS borderline internode of a large myelinated fibre. In contrast to the arrangements in the distal paranode (b) the bands of enzyme activity of the proximal borderline paranode coalesce into one pool (arrows) ($\times 1300$).

Fig. 8 a-d EM. Cross-sections through different levels of the borderline segment.

a) Section level 16 μ m distally to borderline node. Intervoven astrocytic processes of the glial fringe (GF) enclose the fibre with a minute concentric endoneurial space (E) in a tube- or holster-like fashion. The myelin sheath is created. The accumulations of Schwann cell cytoplasm in the furrows between the myelin crests contains mitochondria and one myelinoid body (MB) ($\times 4500$).

b) Section level 3 μ m distally to borderline node. The myelin sheath is of an ovoid outline and has started its uncoiling along the axon. The Schwann cell cytoplasm is accumulated to a large coherent compartment (S) loaded with mitochondria (cf. Fig. 7a) ($\times 6200$).

MATERIAL AND METHODS

Eight adult cats, body weight 3.5 kg, were anaesthetized intraperitoneally with pentobarbital, 40 mg/kg BW, and artificially ventilated by oxygen administered through a tracheal cannula. The lumbosacral spinal cord and its roots were fixed by vascular perfusion with phosphate buffered 5% glutaraldehyde. Dorsal rootlets belonging to the segment S₁ were carefully removed together with small pieces of the adjoining spinal cord white matter postfixed, osmicated, dehydrated in acetone and embedded in Vestopal W (for details see Carlstedt, 1977).

The Vestopal-embedded specimens were before sectioning trimmed into the shape of a fat mass using a LKB 11800 Pyramitome. Ultra-thin cross-sections with an interference colour of gray to pale yellowish-white corresponding to a section thickness of about 500-1000 Å (see Peachey, 1954) were cut on a LKB 4800 Ultratome. Three series of consecutive cross sections comprising 10,000, 6000 and 5,500 sections and four series of 200-1000 longitudinal sections were made from the transitional region. One series of 4,500 cross sections, as well as transverse and longitudinal sections, were manufactured from the part of the root situated halfway between the ganglion and the spinal cord. The section thickness varied between 600-800 Å and was calculated by dividing the height of the mass with the number of sections it had yielded. The loss of sections was less than 1%. The sections were placed on one-hole copper grids coated with a carbon-stabilized formvar film, double-stained with uranyl acetate (Brody, 1958) and lead citrate (Haynolds, 1963) and examined in a Philips 300 EM electron microscope.

The calibre spectra of unmyelinated fibres were estimated in the peripheral and the central nervous compartments of the same rootlet in three cats using a calibrated Zeiss TUX2 particle size analyser (cf. Romero and Skogglund, 1968).

In the case of 27 fibres (9 of each animal) their sizes were measured at 10 µm intervals at levels on each side of the PNS-CNS borderline in the most proximal part of the TR. For this photocopies of x 5000 magnification of the different levels and a scale of preformed circles were used. These fibres were also carefully examined in the electron microscope at 2 µm intervals at a distance of 100 µm proximally to the borderline. In this way the short internodal length observed along the CNS-extension of large C-fibres was estimated.

Schwann cell nuclear length and Schwann cell internuclear distance were estimated in axon bundles of unmyelinated fibres from three cats. The measurements were performed at consecutive 8 µm intervals on photocopies (x 1000-2000). As a control intervening axons representing 2 µm intervals were checked in the electron microscope.

Terminology (see Berthold and Carlstedt, 1977). The transitional region (TR) is the 2-1000 µm long segment in the proximal free part of a rootlet containing both CNS and PNS tissue. A cross section through the TR reveals two concentric compartments: (1) the TR compartment consisting of CNS tissue arranged in two zones: (a) the core zone being situated in the centre of the rootlet and organized like a central fibre tract, (b) the mantle zone forming the PNS-CNS interface composed of astrocytes and nerve fibres; (2) the PNS compartment containing PNS components and the astrocyte processes of the glial fringe, the latter emanating from the mantle zone.

RESULTS

Unmyelinated fibres distal to the transitional region

The unmyelinated axons constituted about 75% of the total number of the nerve fibres in the stereotypic PNS part of S₁ dorsal rootlets. The axons showed a rounded cross-section contour. The axoplasm contained orangellae of the familiar appearance previously described by, for instance, Elfvin (1938, 1968 see also Ochoa, 1975, 1978). The unmyelinated fibres were arranged in bundles connected to Schwann cells (Fig. 1a). The bundles consisted as a mean value of 21 (SD 9, n=30) fibres at the level of the Schwann cell nucleus. As a rule each fibre was separated from adjacent ones by septa of Schwann cell cytoplasm. All fibres of a

bundle could easily be followed in serial cross sections for up to some 200 μm without any major divergencies or shifts in position (size of observation field, $10 \times 12 \mu\text{m}$) (cf. Gasser 1955; Aguayo *et al.*, 1976). Schwann cell internuclear distance was about 100 μm (cf. Gasser 1955; Peyronnard *et al.* 1973; Aguayo *et al.* 1976).

Unmyelinated fibres in the PNS compartment of the TR

In this part of the rootlet a bundle of unmyelinated fibres consisted as a mean value of 9 (SD 4 $n=30$) fibres at the level of the Schwann cell nucleus. Close to the PNS-CNS borderline there was a pronounced exchange and criss crossing of fibres between the different bundles. This was illustrated by the failure to trace the fibres in a bundle for more than some 20 μm using an observation field $10 \times 12 \mu\text{m}$ in size.

In nine bundles investigated, the mean distance from the PNS-CNS borderline to the most proximally situated Schwann cell nucleus was 23 μm (SD 16). The mean distance between successive Schwann cell nuclei along a bundle of unmyelinated fibres was 12 μm (SD 12) and the mean Schwann cell nucleus length 10 μm (SD 3) (see Fig. 2).

The fibre spectrum analysis of three rootlets (Table I) showed a unimodal pattern of distribution with the peak at 0.5 μm . About 70% of the fibres measured 0.35–0.57 μm . Some 5% were 0.8 μm or more in diameter. The largest axons measured 1.2 μm . The maximum variation in individual fibre size with regard to the mean diameter was 36% (Table II).

Unmyelinated fibres in the CNS compartment of the TR

In the CNS compartment of the rootlet the number of unmyelinated fibres was about 70% of the total number of nerve fibres. They were about 5% less than in the PNS part of the rootlet. The axons were of a somewhat angular outline and their axoplasm contained the same constituents as were noted in the PNS part of the fibres. The axons occurred in bundles consisting of 10–40 axons without intervening cytoplasmic septa (Fig. 1b). In the mantle zone of the CNS compartment just proximally to the PNS-CNS borderline, the fibres occurred in bundles consisting of about 10 fibres. Here there was an extensive interchange of fibres between the different bundles. Thus a bundle of fibres existed as a unit only for some 10–20 μm (size of the observation field, $10 \times 12 \mu\text{m}$). More proximally in the core zone the thin bundles aggregated to form larger units consisting of up to 40 individual fibres.

The calibre spectrum analysis (Table I) showed that no CNS-unmyelinated fibres were larger than 0.8 μm . Below this size the fibre spectrum was similar to that of the PNS part of the rootlets. In the fibres analysed at 10 μm intervals, fibre size remained roughly the same on the two sides of the PNS-CNS borderline (Table II).

An unusual observation made in the mantle zone was the occurrence of round myelinated profiles about 5 μm in diameter. They contained swollen mitochondria, round membrane demarcated dense bodies 0.1–0.2 μm in diameter and vesicular entities (Fig. 10b). The surrounding myelin sheath consisted of 2–10 lamellae. Serial section analysis showed that these myelinated profiles measured 5–10 μm in length and diminished in size to 0.5–1 μm in the distal direction where they showed all the characteristics of a small myelinated or unmyelinated axon (Fig. 10a). When traced proximally the profiles were found to taper off (Fig. 10c) and finally to disappear completely (Fig. 10d). The profiles did not send out side branches.

Unmyelinated fibres at the passage of the PNS-CNS borderline

The majority of the unmyelinated fibres crossed the PNS-CNS borderline in the proximal part of the transitional region, then aggregating in the ventrolateral aspect of the rootlet (cf. Berthold and Carlstedt, 1977). A minority of the fibres entered the CNS compartment more distally in the TR. Such fibres either remained in the central parts of the core zone or left the CNS compartment only to re-enter at a more proximal level (Figs. 4 and 6) (see below).

Unmyelinated fibres in the transitional region

Three different modes of C-fibre PNS-CNS transition were observed. The mode of transition appeared to be related to the diameter of the axons.

1) Fibres less than 0.6 μm in diameter These axons continued as unmyelinated into the CNS compartment. At the point where a bundle of C-fibres was about to cross the PNS-CNS borderline the Schwann cell cytoplasm surrounding the individual axons attenuated and terminated (Figs. 3a-d). At the transition some fibres were covered partly by strands of Schwann cell cytoplasm and partly by astrocyte processes (Figs. 3b-c). Other fibres lost their investing Schwann cell coat a few μm distally to the PNS-CNS borderline and were closely apposed to its neighbour axons in the bundle (Fig. 3c) or ran solitarily being covered only by a basement membrane.

At the point of transition several unmyelinated fibres revealed, when cross-cut, a picture similar to that of a cross-cut small node of Ranvier: that is the axon was more or less surrounded by radially arranged delicate 'finger-like' cytoplasmic processes 500-1000 \AA thick (Figs. 3b-4b-c, d, 5-9b). These processes were of astrocytic origin and reached to within less than 100 \AA from the axolemma. Between the tip of a process and the axon membrane there were accumulations of moderately electron dense material. At these sites, on the axoplasmic side of the axolemma, there was material of a high electron density (Figs. 5-9b). In contrast to a genuine node of Ranvier the occurrence of processes was restricted to certain parts of the axonal periphery. Examination of series of consecutive cross and longitudinal sections showed that the astrocytic processes in fact were thin 'leaflets-like' extensions which ran along the axon for distances up to 20 μm (Fig. 7).

The arrangements given above were prevalent and more elaborated outside larger axons ($> 0.4 \mu\text{m}$) than outside smaller ones. The latter were as a rule surrounded by some blunt astrocyte processes lacking membrane specializations (Fig. 3c). Larger axons ($> 0.4 \mu\text{m}$) were at the transitions often separated from their neighbouring axons by astrocyte extensions (Fig. 5) and were closely spaced with other axons a few μm more proximally.

2) Fibres 0.8 μm or more in diameter These fibres which constituted some 5% of all unmyelinated axons in the PNS compartment, could not be recovered as unmyelinated on the CNS side of the borderline. Instead, careful serial section analysis showed that they became myelinated as they crossed the borderline and entered the CNS (Figs. 7 and 9a-c). Their myelin sheaths consisted of up to 10 lamellae. The mean myelin period was 100 \AA (SD 10 \AA , n 35) (cf. Hildebrand, 1972). The internodal length ranged between 10 and 40 μm (Fig. 7). In the approximately 5 μm gap between the PNS Schwann cell covering and the CNS myelin sheath there were astrocytic leaflets arranged as described above in section 1 (Fig. 7).

The nodes of Ranvier situated more proximally along these fibres (Fig. 7) showed a rather simple architecture with broad node-gaps containing occasional astrocyte extensions: i.e. they appeared quite like the commonly described small CNS node of Ranvier in the central nervous system (cf. Bunge, 1968).

3) Fibres some 0.6-0.8 μm in diameter Most of these fibres showed segmental myelination of their CNS part. Here short myelin sheath cuffs 3-20 μm long were intercalated in an irregular manner between unmyelinated stretches (Fig. 8). Some fibres showed the arrangements of axons 0.8 μm or more in diameter at both ends of the myelin investment.

DISCUSSION

Redistribution of C-fibres. In full agreement with earlier observations (e.g. Gasser 1956; Peyronnard *et al.*, 1973; Aguayo *et al.* 1976) the Schwann cell internuclear distance was about 100 μm and no major shifts were noted in the grouping and distribution of C-fibres at their passage along the root halfway between the spinal ganglion and the spinal cord. The passage along the TR, on the other hand, meant that the C-fibres deserted the central parts of the rootlet and became redistributed to its outer layers and in particular to its ventrolateral aspect (Berthold and Carlstedt, 1977). This is illustrated in the present work by the high degree of C-fibre divergence (or cross-crossing) as noted in the glia fringe close to the PNS-CNS borderline, where the average Schwann cell internuclear distance measured about 12 μm . The occurrence of a Schwann cell internuclear distance that is some 0.1 time that of more distal root regions indicate that there are more Schwann cells per unit length unmyelinated axon in the TR than in the stereotype part of the root. It was found that the average number of unmyelinated fibres connected to a Schwann cell perikaryon was about twice as high in the stereotype part of the root than in the TR. Provided that those observations, derived from a small number of observations ($n=30$) are valid, there should be at least 20 times as many Schwann cells per unit length unmyelinated axon in the TR as compared to the stereotype part of the root. Such an unusually high occurrence of C-fibre-related Schwann cells might be an effect of the excessive C-fibre cross-crossing or it might reflect a genuine Schwann cell surplus of obscure origin specific for the TR.

Whether the fibre redistribution implies a regrouping of unmyelinated axons at random or whether the axons become segregated according to some morphological and functional principle is unknown. Nevertheless it should be mentioned that the CNS arrangement of the redistributed unmyelinated axons — close-packing of many fibres without intervening glia might, in pathological conditions, allow interaction. This matter has recently been discussed by Sandersland (1976) as a phenomenon that might be involved in *causalgia*.

C-fibres at the CNS entrance: PNS calibre spectra show that 80-90% of the unmyelinated axons measured 0.4-0.7 μm (Table I). About 5% of the axons measured 0.8 μm or more (upper limit 1.2 μm). CNS spectra show a similar distribution except for the remarkable lack of axons more than 0.7-0.8 μm thick. Serial section analysis showed that the disappearance of large unmyelinated axons on the proximal side of the PNS-CNS borderline was due to the fact that axons 0.8 μm or more in diameter acquired a complete myelin sheath as they entered the CNS compartment. This explains the already reported (Berthold and Carlstedt, 1977) surplus in small myelinated fibres as noted proximally in the TR and also excludes the possibility that discrepancies in the occurrence of unmyelinated and small myelinated fibres at different levels in the TR to any appreciable extent depended on C-fibre termination in combination with branching of small myelinated fibres.

Serial section reconstructions, however revealed that about 1% of the C-fibres did in fact terminate in the CNS compartment close to the borderline (Figs. 10a-d). These axons showed bulbiform terminal swelling with an appearance similar to that observed by Lampert (1967) after transection of the dorsal columns in rats. Thus signs of C-fibre degeneration appear to be part of the normal TR morphology.

A fully myelinated condition of the large C-fibres was followed in the CNS up to a distance of 100 μm proximally to the PNS-CNS borderline. Whether these fibres remained myelinated in the CNS proper is unknown. However since these fibres in analogy with afferent fibres in general should divide into a cranial and a caudal branch and since branching means a decreased fibre size (Lehmann, 1959) it is not unlikely that C-fibre myelination might be a phenomenon peculiar to that fibre

segment which extends between the PNS-CNS borderline and the first branching point in the CNS. The same arguments apply to the segmentally myelinated C-fibres measuring 0.6-0.8 μm in diameter. Several internodes of the latter fibres were less than 10 μm in length, a size comparable to that of the very short internodes as described by Waxman (1970) in the teleost brain. These observations may be of some interest with regard to the debate on the signal for myelination (see, for instance, Speidel 1964; Matthews 1968; Friede 1972; Weinberg and Spencer 1975). They show that this signal whatever it might be, gives rise to a situation which appears to be strikingly dependent on axon size: fine unmyelinated PNS axons (upper size limit 1.5 μm) acquired a more or less complete myelin sheath in the CNS if they measured more than 0.6 μm .

The functional significance of myelin investment of thin axons has been much discussed. Rushton (1951) calculated that axons less than 1 μm in diameter would transmit impulses faster if unmyelinated. It has been suggested that the increase in conduction velocity that takes place during postnatal development is not directly related to myelination (Conway *et al.*, 1969). Koles and Rasminsky (1972) computed the theoretical effects of demyelination on the conduction of impulses and found that even a few myelin lamellae are of importance for conduction properties. Stone and Freeman (1971) found an eightfold increase in conduction velocity between the intraretinal (unmyelinated) and extraretinal (myelinated) part of even the slowest conducting fibres, which in the intraretinal position presumably had a diameter less than 1 μm (see also Stone and Holländer, 1971). According to the theoretical calculations by Waxman and Bennett (1972) conduction velocity shall accelerate when an unmyelinated fibre is myelinated, the conduction velocity was calculated to be approximately 2.6 times larger in an myelinated fibre, 1 μm diameter as compared to a non-myelinated 1 μm axon (Waxman, 1975).

Against this background it can be tentatively suggested that the mode of impulse conduction changes and that conduction velocity increases in large C-fibres as they enter the CNS compartment of the TR. According to the meagre data relating receptive properties to C-fibre size, the large (>1 μm) axons should transmit impulses set up in low-threshold mechanoreceptors (Douglas and Ritchie, 1967; Besson and Perl, 1969).

Whether the relationships noted between astrocytes and the borderline segments of C-fibres 0.4-0.7 μm in size i.e. node-like arrangements (see Fig. 9) are functionally significant for impulse-propagation is unknown. However the ultrastructural organization noted at the transition of medium and large C-fibres become particularly interesting in view of Waxman's (1975) ideas on the correlation between local nerve fibre design and function. Thus Waxman discusses the possibility that the integrative properties of impulse transmission is influenced not only by the nerve cell body, the dendrites and the receptors but also by local arrangements of the interconnecting fibre.

ACKNOWLEDGEMENTS

This investigation was supported by grants from Karolinska Institutet (Reservations-*slaget*) and from the Swedish Medical Research Council (projects No. 12x-3167 and 03157). I am much indebted to doctor Claes-Henric Berthold for his constructive criticism and comments, to doctor Erik Torebjörk for valuable discussions and to Miss Maj Berghman, Mrs. Anita Bergstrand, Mrs. Eva Björkner and Mrs. Anna-Stina Håjer for excellent technical assistance.

Table I
Fibre spectrum of unmyelinated fibres on the peripheral (P) and central (C) side of the PNS-CNS borderline

Specimen	—0.36 μ m 0.46 μ m	0.35 — 0.46 μ m	0.46 — 0.57 μ m	0.57 — 0.66 μ m	0.66 — 0.79 μ m	0.79 — 0.90 μ m	0.90 — 1.01 μ m	1.01 — 1.12 μ m	1.12 — 1.23 μ m	1.23 — 1.34 μ m	No. of fibres
K 1026 P	33	131	133	33	8	8	2	1			257
C	38	146	133	18							234
K 1038 P	47	198	344	267	75	19	8	3	2		860
C	39	264	389	236	36						804
F 1040 P	46	320	361	210	64	11	8	2	1		1010
	42	277	366	229	34						869

Table II

Axon size as found on the two sides of the PNS-CNS borderline in unmyelinated and unmyelinated myelinated axons.

Speed mm	Number of axons	PNS					Border- line		CNS				
		30 μ m	40 μ m	50 μ m	60 μ m	70 μ m	0	10 μ m	20 μ m	30 μ m	40 μ m	50 μ m	
K 1026	1	0.96	0.86	0.96	0.95	0.95		0.77 ^m	0.66 ^m	1.07 ^m	1.07 ^m	1.29 ^m	
	2	0.41	0.1	0.41	0.1	0.36		0.41	0.41	0.41	0.41	0.30	
	3	0.41	0.41	0.41	0.41	0.36		0.41	0.41	0.41	0.82	0.41	
	4	0.63	0.63	0.63	0.63	0.34		0.63	0.63 ^m	0.63 ^m	0.63	0.63	
	5	0.41	0.41	0.41	0.1	0.36		0.36	0.41	0.82	0.41	0.36	
	6	0.1	0.41	0.41	0.36	0.41		0.62	0.41	0.1	0.62	0.62	
	7	0.34	0.34	0.34	0.34	0.34		0.34	0.63	0.63	0.34 ^m	0.34 ^m	
	8	0.62	0.62	0.62	0.62	0.4		0.62	0.62	0.41	0.41	0.41	
	9	0.4	0.62	0.62	0.41	0.36		0.41	0.62	0.62	0.62	0.62	
K 1038	1	0.63	0.62	0.62	0.63	0.63		0.63 ^m	0.34 ^m	0.34 ^m	0.34 ^m	0.34 ^m	
	2	0.63	0.63	0.63	0.63	0.4		0.41	0.41	0.4	0.41	0.36	
	3	0.4	0.62	0.62	0.1	0.1		0.62	0.62	0.62	0.62	0.62	
	4	0.63	0.63	0.63	0.63	0.63		0.63 ^m	0.34 ^m	0.63 ^m	0.63 ^m	0.34 ^m	
	5	0.1	0.41	0.41	0.41	0.41		0.62	0.62	0.1	0.62	0.41	
	6	0.36	0.41	0.41	0.41	0.41		0.62	0.62	0.41	0.62	0.62	
	7	0.63	0.63	0.63	0.63	0.63		0.63 ^m	0.63 ^m	0.63 ^m	0.34 ^m	0.34 ^m	
	8	0.62	0.41	0.41	0.41	0.1		0.62	0.62	0.62	0.62	0.62	
	9	0.62	0.41	0.41	0.41	0.41		0.41	0.62	0.41	0.41	0.41	
040		0.96	0.96	0.96	0.96	0.96		0.66 ^m	1.16 ^m	0.66 ^m	1.07 ^m	1.67 ^m	
	2	0.41	0.63	0.62	0.1	0.4		0.36	0.62	0.41	0.41	0.41	
	3	0.41	0.1	0.41	0.36	0.36		0.41	0.41	0.41	0.41	0.36	
	4	0.63	0.63	0.63	0.63	0.62		0.41	0.62	0.62 ^m	0.34 ^m	0.34 ^m	
	5	0.62	0.41	0.41	0.4	0.41		0.62	0.62	0.41	0.1	0.36	
	6	0.36	0.36	0.36	0.1	0.36		0.41	0.41	0.41	0.41	0.41	
	7	0.62	0.62	0.62	0.41	0.62		0.62	0.62	0.62	0.62	0.41	
	8	0.63	0.63	0.41	0.1	0.62		0.41	0.62	0.36	0.62	0.62	
	9	0.62	0.62	0.62	0.62	0.41		0.1	0.62	0.36	0.62	0.62	

REFERENCES

- Aguayo A.J. Bray, G.M. Terry L.C. and Sweeney E. (1976) Three dimensional analysis of unmyelinated fibres in normal and pathologic autonomic nerves. *Journal of Neurocytopathology and Experimental Neurology* 35, 131-51.
- Berthold, C. H. and Carlstedt, T. (1977) Observations on the morphology at the transition between the peripheral and the central nervous system in the cat. II. General organization of the transitional region in S dorsal rootlets. *Acta Physiologica Scandinavica* suppl. 446, 23-42.
- Bessou, P. and Perl, E.R. (1969) Response of cutaneous sensory units with unmyelinated fibres to noxious stimuli. *Journal of Neurophysiology* 32, 1028-43.
- Burgess, P.R. and Perl, E.R. (1973) Cutaneous mechanoreceptors and nociceptors. In *Handbook of Sensory Physiology II. Somatosensory System* (edited by Iggo A.) pp 29-78. Berlin Heidelberg New York: Springer Verlag.
- Brody L. (1969) The keratinization of epidermal cells of normal guinea pig skin as revealed by electron microscopy. *Journal of Ultrastructure Research* 2, 482-511.
- Bunge, R.P. (1968) Glial cells and the central myelin sheath. *Physiological Review* 48, 197-251.
- Carlstedt, T. (1977) Observations on the morphology at the transition between the peripheral and the central nervous system in the cat. I. A preparative procedure useful for electron-microscopy of the lumbosacral dorsal rootlets. *Acta Physiologica Scandinavica*, suppl. 446 5-22.
- Lawrey G. (1900) *The cell of Schwann*. Edinburgh and London. E. and S. Livingstone Ltd.
- Conway C.L., Wright, F.S. and Bradley W.E. (1969) Electrophysiological maturation of the pyramidal tract in the postnatal rabbit. *Electroencephalography and Clinical Neurophysiology* 28, 565-77.
- Douglas, W.W. and Ritchie, J.M. (1967) Non-medullated fibres in the asphenous nerve which signal touch. *The Journal of Physiology* 130, 383-99.
- Elfvén, L.-G. (1968) The ultrastructure of unmyelinated fibres in the splenic nerve of the cat. *Journal of Ultrastructure Research* 1, 428-54.
- Elfvén, L.-G. (1968) The structure and composition of motor sensory and autonomic nerves and nerve fibres. In *The Structure and Function of Nervous Tissue* (edited by Bourne G.H.) 1 pp. 325-77 London and New York: Academic Press.
- Friede, R.L. (1972) Control of myelin formation by axon caliber (with a model of the control mechanism). *Journal of Comparative Neurology* 144 233-52.
- Gasser H.R. (1952) Discussion in the hypothesis of saltatory conduction. *Symposium on Quantitative Biology The Neuron*, 17 32-6. Pennsylvania: The Science Press.
- Gasser H.S. (1955) Properties of dorsal root unmyelinated fibres on the two sides of the ganglion. *The Journal of General Physiology* 38, 709-28.
- Gräner L.E. (1970) Concerning the fine structure of the trigeminal root and its connections. In *Trigeminal Neuralgia* (edited by Haasler R. and Walker A.E.) pp. 4-19 Stuttgart: Georg Thieme Verlag.
- Hess, A. (1936) The fine structure and morphological organization of non-myelinated nerve fibres. *Proceeding of the Royal Society London*, B 144 498-512.
- Hildebrand C. (1972) Evidence for correlation between myelin period and number of myelin lamellae in fibres of the feline spinal cord white matter. *Journal of Neurocytology* 1, 223-32.
- Kerr F.W. (1966) The ultrastructure of the spinal tract of the trigeminal nerve and the substantia gelatinosa. *Experimental Neurology* 10, 360-76.
- Kerr F.W. (1970) Fine structure and functional characteristics of the primary trigeminal neuron. In *Trigeminal Neuralgia* (edited by Haasler R. and Walker A.E.) pp. 11-17 Stuttgart: Georg Thieme Verlag.
- Koles, Z.J. and Rasminsky M. (1972) A computer simulation of conduction in demyelinated nerve fibres. *The Journal of Physiology* 237 361-64.
- Lampert, P.W. (1967) A comparative electron microscopy study of reactive degenerating, regenerating and dystrophic axons. *Journal of Neuropathology and Experimental Neurology* 26 345-68.
- Lehmann, H.J. (1959) Die Nervenfasern. In *Handbuch der Mikroskopischen Anatomie des Menschen* (edited by Möllendorff v. W.) pp 515-701. Berlin: Springer Verlag.
- Matthews M.A. (1968) An electron microscopic study of the relationship between axon diameter and the initiation of myelin production in the peripheral nervous system. *The Anatomical Record* 161 337-62.

- Ochoa, L. (1975) Microscopic anatomy of unmyelinated nerve fibres. In *Peripheral Neuropathy* (edited by Dyck, P.J., Thomas, P.K. and Lambert, E.H.) pp. 131-150. Philadelphia, London, Toronto W.B. Saunders.
- Ochoa, L. (1976) The unmyelinated nerve fibre. In *The Peripheral Nerve* (edited by Landon, D.N.) pp. 106-158 London. Chapman and Hall.
- Peachey L.D. (1966) Thin sections. I. A study of section thickness and physical distortion produced during microtomy. *The Journal of Biophysical and Biochemical Cytology* 4: 233-42.
- Peyronnard, J.M., Aguayo, A.J. and Bray G.M. (1973) Schwann cell internuclear distance in normal and regenerating unmyelinated nerve fibres. *Archives of Neurology* 29, 56-9.
- Rabson, H.J. (1965) The organization of the substantia gelatinosa Rolandi in the cat lumbosacral spinal cord. *Zeitschrift für Zellforschung* 67: 1-23.
- Reynolds, E. (1963) The use of lead citrate at high pH as an electron opaque stain in electron microscopy. *The Journal of Cell Biology* 17: 209-13.
- Romero, C. and Skoglund, B. (1965) Methodological studies of the technique in measuring nerve fibre diameters. *Acta Morphologica Neerlandica Scandinavica* 5, 107-17.
- Rushton, W.A.H. (1951) A theory of the effects of fibre size in medullated nerve. *The Journal of Physiology* 115, 101-22.
- Spidel, C.C. (1964) *In vivo* studies of myelinated nerve fibres. *International Review of Cytology* 16, 173-231.
- Steier J.M. (1971) Some observations on the fine structure of rat dorsal spinal nerve roots. *Journal of Anatomy* 109, 467-85.
- Stowe, J. and Freeman, R.B. (1971) Conduction velocity groups in the cat's optic nerve classified according to their retinal origin. *Experimental Brain Research* 13, 489-97.
- Stowe, J. and Hollander, H. (1971) Optic nerve axon diameters measured in the cat retina. Some functional considerations. *Experimental Brain Research* 13, 498-503.
- Sunderland, S. (1976) Pain mechanisms in causalgia. *Journal of Neurology Neurosurgery and Psychiatry* 39: 471-80.
- Szentagothai, J. (1964) Neuronal and synaptic arrangement in the substantia gelatinosa Rolandi. *The Journal of Comparative Neurology* 123, 319-39.
- Waxman, S.G. (1970) Closely spaced nodes of Ranvier in the teleost brain. *Nature (London)* 227: 283-4.
- Waxman, S.G. (1975) Integrative properties and design principles of axons. *International Review of Neurobiology* 18, 1-40.
- Waxman, S.G. and Bennett, M.V.L. (1972) Relative conduction velocities of small myelinated and non-myelinated fibres in the central nervous system. *Nature New Biology* 238, 217-219.
- Wedell, G. and Verillo, R.T. (1972) Common sensibility. In *Scientific Foundations of Neurology* (edited by Critchley, M., O'Leary, J.L. and Jennet, B.) pp. 117-25. London. W. H. Freeman Medical Books Ltd.
- Weinberg, H.J. and Spencer, P.S. (1975) Studies on the control of myelinogenesis. I. Myelination of regenerating axons after entry into a foreign unmyelinated nerve. *Journal of Neurocytology* 4: 395-418.

LEGENDS TO FIGURES

Abbreviations used in figures and legends.

Ap	astrocyte process
Ax	axon
BM	basement membrane
C	collagen fibres
G	gliosome
My	myelin
M	mantle zone
R	node of Ranvier
S	Schwann cell cytoplasm

All pictures beside Fig. 2 are electronmicrographs.

Fig. 1a Cross-section. Bundle of PNS unmyelinated axons. Most axons are separated by Schwann cell septa ($\times 33000$)

Fig. 1b Cross-section. Bundle of CNS unmyelinated axons. The axons are closely packed and accompanied by astrocyte processes (Ap) and small myelinated fibres ($\times 37000$).

Fig. 2 Diagrammatic representation of Schwann cell nuclear length and the distribution of Schwann cells along bundles of unmyelinated fibres in the transitional region. Three bundles each of three specimens (K1028, K1039, K1040) were used.

Figs. 3a-d Four different cross levels selected from a complete series of consecutive cross-sections through the transitional region. The section number is given in the lower left corner of each picture. Section thickness is about 700 Å. A bundle of 12 axons is followed from the PNS to the CNS compartment in the proximal part of the TR. Each fibre is indicated by a number. The mantle zone (MZ) of the CNS compartment is observed in the lower part of the pictures. Cross cut collagen fibres (C) are seen in the endoneurial space. The axons are surrounded by Schwann cell cytoplasm (S) distal to the PNS-CNS borderline (Fig. 3a). At the borderline (Fig. 3b) some 25 µm proximal to the level represented in Fig. 3a, fibre 1 is partly invested by slender Schwann cell septa (S) and partly invested by broad irregularly shaped or slender radially arranged finger-like astrocyte processes (Ap). At the place of transition from the PNS to the CNS (Fig. 3c) some 6 µm proximal to the level represented in Fig. 3b, fibres 1, 2, 4, 5, 7 forms a bundle of closely packed axons. The bundle is surrounded partly by slender processes of Schwann cell cytoplasm (S) and partly by delicate astrocyte processes of the mantle zone (MZ). Proximal to the PNS-CNS borderline (Fig. 3d) and some 46 µm from the level represented in Fig. 3a, the axons are closely packed in a bundle surrounded by the astrocyte processes of the mantle zone (MZ) ($\times 28000$).

Fig. 4a-f Six different cross levels selected from a complete series of consecutive cross-section through the TR. Section number is given in the lower left corner of each picture. Section thickness is 700 Å. Two unmyelinated fibres cross the PNS-CNS borderline two times in the distal part of the TR. The fibres are invested by Schwann cell cytoplasm (S) distal to the PNS-CNS borderline (Fig. 4a). At the borderline (Fig. 4b) the basement membrane (BM) of the Schwann cell and the astrocytes of the mantle zone are continuous. Schwann cell (S) and astrocyte derivatives are opposed without intervening basement membranes (Figs. 4b, d, f). Multiple slender astrocyte lamellae derived from gliosome (G) containing astrocyte processes are directed towards the fibres (Fig. 4b, c, d). The fibres are situated in the CNS compartment for some 18 µm (Figs. 4b, c, d). In Fig. 4f some 22 µm proximal to the level represented in Fig. 4a the fibres are again invested by Schwann cell cytoplasm (S) in the PNS compartment ($\times 29000$).

Fig. 5 Cross-section. A bundle of unmyelinated fibres invested by Schwann cell cytoplasm (S) is seen in the upper part of the picture. In the centre of the picture an unmyelinated axon is situated at the PNS-CNS borderline. The fibre is partly surrounded by a basement membrane (BM) and radially arranged delicate finger-like processes some 500-1000 Å thick, derived from gliosome (G) and fibrillae containing astrocytic extensions. There is a material of high electron density on the axoplasmic side of the axolemma where the astrocyte processes point towards the axon (arrows) ($\times 30000$).

Fig. 6 Two cross sectioned unmyelinated axons (Ax) in a process of the glial fringe in the distal part of the transitional region. The axons are surrounded by numerous irregularly shaped, gliosomes (G) and fibrillae containing astrocytic extensions (x38000).

Fig. 7 Photomontage. Longitudinal section through a 0.8 μ m thick nerve fibre crossing the PNC-CNS borderline (hatched line). In the lower part of the picture the fibre is unmyelinated and invested by Schwann cell cytoplasm (S). In its most distal CNS part, the unmyelinated fibre is invested by lamellae like astrocytic processes (Ap). Some 4 μ m proximal to the PNS-CNS borderline the axon is myelinated (My) and thus a small CNS myelinated fibre. The most distally situated node of Ranvier (R) is seen in the upper part of the picture. Occasional glial processes are seen in the broad node gap. The internodal length is 10 μ m and the myelin is seen to terminate at both internodal ends in a conventional manner (x11000).

Fig. 8 Photomontage. Longitudinal section through a segmentally myelinated axon (Ax) in the mantle zone of the transitional region. The fibre is about 0.8 μ m thick. The internode in the lower part of the picture is about 6 μ m long. The fibre is invested by astrocytic processes (Ap) in its unmyelinated part (x11000).

Figs. 9 a, b. Three levels from a complete cross section series through the TR, showing a nerve fibre, 0.9 μ m thick passing the PNS-CNS borderline.

a) The fibre is unmyelinated distal to the borderline and surrounded by Schwann cell cytoplasm (S). The endoneurial space surrounding the fibre is demarcated by astrocytic processes of the mantle zone. Some 3 μ m more proximally (Fig. 9b), the fibre is invested by broad irregularly shaped and slender radially arranged, leaflet-like astrocytic processes (Ap). There is an electron dense material subjacent to the axon membrane at those places where the leaflet-like astrocytic processes are directed towards the axon (arrows). Some 10 μ m proximal to the level shown in Fig. 9b the axon is myelinated (Fig. 9c) (x34000).

Figs. 10 a-d. Series of cross-section. A small myelinated CNS fibre (x) (Fig. 10a) transforms proximally into an enlarged myelinated profile containing mitochondria, dense bodies and vesicular entities (Fig. 10b). About 6 μ m proximal to the level shown in Fig. 10b the fibre has tapered off into a tip (Fig. 10c) and some 2 μ m more proximally the fibre has disappeared completely (x19000).

Figures at the end of this volume

Running title Unmyelinated fibres in the transitional region

Observations on the Morphology at the Transition between the Peripheral and the Central Nervous System in the Cat.

V

A light microscopical and histochemical study of S₁ dorsal rootlets in developing kittens

by

C.H BERTHOLD and T CARLSTEDT

ABSTRACT

C. H. BERTHOLD and T. CARLSTEDT *Observations on the morphology at the transition between the peripheral and the central nervous system in the cat. V. A light microscopical and histochemical study of S₁ dorsal rootlets in developing kittens. Acta physiol. scand. 1977 Suppl. 446 73-85.*

The postnatal development of the transitional region (TR) i.e. the proximal free part of a spinal rootlet that contains both PNS and CNS tissue, was studied light-microscopically in semi-thin sections and after histochemical staining according to the Marchi and OTAN methods for the demonstration of degenerating myelin and according to the Gomori method for the demonstration of acid phosphatase activity. In the newborn kitten the PNS tissue extended well up to the spinal cord surface and the rootlets lacked a transitional region. The CNS tissue entered the root during the second postnatal week, and a transitional region was fully established at the beginning of the second month.

The degree of myelination in the group of large fibres differed on the two sides of the PNS-CNS borderline: well myelinated PNS fibres were transformed into poorly myelinated or apparently unmyelinated CNS-fibres. PNS and CNS myelin sheaths of large fibres appeared to be of equal thickness in the 4 week old kitten.

During the first postnatal month large amounts of Marchi positive material and a high acid phosphatase activity occurred in complex paranodes and very short internodes in the PNS compartment just distally to the PNS-CNS borderline. In the adult cat Marchi positive bodies were numerous in the CNS compartment just proximally to the PNS-CNS borderline.

The results are discussed against previous studies on focal demyelination as found during the normal development of the feline peripheral nervous system.

The systematic investigation of the anatomical correlate of postnatal spinal reflex maturation in the hindlimbs of the cat as initiated by Skoglund more than 15 years ago (Skoglund, 1960a, b, c, d, e, 1966) includes by now treatises on peripheral nerve fibre maturation (Skoglund and Romero 1965; Ekholm, 1967; Schwieler 1967; Berthold, 1968; Nyström, 1968), motor neuron maturation (Conradi 1969; Mellström, 1971; Hammarberg, 1975; Ronnevi, 1976) central nerve fibre maturation (Hildebrand, 1971) and skeletal muscle maturation (Nyström, 1968; Hammarberg, 1975). Common to all these studies is the demonstration of a profound and rapid maturation which includes steps of remodelling and degeneration and which takes place during the first postnatal month. This development is well functional improvements and gives fully or almost fully mature

patterns during the 5th-6th postnatal week. So far no studies at all have been devoted to the postnatal development of the feline transitional region (TR) i.e. that part of the nervous system where the neuronal environment changes from the CNS to the PNS pattern. The only available data on the developing TR seems to be that given by Henschen (1915) in a study on acoustic nerve tumors where he comments that the extent of CNS tissue into the eighth cranial nerve of the infant is considerably shorter than that of the adult.

Against this background and taking into account the fact that the mature feline transitional region ultrastructure has recently for the first time been described (Carlstedt, 1977 a, b; Berthold and Carlstedt, 1977 a, b) the undertaking of a survey study of the developing transitional region becomes more or less a matter of course.

The present communication deals with the development of this region as studied light-microscopically in semi-thin sections of plastic-embedded specimens and reports the outcome of two histochemical tests on the occurrence of myelin degeneration products and acid phosphatase.

The results, which strongly emphasise the need of further ultrastructural analysis of the postnatally developing transitional region are mainly discussed in terms of the focal demyelination previously demonstrated in the peripheral nervous system of the kitten (Berthold and Sjöglund, 1968, Berthold, 1973c).

MATERIAL AND METHODS

In all, 5 adult cats and 31 kittens (0-180 days old) were used. All animals were anaesthetized intraperitoneally with pentobarbital (40 mg/kg body weight). The lower lumbar and sacral spinal cord segments and their spinal roots were fixed by vascular perfusion through the thoracic aorta (Berthold, 1968a).

That preparative procedure which previously has been given for the TR (Carlstedt, 1977a) was used for adult cats and kittens more than 2 months of age. In younger kittens (see Table I) the perfusate consisted of 5% glutaraldehyde dissolved in 300 mM cacodylate buffer containing 2.7% low-molecular dextran (Berthold, 1968a). After perfusion fixation and a laminectomy the 8, dorsal spinal roots and their spinal cord segment were removed. The roots were carefully separated into the individual rootlets with the aid of watchmakers' forceps. After trimming with a razor blade the specimens consisted of the proximal one third of the rootlet and its attachment to the spinal cord together with a small piece of the surrounding white matter. The specimens were placed for 4 hours at +4°C in a glutaraldehyde solution of the same composition as the perfusate and were rinsed overnight in the buffer at 4°C. Three rootlets per animal were used for Marchi and OTAN treatment (see below). Remaining specimens were osmicated in 2% OsO₄ in 300 mM cacodylate buffer for four hours, dehydrated in a graded series of acetone solutions and embedded in Vestopal W (Byter and Hellenberger, 1966). Longitudinal semi-thin sections (0.5 µm thick) were cut at random on a LKB 4800 Ultratome, placed on glass slides and stained with alkaline toluidine blue (Carlstedt, 1977a).

The Marchi and OTAN methods (see Adams 1965) Longitudinal 15-30 µm thick sections obtained on an Oxford Vibratome[®] were immersed overnight (18-20 hours) in a mixture of 1/4 1% OsO₄ in distilled water and 3/4 1% KC10₄ in distilled water (i.e. the Marchi medium, cf. Adams, 1965). In order to obtain OTAN-staining Marchi-stained slices were rinsed for a short time in a phosphate buffer and treated in a prewarmed saturated solution of alphanaphthylamine at 37°C for 5-10 minutes. OTAN staining was performed only in kittens.

Some sections were investigated directly after glutaraldehyde fixation or after additional treatment in 0.25% OsO₄ in distilled water.

The Gomori method (Gomori, 1952) In one cat and 8 kittens (0, 7, 14, 21, 30 and 45 days old) the perfusate consisted of 2.5% glutaraldehyde dissolved in a 0.1 M cacodylate buffer adjusted to 300 mOsm by the addition of NaCl and containing 2.7% low-molecular dextran. The glutaraldehyde stock solution was purified by shaking with active charcoal (Pahimi and Drochmann, 1965). The perfusion fixation, which duration varied from 10 to 20 minutes, was concluded by a rinse with the buffer lacking glutaraldehyde. After removal the specimens were sectioned into longitudinal slices (15-30 μ m thick) on an Oxford Vibratome¹. The slices were incubated in a freshly prepared Gomori medium (Gomori, 1952) with sodium- β -glycerophosphate as substrate for 15 to 30 minutes at 37°C. After a rinse in the cacodylate buffer the specimens were «developed» for 30 seconds in 1% ammonium sulphide and mounted in glycerine on glass slides. Control specimens were either treated with 1% NaF before incubation or were incubated in a medium which lacked substrate.

RESULTS

Toluidine-blue-stained semi thin sections

After toluidine-blue staining all Vestopal-embedded specimens revealed PNS myelin sheaths with fairly smooth internodal contours and of an intense bluish-black colour. CNS-myelin sheaths, on the other hand, showed corrugated contours and appeared with a more pale blue colour. These differences were used for the identification of the PNS-CNS borderline (Figs. 1-7). A picture of the longitudinally cut mature TR and the adopted nomenclature is given in Fig. 1 and its legend (cf. Berthold and Carlstedt, 1977a).

In kittens less than a week of age (Figs. 2-5) the proximal ends of 8 rootlets were completely free of CNS tissue (Fig. 2). PNS-myelinated fibres extended proximally to the very level of the rootlet-cord junction. PNS myelin sheaths were consistently much thicker than CNS sheaths as seen in the same fibres on the two sides of the PNS-CNS borderline. Numerous unmyelinated axon segments measuring up to 50 μ m in length were found intercalated between myelinated PNS and CNS internodes at the borderline. The axons of several large PNS-myelinated fibres (2-3 μ m in diameter) appeared to continue unmyelinated in the CNS (Fig. 3). The occurrence of cell bodies was high on both sides of the borderline: Schwann cells and immature glia cells dominated the picture in the PNS and the CNS respectively. Several mitoses were seen among the glia cells. With the exception of Schwann cells connected to myelinated axons light microscopy did not allow a classification of the various glial and endoneurial cell elements.

At the end of the 1st postnatal week, PNS borderline paranodes, showed a moderate dilatation, a highly tortuous myelin sheath contour and a content of myelinoid bodies, i.e. the characteristics of a complex paranode (see Berthold, 1973c). To this added the occurrence of a few typical short and very short internodes 50-150 and 10-50 μ m in length, respectively (Fig. 5).

During the 2nd and 3rd postnatal weeks CNS-tissue entered and occupied an expanding compartment of the proximal segment of the rootlets (Fig. 4). At the end of the period the CNS compartment measured up to 50 μ m in length and the rootlets displayed a definite transitional region (Fig. 6). The 2nd postnatal week brought a dramatic increase in the occurrence of very short internodes (Fig. 5). The latter together with unclassified endoneurial cells and complex paranodes, contained clusters of myelinoid bodies. Unmyelinated borderline axon segments were rare at the end of the 3rd week. The clear-cut difference between PNS and CNS myelin sheath thickness which was one of the main characteristics of the borderline during the first postnatal fortnight became less pronounced (Fig. 7).

During the subsequent month (postnatal weeks 4 to 8) the CNS compartment increased gradually in length (Fig. 6) and measured well above 100 μ m in several rootlets in the 2 month-old kitten.

A close to mature overall picture seemed to be present already in 4-5-week-old animals. At the beginning of this period, however, it was common to find thin bundles of only a few CNS fibres accompanied by some astrocytes. Such rays of CNS tissue projected further distally than the main part of the CNS compartment (Fig. 7).

Marchi and OTAN staining

In the adult cat Marchi treatment gave pale yellowish-grey myelin sheaths (Figs. 9-11). The PNS-CNS borderline was characterized by the high number of borderline nodes and the less well preserved condition of the adjoining CNS myelin sheaths (cf. Carlstedt, 1977a). In the CNS compartment there were numerous black Marchi-positive bodies 2-10 μ m in size (Fig. 9). The bodies were concentrated in the mantle zone and were less abundant in the core zone. Brownish-black highly refractile Marchi positive granules less than 1 μ m in size, were scarce in the CNS compartment. In the PNS compartment solitary Marchi positive bodies and short rows of Marchi positive granules were confined to the Schwann cell cytoplasm of a few paranodes.

Material reminiscent of Marchi positive bodies and granules were not found in specimens which after the glutaraldehyde fixation were immersed in 0.25% OsO₄ (Fig. 8). Examination of specimens treated only with glutaraldehyde revealed the occurrence, particularly in the mantle zone, of round bodies with a texture similar to that of the myelin sheath (cf. Fig. 16). These bodies measured 2-10 μ m in size and will be referred to as myelinoid bodies (cf. Berthold and Skoglund, 1968; Hildebrand, 1971).

During the first postnatal month Marchi-positive bodies and Marchi-positive granules were observed in large numbers just distally to the PNS-CNS borderline (Table I, Fig. 12). After OTAN staining the blackness of these bodies and granules became more intense and the myelin sheaths appeared redbrown and much more distinct than after staining in the Marchi medium alone. In the first week the Marchi positivity consisted mainly of Marchi positive granules. The highest occurrence of Marchi positivity was noted in the 2nd and 3rd postnatal weeks, then consisting mainly of Marchi positive bodies. From the 4th week onwards the Marchi-positivity of the PNS compartment declined and the mature picture appeared at the beginning of the second postnatal month (Table I).

The Marchi positive bodies were found in complex paranodes (Fig. 13) in very short internodes (Fig. 14) and in unclassified endoneurial cells. A comparison between the more distal parts of a rootlet and the PNS compartment of its transitional region showed that the occurrence of Marchi-positive very short internodes at the latter site indeed was remarkably high.

In the CNS compartment Marchi positive material was scarce during the first postnatal weeks (Figs. 12, 13). It occurred mainly in the form of Marchi positive granules. Marchi positive bodies began to accumulate at the end of the first month. They then became increasingly more numerous and the adult pattern was present at the end of the second month (Table I).

Gomori staining

In the adult cat staining according to the Gomori method (Figs. 15, 16) gave rise to a finely granular dark brown precipitate (reaction product) occurring on a yellowish background.

Ring and crescent-shaped accumulations of the reaction product were related to some myelinoid bodies (Fig. 18). Schwann cell perikarya and the mantle zone contained a few scattered minute reaction product granules.

The precipitates referred to above were not present in control incubations. As noted elsewhere (Berthold, 1973b) control incubations showed the occurrence of a false reaction product at the nodes of Ranvier (see Fig. 15).

Throughout the postnatal period the occurrence of acid-phosphatase positivity was higher in the PNS compartment than in the CNS compartment (Figs. 17-19). The occurrence of activity was at its peak from the end of the 1st postnatal week until the beginning of the 4th week, whereafter it declined, reaching the adult level at about the end of the second month.

In newborn kittens (0-4 days of age) the reaction product appeared as 0.5-2 μ m large solitary brown-black granules or bodies (Fig. 17). Most cells found close to the PNS-CNS borderline contained a few scattered granules of this kind. Accumulations of reaction products forming rings and crescents were rare.

During the 2nd and 3rd postnatal weeks the occurrence of solitary Gomori-positive granules decreased. Instead there was a high occurrence of ring- and crescent-shaped brown-black material surrounding translucent globules 2-5 μ m in size. These characteristic profiles of reaction products were often arranged in clusters or rows situated in the complex paranodes and in very short internodes (Figs. 18, 19).

In the CNS compartment, where the occurrence of acid phosphatase activity remained low during the whole maturation process, the reaction product occurred in the glia cells and consisted of tiny granules and globules.

DISCUSSION

The present results have given the principal features of the postnatal development of the feline transitional region as studied light-microscopically in semi-thin sections and after histochemical incubations according to the Marchi and OTAN methods for the demonstration of degenerating myelin and to Gomori's method for the demonstration of acid phosphatase activity. Methodological aspects on these procedures as applied to PNS and CNS nerve-fibres have been discussed at length elsewhere (Hildebrand and Skoglund, 1971b; Berthold, 1973a). Briefly it has been shown that Marchi-positive bodies occurring in the paranodal regions of Schwann cell cytoplasm and in relation to the outside of the paranodal myelin sheath of CNS fibres ultrastructurally correspond to lamellar myelinoid bodies. The Marchi-positive granules on the other hand are claimed to represent lipid droplets. Further, that light-microscopically observed clumps, rings and crescents of acid phosphatase activity reflect the presence of aggregations of an electron-dense dust-like material — the reaction product — in relation to the myelinoid bodies mentioned above (Berthold, 1973b). Scattered granules of reaction product observed light-microscopically both in Schwann cells and in glial cells can be interpreted as reflecting lysosomal and Golgi cistern phosphatase activity (cf. Friede, 1966; Holtzman and Novikoff, 1967; Berthold 1973b).

In agreement with earlier observations (Berthold 1973a, b) on adult PNS-nerve fibres, only some of the paranodes of the PNS compartment of the mature TR contained Marchi-positive bodies and mere indications of acid phosphatase activity. The CNS-compartment, on the other hand, was more or less outlined by Marchi positive bodies lodging in the mantle zone. (cf. Singer and Münzer 1888). The acid phosphatase activity was low. The high occurrence of myelinoid bodies in the mantle zone as suggested by the high number of Marchi positive bodies is fully consistent with our earlier electron-microscopic analysis of the adult TR (Berthold and Carlstedt, 1977a). The abundance of Marchi-positive material in the

During the subsequent month (postnatal weeks 4 to 8) the CNS compartment increased gradually in length (Fig. 6) and measured well above 100 μm in several rootlets in the 7 month-old kitten.

A close to mature overall picture seemed to be present already in 4-5-week-old animals. At the beginning of this period however it was common to find thin bundles of only a few CNS fibres accompanied by some astrocytes. Such rays of CNS tissue projected further distally than the main part of the CNS compartment (Fig. 7).

Marchi and OTAN staining

In the adult cat Marchi treatment gave pale yellowish-grey myelin sheaths (Figs. 9-11). The PNS-CNS borderline was characterized by the high number of borderline nodes and the less well preserved condition of the adjoining CNS myelin sheaths (cf. Carlstedt, 1977a). In the CNS compartment there were numerous black Marchi positive bodies 2-10 μm in size (Fig. 9). The bodies were concentrated in the mantle zone and were less abundant in the core zone. Brownish-black highly refractile Marchi positive granules less than 1 μm in size, were scarce in the CNS compartment. In the PNS compartment solitary Marchi positive bodies and short rows of Marchi positive granules were confined to the Schwann cell cytoplasm of a few paranodes.

Material reminiscent of Marchi positive bodies and granules were not found in specimens which after the glutaraldehyde fixation were immersed in 0.25% OsO₄ (Fig. 8). Examination of specimens treated only with glutaraldehyde revealed the occurrence, particularly in the mantle zone, of round bodies with a texture similar to that of the myelin sheath (cf. Fig. 16). These bodies measured 2-10 μm in size and will be referred to as myelinoid bodies (cf. Berthold and Skoglund, 1968; Hildebrand, 1971).

During the first postnatal month Marchi positive bodies and Marchi-positive granules were observed in large numbers just distally to the PNS-CNS borderline (Table I, Fig. 12). After OTAN staining the blackness of these bodies and granules became more intense and the myelin sheaths appeared redbrown and much more distinct than after staining in the Marchi medium alone. In the first week the Marchi positivity consisted mainly of Marchi positive granules. The highest occurrence of Marchi-positivity was noted in the 2nd and 3rd postnatal weeks, then consisting mainly of Marchi positive bodies. From the 4th week onwards the Marchi-positivity of the PNS compartment declined and the mature picture appeared at the beginning of the second postnatal month (Table I).

The Marchi positive bodies were found in complex paranodes (Fig. 13) in very short internodes (Fig. 14) and in unclassified endoneurial cells. A comparison between the more distal parts of a rootlet and the PNS compartment of its transitional region showed that the occurrence of Marchi positive very short internodes at the latter site indeed was remarkably high.

In the CNS compartment Marchi positive material was scarce during the first postnatal weeks (Figs. 12, 13). It occurred mainly in the form of Marchi positive granules. Marchi positive bodies began to accumulate at the end of the first month. They then became increasingly more numerous and the adult pattern was present at the end of the second month (Table I).

Gomori staining

In the adult cat staining according to the Gomori method (Figs. 15-16) gave rise to a finely granular dark-brown precipitate (reaction product) occurring on a yellowish background.

Ring- and crescent-shaped accumulations of the reaction product were related to some myelinoid bodies (Fig. 16). Schwann cell perikarya and the mantle zone contained a few scattered minute reaction product granules.

activation or manufacture myelin exceedingly slowly during the first postnatal weeks needs electron-microscopic exploration. An ultrastructural morphometric analysis of developing TR nerve fibres also appears well worth undertaking in view of the intensifying debate on the signal for myelination (see, e.g. Friede 1972; Weinberg and Spencer 1975).

The occurrence of unmyelinated and/or poorly myelinated fibre stretches interconnecting well myelinated parts of an axon is regardless of latent causes of particular interest in terms of impulse propagation. A rough extrapolation of the values calculated by Koles and Rasminsky (1972) for the length of a paranodal demyelination that would induce conduction block in a large rat PNS fibre to developing large TR fibres in the cat indicates that unmyelinated stretches some 30 and 60 μm in length might block the nerve signal in the newborn and the 3-4-week old kitten respectively. Since several axons of the TR during the first month revealed apparently unmyelinated parts 50 μm or more in length the situation in the TR might turn out to be crucial for impulse propagation during the first month after birth. It should be noted that the length of the demyelinated axon segments which are at hand in the dorsal root outside the TR (Berthold, 1973c) rarely exceeds 20 μm . This should induce impulse retardation rather than block.

ad (3) Local demyelination and elimination of supernumerary internodes are claimed to be inherent features of a maturation step — the nodalization process — whereby a certain nerve fibre stretch acquires a fixed number of evenly spaced nodes of Ranvier and whereby the primitive node-paranode regions of the already myelinated axon develop their complex adult organization (Berthold, 1973c). The nodalization process, including local demyelination has been shown to be relevant for feline CNS myelinated nerve fibres (Hildebrand, 1971a) as well as for the PNS of some commonly used laboratory animals like the rabbit and the dog (Berthold, 1974). The high occurrence and the distribution pattern of short and very short internodes and of unmyelinated axon segments, the large amounts of Marchi positive material and the abundant acid phosphatase reaction product in the proximal part of the \square dorsal rootlets during the first postnatal month suggest strongly that local demyelination and Schwann cell elimination are particularly prominent features of nodalization in the transitional region.

It was recently claimed (Berthold, 1973c) that local demyelination and Schwann cell elimination in developing feline lumbosacral spinal roots are the effects of internodal crowding brought about by an increase in internodal length that exceeds that of the root. Conceivably an active outgrowth of glia along already overpopulated axons might well provoke an exaggeration of the degenerative features. The extent of the Schwann cell elimination in the TR needs, however, electron-microscopic evaluation.

The possibility that there might exist a pool of eliminated supernumerary Schwann cells in the transitional region — in a sense a Schwann cell hamartoma — becomes noteworthy for two reasons. First there does exist in the adult transitional region a population of small round to fusiform cells with scanty cytoplasm and of unknown origin (Berthold and Carstedt, 1977a). The presence of a basement membrane outside some of these cells implies an epithelial origin and suggests some sort of relationship with Schwann cells. A thorough discussion regarding the classification of endoneurial cells and the taxonomic significance of the basement membrane is given by, for instance, Abercrombie and Johnson (1942), Nataniel and Pease (1963) and Thomas (1963 1966). Secondly, benign tumors such as the neurinomas and the Schwannomas and the Schwannomas are found in the transitional region of spinal roots and cranial nerves (cf. Henachen, 1955). Thus, for instance, the acoustic neurinoma is claimed to originate in the transitional region of the eighth cranial nerve (cf. Minner 1972). So a straight forward demonstration of dormant Schwann cells in peripheral nerves and spinal roots would obviously be of considerable neuropathological interest.

The occurrence of Marchi-positive material shifted during the first two postnatal months from the PNS side of the borderline to the CNS side. The main part of the PNS Marchi-positive material appeared to have developed as an effect of nodalization and in analogy with the situation in the root proper (Berthold, 1973 c) it was found to decline rapidly towards the end of the first month. Roughly at the same time CNS-paranodal Marchi positivity started to increase (cf Hildebrand and Skoglund, 1971). The close-to-adult picture was at hand in the 8-week-old animal. Thus it seems that the focal demyelinating features of nodalization of the developing TR are restricted to the PNS compartment and do not affect the CNS compartment.

ACKNOWLEDGEMENTS

This investigation was supported by grants from Karolinska Institutet (Reservationsanlaget) and from the Swedish Medical Research Council (projects No 12x-3157 and -03157). We are much indebted to Mrs. Anita Bergstrand, Mrs. Eva Björkner and Mrs. Anna-Stina Htjyer for excellent technical assistance.

Table I

Occurrence of Marchi-positive material (Marchi-positive bodies and Marchi positive granules) in the transitional region of S₁ dorsal roots of kittens and cats

D = distal to the PNS-CNS borderline

P = proximal to the PNS-CNS borderline

Age in days	D	P
1	++	+
1	++	+
3	++	+
3	++	+
3	++	+
4	++	+
6	+++	+
7	+++	+
8	+++	+
10	+++	+
12	+++	+
14	+++	+
16	+++	+
18	+++	+
21	++	+
21	++	+
23	++	++
25	++	++
27	++	++
30	+	++
30	+	++
40	+	++
50	+	+++
80	+	+++
180	+	+++
Adult	+	+++
Adult	+	+++
Adult	+	+++
Adult	+	+++

+ = low occurrence of Marchi-positive material

++ = moderate occurrence of Marchi-positive material

+++ = high occurrence of Marchi-positive material

REFERENCES

- Abercomble, M. and Johnson, M.L. (1942) The outwandering of cells in tissue cultures of nerves undergoing Wallerian degeneration. *The Journal of Experimental Biology* 10 268-83.
- Adams, C.W.M. (1966) *N eurohistochemistry* Amsterdam. Elsevier Publishing Co.
- Berthold, C. H. (1968) Ultrastructural and light-microscopical features of postnatally developing and mature feline peripheral myelinated nerve fibres. Thesis, Karolinska Institutet, Stockholm, Sweden.
- Berthold, C. H. (1968a) A study on the fixation of large mature feline myelinated ventral lumbar spinal root fibres. *Acta Societatis Medicorum Upsalienis* 73, Suppl. 9 1-36.
- Berthold, C. H. (1968b) Ultrastructure of the node-paranode region of mature feline ventral lumbar spinal root fibres. *Acta Societatis Medicorum Upsalienis* 73, Suppl. 9 37-78.
- Berthold, C. H. (1973a) Histochemistry of postnatally developing feline spinal roots. I. A study with the OTAN (osmiumtetroxide-alpha-naphthylamine) method. *Neurobiology* 3, 275-90.
- Berthold, C. H. (1973b) Histochemistry of postnatally developing feline spinal roots. II. Occurrence of acid phosphatase activity as studied by light and electron microscopical methods. *Neurobiology* 3, 291-310.
- Berthold, C. H. (1973c) Local demyelinations in developing feline nerve fibres. *Neurobiology* 3, 339-62.
- Berthold, C. H. (1974) A comparative morphological study of the developing node paranode region in lumbar spinal roots. I. Electron microscopy. *Neurobiology* 4 82-104.
- Berthold, C. H. and Carlstedt, T. (1977a) Observations on the morphology at the transition between the peripheral and the central nervous system in the cat. II. General organization of the transitional region in 8 dorsal rootlets. *Acta Physiologica Scandinavica Suppl.* 446, 23-42.
- Berthold, C. H. and Carlstedt, T. (1977b) Observations on the morphology at the transition between the peripheral and central nervous system in the cat. III. Myelinated fibres in 8₁ dorsal rootlets. *Acta Physiologica Scandinavica Suppl.* 446, 43-60.
- Berthold, C. H. and Skoglund, B. (1968) Postnatal development of feline paranodal myelin sheath segments. II. Electron microscopy. *Acta Societatis Medicorum Upsalienis* 73, 127-44.
- Carlstedt, T. (1977a) Observations on the morphology at the transition between the peripheral and the central nervous system in the cat. I. A preparative procedure useful for electromicroscopy of the lumbosacral dorsal rootlets. *Acta Physiologica Scandinavica Suppl.* 446 5-22.
- Carlstedt, T. (1977b) Observations on the morphology at the transition between the peripheral and the central nervous system in the cat. IV. Unmyelinated fibres in 8₁ dorsal rootlets. *Acta Physiologica Scandinavica Suppl.* 446 61-72.
- Cocardi, B. (1961) On motoneuron synaptology in cats and kittens. Thesis, Karolinska Institutet, Stockholm, Sweden.
- Donnan, D. (1931) The Marchi method. A discussion of some sources of error and the value of this method for studying primary changes in the myelin sheath. *Archives of Neurology and Psychiatry* 25, 327-66.
- Ekholm, J. (1967) Postnatal changes in cutaneous reflexes and in the discharge pattern of cutaneous and articular sense organs. A morphological and physiological study in the cat. Thesis, Karolinska Institutet, Stockholm, Sweden.
- Fraser, J.P. (1976) The growth and myelination of central and peripheral segments of ventral motoneurone axons. A quantitative ultrastructural study. *Brain Research* 106, 193-211.
- Fahimi, H.D. and Drochmans, P. (1965) Essais de standardisation de la fixation au glutaraldehyde. I. Purification et détermination de la concentration du glutaraldehyde. *Journal de Microscopie* 4 725-36.
- Friede, R.L. (1966) *Topographic Brain Chemistry* New York, London. Academic Press.
- Friede, R.L. (1972) Control of myelin formation by axon caliber (with a model of the control mechanism). *Journal of Comparative Neurology* 144 233-62.
- Gomori, G. (1952) *Microscopic Histochemistry Principles and Practice*. Chicago: Chicago Press.
- Hamilton, W.J. Boyd, I.D. and Mossman, H.W. (1945) *Human embryology* Cambridge: W Heffer and sons Limited.

- Hammarberg, C. (1975) On the postnatal differentiation of motor units in the cat ankle muscles. A histochemical and physiological study. Thesis, Karolinska Institutet, Stockholm, Sweden.
- Henachen, F. (1918) Zur Histologie und Pathogenese der Kleinhirnbrücken-winkeln-tumoren. *Archiv für Psychiatrie und Nervenkrankheiten* 58, 20-193.
- Henachen, F. (1955) Tumoren der Hirnnerven III XII. In *Handbuch der Speziellen Pathologischen Anatomie und Histologie* (edited by Scholz, W.) 3 pp. 820-885 Berlin Göttingen, Heidelberg: Springer Verlag.
- Hildebrand, C. (1971) Ultrastructural and lightmicroscopic studies of myelinated nerve fibres in the adult and developing feline central nervous system. Thesis, Karolinska Institutet, Stockholm, Sweden.
- Hildebrand, C. (1971a) Ultrastructural and lightmicroscopic studies of the developing feline spinal cord white matter I. The nodes of Ranvier. *Acta Physiologica Scandinavica* (suppl. 364), 81-109.
- Hildebrand, C. and Aldskogius, H. (1976) Electron microscopic identification of Marchi positive bodies and argyrophilic granules in the spinal cord white matter of the guinea pig. *Journal of Comparative Neurology* 170, 191-204.
- Hildebrand, C. and Skoglund, S. (1971) Histochemical studies of adult and developing feline spinal cord white matter. *Acta Physiologica Scandinavica* (suppl. 364), 145-73.
- Holtzman, E. and Novikoff, A.B. (1965) Lysosomes in the rat sciatic nerve following crush. *Journal of Cell Biology* 27, 551-69.
- Koles, Z.J. and Rasminsky, M. (1972) A computer simulation of conduction in demyelinated nerve fibres. *The Journal of Physiology* 237, 351-64.
- Mellström, A. (1971) Postnatal motoneuron size and excitability changes in the cat. Thesis, Karolinska Institutet, Stockholm, Sweden.
- Münster, J. (1972) Communication disorders. In *Pathology of the Nervous system* (edited by Münster, J.) 3 pp. 2581-3. New York: McGraw-Hill Book Company.
- Natanf, E.J.H. and Pease, D.C. (1963) Collagen and basement membrane formation by Schwann cells during nerve regeneration. *Journal of Ultrastructure Research* 9, 550-60.
- Nyström, B. (1968) Postnatal, structural and functional development in the efferent neuromuscular system of the cat. Thesis, Karolinska Institutet, Stockholm, Sweden.
- Ronnevi, L.-O. (1976) On spontaneous postnatal elimination of boutons from cat spinal motoneurons. An electron microscopical study. Thesis, Karolinska Institutet, Stockholm, Sweden.
- Ryter, A. and Kellenberger, E. (1968) Inclusion au polyester pour l'ultramicrotomie. *Journal of Ultrastructure Research* 2, 200-14.
- Schwiler, G.H. (1967) Respiratory regulations during postnatal development in cats and rabbits and some of its morphological substrates. Thesis, Karolinska Institutet, Stockholm, Sweden.
- Singer, I. and Münster, E. (1888) Beiträge zur Kenntnis der Gehirnverkreuzung. *Denkschriften der Kaiserlichen Akademie der Wissenschaften Mathematisch-Naturwissenschaftliche Klasse* 58, 163-82.
- Skoglund, S. (1969) On the postnatal development of postural reflexes as revealed by electromyography and myography in decerebrate kittens. *Acta Physiologica Scandinavica* 49, 299-317.
- Skoglund, S. (1969b) The spinal transmission of proprioceptive reflexes and the postnatal development of conduction velocity in different hindlimb nerves in the kitten. *Acta Physiologica Scandinavica* 49, 315-29.
- Skoglund, S. (1969c) The activity of muscle receptors in the kitten. *Acta Physiologica Scandinavica* 50, 203-21.
- Skoglund, S. (1969d) Central connections and functions of muscle nerves in the kitten. *Acta Physiologica Scandinavica* 50, 222-37.
- Skoglund, S. (1969e) The reaction to tetanic stimulation of the two-neuron arc in the kitten. *Acta Physiologica Scandinavica* 50, 238-53.
- Skoglund, S. (1969f) Muscle afferents and motor control in the kitten. In *Muscle Afferents and Motor Control* (Edited by Granit, R.) pp. 245-59. Stockholm: Almqvist and Wiksell.
- Skoglund, S. and Romner, C. (1965) Postnatal growth of spinal nerves and roots. A morphological study in the cat with physiological correlations. *Acta Physiologica Scandinavica* 66 (suppl. 200).
- Sturrock, R.R. (1974) Histogenesis of the anterior limb of the anterior commissure of the mouse brain. III. An electron microscopic study of gliogenesis. *Journal of Anatomy* 117, 37-63.

- Tarlov LM. (1937) Structure of the nerve root. II Differentiation of sensory from motor roots; Observations on identification of function in roots of mixed cranial nerves. *Archives of Neurology and Psychiatry* 37 1338-55
- Thomas, P.K. (1963) The connective tissue of peripheral nerve: an electron microscopic study *Journal of Anatomy* 97 35-44
- Thomas, P.K. (1966) The cellular response to nerve injury. 1 The cellular outgrowth from the distal stump of transected nerve. *Journal of Anatomy* 100 287-303.
- Weinberg H.J. and Spencer P.S. (1976) Studies on the control of myelinogenesis. I. Myelination of regenerating axons after entry into a foreign unmyelinated nerve. *Journal of Neurocytology* 4, 393-418
- Wilson, V.J. (1962) Reflex transmission in the kitten. *The Journal of Neurophysiology* 25 265-75.

LEGENDS TO FIGURES

Abbreviations used in figures and legends.

A	astrocyte
BN	borderline node
C	central nervous fibre
CNS	central nervous system
CZ	core zone
MZ	mantle zone
P	peripheral nervous fibre
PNS	peripheral nervous system
N	node of Ranvier
SC	spinal cord

All pictures are light-micrographs of longitudinal sections through the 8 dorsal root-spinal cord junction. Figs. 1-7 are obtained from toluidine-blue-stained semi-thin section of Vestopal-embedded specimens. In Figs. 1, 2, 4, 6 the solid line indicates the plane of rootlet-spinal cord junction and the hatched line the PNS-CNS borderline. In Figs. 3, 5, 7 the CNS is in the upper part of the pictures.

Fig. 1 Adult cat CNS tissue protrudes like a cone from the dorsal rootlet-spinal cord junction into the proximal part of the rootlet. This part of the rootlet, where PNS and CNS tissue occur side by side is denoted the transitional region (TR). The CNS compartment of the TR (CNS) consists of core zone (CZ) surrounded by the mantle zone (MZ) rich in astrocytes. The nerve fibres pass from the PNS to the CNS type of organization through borderline nodes situated at the outer aspect of the mantle zone ($\times 200$).

Fig. 2 Newborn kitten. PNS fibres with distinct myelin sheaths together with an abundance of cellular profiles of various kinds are noted at the rootlet-spinal cord junction. The PNS-CNS borderline is situated at the surface of the spinal cord ($\times 450$).

Fig. 3 Same specimen as in Fig. 2. A myelinated fibre of PNS type (P) is unmyelinated in the CNS (C) ($\times 1400$).

Fig. 4 One-week-old kitten. The CNS tissue bulges out into the proximal part of the rootlet. The central myelinated fibres have thinner myelin sheaths than the peripheral myelinated ones ($\times 450$).

Fig. 5 Same specimen as in Fig. 4. A very short internode of PNS type containing a highly complex and tortuous myelin sheath is situated at the PNS-CNS borderline ($\times 1100$).

Fig. 6 One-month-old kitten. CNS fibres project like a cone from the rootlet-spinal cord junction into the proximal part of the root. The PNS and CNS fibres appear with about evenly thick myelin sheaths ($\times 450$).

Fig. 7 Same specimen as in Fig. 6. A thin bundle of CNS-fibres projects into the PNS compartment. The PNS and CNS myelinated parts of the fibres meet at borderline nodes of Ranvier (arrows). An astrocyte nucleus is found in the upper left corner ($\times 1100$).

Fig. 8 Adult cat. Specimen treated with 0.25% OsO₄ after glutaraldehyde fixation. Spinal cord to the left. The dotted line indicates the PNS-CNS borderline. The CNS compartment (CNS) is stained lighter than the PNS compartment (PNS). No Marchi-positive material is observed (cf. Fig. 9) ($\times 200$).

Fig. 9 Adult cat. Marchi method. There are many Marchi positive bodies in the mantle zone and they mark out the PNS-CNS borderline ($\times 200$).

Fig. 10 Adult cat. Marchi method. Two Marchi positive bodies are situated in the central paranodal region close to the borderline node (BN) ($\times 1100$).

Fig. 11 Adult cat. Marchi method. A Marchi positive body is situated close to the borderline node (BN) ($\times 2200$).

Fig. 12 Eight-day-old kitten. OTAN method. A high occurrence of Marchi positive bodies and Marchi positive granules is observed just distally to the PNS-CNS borderline ($\times 1100$).

Fig. 13 Ten-day-old kitten. OTAN method. Marchi positive bodies are seen in two complex paranodes distal to the borderline nodes (BN) ($\times 1100$).

Fig. 14 Twelve-day-old kitten. OTAN method. A very short internode situated distally to the borderline node (BN) is filled with Marchi positive bodies and Marchi positive granules ($\times 1200$).

Fig. 15 Adult cat. Gomori method. Two PNS paranodes at the PNS-CNS borderline contain ring and crescent like accumulations of reaction product. An accumulation of dark material (false activity) is seen in the axon of the uppermost borderline node (BN) ($\times 1500$).

Fig. 16 Adult cat. Ring and crescent-shaped accumulations of precipitate (arrows) occur outside bodies of the same texture as myelin, e.g. myelinoid bodies at the CNS paranodes proximally to the PNS-CNS borderline ($\times 1300$).

Fig. 17 Newborn kitten. There is a high occurrence of granules and bodies in the PNS compartment of the TR ($\times 1500$).

Fig. 18 Ten-day-old kitten. Ring-like accumulations of precipitate (arrows) are situated in complex paranode close to the borderline node (BN) ($\times 1400$).

Fig. 19 Twelve-day-old kitten. Ring and crescent-shaped accumulations of precipitate are present in a very short internode situated close to the borderline node (BN) ($\times 1400$).

Figures at the end of this volume

Running title: Development of the transitional region

Figures

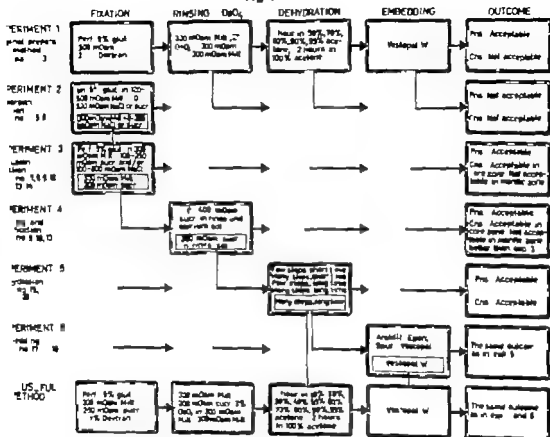
Figures to I

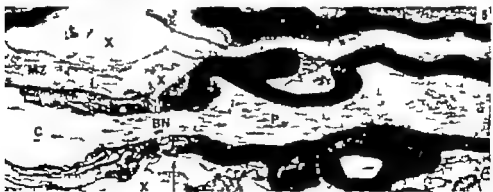
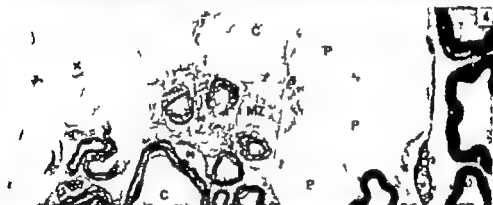
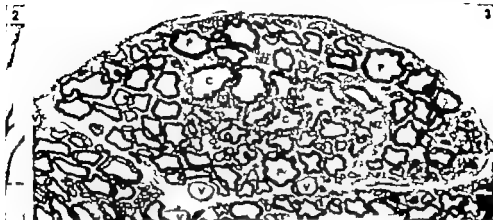
Observations on the morphology at the transition between the peripheral and the central nervous system in the cat. I. A preparative procedure useful for electron microscopy of the lumbosacral dorsal rootlets

Running title EM preparation of the transitional region

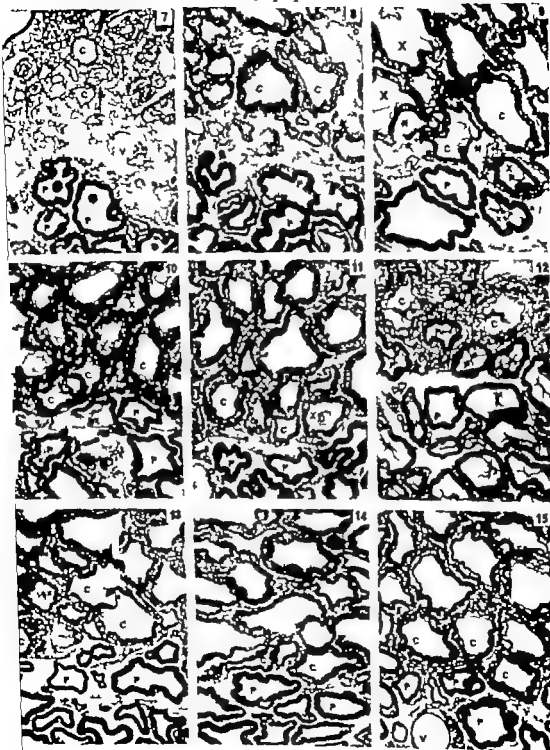
EM preparation of the transitional region

Fig 1

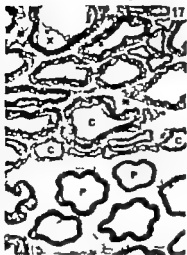


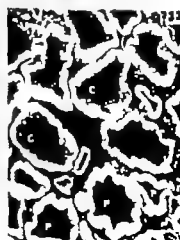
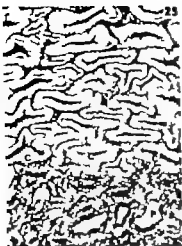


EM preparation of the transitional region



EM preparation of the transitional region





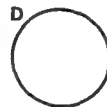
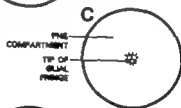
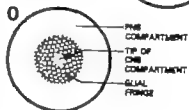
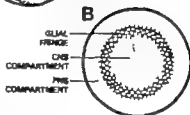
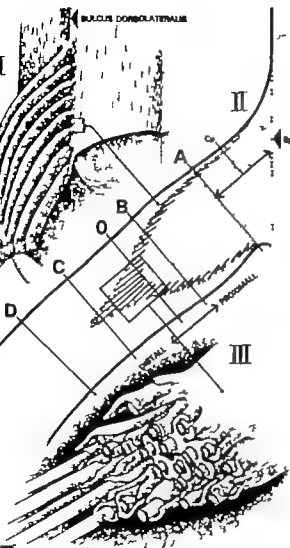
Figures to II

Observations on the morphology at the transition between the peripheral and the central nervous system in the cat. II General organization of the transitional region in S₁ dorsal rootlets

Running title General organization of the transitional region

General organization of the transitional region

Fig.1



General organization of the transitional region

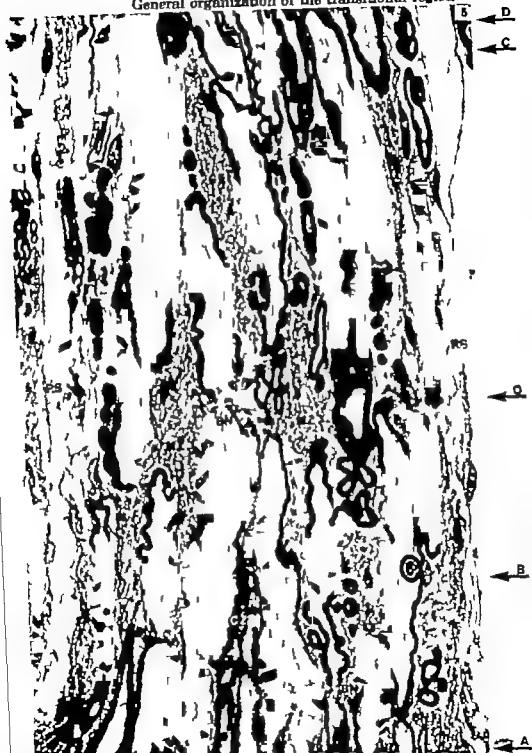
2



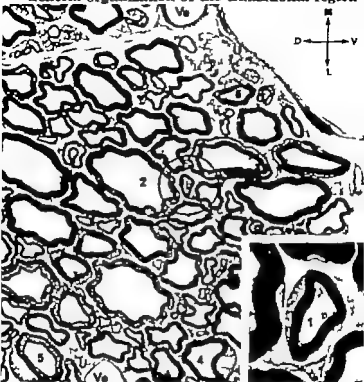
4a

14b

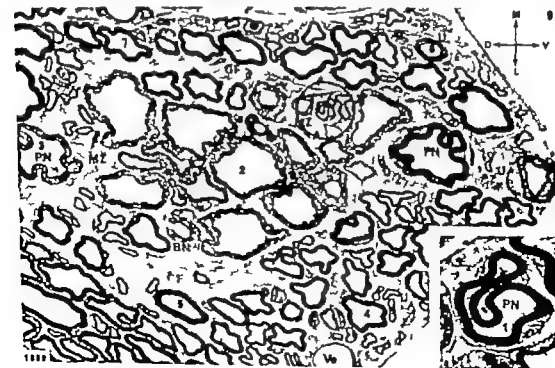
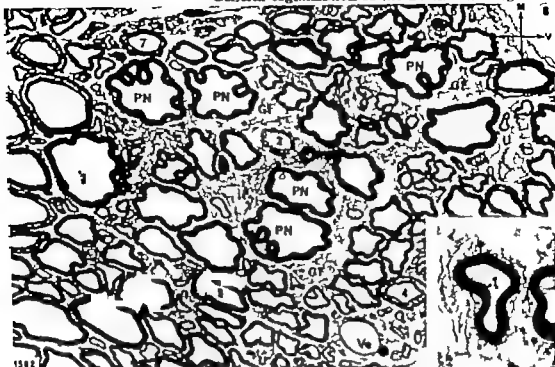
General organization of the transitional region

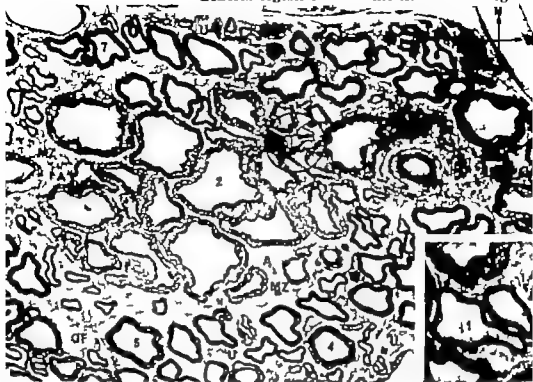


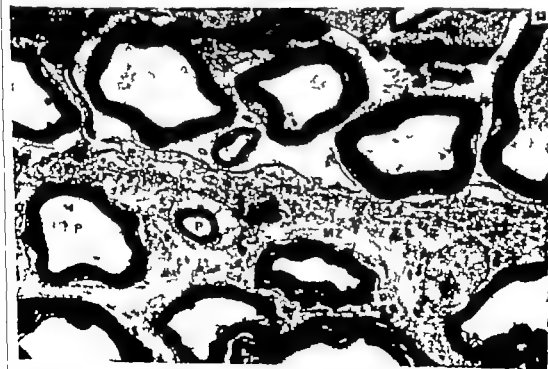
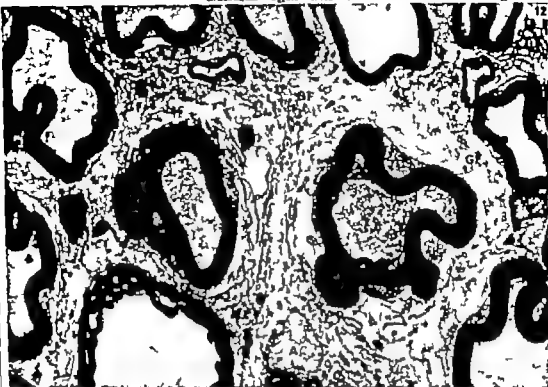
General organization of the transitional region



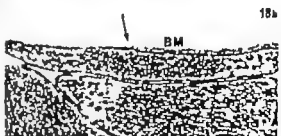
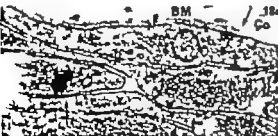
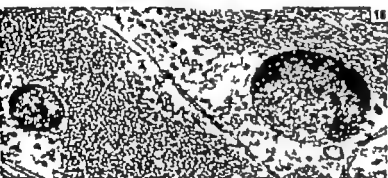
General organization of the transitional region

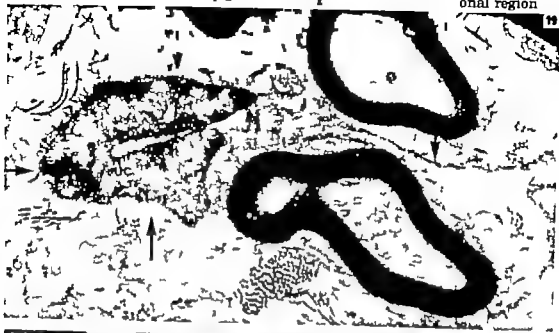






General organization of the transitional region



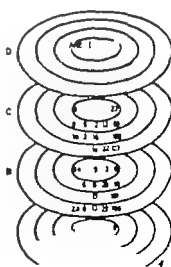
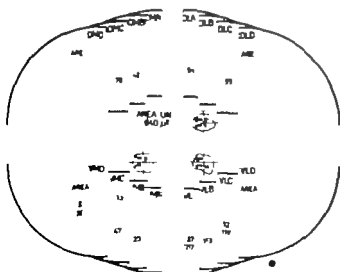
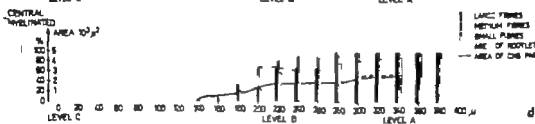
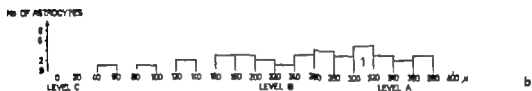


General organization of the transitional region

Fig 21

ROOTLET 1

FIBROBLAST
MICROBLAST
SCHWANN CELL MYELINATED FIBRE
SCHWANN CELL UNMYELINATED AXON
UNCLASSIFIED CELL
PORECYTE



General organization of the transitional region

Fig 22
ROOTLET 2

PERIOBLAST
MIDTLE
SCHWANN CELL MYELINATED FIBRE
SCHWANN CELL UNMYELINATED FIBRE
UNCLASSIFIED CELL
PERICYTE

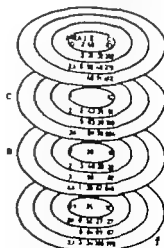
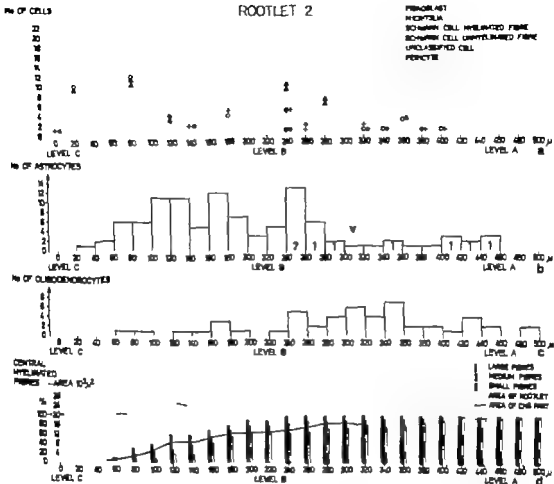
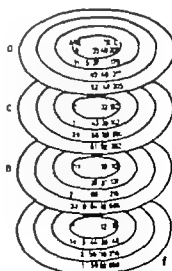
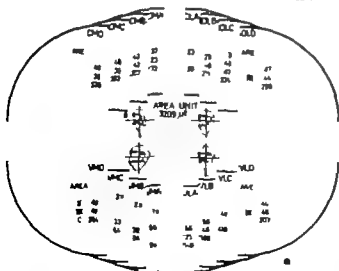
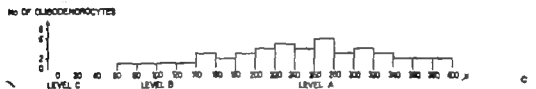
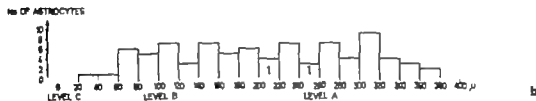


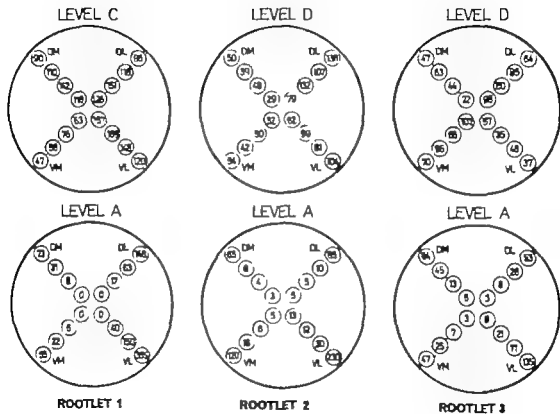
Fig. 23
ROOTLET 3

FIGURE 23
MICROGLIA
SCHWANN CELL MYELINATED FIBRE
BETWEEN CELL UNMYELINATED FIBRE
UNCLASSIFIED CELL
PERICYTE



General organization of the transitional region

Fig 24



Figures to III

Observations on the morphology at the transition between the peripheral and the central nervous system in the cat. III Myelinated fibres in S_1 dorsal rootlets

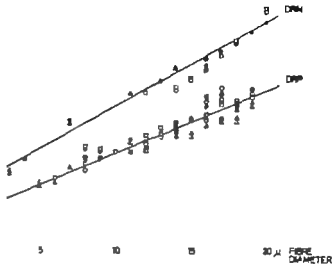
Running title Myelinated fibres in the transitional region

Myelinated fibres in the transitional region

Fig.1

INTERODAL LENGTH

μ
1500
1400
1300
1200
1100
1000
900
800
700
600
500
400
300
200
100



Myelinated fibres in the transitional region

Fig 2

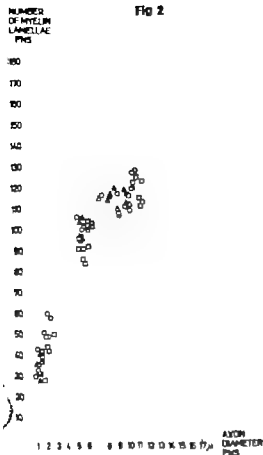
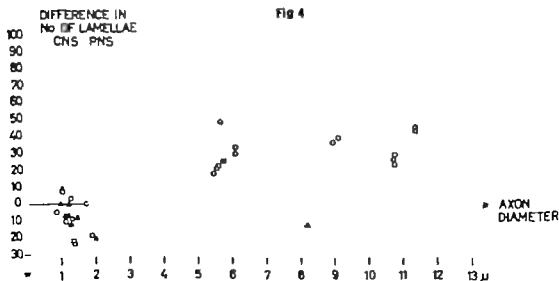


Fig. 3



Fig 4



Myelinated fibres in the transitional region

Fig. 5

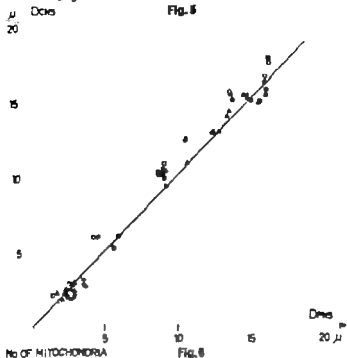
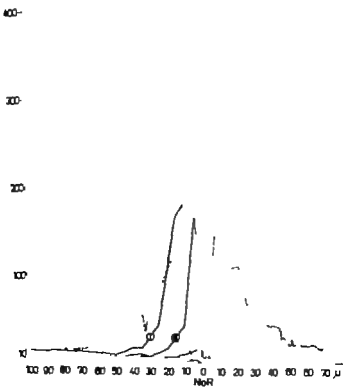
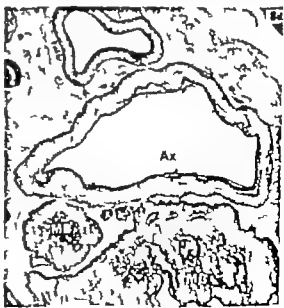
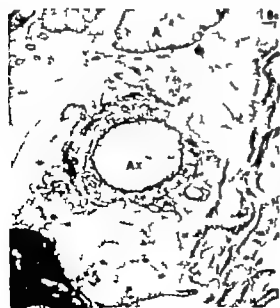


Fig. 6



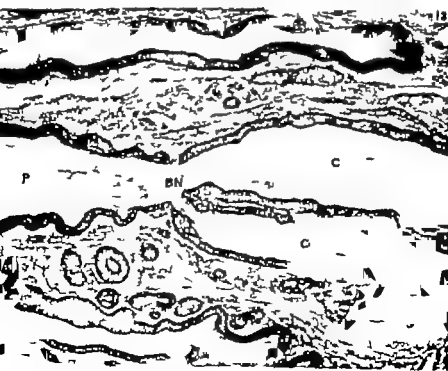


Myelinated fibres in the transitional region



Myelinated fibres in the transitional region





Myelinated fibres in the transitional region



Figures to IV

Observations on the morphology at the transition between the peripheral and the central nervous system in the cat. IV Unmyelinated fibres in S₁ dorsal rootlets

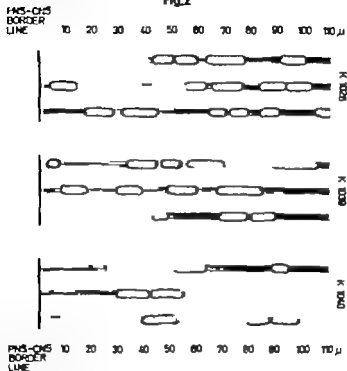
Running title. Unmyelinated fibres in the transitional region

Unmyelinated fibres in the transitional region

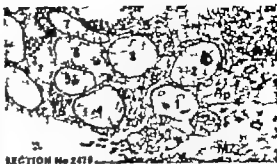
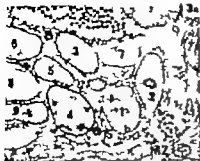


Unmyelinated fibres in the transitional region

Fig.2



Unmyelinated fibres in the transitional region



SECTION No 2479



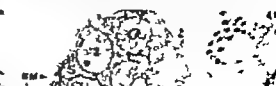
SECTION No 2773



SECTION No 188 E-10

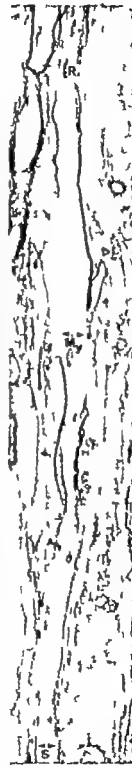


SECTION No 375

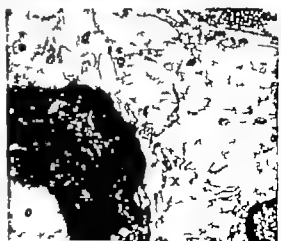
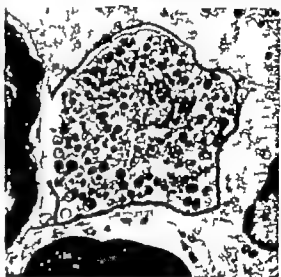


SECTION No 375

Unmyelinated fibres in the transitional region



Unmyelinated fibres in the transitional region

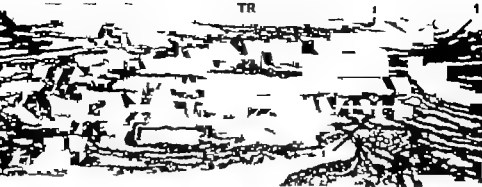


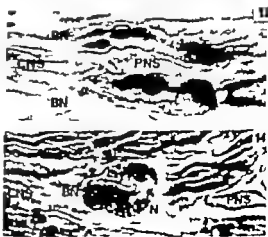
Figures to V

Observations on the morphology at the transition between the peripheral and the central nervous system in the cat. V A light microscopical and histochemical study of S₁ dorsal rootlets in developing kittens

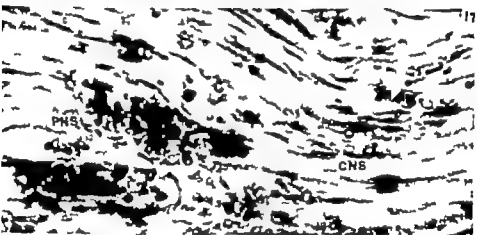
Running title: Development of the transitional region

Development of the transitional region
TR





Development of the transitional region



ACTA PHYSIOLOGICA SCANDINAVICA
Supplement 40

Glomerulotubular balance in the rat kidney

by

Kenneth Steven

Institute of Medical Physiology
Dept. A
University of Copenhagen
Denmark



LEO E. SKOVENINGENS FORLAG

Forsvaret finder sted torsdag den 26. maj 1977 kl. 14
precis i Annexauditorium A, Studiestræde 6 og,
København.

ACTA PHYSIOLOGICA SCANDINAVICA
Supplement 447

Glomerulotubular balance in the rat kidney

*Forsvaret finder sted torsdag den 26. maj 1977 kl. 14
præcis i Annexauditorium A, Studiestræde 6 og,
København.*

To Gunilla ■

SUMMARY OF INVESTIGATIONS

The present study was designed to increase our knowledge of certain aspects of glomerulotubular balance.

1 The relationship between serum protein concentration and colloid osmotic pressure was measured in the rat and found to be in complete agreement with the Landis-Pappenheimer formula derived from measurements made with human plasma. Establishment of the validity of this formula permitted further calculations to be made.

2 A mathematical analysis of the hydrodynamics of the renal corpuscle was used to quantify under steady state conditions, the influence of changes in the following variables on glomerular filtration rate, nephron blood flow and on hydrostatic pressure in the glomerular capillaries

- I arterial haematocrit and plasma protein concentration,
- II hydrodynamic resistance of both the afferent and efferent arterioles
- III ultrafiltration coefficient of the glomerular membrane;
- IV hydrostatic pressure in the proximal tubule
- V hydrostatic pressure in the peritubular capillaries;
- VI arterial blood pressure.

Nephron GFR was predicted to be very sensitive to the concentration of arterial plasma protein. The calculated change in glomerular capillary pressure accompanying a decrease in nephron GFR caused by either an increase in the afferent or decrease in the efferent arteriolar resistance to blood flow agreed with experimentally obtained values. The effect on nephron GFR of changing the hydrostatic pressure in the proximal tubule was calculated and found to agree with the experimental measurements described below

3. The influence of intratubular flow rate on rate of proximal fluid reabsorption (RPFR) was studied using free flow micropuncture techniques. By introducing a small decrease in proximal tubular hydrostatic pressure, nephron GFR was increased. The resulting increase in tubular flow rate was not accompanied by any change in RPFR.

4. The function of proximal convoluted tubules was studied after infusion of angiotensin II into adjacent peritubular capillaries. Infusion of angiotensin II resulted in a substantial reduction in RPFR which was associated with a significant increase in hydrostatic pressure in both the adjacent proximal tubules and the infused capillaries.

5. Similar peritubular infusion experiments were carried out using an antagonist to angiotensin II. The results of these experiments indicated that angiotensin II is a physiological regulator of hydrostatic pressure in the proximal tubule and the peritubular capillaries. No evidence was found of a tonic influence of angiotensin II on RPFR.

GLOMERULOTUBULAR BALANCE IN THE RAT KIDNEY

A nearly constant ratio has been measured between the glomerular filtration rate (GFR) and the rate of fluid reabsorption in the proximal tubule (RPFR), despite the occurrence of large variations in GFR. This ratio, usually termed glomerulotubular balance, remains almost constant regardless of whether the changes in GFR and RPFR occur spontaneously in different nephrons of the same rat or are induced in the same nephron by aortic constriction, renal venous constriction or ureteral obstruction (1, 2, 3, 4, 5). The spontaneous tubule to tubule variations in GFR and RPFR do not, therefore, appear to be caused by differences in glomerular size and tubule length. Furthermore, the hydrostatic pressure in the proximal tubule generally varies very little regardless of large variations in GFR (6, 7, 8, 9, 10, 11).

Accordingly evaluation of the physiological mechanism of glomerulotubular balance requires an examination of the variables influencing GFR, RPFR and hydrostatic pressure in the proximal tubule. For this purpose, it is instructive to make a mathematical analysis of the hydrodynamics of nephron function, and to compare predicted values with experimental results.

Hydrodynamics of nephron function

The decreases in hydrostatic pressure along the proximal and distal tubules are very small (6, 12, 13, 14, 15) leaving only three effective sources of resistance to flow in each nephron:

glomerular resistance; loop of Henle resistance; and collecting duct resistance. For the total number of nephrons within the kidney each of these three resistances is connected in parallel. By analogy with the vascular system, the nephrons within the kidney may logically be regarded as comprising a branched tubular system with respect to their hydrodynamic characteristics. Mathematical analysis may then be simplified by

the concept of »the equivalent« nephron: a hypothetical single nephron which has the same hydrodynamic characteristics as the entire population of nephrons within the kidney

For the equivalent nephron, the pressure head which drives fluid against the nephron resistance, i.e. the glomerular propulsive pressure (16), is equal to the difference between the mean hydrostatic pressure in the glomerular capillaries (less the mean glomerular oncotic pressure) and the pelvic hydrostatic pressure. Equivalent glomerular resistance is found by dividing the glomerular resistance of the single nephron by the total number of nephrons within the kidney approximately 30,000 in the rat (17-18). Equivalent Henle loop resistance is obtained similarly. Collecting duct resistance has been shown to be located mainly in the terminal collecting duct (19, 20). Assuming that the collecting duct resistance is exclusively terminal, an approximate value for the equivalent collecting duct resistance is given by dividing the resistance of the single collecting duct by the number of terminal collecting ducts in the kidney approximately 20 in the rat (18).

Insofar as all nephrons are assumed to function in an identical manner these calculations involve oversimplification. But they do provide an appropriate first approximation as indicated by the recent finding that the hydrostatic pressure in the loop of Henle of the juxtamedullary rat nephron is similar to that of the superficial nephron (19).

From experimental measurements in the hydropenic rat (6, 13, 19-21, 22, 23, 24-25, 26), the following values may be derived. equivalent glomerular resistance 5×10^{-6} mm Hg ml⁻¹ min; loop of Henle resistance 15×10^{-6} mm Hg ml⁻¹ min; collecting duct resistance 700×10^{-6} mm Hg ml⁻¹ min. The hydrodynamic resistance of the glomerular membrane is thus very small compared with distal tubular resistance.

An increase in GFR is known to increase the urine flow rate, but the percentage of additional filtered fluid reabsorbed will be smaller than the percentage of fluid reabsorbed previously. Taking this finding together with the calculated distribution of hydrodynamic resist-

ance within the nephron gives the equivalent nephron definite characteristics (16, 27-28). Hydrostatic pressure in the proximal tubule will be relatively insensitive to changes in RPF_R but will be markedly affected by the most modest perturbations in the glomerular propulsive pressure. Conversely GFR may be considerably changed by quite small alterations in RPF_R while being very insensitive to changes in glomerular propulsive pressure. Any reduction in the tubular resistance will lead to a considerable increase in GFR and urine flow.

An increase in RPF_R will result in an almost identical increase in GFR, because the hydrostatic pressure required to drive an additional quantity of fluid across only the glomerular membrane is negligible in comparison with the pressure that would be required to drive a similar quantity of fluid across the resistance of the entire nephron. It follows that the flow of fluid which overcomes the total nephron resistance, i.e. the urine flow rate, and the hydrostatic pressure in the proximal tubule will be only slightly affected by changes in RPF_R. Even if dramatic changes are induced in RPF_R, the effect on the proximal intratubular pressure will be negligible.

Increasing the glomerular propulsive pressure will increase GFR and urine flow rate, but only a small proportion of the additional fluid filtered will be reabsorbed in the tubules. A large part of the additional fluid filtered must consequently overcome the entire nephron resistance, which is much greater than the average resistance to fluid being reabsorbed. Accordingly the increment in glomerular propulsive pressure required to induce an increment of 1 ml min^{-1} in GFR will be greatly in excess of the unit pressure head previously required, i.e. a given percentage increase in glomerular propulsive pressure results in a much smaller percentage increase in GFR. The increase in hydrostatic pressure in the proximal tubule will be almost as much as the rise in glomerular propulsive pressure, since nephron resistance derives mainly from the distal part of the nephron.

One may conclude that glomerulotubular balance — the nearly constant ratio found to exist between GFR

and RPFR — merely expresses the fact that GFR cannot change significantly unless some alteration occurs in RPFR, assuming tubular resistance to be constant.

Comparison of predicted values with experimental results

Experiments have shown that decreasing the arterial blood pressure below the level of renal autoregulation in the hydropenic rat results in a reduction in the glomerular capillary pressure (9 11 29). This reduction was associated with decreased renal blood flow and hence a reduced glomerular propulsive pressure in the superficial nephron (9 11 29). The percentage decrease in glomerular capillary pressure was considerably smaller than the concurrent reduction in arterial blood pressure (9 11 29). Hydrostatic pressure in the proximal tubule remained almost constant (7 9 11 29). Accordingly a substantial reduction in nephron GFR was recorded (9 29), and RPFR decreased in proportion to the reduction in nephron GFR (29, 30, 31). Hydrostatic pressure in the distal tubule decreased and there was a substantial increase in the collecting duct resistance (7).

EVALUATION OF INTRATUBULAR PRESSURE

Stabilization of the hydrostatic pressure in the proximal tubule must involve changes either in the glomerular propulsive pressure or in the tubular resistance, since the foregoing analysis of nephron hydrodynamics shows that changes in RPFR will only have a very small effect on intratubular pressure. Thus the near constant proximal intratubular pressure observed during aortic constriction, despite a substantial decrease in glomerular propulsive pressure, must have resulted from an increase in tubular resistance. Stabilization of the hydrostatic pressure in the proximal tubule by this mechanism results in a substantial decrease in the flow rate to the distal tubule and in the urine flow rate. These events lead to a reduced loss of body fluid and may serve to maintain the extracellular fluid volume during hypotension. Conversely the decrease in tubular

resistance observed during salt loading (20, 24) may increase sodium and water excretion and restore fluid homeostasis.

Stabilization of the proximal intratubular pressure results mainly from changes in collecting duct resistance, since the resistance of the loop of Henle constitutes only a small part of the tubular resistance. The mechanism proposed for stabilizing the intratubular pressure requires that the tubular resistance is very sensitive to the transmural hydrostatic pressure gradient. The loop of Henle and the collecting duct have a resistance to flow which has been shown to be very sensitive to the intratubular pressure within the physiological range of transmural pressures. These experiments have involved *in vitro* measurements of pressure, flow rate and tubular diameter relationships in thin descending limbs of Henle (32), *in vivo* recordings of pressure and flow in perfused superficial loops of Henle (25, 26), and pressure measurements in the distal tubule and the inner medulla under free flow conditions (20).

Hydrostatic pressure in the proximal tubule during aortic constriction is therefore stabilized mainly by an increase in the tubular resistance. Additionally the results of several studies provide evidence for the existence of a mechanism regulating glomerular propulsive pressure that involves an intrarenal feedback mechanism which stabilizes the supply rate of sodium chloride to the distal tubule. The juxtaglomerular apparatus, having both vascular and tubular constituents, is well disposed to play a role in such a feedback mechanism for compensatory adjustments between glomerular and tubular functions (33, 34, 35). Renin in the juxtaglomerular apparatus could serve to mediate these adjustments with renin activity determining the local formation rate of the potent vasoconstrictor angiotensin II (7, 36, 37, 38, 39, 40, 41). Angiotensin II might control the glomerular propulsive pressure (7, 36, 37, 38, 39, 40, 41, 42, 43) and so stabilize the flow rate to the distal tubule.

Evidence for the existence of this feedback mechanism derives from experiments in which the loop of Henle of the superficial nephron was perfused with a

capillaries (59) (paper V). An angiotensin II antagonist was infused into the peritubular capillaries and hydrostatic pressure was measured both in the infused capillaries and the adjacent proximal tubules. Infusion of this antagonist produced a decrease in hydrostatic pressure in both the capillaries and the proximal tubules; the most striking fall occurred in rats with relatively high levels of plasma renin activity (PRA).

Summary

The increase in tubular resistance accompanying a reduction in arterial blood pressure below the level of renal autoregulation decreases renal fluid excretion and may serve to maintain the extracellular fluid volume. The decrease in tubular resistance associated with extracellular volume expansion may contribute to the maintenance of body fluid homeostasis. Glomerular propulsive pressure has been shown to be regulated by an intrarenal feedback mechanism. This mechanism is capable of depressing the glomerular propulsive pressure when the flow rate to Henle's loop is increased above that of normal but produces no change when the flow rate is reduced below normal. Feedback response is lowered during expansion of the extracellular fluid volume. The feedback mechanism appears to prevent over-elevation of the flow rate in relation to the reabsorptive capacity of the distal tubule and collecting duct hence potentially dangerous losses of salt and water are prevented. For example, circulatory changes during feeding and muscular activity may be expected to change the glomerular propulsive pressure with the result that flow rate to the distal tubule increases. In addition, the intratubular pressure change accompanying increased glomerular propulsive pressure may possibly lead to a reduction in tubular resistance, producing a further increase in fluid excretion.

EVALUATION OF RPFR

The observed decrease in RPFR accompanying the reduced GFR during aortic constriction might be either a direct consequence of decreased GFR or related to changes in the peritubular concentration of some

humoral substance. A slight reduction in GFR might possibly induce a decrease in RPFR, which in turn would result in a further reduction in GFR, i.e. a positive feedback loop. Such an induced decrease in RPFR might be a consequence of an intrinsic or extrinsic tubular mechanism.

INFLUENCE OF TUBULAR FLUID FLOW RATE ON RPFR

The influence of flow rate on RPFR has been examined in several studies employing *in vivo* and *in vitro* pump perfusion of individual segments of proximal convoluted tubules. Most of these studies have shown very little or no influence of perfusion rate on RPFR (60, 61, 62, 63).

Nevertheless, a carefully executed study using plasma ultrafiltrate as perfusion fluid, showed that a 40 per cent decrease in perfusion rate produced a 17 per cent decrease in RPFR (64). In another study aspirating fluid at an early proximal site reduced the flow rate without influencing nephron GFR (65). A 45 per cent reduction in flow rate of tubular fluid was associated with an average reduction of 29 per cent in RPFR. On the other hand, aortic constriction sufficient to decrease the filtration rate by 50 per cent has been shown to reduce RPFR by 50 per cent in pump perfused segments of proximal tubules perfused at a constant flow rate throughout (66). Furthermore, another study (10) (Paper III) indicates that an increase in nephron GFR induced by a decrease in hydrostatic pressure in the proximal tubule does not change RPFR.

Although these results are inconsistent with respect to the magnitude of the change in RPFR induced, they do indicate that a change in the flow rate of tubular fluid is associated with a significant change in the fractional reabsorption of tubular fluid in the proximal tubule. Accordingly changes in the intratubular flow rate alone appear unlikely to account for the balance between filtration rate and proximal reabsorption observed during aortic constriction.

An increase in GFR could conceivably alter RPFR by changing the filtered amount of glucose, amino acids

and bicarbonate, since a proportion of the tubular sodium reabsorption is known to be coupled to the transport of these solutes (67, 68, 69, 70, 71, 72, 73, 74, 75, 76). The concentrations of organic solutes in the ultrafiltrate are low so that only bicarbonate may significantly affect the reabsorption of fluid under physiological conditions.

A mathematical analysis of flow through folded membrane structures has shown that the degree of stirring within the folds may affect the solute concentration profiles within the folds, resulting in altered solute flow through the membrane (77). An increase in the flow rate of tubular fluid has been proposed to increase mixing of the unstirred diffusion barrier within the crypts between the microvilli (65). This mixing might in turn augment the sodium concentration in the diffusion barrier and enhance sodium diffusion into the cells, with the result that sodium reabsorption increases. This theory is fundamentally similar to that of Ketman (78) who suggested that RPFR is proportional to the flow rate of tubular fluid.

EFFECT OF PROTEIN COLLOID OSMOTIC PRESSURE ON RPFR

A decrease in GFR might cause RPFR to decrease under the influence of a mechanism extrinsic to the tubule, for instance, by reducing the peritubular protein concentration. Experiments indicate that aortic constriction reduces the filtration fraction in the superficial rat nephron (9, 29, 79); this will reduce the protein concentration and hence the plasma colloid osmotic pressure in the efferent arteriole.

The influence of colloid osmotic pressure on RPFR has been studied extensively employing both in vitro and in vivo micropuncture techniques. In vitro studies using microperfused fragments of rabbit proximal convoluted tubules have shown that changes in the ambient protein colloid osmotic pressure exert a marked effect on RPFR even when the capillary network is absent (80, 81, 82). This interpretation has been challenged by the results of a similar in vitro microperfusion study which suggested that the effect

on RPFR ascribed to the protein colloid osmotic effect per se was actually caused by unidentified protein accelerators and inhibitors of tubular fluid transport (83).

In vivo studies have been carried out employing either intraluminal application or perfusion of the peritubular capillaries with solutions of differing colloid osmotic pressure. In the first type of experiments RPFR was derived from pump perfusion of tubular segments (84). An effective hydraulic conductivity L_p of $0.05 \text{ nl min}^{-1} \text{ mm tubule length}^{-1} \text{ mm Hg}^{-1}$ was recorded in these experiments.

In the experiments with peritubular perfusion, RPFR in the adjacent proximal convoluted tubules was derived from simultaneous pump perfusion of individual tubular segments (85) from recordings of the t value for the disappearance of a droplet of saline splitting an oil column within the tubule (shrinking droplet technique) (86, 87) or from timed quantitative collections of fluid from the end of the proximal convolution (88, 89, 90, 91).

A change in RPFR of $0.03 \text{ nl min}^{-1} \text{ tubule length}^{-1} \text{ mm Hg}^{-1}$ was found from experiments in which RPFR was estimated by simultaneous tubular microperfusion or by the shrinking droplet technique (85, 86, 87).

The experiments involving peritubular capillary microperfusion and simultaneous fluid collection from the end of the proximal convolution have given inconsistent results (88, 89, 90, 91). Brenner et al found an increase in RPFR of about $0.05 \text{ nl min}^{-1} \text{ mm tubule length}^{-1} \text{ mm Hg}^{-1}$ when the peritubular capillary protein concentration was increased above the control level by vascular microperfusion during aortic constriction (89). According to this study approximately 40 per cent of the decrease in RPFR observed during aortic constriction could be attributed to the associated reduction in peritubular protein concentration. In contrast, Conger et al (88) found RPFR unaffected by varying the peritubular protein concentration between zero and 13 g %.

Similar absence of response was obtained in another carefully executed study (90, 91) nephron GFR

and RPFR were recorded in the same tubules, before and during aortic constriction, employing the recollection micropuncture technique. In one group of nephrons, the peritubular capillary flow rate and protein concentration was kept constant by vascular microperfusion prior to and during aortic constriction. Recordings from these tubules were compared with those obtained from control tubules without vascular microperfusion in which peritubular flow rate and protein concentration were allowed to change. Similar changes in nephron GFR and RPFR were induced in both groups of tubules, suggesting that intraluminal factors mediate the decrease in RPFR during aortic constriction. As mentioned above (page 17) contrasting results have been obtained (66).

Colloid osmotic pressure of efferent arteriolar blood in the superficial rat nephron has been found to decrease by 6 mm Hg associated with a reduction in nephron GFR of 8 nl min^{-1} during aortic constriction, with a decrease in the femoral artery pressure from 120 to 80 mm Hg (9). Given the assumption that the TP/P inulin value of 2.5 was unchanged, RPFR would have decreased by 4.8 nl min^{-1} . With a tubular length of 5 mm and a change in RPFR of $0.05 \text{ nl min}^{-1} \text{ mm tubule length}^{-1} \text{ mm Hg colloid osmotic pressure}^{-1}$ the decrease in efferent arteriolar protein concentration would have resulted in a reduction in RPFR of 1.5 nl min^{-1} which comprises only 31 per cent of the expected decrease in RPFR. Reduction in the peritubular protein concentration therefore appears unlikely to account entirely for the decrease in RPFR during aortic constriction. Nevertheless, the influence of protein colloid osmotic pressure on glomerulotubular balance remains a controversial subject.

EFFECT OF HUMORAL SUBSTANCES ON RPFR

The further possibility exists that the decrease in RPFR associated with aortic constriction is controlled humorally. The diminution in flow rate of tubular fluid to the distal tubule during aortic constriction has been proposed to activate a feedback mechanism resulting in an altered peritubular concentration of a humoral substance

which influences RPFR (3). Angiotensin II has been proposed as a messenger in this feedback mechanism (37). The effect of angiotensin II on RPFR has been the subject of much controversy.

In vivo microperfusion studies have produced evidence against an individual nephron feedback mechanism. Proximal tubules were perfused from an early proximal site and the flow rate to the distal tubule was altered, either by making partial collections of fluid at the end of the proximal convolution (60) or by changing the pump perfusion rate (61). These experiments showed that RPFR in the perfused segments of the proximal tubules did not change when the flow rate to the loop of Henle was altered.

No effect of angiotensin II on RPFR was found during intravenous infusion of subpressor doses of angiotensin II in experiments where the RPFR was determined from timed collections of tubular fluid (92, 93) or by using the shrinking droplet technique (94). Similarly experiments using solutions with very high angiotensin II concentrations administered by intratubular application (94-95) or peritubular perfusion (95) were without effect. Finally RPFR was not affected by angiotensin II in the in vitro perfused proximal tubule (63).

Contrasting results were obtained from experiments in which the occlusion time (the time for complete collapse of the proximal tubular lumen after clamping the renal artery) was used as a measure of RPFR. In these experiments a decrease in RPFR was found after intravenous injections of angiotensin II (96). A marked inhibition of RPFR was also found in a later study employing peritubular infusion with relatively high physiological concentrations of angiotensin II (97) (paper IV). RPFR was derived from timed collections of tubular fluid from the end of the proximal convoluted tubule.

In an attempt to determine whether angiotensin II exerts a tonic influence on RPFR, similar peritubular infusion experiments were carried out with an analogue of angiotensin II L-sarcosine, 8-alanine angiotensin II (59) (paper V). This analogue was found to block the

effect of exogenous angiotensin II on RPFR, but peritubular infusion with the angiotensin II analogue did not increase RPFR. These results fail to provide evidence for a tonic influence of angiotensin II on RPFR.

Summary

The decrease in RPFR during aortic constriction could occur either as a direct consequence of the decrease in GFR or be induced by a humoral substance. A decrease in GFR might influence RPFR by an extrinsic or an intrinsic tubular mechanism. An intrinsic mechanism has been excluded by experiments which demonstrate that altering the flow rate of tubular fluid induces a change in RPFR which is too small to account entirely for the glomerulotubular balance observed during aortic constriction. A mechanism extrinsic to the tubule also appears unlikely to be responsible for glomerulotubular balance: experimental results indicate that the decrease in RPFR caused by a measured reduction in peritubular protein oncotic pressure during aortic constriction is inadequate for this purpose. Angiotensin II has been proposed to mediate changes in RPFR during aortic constriction. Experimental results have not provided evidence of a tonic influence of angiotensin II on RPFR. An as yet unidentified humoral substance may be shown to be responsible for glomerulotubular balance. Alternately glomerulotubular balance may be the result of contributions from all of the above mentioned variables.

Acknowledgements

This study was carried out at the Institute of Medical Physiology A, University of Copenhagen. I wish to express my sincere gratitude to Dr Erik Skadhauge for constant encouragement and for providing excellent working conditions. Thanks to Professor C. Crone, chairman of the institute, for his valuable support.

I wish to thank Professor P. Kruheffer and Professor G. Giebisch, M.D. Yale University New Haven, for many stimulating discussions and much advice.

Thanks to my co-workers Dr S. Ströback, D. Thorpe, M. Sø. and Dr C. Worning for their excellent contributions.

I am especially grateful to my wife Gunilla for expert technical assistance with the micropuncture experiments and to Mrs. Lisa Jessen for skilful technical assistance.

This study was supported by the Danish Medical Research Council, the Danish Foundation for the Advancement of Medical Science, Nordisk Insulin Foundation and J and H. Weimann's legacy.

Copenhagen, May 1976.

References:

1. Walker AM, Bott PA, Oliver J, Mac Dowell MC: The collection and analysis of fluid from single nephrons of the mammalian kidney. *Am J Physiol* 134: 580-595, 1941.
2. Grechich G, Friedberger EE: Renal tubular transfer of sodium, chloride and potassium. *AM J Med* 36: 643-669, 1964.
3. Schermsom J, Wahl M, Lierse G, Flechtbach H: Balance between tubular fluid flow rate and net fluid reabsorption in the proximal convolution in the rat kidney. *Pflügers Arch* 304: 90-103, 1968.
4. Radicio J, Herrera-Acosta J, Salazar JC, Rector FC, Seidus DW: Studies on glomerulotubular balance during aortic constriction, ureteral obstruction and venous occlusion in hydropenic and saline loaded rats. *Nephron* 8: 437-456, 1969.
5. Gertz KH, Boylan J W: Glomerular tubular balance. In: *Handbook of Physiology* Section 8: Renal Physiology. Edited by J. Orloff and RW Berliner. American Physiological Society 1973, pp 763-780.
6. Gottschalk CW, Mylle M: Micropuncture study of pressures in proximal tubules and peritubular capillaries of the rat kidney and their relation to ureteral and renal venous pressures. *Am J Physiol* 185: 430-439, 1956.
7. Leyssac PP: The effect of partial clamping of the renal artery on pressures in the proximal and distal tubules and peritubular capillaries of the rat kidney. *Acta physiol Scand.* 62: 449-456, 1964.

2. Falchek KH, Berliner RW Hydrostatic pressures in peritubular capillaries and tubules in the rat kidney. *Am J Physiol* 220: 1422-1426, 1971.
9. Robertson CR, Deen WM, Troy JL, Brenner BM Dynamics of glomerular ultrafiltration in the rat. III. Hemodynamics and autoregulation. *Am J Physiol* 223: 1191-1200, 1972.
10. Steven K: Influence of nephron GFR on proximal reabsorption in pentobarbital anesthetized rats. *Kidney Int* 5: 204-213, 1974.
11. Kallskog Ö, Lindbom LO, Ulfendahl HR, Wolgast M: The pressure-flow relationship of different nephron populations in the rat. *Acta physiol Scand* 94: 289-300, 1975.
12. Witz H: Die Druckverhältnisse in der normalen Niere. *Schweiz Med Wochr* 88: 377-382, 1956.
13. Gortschak CW, Mylle M: Micropuncture study of pressures in proximal and distal tubules and peritubular capillaries of the rat kidney during osmotic diuretics. *Am J Physiol* 189: 323-328, 1957.
14. Macey R I: Pressure flow patterns in cylinder with reabsorbing walls. *Bull Math Biophys* 25: 1-9, 1963.
15. Macey R I: Hydrodynamics in the renal tubule. *Bull Math Biophys* 27: 117-124, 1965.
16. Kruehler P: Handling of alkali metal ions by the kidney. In: The alkali metal ions in biology. Edited by Ussing H, Kruehler P, Hans Thaysen J, Thore NA. Berlin, Göttingen, Heidelberg, Springer Verlag, 1960, pp 233-423.
17. Ryland DR: The number and size of mammalian glomeruli as related to kidney and body weight with methods for their enumeration and measurements. *Am J Anat* 62: 507-520, 1938.
18. Jamnag RL: Countercurrent systems. In: Kidney and urinary tract physiology. MTP 1:1 Rev Sci, Physiol Series 1, Vol 6, pp 199-243, 1974.
19. Sanyal VM, Johanson PA, Deen WM, Robertson CR, Brenner BM, Jamnag RL: Hydraulic and oncotic pressure measurements in inner medulla of mammalian kidney. *Am J Physiol* 228: 1921-1926, 1975.
20. Marsh DJ, Martin CM: Effects of diuretic states on collecting duct fluid flow resistance in the hamster kidney. *Am J Physiol* 229: 13-17, 1975.
21. Brenner BM, Troy JL, Daugharty TM: Pressures in cortical structures of the rat kidney. *Am J Physiol* 222: 246-251, 1972.
22. Deen WM, Troy JL, Robertson CR, Brenner BM: Dynamics of glomerular ultrafiltration in the rat. IV. Determination of the ultrafiltration coefficient. *J Clin Invest* 52: 1500-1508, 1973.

23. Slonitz RC, Koster FC, Seides DW: Effect of hyperosmotic albumin expansion upon glomerular ultrafiltration in the rat. *Kidney Int* 6: 209-221, 1974.
24. Leyssac PP: Renal salt and water excretion in different states of an intrarenal control system. *Proc Roy Soc Med* 62: 1111-1116, 1969.
25. Schoerman J: Microperfusion study of single short loops of Henle in rat kidney. *Pflügers Arch* 300: 255-282, 1968.
26. Koh YG, Baltes AD: Pressure-flow relationships in Henle's loops and long collapsible rubber tubes. *Kidney Int* 5: 30-36, 1974.
27. Bojarsen E: The renal mechanism of adrenalectomy and salt excretion in dogs. *Acta physiol Scand* 32: 129-147, 1954.
28. Bojarsen E: Den tubulære saltvanderesorption. Christiana Bogtrykkeri, København, Thesis, 1955.
29. Kalkskog Ö, Lindholm LO, Ulfendahl HR, Wolgast M: Kinetics of the glomerular ultrafiltration in the rat kidney. An experimental study. *Acta physiol Scand* 95: 293-300, 1975.
30. Giebisch G, Windhager E E: Electrolyte transport across renal tubular membranes in *Handbook of Physiology* Section 8: Renal Physiology Edited by J. Orloff and RW Berliner. American Physiological Society 1973, pp 315-376.
31. Arrizaola-Machuga ER, Lissiter WE, Liphman EM, Gottschalk CW: Micropuncture study of glomerulotubular balance in the rat kidney. *Nephron* 6: 418-436, 1969.
32. Weisling LW, Weisling DJ: Pressure-flow-diameter relationships in isolated perfused thin limb of Henle. *AM J Physiol* 229: 1-7, 1975.
33. Goormaghtigh N: L'appareil neuro-endo-artériel juxtaglomérulaire du rein; ses réaction en pathologie et ses rapport avec le tube urinaire. *CR Soc Biol (Paris)* 124: 283-296, 1937.
34. Goormaghtigh N: La fonction endocrine des artérioles rénales. *Rev Belge Sc Méd* 16: 85-153, 1943.
35. McManus JFA: Further observations on the glomerular root of the vertebrate kidney. *Quart J Micr Sci* 88: 39-44, 1947.
36. Guyton AC, Langston JR, Naver G: Theory for renal autoregulation by feedback at the juxtaglomerular apparatus. *Circ Res* 14-15, Suppl 1: 187-197, 1984.
37. Leyssac PP: The regulation of proximal tubular reabsorption in the mammalian kidney. *Acta physiol Scand* 70, Suppl. 291: 1-151, 1966.
38. Thomsen K: Fundamentals of renal circulation. *Proc II int Congr Nephrol, Prague, 1963*, pp 51-61.

39. *Thieritz K*: Influence of sodium concentration in macula densa cells on tubular sodium load. *N.Y. Acad Sci* 139: 388-399, 1966.
40. *Vander AJ, Müller R*: Control of renin secretion in the unanesthetized dog. *Am J Physiol* 207: 537-546, 1964.
41. *Vander AJ*: Control of renin release. *Physiol Rev* 47: 359-382, 1967.
42. *Schoenmann J, Levine DZ*: Tubular control of glomerular filtration rate in single nephrons. *Can J physiol pharmacol* 53: 323-329, 1975.
43. *Wright FS*: Intrarenal regulation of glomerular filtration rate. *New Engl. J Med* 291: 135-141, 1974.
44. *Schoenmann J, Persson EG, Ågren B*: Tubuloglomerular feedback. Nonlinear relation between glomerular hydrostatic pressure and loop of Henle perfusion rate. *J Clin Invest* 52: 862-869, 1973.
45. *Wright FS, Schoenmann J*: Interference with feedback control of glomerular filtration rate by furosemide, trifluo-cin, and cyanide. *J Clin Invest* 53: 1695-1708, 1974.
46. *Schoenmann J, Herrule M*: Maintenance of feedback regulation of filtration dynamics in the absence of divalent cations in the lumen of the distal tubule. *Pflügers Arch* 358: 311-323, 1975.
47. *Schoenmann J, Herrule M, Schmidhauser E, Dahlheim H*: Impaired potency for feedback regulation of glomerular filtration rate in DOCA escaped rats. *Pflügers Arch* 358: 325-338, 1975.
48. *Hierholzer K, Müller-Saer R, Gutschke HU, Batz M, Lichtenthan I*: Filtration in surface glomeruli as regulated by flow rate through the loop of Henle. *Pflügers Arch* 352: 315-337, 1974.
49. *Müller-Saer R, Gutschke HU, Samwer KF, Oetters W, Hierholzer K*: Tubuloglomerular feedback in rat kidneys of different renal contents. *Pflügers Arch* 359: 33-36, 1975.
50. *Rector FC, Jameth A, Seklin DW*: Evidence for tubuloglomerular feedback mechanism. Abstracts of Symposium. Sixth Int Congr Nephrol 46-47, 1975.
51. *Schoenmann J, Wright FS, Davis JM, Stackelberg W, Graf G*: Regulation of superficial nephron filtration rate by tubulo-glomerular feedback. *Pflügers Arch* 318: 147-175, 1970.
52. *Burke TJ, Navar G, Clapp JR, Robinson RR*: Response of single nephron glomerular filtration rate to distal nephron microperfusion. *Kidney Int* 6: 230-240, 1974.

53. *Persson AEG, Schnermann J, Wright FS*: Effect of isotonic volume expansion on feedback control of glomerular filtration rate. *Proc Int Union Physiol Sci*, Vol XI, p 119, XXVI Int Congr New Delhi, 1974.
54. *Schnermann J*: Regulation of filtrate formation by feedback. *Abstracts of Symposia*, 6th Int Congr Nephrol; 48-49, 1975.
55. *Wright FS, Persson AEG*: Effect of changes in distal transepithelial potential difference on feedback control of filtration. *Kidney Int* 6: 114 A, 1974.
56. *Steven K, Strabnik S*: Renal corpuscular hydrodynamics: Digital Computer Simulation. *Pflügers Arch* 348: 317-331, 1974.
57. *Thorpe K*: JGA renal activity. *Proc 8th Int Congr Nephrol, Mexico 1972*, Vol 2: 183-192, Karger Basel, 1974.
58. *Schnermann J, Stowe N*: Evaluation of the role of the renin - angiotensin and adrenergic systems and of divalent cations in tubuloglomerular feedback. *INSERM*, Vol 30, Colloque Européen sur la physiologie du néphron, abstracts, p 192, 1974.
59. *Steven K, Thorpe DH*: Angiotensin II: Intratubular and renal capillary pressure regulation in the rat kidney. *Acta physiol Scand*. In press.
60. *Morgan T, Barboer RW*: *In vivo* perfusion of proximal tubules of the rat: glomerulotubular balance. *Am J Physiol* 217: 992-997, 1969.
61. *Moril F, Maruyama Y*: Simultaneous measurement of unidirectional and net sodium fluxes in microperfused rat proximal tubules. *Pflügers Arch* 320: 1-23, 1970.
62. *Radde HW, Rasmick G, Kötter S, Ullrich KJ*: Influence of lumen diameter and flow velocity on the isotonic fluid absorption and ^{51}Cr permeability of the proximal convolution of the rat kidney. *Pflügers Arch* 324: 288-296, 1971.
63. *Berg MB, Orloff J*: Control of fluid absorption in the renal proximal tubule. *J Clin Invest* 47: 2016-2024, 1968.
64. *Barboer E, Early LE*: Importance of ultrafilterable plasma factors in maintaining tubular reabsorption. *Kidney Int* 3: 142-150, 1973.
65. *Barboer E, Early LE*: Effect of intraluminal flow on proximal tubular reabsorption. *J Clin Invest* 52: 843-849, 1973.
66. *Bueno WE, Early LE*: Demonstration of independent roles of proximal tubular reabsorption and intratubular load in the phenomenon of glomerulotubular balance during aortic constriction in the rat. *J Clin Invest* 50: 77-89, 1971.

67. *Ulrich KJ, Radtke HW, Rumrich G*: The role of bicarbonate and other buffers on isotonic fluid absorption in the proximal convolution of the rat kidney. *Pflügers Arch* 330: 149-161, 1971.
68. *Ulrich KJ, Rumrich G, Klotz S*: Specificity and sodium dependence of the active sugar transport in the proximal convolution of the rat kidney. *Pflügers Arch* 351: 35-48, 1974.
69. *Ulrich KJ, Rumrich G, Klotz S*: Sodium dependence of the amino acid transport in the proximal convolution of the rat kidney. *Pflügers Arch* 351: 49-60, 1974.
70. *Frömter E, Göttsche K*: Free-flow potential profile along rat kidney proximal tubule. *Pflügers Arch* 351: 69-83, 1974.
71. *Frömter E, Göttsche K*: Active transport potentials, membrane diffusion potentials and streaming potentials across rat kidney proximal tubule. *Pflügers Arch* 351: 83-98, 1974.
72. *Frömter E*: Electrophysiology and isotonic fluid absorption of proximal tubules of mammalian kidney. In: *Kidney and urinary tract physiology*. K. Thurau, ed., MTP Int Rev Science, Physiol Ser L, Vol 6, pp 1-38, 1974.
73. *Kokko JP*: Proximal tubule potential difference. Dependence on glucose, HCO₃⁻ and aminoacids. *J Clin Invest* 52: 1362-1367, 1973.
74. *Barratt LJ, Rector FC, Kokko JP, Seldin DW*: Factors governing the transepithelial potential difference across the proximal tubule of the rat kidney. *J Clin Invest* 53: 454-464, 1974.
75. *Green R*: Some factors influencing *in vivo* sodium and fluid reabsorption in the proximal convoluted tubule of rats. Abstracts of Symposia, 6th Int Congr Nephrol: 23-24, 1975.
76. *Berg MB*: Mechanism of fluid absorption by proximal convoluted tubules. Abstracts of Symposia, 6th Int Congr Nephrol: 24-25, 1975.
77. *Richardson IW, Licko V, Barish E*: The nature of passive flows through tightly folded membranes. The influence of microstructure. *J Membrane Biol* 11: 293-308, 1973.
78. *Kelman RB*: A theoretical note on exponential flow in the proximal part of the mammalian nephron. *Bull Math Biophys* 24: 303-317, 1962.
79. *Falchuk KH, Brenner BM, Tadokoro AI, Berthier RIV*: Oncotic and hydrostatic pressures in peritubular capillaries and fluid reabsorption by proximal tubule. *Am J physiol* 220: 1427-1433, 1971.
80. *Imai M, Kokko JP*: Effect of peritubular protein concentration on reabsorption of sodium and water in isolated perfused proximal tubules. *J Clin Invest* 51: 314-325, 1972.

81. Kokko JP: Qualitative and quantitative importance of the constituents used in microperfusion experiments. *Yale J Biol Med* 45: 332-338, 1972.
82. Grantham JJ, Quaslika PB, Walling LW: Influence of serum proteins on net fluid reabsorption in isolated proximal tubules. *Kidney Int* 2: 66-75, 1972.
83. Horster M, Borg M, Potts D, Orloff J: Fluid absorption by proximal tubules in the absence of colloid osmotic gradient. *Kidney Int* 4: 6-11, 1973.
84. Persson AEG, Scheerms J, Ågren B, Eriksson NE: The hydraulic conductivity of the rat proximal tubular wall determined with colloidal solutions. *Pflügers Arch* 360: 25-44, 1973.
85. Greco R, Windhager EE, Gieblich G: Protein oncotic pressure effects on proximal tubular fluid movement in the rat. *Am J physiol* 226: 265-276, 1974.
86. Spitzer A, Windhager EE: Effect of peritubular oncotic pressure changes on proximal tubular fluid reabsorption. *Am J physiol* 218: 1186-1193, 1970.
87. Ågren B: Influence of peritubular hydrostatic and oncotic pressures on fluid reabsorption in proximal tubules of the rat kidney. *Acta physiol Scand* 93: 184-194, 1973.
88. Conger JD, Bartoli E, Early LE: No effect of peritubular plasma protein on proximal tubular volume absorption during capillary perfusion in situ. 6th Ann Meet Am Soc Nephrol, Washington DC, p 25, 1973.
89. Brenner BM, Troy JL: Postglomerular vascular protein concentration: Evidence for a causal role in governing fluid reabsorption and glomerulotubular balance by the renal proximal tubule. *J Clin Invest* 50: 336-349, 1971.
90. Holmgren H, Schrier RW: Evaluation of peritubular capillary microperfusion method by morphological and functional studies. *Pflügers Arch* 356: 59-71, 1975.
91. Holmgren H, Schrier RW: Variation of proximal tubular reabsorptive capacity by volume expansion and aortic constriction during constancy of peritubular capillary protein concentration in rat kidney. *Pflügers Arch* 356: 73-86, 1975.
92. Myers BD, Dean WA, Brenner BM: Effects of norepinephrine and angiotensin II on the determinants of glomerular ultrafiltration and proximal tubule fluid reabsorption in the rat. *Circ Res* 37: 101-110, 1975.
93. Eisenbach GM, Van Liew JB, Boylan JW: Effect of angiotensin on the filtration of protein in the rat kidney: A micropuncture study. *Kidney Int* 8: 80-87, 1975.

ACTA PHYSIOLOGICA SCANDINAVICA
SUPPLEMENTUM 482

Aspects of Cardiovascular
Reflex Control in Man
An experimental study

BY

GUNNAR TYDÉN

STOCKHOLM 1977

ACTA PHYSIOLOGICA SCANDINAVICA
SUPPLEMENTUM 448

From the Department of Environmental Physiology
Faculty of Medicine, Karolinska Institutet,
Stockholm, Sweden

Aspects of Cardiovascular Reflex Control in Man

An experimental study

BY
GUNNAR TYDÉN

STOCKHOLM 1977

CONTENTS

PREFACE	5
INTRODUCTION	7
METHODS AND PROCEDURES	14
RESULTS	21
Head-up tilt	21
Increased gravitational force	23
Changes in carotid sinus transmural pressure	25
Lower body negative pressure	26
DISCUSSION	28
A Methodological considerations	28
B General discussion	34
Significance of cardiac effector- mechanisms in cardiovascular homeostasis	34
Effects of posture and exercise on baro- receptor-induced changes in heart rate and mean arterial pressure	42
Relative contributions of sympathetic and parasympathetic influence in reflex heart-rate control	45
SUMMARY	48
REFERENCES	52

The present thesis is based on the following papers:

- I Bjurstedt H G Rosenhamer and G Tydén Acceleration stress and effects of propranolol on cardiovascular responses Acta physiol scand 1974 90 491-500
- II Bjurstedt H G Rosenhamer and G Tydén Cardiovascular responses to changes in carotid sinus transmural pressure in man Acta physiol scand 1975 94 497-505
- III Bjurstedt H G Rosenhamer and G Tydén Gravitational stress and autonomic cardiac blockade Acta physiol scand 1976 96 526-531
- IV Bjurstedt H G Rosenhamer and G Tydén Lower body negative pressure and effects of autonomic heart blockade on cardiovascular responses Acta physiol scand 1977 99 353-360

In the text these papers will be referred to by their Roman numerals I-IV

PREFACE

The present investigation was performed at the Department of Environmental Physiology Karolinska Institutet Stockholm. The experimental part of the investigation was carried out during the years 1972-1973.

I wish to express my profound thanks to Professor Hilding Bjurstedt, Head of the Department of Environmental Physiology, who introduced me into the field of cardiovascular research. He has generously shared with me his experience in this field and has given me continual support throughout this study.

I am further much indebted to Dr. Gunnar Rosenhamer, my instructor and coworker, for invaluable cooperation in the carrying out of the experimental part of the investigation and for stimulating discussions and advice in the processing and interpretation of data.

My thanks are also due to Professor Carl Magnus Hesser and Dr. Dag Linnarsson for stimulating discussions and generous support.

I wish to express my sincere thanks to Irène Unander-Scharin and Margareta Lindborg for expert secretarial help, to Karin Vasser for capable medical assistance, and to Barbro Bergström, Bertil Lindborg, Carl Huldt, Berndt Lennholm, Bertil Lundin and Anders Truvé for skilful technical assistance.

The work has been supported in full by grants from the

The present thesis is based on the following papers:

- I Bjurstedt H G Rosenhamer and G Tydén Acceleration stress and effects of propranolol on cardiovascular responses Acta physiol scand 1974 90 491-500
- II Bjurstedt H G Rosenhamer and G Tydén Cardiovascular responses to changes in carotid sinus transmural pressure in man Acta physiol scand 1975 94 497-505
- III Bjurstedt H G Rosenhamer and G Tydén Gravitational stress and autonomic cardiac blockade Acta physiol scand 1976 96 526-531
- IV Bjurstedt H G Rosenhamer and G Tydén Lower body negative pressure and effects of autonomic heart blockade on cardiovascular responses Acta physiol . scand 1977 99 353-360

In the text these papers will be referred to by their Roman numerals I-IV

INTRODUCTION

Since the demonstration by Hering (1923) of the baroreceptor reflex function of the carotid sinuses knowledge about the physiology of the reflex control of circulation has accumulated at an ever increasing rate. The methods of study of baroreceptors and baroreceptor reflexes have been described and summarized in numerous publications. Notable is the monograph of Heymans and Neil (1958) which provided a much needed full discussion of the role of baroreceptor reflexogenic zones in the control of circulation. Integrated aspects of cardiovascular reflex control have been presented in more recent reviews and monographs e.g. those of Folkow, Heymans and Neil (1965), Henry and Meehan (1971), Korner (1971), Kirchheim (1976) and Öberg (1976).

The information presently available on cardiovascular reflex control has predominantly been derived from experiments performed on anesthetized animals where it has been possible to study separate reflex mechanisms while inputs from other afferent zones have been maintained constant or eliminated (for review see Heymans and Neil 1958). Even though such experiments are basic to any thorough analysis of circulatory control they must be followed by studies on intact conscious man. It is well known that anesthesia as well as surgical trauma can alter the responses of the cardiovascular system to a variety of physiologic stimuli (for recent re-

views see Vatner and Braunwald 1975 Kirchheim 1976) A number of direct and indirect methods have therefore been developed to make possible the study of baroreceptor reflex function in unanesthetized man A physiological and simple way to challenge circulatory homeostasis familiar to all physiologists is to tilt a subject from the supine to the head-up position Indeed many reflex mechanisms involved in postural changes in the circulation have been studied extensively and have been aptly reviewed by Gauer and Thron (1965) To achieve more clearcut but still reversible circulatory responses the gravitational pull in the head-foot direction can be augmented by exposure to increased gravitational force on the human centrifuge The baroreflex involvement in cardiovascular adaptation to accelerative stress has been reviewed by Gauer and Zuidema (1961) and Howard (1965)

Circulatory reflexes evoked by a shift from the recumbent to the head-up position are due mainly to arterial hypotension in the upper portion of the body and to a downward displacement of blood volume from the intrathoracic space Such reflexes can be studied separately The reflex effects on the heart of a drug-induced decrease in arterial pressure have been studied in the supine as well as the erect posture (Robinson et al 1966 Pickering et al 1972a b) However the vasoconstrictor component of the baroreceptor reflex cannot easily be evaluated by this method of drug-induced arterial hypotension since it is masked by the direct effect of depressor drugs on vascular smooth muscle A more physiological method of changing the stimulus to the carotid sinus barore

ceptors in man was first devised by Ernsting and Parry (1957) who increased the carotid sinus transmural pressure by decreasing the pressure in an airtight box enclosing the neck. This method having subsequently been employed in several investigations (Bevegård and Shepherd 1966, Beiser et al 1970, Eekberg et al 1975, 1976, Eekberg 1976) was further developed by Thron et al (1967) to permit also the application of positive pressure on the neck thus simulating carotid sinus hypotension (Wagner et al 1968, Stegemann, Busert and Brock 1974). Finally the effects of direct carotid sinus nerve stimulation have been studied in anesthetized (Carlsten et al 1958) and conscious man (Epstein et al 1969, Eekberg, Fletcher and Braunwald 1972). It must be borne in mind however that the effects of electrical stimulation of the sinus nerve result from both chemoreceptor and baroreceptor nerves which complicates their interpretation.

The circulatory responses to a decrease in intrathoracic blood volume can be studied with the body in the supine position by exposing its lower portion to subatmospheric pressure. This method of applying lower body negative pressure (LBNP) to simulate certain circulatory effects of gravity was first devised by Greenfield et al (1963) and may produce considerable pooling in dependent veins with little if any effects on the arterial blood pressure at head level (for review see Wolthuis, Bergman and Nicogossian 1974). Negative pressures of 40-50 mm Hg have been used to produce physiological changes comparable to those observed during orthostasis and head-up tilt (Gilbert and Stevens 1966).

Samueloff Browse and Shepherd 1966 Murray et al 1968 Molt-huis Hoffer and Johnsson 1970 Musgrave Zechman and Mains 1971 Rowell et al 1972) Indeed pressures of this magnitude have been extensively used in many space missions to simulate the effects of normal gravity on the body in the weightless condition (for review see Pestov and Gerathewohl 1975) Few investigations have involved the application of negative pressures of greater magnitude (Brown et al 1966 Stevens and Lamb 1965)

Since few of the above-mentioned investigations have involved the simultaneous measurement of cardiac output and arterial pressure little is known about the relative contributions of cardiac output and total peripheral resistance in the cardiovascular reflex control in man Thus the effects of increased gravitational force acting in the head-seat direction on cardiac output and total peripheral resistance have previously only been studied by Lindberg et al (1961) who found that exposure to increased gravitational force in the sitting position elevated mean arterial pressure at heart level due to a marked increase in total peripheral resistance while cardiac output was only moderately decreased

Ernsting and Parry (1957) using the direct Fick method and Bevegård and Shepherd (1966) employing the dye dilution technique examined the effects of increased carotid sinus transmural pressure on cardiac output and arterial pressure Ernsting and Parry (1957) found no significant effect on cardiac output; the reduction in arterial pressure evoked by

increased carotid sinus transmural pressure was therefore attributed to vasodilatation probably in the splanchnic area Bevegård and Shepherd (1966) on the other hand who noted a significant decrease in cardiac output when negative pressure was applied to the neck suggested that the decrease in systemic arterial pressure with carotid sinus stimulation results from a slight decrease in cardiac output and some dilatation of resistance vessels Electrical stimulation of the carotid sinus nerves by means of an implanted stimulator was found to reduce mean arterial pressure by reflexly decreasing both vascular resistance and cardiac output in the work of Epstein et al (1969) whereas only cardiac output was reduced in the study of Farrehi (1972)

So far no information is available as to the effect of decreased carotid sinus transmural pressure on the cardiac output in man However Roddie and Shepherd (1957) examined the effects of compression of the carotid arteries below the level of the carotid sinuses on the vascular resistance in the limbs Since vascular resistance in the forearm calf and hand were unchanged or slightly decreased during the increase in arterial pressure elicited by carotid artery compression these authors concluded that the pressor response was due to increased cardiac output or increased peripheral resistance in other vascular beds or both

Measurements of cardiac output and arterial pressure during lower body negative pressure have previously been carried out by Steven and Lamb (1965) Murray et al (1968) and Nowell et al (1972) It was observed that LBNP may produce a

marked decrease in cardiac output with mean arterial pressure essentially unchanged due to a corresponding increase in total peripheral resistance. In the study of Rowell et al (1972) it was concluded that approximately a third of the increase in total vascular resistance was due to splanchnic vasoconstriction. Stevens and Lamb (1965) and Murray et al (1968) extended the exposures to LBNP until the occurrence of presyncopal signs or vasodepressor syncope respectively and found that the fall in mean arterial pressure associated with impending syncope is primarily due to a fall in systemic vascular resistance. It was concluded by Stevens and Lamb (1965) that the individual's ability to maintain his blood pressure through peripheral vascular mechanisms determines the course of events during exposure to LBNP.

Following the introduction of selective beta-adrenergic blocking agents the use of such agents and of atropine has made it possible to pharmacologically isolate the heart from sympathetic or parasympathetic influence or from both. This opportunity has been utilized to study in conscious man the relative roles of the two segments of the autonomic nervous system in the baroreflex control of the heart rate in various conditions. In such studies the tonic restraint exercised from the carotid sinus reflexogenic areas has been deliberately altered by applying some of the methods described above. Likewise autonomic cardiac blockade has been utilized to study the relative roles of cardiac and peripheral effector mechanisms in certain conditions such as hypertension (Julius et al 1971, Ellis and Julius 1973, Körner et al 1973) exercise (Cummings and

Carr 1966 Nordenfelt 1971) and the Valsalva maneuver (Korner Tonkin and Uther 1976) However it seems that beta-adrenergic or combined autonomic cardiac blockade has so far not been utilized to study the relative importance of cardiac effector mechanisms in the circulatory adaptation to such conditions as increased gravitational force bidirectional changes in the carotid sinus transmural pressure or lower body negative pressure

The objectives of the present investigation were to study in conscious man the function of certain cardiovascular reflex mechanisms in experimentally induced disturbances of circulatory homeostasis Such disturbances were brought about by exposing subjects to different experimental conditions vis 70° head-up tilt (II) a threefold increase of the force of gravity (I III) bidirectional changes in the carotid sinus transmural pressure (II) and lower body negative pressure (IV) In this way it has been possible to study different reflex effects on the circulation primarily induced by changes in the transmural pressure at the level of the carotid sinuses and by reductions in central blood volume separately or in combination In order to elucidate the contributions of cardiac effector mechanisms to these effects the cardiovascular adjustments to the above-mentioned conditions were observed before and after beta-adrenergic and/or combined beta-adrenergic and parasympathetic blockade

METHODS AND PROCEDURES

Descriptions of the methods and procedures used in this investigation to challenge circulatory homeostasis and to suppress the participation of cardiac effector mechanisms in certain reflex responses to such challenge have been given in detail in papers I-IV and are therefore only briefly summarized below. The experimental conditions to which the subjects were exposed in the separate studies are presented in Table I.

Subjects In all 20 healthy physically well trained male volunteers were studied. Several of them took part in more than one of the series of experiments. Dimensional and functional data for the subjects have been reported in the individual papers. The subjects were thoroughly acquainted with the experimental procedure before their informed consent was obtained. The design of the investigation has been approved by the Ethical Committee of the Karolinska Institutet.

Normal and increased gravitational force For studies on circulatory responses to the force of normal gravity a tilt table with a foot plate was used where subjects could be passively tilted from the supine to the 70° head-up position. To produce increased gravitational force the human centrifuge (radius = 7.4 m) at the Karolinska Institutet was used. Fig. 1 shows the position of the subject in the centrifuge.

TABLE I Experimental conditions to which the subjects were exposed in the separate studies

Study	n	Type of stress applied	Blockade
II	6	70° head-up tilt	Beta adrenergic and parasympathetic
I	6	Increased gravitational force 3 G resting	Beta-adrenergic
I	6	Increased gravitational force 3 G exercise	Beta-adrenergic
III	8	Increased gravitational force 3 G resting	Beta-adrenergic and parasympathetic
II	8	Changes in carotid sinus trans mural pressure ± 40 mmHg supine	Beta-adrenergic and parasympathetic
II	8	Changes in carotid sinus trans mural pressure ± 40 mmHg erect	Beta-adrenergic and parasympathetic
IV	8	Lower body negative pressure 80 mmHg	Beta-adrenergic
IV	8	Lower body negative pressure 80 mmHg	Beta adrenergic and parasympathetic

gondola The gondola was allowed to swing out freely during the centrifuge runs so that the resultant force was always acting in the head-to-seat direction The speed of rotation was chosen so as to produce a threefold increase in the gravitational force (3 G) this force being well tolerable for subjects which have been made accustomed to the subjective sensations of sustained accelerative stress The gondola was equipped with bidirectional communication facilities as well as with a television camera for continuous supervision of the subject The actual G-force as well as the circulatory variables studied were continuously monitored and recorded outside the centrifuge via a slip-ring arrangement To make leg exercise possible during the centrifuge runs the gondola accommodated an electrically braked cycle ergometer with the crank axis at the level of the gondola seat

Changes in carotid sinus transmural pressure The carotid arterial stretch receptors were exposed to different transmural pressures according to the method of Thron et al (1967) using a plexiglass helmet enclosing the neck and the head The subject breathed air at normal atmospheric pressure through a mouthpiece attached to a hole in the helmet by means of a short rubber tube (II: fig 1) The pressure within the helmet could be changed in either direction and was monitored continuously by a strain gage manometer The time to reach the desired pressure was kept at about 4 sec

Lower body negative pressure (LBNP) The device to produce LBNP consisted of a wooden box with an elliptical opening at one end in the main similar to that described by

Stevens and Lamb (1965) A rubber seal was provided at the opening which fitted hermetically around the waist at the level of the iliac crest. The subject rested supine straddling a narrow padded saddle which provided support during the suction exposures. The box was connected via a pressure regulator to a remotely located preevacuated low pressure chamber which made possible the application of graded negative pressure. The time to reach the desired negative pressure was kept at about 30 sec. A strain-gage manometer was used for continuous monitoring of the pressure in the box. Temperature inside the box was also monitored continuously and was kept at ambient room temperature within $\pm 0.5^{\circ}\text{C}$.

Catheterisation procedures For recording of arterial pressure one radial artery was entered percutaneously at the wrist by a small Teflon catheter (length = 7 cm; O D = 1.15 mm; I D = 0.75 mm). For withdrawal of arterial blood during cardiac output determinations by cuvette densitometry (see below) the contralateral radial artery was catheterized in a similar way using a catheter of somewhat larger caliber (O D = 1.45 mm; I D = 1.05 mm). A venous catheter (length = 30 cm; O D = 1.7 mm; I D = 1.2 mm) was introduced percutaneously into an antecubital vein and advanced so that its tip was located in the axillary vein.

Cardiac output was determined by the indicator dilution technique using indocyanine green (Cardio-Green[®]) and a Waters dichromatic densitometer (Model X-300 in study I D-401 in studies II-IV). Dye injections as well as the subsequent withdrawal and reinfusion of arterial blood through

the densitometer cuvette were made by a remote-controlled injection system described elsewhere (Rosenhamer 1967 1968) The amount of dye injected for each determination was 1 ml of a 0.5% aqueous solution of indocyanine dye and the rate of withdrawal of blood from the radial artery through the cuvette was 20 ml/min In study IV dichromatic earpiece densitometry was used (Reed and Wood 1967) this method having shown satisfactory agreement with results obtained with arterial cuvette densitometry (Reed and Wood 1967; Schneider Cheikhsadeh and Müller 1967 Wallgren 1975) A dichromatic earpiece (Waters XE-302) was then attached to the ear after rubbing the pinna for one minute with rubrifacient ointment (Transvasin[®]) and was secured in position with adhesive tape The method for dye injection and the amount of dye injected was the same as described above

Arterial pressure at heart level was obtained by means of a differential strain-gage manometer (Statham P 23 B) one of the inputs being connected to a radial artery catheter and the other to a plastic tube taped onto the skin along the mid axillary line and filled with saline up to the level of the insertion of the fourth rib This technique afforded automatic compensation for the hydrostatic pressure difference between the heart and the fixed strain gage and thus permitted accurate recordings of the mean arterial pressure and its changes at heart level irrespective of changes in the G level or body position Mean arterial pressure was derived electronically from the arterial pressure recordings

Heart rate was obtained from chest electrodes and recorded

by means of a linear beat-to-beat cardi tachometer (Lindborg Wigertz and Ödman 1969)

Recordings All signals were displayed on a multichannel strip-chart recorder (Brush Mk 200) and recorded on magnetic tape (Ampex FR-100 C) for storage and subsequent detailed analysis of the variables under study. In addition the dye-dilution curves were inscribed on an X-Y recorder (Hewlett-Packard 700 AM) at a paper speed of 4 mm/s

Pharmacological blockade Beta-adrenergic blockade was produced by the i.v. administration of 0.25 mg/kg of propranolol (Inderal®). To achieve parasympathetic blockade atropine sulphate was given i.v. in doses of 0.03 mg/kg (II-III) and 0.04 mg/kg (IV) respectively

General procedures The experimental conditions to which the subjects were exposed in the separate studies may evoke a considerable emotional impact which may influence the reflex circulatory responses. Care was therefore taken to accustom the subjects to the subjective sensations of the circulatory stress to be applied. During the course of 1-5 weeks preceding the day of the experiment several preliminary sessions were therefore conducted on separate days with each subject. No experiment was performed before the subject reported that he was completely familiarized with the subjective sensations involved in the procedure. Furthermore no appreciable apprehension was present during the actual experiment as judged from the subject's resting heart rate

After the catheterization procedures the subject was allowed at least 30 min of rest before any circulatory stress

was applied. Following the administration of propranolol and/or atropine no measurements were made until 10 min had elapsed.

The time of exposure to acceleration stress was 5 min (I) and 4 min (III) respectively to changes in carotid sinus transmural pressure 2 min and to LBMP 4 min.

Calculations Cardiac output was determined from the dye dilution curves according to the method originally devised by Kinsman, Moore and Hamilton (1929). Heart rate and mean arterial pressure were averaged during the inscription of each indicator dilution curve. Total peripheral resistance was calculated as mean arterial pressure (mm Hg) divided by cardiac output (ml/sec). The statistical significance of differences between mean values were evaluated by applying the t-test to the intraindividual differences (of Fisher 1948).

RESULTS

The results are presented in four main sections dealing with circulatory responses to head-up tilt increased gravitational force changes in carotid sinus transmural pressure and lower body negative pressure respectively In each section the effects of beta-adrenergic and/or combined beta-adrenergic and parasympathetic blockade on the circulatory responses are presented Absolute and percentage changes refer to group mean values For detailed additional information the reader should consult the individual papers (I-IV)

Head up tilt (II)

Effects of a shift from the supine position to 70° head-up tilt (6 min) were studied in six subjects before and after combined cardiac effector blockade

Mean arterial pressure at heart level was slightly increased (7%) following change to the head up position this increase not being affected by autonomic blockade The increase in heart rate normally following head up tilt was almost completely abolished by the blockade Cardiac output was decreased by 51% when assuming the upright position after blockade as compared to 26% in the unblocked condition However due to a potent increase in total peripheral resistance (113%) (fig 2) the exaggerated curtailment of cardiac output after blockade was fully compensated

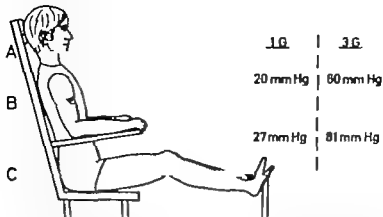


Fig 1 Position of subject in the centrifuge gondola with approximate hydrostatic pressure differences between the hydrostatic indifference point (B) the carotid sinuses (A) and the legs (C) respectively at normal gravity (1 G) and during a threefold increase in the gravitational force (3 G)

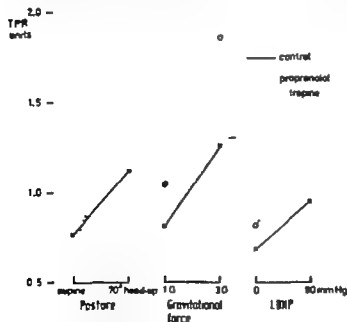


Fig 2 Changes in total peripheral resistance (TPR) induced by 70° head-up tilt (n=6) exposure to increased gravitational force (3 ■ n=8) and lower body negative pressure (LBNP n=8) before and after cardiac effector blockade

Increased gravitational force (I-III)

Two separate experimental series were performed. In the first six subjects were studied in the seated position before and during a 5 min exposure to a threefold increase in the gravitational force (3 G). Cardiovascular responses were investigated before and during leg exercise and before and after beta-adrenergic blockade. The work load was preset individually to correspond to approximately 50% of the subjects' aerobic working capacity. The second series comprised eight subjects exposed to 4 min of 3 G before and after combined cardiac effector blockade.

Exposure to 3 G in the sitting position produced an increase in mean arterial pressure at heart level from 99 to 126 mm Hg (I) and from 102 to 127 mm Hg (III) respectively. Beta adrenergic blockade did not affect the blood pressure response to 3 G (95 to 125 mm Hg) which was however significantly decreased after combined cardiac effector blockade (104 to 118 mm Hg). During exercise exposure to 3 G caused an increase in blood pressure from 115 to 139 mm Hg before and from 105 to 130 mm Hg after propranolol (fig. 3). G-induced increase in heart rate was 52 (I) and 45 (III) beats/min respectively. Propranolol reduced this response by 62% whereas propranolol and atropine reduced it by 78%. During exercise the G-induced heart-rate response was reduced by 92% by propranolol (fig. 4). G-induced reductions in cardiac output were augmented by 25% after propranolol and by 30% after propranolol and atropine. The absolute values during exposure to 3 G were 6.3 and 6.1 l/min (studies

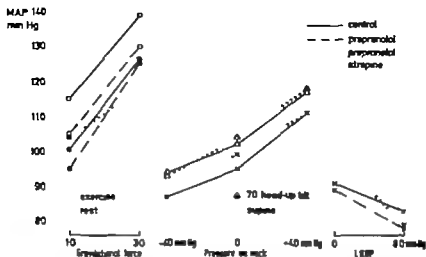


Fig 3 Changes in mean arterial pressure (MAP) at heart level induced by increased gravitational force (3 G) at rest (n=14 before blockade n=6 during propranolol n=8 during propranolol + atropine) and during exercise (n=6) by positive and negative pressures on the neck (n=8) and by lower body negative pressure (LBNP n=8) before and after beta-adrenergic and combined beta-adrenergic and parasympathetic blockade

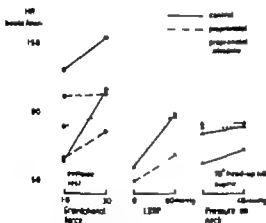


Fig 4 Changes in heart rate (HR) induced by increased gravitational force (3 G) at rest (n=14 before blockade n=6 during propranolol n=8 during propranolol + atropine) and during exercise (n=6) by lower body negative pressure (LBNP n=8) and by pressure on the neck (n=8) before and after beta-adrenergic and combined beta-adrenergic and parasympathetic blockade

I and III) in the unblocked situation 4.2 l/min after beta-adrenergic and 3.9 l/min after combined beta-adrenergic and parasympathetic blockade. Total peripheral resistance increased markedly in all conditions following exposure to 3 G (fig. 2). Although the percentage increase was greater after combined blockade than after propranolol only, the absolute values were almost identical 1.85 and 1.86 units respectively.

Changes in carotid sinus transmural pressure (II)

Eight subjects were studied during 2 min periods of exposure to a 40 mm Hg increase or decrease respectively of the external pressure over the neck both in the supine and 70° head up position. Six of the subjects participated in a second experimental session where the above-mentioned exposures were run after combined cardiac effector blockade.

Positive pressure of 40 mm Hg on the neck produced an increase in mean arterial pressure of 16 mm Hg whereas negative pressure of the same magnitude caused a reduction in arterial pressure of only 8 mm Hg (fig. 3). The arterial pressure responses obtained by changing the transmural pressure were essentially the same in the supine as in the 70° head-up position. Furthermore combined autonomic blockade did not affect the reflex changes in mean arterial pressure in either position. A 16% increase in heart rate accompanied the increase in mean arterial pressure during positive pressure on the neck in the supine position. During head-up tilt the corresponding increase was only 6% (fig. 4). Heart-rate

response to negative pressure on the neck was -6% in the supine position but negligible in the head-up position. Autonomic blockade drastically reduced changes in heart rate accompanying changes in carotid sinus transmural pressure although they were not completely extinguished. Cardiac output increased significantly during positive pressure on the neck (10% in the supine as well as the head-up position). Autonomic blockade completely abolished this increase. During negative pressure there were no changes in cardiac output neither before nor after blockade. Whereas the arterial pressure response to increased carotid sinus transmural pressure was due solely to a reduction in total peripheral resistance, a significant increase in cardiac output thus contributed to the more potent pressor response to decreased transmural pressure. When the increase in cardiac output was abolished by autonomic blockade a compensatory increase in total peripheral resistance maintained the pressor response at the pre-blockade magnitude.

Lower body negative pressure (IV)

Eight subjects were studied before and during 4 min periods of exposure to 50 mm Hg of LBWP before and after beta-adrenergic and combined beta-adrenergic and parasympathetic blockade.

LBWP produced a slight decrease in mean arterial pressure towards the end of the exposure (9%) (fig. 3). Propranolol augmented this decrease, the absolute value at the end of the suction period being significantly lower than before blockade (78 mm Hg and 83 mm Hg respectively). After combined cardiac

effector blockade the pre-LEBP value of mean arterial pressure was significantly increased as compared to the unblocked condition and that with propranolol alone. During LBNP however there was a clearcut reduction (21%) so that the value at the end of the period was the same as with propranolol alone. Heart rate increased gradually during LBNP (+24 beats/min after 30 sec +39 beats/min at the end of the period). Propranolol reduced this response by 51% whereas combined blockade reduced it by 87% (fig. 4). In spite of the increase in heart rate during LBNP cardiac output was reduced by 33% in the unblocked condition due to a 60% decrease in stroke volume at the end of the exposure. Propranolol augmented the decrease in cardiac output during LBNP even though the decrease in stroke volume was less pronounced than before blockade. After combined blockade the percentage decrease in cardiac output was 46% the absolute value during LBNP however not being significantly different from that obtained with propranolol only. Total peripheral resistance showed a prompt increase by 50% at the application of LBNP but then gradually decreased to a final level of 40% at the end of the exposure. This phenomenon which was also observed after combined blockade was responsible for the gradual fall in blood pressure. Absolute values of total peripheral resistance at the end of LBNP were 0.95, 1.16 and 1.20 units before and after propranolol and combined propranolol and atropine respectively.

DISCUSSION

A Methodological considerations

In the experiments with increased gravitational force the 3 g level was chosen since it has been found to produce profound circulatory changes yet being well tolerable to subjects having been made accustomed to the subjective sensations of sustained accelerative stress (Bjurstedt Hansson and Ström 1959 Rosenhamer 1967 Linnarsson and Rosenhamer 1968 Bjurstedt Rosenhamer and Wigertz 1968)

The adjustments of the circulation to an increase in the gravitational force are due largely to the effects of increased hydrostatic pressures below and decreased hydrostatic pressures above the hydrostatic indifference point (HIP) the HIP being defined as the point where the intravascular pressures stay constant when the direction or magnitude of the force of gravity is altered (cf Gauer and Thron 1965) In the sitting position the HIP for the venous as well as the arterial system is located approximately at the level of the diaphragm (cf Gauer and Zuidema 1961) Assuming a hydrostatic pressure difference between the HIP and the level of the carotid sinuses of approximately 20 mm Hg (fig 1) an abrupt threefold increase in the gravitational force will increase this pressure difference to 60 mm Hg 1 e the mean pressure in the carotid sinuses will initially be lowered by 40 mm Hg Likewise the hydrostatic pressure in

the horizontally oriented legs (fig 1) being 25-30 mm Hg higher than that prevailing at the level of the HIP during normal gravity will be increased to approximately 80 mm Hg during the 3 G runs

Evidence has been presented by Thron et al (1967) that with changes in carotid sinus transmural pressure accomplished by the technique employed in the present experiments the pressure transmitted to the walls of the carotid sinuses is linearly related to the applied helmet pressure when the latter is changed in the range -60 to +60 mm Hg Furthermore Eekberg (1976) found that maximum reduction of the internal jugular vein pressure was nearly equal to the reduction in pressure on the neck It can thus be assumed that in the present experiments the application of positive and negative pressures of 40 mm Hg in the helmet produced equal transmural pressure changes over the carotid sinuses in opposite directions from the normal

When the external pressure over the head and neck is decreased the driving pressure in the enclosed vascular segments approximates the difference between inflow and outflow pressures except initially for as long as it takes for the enclosed distensible veins to fill and the pressure in these vessels to approximate the outflow pressure so that flow is resumed Thus at steady state a subatmospheric helmet pressure does not affect the driving pressure in cerebral circuits However with positive pressure in the helmet the pressure in the downstream ends of the enclosed vascular segments is close to that of the surrounding pressure This

is due to the operation of the waterfall effect which characterizes the outflow from collapsible veins when the surrounding pressure is higher than the outflow pressure (cf Permutt and Riley 1963) This means that with a positive pressure in the helmet the transmitted portion of this pressure was lost from the normal driving pressure (inflow pressure minus outflow pressure) The functional implications of such loss of driving pressure have been considered in paper II (p 502)

The technique employed to produce lower body negative pressure has been used extensively during the last ten years (for review see Wolthuis Bergman and Nicogossian 1974) The application of LBNP causes an elevation in lower body vascular transmural pressure the magnitude of which is directly related to the level of reduced pressure applied (Coles 1956) thus producing pooling of blood in the distensible veins of the lower body and a consequent reduction in central blood volume To make possible a comparison between the results obtained in the LBNP experiments and those observed in the experiments with increased gravitational stress a level of negative pressure was chosen that would produce approximately the same increase in vascular transmural pressure in the legs as that obtaining during 3 G in the sitting position with the legs horizontally oriented viz 80 mm Hg (see above and fig 1) Since blood pooling during accelerative stress occurs primarily in the legs with little if any pooling in abdominal vessels (cf Howard 1965) it can be assumed that 80 mm Hg of LBNP will produce

approximately the same degree of blood pooling in the legs as will exposure to 3 G. Such pooling reduces central blood volume and this is reflected by a proportional change in stroke volume (Sjöstrand 1953, Milnor, Jose and McGaff 1960, Levinson, Frank and Helloms 1964, Levinson, Pacifico and Frank 1966, Ellis and Julius 1973). It is of interest that the values of stroke volume during 3 G and LBNP were almost identical (40 and 43 ml respectively) when the heart was deprived of autonomic influence. This observation supports the assumption that the degree of peripheral pooling and reduction of central blood volume was approximately the same during the two experimental conditions.

Since external temperature is known to strongly influence the amount of blood pooled (Henry 1951), care was taken to keep this variable constant during the experiment. This was achieved by means of continuous ventilation of the LBNP-box during the control period as well as during the exposures to negative pressure. Temperature could thus be kept within $\pm 0.5^{\circ}\text{C}$ in the box throughout the experiment.

Beta-adrenergic and parasympathetic blockade of the heart. A salient feature of the present investigation was to study the contribution of cardiac effector mechanisms to circulatory homeostasis in certain conditions of cardiovascular stress. For this purpose, beta-adrenergic and parasympathetic influence on cardiac activity was offset by the intravenous administration of propranolol and atropine, separately and in combination.

Epstein et al (1963) found that 0.15 mg/kg of propranolol

intravenously produced a degree of blockade that caused at least a tenfold reduction in the sensitivity of the heart to infused isoproterenol. Jose and Taylor (1969) found no further decrease in resting heart rate when increasing the dose from 0.20 to 0.25 mg/kg. However, the latter dose would seem preferable in conditions with a high sympathetic background activity such as presumably existed in the present experiments on cardiovascular effects of increased gravitational stress with and without exercise and of LBNP. Robinson et al (1966) who investigated the effects of exercise and postural changes on the heart rate used a dose of 0.25 mg/kg. This dose has been used throughout in the present experiments. Unlike certain other beta-adrenergic blocking agents, propranolol is devoid of any intrinsic sympathomimetic activity in the heart (for review see Gibson 1974).

The primary actions of atropine on the heart are blockade of vagal negative chronotropic and inotropic effects (for review see Higgins, Vatner and Braunwald 1973). However, apart from its cardiac vagal blocking effects, atropine has several other sites of action (see further below) which may interfere with the cardiovascular reflexes. Since these effects of atropine may affect tolerance to stressful stimuli such as those employed in the present experiments, a dose as small as possible to produce effective cardiac vagal blockade was chosen (0.03 mg/kg). The dose required to produce maximum inhibition of vagal control of the sinoatrial node has been reported to be in the range 0.025 to 0.04 mg/kg (Chamberlain, Turner and Sneddon 1967). Jose and Taylor (1969) found that

increasing the dose from 0.03 to 0.04 mg/kg raised the resting heart rate by only 0.8 beats/min. In pilot LBNP experiments (8 subjects unpublished observations) preceding the present investigation a substantial slowing of the heart was noted after release of LBNP during cardiac effector blockade. Since it could not be excluded that this effect on the heart was due to defective vagal blockade the dose of atropine was increased to 0.04 mg/kg in the present LBNP experiments. It was found, however, that the increased dose had no significant influence on the post-LBNP slowing of the heart rate.

It is well known that both propranolol and atropine exerts other influences on the circulation than those resulting from blockade of cardiac effector mechanisms. Thus propranolol as well as atropine may interfere with the circulatory reflex control by prevention of beta-adrenergic and cholinergic vasodilatation respectively even though the significance of such vasodilatation in the baroreflex control of vascular tone in man is uncertain (Brick 1966, Mahon 1966, Johnsson 1967, Price, Cooperman and Warden 1967, Folkow 1955, Roddie and Shepherd 1963, Uvnäs 1967). Furthermore atropine may affect certain cardiovascular reflex responses due to its central ganglionic and peripheral sites of action (for reviews see Ambache 1955, Eger 1969). The importance of these effects of propranolol and atropine will be discussed where relevant in later sections.

intravenously produced a degree of blockade that caused at least a tenfold reduction in the sensitivity of the heart to infused isoproterenol Jose and Taylor (1969) found no further decrease in resting heart rate when increasing the dose from 0.20 to 0.25 mg/kg. However, the latter dose would seem preferable in conditions with a high sympathetic background activity such as presumably existed in the present experiments on cardiovascular effects of increased gravitational stress with and without exercise and of LBNP. Robinson et al. (1966) who investigated the effects of exercise and postural changes on the heart rate used a dose of 0.25 mg/kg. This dose has been used throughout in the present experiments. Unlike certain other beta-adrenergic blocking agents, propranolol is devoid of any intrinsic sympathomimetic activity in the heart (for review see Gibson 1974).

The primary actions of atropine on the heart are blockade of vagal negative chronotropic and inotropic effects (for review see Higgins, Vatner and Braunwald 1973). However, apart from its cardiac vagal blocking effects, atropine has several other sites of action (see further below) which may interfere with the cardiovascular reflexes. Since these effects of atropine may affect tolerance to stressful stimuli such as those employed in the present experiments, a dose as small as possible to produce effective cardiac vagal blockade was chosen (0.03 mg/kg). The dose required to produce maximum inhibition of vagal control of the sinoatrial node has been reported to be in the range 0.025 to 0.04 mg/kg (Chamberlain, Turner and Sneddon 1967). Jose and Taylor (1969) found that

lume by loss of baroreceptor-induced inotropic drive to the heart (Sarnoff et al 1960 De Geest Levy and Zieske 1964 Glick 1971); it has been shown that exercise-induced augmentation of the contractile state of the myocardium is diminished by propranolol (Sonnenblick et al 1965) and that beta-adrenergic blockade diminishes cardiac output also when heart rate is kept constant by fixed rate artificial pacemakers (Bloomfield and Sowton 1967 Donoso et al 1967 Lund-Larsen et al 1968). Since in the present experiment on circulatory adjustments to a change from the supine to the erect posture the exaggerated curtailment of cardiac output after blockade was well compensated for by a concomitant increase in vascular resistance it is concluded that cardiac effector mechanisms are not of essential importance for the maintenance of arterial pressure during orthostasis. This conclusion is in agreement with the results of several investigations concerning orthostatic tolerance in man during beta-adrenergic blockade (Sannerstedt Julius and Conway 1970 Cuthbert and Owusu-Ankomah 1971 Fuccella et al 1971 Mæhrud et al 1971 Spodick Meyer and St Pierre 1972).

When the gravitational force acting in the long axis of the body is further increased (I-III) the circulatory responses are not solely exaggerated but in part qualitatively different from those obtained by head up tilt. Thus at 3 G there is a more pronounced increase in heart rate (Björstedt Hansson and Ström 1959) concomitant with a decrease in stroke volume which leaves cardiac output only slightly or moderately depressed (Lindberg et al 1963 Rosenhamer 1967). Due to a

potent vasoconstrictor response mean arterial pressure at heart level is not only maintained but is actually increased sometimes quite markedly (Lindberg et al 1960) These findings are confirmed by the results obtained in the present experiments (I III)

The fact that the circulatory responses to increased gravitational force before blockade were almost identical in studies I and III makes a comparison between values obtained after beta-adrenergic and combined cardiac blockade respectively in the separate studies justifiable although the experiments were performed on different days and with only some of the subjects participating in both studies After propranolol alone the response of the heart rate to 3 G was only 38% of that obtained without this drug (fig 4) The impaired heart-rate response was accompanied by a more clearcut curtailment of cardiac output than occurred before blockade In spite of this mean arterial pressure at heart level rose to about the same level before and after propranolol due to a more marked vasoconstrictor response after blockade (fig 3) The fact that the G-induced vasoconstrictor response was so precisely adjusted to compensate for the impaired response of the heart indicates not only that the central regulation of the arterial pressure was intact after propranolol; it also implies that cardiac sympathetic drive is not an essential mechanism in the circulatory defense against increased gravitational stress This concept is further emphasized by the observations of the G-induced arterial pressure response during exercise; this response was not affected by proprano-

lol even though the heart rate response to increased gravitational force during exercise was completely abolished by this drug (fig 3 and 4)

After combined cardiac effector blockade the G-induced increase in mean arterial pressure at heart level was significantly reduced (fig 3) Since propranolol alone did not affect the blood pressure response the explanation for the defective regulation of arterial pressure at 3 G after combined blockade must be sought in possible deleterious actions of atropine alone or in combination with propranolol on cardiac output or total peripheral resistance Since the mechanism of action of atropine on the heart is blockade of vagal negative chronotropic and inotropic effects it appears less probable that any reduction in cardiac performance at 3 G after combined heart blockade was due to actions of atropine on the heart On the other hand it has been suggested that atropine may impair cardiac filling in ortho tasis due to increased blood pooling in intracardiac vessels (Kaiser Frye and Gordon 1954) Furthermore other possible actions of atropine such as interference with some of the actions of acetylcholine on various parts of the central nervous system or a partial ganglionic blockade (for reviews see Ambache 1955 Eger 1962) may have acted to prevent the baroreceptor-induced vasoconstrictor response from fully developing as required for the maintenance of arterial pressure homeostasis

One of the salient effects of increased gravitational force in the head-seat direction is a fall of the mean arterial pressure in the cranial portion of the body It was

therefore thought of interest to study certain circulatory responses to primary pressure changes at the level of the carotid sinuses (II) Such changes were produced by altering the pressure in a helmet enclosing the head and neck It was found that a decrease in carotid sinus transmural pressure produced a much stronger arterial pressure response than a corresponding increase in transmural pressure (fig 3) The finding that the carotid baroreflex acts as a predominantly antihypotensive mechanism is in agreement with the results of Thron et al (1967) and Stagemann Busart and Brock (1974) who used a similar technique but contrasts with the generally held concept that the stimulus-response relationship of the carotid sinus reflex is a sigmoid curve which is symmetrical about normal arterial pressure (cf Heymans and Weil 1952) However this concept has arisen from findings in anesthetized vagotomized animals with surgically exposed and isolated open loop carotid sinus preparations; it is generally agreed that anesthesia as well as surgical trauma may interfere with the baroreflex response characteristics (cf Vatner and Braunwald 1975 Kirchheim 1976)

Concomitantly with the stronger pressure response to decreased transmural pressure cardiac output showed a significant 10% increase whereas no change in this variable was observed when the transmural pressure was increased Thus the difference between the magnitudes of the blood pressure responses in the two cases was associated with a change in the relative contributions of cardiac and peripheral effector mechanisms After combined cardiac effector when

any intervention on the part of the cardiac effector mechanisms was prevented the difference in magnitude between the blood pressure responses to increased and decreased transmural pressure was somewhat less evident. However the fact that the reflex blood pressure responses to changes in transmural sinus pressure were not greatly impaired in the absence of cardiac effector mechanisms indicates that these mechanisms are not of critical importance in the buffer function of the carotid sinus baroreceptors (fig 3). This conclusion is in agreement with the results of Ernesting and Parry (1967) who increased the carotid sinus transmural pressure by suction in a box enclosing the neck only. It is also concordant with the observation of Epstein et al (1969) that electrical stimulation of the carotid sinus nerve in man causes a fall in systemic arterial pressure even when cardiac output is kept constant by mild exercise and with that of Eekberg et al (1972) that the arterial pressure response to carotid sinus nerve stimulation is not affected by autonomic heart blockade.

Besides its lowering effect on the arterial pressure at carotid sinus level gravitational stress in the head-down direction produces a downward displacement of blood volume from the intrathoracic space to infracardiac veins. The reflex circulatory responses to a reduction in central blood volume without an accompanying fall in mean arterial pressure may be studied by lowering the external pressure over the lower part of the body. In the supine body position this maneuver may produce considerable pooling of blood in dependant

dent veins with little if any effect on the arterial pressure at head level (for review see Wolthuis Bergman and Nicogossian 1974) In the present experiments a level of negative pressure (80 mm Hg) was chosen that produces blood pooling of an order of magnitude comparable to that produced in the 3 G experiments It was of interest to note that 80 mm Hg of LBNP produced a more clearcut reduction in cardiac output and a less pronounced vasoconstrictor response than did exposure to 3 G (fig 2)

After propranolol tolerance to LBNP was reduced as judged from the blood pressure response i.e mean arterial pressure was significantly lower at the end of the LBNP period than it was before blockade (fig 3) This difference can be explained by the blockade of cardiac sympathetic effector mechanisms and a resulting reduction in cardiac output Although there was a more potent vasoconstrictor response to LBNP after propranolol it was not sufficient to maintain arterial pressure at the same level as before blockade This finding is notable since the exaggerated curtailment of cardiac output following exposure to 3 G after propranolol was well compensated by a concomitant rise in peripheral resistance (1) It is believed therefore that the carotid hypotension associated with exposure to increased gravitational force initiated a stronger overall sympathetic outflow than did exposure to LBNP

With combined cardiac effector blockade heart rate cardiac output and mean arterial pressure increased considerably these findings being concordant with those of other experiments concerning autonomic heart blockage in the ro-

cuscent position (Cummings and Carr 1966 Julius et al 1971 Ellis and Julius 1973 Korner et al 1973 Korner Tonkin and Uthar 1976) However following application of LBSP there was a drastic reduction in cardiac output and mean arterial pressure to the same levels as obtained during LBSP with propranolol only although the heart rate remained elevated (fig 3 and 4) These findings clearly show the dependence of the central blood volume for the capacity of the heart to increase its output by means of an increase in its rate and are in agreement with earlier results concerning atropine and LBSP (Murray and Shropshire 1970) and atropine and posture (Weissler Leonard and Warren 1957) It is thus concluded from the LBSP experiments that cardiac sympathetic effector mechanisms were essential for the maintenance of arterial pressure

In summary the present experiments on the effects of head-up tilt increased gravitational force and locally lowered carotid sinus transmural pressure have shown that cardiac effector mechanisms are not of essential importance for the reflex blood pressure regulation associated with such maneuvers In all these cases carotid sinus transmural pressure was markedly reduced On the other hand cardiac sympathetic drive may be essential for the circulatory homeostasis in conditions with reduced central blood volume such as LBSP when mean arterial pressure at carotid sinus level is only slightly affected

Effects of posture and exercise on baroreceptor-induced changes in heart rate and mean arterial pressure

There is still considerable controversy as to what extent postural changes and exercise may modify baroreflex control of heart rate and arterial pressure. When in the present experiments the carotid sinus transmural pressure was increased or decreased by negative and positive pressure on the neck respectively the ensuing heart-rate responses were markedly altered by a change in posture. Thus during head-up tilt the heart-rate response was only half that obtained in the supine position. This is in accordance with the findings of Pickering et al (1971) that the reflex bradycardia in response to a drug-induced rise of arterial pressure is decreased in the erect posture but is at variance with those of Eckberg, Abboud and Mark (1976) who reported that the decrease in heart rate evoked by negative pressure on the neck is the same in the supine and standing positions. In the latter investigation however observations were limited to the first 5 sec of suction on the neck in order to minimize cardioacceleration resulting from reduction of aortic baroreceptor activity by reflex hypotension. In the present experiments on the other hand measurements were obtained after 30 sec of negative pressure i.e. when the baroreceptor-induced reduction in mean arterial pressure was fully developed. The discrepancy between the results obtained in the two studies may thus be explained by different contributions on the part of the aortic baroreflex on the heart-rate responses.

In the present experiments it was observed that exercise reduced the G-induced cardioacceleration by nearly 50% (fig 4). Analogue results were obtained by Pickering et al (1972a) in their studies on the effects of exercise on the transient increase in heart rate in response to a drug-induced decrease in arterial pressure while Robinson et al (1966) found that the changes in heart rate that followed sustained alterations in arterial pressure were of similar magnitudes at rest and during exercise. However, whereas the changes in heart rate studied by Robinson et al (1966) and Pickering et al (1972a) were induced by alterations in arterial pressure, the G-induced acceleration of the heart is the result of central hypovolemia as well as carotid hypotension. A comparison between results obtained by the two methods is therefore only of limited relevance.

The above observed effects of posture and exercise on the heart-rate responses were not reflected in corresponding alterations in the baroreceptor-mediated changes in arterial pressure. Thus the pressor and depressor responses to positive and negative pressure on the neck respectively were as potent in the supine as in the 70° head-up position. Furthermore, the G-induced increase in mean arterial pressure was almost exactly the same before and during leg exercise (fig 3). It can be concluded therefore that the carotid baroreflex responsiveness in terms of its buffering capacity of acute changes in arterial pressure is not modified by exercise or postural shifts, even though the contribution on the part of the heart rate in the reflex response may be attenuated.

maneuvers. These findings give further support to the conclusion drawn in the previous section viz that cardiac effector mechanisms are not of essential importance for the reflex arterial pressure regulation associated with changes in the carotid sinus transmural pressure or exposure to increased gravitational force.

It was found in the present experiments that the pressor response to a threefold increase in the gravitational force was much more potent than that following positive pressure on the neck although the decrease in carotid sinus transmural pressure was essentially the same in the two situations (fig. 3). Several explanations to this discrepancy must be considered. A more potent G-induced pressor response might be expected from stronger ischemic stimulation of carotid chemoreceptors due to local reduction of perfusion pressure (cf. Landgren and Neil 1951). This seems less probable however since the perfusion pressure at the level of the carotid bodies was essentially the same in the two situations. Furthermore there is no decrease in arterial oxygen tension or increase in arterial carbon dioxide tension during exposure to 3 G (Rosenhamer 1967). The possibility must therefore be considered that the external pressure applied to the neck in study II was not completely transmitted to the walls of the carotid sinuses. However if this were to explain the entire difference in magnitude between the pressor response to 3 G and that of positive pressure on the neck respectively the external pressure must have been greatly attenuated during the transmission through the tissues of the neck to

the walls of the carotid sinuses. This appears less probable since Eckberg (1976) found that maximum reduction of the internal jugular vein pressure is nearly equal to maximum reduction in neck chamber pressure.

The validity of the comparison between exposure to 3 G and 40 mm Hg of neck pressure is based on the assumption that the intrasinus mean pressure was lowered by 40 mm Hg by the transition from 1 G to 3 G (cf fig 1). However if this pressure reduction was in reality greater the pressor response to 3 G would presumably be more potent than that obtained by 40 mm Hg of pressure on the neck. Finally changes in the carotid sinus transmural pressure produced by alterations of the external pressure on the neck will only affect the static component of the carotid baroreflex. Exposure to 3 G on the other hand also alters the dynamic component due to drainage of blood from the intrathoracic space and an ensuing decrease in pulse pressure. It is well known that alterations in intrasinus pulse pressure constitute potent stimuli to the carotid sinus baroreceptors (Ead Greer and Neil 1952, Soher and Young 1963, Gero and Gerova 1967, Angell James and Daly 1970); this may therefore form an explanation why the pressor response to 3 G was more potent than that during 40 mm Hg or neck pressure.

Relative contribution of sympathetic and parasympathetic influence in reflex heart-rate control

Although there has been considerable interest in the mechanism by which the heart rate is altered in response to

postural changes and stimulation of the baroreceptors the question concerning the relative roles of the two divisions of the autonomic nervous system in mediating these changes in conscious man has not yet been settled. When subjects were exposed to 3 G in the seated position on the centrifuge it was observed that propranolol reduced the normal response of the heart rate to increased gravitational force by 62% (fig 4). Thus G-induced cardioacceleration is predominantly but not entirely due to sympathetic stimulation. The fact that the addition of atropine raised heart rate considerably at normal gravity but only slightly at 3 G indicates that there was a considerable vagal restraint at 1 G which was almost completely withdrawn at 3 G (fig 4). When exercise was performed during exposure to 3 G the G-induced heart-rate response was almost entirely of sympathetic origin since propranolol reduced this response by no less than 92%. During exposure to LBNP propranolol reduced the reflex heart-rate response by 51%. However the addition of atropine increased heart rate considerably not only before but also during LBNP indicating the existence of strong vagal restraint even during LBNP (fig 4). It can thus be concluded that the reflex heart-rate response to a reduction in central blood volume separately or in combination with an unloading of arterial baroreceptors is of both parasympathetic and sympathetic origin the ultimate balance however being dependent on the preexisting level of background activity. The observations of a reciprocal control of the heart rate is in agreement with the findings of Glick and Braunwald (1965).

Robinson et al (1966) and Scher et al (1970) but are at variance with those of Leon Shaver and Leonard (1970) and Pickering et al (1972a) who claim that baroreceptor-induced changes in heart rate are entirely of parasympathetic origin. The last-mentioned groups studied transient effects on heart rate whereas the present results refer to effects studied over several minutes. It is well known that parasympathetic control of the heart rate is extremely fast, sympathetic control being considerably slower (Mang and Horison 1947, Warner and Cox 1962); thus the relative contributions of the two divisions of the autonomic system may not be the same for transient as for the sustained heart-rate responses.

The finding that the heart-rate responses to 3 G and LBNP were of similar magnitude whereas those following isolated changes in carotid sinus transmural pressure were much less conspicuous (fig. 4) suggests that the main component responsible for the orthostatic heart-rate control is the decrease in central blood volume, the lowering of intrasinus mean pressure being of less importance. On the other hand, intrasinus mean pressure seems to be an important factor for the vasoconstrictor response to orthostasis since the increase in total peripheral resistance was much more conspicuous following head up tilt and 3 G as compared to LBNP (see above and fig. 2).

SUMMARY

The objectives of the present investigation were to study in conscious man some of the functions of cardiovascular reflex mechanisms in certain experimental conditions viz 70° head-up tilt (II) a threefold increase of the force of gravity (I-III) bidirectional changes (± 40 mm Hg) in the pressure surrounding the neck in the supine and 70° head-up position (II) and lower body negative pressure (LENP 80 mm Hg) (IV). In this way it was possible to study different circulatory effects primarily induced by changes in the transmural pressure at the level of the carotid sinuses and by reductions in central blood volume separately or in combination.

Intraarterial pressure electronically derived mean arterial pressure heart rate and the actual G-level or the external pressure applied to the neck or the lower part of the body were recorded continuously and simultaneously. Cardiac output determinations were obtained by the dye-dilution technique. Stroke volume and total peripheral resistance were calculated from simultaneously obtained values of cardiac output and heart rate or mean arterial pressure respectively.

In order to further elucidate the contributions of cardiac effector mechanisms to the reflex effects on the circulation the above-mentioned circulatory variables were observed before and after beta-adrenergic and/or combined beta-adrenergic and parasympathetic blockade as induced by the i.v. administration

of propranolol separately or in combination with atropine

After combined cardiac effector blockade a shift from the supine to the 70° head-up position caused a greater fall in cardiac output than before blockade. However mean arterial pressure at heart level was not lowered and the exaggerated curtailment of cardiac output was therefore fully compensated by a greater increase in systemic vascular resistance.

The response of the heart rate to increased gravitational force was markedly reduced by propranolol. The impaired heart-rate response was accompanied by a more clearcut curtailment of cardiac output than occurred before blockade. In spite of this mean arterial pressure at heart level rose to the same level as before propranolol due to a more marked vasoconstrictor response after blockade. Combined cardiac effector blockade reduced the G induced arterial pressure response. This effect is discussed in terms of actions of atropine on the baroreceptor-induced vasoconstrictor response and/or on the degree of intracardiac pooling.

A decrease in carotid sinus transmural pressure produced a much stronger arterial pressure response than a corresponding increase in transmural pressure. This indicates that normally the carotid sinus reflex acts as a predominantly antihypotensive mechanism. Whereas the depressor response to increased transmural pressure was due solely to a reduction in vascular resistance, an increase in cardiac output contributed to the more potent pressor response to decreased transmural pressure. The pressor and depressor responses to changes in the transmural pressure were as potent in the supine as in the 70° head-

-up position . Combined cardiac effector blockade abolished the effect of reduced transmural pressure on cardiac output without impairing the blood pressure response

Tolerance to LBNP was reduced by beta-adrenergic blockade as judged from the exaggerated decrease in mean arterial pressure during LBNP after blockade . Combined cardiac effector blockade elevated pre-LBNP values of heart rate , cardiac output and arterial pressure as compared to values obtained after beta-adrenergic blockade alone; however tolerance to LBNP remained impaired

From the experiments on the effects of head-up tilt , increased gravitational force and locally lowered carotid sinus transmural pressure it is concluded that cardiac effector mechanisms were not of essential importance for the reflex blood pressure regulation associated with these maneuvers . In all these cases carotid sinus transmural pressure was markedly reduced . However during LBNP when mean arterial pressure at carotid sinus level is only slightly affected but the central blood volume is effectively reduced , cardiac sympathetic drive seemed to be important for the maintenance of arterial pressure

Experiments with beta-adrenergic and combined autonomic heart blockade showed that G-induced cardioacceleration was predominantly but not entirely due to sympathetic stimulation . When exercise was performed during exposure to 3 G the G induced heart-rate response was almost entirely of sympathetic origin . There was a considerable vagal restraint at 1 G at rest which was almost completely withdrawn at 3 G . The heart-rate response to LBNP was equally attributable to withdrawal of vagal tone and

increase in sympathetic drive a considerable vagal restraint still remaining in this condition. From these findings it is concluded that the reflex heart-rate response to a reduction in central blood volume separately or in combination with an unloading of arterial baroreceptors is of both parasympathetic and sympathetic origin the ultimate balance being dependent on the preexisting level of background activity.

REFERENCES

- AMBACHE N The use and limitations of atropine for pharmacological studies on autonomic effectors *Pharmacol Rev* 1955 7 467-494
- ANGELL JAMES J E and M de B DALY Comparison of the reflex vasomotor responses to separate and combined stimulation of the carotid sinus and aortic arch baroreceptors by pulsatile and non-pulsatile pressure in dog *J Physiol (Lond)* 1970 209 257-293
- BEISER G D R ZELIS S E EPSTEIN D T MASON and E BRAUNWALD The role of skin and muscle resistance vessels in reflexes mediated by the baroreceptor system *J Clin Invest* 1970 49 225-231
- BEVEGÅRD S B and J T SHEPHERD Circulatory effects of stimulating the carotid arterial stretch receptors in man at rest and during exercise *J Clin Invest* 1966 45 132-142
- BJURSTEDT H G ROSENHAMER and O WIGERTZ High-G environment and responses to graded exercise *J Appl Physiol* 1968 25 713-719
- BJURSTEDT H L -E HANSSON and G STRÖM Electrocardiographic heart-rate and subjective responses to prolonged gravitational stress and their relation to some dimensional and functional parameters of the circulatory system *Acta Physiol Scand* 1959 47 97-108
- BLOOMFIELD D A and E SOMTON Rate-independent effects of propranolol The differentiation between chronotropic inotropic and peripheral vascular responses *Circulat Res* 1967 20 Suppl III 243-247

BRICK I W E GLOVER K J HUTCHISON and I C RODDIE Effects of propranolol on peripheral vessels in man Am J Cardiol 1966 18 329-332

BROWN E J S GOEI A D M GREENFIELD and H C PLASSARAS Circulatory responses to simulated gravitational shifts of blood in man induced by exposure of the body below the iliac crests to subatmospheric pressure J Physiol (Lond) 1966 183 607-627

CHRISTEN A B FOLKOW G GRIMBY E -A HANBERGER and O THULESIUS Cardiovascular effects of direct stimulation of the carotid sinus nerve in man Acta Physiol Scand 1958 44 138-145

CHAMBERLAIN D A P TURNER and J W SWEDOM Effects of atropine on heart-rate in healthy man Lancet 1967 2 12-15

COLE D R Observations on the Responses of Human Blood Vessels to Local Alterations in Transmural Pressure (Dr Med Thesis) Bristol Ireland: University of Bristol 1956

COXING G R and W CARR Hemodynamic response to exercise after beta-adrenergic and parasympathetic blockade Can J Physiol Pharmacol 1967 45 813-819

CURRIST M F and K OMOSU AKEOMAR Effect of M&B 17803A a new beta-adrenoceptor blocking agent on the cardiovascular responses to tilting and to isoprenaline in man Brit. J Pharmacol 1971 43 639-648

DE GEEST H M M LEVY and H SIESEKE Carotid sinus baroreceptor reflex effect upon myocardial contractility Circulation Res 1964 15 327-341

DOMOSO E L J COHEN B J NEMMON N S BLOOM W C STEIN and C K FRIEDBERG Effects of propranolol on patients with atrial heart block and implanted pacemakers Circulation 1967 36 534-538

- EAD H W J H GREEN and E NEIL A comparison of the effects of pulsatile and non-pulsatile blood flow through the carotid sinus on the reflexogenic activity of the sinus baroreceptors in the cat J Physiol (Lond) 1952 118 509-51
- ECKBERG D L Temporal response patterns of the human sinus node to brief carotid baroreceptor stimuli J Physiol (Lond) 1976 258 769-782
- ECKBERG D L F M ABBOUD and A L MARK Modulation of carotid baroreflex responsiveness in man: effects of posture and propranolol J Appl Physiol 1976 41 383-387
- ECKBERG D L M B CAVANAUGH A L MARK and F M ABBOUD A simplified neck suction device for activation of carotid baroreceptors J Lab Clin Med 1975 85 167-173
- ECKBERG D L G F FLETCHER and E BRAUNWALD Mechanism of prolongation of the R-R interval with electrical stimulation of the carotid sinus nerves in man Circulat Res 1972 30 131-138
- EGER E I Atropine scopolamine and related compounds Anesthesiology 1962 23 365-383
- ELLIS C N and S JULIUS Role of central blood volume in hyperkinetic borderline hypertension Brit Heart J 1973 35 450-453
- EPSTEIN S E G D BEISER E E GOLDSTEIN M STAMPPER A S WECHSLER G GLICK and E BRAUNWALD Circulatory effects of electrical stimulation of the carotid sinus nerves in man Circulation 1969 40 269-276
- EPSTEIN S E B F ROBINSON R L KAWLER and E BRAUNWALD Effects of beta-adrenergic blockade on the cardiac response to maximal and submaximal exercise in man J Clin Invest 1965 44 1745-1753
- ERNSTING J and D J PARRY Some observations on the effects of stimulating the stretch receptors in the carotid artery of man J Physiol (Lond) 1957 137 45-46P

- FAKREH C Cardiovascular effects of carotid sinus nerve stimulation in resting man Chest 1972 61 121-124
- FISHER R A Statistical Method for Research Workers 10th Ed Edinburgh Oliver and Boyd Ltd 1948 354 pp
- FULKOW H Nervous control of the blood vessels Physiol Rev 1955 35 629-663
- FULKOW B C HEYMANS and E NEIL Integrated aspects of cardiovascular regulation In Handbook of Physiology Circulation Washington D C Am Physiol Soc 1965 Sect 2 III 1787-1823
- FUCCILLA L M J REBAN P BASSINI E LATTES and V MORDELLI Effect of two new beta-blocking drugs on heart rate and blood pressure during passive tilting in man Europ J Clin Pharmacol 1971 4 12-17
- GAUER O H and H L THROM Postural changes in the circulation In: Handbook of Physiology Circulation Washington D C Am Physiol Soc 1965 Sect 2 III 2409-2439
- GAUER O H and G D ZUIDENHA Gravitational Stress in Aerospace Medicine Boston Little Brown & Co 1961 278 pp
- GERO J and M GEROVA Significance of the individual parameters of pulsating pressure in stimulation of baroreceptors In Baroreceptors and Hypertension Ed by D Kozdi Perzson Press Ltd 1967 17-30
- GIBSON D G pharmacodynamic properties of beta-adrenergic receptor blocking drugs in man Drugs 1974 7 8-38
- GILBERT C A and P M STEVENS Forearm vascular responses to lower body negative pressure and orthostasis J. Appl Physiol 1966 21 1266-1272
- GLICK G Importance of the carotid sinus baroreceptors in the regulation of myocardial performance J Clin Invest 1971 50 1116-1123
- GLICK E and K BRAUNNOLD Relative roles of the sympathetic and para sympathetic nervous system in the reflex control of heart rate Circulat Res 1965 16 363-375

- GREENFIELD A H M E BROWN J S GOBI and G E PLASSARAS
Circulatory responses to abrupt release of blood accumulated in the legs *Physiologist* 1963 6 191
- HENRY J H The significance of the loss of blood volume into the limbs during pressure breathing *J Aviation Med* 1951 22 31-38
- HENRY J P and J P MEEHAN The Circulation An Integrative Physiologic Study Year Book Med Publ Inc 1971 208 pp
- HERING H E Der Karotiedruckversuch *Munch Med Wochschr* 1923 70 1287-1290
- HEYMANS C and E NEIL Reflexogenic Areas of the Cardiovascular System London J & A Churchill Ltd 1958 271 PP
- HIGGINS C B S F VAITNER and H BRAUNWALD Parasympathetic control of the heart *Pharmacol Rev* 1973 25 119-155
- HOWARD P The physiology of positive acceleration In: A Textbook of Aviation Physiology Pergamon Press Edited by J A Gillies 1965 551-687
- JOHNSON G The effects of intraarterially administered propranolol and H 56/28 on blood flow in the forearm - a comparative study of two beta-adrenergic receptor antagonists *Acta Pharmacol Toxicol* 1967 25 Suppl 2 63-74
- JOSE A H and H G TAYLOR Autonomic blockade by propranolol and atropine to study intrinsic myocardial function in man *J Clin Invest* 1969 48 2019-2031
- JULIUS S A V PASCUAL R SANNERSTEDT and E MITCHELL Relationship between cardiac output and peripheral resistance in borderline hypertension *Circulation* 1971 43 382-390
- KALSER H H E W FRYE and A S GORDON Postural hypotension induced by atropine sulfate *Circulation* 1954 10 413-422
- KINSMAN J M J W MOORE and W F HAMILTON Studies on the circulation I Injection method Physical and mathematical considerations *Am J Physiol* 1929 89 322-330

- KIRCHHEIM H R Systemic arterial baroreceptor reflexes
Physiol Rev 1976 56 100-177
- KORNER P I Integrative neural cardiovascular control Physiol Rev 1971 51 312-367
- KORNER P I J SHAW J B UTHER M J WEST R J McRITCHIE and J G RICHARDS Autonomic and non-autonomic circulatory components in essential hypertension in man Circulation 1973 48 107-117
- KORNER P I A M TOMKIN and J B UTHER Reflex and mechanical circulatory effects of graded Valsalva maneuvers in normal man J Appl Physiol 1976 40 434-440
- LANDGREN S and E MEIL Chemoreceptor impulse activity following haemorrhage Acta Physiol Scand 1951 23 158-167
- LEON D F J A SHAVER and J J LEONARD Reflex heart rate control in man Am Heart J 1970 80 729-739
- LEVINSON G E M J FRANK and H K HELLEMS The pulmonary vascular volume in man Measurement from atrial dilution curves Am Heart J 1964 67 734-741
- LEVINSON G E A D PACIFICICO and M J FRANK Studies of cardiopulmonary blood volume Measurement of total cardiopulmonary blood volume in normal human subjects at rest and during exercise Circulation 1966 33 347-356
- LINDSTROM Z P W F SUTTERER H W MARSHALL R W HEDLY and E H WOOD Measurement of cardiac output during headward acceleration using the dye-dilution technique Aero space Med 1960 31 817-834
- LINDSTROM B O WIGERTZ and Th ÖDMAN A beat-to-beat heart-rate meter with linear analog output for muscular exercise studies Report Lab Aviat Med Naval Med Karol Inst Stockholm Dec 1969 23 pp
- LINDBLASS H and E ROSENHAMER Exercise and arterial pressure during simulated increase of gravity Acta Physiol Scand 1968 74 50-57

- GREENFIELD A D M E BROWN J S GOEI and H C PLASSARAS
Circulatory responses to abrupt release of blood accumulated in the legs *Physiologist* 1963 6 191
- HENRY J P The significance of the loss of blood volume into the limbs during pressure breathing *J Aviation Med* 1951 22 31-38
- HENRY J P and J E MEEHAN The Circulation An Integrative Physiologic Study Year Book Med Publ Inc 1971 208 pp
- HERING H E Der Karotiedruckversuch *Münch Med Wochschr* 1923 70 1287-1290
- HEYMAES C and E NEIL Reflexogenic Areas of the Cardiovascular System London J & A Churchill Ltd 1958 271 pp
- HIGGINS C B S F VATNER and E BRAUNWALD Parasympathetic control of the heart *Pharmacol Rev* 1973 25 119-155
- HOWARD F The physiology of positive acceleration In: *A Textbook of Aviation Physiology* Pergamon Press Edited by J A Gillies 1965 551-687
- JOHANSSON G The effects of intraarterially administered propranolol and H 56/28 on blood flow in the forearm - a comparative study of two beta-adrenergic receptor antagonists *Acta Pharmacol Toxicol* 1967 25 Suppl 2 63-74
- JOSE A D and R G TAYLOR Autonomic blockade by propranolol and atropine to study intrinsic myocardial function in man *J Clin Invest* 1969 48 2019-2031
- JULIUS S A V PASCUAL R SANHERSTEDT and C MITCHELL Relationship between cardiac output and peripheral resistance in borderline hypertension *Circulation* 1971 43 382-390
- KALSER M H C W FRYE and A S GORDON Postural hypotension induced by atropine sulfate *Circulation* 1954 10 413-422
- KILMAN J H J W MOORE and W F HAMILTON Studies on the circulation I: Injection method; Physical and mathematical considerations *Am J Physiol* 1929 89 322-330

FERMUTT S and R L RILEY Haemodynamics of collapsible vessels with tone: the vascular waterfall J Appl Physiol 1963 18 924-932

FASTOV I D and S J GERATHEWOHL Weightlessness In: Foundations of Space Biology and Medicine U S Government Printing Office Edited by M Calvin and O G Gaxenko 1975 II:1 305-354

PICKERING T G B GRIBBIN E S PETERSEN D J C CUNNINGHAM and P SLEIGHT Comparison of the effects of exercise and posture on the baroreflex in man Cardiovasc Res 1971 5 582-586

PICKERING T G B GRIBBIN E S PETERSEN D J C CUNNINGHAM and P SLEIGHT Effects of autonomic blockade on the baroreflex in man at rest and during exercise Circulat Res 1972a 30 177-185

PICKERING T G B GRIBBIN and P SLEIGHT Comparison of the reflex heart rate response to rising and falling arterial pressure in man Cardiovasc Res 1972b 6 277-283

PRICE H L L H COOPERMAN and J C WARDEN Control of the splanchnic circulation in man Circulat Res 1967 21 333 340

REED J H Jr and E H WOOD Use of dichromatic earpiece densitometry for determination of cardiac output J. Appl. Physiol 1967 23 373-380

ROBINSON B F E E EPSTEIN G D REISER and E BRAUNWALD Control of heart rate by the autonomic nervous system Circulat Res 1966 19 400-411

RODDIE I E and J T SHEPHERD The effects of carotid artery compression in man with special reference to changes in vascular resistance in the limbs J Physiol (Lond) 1957 139 377-384

RODDIE I C and J T SHEPHERD Nervous control of the circulation in skeletal muscle Brit Med Bull 1963 19 115 119

- ROSENHAMER G Influence of increased gravitational stress on the adaptation of cardiovascular and pulmonary function to exercise Acta Physiol Scand 1967 Suppl 267
- ROSENHAMER G Remote-controlled injection system for repeat dye-dilution studies Scand J Clin Lab Invest 1968 21 347-350
- ROWELL L H J R DETRY J R BLACKMON and C WYSS T of the splanchnic vascular bed in human blood pressure regulation J Appl Physiol 1972 32 213-220
- SAMUELOFF S L M L BROWSE and J T SHEPHERD Response of capacity vessels in human limbs to head up tilt and suction on lower body J Appl Physiol 1966 21 47-54
- SANNERSTEDT R S JULIUS and J CONWAY Hemodynamic response to tilt and beta-adrenergic blockade in young patients with borderline hypertension Circulation 1970 42 1057-1064
- SARNOFF E J J P GILMORE S K BROCKMAN J H MITCHELL and R J LINDEN Regulation of ventricular contraction by the carotid sinus: its effect on atrial and ventricular dynamics Circulat Res 1960 8 1123-1136
- SCHENNETTEN F P W Die orthostatisch bedingten Kreislaufumstellungen in ihrer Auswirkung auf Puls Blutdruck und Ekg und ihre Beeinflussung durch Atropin Arch Kreislauff 1943 11 326-372
- SCHER A M W W OHM F BUNGARNER R BOYNTON and A C YOUNG Sympathetic and parasympathetic control of heart rate in the dog baboon and man Fed Proc 1972 31 1219-1225
- SCHER A M and A C YOUNG Servoanalysis of carotid sinus reflex effects on peripheral resistance Circulat Res 1963 12 152-162
- SCHNEIDER K W von A CHEIKHZADEH und W MÜLLER Die Bestimmung des Herzenminutenvolumens mit einem dichromatischen Ohrdensitometer und vereinfachter Berechnung durch Computer Cardiologia (Basel) 1967 51 349-358

SJÖSTRAND T Volume and distribution of blood and their significance in regulating the circulation Physiol Rev 1953 33 202-228

SOMMERBLICK E H E BRAUNWALD J F WILLIAMS and E GLICK Effects of exercise on myocardial force-velocity relations in intact unanesthetized man: relative roles of changes in heart-rate sympathetic activity and ventricular dimensions J Clin Invest 1965 44 2051-2062

SPODICK H H M B MEYER and J R St PIERRE The effect of beta adrenergic blockade on cardiac responses to orthostatic stress Am Heart J 1972 83 719-722

STEGEMANN J A BUSERT and E BROCK Influence of fitness on the blood pressure control system in man Aerospace Med 1974 45 45 48

STEVENS P H and L E LAMB Effects of lower body negative pressure on the cardiovascular system Am J Cardiol 1965 16 506-515

THOM H L W BRECHMAN J WAGNER and K KELLER Quantitative Untersuchungen über die Bedeutung der Gefäßdehnungsrezeptoren im Rahmen des Kreislaufhomeostase beim wachen Menschen Pflügers Arch ges Physiol 1967 293 68-99

UVKES B Cholinergic vasodilator innervation to skeletal muscles Circulat Res 1967 20 Suppl 1 83-90

VATNER S F and E BRAUNWALD Cardiovascular control mechanisms in the conscious state N. Engl J. Med 1975 293 970 976

WAGNER J J WACKERBAUER und H H HILGER Arterielle Blutdruck- und Herzfrequenzverhalten bei Hypertonikern unter Änderung des transmuralen Druckes in Karotissinusbereich Kreislauff 1968 57 701 712

WALLOREN C G J S HANSON G KRETSCHEMAR and P LITVINOVICH Validity of dichromatic earpiece densitometry for pulse rate studies in children with shunt free cardiovascular malformations Acta paediat Scand 1975 Suppl 254 1-6

- WANG S C and H L BORISON An analysis of the carotid sinus cardiovascular reflex mechanism Am J Physiol 1947 150 712-721
- WARNER H R and A COX A mathematical model of heart rate control by sympathetic and vagus efferent information J Appl Physiol 1962 17 349-355
- WEISSLER A M J J LEONARD and J V WARREN Effects of and atropine on the cardiac output J Clin Invest 1957 36 1656-1662
- WOLTHUIS R A S A BERGMAN and A E NICOGLOSSIAN Physiologic effects of locally applied reduced pressure in man (in Rev 1974 54 566-595
- WOLTHUIS R A S W BOFFLER and R L JOHNSON Lower body negative pressure as an assay technique for orthostatic tolerance: I The individual response to a constant level (-40 mm Hg) of LBNP Aerospace Med 1970 41 30-35

PLASMA CHOLINE AND
CHOLINERGIC MECHANISMS
IN THE BRAIN

METHODS FUNCTION AND RÔLE
IN HUNTINGTON'S CHOREA

BY
SVEN-ÅKE ECKERNÄS

Acta Physiologica Scandinavica Supplementum 449

From the Department of Pharmacology Faculty of Pharmacy
University of Uppsala, Biomedical Center
Box 573, S-751 23 Uppsala, Sweden
and

Department of Neurology University Hospital, University of
Uppsala, Fack, S-750 14 Uppsala, Sweden

PLASMA CHOLINE AND CHOLINERGIC MECHANISMS IN THE BRAIN

METHODS FUNCTION AND RÔLE
IN HUNTINGTON'S CHOREA

BY
SVEN ÅKE ECKERNAS

UPPSALA 1977

To Annika

5.2.1 Regional distribution of ChAT in human brain	34
5.3 Some well established central cholinergic tracts	35
5.4 Interaction of cholinergic neurons with other neuronal systems in extrapyramidal nuclei	38
6. Huntington's Chorea	41
6.1 Introduction	41
6.2 Role of different transmitter systems	41
6.2.1 Cholinergic system	41
6.2.2 Catecholaminergic system	41
6.2.3 GABA-ergic system	42
6.2.4 Conclusion	42
6.3 Different therapeutic approaches	43
6.3.1.1 Cholinesterase inhibitors	43
6.3.1.2 Choline	43
6.3.1.3 2 Dimethylaminoethanol	45
6.3.2 Drugs affecting the monoaminergic system	46
6.3.3 Drugs affecting the GABA-ergic system	47
6.4 Early detection	47
7 General Summary	48
8 Acknowledgements	49
9 References	50

The present survey is based on the following papers, which will be referred to by their Roman numbers.

- I Aquilonius, S-M, and Eckernäs, S Å (1976) Cortical and striatal *in vivo* uptake and metabolism of plasma choline in the rat: Effect of haloperidol and apomorphine. *Acta Pharmacol. Toxicol. (Kbh)* 39 129-140.
- II Eckernäs, S-Å, and Aquilonius, S-M (1977) Free choline in human plasma analyzed by a simple radioenzymatic procedure: Age distribution and effect of a meal. *Scand. J. Clin. Lab. Invest.* In press.
- III Eckernäs, S Å, and Aquilonius, S-M (1977) A simple radioenzymatic procedure for the determination of choline and acetylcholine in brain regions of rats sacrificed by microwave irradiation. In manuscript.
- IV Eckernäs, S-Å, Sahlström, L., and Aquilonius, S-M (1977) *In vivo* turnover rate of acetylcholine in rat brain parts at elevated steady state concentration of plasma choline. In manuscript.
- V Aquilonius, S-M, Eckernäs, S Å, and Sundwall, A (1975) Regional distribution of choline acetyltransferase in human brain. Changes in Huntington's chorea. *J. Neurol. Neurosurg. Psychiat.* 38 669-677.
- VI Aquilonius, S-M, and Eckernäs, S-Å (1977): Choline therapy in Huntington's chorea. *Neurology (Minneapolis)* In press.
- VII Aquilonius, S-M and Eckernäs, S Å (1976) Choline acetyltransferase in human cerebrospinal fluid. Non-enzymatically and enzymatically catalysed acetylcholine synthesis. *J. Neurochem.* 27.317-318.

Preface

About six blind men of Indostan who approached an elephant for the first time-

First blind man falling against the elephant's side

"God bless me! but this elephant

Is very like a wall"

Second blind man feeling the tusk

"This wonder of an elephant

Is very like a spear"

Third blind man grasping the squirming trunk

I see quoth he "the elephant

Is very like a snake

The fourth blind man clasping the knee

"This is clear enough the elephant

Is very like a tree

The fifth blind man catching the ear

"This marvel of an elephant

Is very like a fan

The sixth feeling the swinging tail.

I see quoth he the elephant

Is very like a rope

And so these men of Indostan

Disputed loud and long

Each in his own opinion

Exceedingly stiff and strong

Though each was partly in the right

And all were in the wrong

(William Shenstone 1714-1763)

1 A Short History of Cholinergic Biology

The origin of cholinergic biology can be traced back to the experiments by Hunt and Taveau (1906), in which the physiological effects of different choline analogues were examined. They observed that the most potent vasodepressor analogue was the acetyl derivative acetylcholine (ACh).

In 1914 Sir Henry Dale suggested that ACh was a substance of importance for the function of the peripheral nervous system and in 1929 were Dale and Dudley able to isolate ACh from mammalian tissue.

A pupil of Dale, Dikshit, was to my knowledge the first to suggest, on experimental grounds, that ACh had a function as a transmitter substance in the central nervous system (CNS) also (Dikshit 1934). However convincing data were sparse for a long time, but it became more and more generally accepted that ACh was in fact a transmitter in the CNS (Feldberg 1945).

The final identification of ACh in mammalian brain had to await the application of gas chromatography in combination with mass spectrometry (Hammar et al. 1968).

During the last few years there has been a rapid acceleration in the development of new methods for Ch and ACh determination, as well as for sacrifice of animals, turnover calculations, mapping of cholinergic structures within the brain, subcellular fractionating, determination of ACh release, stereotaxic intracerebral application of drugs, and neurophysiological methods for intracerebral stimulation and recording. In combination with neuropharmacological experiments these advances have almost dramatically increased our knowledge of the importance of the central cholinergic mechanisms.

2 Determination of Ch and ACh

2.1 Bioassay

Up to the end of the 1960's bioassay was the only method available for determination of ACh in the small quantities present in most tissues and tissue perfusates. Some of these assays are very sensitive, but the selectivity is always questionable to some degree since it is well known that other endogenous substances (for example serotonin and histamine) will also result in a biological response. In pharmacological experiments drugs will be present, mostly in unknown concentrations, in the test solutions and may increase or decrease the biological response (Hamm and Jenden 1966). Only when the specificity is carefully controlled can bioassay be used with success.

2.2 Radioisotopic Procedures

All radioisotopic methods for determination of Ch and ACh are based on the enzymatic conversion of Ch to a radioactive product whose activity is measured after isolation. The methods began with the development of sensitive radioenzymatic techniques for Ch determination (Smith and Saelens 1967 Schubert et al. 1969 Ewetz et al. 1969) and these principles were originally applied to ACh measurement by Feigenson and Saelens (1969). The different steps in existing radioenzymatic methods are summarized below:

A Separation of Ch and ACh

- Electrophoretically (Feigenson and Saelens 1969)
- Enzymatic conversion of Ch to phosphorylcholine (Goldberg and McCaman 1973 Shea and Aprison 1973)
- Separation not needed (Massarelli et al. 1976 Paper III).

B Hydrolysis of ACh

- Base (Feigenson & Saelens 1969 Massarelli et al. 1976).
- Acetylcholinesterase (AChE Goldberg & McCaman 1973 Paper III).

C Conversion of Ch to radioactive product

- Choline acetyltransferase (ChAT): Ch $\xrightarrow[\text{ChAT}]{\text{labelled Acetyl}}$ 3-labelled ACh (Feigenson & Saelens 1969 Papers II and III Massarelli et al. 1976).
- Choline phosphokinase: Ch $\xrightarrow[\text{choline phosphokinase}]{\text{P, } ^{32}\text{P}}$ ^{32}P phosphorylcholine (Ewetz et al. 1969 Red et al. 1971).

D Separation of labelled precursor from product

- a) Electrophoretically (Feigenson & Saelens 1969).
- b) Liquid cation-exchange chromatography (Shea & Aprison 1973)
- c) Column anion-exchange chromatography (Reid et al. 1971).
- d) Ion-pair extraction, with K_2HgI_4 in heptanone-(3) (Paper II) with tetraphenylboron (Fonnum 1969) in butenitrile (Shea & Aprison 1973) with tetraphenylboron in acetonitrile/toluene (Fonnum 1975 Paper III) with tetraphenylboron in diisobutylketone (Massarelli et al. 1976).

2.3 Gas Chromatographic Procedures

Several gas chromatographic procedures for Ch and ACh determination have been described (Jenden et al. 1968 Hammar et al. 1968 Hanin et al. 1970 Hanin & Skinner 1975 Sallagy et al. 1972). The most specific of all methods for assaying Ch and ACh is probably the application of gas chromatography in combination with mass spectrometry (Hammar et al. 1968 Hanin & Skinner 1975), but in view of the extreme cost of such equipment it cannot be expected to come into use as a routine instrument in most laboratories.

2.4 Other Methodological Approaches

Several other methods for Ch and ACh determination have been described (see Hanin 1974) for example: a) Polarographic (Maslova 1964) b) Photometric (Schumacher & Ehl 1970 Elsborg & Persson 1971a,b c) Fluorometric (Fellman 1969) d) Ion pair partition chromatography (Ulin et al. 1976). None of these methods have yet been of any great importance for the recent development of cholinergic biology

2.5 Methods Used in Present Studies

2.5.1 Bioassay of ACh

In study I a strip of the dorsal muscle of the leech was used in a microbath (Szerb 1961) for the determination of ACh. As pointed out earlier the specificity of the analytical method had to be checked in several ways

- a) When known amounts of ACh were added to the tissue extracts no potentiation or inhibition occurred.
 - b) Extracts treated with alkali (pH 11–12) had no biological effect.
 - c) Addition of drugs (haloperidol and apomorphine) to extracts did not result in any potentiation or inhibition of the biological response to ACh.
 - d) Some aliquots of brain extracts analysed by gas chromatography/mass spectrometry gave values similar to those obtained for bioassayed aliquots.
- The bioassay procedure had a very low capacity however, and further the

progress of our work seemed to be more and more dependent upon a good leech season in Hungary. This inspired us to develop a radioenzymatic method for Ch and ACh assay (Papers II and III see below).

2.5.1.1 Results and discussion. As the experiments in study I were performed before the introduction of microwave irradiation for the stabilization of Ch and ACh levels, the endogenous values of ACh are considerably lower than those obtained in subsequent studies, in which the animals were killed by microwave irradiation (Paper III see below). This is probably due to rapid postmortal hydrolysis of an AChE-sensitive ACh pool (see Nordberg 1977). The levels of endogenous ACh obtained in study I are of the same magnitude (cortex 10 nmol g^{-1} striatum 29 nmol g^{-1}) as those reported earlier by other authors using decapitation or near-freezing methods to kill the animals (for review of all ACh concentrations in rat and mouse brains published earlier see Saelens and Sunke 1976).

2.5.2 Determination of free Ch in plasma (Paper II)

In study II a simple and rapid assay system for plasma Ch based on radioenzymatic determination in an ultrafiltrate was applied in an investigation on healthy volunteers.

2.5.2.1 Ultrafiltration of plasma The concentration of free Ch increased, probably due to an enzymatic process, when plasma and blood were left at room temperature. In plasma and blood kept at $+4^{\circ}\text{C}$ and in a protein-free ultrafiltrate of plasma kept at 22°C no increase in Ch concentration was detected (Fig. 1). Thus, rapid cooling of blood after venepuncture, followed by ultrafiltration of the plasma, seemed to be a good way to obtain a stable plasma sample for further processing. An increase in Ch concentration has also been found to occur in plasma from experimental animals (Wang and Haubrich 1975; Spanner et al. 1976). Spanner et al. (1976) used formic acid/acetone extraction of the precooled plasma sample to obtain a stable value. This method seems to be useful for that purpose, but it is very time-consuming. However the plasma concentrations obtained in their study (Spanner et al. 1976) are extremely low ($\sim 0.8 \text{ nmol ml}^{-1}$ in human plasma). The reason for this seems to be unexplainable at present. Wang and Haubrich (1975) boiled plasma for 15 min in an attempt to get stable Ch values. This method is rapid, but as shown in paper II it seems to result in significantly higher values than those obtained with the ultrafiltration procedure probably due to a rapid initial release of Ch from Ch-containing compounds. Ultrafiltration of plasma, on the other hand, separates low molecular weight Ch-containing compounds from the enzymes catalyzing the Ch liberation without any increase in temperature or changes in other physical properties. The concentration of Ch in the ultrafiltrate probably corresponds to free Ch of plasma, which equilibrates physiologically with other Ch compartments in the body.

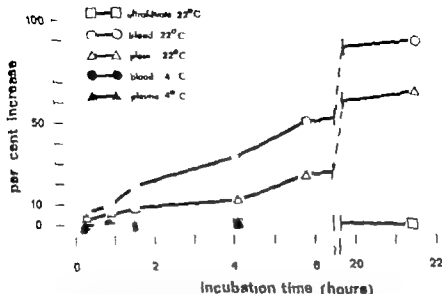


Fig. 1 Choline concentration in ultrafiltrate, blood and plasma left for different times at room temperature (22°C) and at 4°C. The curves of ultrafiltrate (22°C), blood and plasma at 4°C are superimposed in the time interval 0-4 (from Paper II).

Table 1 Choline concentration in ultrafiltrate / human plasma (nmol/l mean \pm S.E.M.)

Group	8 a.m. fasted 10-14 hrs	Confidence limits 95 %	1 p.m. (one hr after meal)	Confidence limits 95 %
Children (4-11 years, 3 d. 59)	9.7 \pm 0.6 n = 8	8.3 - 11.1	xxx 12.1 \pm 0.3 - 8	11.4 - 12.8
Adults (24-57 years, 5 d. 59)	9.7 \pm 0.6 n = 10	8.3 - 10.9	xx 11.0 \pm 0.5 n = 10	9.7 - 12.2
Adults (70-74 years, 3 d. 29)	12.5 \pm 0.3 n = 5	11.7 - 13.6	11.5 \pm 0.9 n = 5	9.1 - 13.9
Mean 11 d. 129	10.6 \pm 0.4 n = 23	9.6 - 11.4	xx 11.5 \pm 0.3 23	10.8 - 12.2

Significantly different (xx $p < 0.01$ x $p < 0.001$ Student's paired t -test) from fasted Ch value (8 a.m.)

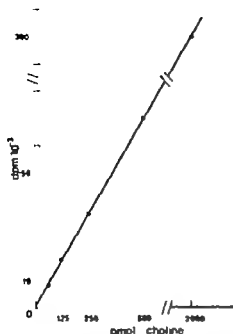


Fig. 2 A typical standard curve used in Ch determination. Each point represents the mean of two determinations. S.E.M. at each point is less than 2% of the mean $r = 0.99$ $k = 1500 \pm 2\%$ (\pm S.D.) (from paper III).

2.5.2.2 Results and discussion. Using two determinations at five different Ch concentrations as standards, the detection limit of Ch in a typical standard curve (fig. 2) at a 95 % confidence level (Hubaux and Vos 1970) is about 25 pmol.

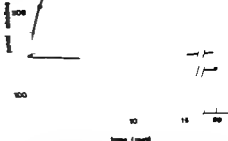
The plasma Ch concentrations in healthy fasting volunteers lay within narrow limits (mean $10.6 \mu\text{mol/l}$). A small but significant increase was noted one hour after a meal ($11.5 \mu\text{mol/l}$) (Table I). The concentration range was similar to that reported in an early investigation by Bligh (1952), who used a bioassay technique for Ch determination.

In three newborn infants the free Ch concentration in plasma (obtained from the umbilical vein) was about double ($24.5 \mu\text{mol/l}$) that in older children and adults. No explanation can be given for this as yet but it is known that the placenta is extremely rich in ACh and the cholinergic enzymes ChAT and AChE (Savory et al. 1976).

2.5.3 Determination of Ch and ACh in rat brain parts (Paper III)

This paper describes a modification of the previously used radioenzymatic procedure for Ch and ACh determination (Feigenson and Saelens 1969 Goldberg and McCaman 1973 Shea and Aprison 1973). After ion pair extraction of the ^1C ACh formed, using tetraphenylboron (Kalignost[®]), directly in the scintillation vial (Foomum 1975), radioactivity is measured by liquid scintillation counting. In one aliquot of a brain extract endogenous ACh is specifically hydrolyzed by

Fig. 3 Free Ch following incubation with acetylcholine esterase (AChE) for different times at 37°C, pH=8. ●—● stratal homogenate; ▼—▼ a solution containing 2000 pmol phosphorylcholine and 200 pmol Ch; □—□ stratal homogenate with no AChE added (from paper III).



means of AChE (Fig. 3) and the total Ch content of the sample is determined. The content of endogenous Ch is measured in an unhydrolyzed aliquot and the ACh level is then obtained as the difference in Ch content between the two aliquots.

2.5.3.1 Microwave irradiation for stabilizing Ch and ACh levels Since the Ch and ACh concentrations in brain change extremely rapidly *post mortem* (Ewetz et al. 1969, Scheiberth et al. 1970, Dross and Kewitz 1972, Nordberg 1977a), it is necessary to use a technique which quickly inactivates the enzymes responsible for these changes. This can be done by rapid heating of the brain by microwave irradiation (Stavinoha et al. 1973, Butcher and Butcher 1974a, Guidotti et al. 1974, Schmidt 1976, Nordberg and Sundwall 1976, Nordberg 1977a). It has been shown that a temperature of 80–85°C is sufficient to inactivate brain AChE and ChAT and thereby eliminate *post mortem* alterations in ACh steady state levels (Schmidt et al. 1972, Schmidt 1976, Stavinoha et al. 1974, Nordberg and Sundwall 1976, Nordberg 1977). However, as shown by Schmidt (1976) a brain temperature of about 95°C must be attained in order to halt the *post mortem* increase in Ch concentration in rat brain. This indicates that the enzyme(s) responsible for producing *post-mortem* increases in Ch are more heat stable than both AChE and ChAT. In studies III and IV a beam of microwave (5kW, 2450 MHz) was focused on the rats' heads for 1.7 s. This resulted in a homogenous brain temperature of about 95°C. However, the possibility cannot be ruled out that changes still take place during the irradiation period or during the time while the animals are being restrained immediately before death. A "stress-free" method of killing cannot be achieved at present (if ever).

2.5.3.2 Results and discussion The radioenzymatic method described in Paper III was found to be a rapid (120 samples/day) and simple procedure for the measurement of Ch and ACh concentrations in small parts of brain tissue. The detection limit of a typical standard curve at a 95 % confidence level (Haubeux

Table II Recently published values for Ch and ACh concentration in rats and mice sacrificed by microwave irradiation

Analytical procedure	Authors	Cortex		Striatum	
		Ch	ACh nmol/g \pm S.E.M.	Ch	ACh
Radioenzymatic	Present paper	23 \pm 2.5 n = 18	16 \pm 1.0 n = 18	33 \pm 1.2 n = 23	76 \pm 2.4 n = 23
	Flisbrich et al. 1975	17	14	29	83
Gas chromatography	Wachtlaub et al. 1976	—	16	—	64
	Raceps et al. 1976	—	—	39	51
	Modak et al. 1976 ^a	—	26	—	81
	Schmidt 1976	28	28	32	64
Gas chromatography/ mass spectrometry	Butcher and Butcher 1974	—	—	27	98
Biossary	Nordberg and Sundwall 1977 ^a	31	24	41	74

Mice

and Vos 1970) is about 25 pmol (Fig. 2). The calculation of ACh concentration as the difference in Ch concentration between a hydrolyzed and an unhydrolyzed aliquot obviates the separation of Ch from ACh by chromatography or electrophoresis, which are time-consuming procedures that sometimes do not give complete separation of the two compounds. The extraction procedure for ACh described by Fonnum (1975), where ^3H ACh is separated from ^3H -acetyl-CoA directly in the scintillation vials prior to liquid scintillation counting, was found to be very convenient and rapid. The partial purification of ChAT takes one day and results in an enzyme batch for more than 4000 determinations. The endogenous Ch and ACh concentrations obtained in study I are in close agreement with those reported by other authors using microwave irradiation for killing the animals (Table II). Recently a similar approach for ACh determination was described by Massarelli et al. (1976).

3 Estimation of Brain ACh Turnover Rate *In Vivo* by Isotopic Procedures

The aim of the estimation of ACh turnover rate *in vivo* is to measure the behavior of cholinergic synapses during normal functioning as well the adaptation of the system to environmental changes. These changes can be imposed by the actions of drugs, external stimuli or perhaps by alterations in precursor availability

3.1 Basic Principles of Turnover Analysis

3.1.1 Concepts and definitions

Zilvermanit and co-workers have published several articles regarding the design and analysis of isotope experiments (for review see Zilvermanit 1960), and some of the concepts and definitions introduced by these authors are summarized below

Specific Activity (S) Represents the amount of radioactivity per unit of substance. It is commonly expressed as dpm per nanomole of the substance measured.

Steady State In a situation in which the rate of entry of a molecule by synthesis or transport equals the rate of exit by breakdown or transport, the concentration of the substance remains constant and a steady state is said to exist. An increase in concentration may result from an increase in the rate of formation and/or from a decrease in the loss of the substance.

Turnover This term refers to the process of renewal of a substance in a given compartment. Renewal may take place in two different ways: 1) a substance may be synthesized in a given compartment, or 2) the substance may be transported to the compartment.

Turnover Rate. The rate at which a substance (X) is being renewed in a given compartment (amount per unit of time, TR_x).

Fractional Rate Constant The turnover rate is always a function of a constant (K_x) termed the fractional rate constant and denoting the state of activity and its value implicates the proportion of the compartment that is metabolized during the unit of time considered. The turnover rate then equals K_x (endogenous concentration of X) ($TR_x = K_x [X]$).

Turnover Time The turnover time of a substance is the time that is required for the turnover of a quantity equal to that present in the compartment. During the turnover time only 63 % of the "old" molecules have been replaced by "new" ones (insert $K_x t = 1$ in equation 4 below).

3.1.2 Definitions of symbols and conditions

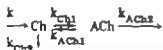
[Ch] and [ACh] represent the total amount of Ch and ACh present in a given compartment, and Ch and ACh represent the total amount of radioactive molecules in the same compartment. Thus $\text{Ch}/[\text{Ch}] = S_{\text{Ch}}$ and $\text{ACh}/[\text{ACh}] = S_{\text{ACh}}$.

TR_{Ch} and TR_{ACh} denote the turnover rates (nmol mm^{-1} of Ch and ACh, respectively) in a given compartment. The fractional rate constants for Ch and ACh are described $K_{\text{Ch}} = \text{TR}_{\text{Ch}}/[\text{Ch}]$ and $K_{\text{ACh}} = \text{TR}_{\text{ACh}}/[\text{ACh}]$ respectively. Thus the fractional rate constant is the fraction of a given compartment that is being renewed per unit of time.

- It is assumed that the following conditions for Ch and ACh in brain exist
- Free Ch in brain tissue is the immediate precursor of ACh.
 - The system is open, i.e. the isotope is continuously lost from the system by dilution with unlabelled material and by subsequent excretion.
 - A steady state exists, which means that the total rate of inflow of ACh equals the rate of outflow (release and hydrolysis, transport etc.) and this rate equals TR_{ACh} .
 - The turnover rates of Ch and ACh are constant during the experimental period.
 - Random break down prevails, i.e. the brain does not distinguish between radioactive and non radioactive molecules, nor does it differentiate between newly synthesized and old molecules.
 - Ch and ACh in brain are each present in a homogeneous pool and radioactive Ch and ACh are evenly distributed in these pools.

3.1.3 Mathematical analyses

The above assumptions have been incorporated into the following model



where $K_{\text{Ch}} = k_{\text{Ch}} + k_{\text{Ch2}}$ and $K_{\text{ACh}} = k_{\text{ACh1}} + k_{\text{ACh2}}$

The rate of entry of radioactive Ch into the Ch pool is indicated by k . The change of S_{ACh} will be expected to take place with time as shown in the following equation

$$\frac{dS_{\text{ACh}}}{dt} = K_{\text{ACh}}(S_{\text{Ch}} - S_{\text{ACh}}) \quad (1)$$

Thus, since K_{ACh} is constant, the change of S_{ACh} with time will depend upon the difference between S_{Ch} and S_{ACh} . The problem is to know how S_{Ch} changes with

time and thus to be able to solve equation (1). This problem can be handled in several ways

a) If it is assumed that S_{Ch} is kept constant during the experimental period, $S_{Ch}=C$ equation (1) will be

$$\frac{dS_{ACh}}{dt} = K_{ACh}(C - S_{ACh}) \quad (2)$$

which after integration gives

$$S_{ACh} = C(1 - e^{-K_{ACh}t}) \quad (3)$$

Since $S_{Ch}=C$ equation (3) can be divided by S_{Ch} on both sides

$$\frac{S_{ACh}}{S_{Ch}} = 1 - e^{-K_{ACh}t} \quad (4)$$

If S_{Ch} and S_{ACh} are measured at a given time point, $K_{ACh}t$ can easily be calculated by means of a small desk computer

b) It may be assumed that S_{Ch} is described by a given function of time, for example when Ch is infused at a constant rate a change in S_{Ch} with time is expected to be described by the following equation.

$$\frac{dS_{Ch}}{dt} = k - K_{Ch}S_{Ch} \quad (5)$$

After determination of k_{Ch} , K_{Ch} can be calculated. However K_{Ch} must first be determined from multiple points during infusion (Racagni et al. 1974).

c) If the equation which describes the S_{Ch} change with time is not known, but it is possible to measure S_{Ch} and S_{ACh} at different time points after introduction of the radioactive precursor into the system, another approach can be used. The function $f(t)_{Ch}$ is assumed to be any function of time which describes the change in S_{Ch} , and this function is inserted in equation (1) to yield

$$\frac{dS_{ACh}}{dt} = K_{ACh}(f(t)_{Ch} - S_{ACh}) \quad (6)$$

Equation (6) may be integrated between two times, t_1 and t_2 , as follows.

$$S_{ACh2} - S_{ACh1} = K_{ACh} \left[\int_{t1}^{t2} f(t)_{Ch} dt - \int_{t1}^{t2} S_{ACh} dt \right] \quad (7)$$

The difference at the left is equal to Δ in Figs 4 and 5 and the quantity between the square brackets is equal to the shaded area in Figs 4 and 6. Thus $K_{ACh} = \Delta / (\text{shaded area})$, which can be solved graphically or by using a computer. With this method it is possible to estimate K_{ACh} and TR_{ACh} without any knowledge about induced changes in Ch kinetics.

How valid are these equations when applied to ACh turnover within the brain?

STRIATUM

plasma Ch 17 pmol l⁻¹

plasma Ch 140 pmol l⁻¹

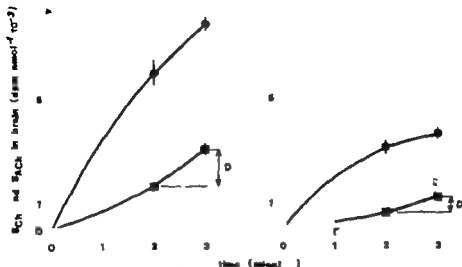


Fig. 4 S_{Ch} and S_{ACh} in the striatum of rats infused with saline or unlabelled Ch for 15 min prior to an infusion of ³H Ch. ○— S_{Ch} ■—■ S_{ACh} $k_{ACh} = \frac{D}{S_{ACh}}$ (from paper IV)

Unknown components are the nature and number of various "pools" of Ch (paper I) and ACh (Jenden et al. 1974 Nordberg 1977a). It is also known, at least *in vitro* that newly synthesized ACh is preferentially released (Collier 1969 Potter 1970, Molenaar and Polak 1976), which thus disagrees with condition e) under paragraph 3.1.2 above. However published data nevertheless appear to fit the model described above, at least during the first 20 min after labelling (Jenden et al. 1974 Saelels et al. 1973 Cheney et al. 1975).

3.2 Various Isotopic Approaches Currently Used to Study ACh Turnover *In Vivo*

The observation that ACh in the brain can be labelled with intravenously injected radioactive Ch (Dross and Kewitz 1966 Schubert et al. 1969) contributed to the development of the isotopic approach to the study of brain ACh turnover *in vivo*. The first application of intravenous injection of labelled Ch for this purpose was made by Dross and Kewitz (1966) and pioneer work in the development of a useful method for the estimation of ACh turnover *in vivo* was carried out by Schubert et al. 1969. The calculations of TR_{ACh} in this method were based on the assumption that an intravenous pulse injection rapidly (within seconds) gives a constant S_{Ch} in brain (in addition to the general assumption for analysis of isotopic experiments given in paragraphs 3.1.2) and that the following relationship

exists during the first minutes after the injection. $TR_{ACh} = ACh \cdot [Ch]/Ch \cdot t$. Since $TR_{ACh} = K_{ACh} \cdot t$ this is an estimation of $K_{ACh} \cdot t$ by the following formula $S_{ACh}/S_{Ch} = K_{Ch} \cdot t$ (compare with equation (4) above), which is only valid when S_{ACh}/S_{Ch} quotients are small (for example at $S_{ACh}/S_{Ch} = 0.2$ the calculated $K_{ACh} \cdot t$ value is 10 per cent too low and at $S_{ACh}/S_{Ch} = 0.5$ $K_{Ch} \cdot t$ is about 30 per cent too low as compared with the values obtained when equation (4) is solved for $K_{ACh} \cdot t$). What also may hamper this method is the fact that S_{Ch} in brain is not constant following an intravenous pulse injection (initial half life ~ 30 s, paper I) and that drug induced changes in Ch kinetics (Nordberg 1977b) may result in misleading alterations in calculated TR_{ACh} . However this method has been used successfully in several investigations in which the effect of drugs on relative changes in ACh synthesis has been studied (Schuberth et al. 1969, Schuberth et al. 1970, Aquilonius et al. 1973b, Nordberg and Sundwall 1975, Nordberg and Sundwall 1976, Nordberg 1977a).

Jenden and co-workers (Jenden et al. 1974) used the following variant of equation (1) for their mathematical analysis of experimental data obtained after a pulse injection of deuterium-labelled Ch: $dACh/dt = TR_{ACh} \cdot (S_{Ch}/S_{ACh})$ (equation (1) multiplied by $[ACh]$). TR_{ACh} was calculated from the slope of the line expressed when $dACh/dt$ was plotted against (S_{Ch}/S_{ACh}) . However since a non tracer amount of deuterated Ch had to be injected in this study the steady-state of brain Ch would be perturbed (Racagni et al. 1975) and this should therefore caution against the validity of applying principles of steady-state tracer kinetics in calculating TR_{ACh} .

Racagni and co-workers (1974), who used a constant intravenous infusion of radioactive phosphorylcholine, which is rapidly hydrolyzed to radioactive choline, made the assumption that S_{Ch} changes with time were described by the following equation: $dS_{Ch}/dt = -k_0 \cdot K_{Ch} \cdot S_{Ch}$, which is inserted in equation (2) above.

Cheney et al. (1975), using an intravenous pulse injection of radioactive phosphorylcholine, applied the same basic equation as above (equation (2)) for calculating TR_{ACh} but they also introduced the Ch kinetic in plasma as a transfer factor in order to compensate for drug-induced alteration of plasma kinetics.

3.3 Present Method (Paper IV)

In study IV a constant intravenous infusion of a tracer dose of tritiated Ch (3H Ch) was given for 2 and 3 min before the animals were killed by focusing a beam of microwave on their heads. K_{ACh} and TR_{ACh} were calculated from equation (7), in which K_{Ch} equals $D/(\text{shaded area})$ in Fig. 4. Under the approximation that the changes in S_{Ch} and S_{ACh} between 2 and 3 min are linear K_{ACh} and TR_{ACh} were calculated in a computer. The theoretical error introduced by this approximation is negligible in consideration of the experimental error in each S_{Ch} and S_{ACh} value. The method makes it possible to calculate K_{ACh} even if the Ch kinetics is altered by infusion of unlabelled Ch or by the effect of drugs. However the system must

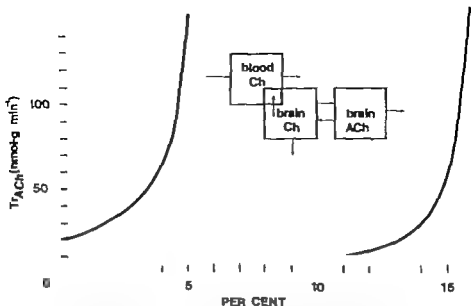


Fig. 5 "True" TR_{ACh} as a function of percentage of unequibrated blood within cerebral blood vessels. The S_{Ch} in arterial blood were subtracted by a computer from S_{Ch} in the brain tissue homogenates prior to calculation of K_{ACh} and TR_{ACh} .

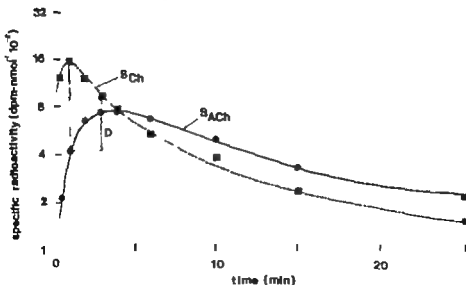


Fig. 6 Time course of S_{Ch} and S_{ACh} in brains of mice given an i.v. pulse injection of phosphoryl ($Me-^{14}C$) choline (data from Cheney et al. 1975).

of course still be at steady state.

When S_{Ch} in brain tissue is being measured it must be kept in mind that the brain is composed of ~94 % parenchyma and ~6 % blood, and that the S_{Ch} in arterial blood is about 10 times as high as the brain S_{Ch} during an intravenous infusion of 3H -Ch (unpublished observations). Thus, if the Ch in brain blood is not completely equilibrated with the Ch in brain tissue, a brain extract can be "contaminated" by a small Ch compartment of high specific activity which does not correspond to the brain Ch compartment used in ACh synthesis (Fig. 5). This will lead to too-low calculated TR_{ACh} values with all known mathematic applications for analysis of isotope experiments (Fig. 5). If the actual brain blood volume is estimated with 3H -dextran (Papers I, IV), it is possible to exclude at least major changes in brain blood volume in drug experiments. However under normal conditions "contaminating blood" is probably not a problem, since a product precursor relationship seems to exist between the total S_{Ch} and S_{ACh} in a brain homogenate (Jenden et al. 1974; Cheney et al. 1975; Nordberg 1977a, Fig. 6).

4 ACh Synthesis

ACh is synthesized by the transfer of an acetyl group from acetyl CoA to Ch. The reaction is catalyzed by the enzyme choline acetyltransferase (ChAT: acetyl CoA: choline *o*-acetyltransferase, E.C. 2.3.1.6). This enzyme probably largely occurs in the cytosol of cholinergic neurons at physiological pH and ionic strength (Fonnum 1973).

4.1 Origin of Ch in the Brain

For optimal ACh synthesis in the perfused cervical ganglia of the rat, the Ch concentration in the perfusion medium is of great importance (Blirks and MacIntosh 1961; Collier and MacIntosh 1969). It seems likely that a major portion of the Ch which acts as a substrate for ACh synthesis is Ch that is produced from ACh hydrolysis and is recaptured by the presynaptic nerve terminal (Collier and MacIntosh 1969).

Brain tissue seems to be unable to synthesize Ch *de novo*. It was shown by Bremer and Greenberg (1961) that the brain has less than 1% of the enzyme system of the liver responsible for the stepwise methylation of phosphatidylethanolamines by adenosylmethionine to form phosphatidylcholine. Intracerebral injection of ^{14}C -ethanolamine in rats leads to the labelling of the ethanolamine phospholipids but not the choline lipids (Ansell and Spanner 1967). A similar procedure with ^{14}C Ch lead to extensive labelling of Ch phospholipids (Ansell and Spanner 1968). *In vitro* studies (Browning and Schulman 1968) also substantiate this view as brain tissue is unable to synthesize Ch from unmethylated precursors such as serine and aminoethanol. Thus, the brain should be dependent upon an exogenous supply of Ch from plasma.

Up to now free Ch in plasma (Schuberth et al. 1969; Sparf 1973; Hamn and Schuberth 1974) and plasma lysophosphatidylcholine (Illingworth and Portman 1972) are the only established precursors of brain Ch *in vitro* (Fig. 7). However, part of the free Ch in brain is probably split off enzymatically from Ch-containing compounds in the brain tissue (Dross and Kewitz 1972; Kewitz et al. 1973; Choi et al. 1975; Browning 1976), which thus might explain the negative arteriovenous difference of free Ch over the brain demonstrated in different species (Kewitz et al. 1973; Aquilonius et al. 1975; Choi et al. 1975).

There are probably two different Ch generating pools, as when a 30 min infusion of labelled Ch is stopped, the total quantity of labelled Ch leaving the brain greatly exceeds the quantity found unbound in the brain (Choi et al. 1975), indicating that a short-term infusion has labelled a source capable of generating Ch. However, the Ch formed *post mortem* (Kewitz et al. 1973) is not labelled following short term infusion (Choi et al. 1975) or after acute feeding of deuterated Ch to mice (Hamn and Schuberth 1974).

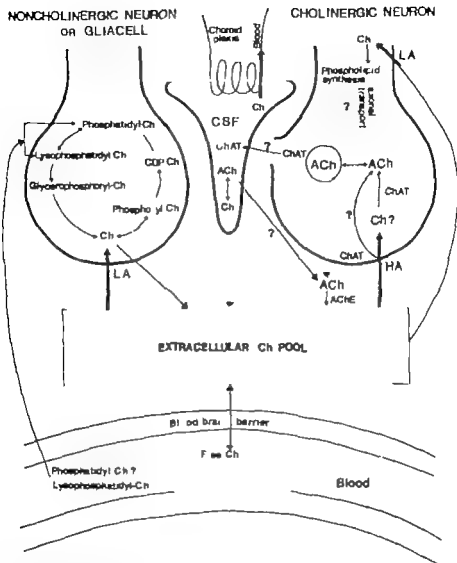


Fig. 7 Schematic diagram of the uptake, compartmentation and metabolism of Ch in the brain. Abbreviations in text.

Recently Kewitz and Pleul (1976), on the basis of the observation that the S_{Ch} in brain was higher than S_{Ch} in blood after administration of labelled methionine and ethanolamine but not after administration of radioactive Ch, suggested that a *de novo* synthesis of Ch occurred in brain. However the authors have not considered the fact that lysophosphatidylcholine in plasma, which is relatively more strongly labelled following the administration of methionine and ethanolamine than after Ch injection (Kewitz and Pleul 1976), can act as a precursor for brain Ch (Illingworth and Portman 1972).

4.1.1 The fate of Ch in plasma

The half life of Ch in plasma is extremely short (Bligh 1953 paper I Freeman et al. 1975 Haubrich et al. 1975a). The clearance of the pool into which the infused Ch is distributed has been estimated to be 75 ml kg^{-1} in the rat (Freeman et al. 1975). The steady state level of plasma Ch is rapidly attained following a constant infusion of Ch and this steady state level seems to be linearly related to the infusion rate (Gardiner and Paton 1972, Freeman et al. 1975 Gardiner and Gwee 1974 paper IV). It also appears that the endogenous plasma concentration of undeuterated Ch is not affected by a large exogenous load of deuterated Ch (Freeman et al. 1975 Chol et al. 1975), which indicates that the efflux of Ch into plasma does not appear to be subject to feedback inhibition. The short half life of Ch at physiological plasma concentrations is due to a rapid uptake into tissues and subsequent metabolism to phosphorylcholine, phospholipids and betaine (Bligh 1953 Sparf 1973 Gardiner 1974 Haubrich et al. 1974 Haubrich et al. 1975a).

Since very little radioactive Ch is detected in the urine after intravenous administration of labelled Ch in tracer amounts (Sparf 1973 Gardiner and Paton 1972), little regulatory contribution has been attributed to the kidney until recently Acara (1975) showed in chickens that the extraurinary clearance of Ch decreased, while the contribution of renal clearance to total clearance of plasma Ch increased when plasma concentrations were elevated by an infusion of Ch. At a plasma Ch concentration of $500 \mu\text{M l}^{-1}$ the kidneys removed more than 70 % of the infused Ch. The author suggested that the renal tubule has a bidirectional transport mechanism such that net tubular reabsorption occurs at low plasma Ch levels and net tubular excretion at high plasma levels of Ch.

4.1.2 Regulation of human plasma Ch

Since the work of Bligh (1953) in which he concluded that it was unlikely that any variation in the level of plasma Ch could occur under normal and pathological conditions, little attention has been paid to the regulation of plasma Ch in man. Aquilonius and Eckernäs (1975) showed that large oral doses of Ch (3–9 g daily) resulted in a long lasting elevation of plasma Ch in patients with Huntington's chorea, and in view of the presence of 500–900 mg Ch in an average daily diet, a dietary influence on plasma Ch could be expected.

In study II a dietary influence on free Ch in plasma was demonstrated. In 20 out of 23 fasting volunteers the plasma Ch concentration ($10.6 \mu\text{mol l}^{-1}$) increased by $1\text{--}2 \mu\text{mol l}^{-1}$ ($11.5 \mu\text{mol l}^{-1}$) following a meal (Table I). Hitherto few data are available on plasma Ch levels in disease or during malnutrition, and nothing is yet known about the clinical significance of any such alterations. Recently a plasma Ch concentration about twice that of normal persons was reported in azotemic subjects before hemodialysis (Remmick et al. 1976), a finding recently confirmed in our own laboratories, (Aquilonius, Eckernäs and Sahlinström, to be published).

4.2 Uptake of and Compartmentation of Ch

Schubert et al. (1969-1970) demonstrated that labelled Ch in the blood is taken up into the brain and is rapidly converted to ACh, an observation which has been verified by a number of investigators (see Freeman and Jenden (1976)). As pointed out earlier free Ch in plasma is not the only source of brain Ch. Plasma lysophosphatidylcholine, for example, is able to pass the blood-brain barrier intact, and 20 % of this seems to be metabolized to free Ch in brain (Illingworth and Portman 1972). The proportions of free and derived Ch from plasma that act as precursors for free Ch in brain show species differences. In the rat derived Ch seems to contribute almost 90 % of the Ch used for ACh synthesis, while the corresponding figures in the rabbit and mouse have been calculated to be 50 % and 20 %, respectively (Schubert and Jenden 1975).

Diamond (1971) and Sparf (1973) reported the observation of a saturable uptake of plasma Ch into mouse brain, while Freeman et al. (1975) recently suggested that a non-saturable uptake of plasma Ch into rat brain existed. However in the latter investigation the plasma Ch concentration was increased to a maximum level of about 10 000 nmol/ml. The observed Ch concentration in brain at this plasma concentration was only about 100 nmol/g. Since about 6 % of the brain weight consists of blood, the observed increase in brain Ch concentration (1 % of the plasma concentration) may be a consequence of unequilibrated blood within the cerebral blood vessels.

Regardless of the original source of free Ch in brain (free Ch in plasma, Ch containing compounds in plasma and Ch liberated from Ch-containing compounds within the brain) the Ch used in the synthesis of ACh appears to be free Ch that is extracellular (Fig. 7) to the site of synthesis (see Barker 1976). This Ch pool seems to be fairly homogeneous, at least on mathematical grounds. For example in the mouse, where about 80 % of brain Ch is derived from free Ch in plasma, the S_{Ca} and S_{ACh} curves following and intravenous injection of labelled precursors (Jenden et al. 1974; Cheney et al. 1975; Nordberg 1977a) seem to fulfil the criteria for brain Ch being an immediate precursor to brain ACh in a homogeneous compartment (Fig. 6, Zilversmit 1960).

All cell membranes appear to possess a low affinity (L.A.) Ch uptake system which supplies Ch for the synthesis of phosphorylcholine (see Barker 1976), while a sodium-dependent high affinity (H.A.) system is specifically associated with the cholinergic nerve terminals and supplies Ch for the synthesis of ACh (Haga and Noda 1973; Dowall and Simon 1973; Yamamura and Snyder 1973; Suzukawa and Pilar 1976, Fig. 7). It has been suggested that the H.A. Ch transport is physically coupled directly to the synthesis of ACh, and that Ch used for the synthesis of ACh thus may not have a free existence within the cholinergic nerve terminals (Barker 1976). However there is also evidence that uptake and synthesis can be kinetically coupled and that a free Ch pool might exist within the cholinergic neuron (Suzukawa and Pilar 1976). No distinction can be made between the two models with the data available today.

4.2.1 Cortical and striatal *in vivo* uptake and metabolism of plasma Ch (Paper I)

In study I was observed that the quotient between brain ^3H -Ch and blood ^3H -Ch increased linearly with time following an intravenous injection of ^3H -Ch, both in the cortex and in the striatum (1.2 % and 6.4 % per min, respectively), thus reflecting a net transport from blood to brain (Fig. 8). The results were explained as a consequence of differences in density of cholinergic neurons between cortex and striatum. This theory is supported by Carrol and Buterbaugh (1975), who have studied the kinetics of Ch accumulation by synaptosomes prepared from different regions of guinea-pig brain. They suggested that the maximal velocity (V_{max}) of the H.A. system reflects the density of cholinergic nerve endings within brain regions. However in view of the suggested coupling between ACh synthesis and Ch transport (see above), it would be tempting to propose that the rate of Ch uptake might reflect the rate of ACh turnover in different brain regions. In view of the turnover rate data obtained in study IV (cortex $3.6 \text{ nmol g}^{-1} \text{ min}^{-1}$ striatum $23.8 \text{ nmol g}^{-1} \text{ min}^{-1}$) the accumulation rates of Ch observed in study I may reflect regional differences in cholinergic activity.

As pointed out earlier it has been suggested that free Ch may not have a free existence within the cholinergic neurons (Barker 1976). If this holds true the accumulation of ^3H -Ch should be regarded as an "affinity" (i.e. there is a greater probability of ^3H -Ch derived from released ^3H ACh being recaptured) for Ch rather than as a transport into the neurons. In the "free pool" model suggested by Suzuki and Pilar (1976) the accumulation of ^3H -Ch could be explained by a compartmentation of Ch within the cholinergic nerve terminals. However a combination of "affinity" and intraneuronal compartmentation is also possible (Fig. 7).

In study I marked differences in the utilization of ^3H -Ch within the brain regions were also demonstrated. Cortical H-Ch was converted into metabolites other than ACh (phosphorylcholine) at a rate of 36 % per min, while the corresponding figure in the striatum was 6 % per min. To explain these differences it was necessary to assume the existence of different pools of free Ch in the brain, one localized close to the H.A. uptake system and another close to the L.A. system. However as pointed out earlier recently published data indicate that brain Ch seems to be distributed to a fairly homogeneous extracellular pool and a possible alternative explanation is thus, that in the cortex, where the value of $\text{TR}_{\text{L.A.}}$ is about six times lower than that in the striatum there should be a six times higher probability that Ch is taken up by the L.A. system and thus mainly used in phospholipid synthesis.

4.3 Regulation of ACh Synthesis

Experiment utilizing the cholinergic system in the periphery (McIntosh 1963 Collier and McIntosh 1969 Potter 1970 Hebb 1972, Collier and Katz 1974) and in the brain (Rommelspacher and Kuhar 1974) have revealed that ACh synthesis

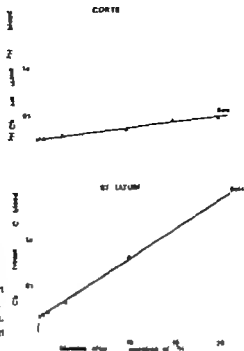


Fig. 8 Time course of the quotient between free H-Ch in blood and in brain tissue following an i.v. injection of tracer H-Ch. Cortex $k=0.012$, $r=0.99$ striatum $k=0.064$, $r=0.98$ (from paper I).

is coupled to ACh release. Most models used to explain this coupling have involved ChAT. The models include feedback inhibition of ChAT by ACh (Kaiba and Goldberg 1969 Morris et al. 1971) and mass action regulation of ChAT (Glover and Potter 1971). However there has been no direct evidence that ChAT is regulated *in vivo*.

Recent observations indicate that the availability of Ch is rate limiting in ACh synthesis (Eisenstadt and Schwartz 1975 Simon et al. 1976). In view of the presumed coupling between H.A. Ch uptake and ACh synthesis described above, an attractive hypothesis would be that the H.A. transport system has a regulatory function. It was thus of great interest when Simon et al. (1976) demonstrated that alterations in the activity of cholinergic pathways *in vivo* caused by lesions or drugs resulted in a change in V_{max} for the H.A. transport of Ch when tested *in vitro*. For example treatment with drugs that increase neuronal activity e.g. pentylenetetrazol or scopolamine, cause an increase in V_{max} of H.A. transport into brain synaptosomes without any change in K_m . Conversely decreased neuronal activity after pentobarbital, or lesion causes a decrease in V_{max} .

Jenden et al. (1976) reported a correlation between the rate of H.A. uptake of Ch and the ACh content of synaptosomes, and suggested that the synaptosomal ACh concentration might regulate H.A. Ch uptake. However Kuhar et al. (1975) found that ACh concentrations in the interpeduncular nucleus did not change after acute lesions or pentobarbital administration, but the Ch uptake in that region was nevertheless reduced. Thus, it remains to be established whether

other regulatory mechanisms exist.

Some reported results do not seem to be explainable on the basis of the H.A. system alone, and in these cases the L.A. system may play a role. For example, it has recently been demonstrated that parenteral administration of Ch can result in increased plasma and brain Ch concentrations and in brain ACh concentration (Haubrich et al. 1974 1975 Cohen and Wurtman 1975). Since the sodium dependent H.A. Ch uptake ($K_m = 0.75 \mu M$ Simon et al. 1976) would already be saturated, it seems that the L.A. Ch uptake could subserve ACh synthesis, since the L.A. system has a K_m value of about $50 \mu M$ (Yamamura and Snyder 1973 Barker and Mittag 1975 Carroll and Goldberg 1975) and would not be saturated at normal Ch levels. Carroll and Goldberg (1975) suggest, on the basis of experiments *in vitro* that when the nerve terminals are depolarized, Ch can be supplied by the L.A. transport system for the synthesis of ACh. This is in contrast to the finding of Simon et al. (1976) however that altered neuronal activity only affected the V_{max} of the H.A. transport system for Ch. Furthermore, Suszkiw and Pilar (1976), who studied synaptosomes from the ciliary cells in the iris, suggested that cholinergic nerve terminals seem to be deficient in the L.A. transport system, while the cell bodies of the same neurons are deficient in the H.A. system. It remains to be established however whether this is a general property of all cholinergic neurons.

4.3.1 Effect of elevated plasma Ch concentration on *in vivo* turnover rate of brain ACh (Paper IV)

The aim of the present paper was to evaluate the proposal recently put forward by several authors (Cohen and Wurtman 1975 Haubrich et al. 1975b, Wurtman and Fernstrom 1976) that increased concentrations of plasma Ch stimulate the synthesis of brain ACh. At steady state an increased transmitter synthesis must be balanced by an increased transmitter outflow and thus result in an increased turnover rate of the transmitter (Zilvervsmil 1960).

Rats were infused intravenously with saline ($0.25 \text{ ml min}^{-1} \text{ kg}^{-1}$) or unlabelled Ch ($15 \mu\text{mol min}^{-1} \text{ kg}^{-1}$) for 15 min and an infusion of ^3H -Ch was then started (Fig. 9). The two infusions were then continued simultaneously for a further two or three minutes. During the infusions the animals were held in place in the holder within a microwave equipment (drawn very schematically in Fig. 10). The rats were killed by focusing a beam of microwave on their heads 2 and 3 min after the ^3H -Ch infusion was started. TR_{ACh} was calculated as described in paragraph 3.3 above.

The elevated steady state concentrations of plasma Ch ($\sim 140 \mu\text{mol l}^{-1}$) were of the same magnitude as the peak values shown to be paralleled by increased brain ACh concentrations in the studies by Haubrich et al. (1975) with use of intraperitoneal administration of Ch.

At the elevated plasma Ch level the Ch concentration was significantly increased both in the cortex and in the striatum, while the ACh concentrations were

Fig. 9 Time course of plasma Ch in rats infused with unlabelled Ch. $\nabla-\nabla$ $15 \mu\text{mol kg}^{-1} \text{ min}^{-1}$ $\nabla-\nabla$ $2.5 \mu\text{mol kg}^{-1} \text{ min}^{-1}$ (from paper IV).

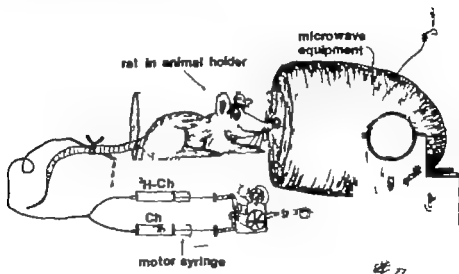
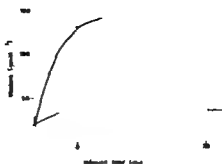


Fig. 10 A very schematic figure of the procedure used in paper IV

Table III Cholinergic parameters in brain regions of the rat at different steady-state concentrations of plasma Ch

Brain part and steady-state concentration of plasma Ch	Ch (nmol g ⁻¹) $\bar{m} \pm \text{S.E.}$	ACh (nmol g ⁻¹) $\bar{m} \pm \text{S.E.}$	Fractional rate constant K_{ACh} (min ⁻¹)	Turnover rate TR _{ACh} (nmol g ⁻¹ min ⁻¹)
Cortex (plasma Ch $17 \mu\text{mol l}^{-1}$ $n=18$)	43 ± 2.4	16 ± 1.6	0.22	3.6
Cortex (plasma Ch $140 \mu\text{mol l}^{-1}$ $n=15$)	$59 \pm 3.7^{**}$	14 ± 1.7	0.26	3.6
Striatum (plasma Ch $17 \mu\text{mol l}^{-1}$ $n=23$)	33 ± 1.22	76 ± 2.9	0.31	23.8
Striatum (plasma Ch $140 \mu\text{mol l}^{-1}$ $n=22$)	$53 \pm 2.0^{**}$	84 ± 3.0	0.26	21.4

$** p < 0.02$
 $** p < 0.001$ (Student's t-test)

increased slightly in the striatum only (Table III). However no conclusive changes in the regional TR_{ACh} were detected (Table III). These findings thus contradict the suggestion that increased plasma levels of Ch are paralleled by enhanced neuronal synthesis of ACh in the brain. These results are not unexpected, since it would be unlikely that neuronal functional activity should normally be regulated by its precursor availability.

The slight and significant increase in striatal ACh concentration and the minute reduction of striatal TR_{ACh} might indicate a direct agonistic effect of Ch itself in some receptor-close compartment. However the present findings do not necessarily rule out a possibility of restoring cholinergic function with Ch under pathological conditions (Paper VI).

5 Cholinergic Mechanisms in the CNS

5.1 Methods for Localization of Cholinergic Neurons

Direct visualization of ACh as achieved by the histochemical fluorescence of catecholamines seems to be impossible in view of the simple chemical structure of ACh. However a variety of methods for identifying and localizing cholinergic tracts have been developed.

5.1.1 Biochemical "markers"

Biochemical "markers" include ACh levels, ChAT and AChE activity H.A. Ch uptake and the presence of cholinergic receptors (see Kuhar 1976). ACh concentration can, in animal experiments, reflect the cholinergic representation at the gross anatomical level if special precautions for stabilization of ACh have been undertaken (see above). However in human studies ACh concentrations probably cannot be used as a cholinergic marker because of the post-mortal changes.

The activity of the cholinergic enzymes ChAT and AChE can easily be measured by sensitive methods (Fonnum 1973). There is little doubt, however that ChAT is a far more relevant marker for cholinergic structures than AChE. In some brain regions, for example, there is no correlation between AChE and ACh concentration, while the ChAT activity is well correlated to ACh concentration in different regions (Koelle 1969 Nordberg and Sundwall 1975).

Sorimachi and Kataoka (1974) and Simon and Kuhar suggested that H.A. uptake of Ch as measured in synaptosomes prepared from different brain regions could be a specific marker for cholinergic neurons, but in view of the recent suggestion that the H.A. transport system is adapted to functional changes in the cholinergic neurons (Simon et al. 1976), regional differences in H.A. uptake of Ch might possibly reflect differences in the functional activity of cholinergic neurons more than the relative density of cholinergic neurons.

Another useful biochemical marker for cholinergic representation is the presence of what appear to be the cholinergic receptors. This is a rather new area of research and will perhaps give additional knowledge about cholinergic anatomy in the future (see Kuhar 1976).

5.1.2 Histochemical methods

There are several workable methods for localization of AChE at light and electron microscopic levels (see Kuhar 1976). However as pointed out earlier AChE does not necessarily represent the cholinergic innervation. Apart from the localization of AChE in the endoplasmatic reticulum, in axons and in synaptic regions, it has

also been suggested that AChE is present in glial cells (Hemminki et al. 1973).

The presumably unique presence of ChAT in cholinergic neurons thus makes it more useful for histochemical localization. The first method described for detection of ChAT was based on the precipitation of CoA, which is produced in the formation of ACh (and also in other biochemical reactions) as a mercaptide (Burt 1970 Kasa et al. 1970). However Burt and Silver (1973) later reinvestigated the specificity and suggested that this histochemical method was not completely reliable.

Another approach recently developed is immunohistochemical methods (Eng et al. 1974 McGeer et al. 1974). However the specificity is not very well established at present (Rossier 1975). In spite of the many problems involved and the need for extensive controls, several laboratories are intensively engaged in trials with these methods (Malthe-Sørensen et al. 1973 McGeer et al. 1975 Singh et al. 1975 Hattori et al. 1976 Rossier 1976), and within the next few years such techniques will probably be more prominent in cholinergic research.

5.2 Distribution of ChAT in CNS

The radioenzymatic procedures for ChAT determinations permit assay in μg amounts of brain tissue (Fonnum 1973), and since ChAT has been shown to be remarkably stable post mortem (Paper V) it can be used in studies on human brain.

The first study on ChAT activity in human brains, though relatively limited, was made by Hebb and Silver (1956), who used bioassay to determine the enzyme activity. They observed that the activity of ChAT showed marked regional differences, with very high values in the striatal system. Similar relative distribution patterns have also been found in lower animals (Hebb and Silver 1956). The first more detailed study in primates (Rhesus monkey) was made by Fahn and Côté (1968) and in human brain by McGeer and McGeer (1971) and Aquilonius et al. (1973). However at this stage all tissue samples consisted of gross anatomical regions removed by free-hand dissection.

5.2.1 Regional distribution of ChAT in human brain (Paper V)

Until recently it was necessary to dissect fresh brain to obtain tissue samples. This method is very inaccurate, the main drawback being that the sample from the area of interest is usually very poorly defined. Possible subnuclear differences in analysed substances in an apparently homogeneous structure cannot be detected.

In paper V a method for obtaining well-defined samples from brain tissue was developed and was applied to ChAT analysis in subregions of human brain. From a frozen brain oriented so that 200 μ cryo sections are taken (LKB 2250 PMW Cryo-Microtome, LKB Produkter AB, Sweden) perpendicular to the intercommissural plane (anterior and posterior commissures) and to the sagittal plane. Tissue samples ($\sim 0.1 \text{ mm}^3$) are then punched out, using a small glass capillary



Fig. 11 The distribution of punchings in a typical section of human brain, 5 mm behind the anterior commissure (from paper V).

(Fig. 11), and the ChAT activity is measured by a radiochemical procedure. The enzyme activity is expressed in relation to unit of volume of brain tissue, which is probably better than wet weight, since the area punched out (and thus original volume of tissue) will not change even if moisture is lost (or added).

Several anatomical regions could be subdivided according to differences in ChAT activity (Fig. 12, Table IV). Especially in the caudate nucleus different populations could be traced sterically through the sections. Little is known as yet about possible physiological correlates to these subnuclear regions, but it may be of interest to note that choreiform hyperkinesia in the cat is induced after local application of dopamine only in the rostromedial part of the caudate nucleus (Cools 1972).

The extreme range (10–140 nmol ACh/min-cm³) of ChAT activity found in the amygdala indicates that some subnucleus might be rich in cholinergic neurons. The highest values seemed to be in the central part of the nucleus. However no statistically significant regions could be distinguished owing to the relatively fewness and scattering of the punchings. Most of our findings in study V concerning intranuclear distribution of ChAT in human brain have recently been confirmed by McGeer (1976).

5.3 Some Well Established Central Cholinergic Tracts

ChAT is synthesized in the cell body of the cholinergic neuron and is transported by axonal flow to the terminal region. Accordingly a lesion of a cholinergic



CAT activity [nmoles ACh formed/minute on tissue]



Table IV ChAT activity in different regions of human brain

Structure	Population area	ChAT activity (nmole ACh/min cm ³)	No
		±SE ()	
Caudate nucleus	Cd1	108.7 ± 8.3	13
	Cd2	194.1 ± 4.0	98
	Cd3	151.3 ± 6.5	43
	Cd4	91.8 ± 4.7	27
Putamen	Pt1	237.5 ± 3.9	147
	Pt2	319.3 ± 7.6	34
	Pt3	180.4 ± 16.5	9
Globus pallidus lateralis	Pl1	12.4 ± 1.0	15
	Pl2	8.7 ± 0.3	41
	Pl3	15.1 ± 1.8	31
Globus pallidus medialis	P.m	4.5 ± 0.2	31
Nucleus ansa lentiformis	Al	35.4 ± 7.1	14
Clastrum+5	Cl	4.9 ± 0.4	9
Clastrum-5 -10 -20	Cl	10.4 ± 0.5	35
Substantia nigra pars compacta	NLc	5.9 ± 0.5	11
Substantia nigra pars reticulata	NLr	3.2 ± 0.1	15
Subthalamic nucleus	Stb	12.3 ± 0.9	15
Nucleus ruber	Ru	5.0 ± 0.1	2
Thalamus medial part	Th.m	10.5 ± 0.6	33
Thalamus lateral part	Th.l	6.4 ± 0.3	73
Substantia reticularis thalami	Rt	4.9 ± 0.5	15
Amygdala	Am	25.6 ± 2.7	61
Gyrus cinguli	G.c	4.5 ± 0.1	5
Gyrus olfactorius	G.ol	10.0 ± 0.8	13
Insula	Cx.in	8.6 ± 0.6	6
Hippocampus	Hipp	13.6 ± 1.5	17
White substance	W	1.9 ± 0.1	14

Fig. 12 Normal distribution of choline acetyltransferase (ChAT) in different regions of human brain (5 mm rostral and 5-10 and 20 mm behind the anterior commissure). Abbreviations: Al—nucleus ansa lenticularis, Am—amygdala, Cd—caudate nucleus, C.c—corpus callosum, Cl—claustrum, C.m.a—anterior commissure, Cp.l—internal capsule, Cx.in—insula, Fx—fornix, G.c—gyrus cinguli, G.ol—gyrus olfactorius, Hipp—hippocampus, NLc—substantia nigra pars compacta, NLr—substantia nigra pars reticulata, Pl—lateral pallidum, P.m—medial pallidum, Pt—putamen, Rt—substantia reticularis thalami, Ru—nucleus ruber, Stb—subthalamic nucleus, Th.l—thalamus, lateral part, Th.m—thalamus, medial part, w—white substance, White areas—not analysed. (From paper V).

neuron is accompanied by accumulation of ChAT proximal to the lesion and depletion of the enzyme in the target area of the neuron.

It is well known that a septal-hippocampal pathway exists (see Kuhar 1976), and since some of these neurons stain for AChE (Lewis and Shute 1967) a cholinergic septal-hippocampal pathway might be present. Consequently lesions in the fimbria result in a large decrease of AChE and ChAT in the hippocampus on the lesioned side (Lewis et al. 1967 McGeer et al. 1969). It has been possible to localize ChAT activity to certain cell layers of the dentate area of the hippocampus (Fonnum 1970). Moreover Kuhar et al. (1973) found that lesions in the medial septal area resulted in a sharp reduction in the H.A. uptake of Ch into crude synaptosomal fractions prepared from the hippocampus, and in a concomitant decrease in activity of ChAT.

Following lesions of the major known afferent pathway to the caudate nucleus in rats no decrease in AChE, ChAT (McGeer et al. 1971a) or ACh (Butcher and Butcher 1974) could be detected in the striatum. Furthermore, when the striatum is destroyed no alteration of ChAT is found in other brain regions (McGeer et al. 1969). These findings suggest that striatal cholinergic neurons mostly are interneurons.

Lesions of the crossed and uncrossed olivocochlear bundle in the cat are accompanied by a 90 % reduction of ChAT activity in the membranous cochlea (Jasser and Guth 1973), thus supporting the existence of a cholinergic efferent tract from the superior olivary complex to the cochlea hair cells.

It is now fairly well established that some of the neurons in the habenulo-interpeduncular tract are also cholinergic (see Kuhar 1976).

5.4 Interaction of Cholinergic Neurons with Other Neuronal Systems in Extrapyramidal Nuclei

The neostriatum has one of the highest densities of cholinergic neurons found in the CNS and, as discussed earlier, there is considerable evidence to suggest that these are interneurons (McGeer et al. 1971a, Butcher and Butcher 1974, McGeer et al. 1975, Hattori et al. 1976). About 95 % of all neurons in the neostriatum seem to be Golgi type II interneurons (Kemp and Powell 1971). The neostriatum also contains dopaminergic terminals originating in the zona compacta of the substantia nigra (Andén et al. 1964, Dalström and Fuxe 1964, Ungerstedt 1971). In the rat it has been estimated that there are about 3 500 dopaminergic neurons in the substantia nigra which produce about 1.6×10^6 nerve terminals in the neostriatum (Andén et al. 1966).

It has long been known that iontophoretic application of ACh enhances the firing rate of cells in the caudate, whereas dopamine depresses the majority of these cells (Bloom et al. 1965). In neuropharmacological experiments dopamine agonists decrease ACh release and turnover in the striatum while dopamine

Table V *Effect of various treatment on cholinergic parameters in the striatum*

Treatment	ACh levels	ACh release	ACh turnover
Dopamine agonists	↑ (1 2 9) ^a ‡ (4)	↓ (6)	↓ (4)
Dopamine receptor blockers	↓ (1 8), ‡ (4)	↑ (6)	↑ (4)
Muscarinic receptor stimulators (Ox. tremorin)	↑ (4 5)	—	↓ (4 5)
Muscarinic receptor blockers	↓ (4)	↑ (11)	‡ (4)
GABA receptor blockers (Picrotoxin)	↑ (10)	—	—
Lesion of the medial forebrain bundle	↓ (7)	—	—
Electrical stimulation of the nigro-neostriatal pathway	—	↓ (6)	—

↑ increase

↓ decrease

‡ no change

^a The number in the parentheses indicate reference source of data

- | | |
|----------------------------------|-----------------------------------|
| (1) Paper I | (6) Bartholomew et al. (1976) |
| (2) Conzoto et al. (1974) | (7) Romachpacher and Kuhar (1975) |
| (3) Himrich et al. (1973c) | (8) Seely and Van Woert (1974) |
| (4) Racagni et al. (1976) | (9) Schmidt (1976) |
| (5) Nordberg and Sundvall (1977) | (10) Laidlaw et al. (1976) |

receptor blocking agents increase ACh release and turnover in this region (Table V). Thus, it seems likely that a dopaminergic input from the substantia nigra has a tonic inhibitory influence on some of the cholinergic interneurons in the neostriatum (see Roth and Bunney 1976).

Data have also been presented that support a theory of a cholinergic system in the substantia nigra (see Roth and Bunney 1976). The origin of the cholinergic system in the substantia nigra may be intrinsic or extrinsic, but in the latter case all that can be said at this time is that it does not arise from the striatum (Hattori et al. 1973 Kataoka et al. 1974 Fonnum et al. 1974).

There is now substantial biochemical evidence of a γ -aminobutyric acid (GABA)-ergic input to the substantia nigra originating in the striatum. A lesion in the strionigral pathway results in a marked decrease in both GABA and glutamic acid decarboxylase in the substantia nigra (Kim et al. 1971 McGeer et al. 1971b, Hattori et al. 1973 Fonnum et al. 1974). Recently Laidlaw et al. (1976) observed that the ACh concentration in rat striatum increased after administration of the GABA-ergic blocking agent picrotoxin. This supports a theory of a GABA-ergic (inhibitory)—dopaminergic (inhibitory)—cholinergic linker

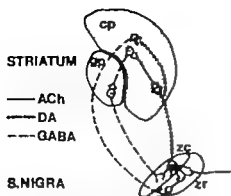


Fig. 13 Possible interactions between cholinergic, dopaminergic, and GABAergic neurons linking the substantia nigra and basal ganglia. cp—caudate nucleus and putamen, gp—globus pallidus, zc—zona compacta of substantia nigra, xr—zona reticulata of substantia nigra.

minating in the striatum. In Fig. 13 a possible model for the interactions between cholinergic, dopaminergic and GABA-ergic neurons in the substantia nigra and basal ganglia is depicted.

6 Huntington's Chorea

6.1 Introduction

Huntington's chorea (H.C.) is a hereditary disorder of unknown etiology characterized by the onset of progressive choreiform movements and dementia usually between the third and fifth decades of life.

The first detailed description and the first account of the hereditary nature of the disease were given on 15th February 1872 by the 22 year-old George Huntington in a lecture before the Meigs and Mason Academy Middleport, Ohio.

The disease is inherited in an autosomal dominant fashion with complete penetrance (see Barbeau et al. 1974) and involves characteristic degeneration of small (Goigi type II) neurons in the neostriatum (Bruyn 1968).

6.2 Rôle of Different Transmitter Systems

6.2.1 Cholinergic system

Several clinical observations compatible with reduced activity of cholinergic neurons in H.C. have been made. It has been demonstrated that central cholinergic stimulation by physostigmine reduce choreatic movements, while blockade of central cholinergic receptors aggravates the symptoms (Aquilonius and Sjöström 1971 Klawans and Rubovits 1971 1972, Davis et al. 1976). Aquilonius et al. (1972) found decreased concentrations of Ch in the lumbar CSF of H.C. patients, which might be reflective of cholinergic dysfunction. Furthermore, there are marked reductions of the cholinergic marker ChAT in the neostriatum of H.C. patients with this disease (McGeer et al. 1973 Aquilonius et al. 1974 Bird and Iversen 1974 Stahl and Swanson 1974 Paper V), especially in the rostromedial part of the caudate nucleus (Fig. 14 Paper V). The morphological basis of the cholinergic hypofunction in H.C. thus seems to be a degeneration of striatal cholinergic interneurons. However loss of muscarinic receptors in the caudate and putamen has also been reported (Hiley and Bird 1974 Wastek et al. 1976). At present, it is not known whether this is primary or secondary to the degeneration of cholinergic neurons.

6.2.2 Catecholaminergic system

There is some controversy regarding involvement of a dopaminergic degeneration in H.C. Unchanged activity of tyrosine hydroxylase, a marker for dopaminergic and noradrenaline terminals, has been found in the striata of H.C. brains (McGeer et al. 1973). Normal levels of dopamine (DA) and homovanillic acid have also been observed by several investigators (Ehringer and Hornykiewicz 1960, Hor

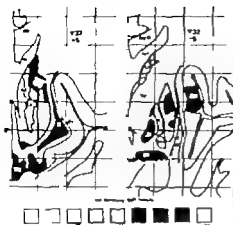


Fig. 14 Brain ChAT (per cent of control values) in a patient with Huntington's chorea. Abbreviations as in Fig. 12. White areas: not analysed (from paper V).

nykiewicz 1966, Bird and Iversen 1974 Mattson 1974), while decreased concentrations of dopamine limited to the caudate were found in one study (Bernheimer and Hornykiewicz 1973).

In an investigation by Lal et al. (1973) the increase in homovanillic acid in CSF following probenecid administration was found to be similar in controls and H.C. patients and may be taken as an indication of a preserved dopaminergic mechanism in H.C. Thus, most data available at present indicate that this mechanism are relatively intact in H.C.

6.2.3 GABA-ergic system

As discussed earlier there is evidence of a DA ACh-GABA linkage between the substantia nigra and the striatum. It is thus interesting to note that deficits in the GABA concentrations in the neostriatum and substantia nigra (Perry et al. 1973) and markedly decreased levels of GABA in CSF (Glaser et al. 1975) have been found in H.C. A significant reduction of glutamic acid decarboxylase in the striatum of H.C. patients has also been reported (Bird et al. 1973), McGeer et al. 1973 Bird and Iversen 1974 Stahl and Swanson 1974 Ungerhart et al. 1975). However glutamic acid decarboxylase deficits are not specific to H.C. and are also seen Parkinson's disease (Lloyd and Hornykiewicz 1973 Laaksonen et al. 1974) and in ageing (Bowen et al. 1974 Ungerhart et al. 1975). Further the decrease in glutamic acid decarboxylase in H.C. seems to be uniform (McGeer et al. 1973b) in striatum and substantia nigra, while ChAT reductions are patchy (McGeer et al. 1973, Paper V).

6.2.4 Conclusion

It may thus be suggested that in H.C. the DA ACh GABA-ergic loop in the basal ganglia might be disturbed owing to degeneration of cholinergic interneurons in the striatum and possibly a parallel or secondary degeneration of GABA-ergic neurons from the striatum to the substantia nigra.

To understand the effect of such degenerative changes it may be relevant to introduce the term "biological buffer capacity" (Gerlach et al. 1974) to express the ability of a neuronal system to maintain normal function under different environmental conditions. Thus, in H.C. it can be assumed that the "buffer capacity" of the basal ganglia is decreased, at least in some parts in a level where choreatho movements appear spontaneously. In asymptomatic relatives with the inherited gene for H.C., provocation with L DOPA can induce hyperkinesia in some cases (Klawans et al. 1972). This could thus be explained by a less pronounced decrease in "buffer capacity" and consequently the hyperkinesia only being manifested when the system is disturbed.

However much more basic studies will be required to delineate the relative importance of different transmitter systems during normal and abnormal function of the basal ganglia.

6.3 Different Therapeutic Approaches

No curative treatment for the progressive dementia and motor disturbances is known at present and all current therapy is symptomatic.

6.3.1 Drugs affecting the cholinergic system

6.3.1.1 Cholinesterase inhibitors Several investigators have shown that physostigmine, a centrally active anticholinesterase, reduces the choreatic movements in H.C. patients (Aquilonus and Sjöström 1971 Klawans and Rubovits 1971 1972 Davis et al. 1976). However not all patients seem to be improved by physostigmine. In a study by Tarry et al. (1974) the chorea was reduced in only two out of twelve patients. Davis et al. (1976) found that one out of four patients was unaffected by physostigmine, and Fahn et al. (1973) saw no improvement in any of four patients treated with physostigmine.

6.3.1.2 Choline It has been demonstrated that parenteral administration of Ch to animals may result in increases in plasma and brain Ch concentrations and in brain concentrations of ACh (Haubrich et al. 1974 1975 Cohen and Wurtman 1975 Paper IV see above). This finding was of course of great interest as it suggested that Ch could be used as a "cholinergic L DOPA" in the treatment of postulated hypocholinergic disorders such as H.C. and tardive dyskinesia.

In 1975 it was shown by Aquilonius and Eckernäs that oral administration of Ch to patients resulted in a long-lasting elevation of the plasma Ch concentration, and in the same year Davis et al. (1975) reported that 16 g of Ch per day had beneficial effect in a case of tardive dyskinesia.

In study VI the effect of high oral doses of Ch (15 g/day) on the hyperkinesia in five patients with H.C. was examined. In spite of the dose-dependent increase in plasma Ch (Fig. 15), little or no clear therapeutic effect was noted following the

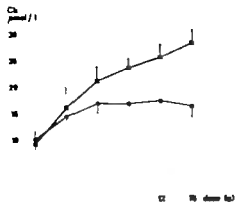


Fig. 15 Plasma Ch in five patients on oral doses of Ch. Plasma samples were taken on the third day following a change in Ch dose. ●—● 16 after the last daily dose; ■—■ 1 h after the second daily dose. Vertical bars indicate S.E.M. (from paper VT).

Ch treatment (Fig. 16). Two patients (AB and BZ) showed a tendency to a dose dependent reduction in their hyperkinetic movements, but only one type of hyperkinesia (no 11 in Fig. 16) in one patient (AB) returned to the premedication level following withdrawal of Ch, while the other hyperkinesias (nos. 2, 4 and 5 Fig. 16) were reduced even more after a two-month withdrawal period. One type of chorea in this patient (no. 5) even disappeared during the withdrawal period and a new type of hyperkinesia appeared instead. Such a spontaneous change in the hyperkinetic pattern might of course give rise to misleading interpretation of results when long-lasting drug effects in H.C. are being studied.

The failure to affect the choreatic movements by Ch treatment can be explained in several ways. Firstly as shown in Paper IV there is no indication of an increased turnover rate of ACh in brains of normal animals when plasma concentrations of Ch are increased. Thus, residual normal neurons in the brain of a patients with H.C. probably cannot increase the ACh release in order to compensate for degenerated neurons. However if the normal availability of Ch at the site of the synthetic reaction is reduced, for example, due to a defect in the HLA-system at early stages of degeneration, treatment with Ch might theoretically restore ACh synthesis. Secondly as shown in study V the degeneration of cholinergic neurons in the striatum is not uniform, and one part with complete degeneration might correspond to one type of refractory hyperkinesia. Muscarinic receptor sites might also be reduced in a patchy manner (Hiley and Bird 1974 Wastek et al. 1976). Finally the complexly disturbed interaction between different possible neuronal systems (DA ACh-GABA) cannot be restored merely by alteration of cholinergic function.

When preparing this survey a similar study was published (Davis et al. 1976), in which Ch in doses of up to 20 g daily was administered to four H.C. patients. Two patients showed a dose-dependent decrease in chorea, but in view of what appears to be spontaneous fluctuation in hyperkinesia, the result must be interpreted with caution. Nevertheless, it is felt that the present data concerning the clinical effects of Ch treatment in H.C. justify further studies. Since part of Ch

Frequency

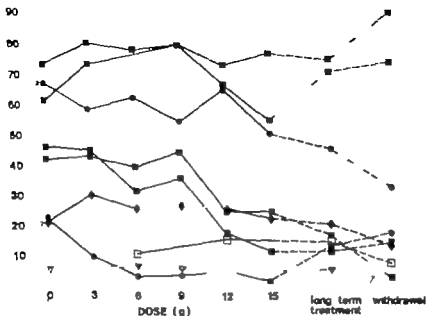


Fig. 16 Frequencies of involuntary movements (movements/min) in five patients suffering from H.C. treated with oral doses of Ch.

■ BZ, ● AB, ◆ MB, □ MN, ▽ PO

Types of hyperkinesia. 1 finger movements, 2 flexion of toes, 3 elevation of right leg, 4 head movements, 5 oral hyperkinesia, 6 abduction of the legs, 7 elevation of the eye brows, 8 maximal time (seconds) for extension of the tongue, 9 widening of the eyes (from paper VI).

seems to be metabolized to trimethylamine in the gut by bacterial action and in view of the possible rôle of trimethylamine in uremic toxicity (Simenbott 1975), studies concerning possible toxicological effects of long-term treatment with high doses of Ch also seem of special importance.

6.3.1.3 2 Dimethylaminoethanol (deanol) There is much controversy concerning deanol as a "cholinergic drug". Despite the evidence that Ch is formed slowly if at all, by methylation of the Ch analogues ethanolamine and dimethylaminoethanol (see above) in the brain, several investigators have described deanol as a precursor of brain Ch (Pfeiffer 1959, Walker et al. 1973, Miller et al. 1974, Miller 1974, Casey and Denny 1975, Haubrich et al. 1975b, Widrow and Heisler 1976). Some authors have reported that deanol increases brain ACh concentrations in animals (Pfeiffer 1959, Danyss et al. 1967, Goldberg and Silbery 1974, Haubrich et al. 1975b), while others have failed to substantiate a conversion of deanol to Ch and ACh (Pepet et al. 1960, Zahler and Hanin 1976).

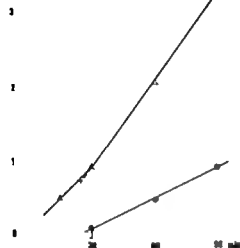


Fig. 17 Time course of ACh formation upon incubation of human CSF
●— untreated CSF ▽—boiled CSF (from paper VII)

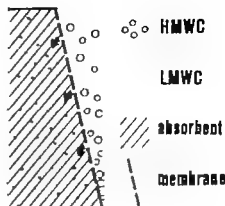


Fig. 18 The use of Minicon B15 (Amicon B.V. Holland) for obtaining a concentration of high molecular weight compounds (HMWC), while low molecular weight compounds (LMWC) are diluted at the same time (used in paper VII).

Despite the controversy regarding the action of deanol there are several reports of the therapeutic efficiency of this drug in tardive dyskinesia (Müller et al. 1974 Casey and Denny 1975 Curran et al. 1975), L DOPA induced hyperkinesia (Miller 1974) and Huntington's chorea (Walker et al. 1973). Other investigators, however, have failed to show any effect of deanol on tardive dyskinesia (Escobar and Kemp 1975) and in L DOPA induced dyskinesia (Klawans et al. 1975).

6.3.2 Drugs affecting the monoaminergic system

Drugs lowering (reserpine, tetrabenazines), displacing (α -methyl-dopa) or blocking (phenothiazines, butyrophenones) the action of catecholamines have all been reported to be of some use, albeit limited, in HC (see Barbeau 1975). On the other hand, L DOPA has generally been shown to aggravate chorea, except in the small number of patients who have the rigid akinetic form (juvenile form) of HC where L DOPA may improve the neurological status (see van Woert 1976).

In animal experiments it has been shown that a dopaminergic blockade increases the turnover of ACh in the striatum (Table V Trabucchi et al. 1973 Cheney et al. 1974) and this could perhaps be the mechanism underlying the improvement of hyperkinesia.

Fig. 19 Time course of ACh formation upon incubating of selectively concentrated human CSF. The high molecular weight (HMVC) fraction is concentrated 10 times while the low molecular weight (LMVC) fraction is diluted 10 times. —●— unboiled CSF, —▽— boiled CSF (from paper VII).



6.3.3 Drugs affecting the GABA-ergic system

Several investigations have failed to show any clear-cut effect on H.C. with different GABA-ergic stimulating drugs (see Barbeau 1975).

6.4 Early Detection

One of the aims of biochemical research in H.C. is the development of a test to permit detection of the disease long before the appearance of symptoms and, if possible, before the child-bearing age. Unfortunately such a goal has not yet been achieved, but several approaches have been tried, for example the L-DOPA load test (Klawans et al. 1972), "physiological test battery" and prolactin secretion following L-DOPA (Barbeau 1975).

Since degeneration of cholinergic neurons in the CNS theoretically would give rise to altered levels of ChAT in CSF assay of the enzyme activity in lumbar CSF might be a possible way of achieving early detection. In study VII a procedure was developed enabling the analysis of the small quantities of ChAT appearing in "normal" CSF. It was shown that a non enzymatically catalyzed synthesis of ACh, which was increased when CSF was boiled, appeared in untreated CSF during analysis (Fig. 17). This could be overcome, however, by a specific concentration of high molecular weight compounds in the CSF by use of a membrane with selective permeability (Figs. 18, 19). The method is now being applied in an investigation of CSF from H.C. patients and relatives of such patients.

7 General Summary

Simple and rapid methods for the determination of free choline (Ch) in plasma and of Ch and acetylcholine (ACh) concentrations in brain tissue have been developed.

Basic principles for turnover analysis are discussed, and these principles were applied in estimation of the turnover rate of ACh in rat brain parts following i.v. infusion of ^3H -Ch is described.

The origin and compartmentation of Ch in the brain and the regulation of ACh synthesis are treated. It is concluded that it seems unlikely that increased concentrations of plasma Ch are paralleled by an increased turnover rate of ACh under physiological conditions.

Different available methods for localization of cholinergic structures within the CNS are discussed. A stereotaxic method for tissue sampling in human brain was applied in a study of regional distribution of the cholinergic marker choline acetyltransferase (ChAT) in human brains. It was found that several nuclei of the basal ganglia could be subdivided according to the density of the cholinergic marker.

Possible pathophysiological mechanisms involved in Huntington's Chorea (H.C.) are discussed. Extreme reductions of ChAT were found in basal ganglia of brains of H.C. patients and it is concluded that a cholinergic hypofunction in the neostriatum due to degeneration of small cholinergic interneurons seems to be of pathophysiological importance.

Patients with H.C. were treated with high oral doses of Ch (15 g daily), but no clear-cut beneficial effect was noted. Some hyperkinesias showed an apparent dose-dependent reduction in frequency. However, this might have been an artefact due to a spontaneous variation in the hyperkinetic pattern. Nevertheless, it is felt that the present data justify further studies.

Early detection of H.C. before child-bearing age is an important aim. Since degeneration of cholinergic structures within the CNS theoretically should result in increased levels of ChAT in lumbar CSF, a method for the determination of the enzyme activity in human CSF was developed.

8 Acknowledgements

The present studies were performed at the Department of Pharmacology Faculty of Pharmacy (Paper I) and at the Department of Neurology University Hospital (Papers II–VII), Uppsala, Sweden.

I wish to express my sincere thanks to

Dr Sten-Magnus Aquilonius, my teacher and collaborator for excellent guidance, generous support and unfailing enthusiasm.

Professor Anders Sundwall, who first introduced me to cholinergic research

Professor Per-Olov Lundberg for the excellent facilities placed at my disposal at the Department of Neurology

Professor Bo Holmstedt, who kindly allowed me to use the microwave equipment at the Department of Toxicology Karolinska Institutet, Stockholm

Professor Sven Ulfberg, for advice concerning the cryomicrotome

My colleague Lena Sahlström, for highly stimulating collaboration

Inger Falk, Lena Persson and Lisbeth Lethipalo for skilful technical assistance

Karin Anter and Gunilla Gradin for excellent assistance in the preparation of manuscripts

Maud Marsden and Dr David Burke for revising the English

The airplane SE-FFI for highly stimulating flying and recreation

My friends at the medical school who encouraged me in my medical studies in parallel with my research

Numerous other friends for help and stimulating discussions.

The financial support of The Swedish Medical Research Council, Tore Nilsson Foundation, Harald and Greta Jeansson Foundation, Anton and Dorothea Bechius Foundation, Swedish Society for Medical Research, the Lernander Fund and Grants from the Faculty of Pharmacy and the Faculty of Medicine, Uppsala University is gratefully acknowledged.

9 References

- Acara, M. The kidney in regulation of plasma choline in the chicken. *Amer J Physiol* 1975 228 645-649
- Andén, N.-E., A. Carlsson, A. Dahlström, K. Fuxe, N.A. Hillarp and N. Larsson, Demonstration and mapping out of nigro-neostriatal dopamine neurons. *Life Sci* 1964 3 523-530
- Andén, N.-E., K. Fuxe, B. Hamberger and T. Hökfelt, A quantitative study on the nigro-neostriatal dopamine neuron system in the rat. *Acta Physiol Scand.* 1966, 67 306-312.
- Ansell, G.B. and S. Spanner. The metabolism of labeled ethanolamine in the brain of the rat *in vivo* *J Neurochem* 1967 14 873-885
- Ansell, G.B. and S. Spanner. The metabolism of [^{14}C] choline in the brain of the rat *in vivo* *Biochem. J* 1968, 110 201-206
- Aquilonius, S.-M. and S.-Å. Eckernäs, Plasma concentration of free choline in Huntington patients on high doses of choline chloride. *New Eng J Med* 1975 293 1105-1106.
- Aquilonius, S.-M. and R. Sjöström, Cholinergic and dopaminergic mechanisms in Huntington's chorea. *Life Sci* 1971 10 405-414
- Aquilonius, S.-M. S.-Å. Eckernäs and A. Sundwall, Topical localization of choline acetyltransferase in human extrapyramidal nuclei. *Acta Physiol Scand* 1973a, Suppl. 396 79
- Aquilonius, S.-M. S.-Å. Eckernäs and A. Sundwall, Brain choline acetyltransferase in hereditary chorea. *Acta Pharmacol. Toxicol* (Kbh) 1974 35 suppl. 1 p. 19
- Aquilonius, S.-M., B. Nyström, J. Schuberth and A. Sundwall, Cerebrospinal fluid choline in extrapyramidal disorders. *J Neurol. Neurosurg Psychiatry* 1972, 35 720-725
- Aquilonius, S.-M., G. Ceder, U. Lyng-Tunell, H. O. Malmund and J. Schuberth, The arteriovenous difference of choline across the brain of man. *Brain Res.* 1975 99 430-433
- Aquilonius, S.-M., F. Flemig, J. Schuberth, B. Sparf and A. Sundwall, Synthesis of acetylcholine in different compartments of brain nerve terminals *in vivo* as studied by the incorporation of choline from plasma and the effect of pentobarbital on this process. *J Neurochem.* 1973b, 20 1509-1521
- Barbeau, A. Progress in understanding Huntington's chorea. *J Can. Sci Neurol.* 1975 May 81-85
- Barbeau, A., T.N. Chase and G.W. Paulson, Huntington's Chorea, 1872-1972. In *Advances in Neurology* Raven Press, New York, 1973 vol. 1
- Bartholini, G., H. Stadler, M. Gadea-Coria and K.G. Lloyd, The use of push-pull canula to estimate the dynamics of acetylcholine and catecholamines within various brain areas. *Neuropharmacol* 1976, 15 515-519

- Barker L.A. Subcellular aspects of acetylcholine metabolism. In *Biology of Cholinergic Function* Eds. A.M. Goldberg and I. Hanin. Raven Press. New York. 1976. pp. 203-238.
- Barker L.A. and T.W. Mittag, Comparative studies of substrate and inhibitors of choline transport and choline acetyltransferase. *J Pharmacol Exp. Ther* 1975 192 86-94
- Bernheimer H. and O. Hornykiewicz, Brain amines and Huntington's chorea. In *Advances in Neurology* Eds. A. Barbeau, T.N. Chase and G.W. Paulson. Raven Press. New York. 1973 pp. 525-531
- Bird, E.D. and L.L. Iversen, Huntington's chorea. Post mortem measurement of glutamic acid decarboxylase, choline acetyltransferase and dopamine in basal ganglia. *Brain*. 1974 97 457-472.
- Bird, E.D. A.V.P. Mackay C.N. Rayner and L.L. Iversen, Reduced glutamic acid-decarboxylase activity of postmortem brain in Huntington's chorea. *Lancet*. 1973 1 1090-1092.
- Birks, R. and F.C. MacIntosh, Acetylcholine metabolism of a sympathetic ganglion. *Can J Biochem. Physiol*. 1961 39 787-827
- Bligh, J. The level of free choline in plasma. *J Physiol (Lond)*. 1952. 117 234-240.
- Bligh, J. The role of the liver and the kidneys in the maintenance of the level of free choline in plasma. *J Physiol (Lond)*. 1953 120 53-62.
- Bloom, F.E., E. Costa and G.C. Salmistraglia, Anesthesia and the responsiveness of individual neurons of the caudate nucleus of the cat to acetylcholine, norepinephrine and dopamine administered by microelectrophoresis. *J Pharmacol. Exp. Ther* 1965 150 244-252.
- Bowen, D.M. P. White and A.N. Davison, Glutamic acid (GAD) and dehydroxy phenylalanine (DOPAD) decarboxylase activities in senile dementia. Proceedings 7th Int. Congress of Neuropathology Akadémiai Kiado Budapest. 1974. p. 41
- Bremer J. and D.M. Greenberg, Methyl transferring enzyme system of microsomes in the biosynthesis of lecithin (phosphatidylcholine). *Biochim Biophys Acta* 1961 46 205-216.
- Browning, E.T., Acetylcholine synthesis: Substrate availability and the synthetic reaction. In *Biology of Cholinergic Function* Eds. A.M. Goldberg and I. Hanin. Raven Press. New York. 1976. pp. 187-201
- Browning, E.T. and M.P. Schulman, [^{14}C] Acetylcholine synthesis by cortical slices of rat brain. *J Neurochem* 1968. 15 1391-1405
- Bruyn, G.W., Huntington's chorea. Historical clinical and laboratory synopsis. In. *Handbook of Clinical Neurology* Vol. 6, Diseases of Basal Ganglia. Eds. P.J. Vinken and G.W. Bruyn. North Holland. Amsterdam. 1968. pp. 295-378.
- Burt, A.M. A histochemical procedure for the localization of choline acetyltransferase activity *J Histochem Cytochem*. 1970 18 408-415

- Burt, A.M. and A. Silver. DFP as a prerequisite in the histochemical demonstration of choline acetyltransferase. *Brain Res* 1973 57 518-521
- Butcher S.H. and L.L. Butcher. Acetylcholine and choline levels in the rat corpus striatum after microwave irradiation. *Proc West Pharmacol Soc* 1974a. 17 37-39
- Butcher S.H. and L.L. Butcher. Origin and modulation of acetylcholine activity in the neostriatum. *Brain Res* 1974b. 71 167-171
- Carroll, P.T. and G.G. Buterbaugh. Regional differences in high affinity choline transport velocity in guinea-pig brain. *J Neurochem* 1975 24 229-232.
- Carroll, P.T. and A.H. Goldberg. Relative importance of choline transport to spontaneous and potassium depolarized release of acetylcholine. *J Neurochem* 1975 25 523-527
- Casey D.E. and D. Denny Deanol in treatment of tardive dyskinesia. *Am J Psychiatry* 1975 132 864-867
- Cheney D.L., E. Costa, G. Racagni and M. Trabucchi. Dopaminergic regulation of acetylcholine turnover rates in rat striatum. *Br J Pharmacol* 1974 52 427P-428P
- Cheney D.L., E. Costa, I. Hanlin, M. Trabucchi and L.T. Wang. Application of principles of steady-state kinetics to the *in vivo* estimation of acetylcholine turnover rate in mouse brain. *J Pharmacol Exp. Ther* 1975 192 288-296.
- Choi, R.L., J.J. Freeman and D.J. Jenden. Kinetics of plasma choline in relation to turnover of brain choline and formation of acetylcholine. *J Neurochem* 1975 24 735-741
- Cohen, E.L. and R.J. Wurtman. Brain acetylcholine. Increase after systemic choline administration. *Life Sci* 1975 16 1095-1102.
- Collier B. The preferential release of newly synthesized transmitter by a sympathetic ganglion. *J Physiol (Lond.)* 1969 205 341-352.
- Collier B. and H.S. Katz. Acetylcholine synthesis from recaptured choline by a sympathetic ganglion. *J Physiol (Lond.)* 1974 238 639-655
- Collier B. and F.C. MacIntosh. The source of choline for acetylcholine synthesis in a sympathetic ganglion. *Can. J Physiol. Pharmacol* 1969 47 127-135
- Consolo, S. H. Ladinsky and S. Garatuni. Effect of several dopaminergic drugs and trihexyphenidyl on cholinergic parameters in rat striatum. *J Pharm. Pharmacol* 1974 26 275-277
- Cools, A.R., Athetoid and choreiform hyperkinesias produced by caudate application of dopamine in cats. *Psychopharmacologia* 1972. 25 229-237
- Curran, D. S. Nagaswami and K. Mohan. Treatment of phenothiazine induced bulbar persistent dyskinesia with deanol acetamidobenzoate. *Dis Nerv Sys* 1975 36 71-73
- Dahlström, A. and K. Fuxe. Evidence for the existence of monoamine-containing neurons in the central nervous system. I. Demonstration of monoamines in the cell bodies on brain stem neurons. *Acta Physiol Scand* 1964 Suppl. 232. 1-55

- Dale, H.H., The action of certain esters and ethers of choline, and their relation to muscarine. *J Pharmacol Exp. Ther* 1914 6 147-190
- Dale, H.H. and H.W. Dudley The presence of histamine and acetylcholine in the spleen of the ox and the horse. *J Physiol (Lond.)* 1929 68 97-123
- Danyuz, A., D. Kocmieraka-Grodzka, B. Kostro, B. Polocki and J. Kruszewska, Pharmacological properties of 2-dimethylaminoethanol. *Dissert Pharm Pharmacol* 1967 19 469-477
- Davis, K.L., P.A. Berger and L.E. Hollister Choline for tardive dyskinesia. *New Eng J Med* 1975 293
- Davis, K.L., L.E. Hollister J.D. Barchas and P.A. Berger Choline in tardive dyskinesia and Huntington's disease. *Life Sci* 1976. 19 1507-1516.
- Diamond, L. Choline metabolism in brain. *Arch Neurol* 1971 24 333-339
- Dikshik, B.B. Action of acetylcholine on the brain and its occurrence therein. *J Physiol (Lond.)* 1934 80 409-421
- Dowdall, M.J. and E.J. Simon, Comparative studies on synaptosomes Uptake of [N-Me ³H] choline by synaptosomes from squid optic lobes. *J Neurochem* 1973 21 969-982.
- Dross, V.K. and H. Kewitz, Das Einbau von $\text{L}\alpha$ zugefuhrtem Cholin in das Acetylcholin des Gehirns. *Neuromy Schmeldebergs Arch Pharmacol* 1966. 255 10
- Dross, H. and H. Kewitz, Concentration and origin of choline in rat brain. *Neuromy Schmeldebergs Arch Pharmacol. Exp Pathol* 1972. 274 91-106.
- Ehringer H. and O. Hornykiewicz, Verteilung von Noradrenalin und Dopamin (3-hydroxytyramin) im Gehirn des Menschen und ihr Verhalten bei Erkrankungen des Extrapyramidale Systems. *Klin Wschr* 1960 38 1236-1239
- Eisenstadt, M.L. and J.H. Schwartz, Metabolism of acetylcholine in the nervous system of *Aplysia californica*. III Studies of an identified cholinergic neuron. *J Gen. Physiol* 1975 65 293-313
- Eksborg, S. and B.A. Persson, Photometric determination of acetylcholine in rat brain after selective isolation by ion pair extraction and micro column separation. *Acta Pharm Suec* 1971a. 8 205-216
- Eksborg, S. and B.A. Persson, Photometric determination of choline in biological objects by ion pair extraction technique. *Acta Pharm Suec* 1971b. 8 605-608.
- Eng, L.F. C.T. Uyeda, L.P. Chao and F. Wolfgram, Antibody to bovine choline acetyltransferase and immunofluorescent localization of the enzyme in the neuroax. *Nature (Lond.)* 1974 250 243-245
- Escobar J.J. and K.F. Kemp, Dimethylaminoethanol for tardive dyskinesia. *New Eng J Med* 1975 292 317-318
- Ewetz, L., B. Sparf and B. Sörbo, Enzymatic determination of choline in brain with choline phosphokinase and ³²P-labelled ATP In *Symposium on in vitro procedures with radiotopes in clinical medicine and research* International Atomic Energy Agency 1969 pp. 175-183

- Fahn, S. and L.J. Côté, Regional distribution of choline acetylase in the brain of the rhesus monkey *Brain Res* 1968, 7 323-325
- Fahn, S., M.M. Mishkin and R.R. Hoffman, Pharmacological and radiologic investigations in Huntington's chorea. In *Advances in Neurology* Eds. A. Barbeau, T.N. Chase and G.W. Paulson. Raven Press. New York 1973 1 pp. 581-597
- Felgenson, M.F. and J.K. Saelens, An enzyme assay for acetylcholine. *Biochem Pharmacol* 1969 18 1479-1486.
- Feldberg, W., Present views on the mode of action of acetylcholine in the central nervous system. *Physiol. Rev* 1945 25 596-642.
- Fellman, J.H. A chemical method for the determination of acetylcholine. Its application in a study of presynaptic release and a choline acetyltransferase assay *J Neurochem.* 1969 16 135-143.
- Fonnum, F., Isolation of choline esters from aqueous solutions by extraction with sodium tetraphenylboron in organic solvents. *Biochem. J* 1969 113 291-298.
- Fonnum, F., Topographical and subcellular localization of choline acetyltransferase in rat hippocampal region. *J Neurochem.* 1970. 17 1029-1037
- Fonnum, F., Recent developments in biochemical investigations of cholinergic transmission. *Brain Res* 1973 62 497-507
- Fonnum, F., A rapid radiochemical method for the determination of choline acetyltransferase. *J Neurochem* 1975 24 407-409
- Fonnum, F. I. Grofova, E. Rinvik, J. Storm-Mathisen and F. Wolberg, Origin and distribution of glutamate decarboxylase in substantia nigra of the cat. *Brain Res.* 1974 71 77-92.
- Freeman, J.J. and D.J. Jenden, The source of choline for acetylcholine synthesis in brain. *Life Sci* 1976. 19 949-962.
- Freeman, J.J. R.L. Choi and D.J. Jenden, Plasma choline: Its turnover and exchange with brain choline. *J Neurochem* 1975 24 729-734
- Gardiner J.E., The infusion of choline into the carotid circulation of the cat. *Arch. Int. Pharmacodyn.* 1974 209 150-161
- Gardiner J.E. and M.C.E. Gwee, The distribution in the rabbit of choline administered by injection or infusion. *J Physiol (Lond.)* 1974 239 459-476
- Gardiner J.E. and W.D.M. Paton, The control of the plasma choline concentration in the cat. *J Physiol (Lond.)* 1972. 227 71-86
- Gerlach, J., N. Reusby and A. Randrup, Dopaminergic hypersensitivity and cholinergic hypofunction in the pathophysiology of tardive dyskinesia. *Psychopharmacologia (Berl.)* 1974 34 21-35
- Glaeser B.S., W.H. Vogel D.B. Olewiler and T.A. Hare, GABA levels in cerebrospinal fluid of patients with Huntington's chorea: A preliminary report. *Biochem Med.* 1975 12 380-385
- Glover V.A.S. and L.T. Potter Purification and properties of choline acetyltransferase. *J Neurochem* 1971 18 571-580.

- Goldberg, A.M. and R.E. McCaman, The determination of picomole amounts of acetylcholine in mammalian brain. *J Neurochem.* 1973 20 1-8.
- Goldberg, A.M. and E.K. Silbergeld, Neurological aspects of lead induced hyperactivity *Trans. Am Soc Neurochem.* 1974 5 185
- Gundolf, A., D.L. Cheney, M. Trabucchi, M. Doteuchi and C. Wang, Focussed microwave radiation. A technique to minimize post mortem changes of cyclic nucleotides, DOPA, and choline and to preserve brain morphology *Neuropharmacol* 1974 13 1115-1122.
- Haga, T. and H. Noda, Choline uptake systems of rat brain synaptosomes. *Biophys Acta* 1973. 291 564-575
- Hammar C.G. L. Hanin, B. Holmstedt, R.J. Kitz, D.J. Jenden and B. Karlén, Identification of acetylcholine in fresh rat brain by combined gas chromatography-mass spectrometry *Nature (Lond.)* 1968. 220 915-917
- Hanin, I. *Choline and acetylcholine Handbook of chemical assay methods.* Raven Press, New York. 1974
- Hanin, I. and D.J. Jenden, The effect of perchlorate ion and some pharmacological agents on the sensitivity of the frog (*Rana pipiens*) rectus abdominis to acetylcholine. *Experientia* 1966. 22 537-539
- Hanin, I. and J. Schuberth, Labelling of acetylcholine in the brain of mice fed on a diet containing deuterium labelled choline Studies utilizing gas chromatography-mass spectrometry *J Neurochem* 1974 23 819-824
- Hanin, I. and R.F. Skinner Analysis of microquantities of choline and its esters utilizing gas chromatography-chemical ionization mass spectrometry *Anal Biochem.* 1975 66 568-583
- Hanin, I., R. Massarelli and E. Costa, Environmental and technical preconditions influencing choline and acetylcholine concentrations in rat brain. In *Drug and Cholinergic Mechanisms in the CNS* Eds. E. Hellbrom and A. Winter Försvarets forskningsanstalt, Stockholm. 1970 pp 33-54
- Hattori, T. P.L. McGeer H.C. Ffifiger and E.G. McGeer On the source of GABA-containing terminals in the substantia nigra Electron microscopic autoradiographic and biochemical studies. *Brain Res* 1973 54 103-114
- Hattori, T. V.K. Singh, E.G. McGeer and P.L. McGeer Immunohistochemical localization of choline acetyltransferase containing neostriatal neurons and their relationship with dopaminergic synapses. *Brain Res.* 1976 102 164-173
- Haubrich, D.R., Choline acetyltransferase and its inhibitors. In *Biology of Cholinergic Function.* Eds. A.M. Goldberg and I. Hanin. Raven Press, New York. 1976. pp. 239-268.
- Haubrich, D.R., P.F.L. Wang and D.E. Clody Increase in tissue concentration of acetylcholine in guinea pigs *in vivo* induced by administration of choline *Life Sci* 1974 14 921-927
- Haubrich, D.R. P.F.L. Wang and P.W. Wedeking, Distribution and metabolism of intravenously administered choline[methyl-³H] and synthesis *in vivo* of

- Lewis, P.R. and C C D Shute, The cholinergic limbic system. Projections to hippocampal formation, medial cortex, nuclei of the ascending cholinergic reticular system and the subfornical organ and supra-optic crest. *Brain* 1967 90 521-540
- Lewis, P.R., C C D Shute and A Silver. Confirmation from choline acetylase of a massive cholinergic innervation to rat hippocampus. *J Physiol* (Lond.) 1967 191 215-224
- Lloyd, K G and O Hornykiewicz, L. glutamic acid decarboxylase in Parkinson's disease. Effect of L DOPA therapy. *Nature* (Lond.) 1973 243 521-523
- MacIntosh, F C. Synthesis and storage of acetylcholine in nervous tissue. *Can. J Biochem Physiol* 1963 41 2555-2571
- Mahle Sorensen, D., T Eskeland and F Fonnum. Purification of rat brain choline acetyltransferase: some immunochemical properties of a highly purified preparation. *Brain Res* 1973 62 517-522
- Mastova, A.F., Quantitative determination of acetylcholine in biological materials by polarographic analysis. *Vopr Med. Khim* 1964 10 311 (see *Fed Proc* 1965 24 P548-550.)
- Massarelli, R., T Durkin, C. Niedergang and P Mandel, A simple radioenzymatic determination of choline and acetylcholine concentrations. *Pharmacol. Res Commun* 1976. 8 407-416.
- Mattsson, H. Clinical, genetic and pharmacological studies in Huntington's chorea. *University of Umea Medical Dissertations* 7 1974
- McGeer P.L. and E.G. McGeer. Cholinergic enzyme systems in Parkinson's disease. *Arch Neurol* (Chic.) 1971 25 265-268.
- McGeer P.L. and E.G. McGeer. Enzymes associated with the metabolism of catecholamines, acetylcholine and GABA in human controls and patients with Parkinson's disease and Huntington's chorea. *J Neurochem* 1976 26 65-76.
- McGeer P.L., E.G. McGeer and H C Fibiger. Choline acetylase and glutamic acid decarboxylase in Huntington's chorea. *Neurology* (Minncap.) 1973 23 912-917
- McGeer P.L., E.G. McGeer H C Fibiger and V Wickson, Neonatal choline acetylase and cholinesterase following selective brain lesions. *Brain Res* 1971a. 35 308-314
- McGeer E.G. P.L. McGeer D.S. Grewal and V.K. Singh, Striatal cholinergic interneurons and their relation to dopaminergic nerve endings. *J Pharmacol* (Paris) 1975. 6 143-152.
- McGeer P.L., E.G. McGeer V.K. Singh and W.H. Chase, Choline acetyltransferase localization in the central nervous system by immunohistochemistry. *Brain Res* 1974 81 373-379
- McGeer P.L. E.G. McGeer J.A. Wada and E. Jung, Effect of globus pallidus lesions and Parkinson's disease on brain glutamic acid decarboxylase. *Brain Res* 1971b. 32 425-431
- McGeer E.G. J.A. Wada, A. Terao and E. Jung, Amine synthesis in various

- brain regions with caudate or septal lesions. *Exptl Neurol* 1969 24 277-284
- Müller E., Deanol in the treatment of levodopa-induced dyskinesias. *Neurology (Minneapolis)* 1974. 24 116-119
- Müller E., D.E. Casey and D. Denney Deanol A solution for tardive dyskinesia. *New Eng J Med* 1974 291 796-797
- Modak, A.T. S.T. Weintraub, T.H. McCoy and W.B. Stavinocha, Use of 300-msec microwave irradiation for enzyme inactivation. A study of effects of sodium pentobarbital on acetylcholine concentration in mouse brain regions. *J Pharmacol. Exp. Ther* 1976. 197 245-252.
- Molenaar P.C. and R.L. Polak, Analysis of the preferential release of newly synthesized acetylcholine by cortical slices from rat brain with the aid of two different labelled precursors. *J Neurochem* 1976 26 95-99
- Morris, D. A. Manockjee and C. Hebb, Kinetic properties of human placental choline acetyltransferase. *Biochem J* 1971 125 857-863
- Nordberg, A. Apparent regional turnover of acetylcholine in mouse brain. Methodological and functional aspects. *Acta Physiol Scand* 1977a. Suppl. 445. 1-51
- Nordberg, A., Effect of oxotremorine and sodium pentobarbitone on the pharmacokinetics of intravenous tracer doses of radioactive choline. *J Pharm Pharmacol.* 1977b. 29 96-98.
- Nordberg, A. and A. Sundwall, Effect of pentobarbital on endogenous acetylcholine and biotransformation of radioactive choline in different brain regions. In: *Cholinergic Mechanisms* Ed. P.G. Waser Raven Press. New York. 1975 pp 229-239
- Nordberg, A. and A. Sundwall, Biosynthesis of acetylcholine in different brain regions *in vitro* following alternative methods of sacrifice by microwave irradiation. *Acta Physiol. Scand* 1976 98 307-317
- Pepen, G., D.X. Freedman and N.J. Glarman, Biochemical and pharmacological studies of dimethylaminoethanol (denol). *J Pharmacol Exp. Ther* 1960 129 291-295
- Perry T.L., S. Hansen and M. Kloster Huntington's chorea. Deficiency of γ aminobutyric acid in brain. *New Eng J Med* 1973 288 337-342.
- Pfeiffer C.C., Parasympathetic neurohumors, possible precursors and effect on behaviour *Int Rev Neurobiol* 1959 1 195-244
- Potter L.T. Synthesis, storage and release of (1 C)-acetylcholine in isolated rat diaphragm muscles. *J Physiol (Lond.)* 1970. 206 145-166.
- Racagni, G. M. Trabucchi and D.L. Cheney Steady state concentrations of choline and acetylcholine in rat brain parts during a constant rate infusion of deuterated choline. *Naunyn-Schmiedeberg's Arch Pharmacol* 1975 290 99-105.
- Racagni, G. D.L. Cheney M. Trabucchi and E. Costa, *In vitro* actions of clozapine and haloperidol on the turnover rate of acetylcholine in rat striatum. *J Pharmacol. Exp. Ther* 1976. 196 323-332.

- Racagni, G. D.L. Cheney M. Trabucchi, C. Wang and E. Costa, Measurement of acetylcholine turnover rate in discrete areas of rat brain. *Life Sci* 1974 15 1961-1975
- Reid, W.D. D.R. Haubrich and G. Krishna, Enzymatic radioassay for acetylcholine and choline in brain. *Anal Biochem* 1971 42 390-397
- Rennick, B., M. Acara, P. Hysert and B. Mookerjee, Choline loss during hemodialysis. Homeostatic control of plasma choline concentrations. *Kidney Int* 1976. 10 329-335
- Rommelspacher H. and M.J. Kuhar. Effect of electrical stimulation on acetylcholine levels in the central cholinergic nerve terminals. *Brain Res.* 1974 81 243-251
- Rommelspacher H. and M.J. Kuhar. Effect of dopaminergic drugs and acute medial forebrain bundle lesions on striatal acetylcholine levels. *Life Sci* 1975 16 65-70.
- Rossier J. Immunohistochemical localization of choline acetyltransferase: real or artefact? *Brain Res* 1975 98 619-622.
- Rossier J. Purification of rat brain choline acetyltransferase. *J Neurochem* 1976 26 543-548.
- Roth, R.H. and B.S. Bunney. Interaction of cholinergic neurons with other chemically defined neuronal systems in the CNS. In *Biology of Cholinergic Function*. Eds. A.M. Goldberg and I. Hanin. Raven Press. New York 1976 pp. 379-394
- Saelens, J.K. and J.P. Smke, Effects of various drugs on acetylcholine and choline concentrations in various biological tissues. In *Biology of Cholinergic Function* Eds. A.M. Goldberg and I. Hanin. Raven Press. New York. 1976 pp. 683-706.
- Saelens, J.K. J.P. Smke, M.P. Aden and C.A. Conroy. Some of the dynamics of choline and acetylcholine metabolism in rat brain. *Arch Int Pharmacodyn. Ther* 1973 203 305-312.
- Sastry B.V.R. J. Oluwadewo, R.D. Harbison and D.E. Schmidt, Human placental cholinergic system. Occurrence, distribution and variation with gestational age of acetylcholine in human placenta. *Biochem Pharmacol* 1976 25 425-431
- Schmidt, D.E., Regional levels of choline and acetylcholine in rat brain following head focussed microwave sacrifice. Effect of (+)amphetamine and (\pm) parachloroamphetamine. *Neuropharmacol.* 1976. 15 77-84
- Schmidt, D.E., H.C. Speth, F. Welsch and M.J. Schmidt, The use of microwave radiation in the determination of acetylcholine in the rat brain. *Brain Res* 1972. 38 377-389
- Schuberth, J. and D.J. Jenden, Transport of choline from plasma to cerebrospinal fluid in the rabbit with reference to the origin of choline and to acetylcholine metabolism in the brain. *Brain Res* 1975 84 245-256.
- Schuberth, J., B. Sparf and A. Sundwall, A technique for the study of

- acetylcholine turnover in mouse brain *in vitro*. *J Neurochem.* 1969 *16* 695-700.
- Schubert, J., B Sparf and A Sundwall, On the turnover of acetylcholine in nerve endings of mouse brain *in vitro*. *J Neurochem* 1970. *17* 461-468.
- Schumacher H and R. Ehl, Influence of diethyl-p-nitrophenyl phosphate on the acetylcholine content of aqueous humor *1rnselm Forsch* 1970. *20* 1476-1479
- Sethy V.H. and M.H. Van Woert, Regulation of striatal acetylcholine concentration by dopamine receptors. *Nature (Lond.)* 1974 *251* 529-530
- Shea, P.A. and M.H. Aprison, An enzymatic method for measuring picomole quantities of acetylcholine and choline in CNS tissue. *Anal. Biochem* 1973 *56* 165-177
- Siroenhoff, M.L., Metabolism and toxicity of aliphatic amines. *Kidney Int* 1975 *7* S314-S317
- Simon, J.R. and M.J. Kuhar Impulse-flow regulation of high affinity choline uptake in brain cholinergic nerve terminals. *Nature* 1975 *255* 162-163
- Simon, J.R., S Atweh and M.J. Kuhar Sodium dependent high affinity choline uptake: A regulatory step in the synthesis of acetylcholine. *J Neurochem.* 1976. *26* 909-922.
- Singh, V.K. E.G. McGeer and P.L. McGeer Two immunological different choline acetyltransferase in human neostriatum. *Brain Res* 1975 *96* 187-191
- Smith, J.C. and J.K. Saelens, Determination of tissue choline with choline acetyltransferase. *Fed Proc* 1967 *26* 296.
- Sorimachi, M. and K. Katsuka, Choline uptake by nerve terminals: A sensitive and specific marker of cholinergic innervation. *Brain Res* 1974 *72* 350-353
- Spanner S R.C. Hall and G.B. Ansell, Arterio-venous differences of choline and choline lipids across the brain of rat and rabbit. *Biochem J* 1976. *154* 133-140.
- Sparf, B. On the turnover of acetylcholine in the brain. *Acta Physiol Scand* 1973. Suppl. 397 1-47
- Stahl, W.L. and P.D. Swanson, Biochemical abnormalities in Huntington's chorea. *Neurology (Minneapolis)* 1974 *24* 813-819
- Stavrohs, W.B. S.T. Wentraub and A.T. Modak, The use of microwave heating to inactivate cholinesterase in the rat brain prior to analysis for acetylcholine. *J Neurochem.* 1973 *20* 361-371
- Suzukiw J.B. and G. Pilar Selective localization of a high affinity choline uptake system and its role in ACh formation in cholinergic nerve terminals. *J Neurochem* 1976 *26* 1133-1138
- Szerb, J. The estimation of acetylcholine using leech muscle in a microbath. *J Physiol* 1961 *158* 8-9
- Szilagyi, P.I.A. J.P. Green, O.M. Brown and S. Margolis, The measurement of nanogram amounts of acetylcholine in tissues by pyrolysis gas chromatography *J Neurochem* 1972, *19* 2555-2566.

- Tarsy D., N Leopold and D.S. Sax, Physostigmine in choreiform movement disorders. *Neurology (Minneapolis)* 1974 24 28-33
- Trabucchi, M., D.L. Cheney G Racagni and E. Costa, Involvement of brain cholinergic mechanisms in the action of chlorpromazine. *Nature (Lond.)* 1973 249 664-666.
- Ulin, B K Gustavii and B A Persson, Bioanalysis of picomole amounts of acetylcholine by ion pair partition chromatography applied to rat striatic nerve. *J Pharm. Pharmacol.* 1976. 28 672-675
- Ungerstedt, U., Stereotaxic mapping of the monoamine pathways in the rat brain. *Acta Physiol. Scand.* 1971 Suppl. 267 1-48.
- Urguhart, N., T.L. Perry S. Hansen and J Kennedy GABA content and glutamic acid decarboxylase activity in brain of Huntington's chorea patients and control subjects. *J Neurochem* 1975 4 1071-1075
- Van Woert, M.H Parkinson's disease, tardive dyskinesia, and Huntington's chorea. In *Biology of Cholinergic Function*. Eds. A.M Goldberg and L. Hanin. Raven Press. New York 1976. pp. 583-601
- Walker J.E., M Hoehn, E. Sears and J Lewis, Dimethylaminoethanol in Huntington's chorea. *Lancet* 1973 1 1512.
- Wang, P.F.L. and D.R. Haubrich, A simple, sensitive and specific assay for free choline in plasma. *Anal. Biochem.* 1975 63 195-201
- Wastek, G.J L.Z. Stern, P.C Johnson and H.I Yamamura, Huntington disease: Regional alternation in muscarinic cholinergic receptor binding in human brain. *Life Sci.* 1976. 19 1033-1040.
- Weintraub, S.T A.T Modak and W.B Stavinoch, Acetylcholine postmortem increase in rat brain regions. *Brain Res.* 1976. 105 179-183
- Widroe, H.J and S. Heisler Treatment of tardive dyskinesia. *Diseases of nervous system* 1976. 37 162-164
- Wurtman, R.J and J.D Fernstrom, Control of brain neurotransmitter synthesis by precursor availability and nutritional state. *Biochem. Pharmacol.* 1976 25 1691-1696
- Yaksh, T.L. and H.I Yamamura, The release *in vitro* of [³H] acetylcholine from cat caudate nucleus and cerebral cortex by atropine, pentylenetetrazol, II depolarization and electrical stimulation. *J Neurochem.* 1975 25 123-130.
- Yamamura, H.I. and S. Snyder High affinity transport of choline into synaptosomes of rat brain. *J Neurochem* 1973 21 1355-1374
- Zahniser N.R. and L. Hanin, Deanol and the cholinergic system A gas chromatographic evaluation. *Fed Proc* 1976. 35 801 Abstract No 3286.
- Zilversmit, D.B The design and analysis of isotope experiments. *Am J Med.* 1960. 29 832-848.

ACTA PHYSIOLOGICA SCAN
SUPPLEMENTUM 450

Local Sympathetic Reflex Mechanisms
in Regulation of Blood Flow in
Human Subcutaneous Adipose Tissue

BY
OLE HENRIKSEN

COPENHAGEN 1977

Forsvaret finder sted tirsdag den 7 juni 1977
kl. 14 præcis i Universitetets annex-auditorium A,
Studiestræde 6 (over gården).

ACTA PHYSIOLOGICA SCANDINAVICA
Supplement 450

From the Department of Nuclear Medicine Rigshospitalet, Copenhagen, Denmark

Local Sympathetic Reflex Mechanism in Regulation
of Blood Flow in Human Subcutaneous
Adipose Tissue

by

OLE HENRIKSEN

COPENHAGEN 1977

Denne afhandling er i forbindelse med omstående tidligere publicerede afhandlinger af det lægevidenskabelige fakultet ved Københavns Universitet antaget til offentlig at forsvares for den medicinske doktorgrad

København den 4 marts 1977

J C Melchior dekan

The present thesis is based on the following publications

- I. Henriksen, O S L. Nielsen and W P Paaske Autoregulation of blood flow in human adipose tissue *Acta physiol scand* 1973 89 531-537
- II. Henriksen, O and T Alsner Effect of spinal sympathetic blockade upon local regulation of blood flow in subcutaneous tissue. *Acta physiol scand* 1975 95 83-88
- III. Henriksen O Effect of somesthetic denervation upon the vasoconstrictor response in human subcutaneous tissue *Acta physiol scand* 1976 96 431-432.
- IV. Henriksen, O Effect of chronic sympathetic denervation upon blood flow in human subcutaneous tissue. *Acta physiol. scand* 1976 97 377-384
- V. Henriksen, O Local reflex in microcirculation in human subcutaneous tissue *Acta physiol. scand* 1976 97 447-456.
- VI. Henriksen, O Local nervous mechanism in regulation of blood flow in human subcutaneous tissue *Acta physiol scand* 1976 97 385-391

Preface

I wish to express my deepest gratitude to P. Sejrnsen, M.D. Ph.D. Institute of Medical Physiology II University of Copenhagen, for his great interest, active support and many invaluable and inspiring discussions during the whole course of the present study.

I further wish to thank W. Paaske, M.D. Institute of Medical Physiology B for his exceedingly valuable collaboration and constructive criticism of the manuscript.

The investigations have been carried out in the Dept. of Nuclear Medicine Rigshospitalet, and the Institute of Medical Physiology B University of Copenhagen and I wish to thank the heads of these departments: T. Munkner, M.D. Ph.D. S. Solvsten Sørensen, M.D. and Professor P. Krüthoffer, M.D. Ph.D. for their interest and their offering of favourable working conditions.

I further want to thank S. Levin Nielsen, M.D. Dept. of Clinical Physiology Herlev Hospital, and N. A. Laasen, M.D. Ph.D. Dept. of Clinical Physiology Bispebjerg Hospital, for valuable assistance.

Finally I wish to offer my sincere thanks to my wife Annie who supported and encouraged me throughout the course of the study.

*Ole Henriksen
Rødovre 1977*

Introduction

Adjustment of vascular resistance to changes in arterial pressure (autoregulation) and/or changes in venous pressure plays an important role in regulation of blood flow and transcapillary fluid exchange

Autoregulation of blood flow

Autoregulation of blood flow *i.e.* tendency towards maintenance of constant blood flow during changes in arterial perfusion pressure head has been demonstrated in various tissues and organs in animals: brain (Fog 1934 Rapola and Green 1964) kidneys (Rein 1931 Sefkurt 1946) skeletal muscle (Folkow 1949 Stainsby and Renkin 1961 Jones and Berne 1964) myocardium (Berne 1959) intestine (Bürgi 1944 Johnson 1960) liver (Torrance 1958) and adipose tissue (Heuriksen, Nielsen, and Pauske 1976)

Human studies indicate that autoregulation is present in brain (Lassen 1959 Paulson Olesen, and Stig Christensen 1972) and cutaneous tissue (Heuriksen *et al* 1973)

The mechanism responsible for adjustment of vascular resistance has been a matter of much controversy. The mechanism appears to be very sensitive to local surgical trauma and to changes in local carbon dioxide tension (Häggendahl and Johansson 1965 Paulson Olesen and Stig Christensen 1972). Autoregulation was not abolished by acute and chronic sympathectomy in cat skeletal muscle (Folkow 1949 Jones and Berne 1964) and vasomotoric activity was still present in reserpinized cats (Folkow and Öberg 1961). This indicates that local nervous mechanisms are not involved.

As originally proposed by Bayliss (1902) intrinsic myogenic smooth muscle reactions related to stretch might be involved (Folkow 1962 and 1964). Another possible explanation is that vascular resistance adjustments are due to changes in local concentration of vasoactive metabolites liberated from the tissues (Anrep 1912, Berne 1964 Hilton 1971) or variation of local oxygen tension (Ross *et al* 1962). Other theories have been proposed but the fundamental nature of the mechanism is still unsettled (Johnson 1964).

Venous pressure elevation

Venous pressure elevation of 20 mm Hg caused a pronounced increase in vascular resistance in adipose tissue of rabbits (Heuriksen, Nielsen and Pauske 1976). Similar findings have been obtained in rabbit ear (Burton and Rosenberg 1956 Rosenberg 1956) cat skeletal muscle (Folkow and Öberg 1961 Mellander Odehman and Öberg 1964) dog limb (Haddy and Gilbert 1956) kidney (Haddy 1956) and in mesentery of different animal species (Sefkurt and Johnson 1958 Johnson 1959 Richardson and Zweifach 1970). It was concluded that increase in vascular resistance was due to arteriolar constriction (Haddy

and Gilbert 1936 Haddy and Scott 1964 Richardson and Zwelfach 1970 Johnson 1968 Bacz *et al* 1974)

In humans venous stasis of 40 mm Hg caused decrease of blood flow in skeletal muscle and cutaneous tissue (Henriksen and Sejrten 1976 and 1977 a)

Parallel elevation of arterial and venous pressures

Parallel increase in arterial and venous pressures was accompanied by decrease in blood flow in cat skeletal muscle (Folkow and Öberg 1961)

In humans parallel increase in arterial and venous transmural pressures can be produced either by lowering of a limb or by applying external negative pressure. Limb blood flow measured by venous occlusion plethysmography decreased when vascular transmural pressure was elevated (Gaskell and Burton 1963 Greenfield and Patterson 1954 a, Beaconsfield and Ginsburg 1955 Coles and Greenfield 1956 Mellander Odehram and Öberg 1964). The phenomenon has been demonstrated in human skeletal muscle (Golenhofen and Hildebrandt 1962 Balldin *et al* 1971 Amery *et al* 1973) and human cutaneous tissue (Henriksen *et al* 1973)

Mechanism

Arteriolar constriction in response to vascular distension might be due to *central reflex mechanisms*. Passive tilting of a subject (feet down) caused decrease in blood flow in forearm remaining at heart level. The decrease did not occur following sympathectomy (Brigden *et al* 1950). Roddile and Shepherd (1956) and Roddile *et al* (1958) concluded that blood flow in skeletal muscle only was affected by baroreceptor activity. Delius *et al* (1972) observed that changes in baroreceptor activity did not influence electrical activity in sympathetic fibres of skin fascicles. Also carotid artery occlusion did not affect blood flow in subcutaneous adipose tissue (Ngal *et al* 1966 Hanley Sachs, and Skinner 1971). However DiSalvo *et al* (1971) found that blood flow in subcutaneous tissue was influenced. Similarly other investigators concluded based on indirect evidence, that skin vessels were affected (Mosley 1969 Beiser *et al* 1970 Zoller *et al* 1972 Rowell *et al* 1973)

In animals it has been shown that the local vasoconstrictor response to venous stasis was not affected by central blockade (Rosenberg 1956 Haddy and Scott 1964) indicating that *local mechanisms* are responsible. Haddy (1956) found that the response in kidney was abolished in the denervated organ which suggests that the response might be due to a *local nervous mechanism* as originally proposed by Gaskell and Burton (1953). However Johnson (1959) found in dog mesentery that vascular response to venous stasis was unaffected by procaine and phenoxybenzamine and concluded that the response was due to an *intrinsic myogenic mechanism* (Bayliss 1902). In humans, Gaskell and Burton (1953) and Beaconsfield and Ginsburg (1955) observed that the effect of postural changes upon limb blood flow was unaffected by chronic sympathetic denervation in patients suffering from occlusive arterial diseases as measured by venous occlusion plethysmography

Results obtained in animal studies indicate that vascular response to increase in vascular transmural pressure is due to local mechanisms. Otherwise, the results are conflicting. Venous occlusion plethysmography studies of limb blood flow in humans indicated that nervous mechanisms are not involved in vascular reaction to increase in vascular transmural pressure. However the results may not be conclusive because venous occlusion plethysmography does not give reliable estimates of blood flow when veins are distended (Greenfield and Patterson 1954b). Venous capacity decreases markedly when venous pressure exceeds 10 mm Hg (Wood and Eckstein 1958). The error may be influenced by the magnitude of blood flow because when blood flow is high the duration of the "initial slope" of the curves becomes very short due to fast filling of veins. The problem is further complicated by the fact that perfusion through shunt vessels is included when the region in which blood flow is determined comprises hand or foot.

The mechanism responsible for the vascular response to increase in vascular transmural pressure is still unsettled.

The local isotope washout technique (Kety 1949, Lassen, Lindbjerg, and Munck 1964) makes it possible to estimate relative blood flow in a single tissue during venous distension. In the present study ^{133}Xe was used as tracer which was introduced atraumatically into subcutaneous adipose tissue (Sejrsen 1969, Nielsen 1972b).

The purpose of the present study was to investigate effects of changes in vascular transmural pressure upon blood flow in human subcutaneous adipose tissue in an attempt to clarify underlying mechanisms.

Methods

Measurement of blood flow in subcutaneous adipose tissue

Theoretical considerations When washout of tracer from a homogeneous tissue with homogeneous perfusion is entirely perfusion limited ($Q \gg$ diffusion equilibrium is achieved between tissue and effluent blood) alteration in mean concentration of tracer in tissue with time $C(t)$ can be expressed as

$$C(t) = C(0) \exp -((f/\lambda)t) \quad (1)$$

$C(0)$ is concentration in tissue at time zero f perfusion coefficient in ml/g-min and λ tissue to blood partition coefficient in ml/g. Assumptions are zero concentration of tracer in inflowing blood and tracer must leave tissue exclusively by effluent blood. Rearrangement of the equation to express f per 100 g of tissue gives

$$f = k \cdot \lambda \cdot 100 \text{ (ml/100 g min)} \quad (2)$$

(Kety 1949 and 1951) where k is fractional washout rate constant in min. As shown by Sejrsen (1971) $^{133}\text{Xenon}$ washout from inguinal fat pad in cats follows a monoexponential course. Nielsen (1972a and b) demonstrated that the $^{133}\text{Xenon}$ washout method gives a reliable estimate of blood flow in adipose tissue when λ is known. λ is very sensitive to variations in lipid concentration of tissue. However relative blood flow can be determined without knowledge of λ , if λ remains constant. Intravascular blood volume in adipose tissue was found by Paaske and Nielsen (1976) to be about 3 per cent (0.03 ml/g). If vascular volume increases with a factor of 2 during venous distension of 40 mm Hg this implies a change in λ of less than 3 per cent.

A detailed discussion of the $^{133}\text{Xenon}$ washout method has been given previously by Sejrsen (1971).

Sources of error Due to decrease in linear velocity of the blood during venous stasis $^{133}\text{Xenon}$ might be redistributed to adipose tissue around veins proximally to the site of application. However when the detectors were collimated to record only from the distal half of the labelled area a decrease in calculated blood flow of same magnitude was obtained indicating that this error was insignificant.

In experiments where lidocaine or phenolamine is injected directly into subcutaneous tissue vascular reactions might be influenced by injection trauma. Nielsen (1972a) showed that blood flow in adipose tissue returned to normal resting values between 10 and 30 minutes after subcutaneous injection of $^{133}\text{Xenon}$ in saline. The measurements of the present study were therefore not started until 30 minutes after the subcutaneous injections. Control experiments were performed with subcutaneous injection of isotonic saline. Results obtained were almost similar to those obtained from non-traumatized areas. This

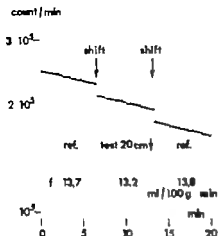


Fig. 1 Example of $^{125}\text{Xenon}$ washout curves from distal part of forearm placed 1) at reference level (jugular notch), f_{ref} , 2) lowered 20 cm, f_{test} , and 3) placed at reference level, f_{ref} . f denotes perfusion coefficients (ml/100 g min).

indicates that trauma due to infiltration procedures was insignificant at the time of measurement.

Procedure $^{125}\text{Xenon}$ in isotonic saline (3 mCi/ml) was injected intracutaneously into an area located on distal part of forearm or crus. About 90 minutes after injection remaining activity is located exclusively in subcutaneous adipose tissue (Sejrsen 1971). At this time measurements were started. The limb under study was carefully immobilized in order to avoid changes in counting geometry due to movements. γ -emission of $^{125}\text{Xenon}$ was detected by a scintillation detector (NaI(Tl)). The detector was placed about 15 cm above the radioactive field and collimated to see more than the labelled area. Pulses were fed into a gamma-spectrometer with a window set around the 81 keV photopeak of $^{125}\text{Xenon}$. Activity was recorded in intervals of 10 or 20 seconds, and results were punched out. $^{125}\text{Xenon}$ washout rate constant k (Eq. 2) was computed from the regression line calculated from the "least square" method, using logarithmically transformed count rates corrected for background activity. In calculations a λ value of 10 ml/g was used (Sejrsen 1971).

A single investigation consisted of 3 periods of measurement, and each blood flow determination had a duration of about 6 minutes. The sequence of the measurements was 1) reference f_{ref} , 2) test, f_{test} , and 3) reference f_{ref} (see Fig. 1). Relative blood flow was calculated as $f_{\text{test}}/f_{\text{ref}}$, where f_{test} denotes mean perfusion coefficient (ml/100 g min) obtained under test conditions. f_{ref} denotes calculated mean value of two measurements obtained under reference conditions just before and after the test.

Changes in vascular transmural pressure were induced by three different techniques, 1) postural changes of a limb, 2) local subatmospheric pressure, or 3) venous stasis induced by inflating a cuff placed on upper arm or thigh.

Venous pressure

Venous pressure was measured directly in a superficial vein on the dorsum of the hand in a sitting subject. When the hand was elevated from 5 cm below jugular notch, venous pressure remained constant at about 3 mm Hg. When the hand was lowered venous

pressure increased by an amount equivalent to the pressure of a blood column of similar height. During induced local subatmospheric pressure, venous transmural pressure was assumed to increase corresponding to induced negative pressure. During venous stasis venous pressure was found to become close to cuff pressure.

Arterial pressure

Systolic and diastolic arterial pressures were measured on upper arm by means of a cuff. Arterial mean pressure was calculated as diastolic pressure plus 1/3 of the pulse amplitude. During postural changes of the limb, pressure in arterial system of the limb and thus the transmural pressure, was assumed to vary corresponding to the hydrostatic pressure exerted by the column of blood. During application of local suction transmural arterial pressure was assumed to increase corresponding to applied negative pressure. During venous stasis arterial pressure was assumed to remain constant.

Relative vascular resistance

Relative vascular resistance $R_{\text{test}}/R_{\text{ref}}$ was calculated from obtained relative blood flow $I_{\text{test}}/I_{\text{ref}}$ and estimated arterial and venous pressures. R_{test} denotes vascular resistance during test conditions and R_{ref} signifies average vascular resistance calculated for the two reference periods.

Statistics

I_{test} and I_{ref} were compared by means of Student's t-test for paired samples. Relative blood flow $I_{\text{test}}/I_{\text{ref}}$ obtained under different conditions were compared by randomization test for unpaired samples. As level of significance was chosen 0.05. In figures and text, SD denotes standard deviation, and SE signifies standard error of the mean.

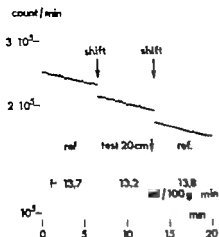


Fig. 1. Example of $^{133}\text{Xenon}$ washout curves from distal part of forearm placed 1) at reference level (jugular notch), f_{ref} ; 2) lowered 20 cm, f_{test} , and 3) placed at reference level, f_{ref} . f denotes perfusion coefficient (ml/100 g min).

indicates that trauma due to infiltration procedures was insignificant at the time of measurement.

Procedure $^{133}\text{Xenon}$ in isotonic saline (3 mCi/ml) was injected intracutaneously into an area located on distal part of forearm or crus. About 90 minutes after injection remaining activity is located exclusively in subcutaneous adipose tissue (Sejrsen 1971). At this time measurements were started. The limb under study was carefully immobilized in order to avoid changes in counting geometry due to movements. γ -emission of $^{133}\text{Xenon}$ was detected by a scintillation detector (NaI(Tl)). The detector was placed about 15 cm above the radioactive field and collimated to see more than the labelled area. Pulses were fed into a gamma-spectrometer with a window set around the 81 keV photopeak of $^{133}\text{Xenon}$. Activity was recorded in intervals of 10 or 20 seconds and results were punched out. $^{133}\text{Xenon}$ washout rate constant k (Eq. 2) was computed from the regression line calculated from the "least square" method using logarithmically transformed count rates corrected for background activity. In calculations a λ value of 10 ml/g was used (Sejrsen 1971).

A single investigation consisted of 3 periods of measurement, and each blood flow determination had a duration of about 6 minutes. The sequence of the measurements was: 1) reference f_{ref} , 2) test f_{test} , and 3) reference f_{ref} (see Fig. 1). Relative blood flow was calculated as $f_{\text{test}}/f_{\text{ref}}$, where f_{test} denotes mean perfusion coefficient (ml/100 g min) obtained under test conditions, f_{ref} denotes calculated mean value of two measurements obtained under reference conditions just before and after the test.

Changes in vascular transmural pressure were induced by three different techniques: 1) postural changes of a limb; 2) local subatmospheric pressure; or 3) venous stasis induced by inflating a cuff placed on upper arm or thigh.

Venous pressure

Venous pressure was measured directly in a superficial vein on the dorsum of the hand in a sitting subject. When the hand was elevated from 5 cm below jugular notch venous pressure remained constant at about 3 mm Hg. When the hand was lowered venous

pressure increased by an amount equivalent to the pressure of a blood column of similar height. During induced local subatmospheric pressure venous transmural pressure was assumed to increase corresponding to induced negative pressure. During venous stasis venous pressure was found to become close to cuff pressure.

Arterial pressure

Systolic and diastolic arterial pressures were measured on upper arm by means of a cuff. Arterial mean pressure was calculated as diastolic pressure plus 1/3 of the pulse amplitude. During postural changes of the limb pressure in arterial system of the limb and thus the transmural pressure was assumed to vary corresponding to the hydrostatic pressure exerted by the column of blood. During application of local suction transmural arterial pressure was assumed to increase corresponding to applied negative pressure. During venous stasis arterial pressure was assumed to remain constant.

Relative vascular resistance

Relative vascular resistance $R_{\text{limb}}/\bar{R}_{\text{limb}}$ was calculated from obtained relative blood flow $Q_{\text{limb}}/\bar{Q}_{\text{limb}}$ and estimated arterial and venous pressures. R_{limb} denotes vascular resistance during test conditions and \bar{R}_{limb} signifies average vascular resistance calculated for the two reference periods.

Statistics

Q_{limb} and \bar{Q}_{limb} were compared by means of Student's t-test for paired samples. Relative blood flow $Q_{\text{limb}}/\bar{Q}_{\text{limb}}$ obtained under different conditions were compared by randomization test for unpaired samples. As level of significance was chosen 0.05. In figures and text, SD denotes standard deviation, and SE signifies standard error of the mean.

Results

1 Effect of changes in vascular transmural pressure (I V)

The experiments were performed on 6 healthy subjects. Changes in vascular transmural pressure were induced by three different techniques.

(a) Postural changes of a limb

Blood flow was measured either on distal part of forearm with the subject placed in a sitting position or on distal part of crus with the volunteer placed in a supine position. Measurements were undertaken at different test levels below or above heart level.

Results obtained in one subject are shown in Fig. 2. Blood flow remained constant within 20 cm above and 20 cm below reference level (jugular notch). Raising the arm above this range was followed by decrease in blood flow. When the arm was lowered 30 cm below jugular notch, blood flow suddenly decreased 40 per cent of the control value. When the arm was further lowered, blood flow remained constant. Calculated vascular resistance at maximum elevation of the arm decreased to 70 per cent of the reference value (venous pressure remained constant). When the arm was lowered to 20 cm below the jugular notch, vascular resistance remained constant (arterial and venous pressures increased in parallel). But when the arm was lowered 30 cm (or more) blood flow suddenly decreased by about 40 per cent. Results were qualitatively similar in all 6 subjects. However in one subject blood flow remained constant when the arm was lowered 40 cm (1), and further studies revealed that blood flow decreased in this subject, too when the arm was lowered 50 and 60 cm. Similar results were obtained in the leg.

(b) Local subatmospheric pressure

Effect of local subatmospheric pressure upon blood flow was studied in one subject (1). Blood flow measured on distal part of forearm decreased by about 30 and 50 per cent during negative pressure of -30 and -60 mm Hg, respectively.

(c) Venous stasis

Three subjects were studied and blood flow was measured on the distal part of crus. During venous stasis of 15 mm Hg blood flow remained constant. During venous stasis of 30 and 40 mm Hg, blood flow decreased by about 50 per cent corresponding to an increase in calculated vascular resistance of about 30 per cent.

Comments

During elevation corresponding to decrease in arterial mean pressure of about 70 mm Hg blood flow remained constant due to a decrease in vascular resistance. Thus, autoregulation of blood flow is present in human subcutaneous adipose tissue.

ADIPOSE TISSUE

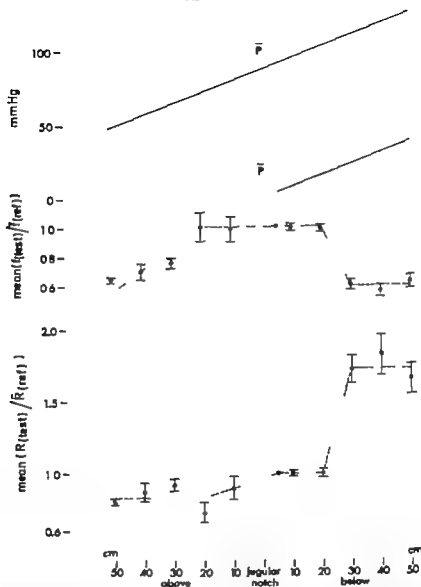


Fig. 2 Mean arterial pressure (\bar{P}_a), mean venous pressure (\bar{P}_v), relative blood flow ($Q_{\text{test}}/Q_{\text{ref}}$) and relative total vascular resistance ($R_{\text{test}}/R_{\text{ref}}$) obtained from distal part of forearm placed at different test levels below or above reference level (jugular notch). Vertical lines with bars denote 1 SD.

When the arm was lowered 20 cm corresponding to an increase in vascular transmural pressure of 15 mm Hg, blood flow and vascular resistance remained constant. This indicates that vascular smooth muscle cells of resistance vessels had increased their active force of contraction just sufficiently to balance the increase in passive distending forces corresponding to the rise in vascular transmural pressure.

When vascular transmural pressure was elevated about 25 mm Hg blood flow decreased due to increase in vascular resistance. This response was seen during lowering of the limb during induced local subatmospheric pressure and during venous stasis. When the tissue was infiltrated by histamine which presumably paralyzes smooth vascular musculature venous stasis of 40 mm Hg which reduces arteriovenous pressure difference by some 45 per cent. Also it produces a decrease in blood flow of only 18 per cent instead of 50 per cent. This indicates that the decrease in blood flow observed in normal subcutaneous adipose tissue is only partly produced by the drop in driving pressure. To a considerable extent the decrease is caused by an increase in vasoconstrictor activity. An increase in total vascular resistance is in agreement with this.

Hence moderate change in vascular transmural pressure is followed by regulatory changes in vascular smooth muscle activity keeping blood flow constant (autoregulation). An increase in vascular transmural pressure above a certain threshold about 25 mm Hg is followed by an additional vasoconstriction causing a decrease in blood flow of about 50 per cent. This latter phenomenon will for the sake of brevity in the following be referred to as the "vasoconstrictor response" to an increase in vascular transmural pressure.

Such changes in vascular smooth muscle activity might be due to

- 1) Reflex changes in sympathetic vasoconstrictor activity due to changes in distension of central veins and of the right atrium of the heart (low pressure baroreceptors)
- 2) Spinal reflex mechanisms of local origin e.g. distension of veins in the extremity might cause arteriolar constriction by way of a reflex arch comprising the spinal cord
- 3) Local nervous mechanisms
- 4) Intrinsic vascular adjustments to changes in vascular transmural pressure (myogenic metabolic)

In order to study the possible role of central mechanisms in the observed changes in vascular resistance during postural changes of a limb experiments were performed before and after an acute spinal sympathetic blockade.

2. Acute spinal sympathetic blockade (II)

Both legs of four normal subjects placed in a supine position, were studied. Spinal sympathetic blockade was achieved by epidural anaesthesia induced by marcaine 0.5 per cent, without adrenaline. The blockade was extended to involve 6th to 8th thoracic segment. Increase in skin temperature (Rou *et al.* 1973), disappearance of sympathico-adrenergic reflex (Daos *et al.* 1963) and abolished sweat production as tested by the minhydrin test (Dünér *et al.* 1960) were taken as evidence of effective central sympathetic blockade.

Arterial blood pressure was measured and remained almost constant throughout the whole investigation.

Plasma concentrations of adrenaline and nor-adrenaline were measured (Valeri *et al.* 1970) before and after blockade.

VENOUS STASIS

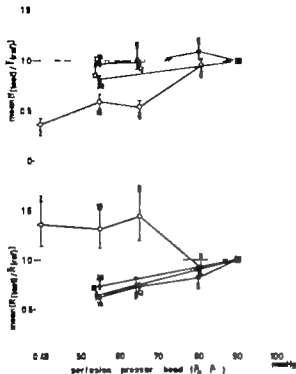


Fig. 11. Mean relative blood flow ± 1 SE and total vascular resistance ± 1 SE on the distal part of the leg during induced venous stasis plotted as functions of perfusion pressure head. Venous pressure was close to cuff pressure. \circ —control area infiltrated with isotonic saline, \bullet —area infiltrated with phentolamine, \square —area infiltrated with lidocaine, \triangle —area infiltrated with heptamine. Figures denote number of experiments.

A scintigram of the area obtained after conclusion of an experiment showed that activity of ^{133}Xe remaining in the field was confined to this area. Analgesia of skin was taken as evidence that effective lidocaine blockade had been achieved.

(a) When the limb was lowered 40 cm, blood flow under control conditions decreased about 60 per cent. This corresponds to increase in calculated vascular resistance of about 200 per cent. In areas infiltrated with lidocaine or phentolamine blood flow remained constant. When the limb was elevated 30 cm blood flow under both control and experimental conditions remained constant (Fig. 7). This corresponds to a decrease in vascular resistance of about 30 per cent.

(b) During induced external negative pressure of -30 and -60 mm Hg in one subject, blood flow decreased 30 and 54 per cent respectively in control experiments. In areas infiltrated with phentolamine blood flow remained constant.

(c) During venous stasis of 15 mm Hg, blood flow remained constant. This corresponds to decrease in vascular resistance of about 11 per cent in control experiments. However under control conditions venous stasis of 30 and 40 mm Hg induced decrease in blood flow of about 50 per cent corresponding to an increase in vascular resistance of about 30 per cent (Fig. 11). Blood flow remained constant in areas infiltrated with lidocaine or phentolamine where decrease in vascular resistance of about 30–40 per cent was found. In order to test effect of low doses of the drugs used, another series of experiments was

XENON WASHOUT CURVES

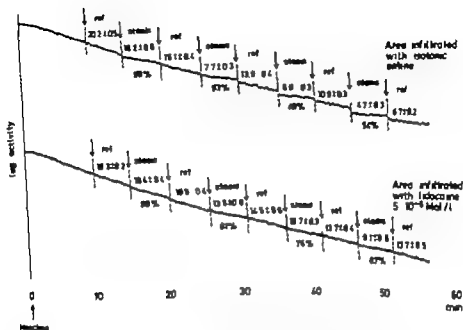


Fig. 9 ^{135}Xe washout curves obtained on distal part of forearm. Upper curve shows control experiments with the area infiltrated with isotonic saline. Lower curve shows findings with the area infiltrated with lidocaine (5×10^{-4} Mol/l). Venous stasis (30 mm Hg) was induced consecutively 15 25 35 and 45 minutes after injections. Figures above each curve represent deceleration perfusion coefficient ± 1 SD. Figures below the curves denote relative blood flow f_{rel} during venous stasis. f_{rel} denotes average value of perfusion coefficient obtained just before and after the stasis period.

performed on one subject. Lidocaine was used in concentrations of 3×10^{-4} Mol/l and 5×10^{-4} Mol/l. Control experiments with injection of saline were also performed. Experiments were performed on the distal part of a forearm. Venous stasis of 30 mm Hg was induced consecutively about 15 25 35 and 45 minutes after injections.

135XENON WASHOUT CURVES venous stasis area infiltrated with phenylephrine 5×10^{-4} Mol/l



Fig. 10 ^{135}Xe washout curves obtained from an area on distal part of forearm infiltrated with phenylephrine (5×10^{-4} Mol/l). Venous stasis of 30 mm Hg was induced 15 minutes after injections. Figures above the curves denote mean perfusion coefficient ± 1 SD. Figure below the curve obtained during venous stasis denotes relative blood flow during venous stasis.

VENOUS STASIS

in subcutaneous tissue infiltrated
with lidocaine or isotonic saline

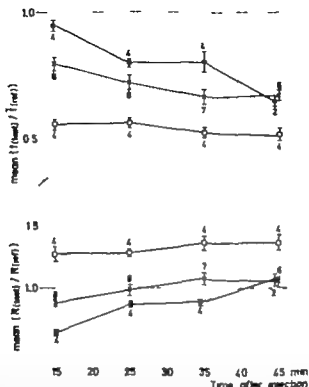


Fig. 11. Mean relative blood flow ± 1 SE and mean relative total vascular resistance ± 1 SE plotted as functions of time after subcutaneous injection of lidocaine or isotonic saline. Venous stasis of 30 mm Hg was induced 15 \blacksquare \square and 45 minutes after injection. \blacksquare —area infiltrated with lidocaine 3×10^{-4} Mol/l. \square —area infiltrated with lidocaine, 5×10^{-4} Mol/l. \circ —area infiltrated with isotonic saline. Figures denote number of experiments.

An example is shown in Fig. 9. Hyperaemia due to injection trauma was almost identical in areas infiltrated with saline and lidocaine. In areas infiltrated with saline blood flow decreased about 60 per cent in all stasis periods corresponding to increase in total vascular resistance of about 30 per cent. Lidocaine (3×10^{-4} Mol/l) blocked response to venous stasis 15 minutes after injection as blood flow remained constant corresponding to decrease in total vascular resistance of about 35 per cent. Lidocaine (5×10^{-4} Mol/l) reduced the response by approximately 50 per cent corresponding to a decrease in vascular resistance of about 15 per cent. However the effect of lidocaine became less pronounced with time. Similarly phenolamine (5×10^{-6} Mol/l) in two experiments reduced the effect of venous stasis upon blood flow by 50 per cent 15 minutes after the injection (Fig. 10). Results obtained in series with lidocaine and saline are summarized in Fig. 11.

Thus, in presence of lidocaine or phenolamine in very low concentrations venous stasis evoked a decrease in total vascular resistance whereas venous stasis evoked an increase in vascular resistance during control condition.

RIGHT FOREARM

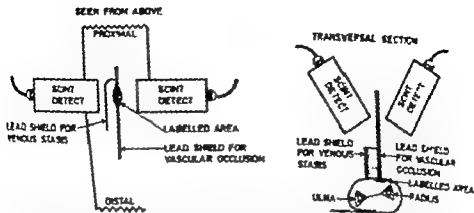


Fig 11. Experimental set up. Right: The distal part of the forearm as seen in transversal section. Left: Diagram of forearm seen from above. A lead shield (14 cm long, 13.5 cm high, and 0.3 cm thick with lower edge narrowed to 1 mm) for vascular occlusion was placed on the skin on dorsal side of forearm. The radioactive field was then separated into two parts. Venous stasis on one side of this shield was induced by another L-shaped lead shield (9 cm long, 5 cm high, and 0.3 cm thick). For details, see text.

Comments

Lidocaine and phentolamine blocked the "vasoconstrictor response" to increase in vascular transmural pressure. This finding speaks against the possibility that sympathetic fibres play a permissive role by exerting a trophic effect on vascular smooth muscle cells. A direct effect of phentolamine and lidocaine on the vascular smooth muscle cells seems to be without significance for the following reasons.

When the areas were elevated 30 cm above mid-axillary line blood flow remained constant corresponding to decrease in vascular resistance of about 10 per cent. This indicates that autoregulation was still present in spite of drugs (Fig. 7). Blood flow and vascular resistance remained constant when the leg was lowered or during local occlusion (Fig. 7). Thus, vascular smooth muscle cells had increased their force of contraction just enough to counteract the passive distension of the vessels due to increase in transmural pressure. Under these conditions arterial and venous transmural pressures increased in parallel.

Significant difference in response was found between areas infiltrated with lidocaine in low concentrations and control areas infiltrated with saline (randomization test for paired samples). Hyperaemia due to injection trauma was almost identical indicating that difference in response was due to presence of lidocaine. The decrease with time in effect of lidocaine was probably due to washout of drug from the area.

Hence even in very low concentrations lidocaine and phentolamine block the "vasoconstrictor response". This indicates that the response is due to a sympathetic reflex mechanism. In combination with absence of effect of central sympathetic blockade (24a), somesthetic denervation (23) these findings indicate that the response is of

LOCAL VENOUS STASIS

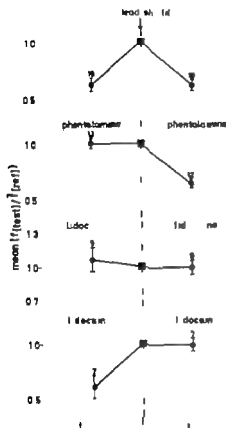


Fig. 13 Mean relative blood flow \pm SE in human subcutaneous adipose tissue increased simultaneously on both sides in^{133}Xe lead shield during venous stasis on one side. The figures denote number of investigations.

sympathetic axon reflex mechanism. If the reflex operates in an area of a certain size the vasoconstrictor response should be transmitted from an area with local venous stasis to adjoining areas without stasis.

6 Local venous stasis (VI)

Three normal subjects were studied together with two patients who had been bilaterally sympathectomized about two years previously. A diagram of experimental "set-up" is shown in Fig. 12. ^{133}Xe was injected intracutaneously into an area of 3×1 cm which was located longitudinally in the midline on the dorsal side of forearm halfway between elbow and wrist. A lead shield (14 cm long, 13.5 cm high and 0.3 cm thick, with the lower edge narrowed to a thickness of 1 mm) was placed longitudinally in the midline on the forearm, thus separating the labelled area into two parts. The shield exerted a pressure on the skin of about 360 mm Hg. Venous stasis on one side of the shield was induced by means of a second lead shield (9 cm long, 5 cm high and 0.3 cm thick) which was bent into L-shape. The second shield was placed proximally and laterally to the labelled area to exert a pressure on the skin of about 40 mm Hg. By this technique venous pressure will rise to

CHRONIC SYMPATHECTOMY

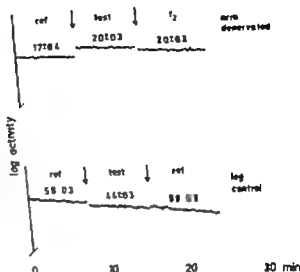


Fig 14 ^{86}K venous washout curves obtained on the same stasis side in a patient who had been bilaterally sympathectomized about 2 years earlier. The curves were obtained during reference conditions, t_{ref} , during venous stasis on opposite side of the lead shield, t_{stasis} , and during reference conditions, t_{ref} . Measurements were performed on denervated forearm (upper curve) and on non-operated leg used as control (lower curve). Figures denote mean perfusion coefficients \pm SD (ml/100 g min). Arrows $p < 0.05$. Lag $p < 0.01$.

about 40 mm Fig in the area between the two lead shields because retrograde venous drainage to veins outside the shields is prevented by venous valves. Blood flow was measured simultaneously on both sides of the lead shield for vascular occlusion.

Results are summarized in Fig. 13. Venous stasis on one side of the shield induced a decrease in blood flow of 40 per cent on both sides. Nerve block was without effect when induced by infiltrating the tissue with lidocaine 3 cm proximally to the labelled area. Response on the non-stasis side could still be demonstrated when venous stasis was induced 1.5 cm in radial direction from the centre of the labelled area. However blood flow was unaffected when the shield for vascular occlusion was placed 3 cm radially to the centre of the labelled area. Blood flow on the non-stasis side was also unaffected when the proximal border of the stasis shield was placed corresponding to the centre of the labelled area.

Phentolamine (10 mg/ml) was injected on the stasis side and blocked the response on this side. The response was still present on the non-stasis side. Lidocaine (20 mg/ml 3×10^{-4} Mol/l) injected on the stasis side blocked the response to venous stasis on both sides (Fig 13). When lidocaine was injected on the non-stasis side blood flow remained constant on this side but decreased on the side of stasis.

In the sympathetically denervated forearm, blood flow remained constant on the non-stasis side during venous stasis on the opposite side of the lead shield. Blood flow however decreased in the non-operated control leg during venous stasis (Fig 14).

Comments

Phentolamine or lidocaine injected prior to stasis induced an increase in blood flow on the side of application only. This shows that the longitudinal shield fulfilled its purpose to separate the two sides on microvascular level. Hence induced increase in vascular trans-

mural pressure on one side was not transferred to the other side of the lead shield used for vascular occlusion.

Results indicate that a vasoconstrictor stimulus elicited during venous stasis can be transmitted to a surrounding non-affected area over a distance of about 1.5 cm in the transversal but not in the proximal direction. Nerve block induced 3 cm proximally was without effect, indicating that the "vasoconstrictor response" depends upon a local transmission mechanism.

Transmission was unaffected by phentolamine on stasis side whereas by lidocaine and chronic sympathetic denervation transmission was blocked. This indicates that the impulse is transmitted through local nerves.

General discussion

Results obtained in the present study indicate that elevation of vascular transmural pressure causes a "vasoconstrictor response" in human subcutaneous tissue. Similar results were obtained during lowering of the limb during external negative pressure as well as during venous stasis. Same response has also been demonstrated in human cutaneous tissue (Henriksen *et al.* 1973) and in human skeletal muscle (Golenhofen and Hildebrandt 1964 Balzli *et al.* 1971 Amery *et al.* 1973). In animal experiments vasoconstrictor response has been demonstrated in adipose tissue of rabbits (Henriksen Nielsen and Poulsen 1976) in skeletal muscle (Folkow and Öberg 1961), in dog limb (Haddy and Gilbert 1956 Haddy and Scott 1964) in rabbit ear (Burton and Rosenberg 1956) in rabbit limb (Rosenberg 1956) and in mesentery of various species of animals (Sefkurt and Johnson 1958 Johnson 1959 Richardson and Zweifach 1970 Baez *et al.* 1974).

Nature of the "vasoconstrictor response"

The "vasoconstrictor response" in human subcutaneous adipose tissue was elicited when vascular transmural pressure increased by more than some 25 mm Hg (I-V). The response could be transmitted over a distance of about 1.5 cm in transversal direction (VI). The response was abolished by induced local counterpressure (V).

Mechanism

The response was not affected by spinal sympathetic blockade (II) by sympathectomy as measured one day postoperatively (IV) or by local nerve block when induced 3 cm proximally laterally and medially to the area under study (VI). These findings indicate that local mechanisms are responsible.

A myogenic response (Bayliss 1902, Folkow 1962 and 1964) to increase in vascular transmural pressure might be responsible. Folkow and Öberg (1961) showed that vasomotor activity was still present in gastrocnemius muscle in reserpinized cats. Passive stretching of a portal vein studied *in vitro* was followed by an increase in electrical and mechanical activity (Johansson and Mellander 1975). The response was not affected by phenoxylbenzamine (5×10^{-6} Moll/l) *in vitro* studies of small subcutaneous arteries from dogs showed rhythmic activity and coordination, indicating a cell-to-cell transmission of electrical activity (single unit behaviour) (Johansson and Bohr 1966).

Transmission of impulse might be ascribed to longitudinal cell-to-cell transmission of myogenic activity *in vitro* studies of turtle arteries and veins by Roddie (1962) indicated that induced electrical activity could be propagated several centimetres. In mammals, peripherally induced vasodilatation was followed by dilatation of femoral artery in dogs

(Hilton 1959) Sympathetic and somesthetic denervation was without effect. The response was abolished when the artery was divided distally to site of measurement indicating that the dilatator response was conducted longitudinally *via* smooth muscle cells. However when repeating the same experiments Mons Lie Sejersted and Khl (1970) found that dilatator response was still present following transection of the artery distally to site of measurement. In larger mammalian arteries cell-to-cell propagation of myogenic activity seems to be of minor significance (Burnstock and Prosser 1960 a and b Keatinge 1966). However vascular smooth muscle cells might behave differently in small vessels. Vascular smooth muscle cells showed single unit behaviour and myogenic activity could be transmitted for some distance in rat portal vein (Johansson and Ljung 1967 and 1968 Ljung and Stage 1970 Hermansmeyer 1973). Based on indirect evidence Bevan and Ljung (1974) concluded that myogenic activity could be transmitted over short distances in small arteries of rabbits.

Another possibility is that the "vasoconstrictor response" is due to a local nervous mechanism (Gaskell and Burton 1953). The "vasoconstrictor response and impulse transmission was abolished four days and later after sympathectomy (IV-VI). Postoperative sweating on third to fourth day following surgery was probably of same nature as degeneration secretion from cat salivary gland (Coats and Emmelin 1962) and to temporary reversion of ptosis 13-15 hours after removal of the superior ganglion in rats (Lundberg 1969). Contents of nor-adrenaline in cat gastrocnemius muscle declined to very low levels four days after sympathectomy (Sedwall 1964). In rat iris only one per cent of sympathetic nerve terminals appeared normal 29 hours after axotomy (Malmfors and Sachs 1965). Postoperative sweating therefore indicates that sympathetic fibres in forearm had lost their ability to function four days after sympathectomy.

The effect of sympathectomy upon the "vasoconstrictor response" might be due to the fact that degeneration of sympathetic fibres causes changes of vascular smooth muscle cells and affects muscular reactivity and impulse propagation. However initiation and propagation of rhythmic activity in smooth muscles from small subcutaneous arteries in dogs were not affected (Johansson and Bohr 1966). Also reactivity of rat portal vein to yohimbine was not diminished (Johansson *et al* 1969) by chronic sympathectomy. Autoregulation of blood flow was still present following sympathetic denervation (IV). Sympathectomy might change lipid metabolism in adipose tissue to affect vascular smooth muscles. However in human cutaneous tissue and human skeletal muscle (Henriksen and Sejrsten 1976 and 1977 a) similar results have been obtained which are not compatible with this theory.

Local blockade with lidocaine blocked "vasoconstrictor response" and underlying impulse transmission. The latter was not affected by phenolamine (V-VI). Selkurt and Johnson (1958) and Johnson (1959) studied the influence of venous pressure elevation upon blood flow and vascular resistance in isolated perfused small intestine in dogs. Total vascular resistance increased during venous stasis. The response was not affected by acute denervation or intraarterially infused phenoxybenzamine or procaine (Johnson 1959). However it seems that blood flow decreased gradually with time in the control experiment presented, and when venous pressure finally was lowered blood flow only increased

corresponding to the increase in perfusion pressure (Selkurt and Johnson 1958). The gradual increase in vascular resistance might therefore be due to intravascular clotting. In an interesting Lutz (1966) found that veno-arteriolar response was diminished but not abolished, by guanethidine.

Folkow and Öberg (1961) found that venous stasis of 10 mm Hg induced a decrease in blood flow in skeletal muscle in reserpinized cats. Indicating that vascular reactivity is still present in more or less complete catecholamine depleted tissue. The duration of measurement was less than 40 seconds. Jones and Barnes (1964) observed a transient decrease of blood flow in the thigh muscle of dogs during venous stasis of 20 mm Hg, lasting about 40 seconds, whereafter blood flow almost returned to the level found before stasis. Lundvall and Mellander (1976) made similar observations in skeletal muscle of cats during external isoprene pressure of -40 mm Hg. Contrary to these findings venous stasis in humans caused a steady decrease in blood flow. Indicating that the phenomena observed in cat skeletal muscle and the "vasoconstrictor response" to venous stasis in humans are not directly comparable.

Thus the findings in reserpinized cats (Folkow and Öberg 1961) do not exclude an overlying nervous reinforcement mechanism.

Local anaesthetics block conduction of the nervous impulse (Taylor 1959) and phentolamine blocks adrenergic stimulation of "alpha-receptors" in vascular walls (Ahlqvist 1948, Roberts *et al.* 1957, Walker *et al.* 1959). The observed effects of local application of these drugs indicate that the "vasoconstrictor response" is due to a local nervous mechanism involving sympathetic adrenergic fibres. However the effect of phentolamine and lidocaine might be due to direct action on vascular smooth muscle cells (Djafarzadeh *et al.* 1968) to suppress myogenic activity.

As discussed previously the drugs did not hamper the capability of vascular smooth muscle cells to produce autoregulatory response. Lidocaine (3×10^{-4} Mol/l) did not affect myogenic activity in rat portal vein, but blocked impulse transmission in sympathetic fibres effectively (Johansson and Ljung 1967). In this concentration, lidocaine blocked the "vasoconstrictor response" 11 minutes after injection. Even when lidocaine (or phentolamine) were applied in concentrations of 5×10^{-4} Mol/l the response was reduced significantly by about 55 per cent.

Furthermore, actual concentrations of drugs in tissue were probably smaller due to dilution. Transmission of the vasoconstrictor stimulus was also blocked by lidocaine (1×10^{-4} Mol/l).

Hence the effect of lidocaine is due to blockade of impulse transmission in sympathetic fibres and the effect of phentolamine is due to blockade of alpha-receptors in vascular wall. This indicates that the "vasoconstrictor response" to an increase in vascular transmural pressure is due to a local nervous mechanism involving sympathetic adrenergic fibres.

Sites of the reflex

The "effector site" of the reflex is probably located in arterioles. Pressure measurements in microvascular system of human cutaneous tissue during changes in orthostatic pressure

and in cat mesentery indicate that precapillary resistance increases during venous stasis (Landis 1929 Richardson and Zwelfach 1970) Similarly precapillary resistance increased whereas postcapillary resistance decreased in autoperfused dog forelimb during venous stasis (Haddy and Scott 1964) In rat mesentery *Bacz et al* (1974) observed that arteriolar diameter decreased whereas venular diameter increased during venous stasis.

The "receptor site" is probably located in small veins Evidence is obtained from comparison of arterial and venous pressures under various conditions. Thus the response was produced by venous stasis of 30 mm Hg and by lowering the area 40 cm Both procedures produce increase of 30 mm Hg in venous transmural pressure However whereas similar increase in arterial transmural pressure is produced by lowering the extremity increase of maximally 15 mm Hg will occur during venous stasis of 30 mm Hg (Landis 1929) but this increase has already been produced by 20 cm lowering. In this position, blood flow remained constant (I) which contradicts precapillary location of receptor site When increase in venous transmural pressure during 40 cm lowering of the limb was prevented by letting the subject tip his foot, blood flow in subcutaneous adipose tissue remained constant (Henriksen and Sejrsen 1977b) In this situation, total vascular resistance increased only by 48 per cent corresponding to increase in arterial perfusion pressure head (autoregulation) This is contrary to the increase of about 200 per cent observed in the lowered resting limb Abolishment of the "vasoconstrictor response" during exercise might be due to metabolic changes in subcutaneous adipose tissue. However blood flow at reference conditions was not changed significantly by exercise. Furthermore, when venous pressure was elevated during exercise in the lowered limb by inflating a thigh cuff to 40 mm Hg, blood flow decreased by 50 per cent. This corresponds to an increase in vascular resistance of same magnitude as in the lowered resting leg. In patients with venous insufficiency exercise did not prevent the increase in venous transmural pressure and did not abolish the vasoconstrictor response

Therefore it is concluded that elevation of venous transmural pressure is the factor that elicits the vasoconstrictor response and that the response depends on impulse transmission from veins to arterioles (veno-arteriolar reflex)

The receptors are probably "stretch receptors" because the reflex was abolished when venous distension was counteracted by inducing local counterpressure (V)

Katz (1950) found that mechanical stretch of free nerve terminals of frog muscle spindles produced a local depolarization in the terminals. When stretch exceeded a certain level, discharge of action potential was elicited in stem axon. This is in agreement with the observation that the vasoconstrictor response was not elicited until the venous wall was distended to a degree which corresponds to an increase in venous transmural pressure of about 25 mm Hg. There is however so far no evidence of presence of a similar phenomenon in sympathetic fibres.

Nature of the impulse transmission

The "vasoconstrictor response" was not affected by somesthetic denervation (III) indicating that the impulse is transmitted only in sympathetic fibres. One possibility is that

impulses are transmitted from veins to arterioles in peripheral branches of efferent sympathetic fibres (sympathetic axon reflex). If so it is necessary to assume that a single efferent sympathetic axon innervates both veins and arterioles. Lumbar sympathetic nerve stimulation produced an increase in vascular resistance in perfused hind paw of dogs (Zimmerman 1966). The response in arteries and small vessels was blocked by section of somatic nerve bundles accompanying main arterial supply to the paw. The response in greater veins was unaffected. This indicates that sympathetic fibres supplying arterioles, arterioles, and small veins follow the same route. At present, there is no anatomical evidence that a single axon supplies both arterioles and veins.

Another possibility is an axo-axonal (ephaptic) transmission (Furshpan and Potter 1969) between afferent and efferent sympathetic fibres. However this seems to be of little significance in mammals. In the author's opinion the mechanism is most likely a sympathetic axon reflex. Later studies indicate that the reflex is present in human cutaneous tissue and human skeletal muscle too (Henriksen and Sejrsen 1976 and 1977 a).

Methodological implications of the reflex

Determination of blood flow by venous occlusion plethysmography

Blood flow measured by venous occlusion plethysmography might be influenced by the reflex. When a cuff placed on upper arm was inflated to 40 mm Hg between 40 and 60 seconds were necessary for venous pressure of distal forearm to increase to the threshold level of the reflex (25 mm Hg) (Henriksen and Sejrsen 1977 a). This indicates that existence of the reflex does not interfere with measurements of blood flow by venous occlusion plethysmography as long as preocclusion venous pressure is kept low.

Determination of capillary filtration capacity

Mellander, Odén, and Öberg (1964) determined capillary filtration capacity in human limbs by venous occlusion plethysmography. The subject was placed in a supine position and end-diastolic pressure was elevated 20–30 mm Hg above control values. The vasoconstrictor response, which increases pre- to postcapillary resistance ratio was probably elicited in these experiments. Estimated capillary pressure was therefore too high which leads to underestimation of capillary filtration capacity ($0.0077 \text{ ml}/100 \text{ g min mm Hg}$). Possible involvement of the veno-arteriolar reflex may also be taken into consideration when isogravimetric technique (Pappenheimer and Soto-Rivera 1948) is used. Using transmucosal osmotic technique (Pappenheimer, Renkin, and Borrero 1951) the vasoconstrictor response is not elicited.

Hæmodynamic implications of the reflex

Autoregulation of blood flow

Blood flow remained constant during elevation of the forearm despite decrease in arterial perfusion pressure head (venous pressure constant). This indicates that autoregulation of blood flow is maintained in subcutaneous adipose tissue. During increase in vascular

transmural pressure autoregulation was also observed but when venous transmural pressure exceeded a certain magnitude the veno-arteriolar reflex was superimposed. However when the reflex was blocked, autoregulation became evident in the whole range of changes in transmural pressure during lowering the limb as well as during external negative pressure. Similar findings have been obtained in adipose tissue of rabbits (Henriksen Nielsen and Paaske 1976) Ballard and Allapouhous (1975) found no evidence of autoregulation during arterial hypotension in adipose tissue of dogs. Difference in results obtained might be due to the fact that changes in carbon dioxide tension in tissue, surgical trauma, and mechanical manipulation might affect delicate mechanisms underlying autoregulatory responses (Johnson 1964 Rapela and Green 1964)

Autoregulation was present in denervated tissue (IV) and local nerve block was without effect (V) These findings indicate that intrinsic mechanisms are responsible This is compatible with results in skeletal muscle (Folkow 1949) The exact mechanism cannot be deduced from the present study

Autoregulation might be caused either by myogenic smooth muscle reactions that are related to stretch (Bayliss 1902, Folkow 1962 and 1964 Johnson 1968 Johansson and Mellander 1975) or due to changes in metabolic environment in the tissue (Anrep 1912, Hilton 1971) or both. Stansby and Renkin (1961) observed that blood flow in skeletal muscle was autoregulated at different levels that correlated to metabolic rate. Furthermore potassium (Kjellmar 1965) and hyperosmolality (Mellander *et al* 1967) seem to play a role in hyperaemia during exercise Cobbold *et al* (1963) showed that effect of sympathetic stimulation was abolished during ischaemia. In human skeletal muscle (Lindbjerg 1969) human cutaneous tissue (Paaske and Henriksen 1975) and human subcutaneous adipose tissue (Nielsen and Sejrsoen 1972) "cumulative" blood flow during postischæmic hyperaemia (repayment) was correlated to duration of ischaemia. Fairchild Ross and Guyton (1966) observed that there was no recovery from reactive hyperaemia in the absence of oxygen. It seems more and more evident that oxygen tension influences arteriolar diameter (Duling and Berne 1970 Duling 1972 Hutchins, Bond, and Green 1974) Studies by Gentry and Johnson (1972) indicate that blood flow through capillaries is ned by the condition of arteriolar smooth musculature.

Thus, a basal locus can probably be ascribed to myogenic reactivity related to stretch whereas autoregulation of blood flow is coupled to metabolic rate via metabolites and oxygen tension affecting arteriolar smooth muscle cells. However when venous transmural pressure is elevated about 25 mm Hg a veno-arteriolar reflex is superimposed to cause decrease in blood flow of about 50 per cent. It is important to emphasize that blood flow is still autoregulated at this lower level (I) Oxygen uptake in tissues probably remains constant As determined in blood from femoral artery and vein in humans arteriovenous oxygen difference increased from 43 ml/l to 120 ml/l during passive tilting to 70° and during standing with one leg hanging passively (Reeves *et al* 1961) If oxygen uptake in tissue remains constant this will correspond to a mean decrease in blood flow of about 65 per cent. This would be compatible with findings in subcutaneous adipose tissue of leg (V) and in skeletal muscle (Baldin *et al* 1971 Amery *et al* 1973)

Nicoli and Webb (1955) studied subcutaneous vessels and found that terminal arterioles

were seemingly unaffected by sympathetic innervation. However small arterioles were most sensitive to changes in oxygen tension (Duling 1972 Hutchins Bond and Green 1974). The veno-arteriolar reflex might affect greater arterioles which are richly innervated by adrenergic sympathetic fibres (Ehinger Falck, and Sporrang 1966) whereas intrinsic vascular reactions preferably take place in the smallest arterioles.

Trans-capillary fluid transfer

Vascular responses to changes in vascular transmural pressure seem closely connected with regulation of capillary hydrostatic pressure. Gore *et al* (1974) found that capillary pressure remained almost constant during arterial hypotension in cat mesentery. Järbult and Mellander (1974) studied net transcapillary fluid movements in response to variations in arterial perfusion pressure in acutely sympathectomized cat skeletal muscle. Results indicate that within a considerable range capillary hydrostatic pressure remained nearly constant due to resetting of pre- to postcapillary resistance ratio. In the lowest pressure range postcapillary resistance suddenly increased. Hanson and Johnson (1962) made similar observations in mesentery of cats. However increase in postcapillary resistance was abolished by local infusion of phenoxybenzamine phentolamine or in chronically sympathectomized animals. The increase was present after acute sympathectomy which indicates that this response, too, might be due to a sympathetic axon reflex. Thus local nervous mechanisms (veno-arteriolar arterio-venous reflexes) seem to participate in regulation of capillary hydrostatic pressure to supplement intrinsic vascular reactions. Local nervous reflexes counteract increased fluid filtration induced by augmented vascular transmural pressure under postural changes and venous stasis as edema protecting mechanisms.

Cardio-vascular adjustments to postural changes

Changing from supine to upright position caused an average decrease in cardiac output of about 1.7 l/min in resting human subjects (Hanson Tabakin, and Levy 1968). Average body weight was 77 kg. Assuming that mean arterial pressure remains constant at heart level, this decrease in cardiac output corresponds to a reduction in total vascular conductance of about 22 per cent. Venous transmural pressure probably increases more than 25 mm Hg in tissues constituting 30 per cent of body weight. Assuming that average decrease in blood flow is 2 ml/100 g min in these tissues the local veno-arteriolar reflex responds to a decrease in cardiac output of approximately 0.77 l/min. This corresponds to a decrease in vascular conductance of about 10 per cent, which is about 45 per cent of total change. The remaining 55 per cent are probably due to central reflex mechanisms elicited from baroreceptors located in arteries central veins and heart (Rod-Di Salvo *et al* 1971). Increase in plasma renin activity (Oparril *et al* 1970) and liberation of adrenaline and nor-adrenaline from adrenal medulla (Celander 1954) might also contribute. Hence 45 per cent of increase in vascular resistance due to postural compensation can be ascribed to the veno-arteriolar reflex mechanism that occurs independently of central nervous system.

Control of vascular tonus in human subcutaneous adipose tissue

Evidence obtained indicates that vascular tonus is influenced by intrinsic myogenic activity related to stretch by vasoactive metabolites liberated in tissue, and to periarteriolar oxygen tension. However venous distension corresponding to increase in venous pressure of 25 mm Hg or more elicits a veno-arteriolar reflex mechanism which increases arteriolar tonus to supplement effect of myogenic activity. These local mechanisms can then be influenced by changes in centrally elicited activity of sympathetic fibres as well as changes in plasma concentration of nor-adrenaline and adrenaline (Celander 1954, Mellander 1960, Mellander and Johansson 1968).

Pathophysiological implications

Arterial insufficiency of legs

The effect of lowering the leg on blood flow in subcutaneous tissue was studied in patients suffering from arterial insufficiency due to iliofemoral occlusion or severe stenosis (Henriksen 1974). Both vasoconstrictor response and autoregulation of blood flow were present in patients with intermittent claudication without resting pains. However in patients with resting pains blood flow increased at base of toes during lowering of leg whereas blood flow decreased at lateral malleolus and fibular head. In these patients "vasoconstrictor response" and autoregulation of blood flow were present in less affected areas whereas both responses were lacking in ischaemic areas. Increase of blood flow in ischaemic areas is probably due to decrease in vascular resistance caused by passive distension of vessels due to increase in vascular transmural pressure. Furthermore due to the veno-arteriolar reflex blood flow in the leg is redistributed from less affected areas to ischaemic areas creating an inverse steal syndrome (cf Lassen and Weastling 1969). Abolishment of reflex and autoregulatory mechanisms is probably due to accumulation of vasodilating metabolites in ischaemic areas to make arteriolar smooth muscle cells less sensitive to constrictor stimuli. In ischaemic areas, it has been shown that these vessels are less sensitive to the vasoconstrictor effect of angiotensine compared to vessels in less affected areas located proximally on the crus (Henriksen and Wisborg 1975).

Venous insufficiency

In normal subjects blood flow in subcutaneous adipose tissue remained constant when the limb was lowered 40 cm if increase in venous transmural pressure was avoided by letting the subject tip the foot continuously. However when venous pressure was elevated to about 40 mm Hg by inducing venous stasis blood flow decreased 50 per cent as in lowered resting leg (Henriksen and Sejrsen 1977b). In two patients with venous insufficiency exercise did not abolish the reflex in lowered position. In such patients—contrary to normals—blood flow in subcutaneous tissue of legs is reduced by 50 per cent during walking. This is probably also the case in cutaneous tissue. This might play a role in development of crural ulcers in these patients.

Conclusions

The present study provided a number of observations of physiological and clinical significance

- 1 Activity in sympathetic vasoconstrictor fibres participates in maintenance of vascular tones in human subcutaneous adipose tissue
- 2 Following sympathectomy blood flow in human subcutaneous adipose tissue increases by approximately 100 per cent, but vascular tone is reestablished about 8 days post-operatively
- 3 Autoregulation of blood flow *i.e.* maintenance of constant blood flow during changes in arterial perfusion pressure head or in arterial and venous transmural pressures is present in human subcutaneous adipose tissue.
- 4 Autoregulation of blood flow was still present in sympathetically denervated tissue and during acute local nervous blockade indicating that intrinsic mechanisms are responsible.
- 5 Increase in venous transmural pressure of 25 mm Hg or more elicits arteriolar constriction ("vasoconstrictor response" to increase in vascular transmural pressure) which reduces blood flow by approximately 50 per cent.
- 6 The vasoconstrictor response is in all probability due to a local sympathetic axon reflex mechanism.

Further studies

- 1 Electrical activity in single sympathetic vasoconstrictor fibres should be recorded in order to evaluate whether venous distension is in fact followed by peripherally elicited action potentials.
- 2 Furthermore it should be tested whether the vasoconstrictor impulse is transmitted from veins to arterioles via an afferent sympathetic fibre which plays in spinal ganglia and an efferent sympathetic fibres with ephaptic coupling. It will be necessary to make unilateral extirpation of spinal ganglia in animal experiments and then await degeneration of peripheral fibres
- 3 Relative importance between local regulation mechanisms central influence via centrally elicited nervous reflexes and humoral factors should also be studied.

Clinical aspects

- 1 Effect on blood flow in subcutaneous tissue of lowering the extremity might give information about vascular reactivity in patients with arterial insufficiency ("dependency test") Based on this, it might be possible to predict the effect of vasoactive

Control of vascular tonus in human subcutaneous adipose tissue

Evidence obtained indicates that vascular tonus is influenced by intrinsic myogenic activity related to stretch by vasoactive metabolites liberated in tissue and to periarteriolar oxygen tension. However venous distension corresponding to increase in venous pressure of 25 mm Hg or more elicits a veno-arteriolar reflex mechanism, which increases arteriolar tonus to supplement effect of myogenic activity. These local mechanisms can then be influenced by changes in centrally elicited activity of sympathetic fibres as well as changes in plasma concentration of nor-adrenaline and adrenaline (Celander 1954, Mellander 1960, Mellander and Johansson 1968).

Pathophysiological implications

Arterial insufficiency of legs

The effect of lowering the leg on blood flow in subcutaneous tissue was studied in patients suffering from arterial insufficiency due to iliofemoral occlusion or severe stenosis (Henriksen 1974). Both "vasoconstrictor response" and autoregulation of blood flow were present in patients with intermittent claudication without resting pains. However in patients with resting pains blood flow increased at base of toes during lowering of leg, whereas blood flow decreased at lateral malleolus and fibular head. In these patients, vasoconstrictor response and autoregulation of blood flow were present in less affected areas whereas both responses were lacking in ischaemic areas. Increase of blood flow in ischaemic areas is probably due to decrease in vascular resistance caused by passive distension of vessels due to increase in vascular transmural pressure. Furthermore due to the veno-arteriolar reflex blood flow in the leg is redistributed from less affected areas to ischaemic areas creating an "inverse steal syndrome" (cf Lassen and Westling 1969). Abolishment of reflex and autoregulatory mechanisms is probably due to accumulation of vasodilating metabolites in ischaemic areas to make arteriolar smooth muscle cells less sensitive to constrictor stimuli. In ischaemic areas it has been shown that these vessels are less sensitive to the vasoconstrictor effect of angiotensine compared to vessels in less

¹ areas located proximally on the crus (Henriksen and Wisborg 1975).

Venous insufficiency

In normal subjects blood flow in subcutaneous adipose tissue remained constant when the limb was lowered 40 cm if increase in venous transmural pressure was avoided by letting the subject tip the foot continuously. However when venous pressure was elevated to about 40 mm Hg by inducing venous stasis blood flow decreased 50 per cent as in lowered resting leg (Henriksen and Sejrén 1977b). In two patients with venous insufficiency exercise did not abolish the reflex in lowered position. In such patients—contrary to normals—blood flow in subcutaneous tissue of legs is reduced by 50 per cent during walking. This is probably also the case in cutaneous tissue. This might play a role in development of crural ulcers in these patients.

Summary

Effect of changes in vascular transmural pressure upon blood flow in human subcutaneous adipose tissue was studied in normal subjects. Changes in transmural pressure were obtained either by postural changes of a limb by inducing external negative pressure or by inducing venous stasis. Blood flow in subcutaneous adipose tissue was measured by means of the local ^{133}Xe washout technique.

Blood flow remained constant during elevation of a limb 30 cm above heart level corresponding to a decrease in vascular resistance of about 30 per cent (venous pressure remained constant). This indicates that autoregulation of blood flow / maintenance of constant blood flow during changes in arterial perfusion pressure head is present in human subcutaneous adipose tissue. Neither chronic sympathetic denervation nor local nervous blockade influenced the autoregulatory response indicating that local intrinsic mechanisms are responsible.

Blood flow remained constant when vascular transmural pressure was elevated 15 mm Hg by lowering the limb 20 cm or by inducing venous stasis of 15 mm Hg. However when vascular transmural pressure was elevated 25 mm Hg or more blood flow suddenly decreased about 50 per cent due to an increase in vascular resistance ("vasoconstrictor response"). Similar results were obtained during lowering of the limb during negative external pressure, as well as during venous stasis. The vasoconstrictor stimulus could be transmitted to an adjoining non-affected area over a distance of about 1.5 cm.

The vasoconstrictor response was blocked when passive distension of the vessels was counteracted by inducing local counterpressure indicating that the vasoconstrictor response is elicited by distension of vessels. Blood flow in contralateral leg remained constant.

The vasoconstrictor response to increase in vascular transmural pressure was not affected by acute spinal sympathetic blockade indicating that local mechanisms are responsible. Chronic somesthetic denervation was without effect too. The response was still present one day after sympathectomy. However four days or later after surgery both the "vasoconstrictor response" and the impulse transmission were abolished. Local "alpha-receptor" blockade induced by phentolamine blocked vasoconstrictor response but not impulse transmission, whereas lidocaine blocked both.

These findings indicate that the vasoconstrictor response to increase in vascular transmural pressure in human subcutaneous adipose tissue is due to local nervous mechanism involving sympathetic adrenergic fibres probably sympathetic axon reflex. The receptor site is most likely located in small veins whereas the effector site is located in arterioles (veno-arteriolar reflex).

The increase in pre to postcapillary resistance ratio induced by the reflex will counteract increase in capillary hydrostatic pressure and supplement intrinsic my

drugs upon blood flow in subcutaneous and presumably in cutaneous tissues too (Henriksen and Wisborg 1975)

2. The "dependency test" might indicate whether functioning sympathetic vasoconstrictor fibres are present in the area in question.
3. Vessels in the leg which are subjected to local orthostatic hypertension compared to those in the arm show an augmented "vasoconstrictor response" (Paaske and Henriksen 1975). Effect of treatment of arterial hypertension might be tested by measuring vascular reactivity.
4. In relation to the above-mentioned aspects, it would be interesting to study effect of *temporary hydrostatic hypotension upon the vasoconstrictor response* in vessels of the leg with special reference to the time course.
5. It might also be very interesting to study local regulation of blood flow in subcutaneous tissue in patients with vasospastic disorders and in patients with various skin diseases.

Resumé

Effekten af ændringer i blodkarenes transmurale tryk på gennemblødningen i underhudens fedtvæv er undersøgt i forsøg udført på raske mennesker. Transmurale trykændringer blev fremkaldt på tre forskellige måder: 1) stillingsændringer af en ekstremitet, 2) lokalit. eksternt, negativt tryk og 3) venestase. Gennemblødningen i subcutant fedtvæv blev målt ved hjælp af den lokale ^{149}Xe on udvaskningsteknik.

Gennemblødningen forblev uændret, når en ekstremitet blev elevet 30 cm, hvilket svarer til et fald i den totale karmodstand på ca. 30%. Dette fund tyder på, at gennemblødningen i subcutant fedtvæv er autoreguleret, dvs. uændret gennemblødning trods ændringer i det arterielle perfusionstryk (venetrykket forbliver uændret under elevation). Det autoregulatoriske respons kunne stadig påvises efter kronisk sympatisk denervering og under lokal nerveblokade. Dette taler for at autoregulation af gennemblødningen skyldes ændringer i arteriolerne tonus på grund af lokale ikke-nervøse faktorer. Gennemblødningen blev ikke påvirket af 20 cm's nedsenkning af et malleområde på en ekstremitet eller af 15 mm Hg venestase. Derimod blev gennemblødningen pludselig reduceret med ca. 50% på grund af en stigning i karmodstanden, når det transmurale tryk blev øget med 25 mm Hg eller mere, såvel under senkning af ekstremiteten ved eksternt lokalt undertryk, som ved venestase (vasokonstriktor respons). Et vasokonstriktor stimulus kunne transmitteres til et omgivende, ikke-påvirket område over en afstand af omkring 1,5 cm. Vasokonstriktor responset bliver sandsynligvis udløst ved passiv distension af karrene, da responset kunne blokeres, når man modvirkede distensionen ved at påføre lokalt modtryk over malleområdet. Gennemblødningen i det modsatte ben, der brugtes som kontrol, forblev uændret.

Akut spinal sympaliktablokade havde ingen effekt, hvilket tyder på, at vasokonstriktor responset skyldes lokale faktorer. Kronisk somatisk denervering havde ligeledes ingen effekt. Responset kunne stadig påvises dagen efter sympatektomi, men hverken vasokonstriktor responset eller impulstransmissionen kunne påvises på fjerde postoperative dag eller senere. Lokal alf α -receptor blokade med phentolamin blokerede vasokonstriktor responset, men ikke impulstransmissionen, mens lokalt indgivet lidocain blokerede begge dele. Disse fund tyder på at det vasokonstriktoriske respons over for stigning i det vaskulære transmurale tryk på 25 mm Hg eller mere skyldes en lokal nerves refleksmekanisme: sympatiske fibre d. s. en sympatisk aconrefleks. Receptorstedet er sandsynligvis placeret de små vener, mens effektorstedet er placeret i arteriolerne (veno-arterioler refleks).

Stigningen i forholdet mellem pre- og postkapillær modstand, som induceres af refleks ven., vil modvirke en stigning i det kapillære hydrostatiske tryk og vil dermed sammen med den myogene reaktion modvirke en stigning i den transkapillære filtrationsh α (beskyttelse mod ødemdannelse).

- Bern, R. M. Metabolic regulation of blood flow. *Circulat. Res.* 1964, 15, Suppl. 1, 261-267.
- Bern, J. A. and B. Ljung. Longitudinal propagation of myogenic activity in rabbit arteries and the rat portal vein. *Acta physiol. scand.* 1974, 98, 703-715.
- Brady, W. S. Howarth and E. P. Sharpey-Shafer. Postural changes in the peripheral blood flow of normal subjects in observation on reseroling following reactions as a result of lifting, the lordotic posture, pregnancy and spinal anesthesia. *Chir. Sci.* 1959, 9, 79-81.
- Burnstock, G. and C. L. Prosser. Responses of smooth muscles to quick stretch; relation of stretch to conduction. *Amer. J. Physiol.* 1960a, 198, 971-975.
- Burnstock, G. and C. L. Prosser. Conduction in smooth muscles; comparative electrical properties. *Amer. J. Physiol.* 1960b, 198, 337-359.
- Burton, A. C. and E. Rosenberg. Effects of raised venous pressure in the circulation of the halothane perfused rabbit. *Am. J. Physiol.* 1956, 143, 465-470.
- Bürg, S. Zur Physiologie und Pharmakologie der sterischen Arterio. *Helv. Physiol. Pharmacol. Acta* 1944, 2, 345-363.
- Chamber, O. The range of control exercised by the "sympathico-adrenal system". *Acta physiol. scand.* 1954, 29, Suppl. 116, 1-132.
- Cost, D. A. and N. Easwell. The short term effect of sympathetic ganglionectomy on the cat salivary secretion. *J. Physiol. (Lond.)* 1962, 162, 283-292.
- Cotfield, A., B. Folkow, L. Kjellner and S. Mellander. Nervous and local chemical control of pre-capillary sphincters in skeletal muscle as measured by changes in filtration coefficient. *Acta physiol. scand.* 1961, 37, 180-192.
- Cole, D. R. and A. D. M. Greenfield. The function of the blood vessels of hand during increases in transmural pressure. *J. Physiol. (Lond.)* 1956, 131, 277-299.
- Diaz, F. G. and R. W. Vane. Sympathetic block persistence after spinal or epidural analgesia. *J. Amer. Med. Ass.* 1963, 191, 283-287.
- Debus, W., R. E. Hagerth, A. Høegsø and B. G. Wallen. Massage reducing sympathetic outflow in human skin nerves. *Acta physiol. scand.* 1972, 94, 177-190.
- Diaz, K. G., S. Edelman and A. Winkler. Naloxone test—an objective method for testing local anesthetic drugs. *Acta anaesth. scand.* 1962, 4, 189-198.
- De Zeeuw, J. P. E., Parker, I. B., Scott and P. J. Haddy. Carotid baroreceptor influence on total and regional resistances in skin and muscle vasculature. *Amer. J. Physiol.* 1971, 220, 1970-1978.
- Dijkman, A. M., B. Folkow, B. Lissander and H. Sjöberg. Mechanism of escape of skeletal muscle resistance vessels from the influence of sympathetic cholinergic vasomotor fibre activity. *Acta physiol. scand.* 1968, 72, 148-156.
- Dilling, B. E. and R. M. Berne. Longitudinal gradients in perivascular oxygen tension. *Circulat. Res.* 1970, 27, 686-678.
- Dilling, B. E. Microvascular responses to alterations in oxygen tension. *Circulat. Res.* 1972, 31, 421-439.
- Elanger, B., R. Falck and B. Sperroed. Adrenergic fibres to the heart and to peripheral blood vessels. *Behv. Anal.* 1966, 8, 35-43.
- Fairchild, H. M., J. Ross and A. C. Guyton. Pattern of recovery from reactive hypotension in the presence of oxygen. *Amer. J. Physiol.* 1966, 210, 495-502.
- Fog, M. On postreceptor vasomotoric reactions. *Thromb. Coagulagene* 1954.
- Folkow, B. (intravascular pressure as a factor regulating the tone of small vessels. *Acta physiol. scand.* 1965, 289-310.
- Folkow, B. and B. Öberg. Autoregulation and local tone in cardiovascular vascular sections of the skeletal muscle in response to small changes in arterial pressure. *Acta physiol. scand.* 1961, 53, 105-113.
- Folkow, B. Transmural pressure and vascular tone—some aspects of an old controversy. *Arch. Int. Pharmacodyn.* 1962, 179, 435-468.
- Folkow, B. Description of the myogenic hypothesis. *Circulat. Res.* 1964, 15, Suppl. 1, 279-281.
- Farquhar, E. I. and D. D. Posner. Transmural pressure in the glomerular capillaries of the rat. *J. Physiol. (Lond.)* 1955, 105, 289-315.
- Geisler, P. and A. C. Berne. Local peripheral vasomotor reflexes arising from the body wall. *Circulat. Res.* 1961, 10, 27-39.
- Gentry, R. M. and P. C. Johnson. Reactive hypotension in arterioles and capillaries of frog skeletal muscle. *Circulat. Res.* 1972, 31, 953-963.
- Göthberg, K. and G. Haldbrandt. Probleme der Haut- und Muskeldurchblutung. *Leb. Dokum.* 1961, 15, 79-87.

- Pappasbalester J. R., E. M. Renkin and L. M. Borrero, Filtration, diffusion and molecular sieving through perip capillary membranes. *Amer J Physiol* 1951 167 13-46.
- Parkson, G. B. J. Olesen and S. Christensen, Restoration of autoregulation of cerebral blood flow by a Neurology 1972 22 286-293.
- Pasake W. P. and O. Reardon, Vascular resistance in nonocclusive vessels and vessels subjected to 1 orthostatic hypertension. *Acta physiol. scand* 1973 95 463-469.
- Pasake, W. P. and S. L. Nielsen, Capillary permeability in adipose tissue. *Acta physiol. scand*, 1976, 98 116-122.
- Rapch, C. E. and H. D. Green, Autoregulation of canine cerebral blood flow. *Circulat Res* 1964 14 Suppl. 1 205-211.
- Reeves, J. T. R. P. Grover, S. G. Blount and G. F. Filley, Cardiac output response to standing and treadmill walking. *J Appl Physiol* 1961 162 283-288.
- Rein, H. Vasomotorische Regulationen. *Ergebn. Physiol* 1931 32 28-72.
- Richardson D. R. and B. W. Zweiflich, Pressure relationships in the macro- and microcirculation of the mesentery. *Microvasc Res* 1976 2 474-488.
- Roberts, A. W. Richardson and H. D. Green, Effect of Regimine (C 7337) upon the blood flow responses to epinephrine in the unsensitized hind limb of the dog. *J Pharmacol. exp Ther* 1952 105 446-476.
- Roddie I. C. and J. T. Shepherd, The reflex nervous control of human skeletal muscle blood vessels. *Can. Sci.* 1956, 15 433-440.
- Roddie I. C. and J. T. Shepherd, The effects of carotid artery compression in man with special reference to changes in vascular resistance in the limbs. *J Physiol (Lond)* 1957 139 377-384.
- Roddie I. C. J. T. Shepherd and R. F. Wierman, Reflex changes in human skeletal muscle blood flow associated with intrathoracic pressure changes. *Circulat Res* 1976, 6 23-238.
- Roddie, I. C., The transmembrane potential changes associated with smooth muscle activity in turtle arteries and veins. *J Physiol. (Lond)* 1962, 163 138-150.
- Ros, P. C. and P. L. Coles, Sympathetic blockade during spinal anaesthesia. *Surg Gynecol Obstet* 1973 136, 265-268.
- Rosenberg, E. Local character of the vaso-vasomotor reflex. *Amer J Physiol* 1926, 155 471-473.
- Ross, J. M. H. M. Peirchald, J. Welch and A. C. Ouyson, Autoregulation of blood flow by oxygen lack. *Amer J Physiol* 1962, 202, 21-24.
- Rosell, L. B. C. R. Wyne and G. L. Brengelmann, Sustained isometric work and muscle vasoconstriction with reduced baroreceptor activity. *J Appl Physiol* 1973 5 639-643.
- Sedwell, G. Norepinephrine storage in skeletal muscle. *Acta physiol. scand* 1964, 60 39-50.
- Seymour, P. Blood flow in cutaneous tissue in man studied by washout of radioactive xenon. *Circulat Res* 1969 24 215-229.
- Seymour, P. Measurements of cutaneous blood flow by freely diffusible radioactive isotopes. Thesis, Copenhagen. } 1971 *Danish Medical Bulletin* 1971 Suppl. 18.
- Sellart, E. E. and P. C. Johnson, Effect of acute elevation of portal venous pressure on mesenteric volume, interstitial fluid volume and hemodynamics. *Circulat Res*, 1958, 6, 592-599.
- Sellart, E. E. The reflexes of renal blood flow to effective arterial pressure in the intact kidney of the dog. *Amer J Physiol* 1946 147 537-549.
- Stansby W. N. and E. M. Renkin, Autoregulation of blood flow in peripheral vascular beds. *Amer J Physiol* 1961 201 741-747.
- Taylor R. E. Effect of procaine on electrical properties of squid axon membrane. *Amer J Physiol* 1959 196 1071-1078.
- Tormaa, H. B. The control of hepatic circulation. *J Roy Coll. Surg. Edinb*, 1958, 4 147.
- Valon C. C. A. Brunon, V. Rezzato and L. Cares, Improved procedure for formation of epinephrine and nor-epinephrine fluorophores by the trihydroxymethole reaction. *Anal. Biochem* 1970, 33 158-167.
- Walker H. A., C. Heymann, E. Wilson and A. P. Richardson, The effect of C 7337 on carotid sinus reflex on pressure and peripheral vascular actions of epinephrine and nor-epinephrine. *J Pharmacol. exp Ther* 1970 198 33-34.
- Wood, J. E. and J. W. Eckstein, A tandem forearm plethysmograph for study of acute responses of the peripheral veins of man: the effect of environmental and local temperature change and the effect of pooling blood in the extremities. *J Clin Invest* 1976, 57 41-50.
- Zimmerman, B. O. Separation of responses of arteries and veins to sympathetic stimulation. *Circulat Res* 1966 18 429-436.
- Zoller R. P. A. L. Mark, F. M. Abboud, P. G. Schmid and D. D. Herstad, The role of low pressure baroreceptors in reflex vasoconstrictor responses in man. *J Clin. Invest* 1972 51 2967-2972.

